THE DENSE PHASE HYDRAULIC TRANSPORT OF HIGH CONCENTRATION CYCLONE CLASSIFIED TAILINGS IN PIPELINES

by

ROBERT COOKE

BSc (Eng.), MSc. (Eng.) in Civil Engineering

A thesis submitted in fulfilment of the requirements
for the degree of Doctor of Philosophy

Department of Civil Engineering
University of Cape Town

February 1991

DECLARATION

I, Robert Cooke, declare that this thesis is essentially my own work and has not been submitted for a degree at another university.

R COOKE

February 1991

DEDICATION

In memory of my sister, Frances

ABSTRACT

THE DENSE PHASE HYDRAULIC TRANSPORT OF HIGH CONCENTRATION CYCLONE CLASSIFIED TAILINGS IN PIPELINES

ROBERT COOKE

Department of Civil Engineering, University of Cape Town,
Private Bag, Rondebosch, 7700, South Africa

February 1991

Dense phase flow is defined to exist when the concentration of the solid particles equals or exceeds the freely settled particle concentration, and the dominant mechanism supporting the particles is interparticle contact. The hydraulic transport of high concentration dense phase mixtures is investigated, with particular reference to the transport of cyclone classified tailings for gold mines.

The experimental test procedures for the pipeline test facilities developed for the flow of high concentration slurries in horizontal and vertical pipelines are discussed and experimental errors evaluated for each measurement. The methods used to characterise the solid particles are described. A data base of pipeline tests of cyclone classified tailings materials is presented. At high solids concentration the mean mixture velocity versus pressure gradient curves become linear indicating that the mixture shear stress consists of viscous fluid shear stress and mechanical frictional stresses. The pressure gradient increases sharply for solids concentrations greater than the freely settled particle concentration.

The operating procedure for the rotating disc apparatus developed to investigate the submerged dynamic coefficient of friction between fine grained solid particles and a solid boundary is described, and experimental errors are evaluated for all measurements. Measured values of the dynamic coefficient of friction are presented which remain constant with speed.

A mechanistic model developed for dense phase flow is described. Fluid and solid particle friction mechanisms are used to establish stress relations for the mixture. The governing differential equation for the velocity distribution of the mixture is derived from the Cauchy momentum equation and solved using the finite element method. The model is extended to deal with mixtures with wide particle size distributions such as cyclone classified tailings. The model is evaluated by examining the influence of mean mixture velocity, solids concentration and pipe diameter on the velocity profiles and pressure gradients. The log standard error between the calculated and measured pressure gradients are generally less than 0,04 (average error less than 10%) for all tests above the freely settled particle concentration.

ACKNOWLEDGEMENTS

Professor J H Lazarus, thesis supervisor, for his guidance, encouragement and tremendous insight in the field of hydraulic transport.

The Chamber of Mines of South Africa for funding much of the research contained in this thesis.

The Council for Scientific and Industrial Research of South Africa and the University of Cape Town for financial support.

Mr P E Goosen, MSc student, with whom the author conducted the pipeline test work.

Dr A W Sive, who inspired the author to start the research that produced this thesis.

Professor D Reddy and Dr N J Marais for their discussions concerning numerical techniques.

Professor F A Kilner, Professor A D W Sparks and Dr F Scheele for the many stimulating discussions.

The Department of Civil Engineering workshop and laboratory staff for their assistance throughout the research project.

Mr D Nock of Warman pumps for the donation of equipment and valuable discussions.

Mrs C Wright for her remarkably accurate and efficient typing of this document.

Sieggy for her patience.

CONTENTS

CHAPTER 1 - INTRODUCTION

ABSTRACT

The objective of this investigation is to develop a mechanistic model to predict pressure gradients for the pipeline flow of high concentration backfill slurries to aid backfill system design. Hydraulic backfill transportation systems are described, and the lack of adequate pressure gradient prediction methods discussed. The methodology used in the investigation is described.

CHAPTER 2 - EXPERIMENTAL INVESTIGATION I - PIPELINE TESTS

ABSTRACT

The three pipe loops built to investigate the hydraulic transport of high concentration cyclone classified tailings are described. The methods used for measuring the variables (mean mixture velocity, slurry relative density, pressure gradient and slurry temperature) are discussed and experimental errors evaluated for each measurement. The experimental test procedure is described.

The methods used to characterise the solid particles for each material tested are discussed. The solid particle properties evaluated are: solids relative density, particle size distribution, particle shape factor, freely settled particle concentration, internal angle of friction of the solid particle matrix and the dynamic coefficient of sliding friction.

Test results for cyclone classified tailings from four mines (Blyvooruitsig, East Driefontein, Vaal Reefs and Western Deeps) are presented in a data base (Appendix A).

The variation of pressure gradient with velocity becomes linear at high concentration indicating that the pipe wall shear stress consists of viscous fluid shear stresses and mechanical sliding frictional stresses. The pressure gradient increases sharply with solids concentration above a solids concentration corresponding to the freely settled particle concentration. The rate of increase of pressure gradient with decrease in pipe diameter increases with increased solids concentration. The transition solids concentration between heterogeneous flow and homogeneous flow increases with increasing pipe diameter. The horizontal and vertical down friction pressure gradients are similar, while the vertical down friction pressure gradient is slightly greater than the vertical up friction loss.

CHAPTER 3 - EXPERIMENTAL INVESTIGATION II
MEASUREMENT OF SOLID PARTICLE SLIDING FRICTION

ABSTRACT

Methods used to determine the dynamic coefficient of sliding friction are reviewed. The development of a solid particle sliding friction apparatus for fine grained particles based on the design of a rotary shear meter is discussed. The measurement procedure is described and experimental errors evaluated for all measurements.

Measured values of the dynamic coefficient of friction are presented for the Blyvooruitsig, East Driefontein and Vaal Reefs materials. No values for the Western Deeps material are reported, as the material formed a non-Newtonian mixture which influenced the normal loading on the solid particles.

The measured dynamic coefficient of friction is constant with respect to the relative speed between the particles and the rotating disc. No clear trend regarding the effect of particle size distribution on the coefficient of friction was observed for the materials tested. The variation of the coefficient of friction with solids concentration is assumed to be similar to the variation of the internal angle of friction with concentration.

CHAPTER 4 - DENSE PHASE FLOW - A REVIEW OF ANALYTICAL METHODS

ABSTRACT

The term dense phase flow is defined in the context of this investigation. The Streat dense phase model for horizontal pipes and the Wilson, Brown and Streat model for high concentration flow in vertical pipes are reviewed and discussed. Streat's analysis of the vertical flow of solids-liquid mixtures in pipes is examined.

CHAPTER 5 - MECHANISTIC MODEL FOR THE DENSE PHASE FLOW OF CYCLONE CLASSIFIED TAILINGS

ABSTRACT

The development of a mechanistically based model for predicting pressure gradients of dense phase mixtures is presented. The model uses fluid and solid particle friction mechanisms to develop stress relations for the mixture. The governing differential equation for the velocity distribution of the mixture is derived from the Cauchy momentum equation and solved using the finite element method. The model is extended to deal with mixtures with wide particle size distributions such as cyclone classified tailings.

CHAPTER 6 - EVALUATION OF DENSE PHASE MODEL

ABSTRACT

The input parameters required by the dense phase mechanistic model are discussed and the values used for the model evaluation presented.

The dense phase model is evaluated by considering the influence of mean mixture velocity, solids concentration and pipe diameter on the velocity profiles and pressure gradients. The various dense phase flow regimes are examined. The model is numerically evaluated by calculating the log standard error between the predicted pressure gradients and the experimentally measured data points.

CHAPTER 7 - CONCLUSIONS

ABSTRACT

The main conclusions drawn from the experimental investigations, mechanistic model, and the evaluation of the mechanistic model are presented. The contributions made by the thesis are highlighted.

CHAPTER 8 - FUTURE RESEARCH

ABSTRACT

Research topics that could form an extension of the work done in this thesis are highlighted and discussed. Suggestions are made as to further experiments that may be conducted using the rotating disc friction apparatus, and a method of measuring the normal interparticle stress at the pipe wall is proposed. It is suggested that the velocity and concentration distribution within the pipe be measured to verify the mechanistic model. Further development of the mechanistic model and the evaluation of local pipeline wear rates are discussed.

NOMENCLATURE

		Units
a	area	m^2
A	internal area of pipe	m^2
c	local concentration of solids by volume	
C	mean concentration of solids by volume	
C_{min}	minimum concentration with solid particles in contact (freely settled concentration)	
C_{max}	maximum attainable concentration	
d	particle diameter	m
d_{50}	particle diameter such that 50% by mass of solids are less than d_{50}	m
d_t	transition particle diameter between fine and coarse particles	m
D	internal diameter of pipe	m
E	energy	Nm/s
f	friction factor	
F_i	external body force per unit mass in i direction	m/s^2
g	gravitational acceleration	m/s^2
G	dimensionless parameter	
h	thickness of boundary fluid shear layer	m
Δh	water level difference	m
i	hydraulic gradient in metres of water per metre	m/m
k	pipe roughness	m
K	fluid consistency index	$Pa.s^n$
L	length along pipe	m
m	coefficient in Landel *et al* viscosity equation	
M	mass	kg
n	flow behaviour index	
p	fluid pressure	Pa
P	percentage of solid particles	
ΔP	pressure gradient drop	Pa
Q	volumetric flow rate	m^3/s
r	radial position in pipe = $\sqrt{y^2 + z^2}$	m
Re_{CF}	Couette flow Reynolds number	

S	relative density	
S_f	particle settling shape factor	
t	time	s
T	temperature	°C
v	local velocity	m/s
V	mean velocity	m/s
V_{set}	particle settling velocity	m/s
V^*	shear velocity	m/s
x,y,z	coordinate system relative to pipe	m
X,Y,Z	global coordinate system	m
y	radial distance from pipe wall	m
z	vertical distance below top of sliding bed	m
α	turbulence coefficient	m
α	half angle defining position on pipe wall	rad.
β	angle defining intersection of sheared and unsheared zones at pipe wall	rad.
δ	internal angle of solids friction	rad.
ς	distance from pipe wall	m
θ	half angle defining sliding bed	rad.
κ	coefficient of lateral interparticle stress	
λ	linear concentration	
μ	dynamic coefficient of viscosity	Ns/m²
μ_d	dynamic coefficient of sliding friction	
μ_i	coefficient of incipient sliding friction	
ν	kinematic coefficient of viscosity	m²/s
ρ	bulk density	kg/m³
τ	stress	Pa
τ_y	yield shear stress	Pa
ϕ	angle defining pipe slope	rad.
Ψ	ratio of sheared stresses in a sheared particle matrix	rad.
ω	angular velocity	rad./s
$\mathcal{V}$	volume	m³

Subscripts

A	axial
B	sliding bed
C	coarse fraction
d	delivered
f	friction
F	fine fraction
h	hydrostatic
i	interface between sliding bed and suspension
ℓ	liquid phase
m	solid-liquid mixture
N	normal
p	fluid pressure
R	radial
s	solid phase
S	suspension
t	transition between fine and coarse particles
t	in situ
T	total
V	vehicle
w	pipe wall
w	water
W	weight

Superscripts

$\bar{f}$	mean value of f

COORDINATE SYSTEM

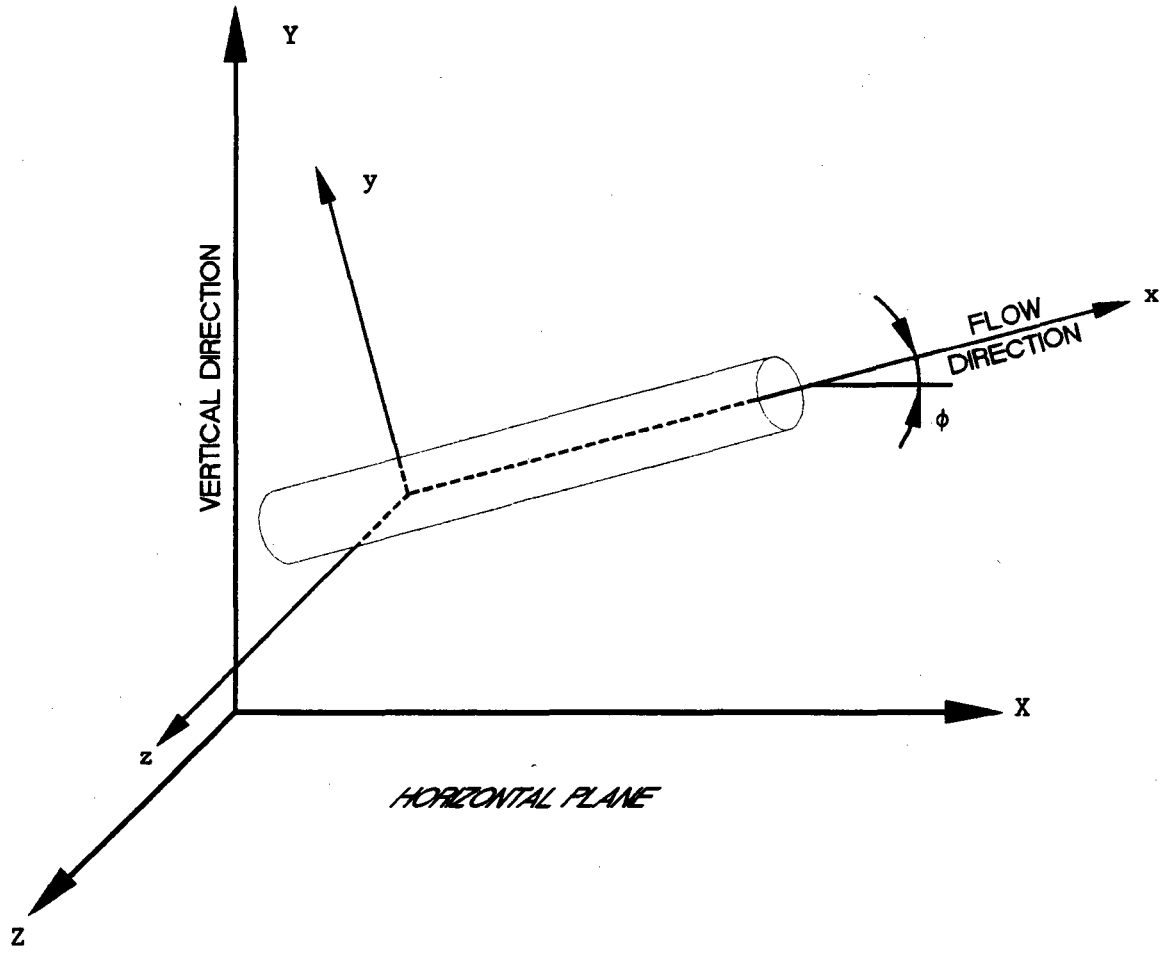

LIST OF FIGURES

LIST OF TABLES

REFERENCES

BAGNOLD, R.A. (1954) : "Experiments on a gravity-free dispersion of large solid spheres in a Newtonian fluid under shear", *Proc. Royal Society of London*, Series A, Vol. 225, p.49-63.

BAGNOLD, R.A. (1956) : "The flow of cohesionless grains in fluids", *Phil. Trans. Royal Society of London*, Series A, Vol. 249, p.235-297.

BANTIN, R.A., STREAT, M. (1970) : "Dense-phase flow of solids-water mixtures in pipelines", *Proc. 1st International Conference on the Hydraulic Transport of Solids in Pipes* (Warwick, England, 1-4 September), paper G1, p.G1-1 to G1-23.

BANTIN, R.A., STREAT, M. (1972) : "Mechanism of hydraulic conveying at high concentration in vertical and horizontal pipes", *Proc. 2nd International Conference on the Hydraulic Transport of Solids in Pipes* (Warwick, England, 20-22 September), paper B2, p.B2-11 to B2-24.

BLEVINS, R.D. (1984) : *Applied Fluid Dynamics Handbook*, New York, Van Nostrand Reinhold.

BOWDEN, F.P., TABOR, D. (1964) : *The Friction and Lubrication of Solids*, Clevedon Press, Oxford.

BRANDT, H.L., JOHNSON, B.M. (1963) : "Forces in a moving bed of particulate solids with interstitial fluid flow". *American Institute of Chemical Engineers Journal*, Vol. 9, No. 6, p.771-777.

BRINKWORTH, B.J. (1968) : *An introduction to experimentation*, English University Press, London.

BRISCOE, B.J., RADWEN, M., STREAT, M. (1983) : "Model Experiments on Sliding Friction for Application in Hydraulic Conveying of Solids". *Canadian Journal of Chemical Engineering*, Vol. 61, Dec., p.769-775.

BROWN, N.P., SHOOK, C.A., PETERS, J. (1983) : "A probe for point velocities in slurry flows". *Canadian Journal of Chemical Engineering*, Vol. 61, August, p.597-602.

BS 1377 (1975) : "Methods of test for soils for Civil Engineering purposes", *British Standards Institution*, London.

BUTTERFIELD, R., ANDRAWES, K.Z. (1972) : "On the Angles of Friction Between Sand and Plane Surfaces". *Journal of Terramechanics*", Vol. 8, No. 4, p.15-23.

CLOETE, F.L.D., MILLER, A.I., STREAT, M. (1967) : "Dense phase flow of solids-water mixtures through vertical pipes", *Trans. Institution of Chemical Engineers*, Vol. 45, p.T392-T400.

COOKE, R., LAZARUS, J.H. (1988) : "Isokinetic sampling probe for slurry flows". *Proc. 11th International Conference on the Hydraulic Transport of Solids in Pipes* (Stratford, England, 19-21 October), Paper C1, p.117-130.

GOVIER, G.W., CHARLES, M.E. (1961) : "The Hydraulics of the Pipeline Flow of Solid-Liquid Mixtures". *Engineering Journal*, Vol. 44, No. 8, August, p.50-57.

GOVIER, G.W., AZIZ, K. (1972) : *The Flow of Complex Mixtures in Pipes*, Van Nostrand Reinhold, New York.

HANKS, R.W. (1981) : *Hydraulic design for flow of complex fluids*, Hanks Associates, Utah.

HINDE, A.L., KRAMERS, C.P., KRUGER, F.J.A., LAMOS, A.W., NAMI, M. (1990) : "The development of backfill technology for deep South African Gold Mines: past, present and future", *Proc. International Deep Mining Conference: Technical Challenges in Deep Level Mining*, Johannesburg, South African Institute of Mining and Metallurgy, p.483-495.

HINTON, E., OWEN, D.R.J. (1980) : *An Introduction to Finite Element Computations*, Swansea, Pineridge Press, p.173-202.

JACOBS, B.E.A., TATSIS, A. (1986) : "Measurement of Wall Shear Stresses for High Concentration Slurries". *Proc. 10th International Conference on the Hydraulic Transport of Solids in Pipes* (Innsbruck, Austria, 29-31 October), Paper H1, p.267-273.

LAZARUS, J.H., NEILSON, I.D. (1978) : "A generalised correlation for friction head losses of settling mixtures in horizontal smooth pipes", *Proc. 5th International Conference on the Hydraulic Transport of Solids in Pipes* (Hanover, Germany, 8-11 May) Paper B1, p.B1-1 to B1-32.

LAZARUS, J.H. (1986) : *Hydraulic Transport of Solids in Pipelines*, Final year course notes, University of Cape Town.

LAZARUS, J.H. (1989) : "Mixed regime slurries in pipelines. I: Mechanistic model", *Journal of Hydraulic Engineering*, A.S.C.E., Vol. 115, No. 11, Nov, p.1496-1509.

LEUNG, L.S., WILES, R.J., NICKLIN, D.J. (1969) : "Transition from fluidised to packed bed flow in vertical hydraulic conveying", *Trans. Institution of Chemical Engineers*, Vol. 47, p.T271-T278.

LIU, B.L., SCHMIDT, H.J. (1985) : "Dense Phase Transport of Pulverised Coal - Modelling and Evaluation". *Proc. 8th Annual Energy Sources Technology Conference*, p.67-73.

NASR-EL-DIN, H., SHOOK, C.A., COLWELL, J. (1987) : "A conductivity probe for measuring local concentrations in slurry systems". *International Journal of Multiphase Flow*, Vol. 13, No. 3, p.365-378.

OWEN, D.R.J., HINTON, E. (1979) : *A Simple Guide to Finite Elements*, Swansea, Pineridge Press, p.47-68.

ROCO, M.C., SHOOK, C.A. (1982) : "Calculation approach for coal slurry pipelines". *Proc 7th International Technical Conference on Slurry Transportation*, STA, March 1982.

ROCO, M.C., SHOOK, C.A. (1983) : "Modelling of slurry flow: The effect of particle size". *Canadian Journal of Chemical Engineering*, Vol. 61, August, p.494-503.

ROCO, M.C., SHOOK, C.A. (1984) : "A model for turbulent slurry flow". *Journal of Pipelines*, Vol. 4, p.3-13.

ROCO, M.C., BALAKRISHNAM, N. (1985) : "Multi-dimensional flow analysis of solid-liquid mixtures". *Journal of Rheology*, Vol. 29, No. 4, p.431-456.

ROCO, M.C., SHOOK, C.A. (1985a) : "Critical deposit velocity in slurry flow". *American Institute of Chemical Engineers Journal*, Vol. 31, No. 8, p.1401-1404.

ROCO, M.C., SHOOK, C.A. (1985b) : "Turbulent flow of incompressible mixtures". *American Society of Mechanical Engineers*, Vol. 107, June, p.224-231.

ROCO, M.C., MAHADEVAN, S. (1986a) : "Scale-up technique of slurry pipelines - Part 1: Turbulence modelling". *Journal of Energy Resources Technology*, Vol. 108, December, p.269-277.

ROCO, M.C., MAHADEVAN, S. (1986b) : "Scale-up technique of slurry pipelines - Part 2: Numerical integration". *Journal of Energy Resource Technology*, Vol. 108, December, p.278-285.

ROCO, M.C., SHOOK, C.A. (1987) : "New approach to predict concentration distribution in fine particle slurry flows". *PhysicoChemical Hydrodynamics*, Vol. 8, No. 1, p.43-60.

ROCO, M.C., CADER, T. (1989) : "Approach to compute and scale up wear distribution in slurry pipelines". *Proc. 6th Freight Pipelines Symposium*.

SCHLICHTING, H. (1968) : *Boundary-Layer Theory*, 6th ed., McGraw Hill, New York.

SHOOK, C.A., DANIEL, S.M. (1965) : "Flow of suspensions of solids in pipelines - Part I: Flow with a stable stationary deposit", *Canadian Journal of Chemical Engineering*, Vol. 43, April, p.56-61.

SHOOK, G.A., DANIEL, S.M., SCOTT, J.A., HOLGATE, J.P. (1968) : "Flow of suspensions in pipelines - Part II: Two mechanisms of particle suspension", *Canadian Journal of Chemical Engineering*, Vol. 46, August, p.238-244.

SIVE, A.W. (1988) : "An analytical and experimental investigation of the hydraulic transport of high concentration mixed regime slurries", *PhD Dissertation - University of Cape Town*.

SIVE, A.W. & LAZARUS, J.H. (1989) : "Mixed regime slurries in pipelines. II: Experimental evaluation", *Journal of Hydraulic Engineering*, A.S.C.E., Vol. 115, No. 11, Nov, p.1510-1520.

SPEARING, A.J.S. & SMART, R.M. (1990) : "The potential benefits of (silicated) cemented backfill systems", *Proc. International Deep Mining Conference: Technical Challenges in Deep Mining*, Johannesburg, South African Institute of Mining and Metallurgy, p.1241-1246.

STREAT, M., TELEVANTOS, Y., CARLETON, A.J. (1976) : "Pilot-Plant Studies of Hydraulic Conveying of Coarse Materials at High Concentration in Pipelines". *Proc. 4th International Conference of the Hydraulic Transport of Solids in Pipes* (Alberta, Canada, 18-21 May), Paper F2, p.F2-21 to F2-30.

STREAT, M. (1982) : "A comparison of specific energy consumption in dilute and dense phase conveying of solids-water mixtures", *Proc. 8th International Conference on Hydraulic Transport of Solids in Pipes* (Johannesburg, South Africa, 25-27 August), paper B3, p.111-122.

STREAT, M. (1986) : "Dense Phase Flow of Solids-Water Mixtures in Pipelines: A state-of-the-art Review". *Proc. 10th International Conference on the Hydraulic Transport of Solids in Pipes* (Innsbruck, Austria, October 29-31), BHRA, Cranfield, UK, Paper B9, p.39-54.

TATSIS, A., JACOBS, B.E.A. (1987) : "Slip-Model Correlation for Semi-Stabilized Slurries". *Proc. 12th International Conference on Slurry Technology*, (New Orleans, USA, 31 March - 3 April), p.79-85.

TELEVANTOS, Y., SHOOK, C., CARLETON, A., STREAT, M. (1979) : "Flow of slurries of coarse particles at high solids concentrations", *Canadian Journal of Chemical Engineering*", Vol. 57, p.255-262.

WALLIS (1969) : *One-Dimensional Two-Phase Flow*, McGraw-Hill, New York.

WILSON, K.C. (1970) : "Slip Point of Beds in Solid-Liquid Pipeline Flow". *Journal of Hydraulic Engineering*, A.S.C.E., HY1, January, p.1-12.

WILSON, K.C., STREAT, N., BANTIN, R.A. (1972) : "Slip-Model Correlation of Dense Two-Phase Flow". *Proc. 2nd International Conference on the Hydraulic Transport of Solids in Pipes*, (Warwick, UK, September 20-22), BHRA, Cranfield, UK, Paper B1, p.B1-1 to B1-10.

WILSON, K.C., BROWN, N.P., STREAT, M. (1979) : "Hydraulic Hoisting at High Concentration: A New Study of Friction Mechanisms". *Proc. 6th International Conference on the Hydraulic Transport of Solids in Pipes*, (Canterbury, U.K., September 26-28), BHRA, Cranfield, U.K., Paper F2, p.269-282.

WILSON, K.C. (1981) : "Analysis of slip of a particulate mass in a horizontal pipe", *Bulk Solids Handling*, Vol. 1, No. 2, May, p.295-299.

WILSON, K.C. (1982) : "The dense phase option for coarse coal pipelining", *Journal of Pipelines*, Vol. 2, p.95-101.

WINGROVE, A.C. (1989) : "Backfill development at JCI", *Proc. Slurry Transport in the Mining Industry: Current Technology*, Hydraulic Conveying Association of South Africa, Sandton, 6 September.

ZENZ, A.F. & OTHMER, D.F. (1960) : *Fluidization and Fluid-Particle Systems*, Reinhold, New York.

CHAPTER 1

INTRODUCTION

1. BACKGROUND

As South African gold mines reach ever increasing depths it has become necessary to backfill stopes to control rock bursts and stope convergence due to excessive over burden pressures. Backfilling involves the placement of waste material (termed backfill) in mined out areas of the mine. Additional reasons for backfilling, apart from rock bursts, are that backfill (Hinde *et al* (1990)) :

(i) reduces labour requirements for handling timber props,

(ii) offsets shortfalls in timber supply and reduces fire hazards,

(iii) improves mine ventilation,

(iv) improves ore extraction.

Backfill material is hydraulically transported from the surface level, where it is produced, to stopes underground where the backfill is placed in paddocks. Figure 1.1 shows the layout of a "free fall" hydraulic transport system. The backfill slurry is supplied to the shaft column in which it falls freely under gravity until it reaches the air-slurry interface. The height of the air-slurry interface is established such that the pressure head available (due to height H_i in Figure 1.1) balances the pipeline friction losses for a particular flow rate. Thus if the supply flow rate is increased the level of the air-slurry interface will rise. Disadvantages of the free fall system are :

(i) Very high velocities are attained in the free fall zone resulting in extremely high pipeline wear rates.

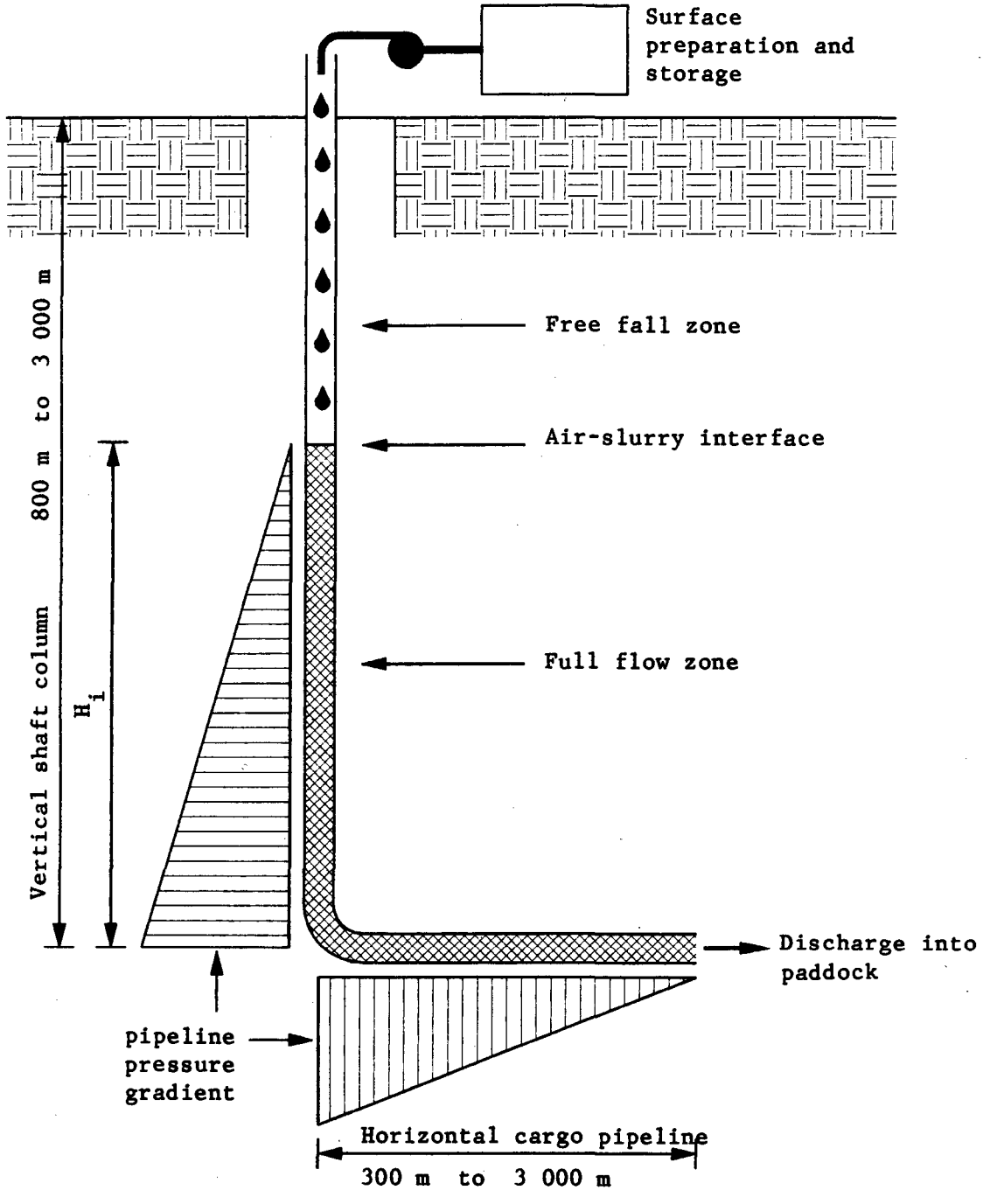

Figure 1.1 : Free fall backfill hydraulic transport system

(ii) The high impact pressures generated at the air-slurry interface may lead to pipeline "bursting" failure.

Figure 1.2 illustrates the layout of a "full-flow" backfill hydraulic transport system. The air-slurry interface is maintained at surface level by ensuring that the pressure head available is matched by the system friction losses. The advantage of the full flow system is that pipeline wear rates, and thus failures, are minimised. The difficulty of implementing such a system is that generally for slurry velocities below 3 m/s the pressure head available is far greater than the frictional losses. Proposals and methods used to dissipate the excess energy are as follows :

(i) Ceramic choke sections have been installed at pipeline flanges. These chokes have led to localised wear downstream of the choke and consequently pipeline failure.

(ii) Lengths of small bore pipe have been installed and successfully used to dissipate excess energy, although the pipeline wear rate is high due to the high slurry velocities.

(iii) Energy dissipators are being developed to dissipate a large amount of energy in a short length of pipeline. One such design incorporates ceramic balls in a housing (Wingrove (1989)). This design has been tested successfully with stabilised slurries, but was found to block with settling mixtures.

(iv) Pressure breaks in the form of storage reservoirs at intermediate levels have been successfully used. Future designs incorporate these pressure breaks (Hinde *et al* (1990)).

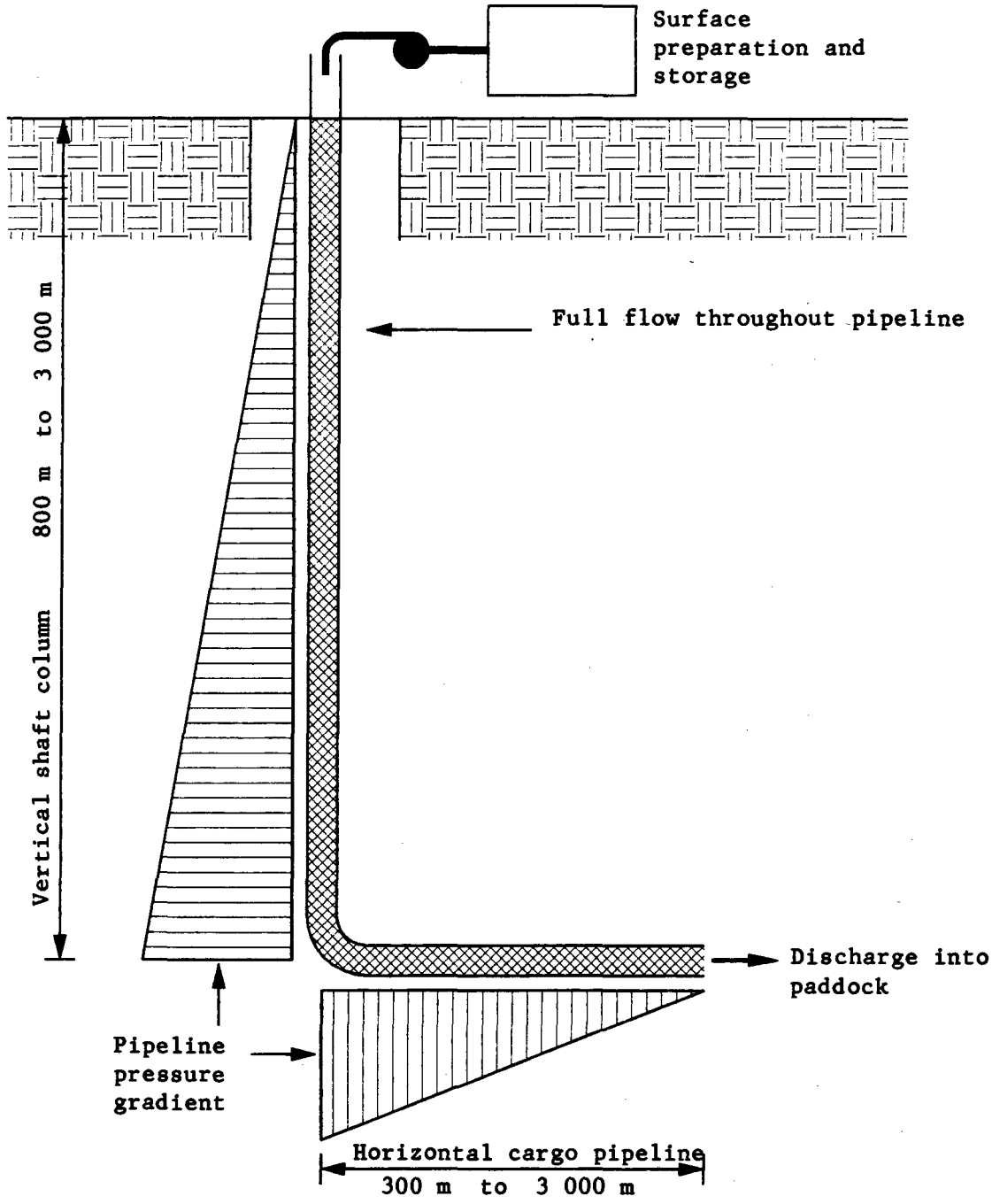

Figure 1.2 : Full flow backfill hydraulic transport system

(v) Most backfill systems operate at a concentration of 36% to 42% by volume. Increasing the solids concentration to 50% by volume will result in the following benefits :

- The pipeline friction losses will be substantially increased, thus reducing the amount of excess energy available.

- There will be less water run-off after placement, which will reduce water handling problems in the mine.

- The backfill consolidation time will be reduced.

There are many types of backfill materials presently being used in gold mines. Table 1.1 shows that cyclone classified tailings account for 73% of the total quantity of fill placed (Spearing and Smart (1990)). Cyclone classified tailings are produced by removing the fine fraction of full plant tailings (all tailings from the mineral extraction process) through a cycloning process. Figure 1.3 compares typical particle size distributions of full plant tailings and cyclone classified tailings.

TABLE 1.1 : Backfill materials (Spearing and Smart (1990))

Material	% of Total Placed
Cyclone classified tailings	73,0
Cemented tailings	25,0
Dewatered tailings	1,5
Comminuted (crushed) waste	0,5

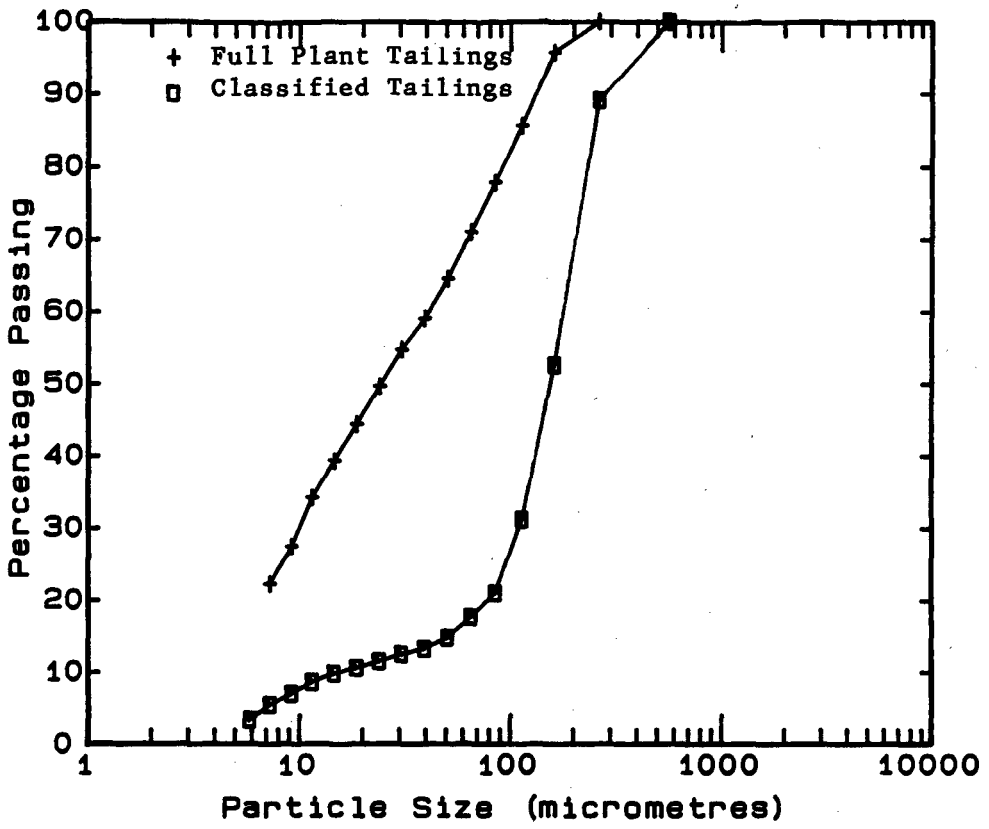

Figure 1.3 : Full plant tailings and cyclone classified tailings particle size distributions

2. STATEMENT OF PROBLEM

In order to design backfill systems with confidence it is vital that the pipeline pressure gradients be predicted accurately. This is especially true for full flow systems.

Figure 1.4 shows the variation of the experimentally measured horizontal pressure gradient with solids concentration for cyclone classified tailings in a 40 mm NB pipeline at a mean mixture velocity of 2 m/s. It is seen that the measured pressure gradient increases very steeply above a solids concentration of 40% by volume. The Lazarus (1989) sliding bed model for mixed regime slurries (i.e. wide particle size distributions) has been shown to accurately predict pressure gradients for solids concentrations less than 40% by volume. It is apparent from Figure 1.4 that the Lazarus analysis does not model the flow mechanisms of high concentration flows satisfactorily enough to predict the sharp increase in pressure gradient for solids concentrations greater than 40% by volume. Also shown in Figure 1.4 is the predicted pressure gradient calculated using Streat's (1986) dense phase model, Equation (4.15) page 4.8, for horizontal pipelines. It is clear that the Streat dense phase model does not adequately predict the pipeline pressure gradient for design use.

The variation of the measured pressure gradient with solids concentration for the vertical downward flow of classified tailings is shown in Figure 1.5. As with horizontal flow the pressure gradient increases steeply for solids concentrations greater than 40% by volume. The predicted pressure gradient calculated using Streat's (1986) analysis, Equation (4.25) page 4.13, for vertical flows is shown in Figure 1.5. Vertical pressure gradients are defined in Figure 2.17 on page 2.43. It is clear that Streat's assumption in his analysis that the friction losses in a vertical pipe may be approximated by that due to clear water alone is not valid for high concentration mixtures.

Thus the primary problem facing the designer of a backfill system is how to predict pipeline pressure gradients for the flow of high concentration backfill slurries.

Very little work has been done on the investigation of high concentration (greater than 40% by volume) settling mixtures. The reason for this paucity of work is that in most cases the high pipeline pressure gradients render high concentration hydraulic transport systems uneconomic. This is not true of backfill hydraulic transport systems where the high pipeline pressure gradients may be advantageously used to dissipate the excess energy available.

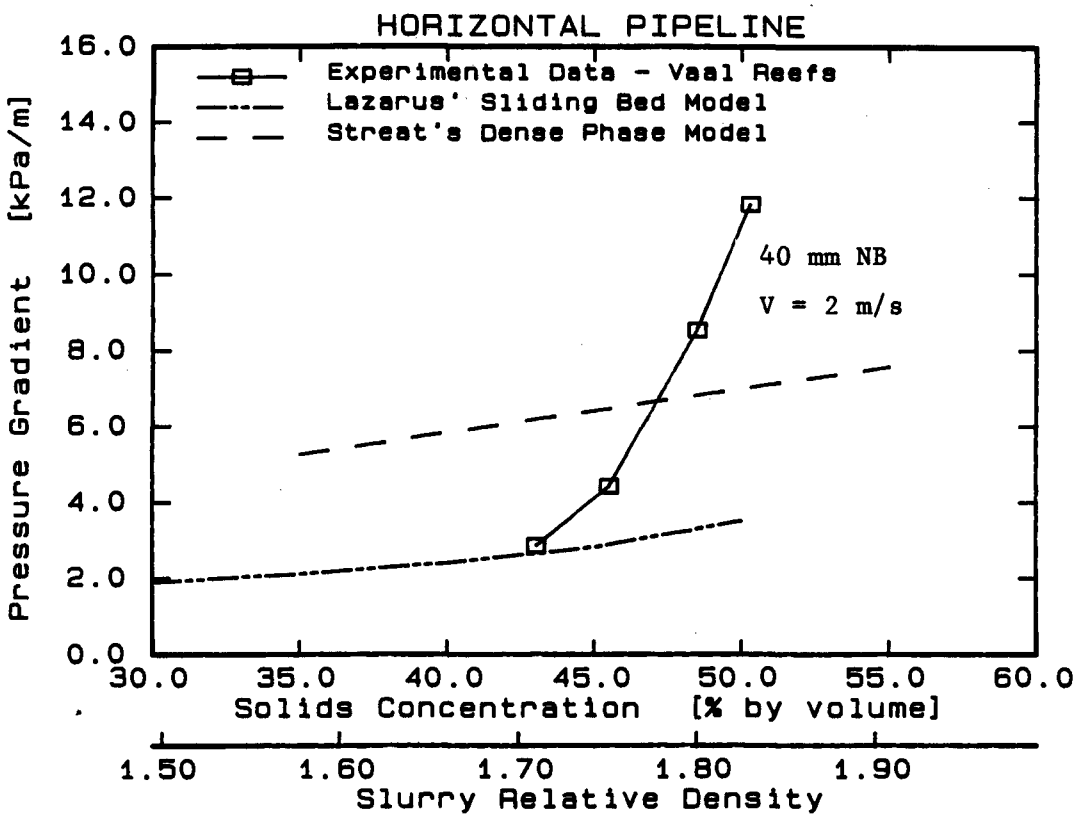

Figure 1.4 : Horizontal pipeline experimental data and model comparison

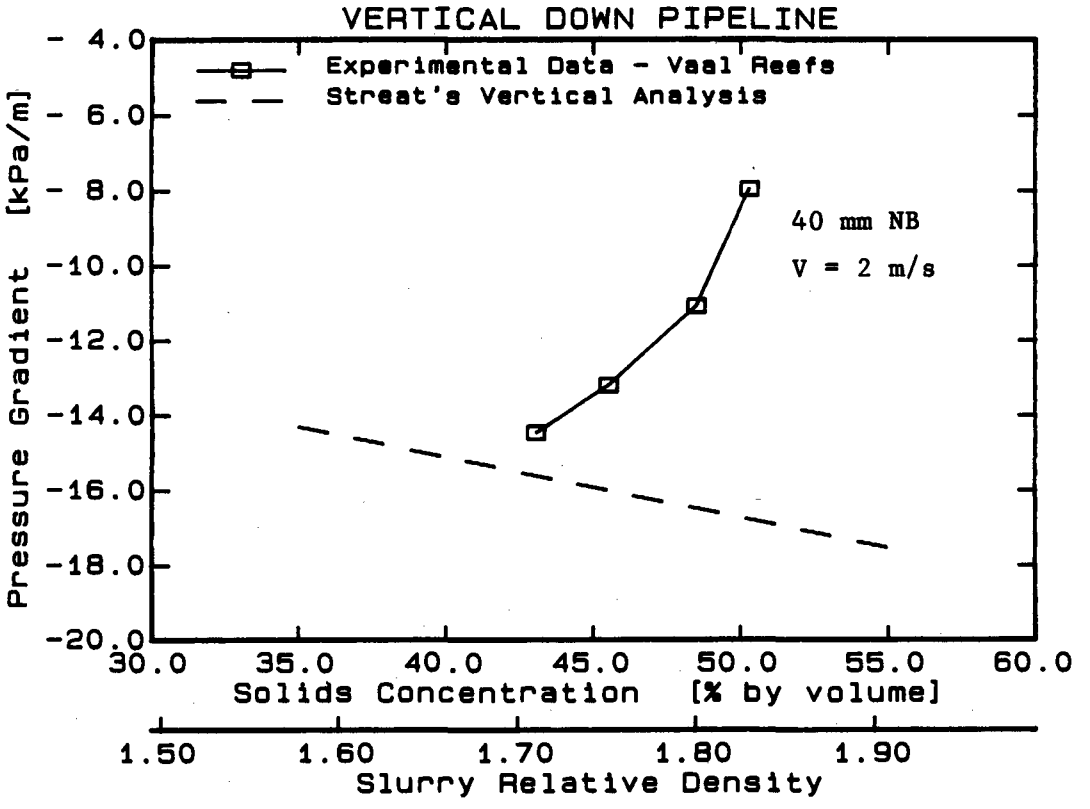

Figure 1.5 : Vertical down pipeline experimental data and model comparison

3. OBJECTIVE AND SCOPE OF INVESTIGATION

The objective of this investigation is to determine the flow mechanisms of high concentration settling slurries, and to develop a model to predict pressure gradients for the pipeline flow of these slurries.

In particular it is required that a model be developed to predict pressure gradients for the design of backfill systems conveying cyclone classified tailings.

4. METHODOLOGY

4.1 Pipeline tests - Chapter 2

The first goal of the investigation is to establish a data base of measured pressure gradients to be used to evaluate the pressure gradient prediction model. In addition to quantitative measurements, valuable qualitative information concerning flow mechanisms and behaviour was obtained from visual observations of the mixtures during tests.

Pipeline pressure gradients were measured for horizontal and vertical down flow in 25 mm, 40 mm and 80 mm nominal bore pipelines. Pressure gradients for vertical up flow were also measured in the 25 mm nominal bore pipe loop. Cyclone classified tailings were tested from four mines (Blyvooruitsig, East Driefontein, Vaal Reefs and Western Deeps).

The following measurements were made during the tests - pressure gradient, mean mixture velocity, solids concentration and slurry temperature. Solid particle properties such as particle size distribution, particle shape factor, solids relative density, angle of internal friction and the dynamic coefficient of sliding friction were determined for each material.

4.2 Coefficient of sliding friction between solid particles and pipe wall - Chapter 3

Due to the importance of mechanical sliding friction to the energy loss of high concentration mixtures, an apparatus was built to investigate the dynamic coefficient of sliding friction. The parameters investigated were particle size distribution, speed of sliding and solids concentration.

4.3 Review of existing dense phase models - Chapter 4

The Streat (1986) dense phase model for horizontal flow is reviewed. Streat (1986) and Wilson *et al* (1979) analyses of high concentration vertical flow are discussed. The models are compared with experimental data.

4.4 Development of mechanistic model - Chapter 5

The mechanistic model for the high concentration flow of settling mixtures is based on the governing differential equation describing the velocity distribution in a pipeline conveying a solid liquid mixture. The differential equation is derived by considering the Cauchy momentum equations for the solid and liquid phases of the flow. Boundary conditions particular to high concentration slurries are applied to the differential equation which is solved using the finite element method.

4.5 Evaluation of model - Chapter 6

The mechanistic dense phase model is compared with the experimental data and discussed.

5. CHAPTER SUMMARY

The objective of this investigation is to develop a mechanistic model to predict pipeline pressure gradients for the flow of high concentration cyclone classified tailings backfill slurries.

The investigation consists of experimental and analytical components. Pipeline pressure gradients and the dynamic coefficient of sliding friction between the particles and pipe wall are experimentally measured. An analytical model which describes the flow mechanisms of high concentration settling mixtures and predicts pipeline pressure gradients is developed. This model is evaluated using the experimentally measured pipeline pressure gradients.

CHAPTER 2

EXPERIMENTAL INVESTIGATION I

PIPELINE TESTS

1. INTRODUCTION

The experimental investigation of the flow of high concentration backfill slurries entailed the development of new pipeline test loops and operating procedures compared with previous experimental work done with lower concentration mixtures (Sive and Lazarus (1989)). Two test facilities were built for the investigation - a 25 mm nominal bore test loop, and a test facility with 40 mm and 80 mm nominal bore pipelines. These test loops are described and the operating procedures discussed. Experimental errors are evaluated for all measurements.

The methods used to characterise the solid particles (particle size distribution, particle relative density, particle shape factor, angle of internal friction and the coefficient of sliding friction between the sliding particles and pipe wall) are discussed. The properties of the cyclone classified tailings from four mines (Blyvooruitsig, East Driefontein, Vaal Reefs and Western Deeps) tested in this investigation are presented and discussed.

The pressure gradient data and flow observations from the pipeline tests are graphically presented as summaries of the test data base. The results are discussed and evaluated.

2. PIPELINE TEST APPARATUS AND OPERATING PROCEDURE

2.1 Description of test loops

Figure 2.1 shows the layout of the 25 mm NB test loop, while the 40/80 mm NB test facility is illustrated in Figure 2.2. The design and layout of the two facilities is similar. Table 2.1 shows the relevant parameters for each pipe loop. Each facility has the following components :

(i) Slurry hopper

The hoppers are circular with conical bases. The slurry in each hopper is mixed using a mechanical agitator to ensure a consistent slurry mixture.

(ii) Sampling tank

The total flow from the pipe loop may be diverted to the sample tank to determine the slurry relative density and verify the flow rate. The sampling tank is suspended from a mass scale.

(iii) Centrifugal pump

The slurry is pumped around the test loop using a centrifugal pump driven by a variable speed hydraulic motor.

(iv) Heat exchanger

An inline heat exchanger is used to reduce the heat build-up in the system in order to maintain a constant slurry temperature during a test.

(v) Pipeline

The pipe loops are constructed from ASTM A106 Grade B seamless carbon steel pipe.

(vi) Clear section

The clear section of polyvinyl chloride (PVC) pipe permits visual observation of the solid liquid mixture.

TABLE 2.1 : Pipe loop parameters

System Parameter	25 mm NB Loop	40/80 mm NB Facility	
		40 mm NB	80 mm NB
Slurry hopper volume (ℓ)	80	450	
Sample tank volume (ℓ)	8	30	
Pipe schedule	40	40	80
Internal diameter (mm)	26,6	40,0	73,4
Internal diameter of clear section (mm)	28,0	46,0	71,0
Length of clear section (mm)	200	2050	1950
Centrifugal pump	Warman 1½/1 steel casing	Warman 3/2 rubber lined	
Rotational speed of agitation impellor (rpm)	29	30	
Diameter of agitation impellor (mm)	420	900	

(vii) Pressure tappings

Differential pressure measurements are made at three locations (horizontal, vertical up and vertical down) in the 25 mm NB loop, and at two locations (horizontal and vertical down) in the 40/80 mm NB facility. The pressure measurements are made using static pressure tappings located in the pipe wall. To ensure accurate pressure measurements the tappings have length to diameter ratios greater than four (Sive 1988). The tappings were drilled to a diameter of 3 mm. Great care was taken to ensure that the tappings were burr free inside the pipe. Each tapping is connected to a solids trap to ensure that the manometers are isolated from the slurry in the pipeline.

Hanks (1981) recommends that a length of unobstructed straight pipe be installed prior to the measuring section to ensure that all disturbances introduced by the pump and fittings are completely damped. This flow development or "calming length" should be at least 50 pipe diameters long for turbulent flow of Newtonian fluids. The pipe loops were designed to meet this requirement as closely as possible.

25 mm NB TEST FACILITY

Pipe loop dimensions (mm)

Loop	D	a	b	c	d	e	f	g	h	i
25 mm NB	26.6	1350	800	650	1700	500	650	950	500	500

Ratio of pipeline dimensions to internal pipe diameter

Loop	a/D	b/D	c/D	d/D	e/D	f/D	g/D	h/D	i/D
25 mm NB	50.8	30.1	24.4	63.9	18.8	24.4	35.7	18.8	18.8

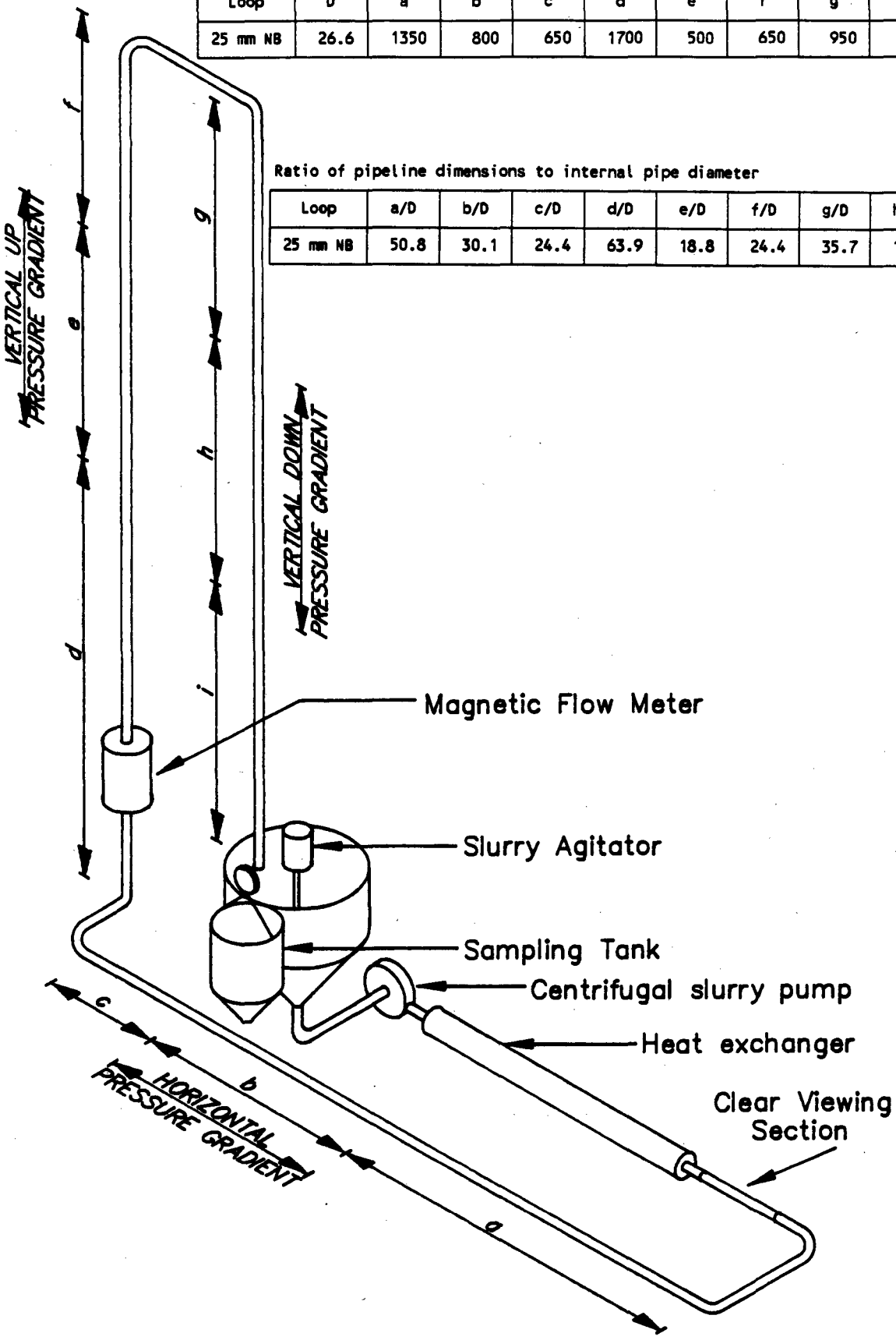

Figure 2.1

40 mm / 80 mm NB TEST FACILITY

Pipe loop dimensions (mm)

Loop	D	a	b	c	d	e	f
40 mm NB	40.0	4885	1000	3270	3020	1000	700
80 mm NB	73.4	3845	1500	3200	3220	1500	1300

Ratio of pipeline dimensions to internal pipe diameter

Loop	a/D	b/D	c/D	d/D	e/D	f/D
40 mm NB	122.1	25.0	81.8	75.5	25.0	17.5
80 mm NB	52.4	20.4	44.0	43.9	20.4	17.7

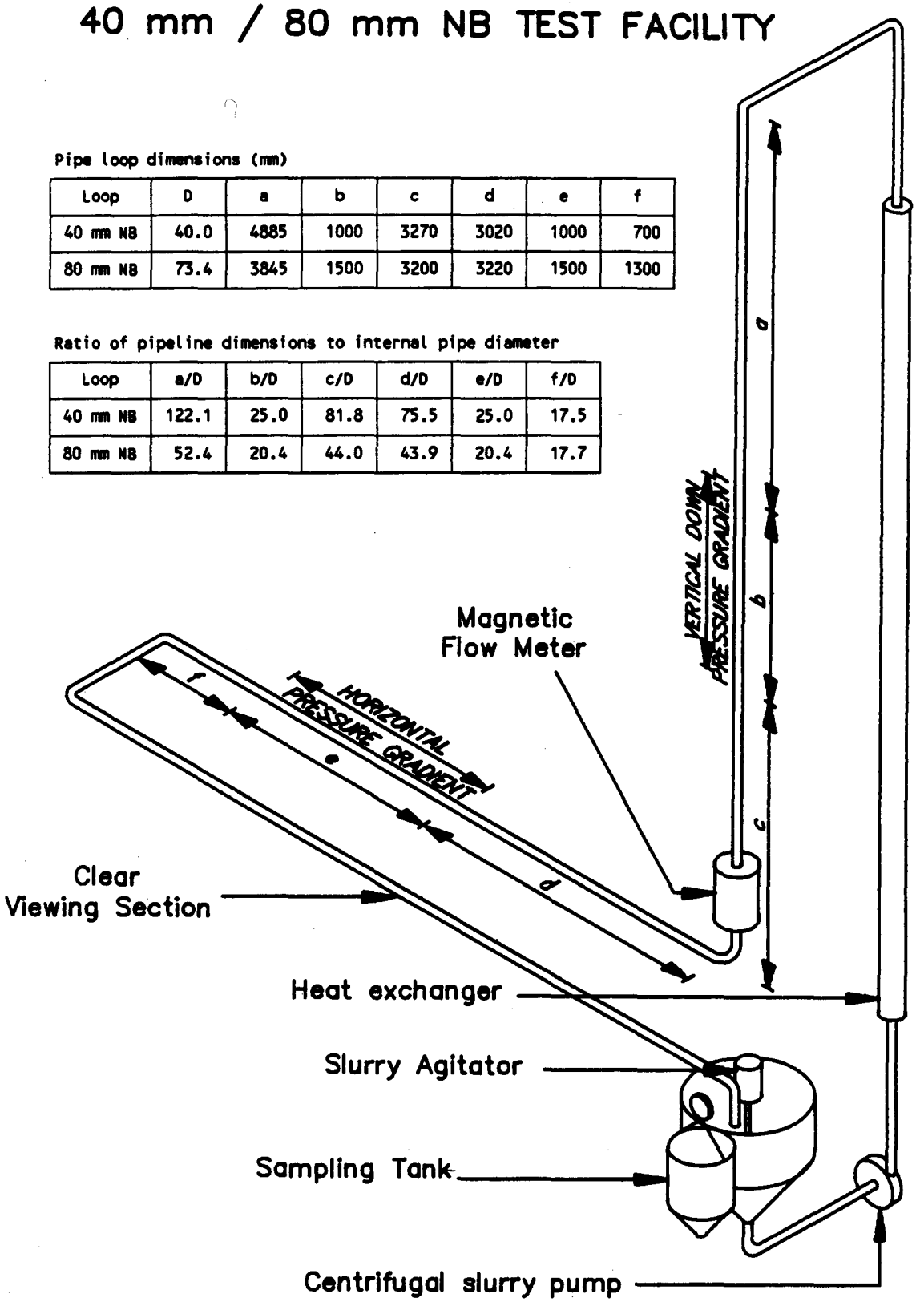

Figure 2.2

(viii) Magnetic flow meter

The magnetic flow meter which consists of a detection head and signal converter, provides a current output which is proportional to the mean flow rate regardless of the fluid.

(ix) Manometer board and differential pressure transducers

Figure 2.3 shows the connection of the air over water manometer board, differential pressure transducers and static pressure tappings for one differential pressure measurement. The glass manometer tubes have an internal diameter of 6 mm and a length of 1,8 m. The following operations are performed from the manometer board :

(a) The air is flushed out of the manometer tubes.

(b) The differential pressure transducer is flushed to remove any trapped air.

(c) The connection lines and isolation pods are flushed to remove any solids or air.

(d) The differential pressure transducer is calibrated by setting up differential heads Δh .

(e) The differential tapping pressure may be read using the air over water manometer. The air pressure in the manometer tubes is matched to the pipeline pressure to ensure that Δh is visible.

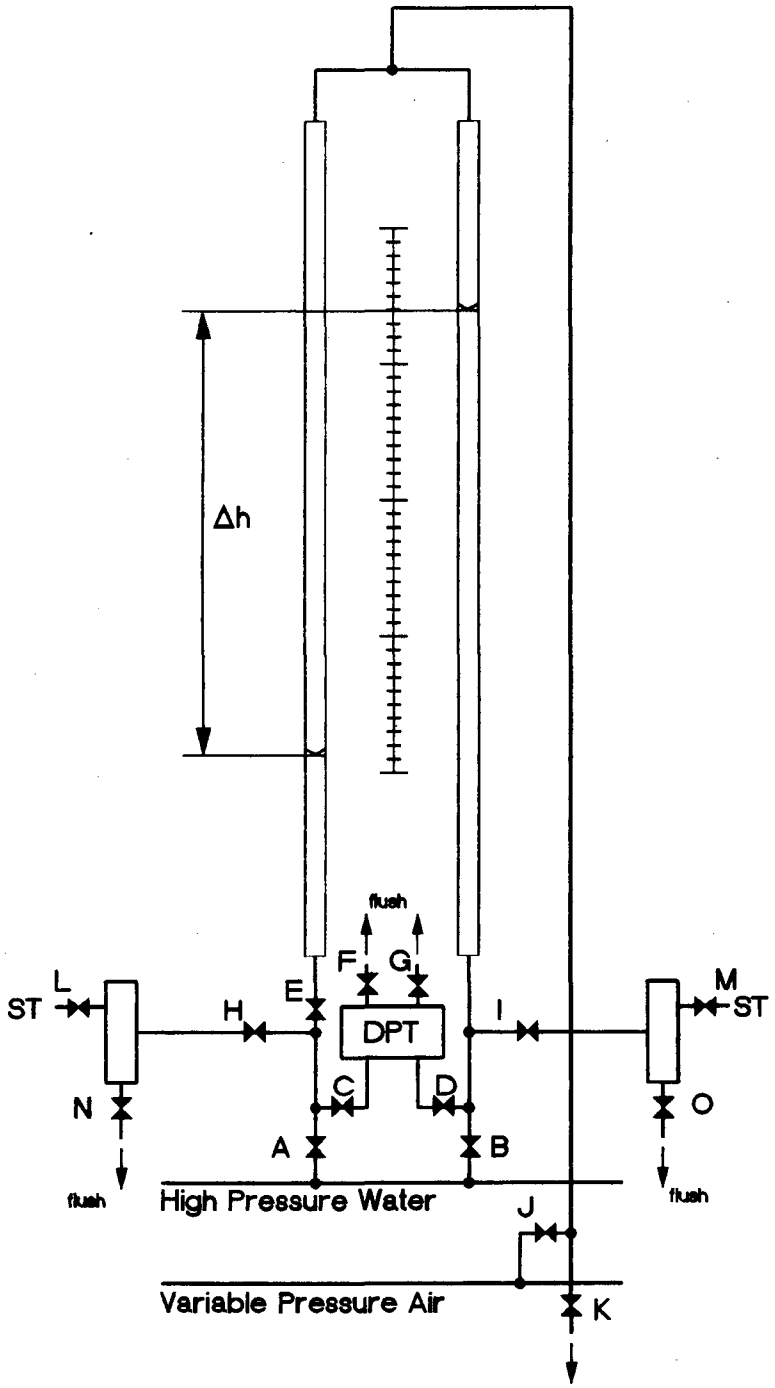

ST : Static Pipewall Pressure Tapping
DPT : Differential Pressure Transducer

Figure 2.3 : Manometer and pressure tapping layout

(f) Read differential tapping pressures using the pressure transducer.

(g) Read the differential tapping pressures using both the air over water manometer and the pressure transducer.

Table 2.2 shows the valve positions for these operations.

TABLE 2.2 : Manometer valve positions

O = Open C = Closed V = Variable

Operation	Valve (see Figure 2.3)														
	A	B	C	D	E	F	G	H	I	J	K	L	M	N	O
(a)	O	O	C	C	O	C	C	C	C	C	O	C	C	C	C
(b)	O	O	O	O	O	O	O	C	C	C	C	C	C	C	C
(c)	O	O	C	C	C	C	C	O	O	C	C	V	V	V	V
(d)	V	V	O	O	O	C	C	V	V	V	C	V	V	C	C
(e)	C	C	C	C	O	C	C	O	O	V	C	O	O	C	C
(f)	C	C	O	O	C	C	C	O	O	C	C	O	O	C	C
(g)	C	C	O	O	O	C	C	O	O	V	C	O	O	C	C

2.2 Measured variables

2.2.1 *Slurry relative density*

This investigation is concerned with the dense phase flow of high concentration slurries. For these mixtures the concentration distribution is taken to be homogeneous across the pipe section, thus the delivered and *in situ* mixture relative densities (and volumetric concentrations) are taken to be equal.

The relative density of the slurry is found by diverting the flow to the sample tank and performing a relative density test. Referring to Figure 2.4 the relative density test is conducted as follows :

Step 1 : Determine the empty mass of the sample tank M_{Te} .

Step 2 : Fill the sample tank with water to a predetermined level AA (a hole in the side of the tank), and obtain the mass of the tank and water M_{Tw} . Thus the volume of the tank is

$$\mathcal{V}_T = \frac{(M_{Tw} - M_{Te})}{\rho_w} , \tag{2.1}$$

where ρ_w = density of water at measurement temperature.

Step 3 : Empty the tank of water and fill with a sample of slurry, ensuring that the slurry does not rise above level AA. Measure the mass of the tank and slurry sample M_{Tm} . The mass of the slurry sample is

$$M_m = M_{Tm} - M_{Te} . \tag{2.2}$$

Step 4 : Fill tank up to level AA with water. Measure the mass of the tank plus sample plus added water M_{Tw} . The volume of water added is

$$\mathcal{V}_w = \frac{(M_{Tmw} - M_{Tw})}{\rho_w} . \tag{2.3}$$

Thus the volume of the slurry sample is

$$\mathcal{V}_m = \mathcal{V}_T - \mathcal{V}_w , \tag{2.4}$$

and slurry relative density is

$$S_m = \frac{M_m}{\mathcal{V}_m \rho_w} . \tag{2.5}$$

This procedure is repeated from Step 3 for subsequent slurry relative density measurements. To ensure an accurate measurement for slurry relative densities greater than 1,80 it is necessary to vibrate the sample to remove air entrained during sampling. The sample is vibrated using a concrete poker vibrator.

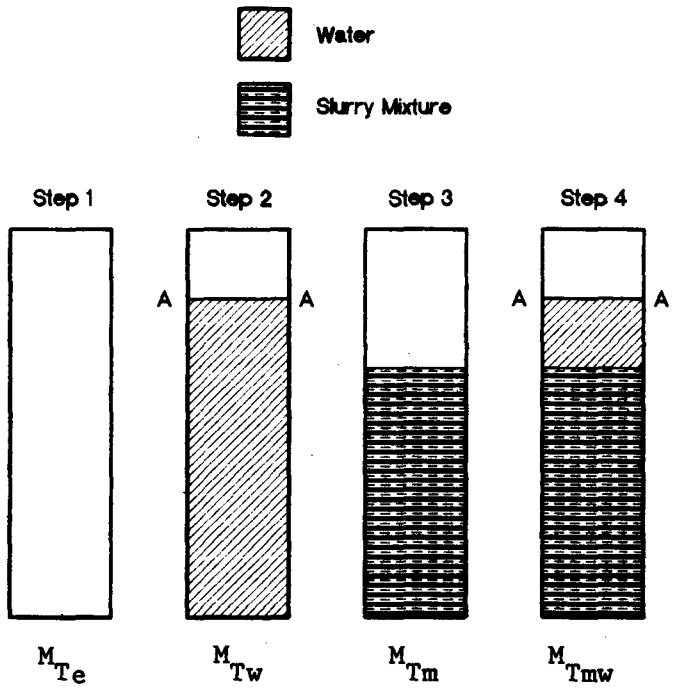

Figure 2.4 : Slurry relative density test

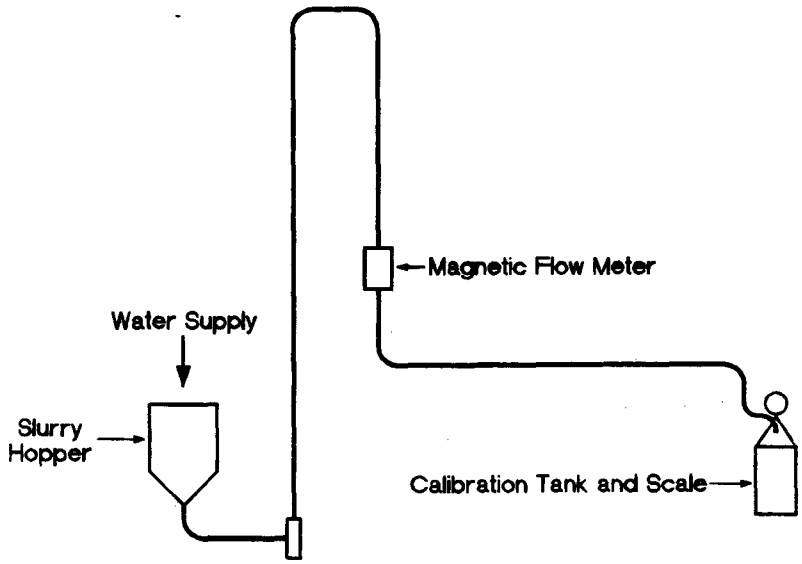

Figure 2.5 : Calibration of magnetic flow meter

2.2.2 *Slurry flow rate*

The slurry flow rate is primarily determined from the output of the magnetic flow meter. The accuracy of the magnetic flow meter output the is checked by timing (t) the collection of a known volume ($\forall_m$) of sample. The flow rate is calculated as follows :

$$Q_m = \frac{\forall_m}{t} , \qquad (2.6)$$

where t = sampling duration.

The magnetic flow meters have a linear relationship between the flow rate and current output, i.e.

$$Q_m = m_{mag}\, i + c_{mag} , \qquad (2.7)$$

where i = current output
m_{mag} = slope of calibration line
c_{mag} = calibration line intercept.

The magnetic flow meter is calibrated with clear water flowing through the pipe loop as shown in Figure 2.5. Water is supplied to the slurry hopper which is pumped through the pipe loop (the water is not recirculated). The flow at the end of the pipe loop is diverted to a 100 ℓ calibration tank to determine the flow rate corresponding to a particular magnetic flow meter output. The flow rate is calculated from the mass of the water sample and the sampling duration. To ensure that the flow rate does not vary during sampling the following precautions are adopted :

(i) The water level in the slurry hopper is kept constant by matching the water supply rate and the pump rotational speed.

(ii) The pipeline outlet is kept at a fixed level.

Calibration data points (magnetic flow meter output and flow rate) are obtained for the required flow range.

The flow range is from zero to a flow rate corresponding to a mean mixture velocity of 4 m/s. The calibration curve is obtained from a least squares linear regression analysis. For the calibration to be accepted the correlation coefficient R should be between 0,99 and 1. The correlation coefficient is defined as :

$$R = \frac{n \Sigma xy - \Sigma x \Sigma y}{[(n \Sigma x^2 - (\Sigma x)^2) (n \Sigma y^2 - (\Sigma y)^2)]^{1/2}} , \qquad (2.8)$$

where, in this case,

x = flow rate

y = magnetic flow meter output

n = number of data points.

2.2.3 *Mixture head loss*

The head loss of mixture in units of water i_m , shown in Figure 2.6, is defined as :

$$i_m = \frac{\Delta h}{L} \qquad (2.9)$$

where Δh = measured water head difference

L = distance between pressure tappings.

The water head difference Δh is measured with a differential pressure transducer. The output of the differential pressure transducer may be verified by simultaneously reading Δh with the air over water monameter.

The differential pressure transducers have a linear relationship between applied water head differential and current output, i.e.

$$\Delta h = m_{press} \, i + c_{press} \qquad (2.10)$$

where m_{press} = slope of calibration line

c_{press} = calibration line constant.

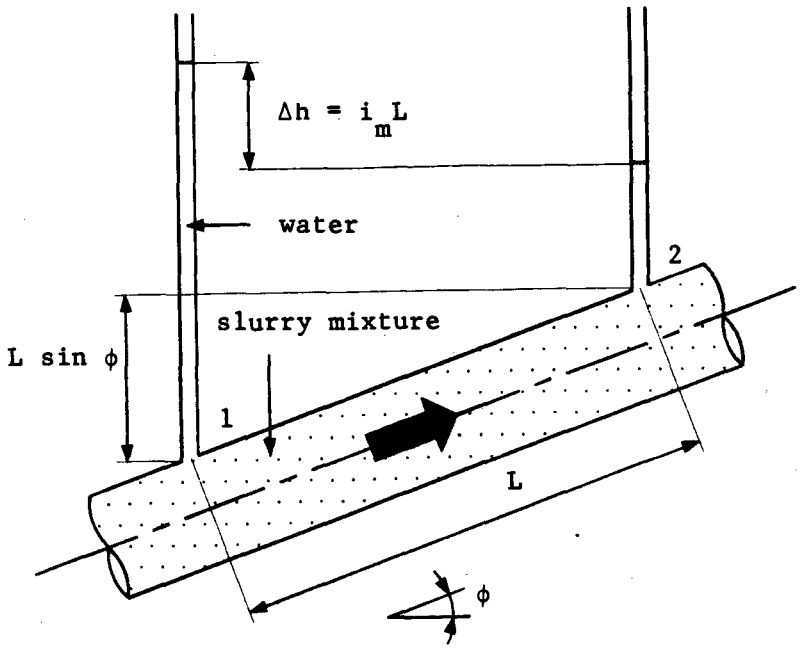

Figure 2.6 : Definition of mixture head loss

The differential pressure transducers are calibrated by setting up various water height differentials on the manometers and recording the transducer current output. The Δh range used for the calibration is 0 to 1 800 mm. The calibration curve is obtained from a least squares linear regression analysis, and checked using the correlation coefficient R (equation 2.8).

Note that Δh includes components due to friction losses as well as the weight component of the solids liquid mixtures. In downward sloping pipes ($\phi < 0$) Δh may be negative.

2.2.4 *Internal pipe diameter*

The internal pipe diameter is obtained by determining the mass of water required to fill a known length of pipeline. The internal pipe diameter is calculated as follows :

$$D = \sqrt{\frac{4\,M_w}{\rho_w \pi\, L}}\ , \qquad (2.11)$$

where M_w = mass of water to fill pipe length

ρ_w = density of water at measurement temperature

L = length of pipeline.

2.2.5 *Slurry temperature*

The slurry temperature is measured using a temperature probe located in the slurry hopper. The probe has a linear relationship between temperature and current output. The probe is calibrated by comparing temperatures measured using a mercury thermometer with the probe's current output. The calibration curve is obtained from a least squares linear regression analysis. The linearity is verified using the correlation coefficient R (equation 2.8).

2.3 Derived variables

2.3.1 *Solids volumetric concentration*

The solids volumetric concentration C is calculated from the following relation :

$$C = \frac{S_m - S_w}{S_s - S_w} \quad , \tag{2.12}$$

where S_m = relative density of slurry
S_w = relative density of water at measurement temperature
S_s = relative density of the solid particles.

2.3.2 *Mean mixture velocity*

The mean mixture velocity V_m is determined from the continuity equation :

$$V_m = \frac{4\,Q_m}{\pi\,D^2} \quad . \tag{2.13}$$

2.3.3 *Pressure gradient*

Referring to Figure 2.6 the pressure difference between points 1 and 2 is :

$$\Delta P = P_1 - P_2$$

$$= (\Delta h + L \sin \phi)\, \rho_w\, g \quad .$$

Thus the pressure gradient may be written as :

$$\frac{\Delta P}{L} = (i_m + \sin \phi)\, \rho_w\, g \quad , \tag{2.14}$$

where $i_m = \frac{\Delta h}{L}$.

The pressure gradient to overcome frictional forces (total pressure gradient - weight component) is found from :

$$\left(\frac{\Delta P}{L}\right)_{fric} = \frac{\Delta P}{L} - S_m \rho g \sin \phi \quad , \qquad (2.15)$$

where ϕ = slope of pipeline.

2.3.4 *Pipe roughness*

The hydraulic roughness of the pipe, k is determined from a clear water test. The hydraulic gradient is measured for velocities ranging from 0 to 4 m/s, and the pipe roughness evaluated using the Colebrook White formulation :

$$\frac{1}{\sqrt{f}} = -4 \log \left[\frac{k}{3{,}7\ D} + \frac{1{,}26}{Re \sqrt{f}} \right] \quad , \qquad (2.16)$$

where f = friction factor = $\dfrac{i_w g D}{2 V^2}$

Re = Reynolds number = $\dfrac{VD}{\nu}$

i_w = water hydraulic gradient

V = mean water velocity

ν = kinematic coefficient of viscosity for water.

2.4 Experimental procedure

The data logging configuration used for recording the test data is shown in Figure 2.7. The data logger converts the analogue signals from the pressure transducers, magnetic flow meter and temperature probe to digital signals which are read by the computer. These readings are then converted to engineering units using the calibration constants. Output from the computer may be to the monitor, printer or plotter.

Sive (1988) and Sive and Lazarus (1989) statistically evaluated each data point during a test run to determine whether it should be accepted or rejected. This procedure, developed by Sive, was found to be inappropriate for data logging high concentration slurry tests due to the long period required to complete a set of data points (90 minutes to 2 hours). When pumping high concentration slurries in a recirculating

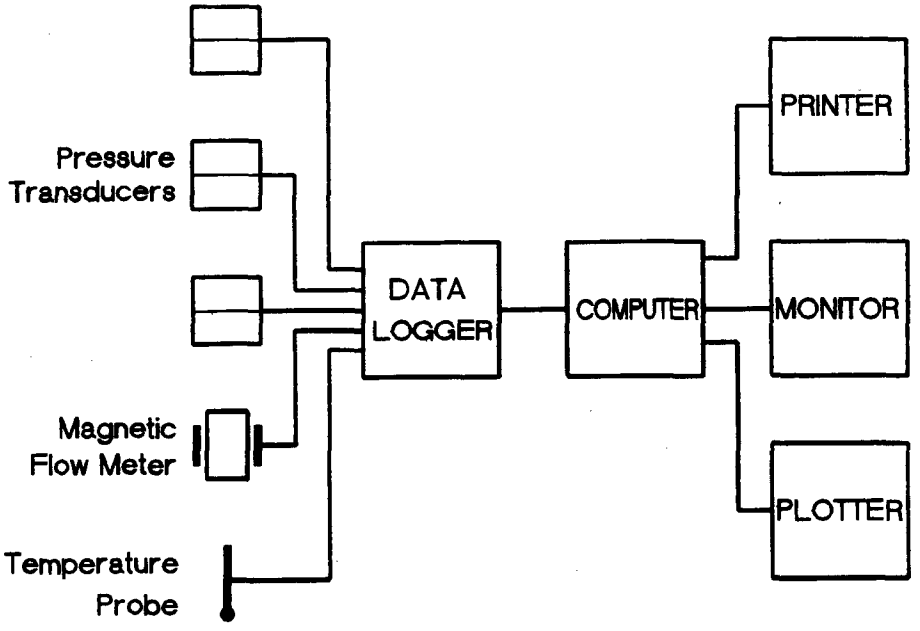

Figure 2.7 : Data logging configuration

pipe loop it was found to be of utmost importance to keep the test duration short to minimise particle degradation and the subsequent change in particle size distribution. Thus the measurement philosophy adopted is to read as much data as possible in as short a time period as possible. Outliers, for example caused by a blocked pressure tapping, are removed from the data set after the test. The test procedure described below keeps the average test time to 20 minutes, thus minimising the effect of particle degradation.

The experimental test procedure is presented in Figure 2.8. The main test activities are as follows :

(i) Calibration

The magnetic flow meter, differential pressure transducers and temperature probe are calibrated prior to testing. These calibrations are verified on completion of the test series.

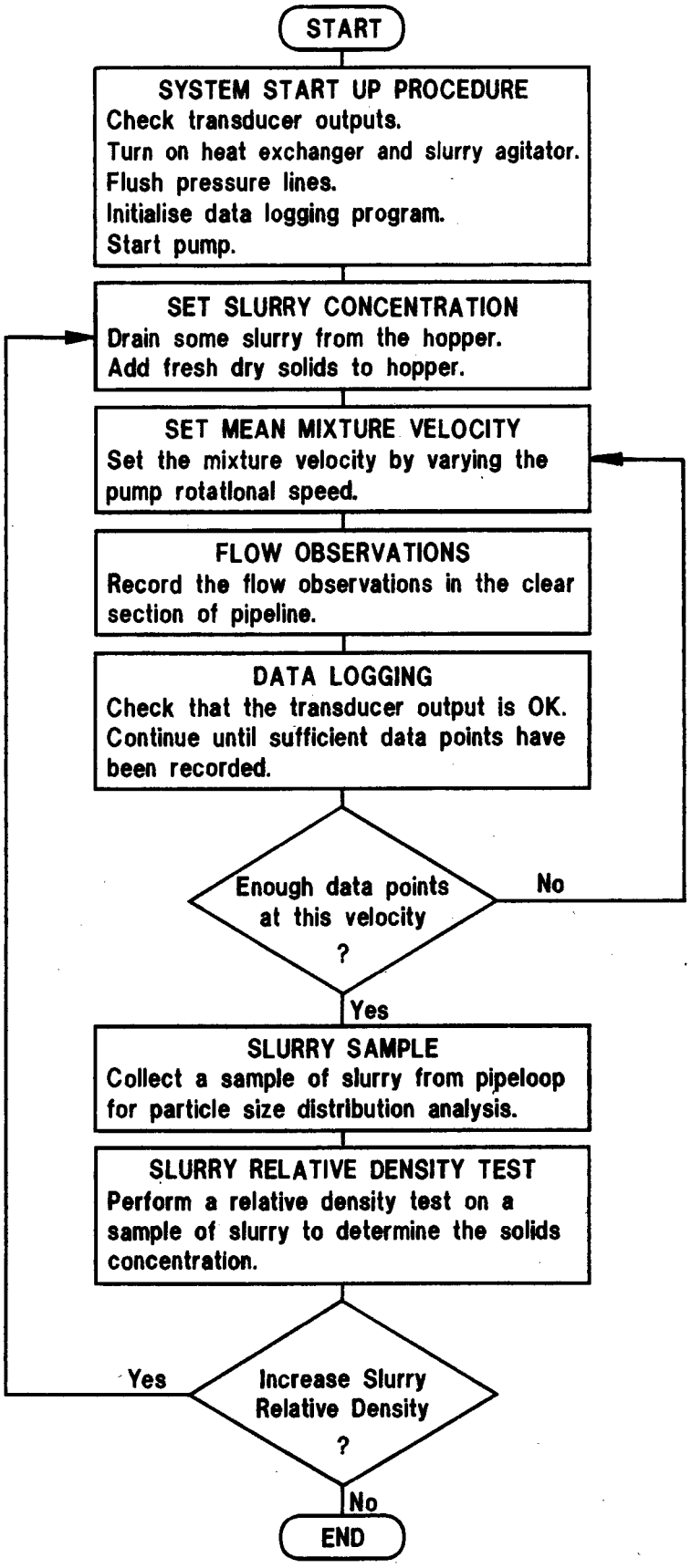

Figure 2.8 : Pipeline experimental test procedure

(ii) System start up

The system is filled with water and the transducer outputs checked. The heat exchanger and slurry agitator are turned on. The manometer tubes, connection lines and isolation pods are flushed. The pressure tapping valves M and L (Figure 2.3) are closed. The data logging program is loaded and initialised, and the pump started.

(iii) Concentration

The starting concentration is obtained by draining water from the hopper and loading solid material into the hopper while the pump is running. The system is always operated with the pipe loop outlet submerged below the water level in the hopper to avoid air entrainment.

The concentration is increased by draining some slurry from the hopper (done by diverting the pipe loop flow), and adding fresh solids to the hopper. In this way new solids are introduced into the system for each data set (one slurry relative density) in an attempt to maintain a constant particle size distribution for the test series (i.e. some of the degraded particles are replaced with fresh particles).

This procedure for increasing the slurry concentration is continued until the maximum pumpable concentration is reached. Note that this is a characteristic of the system - i.e. dependent on the pump discharge pressure and the total pipeline friction losses.

(iv) Velocity

The slurry velocity is set by varying the pump speed using the variable speed hydraulic drive. The test is started at the maximum velocity required (3,5 m/s) or the maximum attainable, and reduced for each new velocity setting.

After the velocity has been set the pressure tapping valves M and L (Figure 2.3) are opened and water flushed through the tapping to remove any solids. The manometer board is set to read the differential pressures with the transducers only. It was found that if the air over water manometers were used the tappings blocked with solids due to the fluctuating water levels in the manometer tubes. For the clear water tests the air over water manometers were also used as the air helped dampen the pressure fluctuations.

The tubes connecting the pressure tappings to the manometer board are slightly expandable. It was found that if the test was started at a low velocity and increased solids were forced through the tapping by the increased pipeline pressure. By starting at the maximum velocity this effect is reversed thus avoiding tapping blockage.

(v) Flow observations

Observations are made of the mixture flow behaviour in the clear horizontal section of pipeline. The length of the clear section of pipeline in the 25 mm NB loop was found to be too short to yield reliable results.

(vi) Data logging

The data logging program reads output from the pressure transducers, magnetic flow meter and temperature probe. A data point comprises the average of 10 readings recorded over a 3 second time period. The channels are read sequentially - i.e. all the instrumentation outputs are recorded over the 3 second period.

The results of each group of average values is printed. A graphical output of the variation of the pressure differences with velocity may be obtained on the computer monitor at any stage of the test. The operator decides whether sufficient data points have been made at a velocity setting by examining the spread of data and comparing the current data points with those obtained at previous velocity settings. Normally 3 to 4 groups of readings are recorded at each velocity.

If it is apparant that there is a problem with one of the transducer outputs (e.g. blocked pressure tapping) corrective action is taken by operator (flushing water through the tapping) before proceeding with the test.

(vii) Slurry sample

On completion of each set of data points (one concentration with a range of velocities) a sample of slurry is taken from the discharge of the pipe loop for particle size distribution analysis. The volume of sample taken is one litre.

(viii) Slurry relative density

On completion of each set of data points a slurry relative density test is performed as described in Section 2.2.1. The volumetric concentration of the mixture is calculated using equation (2.12).

2.5 Experimental errors

Considering quantity X to be a function of several measurements, i.e.

$$X = fn\ (a, b, c, \ldots\ldots n) \quad , \tag{2.17}$$

Brinkworth (1968) defines the highest expected error as :

$$\left(\frac{\delta X}{X}\right)^2_{exp} = \sum \left(\frac{\partial X}{\partial n}\right)^2 \left(\frac{n}{X}\right)^2 \left(\frac{\delta n}{n}\right)^2 \quad , \tag{2.18}$$

where X = value of quantity

δX = error in X

n = measured variable value

δn = error in n.

2.5.1 *Slurry relative density*

The slurry relative density is calculated using equation (2.5) :

$$S_m = \frac{M_m}{\forall_m \rho_w} \quad ,$$

Thus from equation (2.18) we get :

$$\left[\frac{\delta S_m}{S_m}\right]^2_{exp} = \left[\frac{\partial S_m}{\partial M_m}\right]^2 \left[\frac{M_m}{S_m}\right]^2 \left[\frac{\delta M_m}{M_m}\right]^2 + \left[\frac{\partial S_m}{\partial \forall_m}\right]^2 \left[\frac{\forall_m}{S_m}\right]^2 \left[\frac{\delta \forall_m}{\forall_m}\right]^2 + \left[\frac{\partial S_m}{\partial \rho_w}\right]^2 \left[\frac{\rho_w}{S_m}\right]^2 \left[\frac{\delta \rho_w}{\rho_w}\right]^2 \quad , \tag{2.19}$$

where $$\frac{\partial S_m}{\partial M_m} = \frac{1}{\forall_m \rho_w}$$

$$\frac{\partial S_m}{\partial \forall_m} = \frac{- M_m}{\forall_m^2 \rho_w}$$

$$\frac{\partial S_m}{\partial \rho_w} = \frac{- M_m}{\forall_m \rho_w^2} \quad .$$

The volumetric concentration of the solid particles is calculated from equation (2.12) :

$$C = \frac{S_m - S_w}{S_s - S_w} \quad .$$

The highest expected error in C from equation (2.18) is :

$$\left[\frac{\delta C}{C}\right]_{exp} = \left[\frac{\partial C}{\partial S_m}\right]^2 \left[\frac{S_m}{C}\right]^2 \left[\frac{\delta S_m}{S_m}\right]^2 + \left[\frac{\partial C}{\partial S_s}\right]^2 \left[\frac{S_s}{C}\right]^2 \left[\frac{\delta S_s}{S_s}\right]^2 \quad , \qquad (2.20)$$

where $$\frac{\partial C}{\partial S_m} = \frac{1}{S_s - S_w}$$

$$\frac{\partial C}{\partial S_s} = \frac{- (S_m - S_w)}{(S_s - S_w)^2} \quad .$$

Table 2.3 shows the measurement accuracies and the highest expected errors in S_m and C for a typical relative density test. Figure 2.9 shows the variation of the highest expected error in C with solids concentration for the two test facilities.

TABLE 2.3 : Expected highest error - S_m and C

Variables	25 mm NB loop	40/80 mm NB loops
S_m	1,80	1,80
M_m (kg)	17,94 ± 0,05	53,84 ± 0,05
γ_m (kg)	10,00 ± 0,05	30,00 ± 0,05
ρ_w (kg/m³) 25° ± 1°C	997,1 ± 0,3	997,1 ± 0,3
δS_m	0,010	0,003
% Error in S_m	0,57	0,19
C (%)	48,48	48,48
S_s	2,65 ± 0,01	2,65 ± 0,01
δ C (%)	± 0,69	± 0,35
% Error in C	1,42	0,71

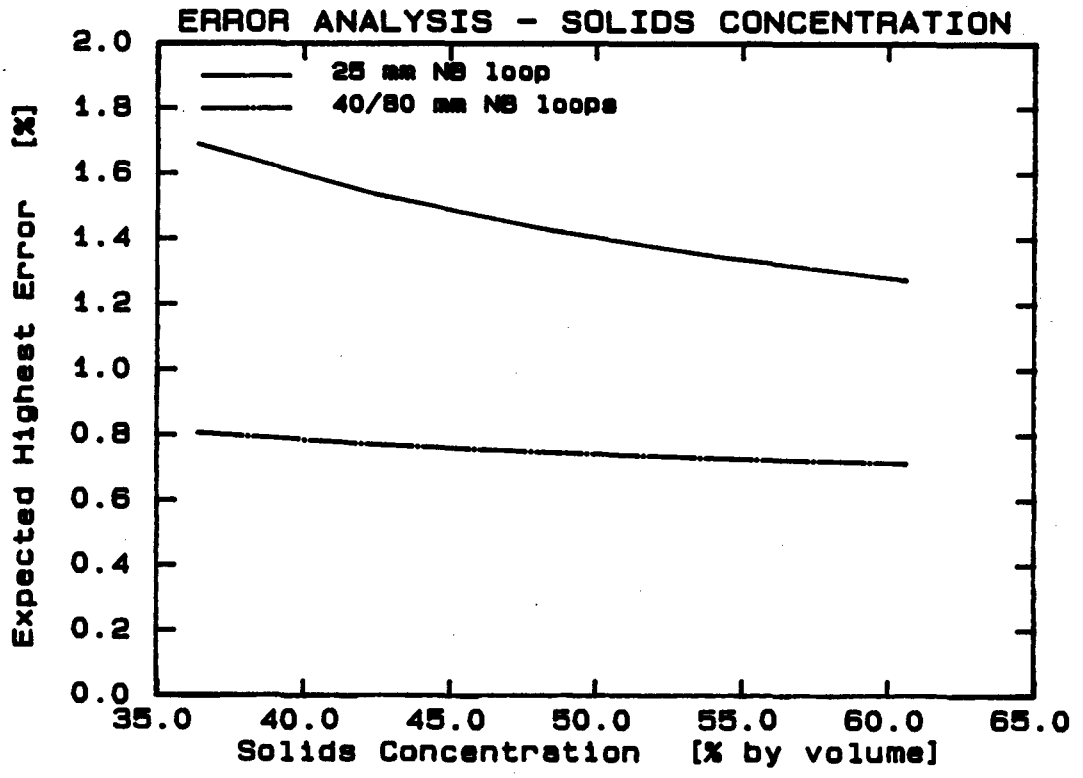

Figure 2.9

2.5.2 *Slurry flow rate and mean mixture velocity*

The magnetic flow meter is calibrated by diverting the flow to a calibration tank and determining the mixture flow rate. The mixture flow rate is calculated from equation (2.6) :

$$Q_m = \frac{M_w}{\rho_w t} \quad .$$

The highest expected error in the magnetic flow meter calibration is found from equation (2.18) :

$$\left[\frac{\delta Q_m}{Q_m}\right]^2_{exp} = \left[\frac{\partial Q_m}{\partial M_w}\right]^2 \left[\frac{M_w}{Q_m}\right]^2 \left[\frac{\delta M_w}{M_w}\right]^2 + \left[\frac{\partial Q_m}{\partial \rho_w}\right]^2 \left[\frac{\rho_w}{Q_m}\right]^2 \left[\frac{\delta \rho_w}{\rho_w}\right]^2 + \left[\frac{\partial Q_m}{\partial t}\right]^2 \left[\frac{t}{Q_m}\right]^2 \left[\frac{\delta t}{t}\right]^2 , \qquad (2.21)$$

where $$\frac{\partial Q_m}{\partial M_m} = \frac{1}{\rho_w t}$$

$$\frac{\partial Q_m}{\partial \rho_w} = \frac{- M_w}{\rho_w^2 t}$$

$$\frac{\partial Q_m}{\partial t} = \frac{- M_w}{\rho_w t^2} \quad .$$

The highest expected error in the magnetic flow meter output is found by adding the transducer error to the highest expected calibration error. The mean mixture velocity is found from equation (2.13) :

$$V_m = \frac{4 Q_m}{\pi D^2} \quad .$$

The highest expected error in the mean mixture velocity is obtained from equation (2.18) :

$$\left[\frac{\delta V_m}{V_m}\right]_{exp} = \left[\frac{\partial V_m}{\partial Q_m}\right]^2 \left[\frac{Q_m}{V_m}\right]^2 \left[\frac{\delta Q_m}{Q_m}\right]^2 + \left[\frac{\partial V_m}{\partial D}\right]^2 \left[\frac{D}{V_m}\right]^2 \left[\frac{\delta D}{D}\right]^2 , \qquad (2.22)$$

where $$\frac{\partial V_m}{\partial Q_m} = \frac{4}{\pi D^2}$$

$$\frac{\partial V_m}{\partial Q_m} = \frac{-8 Q_m}{\pi D^3} .$$

Table 2.4 shows the measurement accuracies, transducer accuracies and highest expected errors in Q_m and V_m at a mean mixture velocity of 3 m/s. Figure 2.10 shows the variation of the expected highest error for the three pipe loops with mean mixture velocity.

TABLE 2.4 : Expected highest errors - Q_m and V_m

Variables	25 mm NB	40 mm NB	80 mm NB
Q_m (ℓ/s)	1,67	3,77	12,69
M_m (kg)	70,00 ± 0,05	70,00 ± 0,05	70,00 ± 0,05
ρ_w (kg/m³) 18° ± 1°C	998,7 ± 0,3	998,7 ± 0,3	998,7 ± 0,3
t (s)	36,0 ± 0,25	15,0 ± 0,25	4,7 ± 0,25
δQ_m (ℓ/s)	± 0,009	± 0,050	± 0,574
% Q_m Calibration error	0,60	1,35	4,53
Transducer error (%)	1,00	1,00	1,00
% Error in Q_m	1,60	2,35	5,53
Total δQ_m (ℓ/s)	± 0,03	± 0,09	± 0,70
V_m (m/s)	3,00	3,00	3,00
D (mm)*	26,6 ± 0,12	40,0 ± 0,08	73,4 ± 0,22
δV_m (m/s)	0,017	0,040	0,135
% Error in V_m	0,58	1,33	4,52

* See Table 2.6

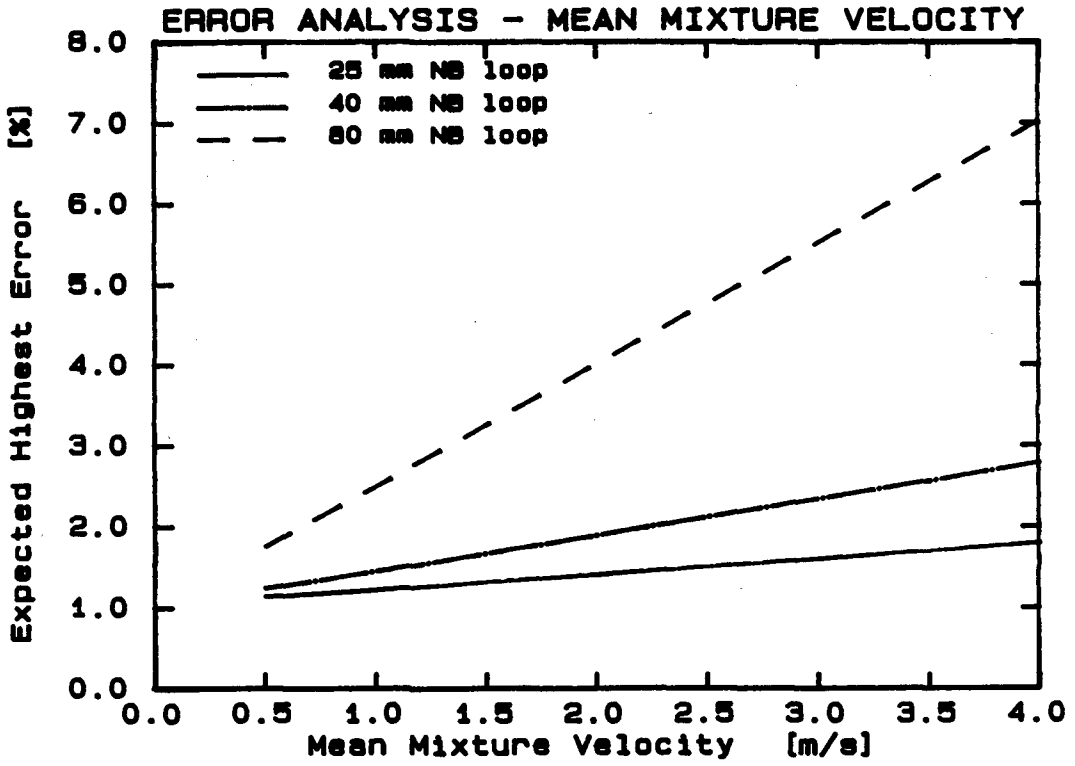

Figure 2.10

2.5.3 *Hydraulic gradient and pressure gradient*

The mixture hydraulic gradient is evaluated from equation (2.9) :

$$i_m = \frac{\Delta h}{L} \quad .$$

As the water head differential Δh is measured using a differential pressure transducer, the measurement of Δh will contain a calibration error and a transducer error. The calibration error in reading Δh from the manometer is $\pm$ 2 mm. The transducer error is 0,1% of the full scale transducer calibration (2 m), i.e. $\pm$ 2 mm. Thus the total error in measurement Δh is $\pm$ 4 mm. From equation (2.18) the highest expected error in i_m is

$$\left[\frac{\delta i_m}{i_m}\right]^2_{exp} = \left[\frac{\partial i_m}{\partial \Delta h}\right]^2 \left[\frac{\Delta h}{i_m}\right]^2 \left[\frac{\delta \Delta h}{\Delta h}\right]^2 + \left[\frac{\partial i_m}{\partial L}\right]^2 \left[\frac{L}{i_m}\right]^2 \left[\frac{\delta L}{L}\right]^2 , \qquad (2.23)$$

where $\frac{\partial i_m}{\partial \Delta h} = \frac{1}{L}$

$$\frac{\partial i_m}{\partial L} = \frac{-\Delta h}{L^2} \quad .$$

The pressure gradient is calculated from equation (2.14) which may be written as

$$\Delta P = \rho_w g i_m \quad .$$

From equation (2.18) the highest expected error in ΔP is :

$$\left[\frac{\delta\,\Delta P}{\Delta P}\right]^2_{exp} = \left[\frac{\partial\,\Delta P}{\partial\,\rho_w}\right]^2 \left[\frac{\rho_w}{\Delta P}\right]^2 \left[\frac{\delta\,\rho_w}{\rho_w}\right]^2 + \left[\frac{\partial\,\Delta P}{\partial\,i_m}\right]^2 \left[\frac{i_m}{\Delta P}\right]^2 \left[\frac{\delta\,i_m}{i_m}\right]^2 , \qquad (2.24)$$

where $\frac{\partial\,\Delta P}{\partial\,\rho_w} = g\,i_m$

$$\frac{\partial\,\Delta P}{\partial\,i_m} = \rho_w\,g \quad .$$

The measurement accuracies, transducer accuracies and highest expected errors in i_m and ΔP are presented in Table 2.5 for a Δh reading of 500 mm. Figure 2.11 shows the variation of the expected highest error for the three pipe loops with pressure gradient.

TABLE 2.5 : Expected highest errors - i_m and ΔP

Variables	25 mm NB	40 mm NB	80 mm NB
i_m (m/m)	1,000	0,500	0,333
Δh (mm)	500 ± 4	500 ± 4	500 ± 4
L (mm)	500 ± 1	1000 ± 1	1500 ± 1
δi_m (m/m)	0,008	0,004	0,003
% Error in i_m	0,82	0,81	0,80
ΔP (kPa/m)	9,797	4,898	3,265
ρ_w (kg/m³) 18° ± 1°C	998,7 ± 0,3	998,7 ± 0,3	998,7 ± 0,3
$\delta \Delta P$ (kPa/m)	0,080	0,039	0,026
% Error in ΔP	0,83	0,81	0,80

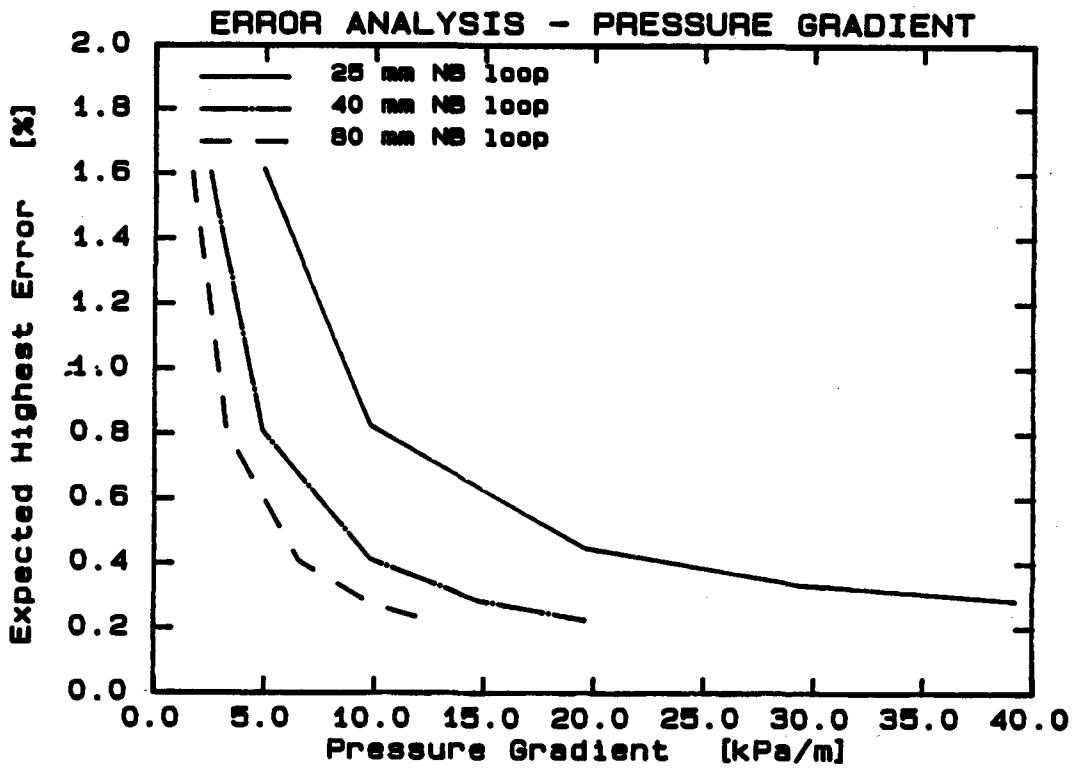

Figure 2.11

2.5.4 *Pipe diameter*

The internal pipe diameter is calculated using equation (2.11) :

$$D = \sqrt{\frac{4\,M_w}{\rho_w\,\pi\,L}} \quad .$$

The expected highest error is found using equation (2.18) :

$$\left[\frac{\delta D}{D}\right]^2_{exp} = \left[\frac{\partial D}{\partial M_w}\right]^2 \left[\frac{M_w}{D}\right]^2 \left[\frac{\delta M_w}{M_w}\right]^2 + \left[\frac{\partial D}{\partial L}\right]^2 \left[\frac{L}{D}\right]^2 \left[\frac{\delta L}{L}\right]^2 + \left[\frac{\partial D}{\partial \rho_w}\right]^2 \left[\frac{\rho_w}{D}\right]^2 \left[\frac{\delta \rho_w}{\rho_w}\right]^2 , \qquad (2.25)$$

where $$\frac{\partial D}{\partial M_w} = \sqrt{\frac{1}{\rho_w\,\pi\,L\,M_w}}$$

$$\frac{\partial D}{\partial L} = -\sqrt{\frac{M_w}{\rho_w\,\pi\,L^3}}$$

$$\frac{\partial D}{\partial \rho_w} = -\sqrt{\frac{M_w}{\rho_w^3\,\pi\,L}} \quad .$$

The measurement accuracies and expected highest errors for the three pipelines are presented in Table 2.6.

TABLE 2.6 : Expected highest errors - D

Variables	25 mm NB	40 mm NB	80 mm NB
D (m)	0,0266	0,0400	0,0734
M_w (kg)	2,22 ± 0,02	5,02 ± 0,02	16,90 ± 0,1
L (m)	4,00 ± 0,005	4,00 ± 0,05	4,00 ± 0,05
ρ_w (kg/m³) 18° ± 1°C	998,7 ± 0,3	998,7 ± 0,3	998,7 ± 0,3
δ D (mm)	0,12	0,08	0,22
% Error in D	0,45	0,21	0,30

2.5.5 *Slurry temperature*

The slurry temperature is measured using a temperature probe. The error in the measurement will contain components due to the calibration and the transducer errors. The calibration error in reading the mercury thermometer is 1°C. The transducer error is 1% of the full scale calibration (100°C) i.e. 1°C. Thus the accuracy of the temperature reading is ± 2°C.

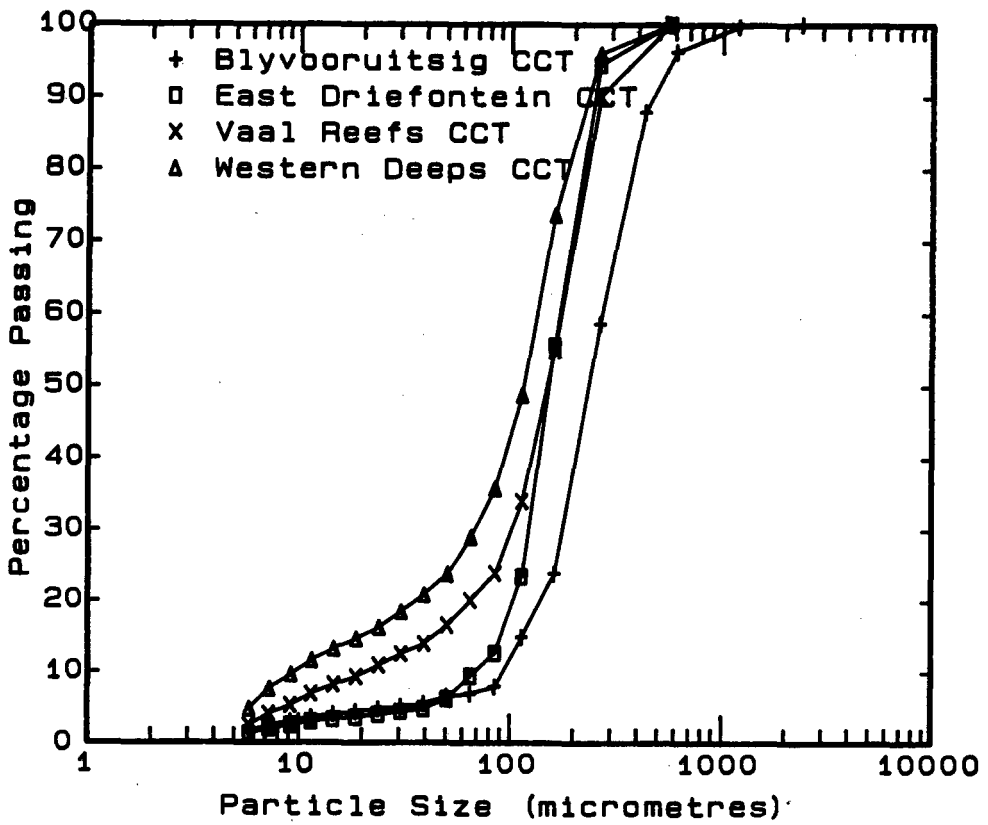

Figure 2.12

3. EVALUATION OF SOLID PARTICLE CHARACTERISTICS

The following tests to characterise the solid particles were measured independent of the pipe loop tests. Table 2.7 summarises the test results.

3.1 Solids relative density

The relative density of the solid particles is obtained using the procedure specified in BS1377 (1975), Methods of test for soils for Civil Engineering purposes, Test 6(B): Determination of the specific gravity of fine grained soils. The Blyvooruitsig solid particles have a relative density of 2,66 compared with 2,65 for the other materials.

3.2 Particle size distribution

The particle size distributions of samples taken, after each pipeline test, were obtained using a Malvern 2600/3600 particle sizer. The particle size distributions for each test are included in the pipeline test data base in tabular and graphical form. As the Blyvooruitsig material contained particles greater than 564 μm, this material was sieved and the particle size distribution of the -425 μm fraction obtained using the Malvern particle sizer.

Figure 2.12 compares the four classified tailings materials tested by plotting the mean particle size distribution of each material. The Western Deeps material contains the highest percentage of fines (10,4% less than 10 μm) and has the smallest d_{50} particle size (115 μm), while the Blyvooruitsig material has the least percentage of fines (3,3% less than 10 μm) and the largest d_{50} particle size (232 μm). The East Driefontein and Vaal Reefs materials have similar d_{50} particle sizes (151 μm and 148 μm respectively), although Vaal Reefs has a higher percentage of fines (6,0% less than 10 μm compared with 2,7%). Table 2.7 compares the d_{10}, d_{50} and d_{90} particle sizes of the four materials.

TABLE 2.7 : Solid Particle Properties

Material :	Blyvooruitsig	East Driefontein	Vaal Reefs	Western Deeps
Ss	2.66	2.65	2.65	2.65
d_{10}* (μm)	92	68	21	10
d_{50}* (μm)	232	151	148	115
d_{90}* (μm)	465	248	262	230
S_f (211-300μm)	0.88	0.80	0.79	0.71
S_f (300-355μm)	0.89	0.75	0.73	0.73
S_f (355-425μm)	0.90	0.77	0.77	0.69
C_{min} (% by vol)	48.0	45.6	46.0	49.0
$\delta_{50\%}$+ (deg)	27.3	28.2	26.3	33.8
μ_d	0.44	0.37	0.46	-

* typical values
\+ extrapolated values for 50 % by volume solids concentration from Figure 2.16

Ss = Relative density of solid particles
Sf = Particle shape factor
C_{min} = Freely settled particle concentration
d_{50} = particle size such that 50 % by weight of particles are < than d_{50}
δ = internal angle of friction
μ_d = dynamic coefficient of friction

3.3 Particle shape factor

The settling velocities of particles were determined by measuring the travel time through water over a known distance. The settling velocity of an equivalent diameter sphere is calculated and hence the particle shape factor obtained. The shape factor is defined as the ratio of the particle settling velocity to the settling velocity of an equivalent diameter sphere.

The particle shape factor was obtained for various size fractions (i.e. between two sieve sizes d_1 and d_2). The representative particle diameter is calculated as the geometric mean,

$$d = \sqrt{d_1 d_2} \quad .$$

Table 2.7 shows the measured shape factors for the four materials in three size ranges (211 μm to 300 μm, 300 μm to 355 μm, and 355 μm to 425 μm). The Blyvooruitsig materials has the highest shape factor (most spherical) and the Western Deeps materials the lowest shape factor (least spherical).

3.4 Particle micrographs

To obtain a qualitative indication of the particle shapes, micrographs were taken of the samples using an electron microscope. Figures 2.13 and 2.14 show micrographs of the East Driefontein and Vaal Reefs classified tailings materials. The scale is located in the top border of each photograph. The particles are seen to be highly angular due to the crushing and grinding stages of the mineral extraction process.

3.5 Freely settled particle concentration

The freely settled concentration of the solid particle matrix is determined using the following procedure :

(i) From the oven dry mass and solids relative density of a sample of material calculate the sample volume.

(ii) Fill a measuring cylinder to 75% of its volume with de-aired water.

(iii) Slowly pour the solid particles into the measuring cylinder. The particles settle freely through the water and assume their freely settled (or loose poured) concentration. This concentration is taken to be the minimum possible with the solid particles in contact.

(iv) After 24 hours, read the volume occupied by the solid particle matrix from the measuring cylinder. The freely settled concentration is calculated as follows :

$$C_{min} = \frac{\mathcal{V}_s}{\mathcal{V}_{occ}} \quad , \qquad (2.26)$$

where $\mathcal{V}_s$ = volume of solid particles
$\mathcal{V}_{occ}$ = volume occupied by solid particle matrix.

Table 2.7 shows the measured values for the freely settled particle concentration. The Blyvooruitsig and Western Deeps materials have the highest values (48,0% and 49,0% respectively), while the values for East Driefontein and Vaal Reefs are similar (45,6% and 46,0% respectively).

3.6 Internal angle of friction of solid particle matrix

The submerged internal angle of friction is obtained using a rectangular box with a central opening in its base as shown in Figure 2.15. This apparatus has been described by Zenz and Othmer (1960) for determining the internal angle of friction for dry particulate materials. The box is made from clear perspex and has dimensions of 300 mm long, 75 mm high and 20 mm wide, with a 12 mm central opening in the base. The test procedure is as follows :

(i) The hole in the base is plugged, and the box half filled with de-aired water.

(ii) A predetermined volume of solid particles are slowly poured into the box. Care is taken to ensure that the solid particles are evenly distributed in the box.

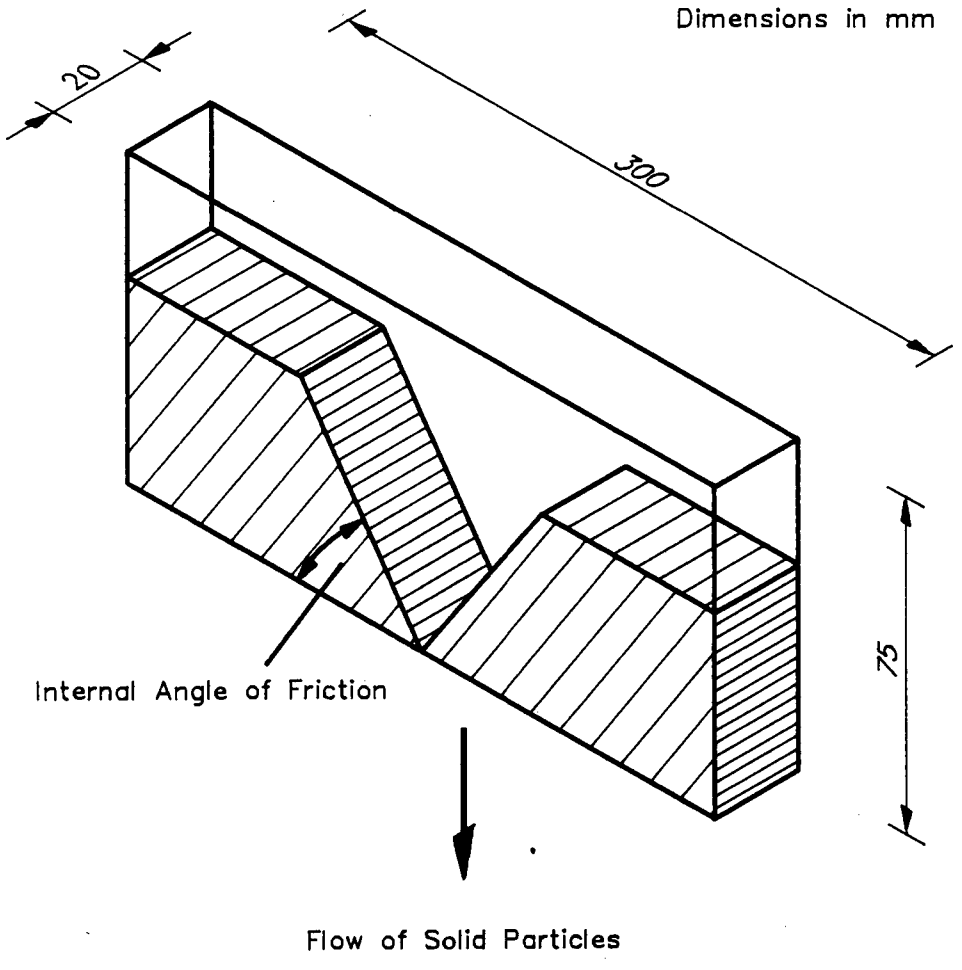

Figure 2.15 : Apparatus to measure internal angle of friction

(iii) The packing density is varied by placing the box on a vibrator to compact the solid particles for various time periods. The volume occupied by the solid particles is determined from the height of the solid particle sample and the geometry of the box. The concentration is calculated using equation (2.26).

(iv) The box is submerged in a tank filled with water and the plug in the opening in the base removed. The solid particles pour out and form a v-shape as shown in Figure 2.15. The internal angle of friction is measured using a protractor.

Figure 2.16 shows the submerged internal angle of friction increases with solids concentration for the four samples tested. The measured values for the Western Deeps material are much higher than the values for the other materials. The Western Deeps material contains a high percentage of fines and appears to form a non-Newtonian mixture at high solids concentrations. It is likely that the high observed "apparent" angles of friction are caused by the yield stress of the mixture. Table 2.7 compares the internal angles of friction of the four materials by extrapolating the curves to a solids concentration of 50% by volume.

3.7 Dynamic coefficient of sliding friction of solid particles

The dynamic coefficient of sliding friction is measured using the rotating disc apparatus described in detail in Chapter 3. The frictional resistance between the particles (held stationary in annular channel) and the rotating disc is measured for various normal loadings. The coefficient of friction, μ_d is calculated as the slope of the frictional resistance - normal loading curve.

The dynamic coefficient of friction was found to be independent of velocity. Table 2.7 shows the measured values of the dynamic coefficient of sliding friction μ_d . No reliable measurements were obtained for the Western Deeps slurry due to its non-Newtonian characteristics.

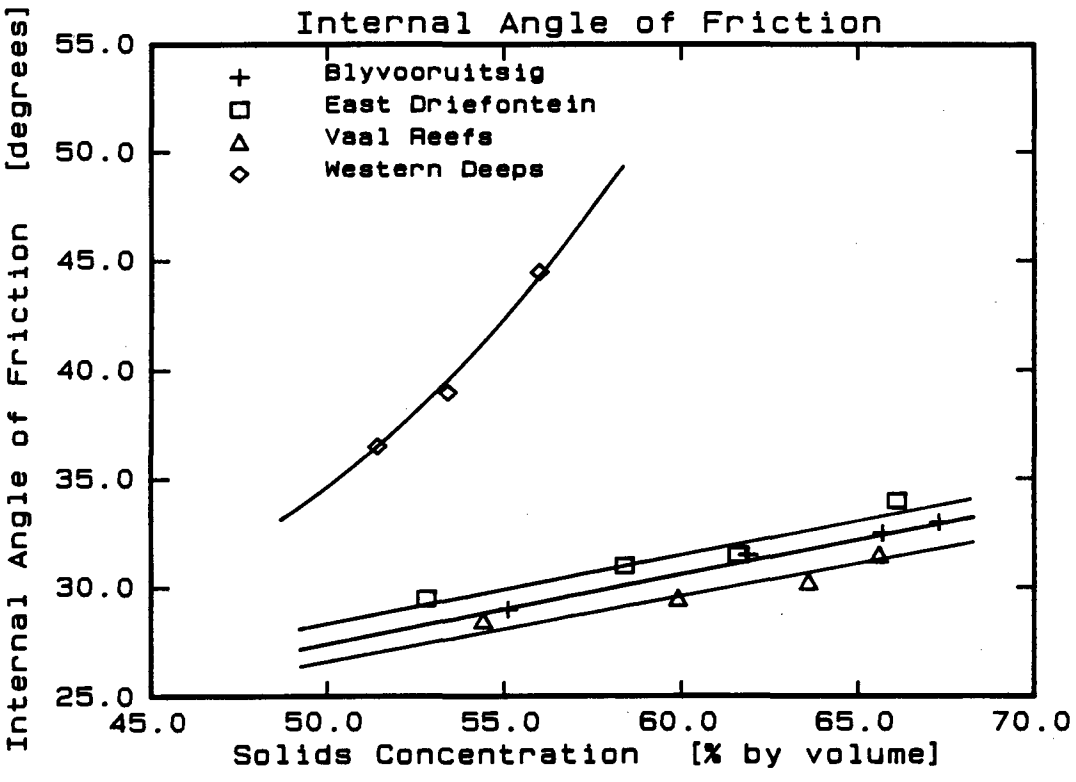
Internal Angle of Friction
Blyvooruitsig
East Driefontein
Vaal Reefs
Western Deeps
Internal Angle of Friction [degrees]
55.0
50.0
45.0
40.0
35.0
30.0
25.0
45.0
50.0
55.0
60.0
65.0
70.0
Solids Concentration [% by volume]

Figure 2.16

4. PIPELINE TEST RESULTS AND DISCUSSION

The pipeline test results are presented in Appendix A - Cyclone Classified Tailings Pipeline Test Data Base. Table 2.8 presents the key to the data base. Each test result contains the following :

(i) A table of experimental measured data points, i.e. mean mixture velocity, pressure gradient and slurry temperature. Figure 2.17 shows how the pressure gradient is defined for horizontal and vertical downward flow.

(ii) A table showing the particle size distribution of the sample taken at the end of the test.

(iii) In the case of the results for horizontal flow in the 40 mm and 80 mm NB pipe loops, a table of observed flow conditions versus mean mixture velocity.

(iv) A graph of measured pressure gradient versus mean mixture velocity.

(v) A plot graphically showing the particle size distribution of the sample taken at the end of the test.

Each test result has an associated data file name which is used to refer to the test data. The file name has the following format :

TABLE 2.7.2

General Format : MTDIGSMF

Code	Field Description	Example
MT	Material type	VR = Vaal Reefs
DI	Pipe diameter	80 = 80 mm NB
G	Pipeline gradient	H = horizontal D = vertical down
SM	Mixture relative density	75 = 1,75
F	Test facility	U = UCT

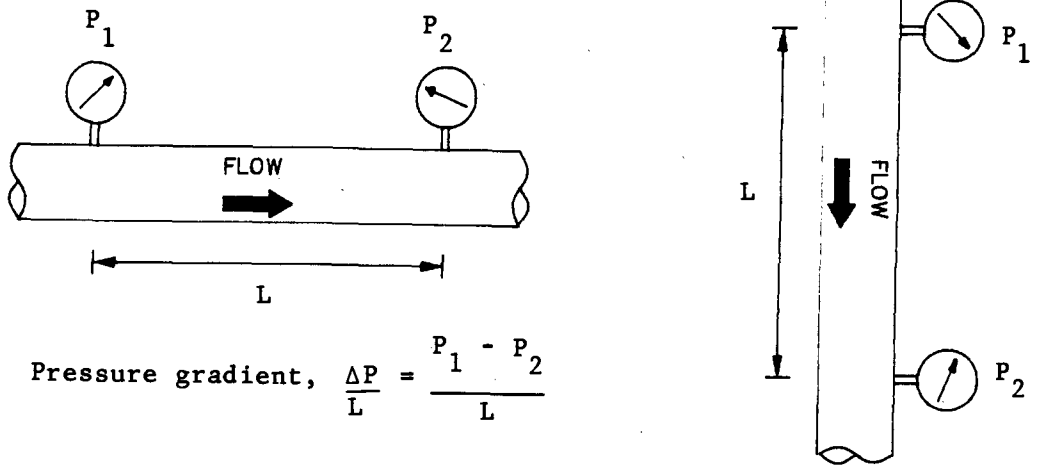

Figure 2.17 : Pressure gradient definition

Figure 2.18 shows the particle size distribution of samples taken at the beginning and end of the series of tests on the Vaal Reefs slurry in the 40 mm NB pipeline. There is a slight increase in the fines content of the sample taken after the last test (relative density 1,86) compared with the sample taken after the first test (relative density 1,71). A similar trend is seen for the Western Deeps test series in the 80 mm NB pipeline as shown in Figure 2.19.

In the following discussion of the test results all the tests corresponding to a particular backfill material are considered to be of a similar material. The mechanistic analysis (Chapters 5 and 6) uses the particle size distribution corresponding to each data file.

TABLE 2.8 : Key to Cyclone Classified Tailings Data Base

Classified Tailings Material	Nominal Pipe Bore (mm)	Pipeline Slope (degrees)	Solids Conc. (% by vol)	Data Base File Name	Data Base Page Number
Blyvooruitsig	25	0	37.3	BV25H62U	A. 2
Blyvooruitsig	25	0	39.2	BV25H65U	A. 3
Blyvooruitsig	25	0	44.6	BV25H74U	A. 4
Blyvooruitsig	25	0	46.4	BV25H77U	A. 5
Blyvooruitsig	25	0	48.8	BV25H81U	A. 6
Blyvooruitsig	25	-90	37.3	BV25D62U	A. 7
Blyvooruitsig	25	-90	39.2	BV25D65U	A. 8
Blyvooruitsig	25	-90	44.6	BV25D74U	A. 9
Blyvooruitsig	25	-90	46.4	BV25D77U	A. 10
Blyvooruitsig	25	-90	48.8	BV25D81U	A. 11
Blyvooruitsig	25	90	37.3	BV25U62U	A. 12
Blyvooruitsig	25	90	39.2	BV25U65U	A. 13
Blyvooruitsig	25	90	44.6	BV25U74U	A. 14
Blyvooruitsig	25	90	46.4	BV25U77U	A. 15
Blyvooruitsig	25	90	48.8	BV25U81U	A. 16
Blyvooruitsig	40	0	44.0	BV40H73U	A. 17
Blyvooruitsig	40	0	47.0	BV40H78U	A. 18
Blyvooruitsig	40	0	48.8	BV40H81U	A. 19
Blyvooruitsig	40	0	51.8	BV40H86U	A. 20
Blyvooruitsig	40	0	52.4	BV40H87U	A. 21
Blyvooruitsig	40	-90	44.0	BV40D73U	A. 22
Blyvooruitsig	40	-90	47.0	BV40D78U	A. 23
Blyvooruitsig	40	-90	48.8	BV40D81U	A. 24
Blyvooruitsig	40	-90	51.8	BV40D86U	A. 25
Blyvooruitsig	40	-90	52.4	BV40D87U	A. 26
Blyvooruitsig	80	0	31.3	BV80H52U	A. 27
Blyvooruitsig	80	0	36.1	BV80H60U	A. 28
Blyvooruitsig	80	0	42.2	BV80H70U	A. 29
Blyvooruitsig	80	0	45.2	BV80H75U	A. 30
Blyvooruitsig	80	0	50.0	BV80H83U	A. 31
Blyvooruitsig	80	0	51.8	BV80H86U	A. 32
Blyvooruitsig	80	0	53.6	BV80H89U	A. 33
Blyvooruitsig	80	-90	31.3	BV80H52U	A. 34
Blyvooruitsig	80	-90	36.1	BV80D60U	A. 35
Blyvooruitsig	80	-90	42.2	BV80D70U	A. 36
Blyvooruitsig	80	-90	45.2	BV80D75U	A. 37
Blyvooruitsig	80	-90	47.6	BV80D79U	A. 38
Blyvooruitsig	80	-90	50.0	BV80D83U	A. 39
Blyvooruitsig	80	-90	51.8	BV80D86U	A. 40
Blyvooruitsig	80	-90	53.6	BV80D89U	A. 41
East Driefontein	25	0	33.3	ED25H55U	A. 42
East Driefontein	25	0	40.0	ED25H66U	A. 43
East Driefontein	25	0	41.8	ED25H69U	A. 44
East Driefontein	25	0	45.5	ED25H75U	A. 45
East Driefontein	25	0	47.9	ED25H79U	A. 46
East Driefontein	25	-90	33.3	ED25D55U	A. 47
East Driefontein	25	-90	40.0	ED25D66U	A. 48

TABLE 2.8 : Key to Cyclone Classified Tailings Data Base cont.

Classified Tailings Material	Nominal Pipe Bore (mm)	Pipeline Slope (degrees)	Solids Conc. (% by vol)	Data Base File Name	Data Base Page Number
East Driefontein	25	-90	41.8	ED25D69U	A. 49
East Driefontein	25	-90	45.5	ED25D75U	A. 50
East Driefontein	25	-90	47.9	ED25D79U	A. 51
East Driefontein	25	90	33.3	ED25U55U	A. 52
East Driefontein	25	90	40.0	ED25U66U	A. 53
East Driefontein	25	90	41.8	ED25U69U	A. 54
East Driefontein	25	90	45.5	ED25U75U	A. 55
East Driefontein	25	90	47.9	ED25U79U	A. 56
East Driefontein	40	0	41.8	ED40H69U	A. 57
East Driefontein	40	0	43.6	ED40H72U	A. 58
East Driefontein	40	0	45.5	ED40H75U	A. 59
East Driefontein	40	0	47.9	ED40H79U	A. 60
East Driefontein	40	0	49.7	ED40H82U	A. 61
East Driefontein	40	0	52.7	ED40H87U	A. 62
East Driefontein	40	-90	41.8	ED40D69U	A. 63
East Driefontein	40	-90	43.6	ED40D72U	A. 64
East Driefontein	40	-90	45.5	ED40D75U	A. 65
East Driefontein	40	-90	47.9	ED40D79U	A. 66
East Driefontein	40	-90	49.7	ED40D82U	A. 67
East Driefontein	80	0	35.8	ED80H59A	A. 68
East Driefontein	80	0	35.8	ED80H59B	A. 69
East Driefontein	80	0	41.2	ED80H68U	A. 70
East Driefontein	80	0	42.4	ED80H70U	A. 71
East Driefontein	80	0	43.0	ED80H71U	A. 72
East Driefontein	80	0	47.9	ED80H79U	A. 73
East Driefontein	80	-90	35.8	ED80D59A	A. 74
East Driefontein	80	-90	35.8	ED80D59B	A. 75
East Driefontein	80	-90	41.2	ED80D68U	A. 76
East Driefontein	80	-90	42.4	ED80D70U	A. 77
East Driefontein	80	-90	43.0	ED80D71U	A. 78
East Driefontein	80	-90	44.8	ED80D74U	A. 79
East Driefontein	80	-90	47.9	ED80D79U	A. 80
East Driefontein	80	-90	50.9	ED80D84U	A. 81
Vaal Reefs	25	0	33.3	VR25H55U	A. 82
Vaal Reefs	25	0	40.0	VR25H66U	A. 83
Vaal Reefs	25	0	45.5	VR25H75A	A. 84
Vaal Reefs	25	0	45.5	VR25H75B	A. 85
Vaal Reefs	25	0	46.7	VR25H77U	A. 86
Vaal Reefs	25	0	52.1	VR25H86U	A. 87
Vaal Reefs	25	-90	33.3	VR25D55U	A. 88
Vaal Reefs	25	-90	40.0	VR25D66U	A. 89
Vaal Reefs	25	-90	45.5	VR25D75A	A. 90
Vaal Reefs	25	-90	45.5	VR25D75B	A. 91
Vaal Reefs	25	-90	46.7	VR25D77U	A. 92
Vaal Reefs	25	-90	52.1	VR25D86U	A. 93
Vaal Reefs	25	90	33.3	VR25U55U	A. 94
Vaal Reefs	25	90	40.0	VR25U66U	A. 95
Vaal Reefs	25	90	45.5	VR25U75A	A. 96

TABLE 2.8 : Key to Cyclone Classified Tailings Data Base cont.

Classified Tailings Material	Nominal Pipe Bore (mm)	Pipeline Slope (degrees)	Solids Conc. (% by vol)	Data Base File Name	Data Base Page Number
Vaal Reefs	25	90	45.5	VR25U75B	A. 97
Vaal Reefs	25	90	46.7	VR25U77U	A. 98
Vaal Reefs	25	90	52.1	VR25U86U	A. 99
Vaal Reefs	40	0	43.0	VR40H71U	A.100
Vaal Reefs	40	0	45.5	VR40H75U	A.101
Vaal Reefs	40	0	48.5	VR40H80U	A.102
Vaal Reefs	40	0	50.3	VR40H83U	A.103
Vaal Reefs	40	0	52.1	VR40H86U	A.104
Vaal Reefs	40	-90	43.0	VR40D71U	A.105
Vaal Reefs	40	-90	45.5	VR40D75U	A.106
Vaal Reefs	40	-90	48.5	VR40D80U	A.107
Vaal Reefs	40	-90	50.3	VR40D83U	A.108
Vaal Reefs	40	-90	52.1	VR40D86U	A.109
Vaal Reefs	80	0	42.4	VR80H70U	A.110
Vaal Reefs	80	0	45.5	VR80H75U	A.111
Vaal Reefs	80	0	47.9	VR80H79U	A.112
Vaal Reefs	80	0	49.1	VR80H81U	A.113
Vaal Reefs	80	0	51.5	VR80H85U	A.114
Vaal Reefs	80	0	53.9	VR80H89U	A.115
Vaal Reefs	80	-90	42.4	VR80D70U	A.116
Vaal Reefs	80	-90	45.5	VR80D75U	A.117
Vaal Reefs	80	-90	47.9	VR80D79U	A.118
Vaal Reefs	80	-90	49.1	VR80D81U	A.119
Vaal Reefs	80	-90	51.5	VR80D85U	A.120
Western Deeps	25	0	40.6	WD25H67U	A.121
Western Deeps	25	0	44.2	WD25H73U	A.122
Western Deeps	25	0	46.1	WD25H76U	A.123
Western Deeps	25	0	47.9	WD25H79U	A.124
Western Deeps	25	0	49.7	WD25H82U	A.125
Western Deeps	25	0	51.5	WD25H85U	A.126
Western Deeps	25	-90	40.6	WD25D67U	A.127
Western Deeps	25	-90	44.2	WD25D73U	A.128
Western Deeps	25	-90	46.1	WD25D76U	A.129
Western Deeps	25	-90	47.9	WD25D79U	A.130
Western Deeps	25	-90	49.7	WD25D82U	A.131
Western Deeps	25	-90	51.5	WD25D85U	A.132
Western Deeps	25	90	40.6	WD25U67U	A.133
Western Deeps	25	90	44.2	WD25U73U	A.134
Western Deeps	25	90	46.1	WD25U76U	A.135
Western Deeps	25	90	47.9	WD25U79U	A.136
Western Deeps	25	90	49.7	WD25U82U	A.137
Western Deeps	25	90	51.5	WD25U85U	A.138
Western Deeps	40	0	38.2	WD40H63U	A.139
Western Deeps	40	0	43.0	WD40H71U	A.140
Western Deeps	40	0	46.1	WD40H76U	A.141
Western Deeps	40	0	48.5	WD40H80U	A.142
Western Deeps	40	0	52.1	WD40H86U	A.143
Western Deeps	40	0	53.3	WD40H88U	A.144

TABLE 2.8 : Key to Cyclone Classified Tailings Data Base cont.

Classified Tailings Material	Nominal Pipe Bore (mm)	Pipeline Slope (degrees)	Solids Conc. (% by vol)	Data Base File Name	Data Base Page Number
Western Deeps	40	-90	38.2	WD40D63U	A.145
Western Deeps	40	-90	43.0	WD40D71U	A.146
Western Deeps	40	-90	46.1	WD40D76U	A.147
Western Deeps	40	-90	52.1	WD40D86U	A.148
Western Deeps	40	-90	53.3	WD40D88U	A.149
Western Deeps	80	0	41.8	WD80H69U	A.150
Western Deeps	80	0	44.2	WD80H73U	A.151
Western Deeps	80	0	47.3	WD80H78U	A.152
Western Deeps	80	0	49.1	WD80H81U	A.153
Western Deeps	80	0	52.1	WD80H86U	A.154
Western Deeps	80	0	54.5	WD80H90U	A.155
Western Deeps	80	-90	41.8	WD80D69U	A.156
Western Deeps	80	-90	44.2	WD80D73U	A.157
Western Deeps	80	-90	47.3	WD80D78U	A.158
Western Deeps	80	-90	49.1	WD80D81U	A.159
Western Deeps	80	-90	52.1	WD80D86U	A.160
Western Deeps	80	-90	54.5	WD80D90U	A.161

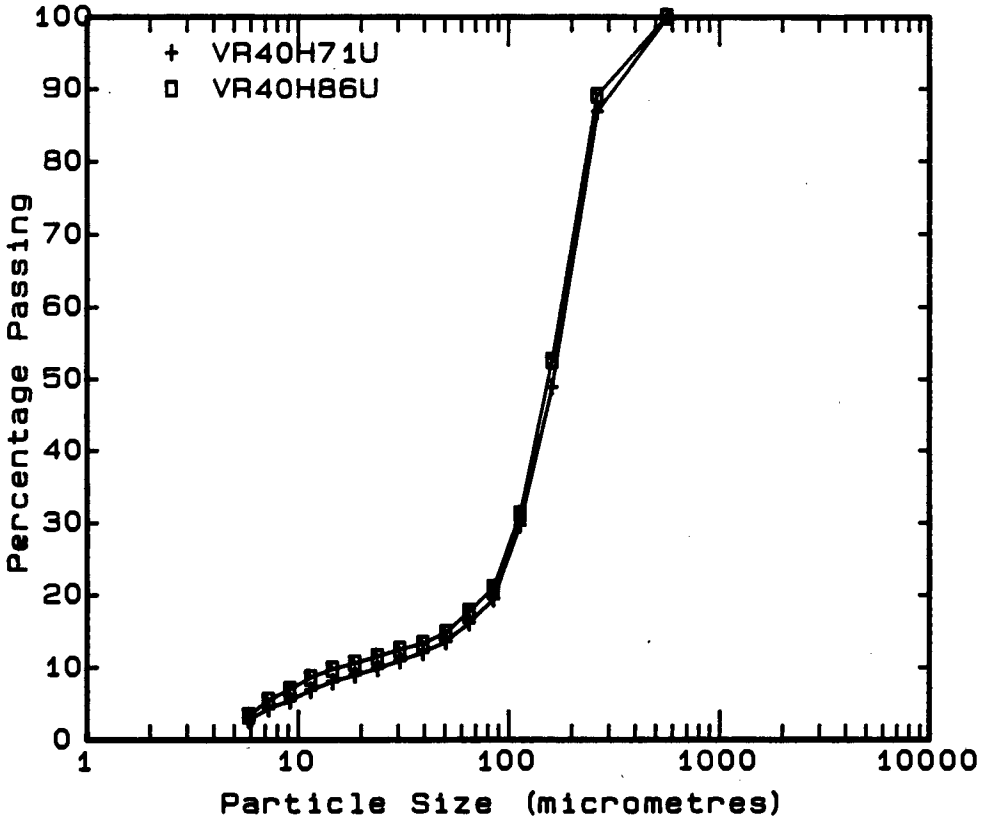

Figure 2.18

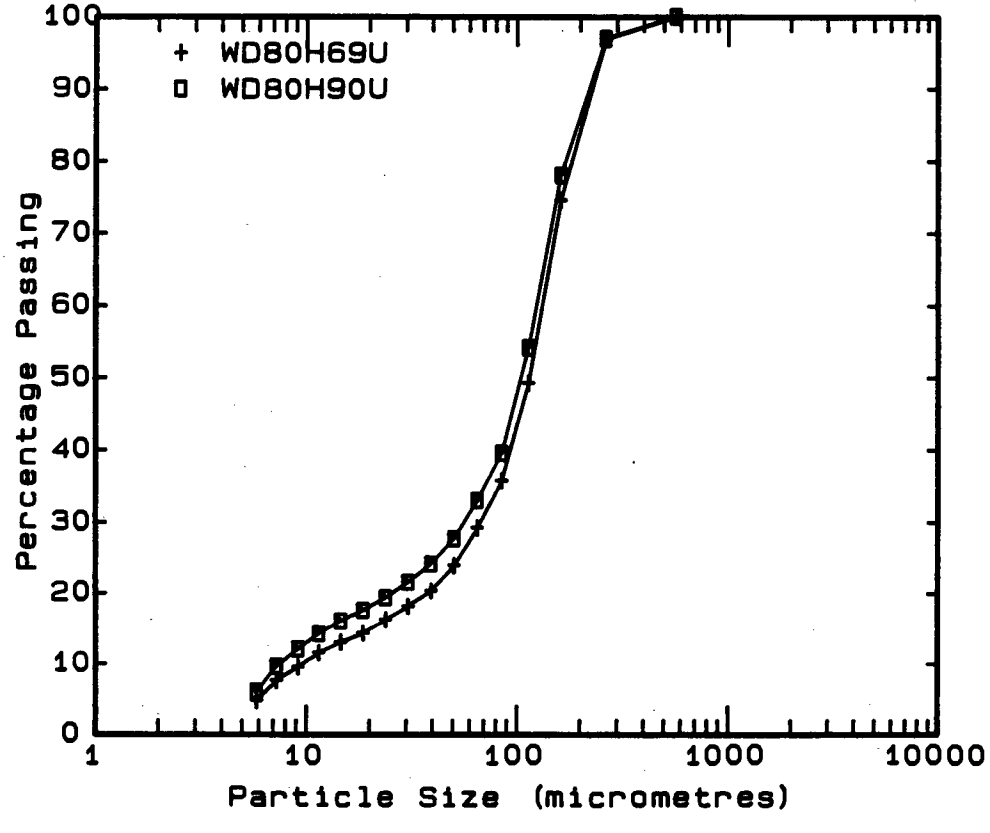

Figure 2.19

4.1 Influence of mean mixture velocity on pressure gradient

Figure 2.20 shows the variation of the horizontal pressure gradient with mean mixture velocity for the Vaal Reefs backfill slurry in a 40 mm NB pipeline for various solids concentrations. The experimental data points show that as the mixture relative density is increased the rate of increase of pressure gradient with velocity is increased. The pressure gradient - velocity curves become linear at higher concentrations. This indicates that at higher concentrations turbulence may be negligible due to dampening by the solid particle matrix.

The same trends are seen in Figure 2.21 for the vertical downward flow of Vaal Reefs slurry in a 40 mm NB pipeline. Figures 2.22 and 2.23 show similar trends for the horizontal and vertical downward flow of Western Deeps slurry in a 25 mm NB pipeline.

4.2 Influence of solids concentration on pressure gradient

Figure 2.24 shows the variation of the horizontal pressure gradient with solids concentration for Vaal Reefs slurry in a 40 mm NB pipeline for mean mixture velocities of 1 m/s, 2 m/s and 3 m/s. The pressure gradient is seen to sharply increase with concentration above a solids concentration of 45% by volume for all velocities. Note that this concentration corresponds closely to the freely settled concentration of the solid particles.

Figure 2.25 depicts the variation of the vertical down pressure with solids concentration for the Vaal Reefs slurry. The trends are similar to that of the horizontal pipeline.

Figure 2.26 shows the variation of the horizontal pressure gradient with solids concentration for the Blyvooruitsig slurry in an 80 mm NB pipeline. As with the Vaal Reefs slurry in a 40 mm pipeline, the pressure gradient is seen to increase with solids concentration above a concentration of 45% by volume. The cross over of the curves representing mean mixture velocities of 1 m/s and 2 m/s is due to the formation of a stationary bed at solids concentrations below 40% by volume and mean mixture velocities less than 2 m/s.

The variation of the vertical down pressure gradient with solids concentration for the Blyvooruitsig slurry is shown in Figure 2.27. The solid straight line represents the calculated pressure gradient assuming no friction, i.e. pressure gradient due to the weight of the slurry only. At low concentrations the mean mixture velocity curves are parallel to the pressure gradient curves calculated assuming no friction (i.e. the contribution of the increased concentration to the weight component is greater than the contribution to the frictional resistance). Above a concentration of 45% by volume the pressure gradient increases with concentration in a similar fashion to that of the horizontal pipeline (i.e. the contribution of the increased concentration to the frictional resistance exceeds the contribution to the weight component).

4.3 Influence of pipe diameter on pressure gradient

Figure 2.28 shows the influence of pipe diameter on the horizontal pressure gradient for the Vaal Reefs slurry at a solids concentration of 45,5% by volume. The pressure gradient for the 80 mm NB pipeline is relatively constant with mean mixture velocity compared with the pressure gradient curves for the 25 mm NB and 40 mm NB pipelines. Figure 2.29 shows that the 80 mm NB pipeline pressure gradient curve for the vertical down pipeline is steeper than that for the horizontal pipeline. The slope of the vertical down pressure gradient curve increases with decreasing pipe diameter.

Figure 2.30 shows how the horizontal pressure gradient varies with pipe diameter for the Vaal Reefs slurry. The pressure gradient increases with decreasing pipe diameter for mean mixture velocities of 2 m/s and 3 m/s. Due to the formation of a stationary bed the pressure gradient at a mean mixture velocity of 1 m/s increases slightly for a pipe diameter greater than 50 mm. Figure 2.31 shows the variation of the vertical down pressure gradient with pipe diameter. The trends are similar to that in the horizontal pipe.

The variation of the Vaal Reefs horizontal pressure gradient with pipe diameter is shown for various solids concentration in Figure 2.32. The variation of the slurry pressure gradient curves are compared with the clear water pressure gradient curve. The rate of increase of pressure gradient with decrease in pipe diameter increases with increased solids concentration. Figure 2.33 shows similar trends for vertical downward flow.

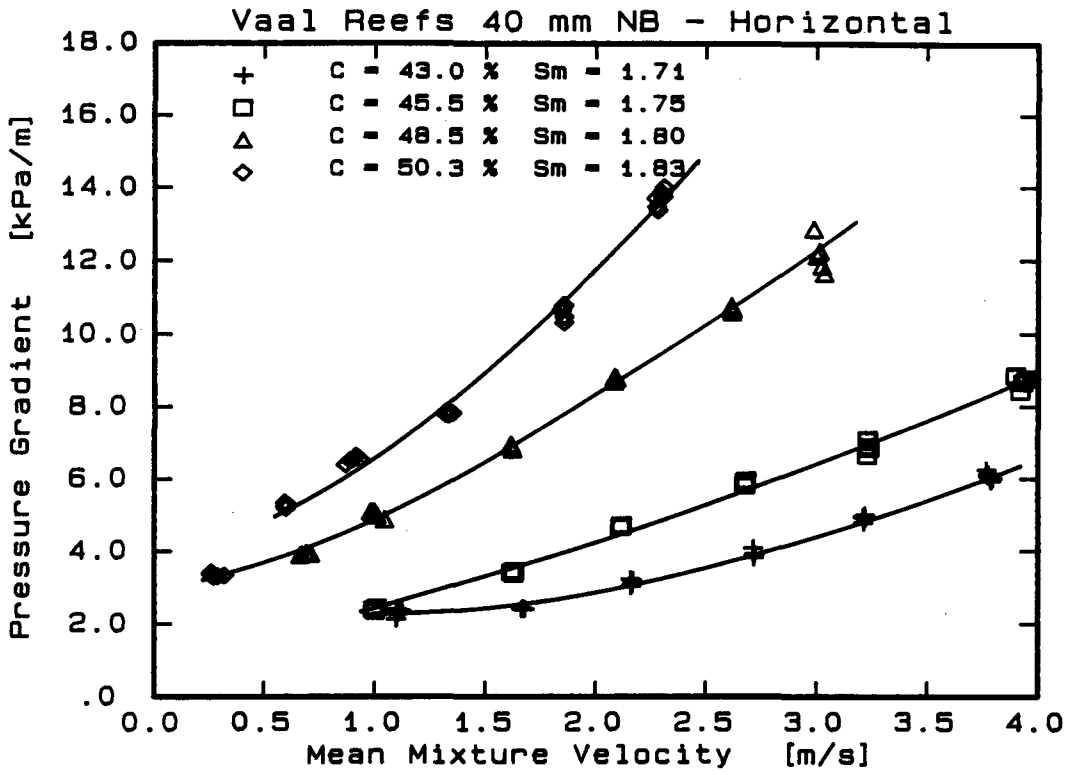

Figure 2.20

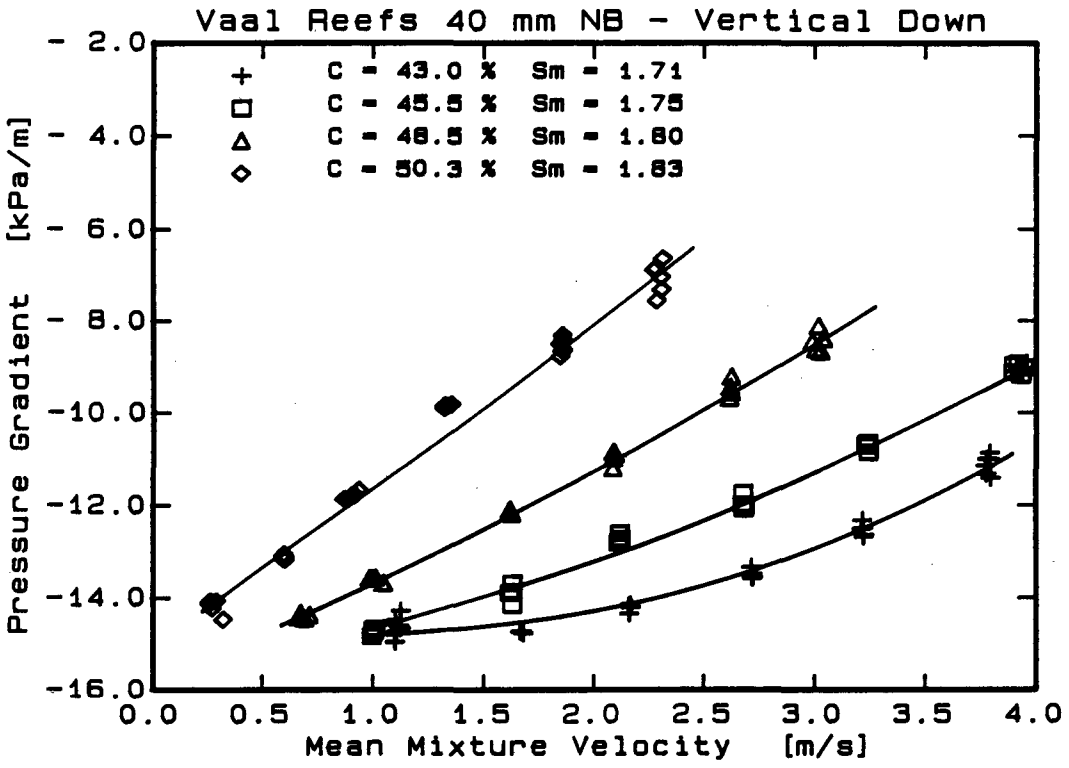

Figure 2.21

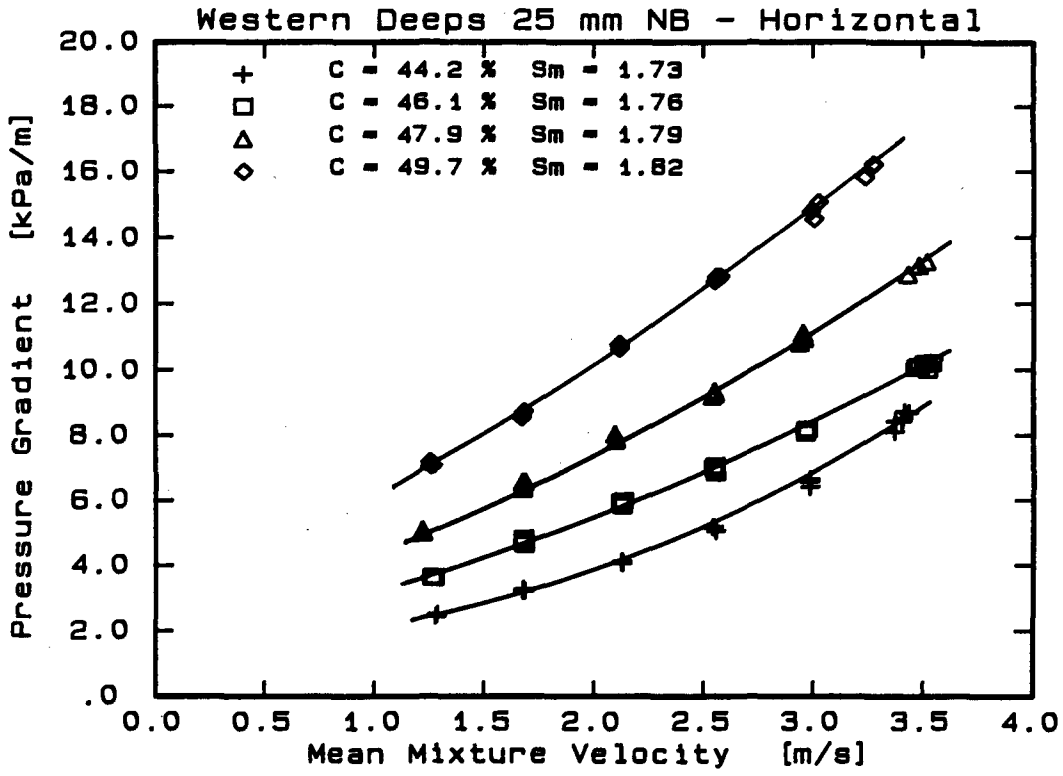

Figure 2.22

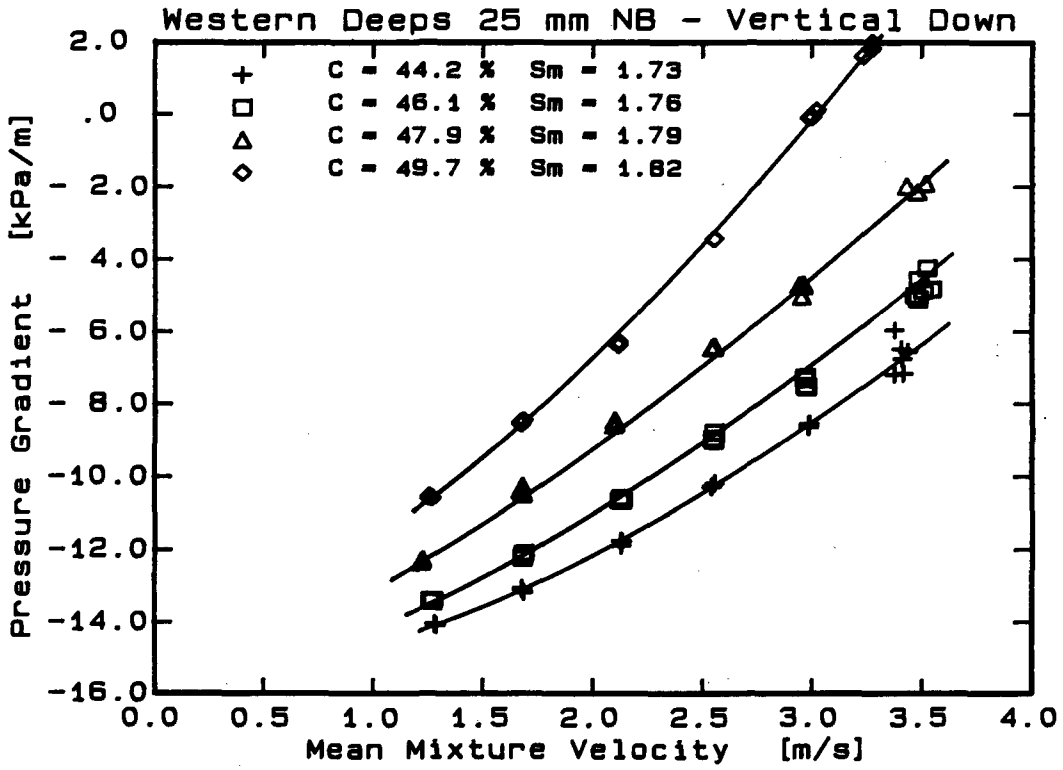

Figure 2.23

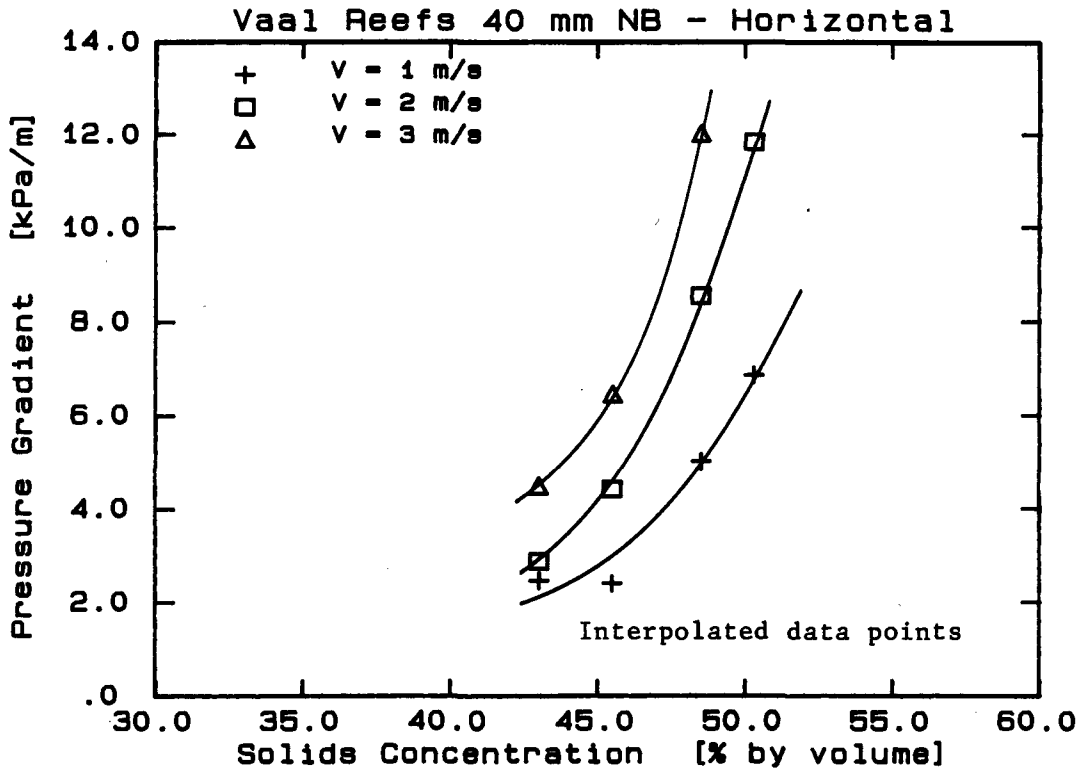

Figure 2.24

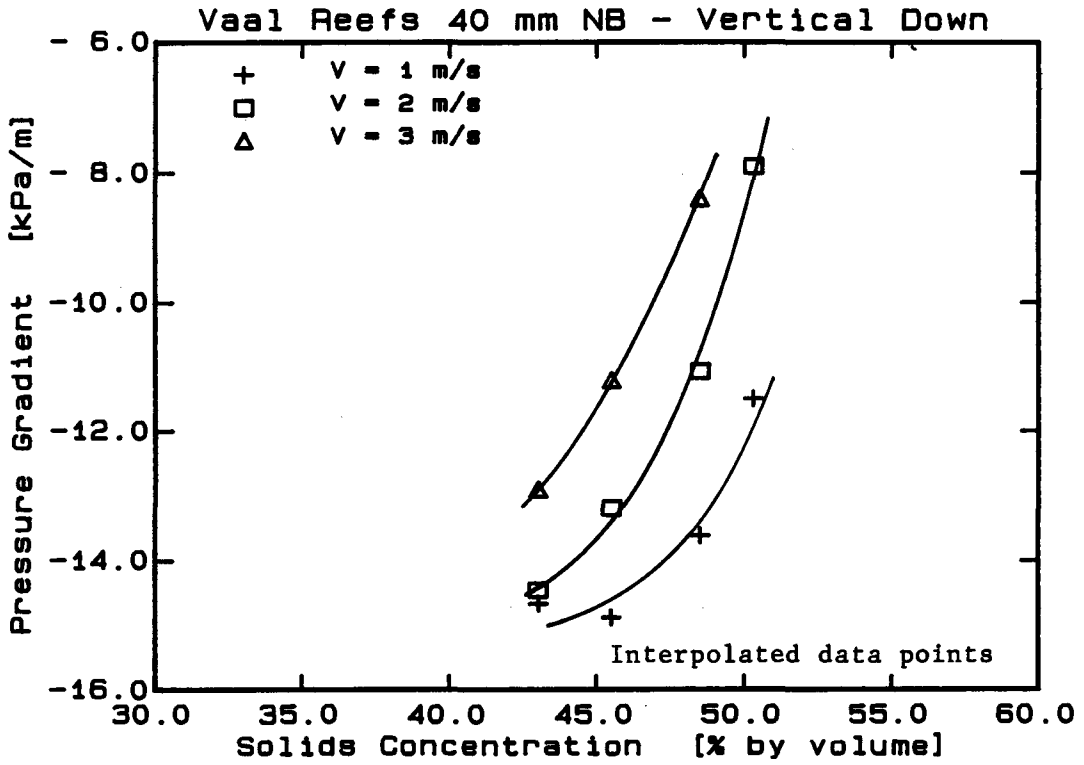

Figure 2.25

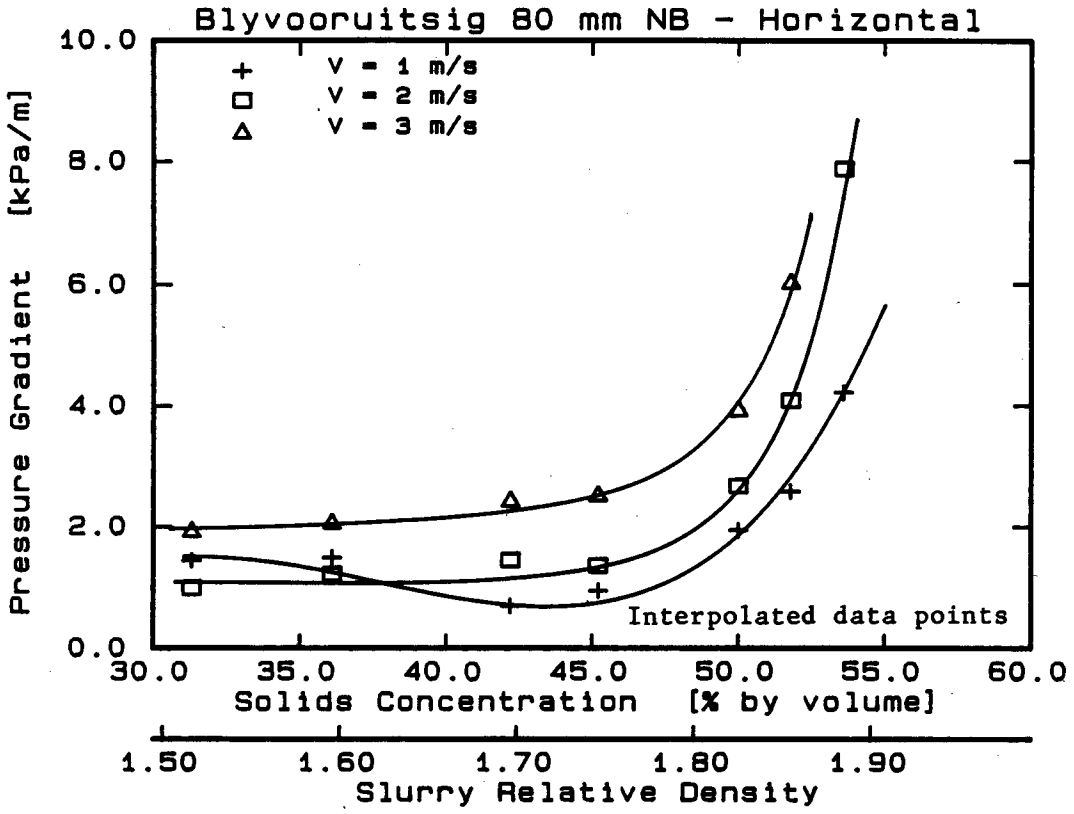

Figure 2.26

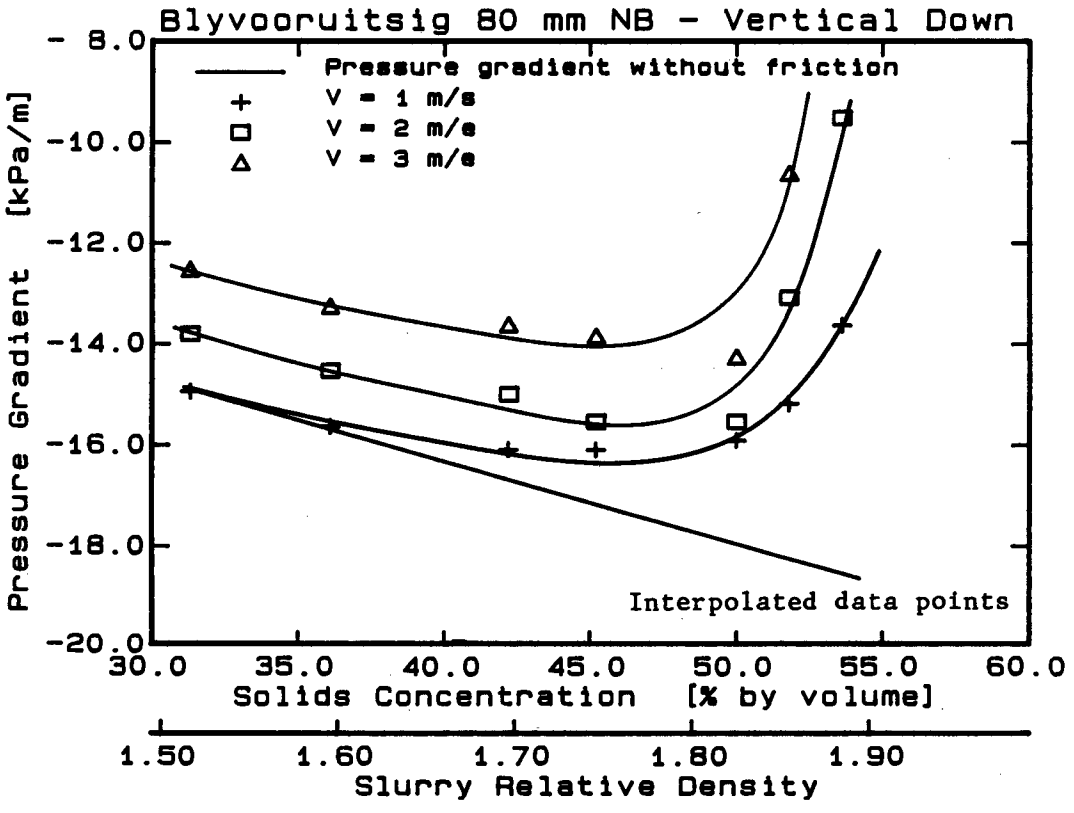

Figure 2.27

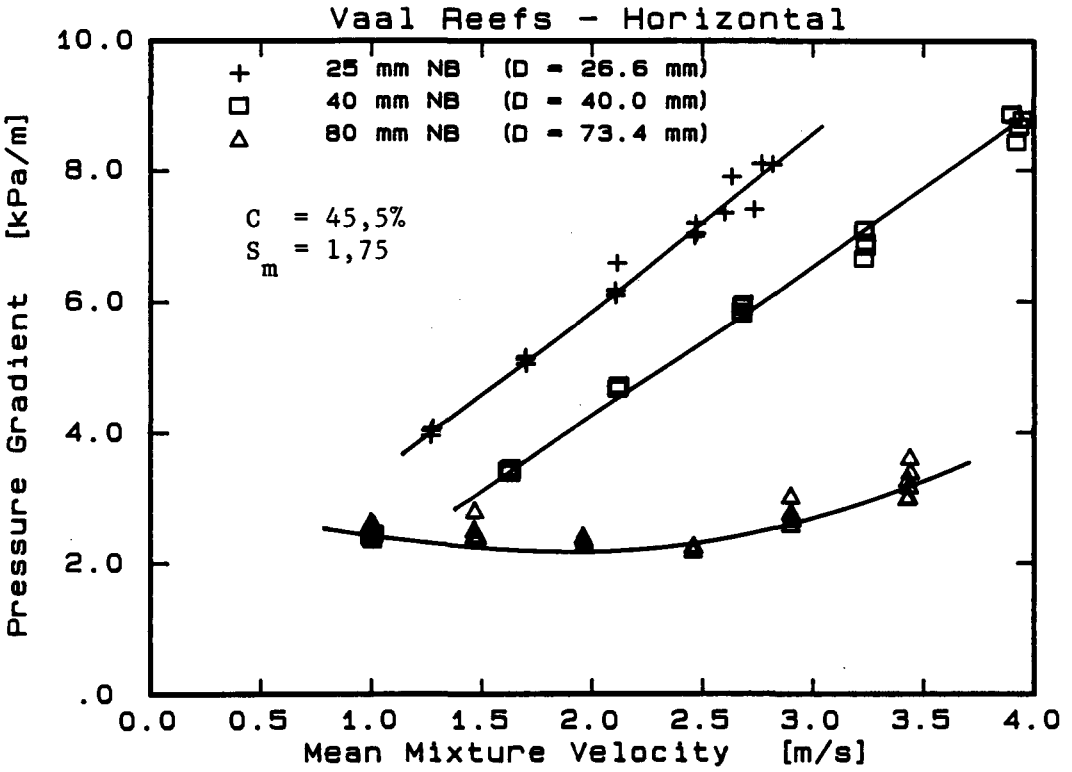

Figure 2.28

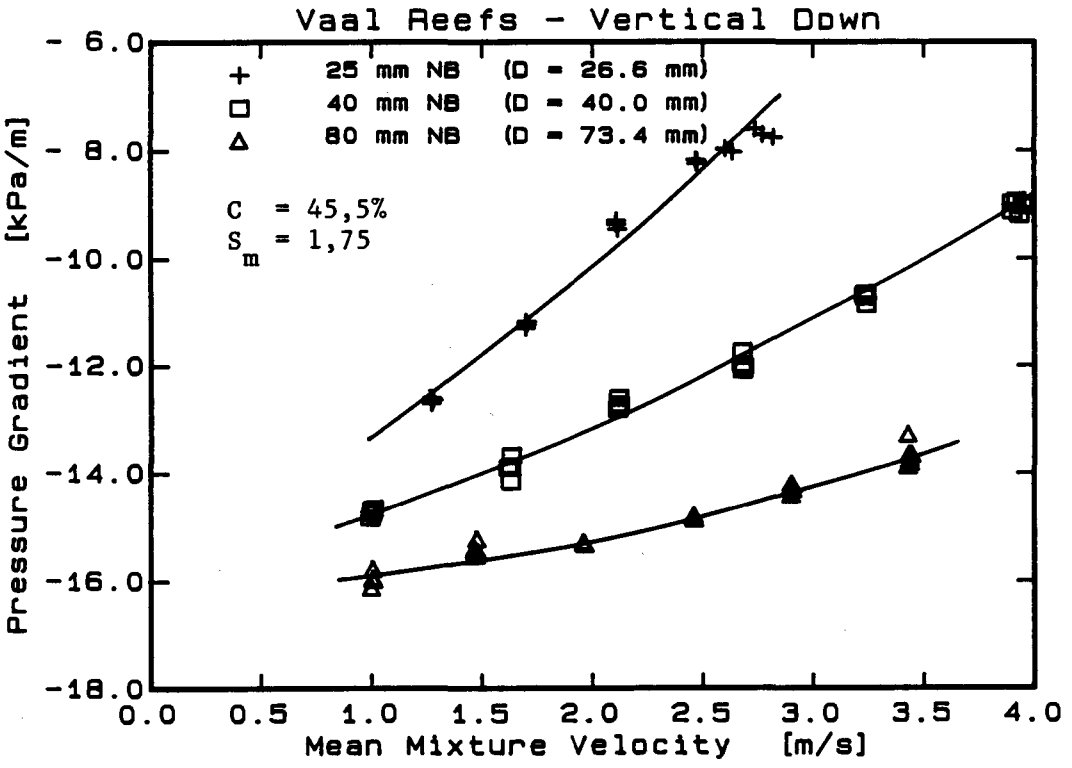

Figure 2.29

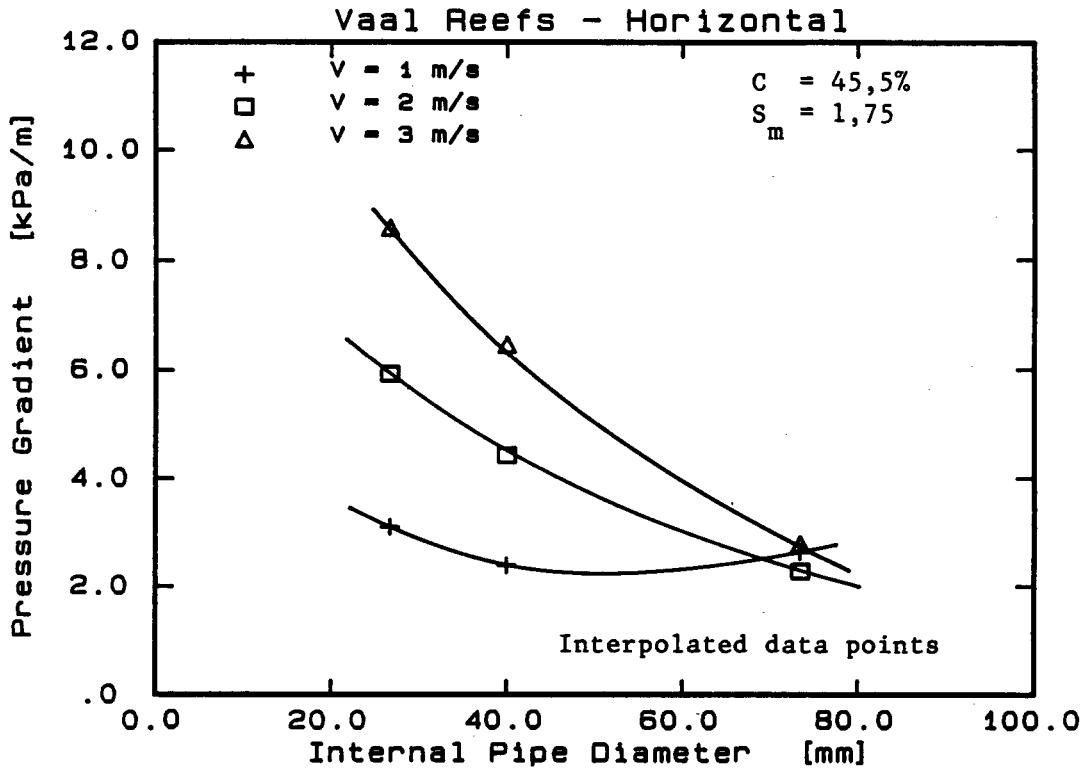

Figure 2.30

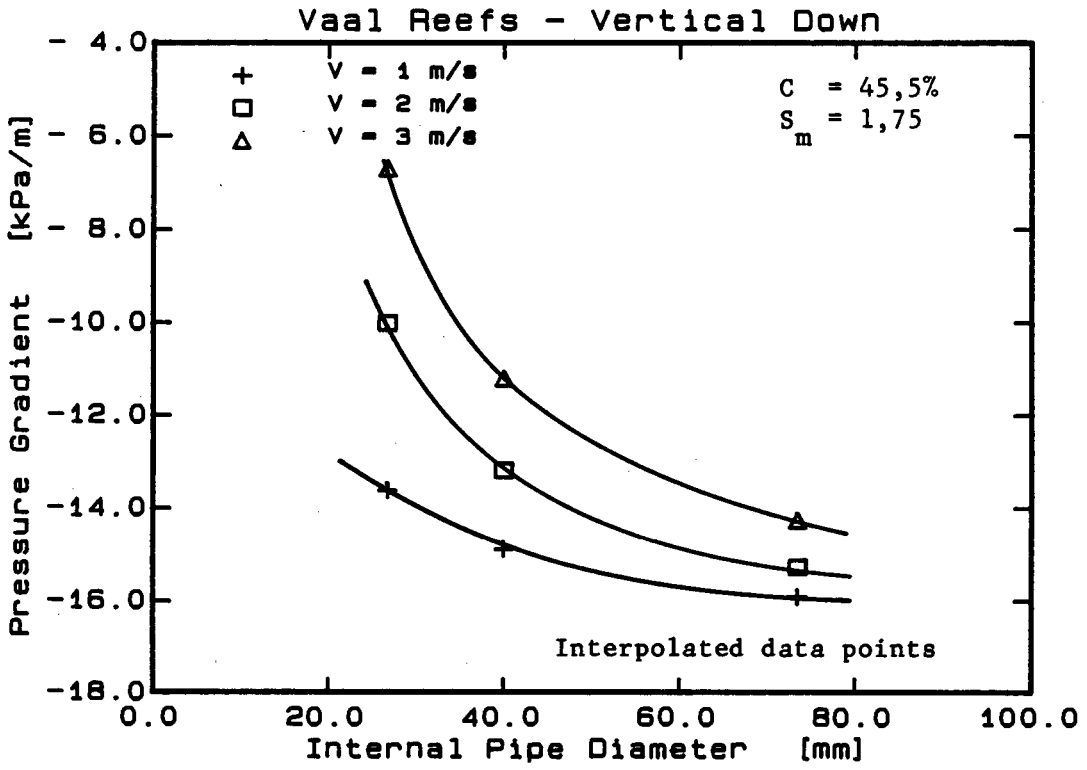

Figure 2.31

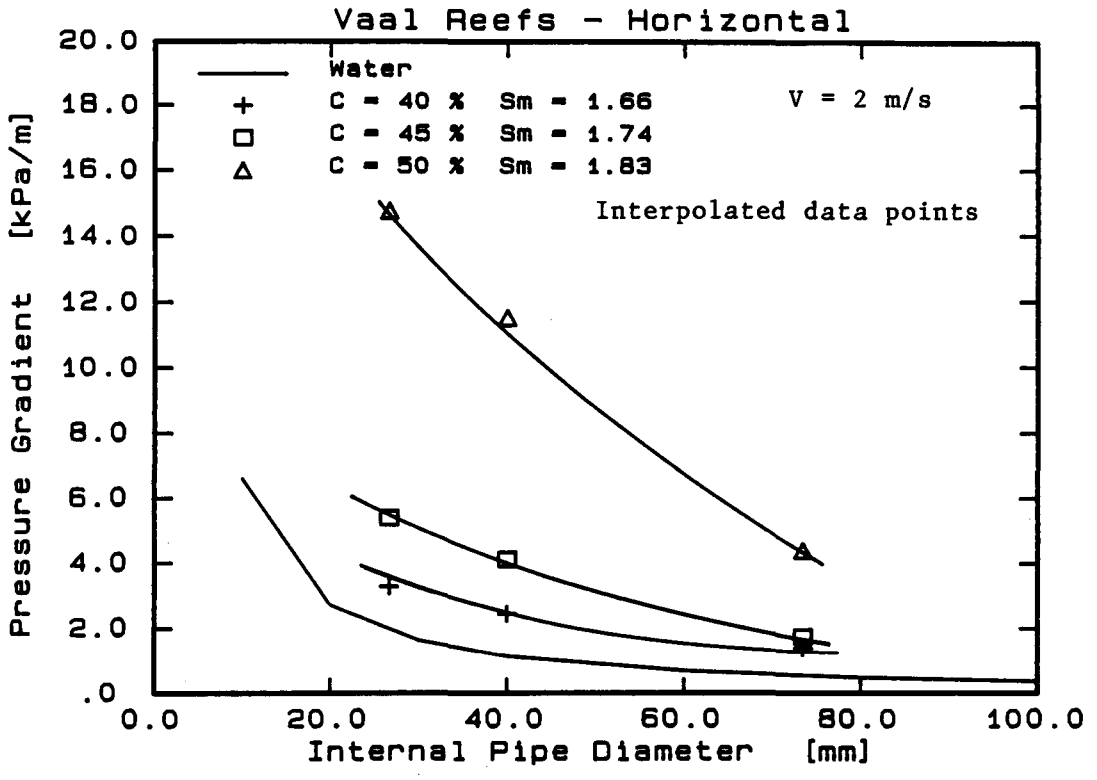

Figure 2.32

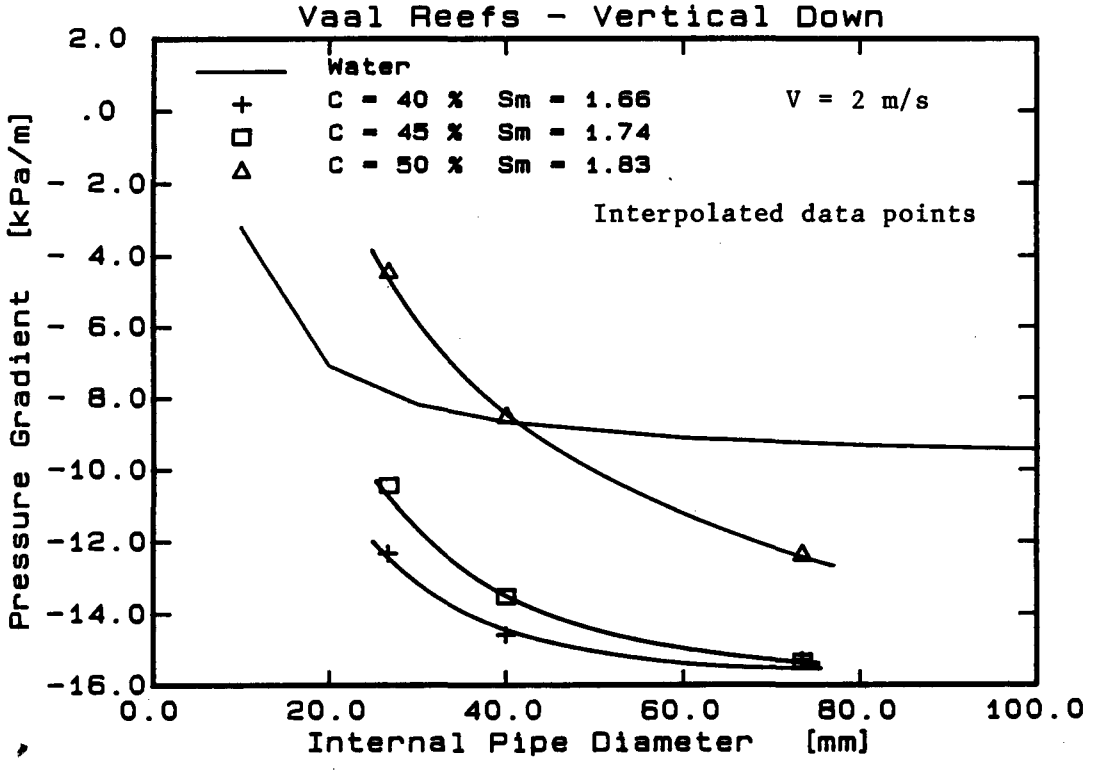

Figure 2.33

4.4 Flow observations

Figure 2.34 shows a plot of flow observations for the Blyvooruitsig slurry in a 40 mm NB horizontal pipeline. The observations are grouped into three categories :

(i) **Stationary bed** - a bed of stationary particles or solitary particles observed on the pipe invert.

(ii) **Asymmetric flow** - an asymmetric concentration and/or velocity profile observed.

(iii) **Symmetric flow** - no asymmetric concentration or velocity profile evident.

Each flow observation in Figure 2.34 is plotted at the intersection of the corresponding solids concentration and mean mixture velocity. The flow observation plot is divided into four flow regimes.

(i) **Stationary bed** - zone in which the combination of solids concentration and mean mixture velocity is likely to result in a stationary bed.

(ii) **Heterogeneous** - flow conditions where asymmetric velocity and/or concentration profiles were observed.

(iii) **Pseudo homogeneous** - zone in which the flow appears to have symmetric velocity and concentration profiles. Slurries in this zone behave as heterogeneous mixtures at lower mean mixture velocities.

(iv) **Homogeneous** - flow appears homogeneous for all mean mixture velocities at a particular solids concentration.

Table 2.9 shows the key to the Figures corresponding to the flow observation plots for the four backfill slurries in 40 mm and 80 mm NB pipes. The flow observation plots for the four materials are similar. Note that no stationary bed was observed for the Western Deeps slurry.

TABLE 2.9 : Key to flow observation plots

Slurry	Figure Number	
	40 mm NB	80 mm NB
Blyvooruitsig	2.34	2.35
East Driefontein	2.36	2.37
Vaal Reefs	2.38	2.39
Western Deeps	2.40	2.41

In Figure 2.42 the solids concentration corresponding to the transition between the heterogeneous flow regime and the homogeneous flow regime of the flow observation plots is plotted against internal pipe diameter. The curves for the Blyvooruitsig, East Driefontein and Vaal Reefs slurries are parallel and show an increasing transition concentration with increasing pipe diameter. The Western Deeps slurry curve also shows an increase in transition solids concentration with pipe diameter, although with a steeper slope than for the other materials. This is probably due to the Western Deeps material forming a stabilised mixture with non-Newtonian characteristics at high concentration (due to the high percentage of fine particles), compared with the settling slurries formed by the other backfill materials.

The ratio of the transition solids concentration between heterogeneous and homogeneous flow to the freely settled solids concentration is plotted against internal pipe diameter in Figure 2.43. The transition data points for the three settling slurries lie on a single curve, while the curve for the Western Deeps slurry has a steeper slope.

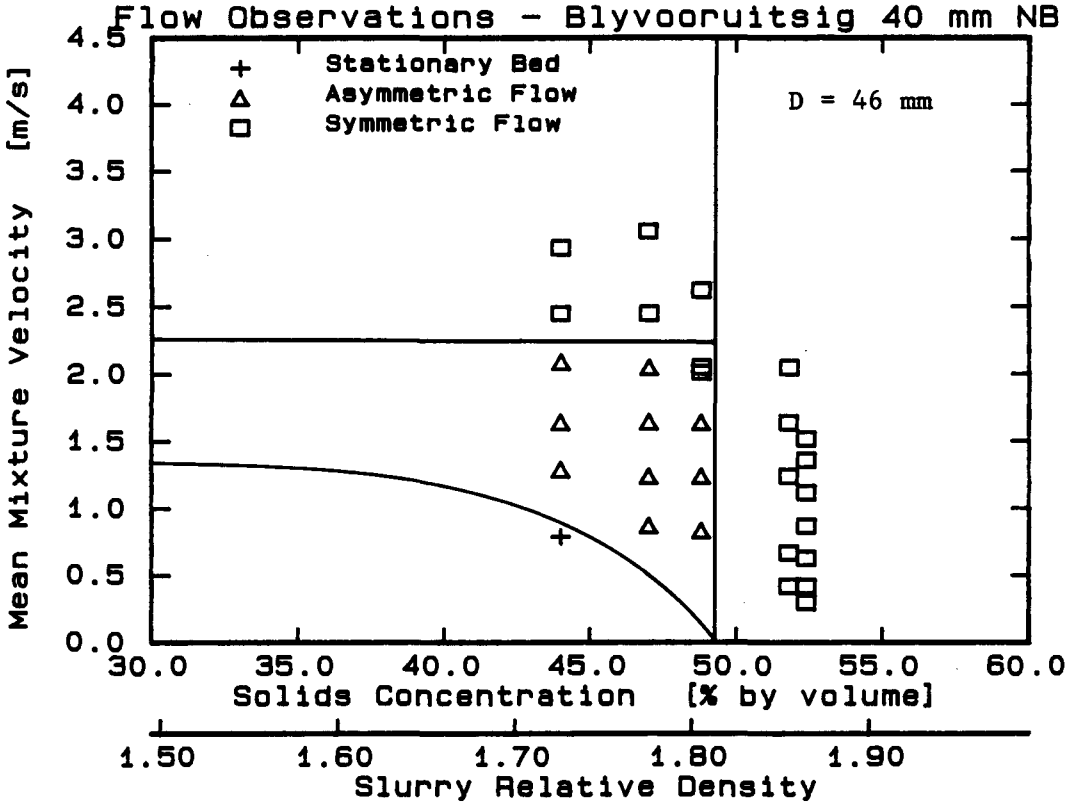

Figure 2.34

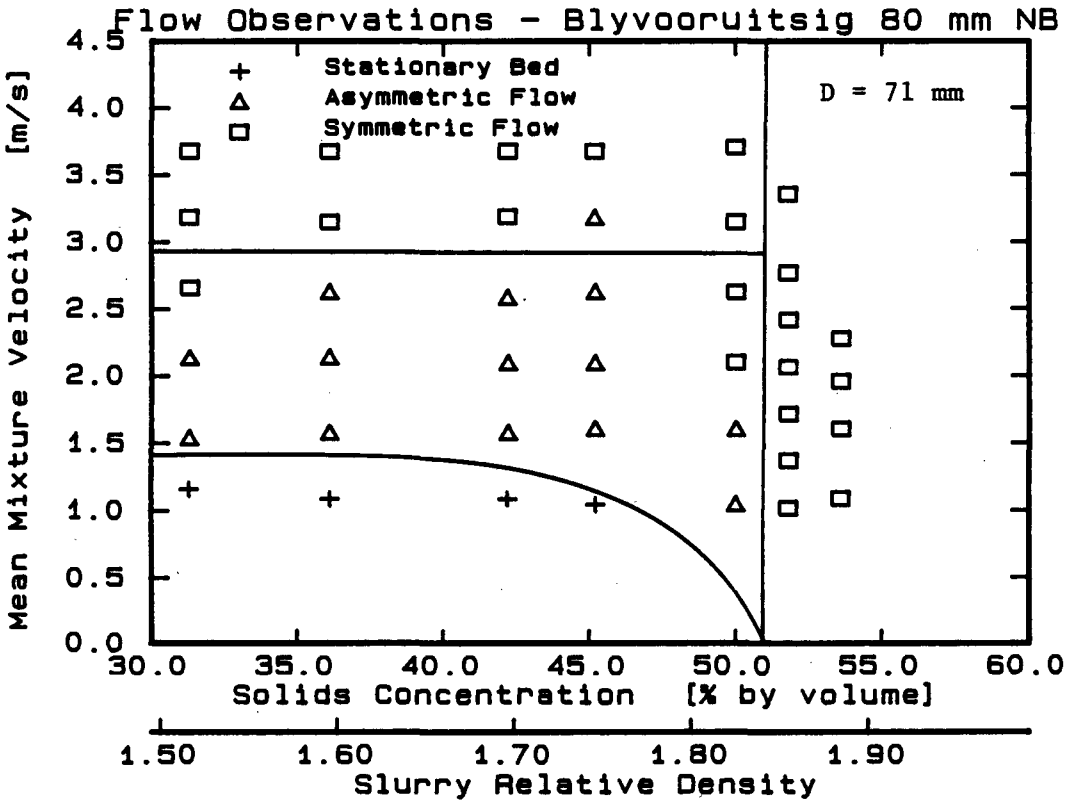

Figure 2.35

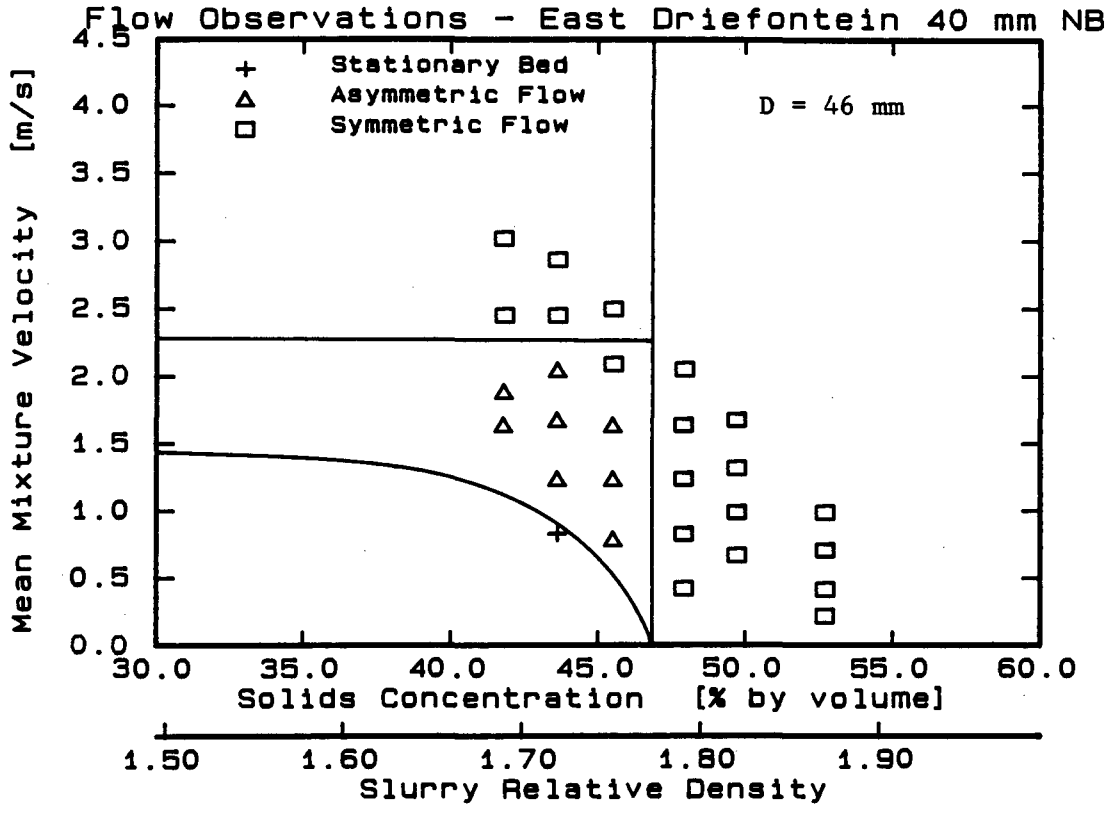

Figure 2.36

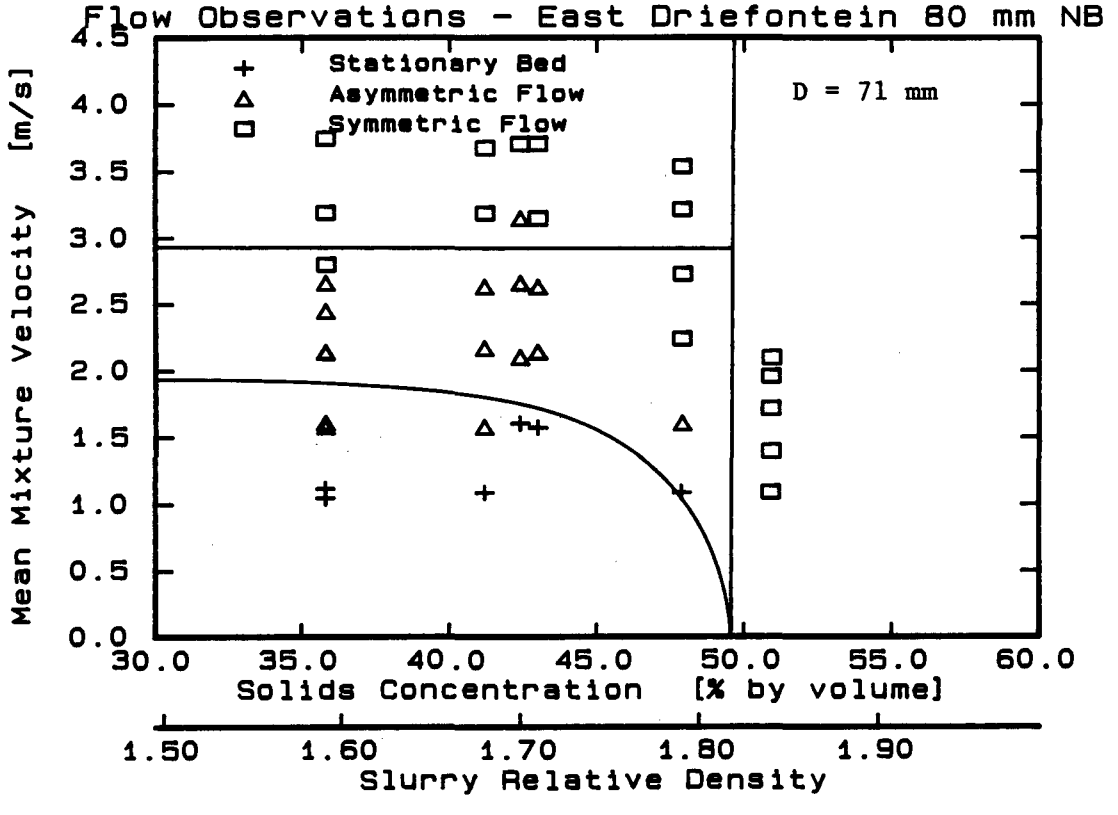

Figure 2.37

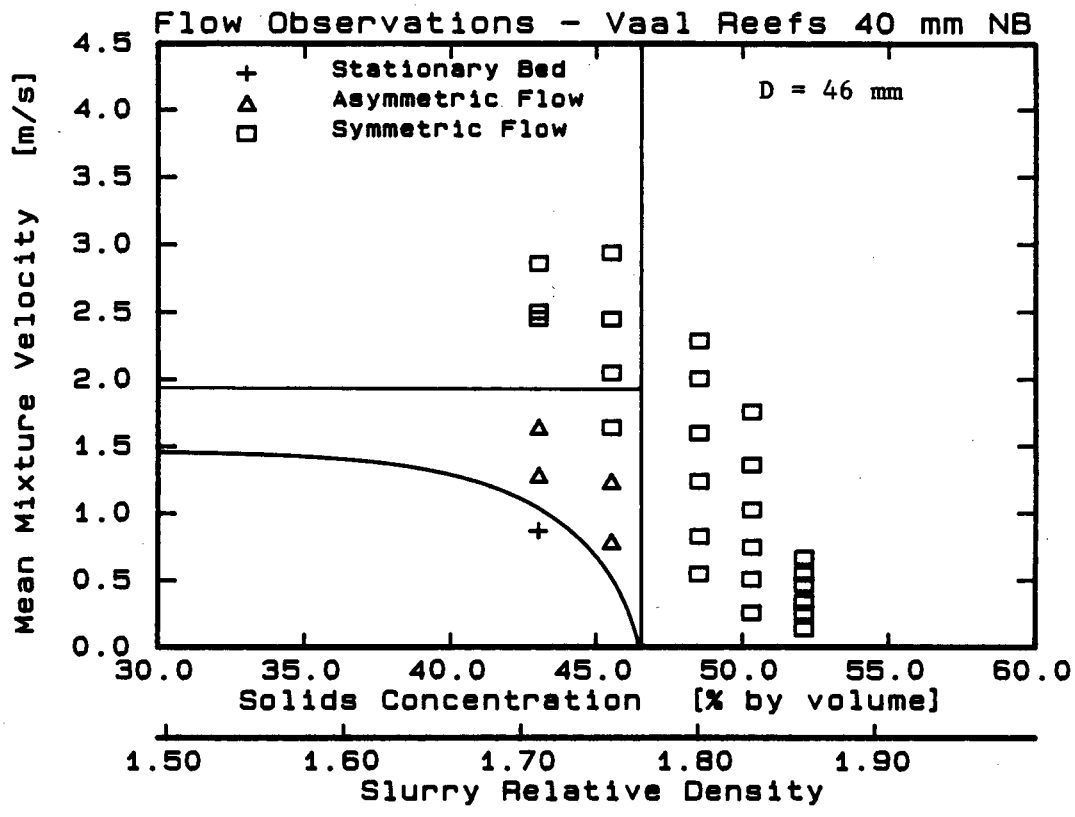

Figure 2.38

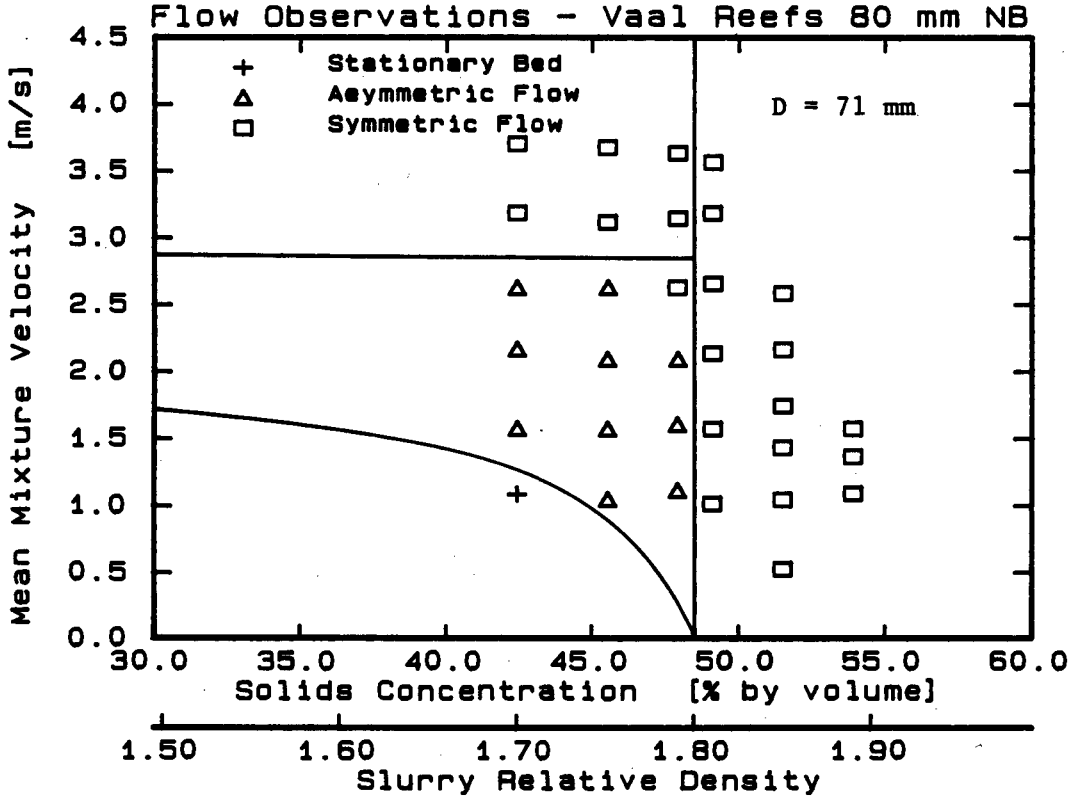

Figure 2.39

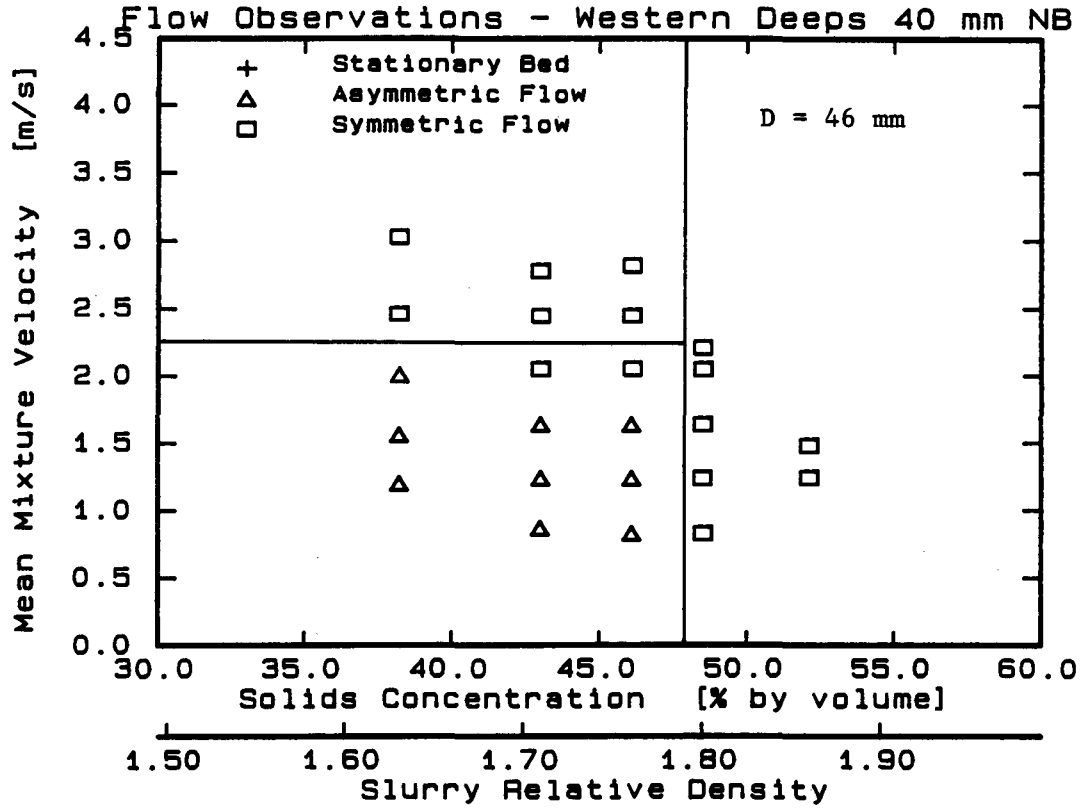

Figure 2.40

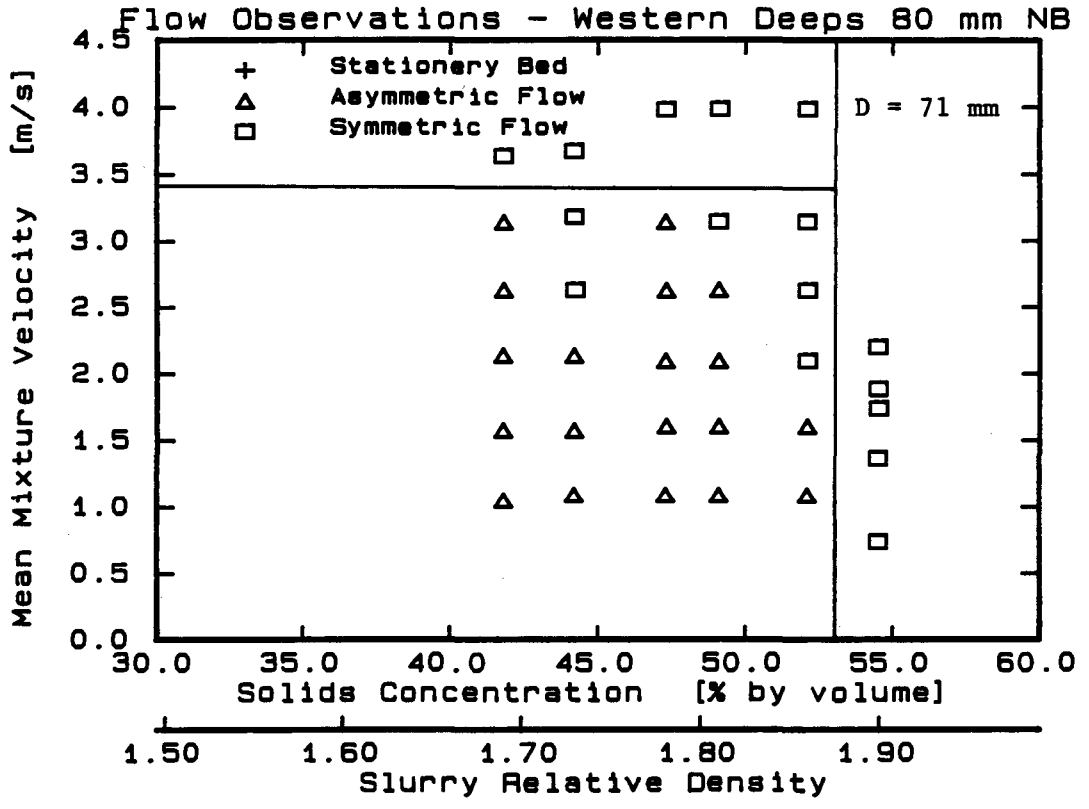

Figure 2.41

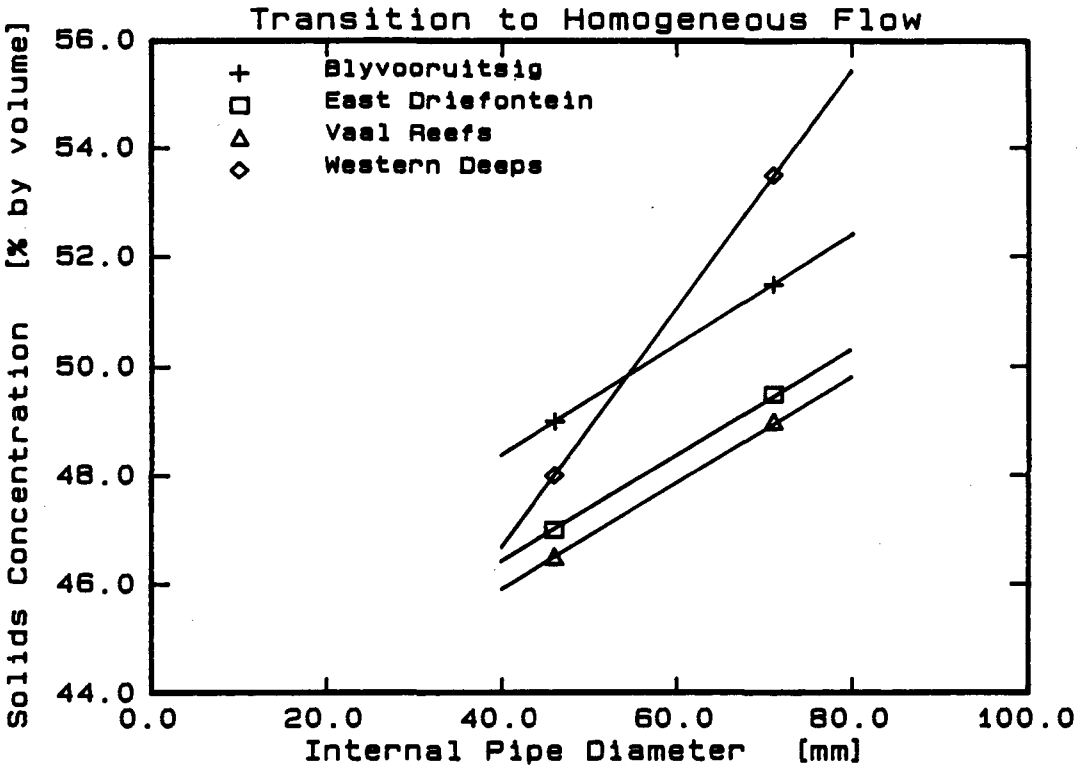

Figure 2.42

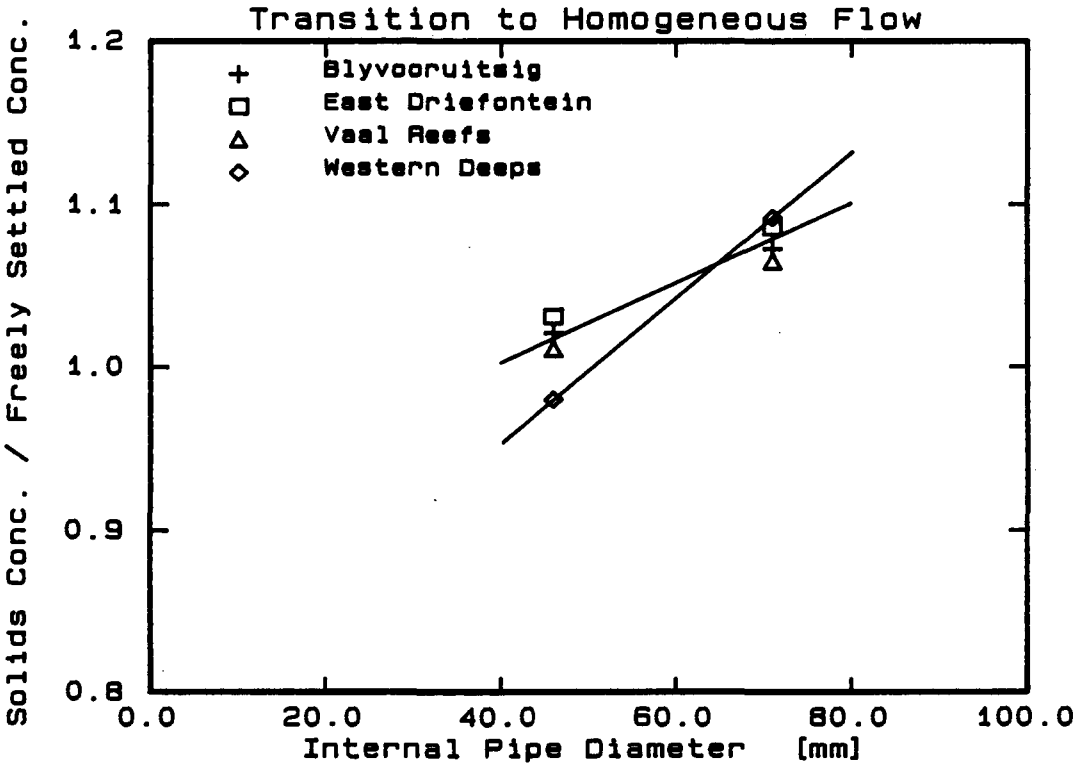

Figure 2.43

4.5 Comparison of backfill pressure gradients

Figure 2.44 compares the horizontal pressure gradients for the four backfill slurries in a 40 mm NB pipeline at a mean mixture velocity of 2 m/s. The East Driefontein and Vaal Reefs slurries have similar pressure gradients which are higher than those for the Western Deeps and Blyvooruitsig slurries. For a particular concentration the Blyvooruitsig slurry has the lowest pressure gradient, with the pressure gradients due to East Driefontein and Vaal Reefs the highest. Figure 2.45 shows the same trend for vertical downward flow.

Figure 2.46 shows the horizontal pressure gradient for the four backfill slurries plotted against the ratio of the solids concentration to the freely settled concentration of each material. The settling mixtures' (Blyvooruitsig, East Driefontein and Vaal Reefs) pressure gradients form a single curve. The pressure gradient curve for the stabilised Western Deeps material lies to the left of the other three backfill slurries. Figure 2.47 shows the same trend for vertical downward flow.

The ratio of the solids concentration to the freely settled concentration of the solid particles appears to be an important parameter, and may be interpreted as indication of the mobility of a particle within the mixture.

4.6 Comparison of horizontal and vertical down friction pressure losses

Figure 2.48 compares the horizontal and vertical down friction pressure gradients (i.e. total pressure gradient less weight component) for the Vaal Reefs slurry in three pipe diameters at a mean mixture velocity of 2 m/s. The horizontal and vertical down pressure gradients are shown to be similar. Figure 2.49 shows similar data for the Blyvooruitsig slurry.

4.7 Comparison of vertical up and down friction pressure losses

Figure 2.50 compares the vertical up and vertical down friction pressure losses for the Vaal Reefs slurry in the 25 mm NB pipeline at a mean mixture velocity of 2 m/s. The vertical down friction loss is slightly greater than the vertical up friction loss. Figure 2.57 shows the same trend for the East Driefontein slurry. The difference between the vertical up and vertical down friction losses may be due to submerged particle weight effects as discussed in Section 2.4.3 of Chapter 5.

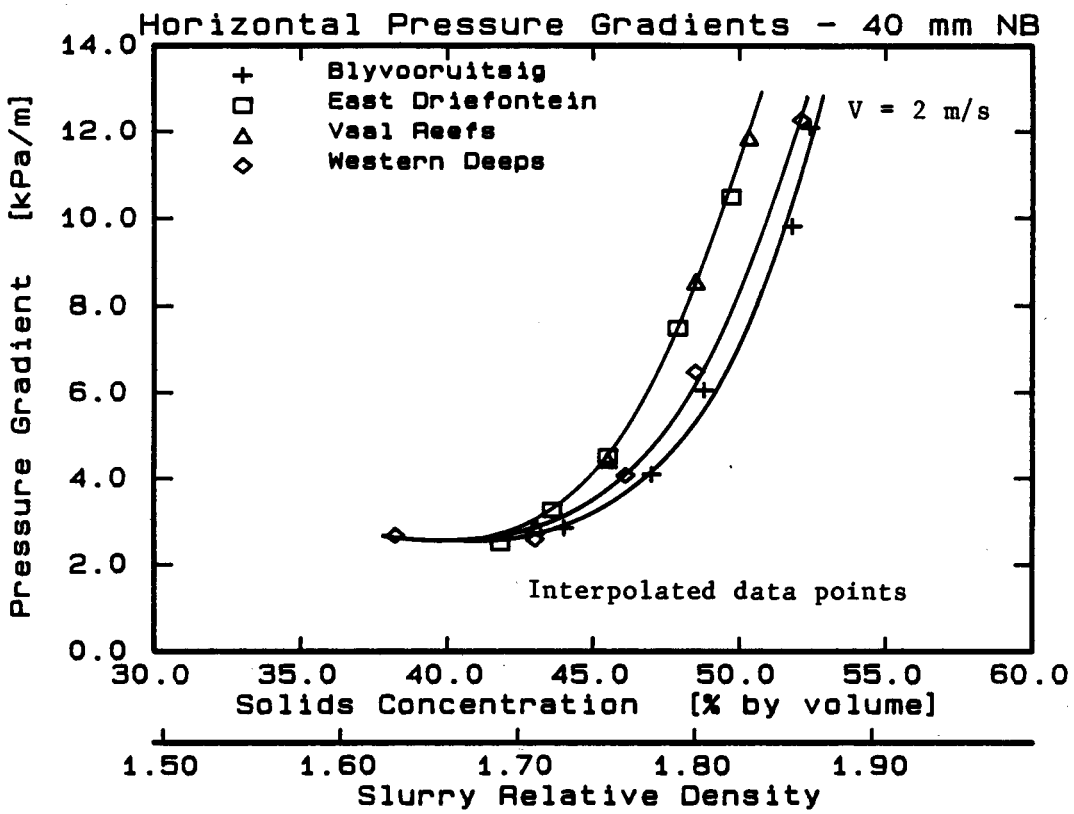

Figure 2.44

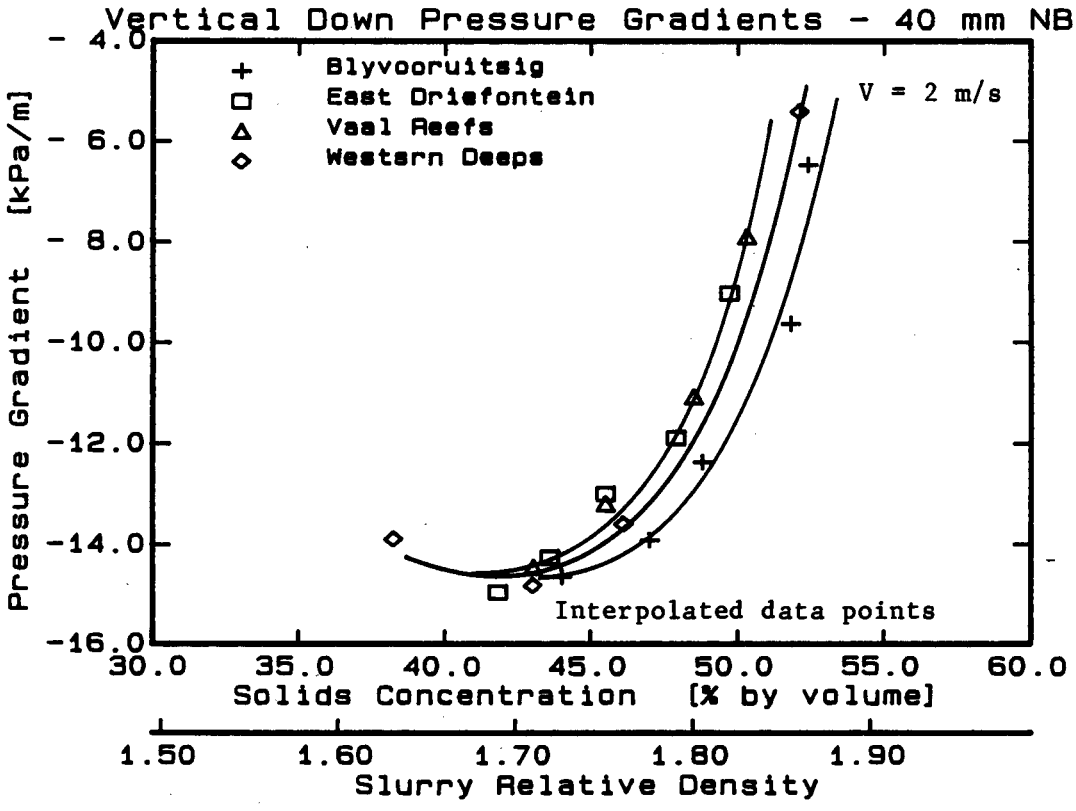

Figure 2.45

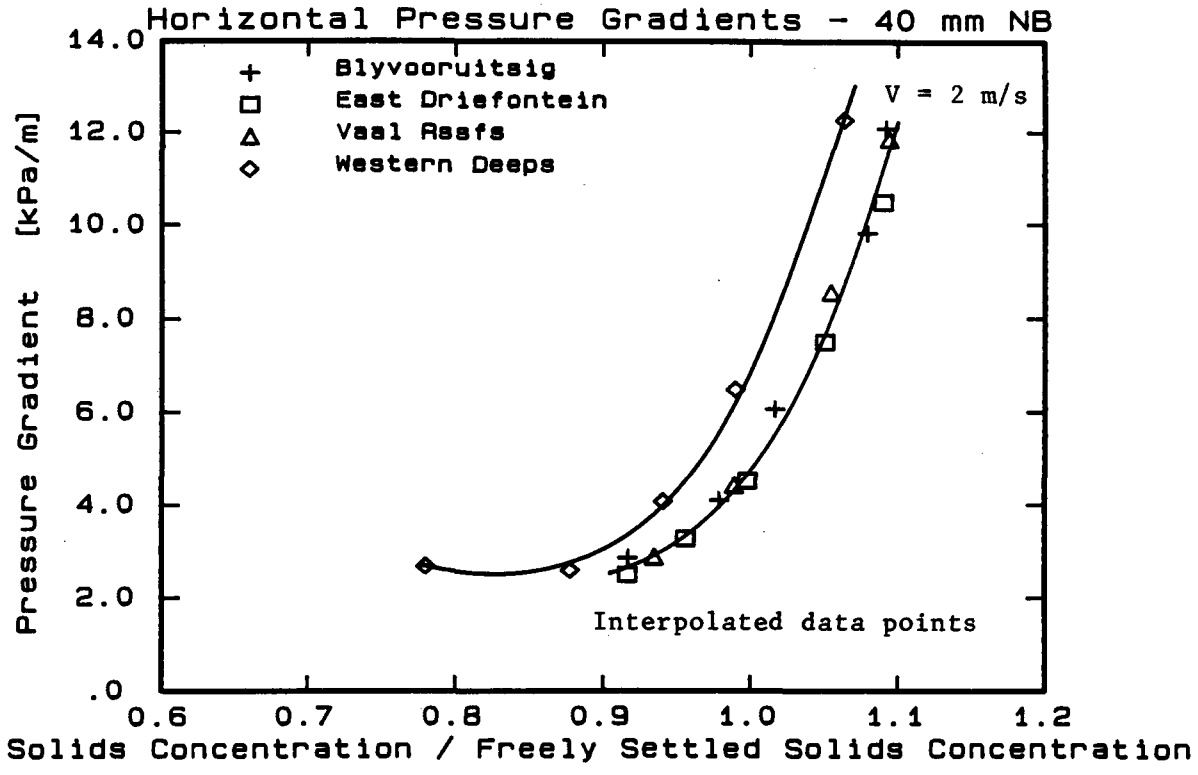

Figure 2.46

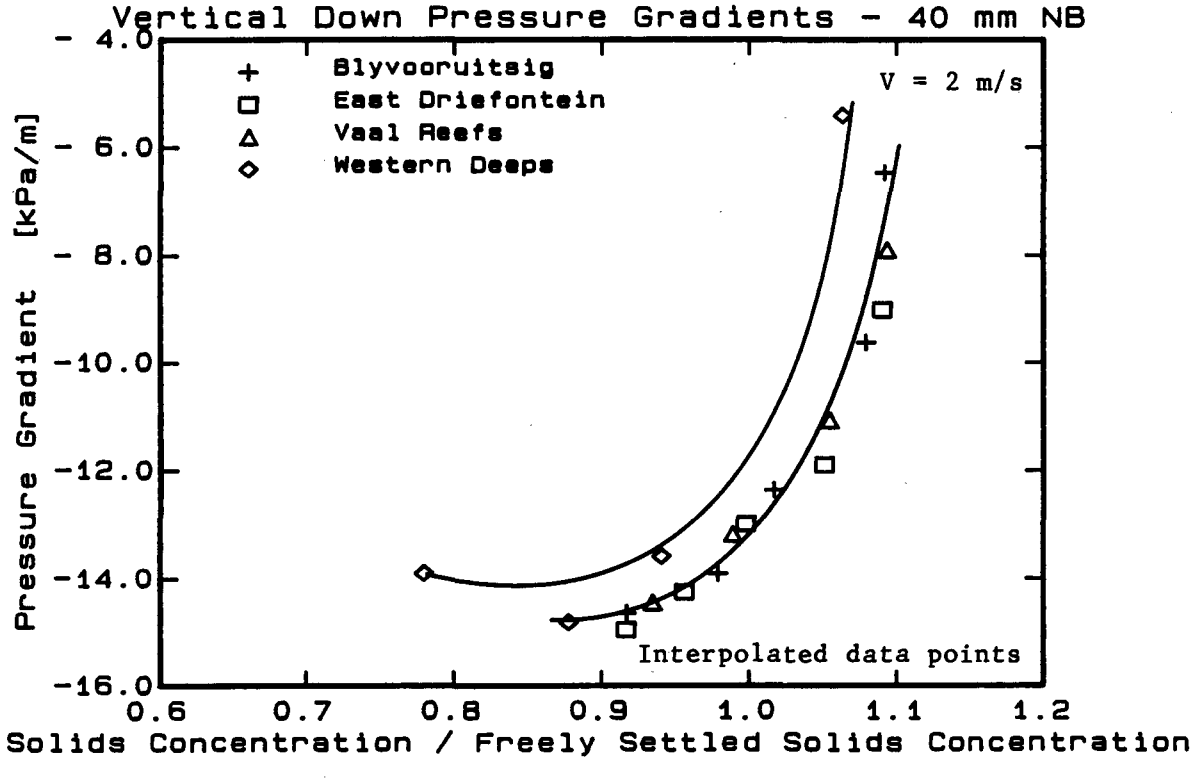

Figure 2.47

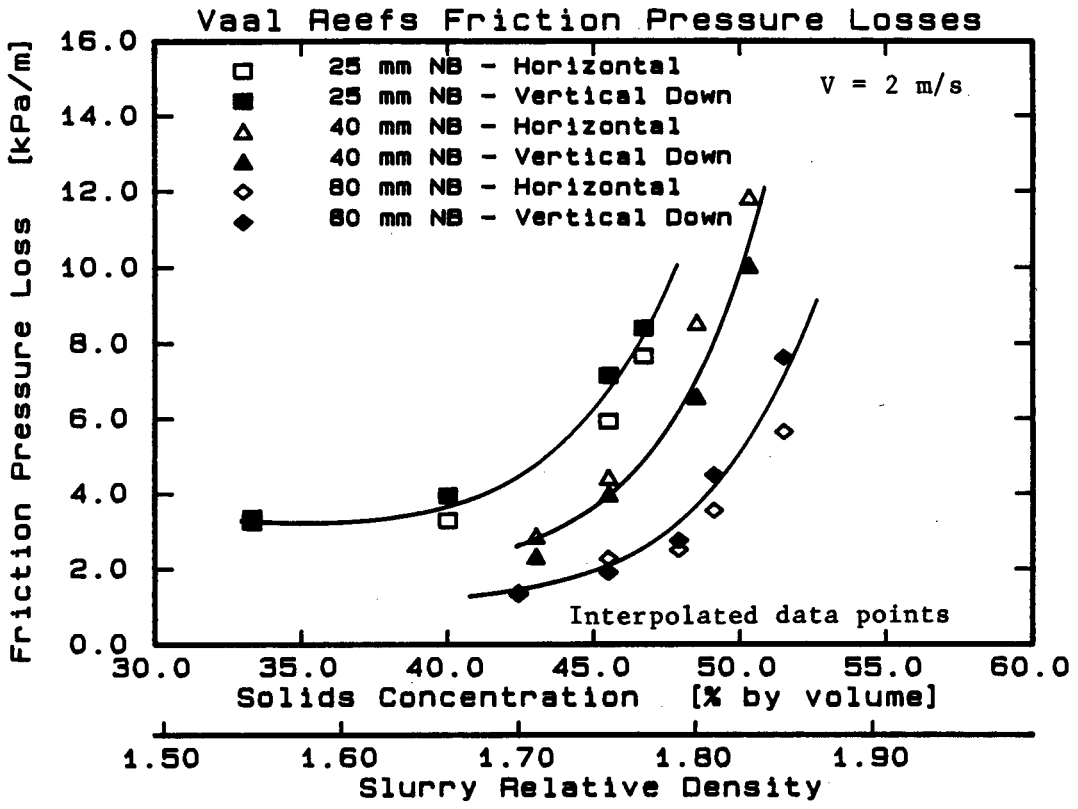

Figure 2.48

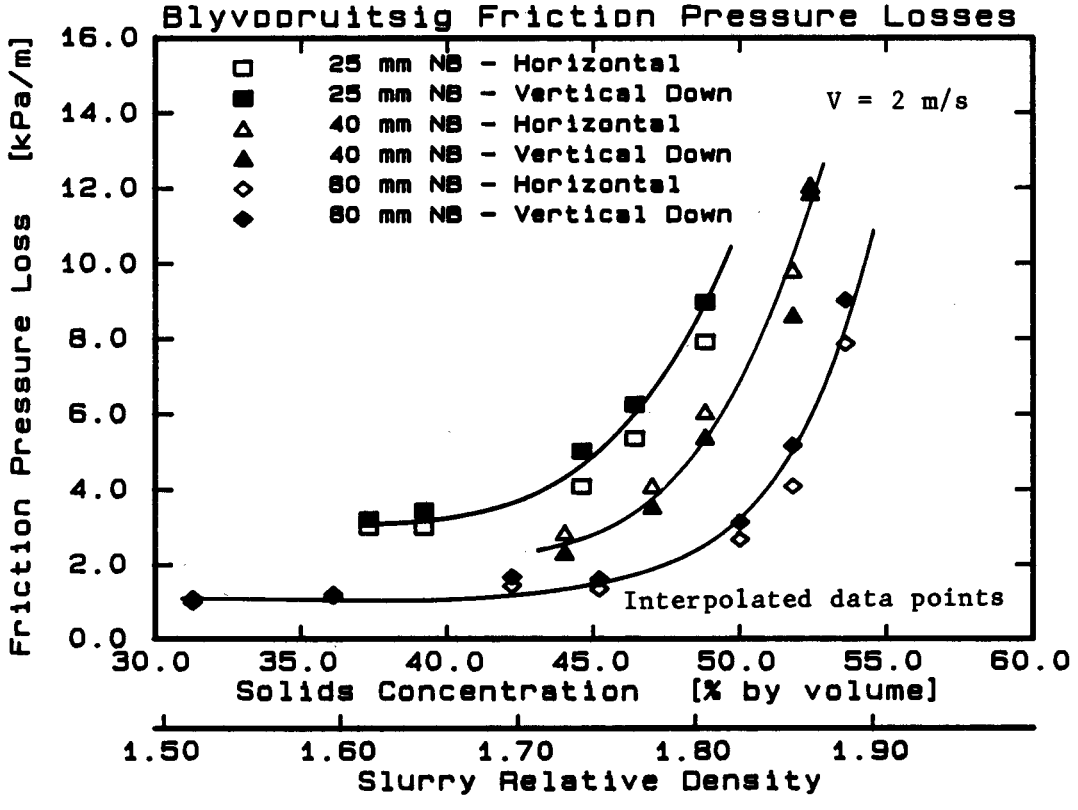

Figure 2.49

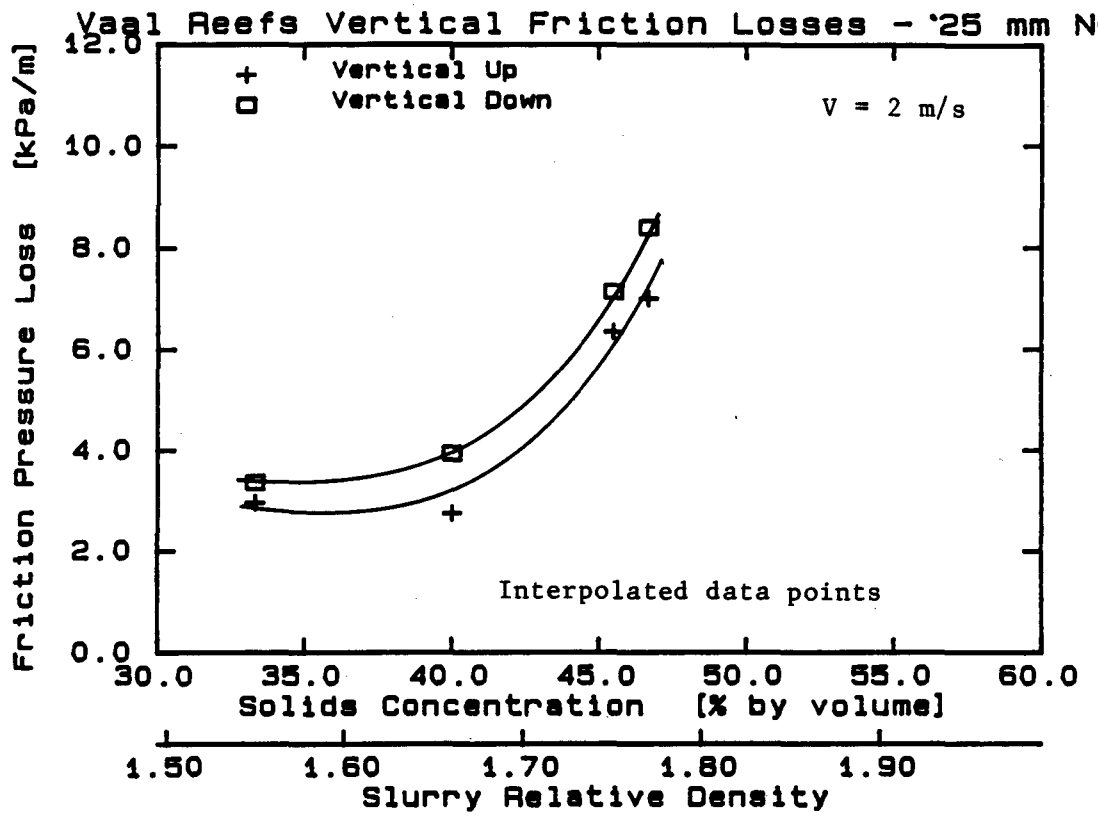

Figure 2.50

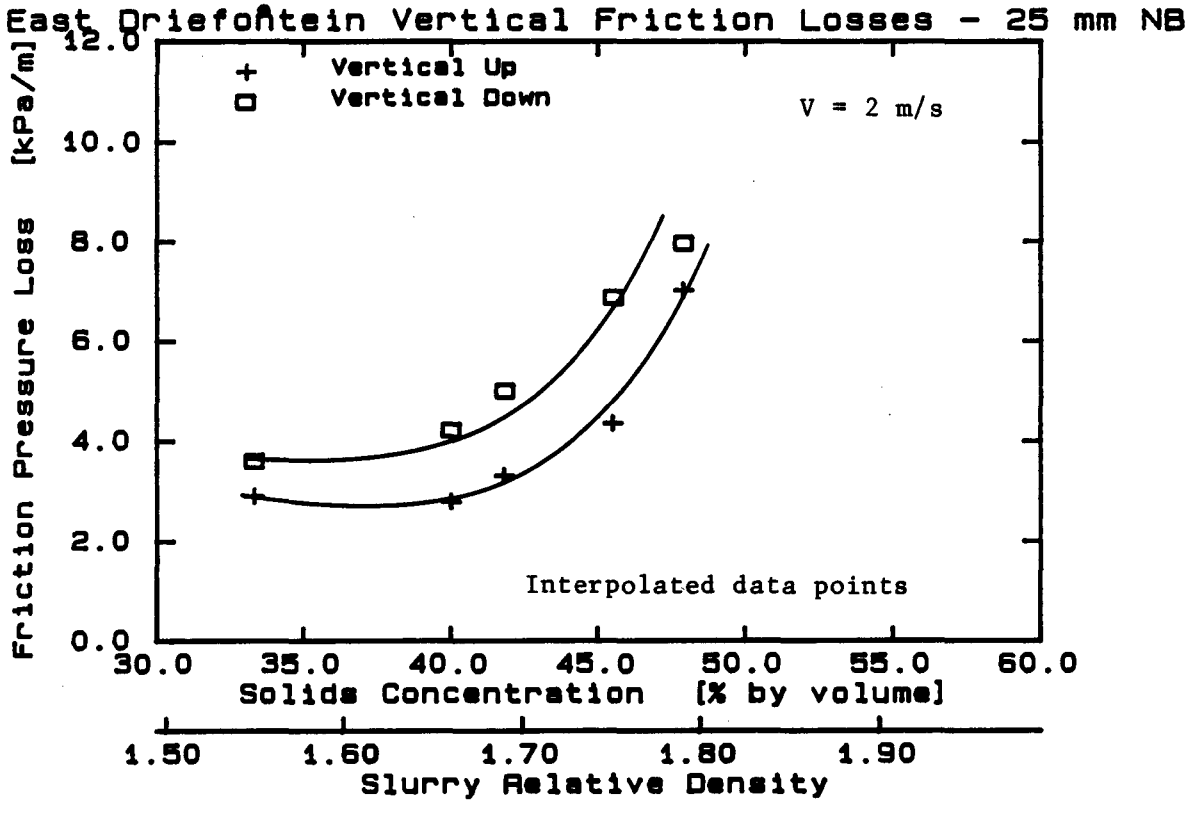

Figure 2.51

5. CHAPTER SUMMARY AND CONCLUSIONS

Pipeline test facilites have been constructed to investigate the hydraulic transport of high concentration cyclone classified tailings for backfilling in gold mines. The test loops consist of 25 mm, 40 mm and 80 mm nominal bore pipelines. The test facilities have been described, test operating procedures discussed and experimental measurement errors evaluated. The mean mixture velocity, horizontal and vertical pressure gradients, slurry relative density and slurry temperature are measured for each test. Visual observations of the slurry flow behaviour in clear pipeline sections are noted.

The methods used to characterise the solid particles are described. The solid particle properties evaluated are :

- solids relative density
- particle size distribution
- particle shape factor
- freely settled particle concentration
- internal angle of friction of solid particle matrix
- dynamic coefficient of sliding friction of solid particles.

Pipeline tests were conducted on cyclone classified tailings materials from four gold mines (Blyvooruitsig, East Driefontein, Vaal Reefs and Western Deeps). The measured solid particle properties for each of these materials is presented in Table 2.7 (page 2.34). The Western Deeps materials forms a stabilised mixture at high solids concentrations, while the three other materials form settling slurries.

A data base of pipe loop test results for cyclone classified tailings has been established (Appendix A). The pipeline pressure gradients and particle size distribution for each test are presented in tabular and graphical form. The conclusions drawn from the pipe loop test results are :

(i) The mean mixture velocity versus pressure gradient curves become linear at high solids concentrations. This indicates that turbulence may be negligible due to dampening by the solid particle matrix. Thus at high solids concentration the pipe wall shear stress consists of viscous fluid shear stresses and mechanical sliding frictional stresses.

(ii) The pressure gradient increases sharply above a solids concentration of 45% by volume (corresponding closely to the freely settled particle concentration) for both horizontal and vertical flow.

(iii) The pressure gradient increases with decreasing pipe diameter. The rate of increase of pressure gradient with decrease in pipe diameter increases with increased solids concentration.

(iv) The transition solids concentration between observed heterogeneous flow and observed homogeneous flow (at all mean mixture velocities) increases with increasing pipe diameter. The ratio of the transition solids concentration to the freely settled particle concentration is similar for the three settling slurries (Blyvooruitsig, East Driefontein and Vaal Reefs).

(v) The pressure gradient versus solids concentration curves for all the backfill materials have a similar shape. The pressure gradient data points for the three settling slurries lie in a single line when plotted against the ratio of solids concentration to the freely settled concentration of the solid particles.

(vi) The ratio of the solids concentration to the freely settled concentration is identified as an important parameter~~, and may be interpreted as an indication of the mobility of a particle within the mixture.~~

(vii) The horizontal and vertical down friction pressure gradients are similar.

(viii) The vertical down friction pressure gradient is slightly greater than the vertical up friction loss.

CHAPTER 3

EXPERIMENTAL INVESTIGATION II

MEASUREMENT OF SOLID PARTICLE SLIDING FRICTION

1. INTRODUCTION

1.1 Shear stress at pipe wall due to solid phase

The total shear stress at the pipe wall in a pipeline transporting a solids liquid mixture consists of shear stresses due to both the liquid and solid phases. As the concentration of solid particles in the mixture increases and the number of solid particles in contact with the pipe wall increases, the contribution of the solid phase to the total pipe wall shear stress increases. There are two mechanisms by which solid particles impart shear stress to the pipe wall - mechanical sliding friction against the pipe wall, and random collisions with the pipe wall due to turbulence. In *high concentration* mixtures the sliding friction mechanism is dominant as the random movement of particles is restrained due to the presence of other solid particles.

For the dense phase mixtures considered in this investigation the solid particles are assumed to be in contact, thus no random motion of particles is possible and all the solid phase shear stress at the pipe wall is due to mechanical sliding friction.

1.2 The nature of solid particle - solid surface sliding friction

Before considering the nature of a granular matrix of solid particles sliding over a solid surface it is useful to first examine solid surfaces sliding relative to each other.

Solid surface - solid surface sliding friction

The simplest model for the frictional forces between two surfaces in contact states that there is a linear relationship between the total normal force N and the frictional resisting force F (see Figure 3.1).

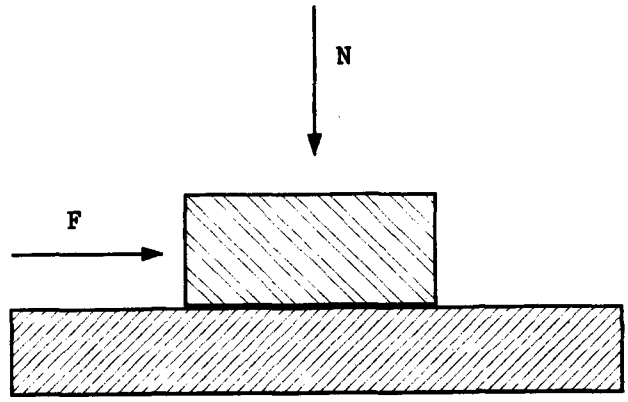

Figure 3.1 : Normal and frictional forces acting on a sliding block

The coefficient of friction between the two surfaces is defined as :

$$\mu = \frac{F}{N} \quad . \tag{3.1}$$

It is found that the force required to initiate movement is generally greater than the force required to maintain steady relative motion. Thus coefficients of incipient sliding friction μ_i , and of dynamic sliding friction μ_d are defined.

Bowden and Tabor (1950) presented a more detailed interpretation of the friction mechanism between two surfaces. They consider all surfaces to be rough on a micro-scale, and thus contact between the surfaces occurs at the tips of asperities over a contact area which is much smaller than the apparent area of contact. The normal stresses at points of contact reach the yield pressure Y of the asperities and they flow plastically until a true area of contact A is developed such that

$$A = \frac{N}{Y} \quad . \tag{3.2}$$

At the points of contact junctions are formed through cold welding. The strength of the junction is equal to that of the solid. During sliding the junctions are sheared. The shearing will occur in the softer material of shear strength S. In addition to the shearing of junctions, asperities of the harder material will plough into the softer material and produce an additional ploughing resistance P. Thus the total frictional resistance is

$$F = SA + P \quad . \tag{3.3}$$

Bowden and Tabor showed that for hard surfaces the ploughing term is usually much smaller than the shearing term and, for a fixed normal load, decreased as the number of contact points increased. Neglecting the ploughing term we get from Equations (3.2) and (3.3)

$$\mu = \frac{F}{N} = \frac{S}{Y} \tag{3.4}$$

Butterfield and Andrawes (1972) note that in practice contaminating films will prevent the formation of strong idealised junctions. Consequently, there is likely to be a combination of sliding and plastic yielding occurring at the asperity contacts. It is also probable that during sliding the surface films will tear producing torn fragments which will influence junction formation. They state that the friction mechanism between two surfaces will involve not only plastic deformation of asperities but also relative motion over asperities and debris. Thus this mechanism is analogous to interlocking phenomena associated with granular materials.

Solid particle matrix - solid surface sliding friction

Butterfield and Andrawes (1972) use the modified Bowden and Tabor model (plastic deformation of asperities and an interlocking phenomena) to explain the mechanism of friction between a solid particle matrix and a solid surface. The efficiency of the interlocking and ploughing contributions to the frictional resistance are strongly dependant on the compressibility of the two surfaces. The solid particle matrix will always be the most compressible of the two surfaces. As the

compressibility of the solid particle matrix will decrease with packing density, so the frictional resistance will be expected to increase. Butterfield and Andrawes extrapolate these concepts developed for micro-scale roughness to macro-scale roughness of the solid particle matrix. They state that the friction between a matrix of solid particles and a solid surface is governed by :

(i) **Microscopic roughness**
The frictional forces will increase with an increase in the microscopic roughness of the two solid materials.

(ii) **Angularity**
The greater the angularity of the particles, the greater the frictional forces will be.

(iii) **Irregularity**
The greater the irregularity (macroscopic roughness) of the solid surface in relation to the irregularity of the surface of the solid particle matrix, the greater the frictional forces. Thus a decrease in particle size will decrease the frictional forces for a given solid surface.

(iv) **Packing density**
As the packing density of the solid particle matrix is increased, so will the frictional forces as the compressibility of the solid particle matrix is reduced.

(v) **Hardness**
The harder the solid particles are, relative to the solid surface, the higher the frictional forces. For soft solid surfaces both the plastic deformation of asperities and the ploughing term become important.

1.3 Coefficient of dynamic sliding friction μ_d

For our purposes, i.e. the investigation of the hydraulic transport of solids in pipelines, we define the dynamic coefficient of sliding friction as

$$\mu_d = \frac{\text{Solid phase shear stress at pipe wall}}{\text{Normal interparticle stress at pipe wall}}$$

$$= \frac{\tau_{sw}}{\sigma_{sw}} \quad . \tag{3.5}$$

The evaluation of μ_d, and consequently the solid phase frictional forces, is an important parameter in the investigation and the understanding of the mechanism of high concentration hydraulic transport. Thus it is considered vital that a bench top test procedure be developed to investigate the nature of the frictional forces between a solid particle matrix and a moving boundary. The test should be able to determine the effect of the following variables on μ_d :

(i) particle size distribution
(ii) particle packing density
(iii) solid boundary roughness and material type
(iv) relative velocity between solid particles and boundary.

It is envisaged that such a bench top test for μ_d will, together with the particle size distribution, shape factor, freely settled packing density, solids relative density and internal angle of friction of solid particle matrix, provide a more complete characterisation of the solid particles.

2. SOLID PARTICLE SLIDING FRICTION MEASUREMENT TECHNIQUES

2.1 Tilting tube

Wilson (1970) pioneered the use of the tilting tube apparatus to evaluate the coefficient of friction between solid particles and the pipe wall.

The apparatus consists of a length of clear perspex pipe stoppered at both ends. The tube may be set to any angle to the horizontal as shown in Figure 3.2(a). The tube is filled with water and solid particles placed at one end of the tube on the pipe invert. The tube is slowly tilted and the angle of the tube to the horizontal ϕ at the point of incipient motion of the particles recorded. Wilson (1970) noted that the tube angle corresponding to the point of slip increased with increasing depth of the particle bed, and presented the hydrostatic assumption for interparticle stresses within a bed of particles. To obtain measurements at large bed depths and tube inclinations the solid particles were placed between bulkheads connected by wires. The coefficient of friction between the solid particles and pipe wall is evaluated from :

$$\mu = \frac{(\theta - \sin\theta \cos\theta)}{2\,(\sin\theta - \theta\cos\theta)} \tan\phi \quad , \tag{3.6}$$

where θ = half angle defining size of the bed

ϕ = tube inclination.

Wilson *et al* (1972) presented a modified test procedure for the tilting tube apparatus. A movable diaphragm of fine mesh screening is attached to a rod passing through a hole in the lower stopper as shown in Figure 3.2(b). The test starts with a diaphragm above the midway position and the solid particles behind the diaphragm. The diaphragm is slowly moved down the tube and the behaviour of the solid particles observed. The procedure is repeated for several tube inclinations. The tube inclination corresponding to a sliding bed of constant height moving *en bloc* with the diaphragm is taken as the slip point angle. The coefficient of friction is calculated from Equation (3.6).

The advantage of the tilting tube apparatus is that it is relatively simple to construct and operate. The results are, however, subjective and care must be taken to distinguish between the incipient coefficient of friction and the dynamic coefficient of friction. The apparatus does not permit measurement of steady state frictional forces unless a very long tube is used.

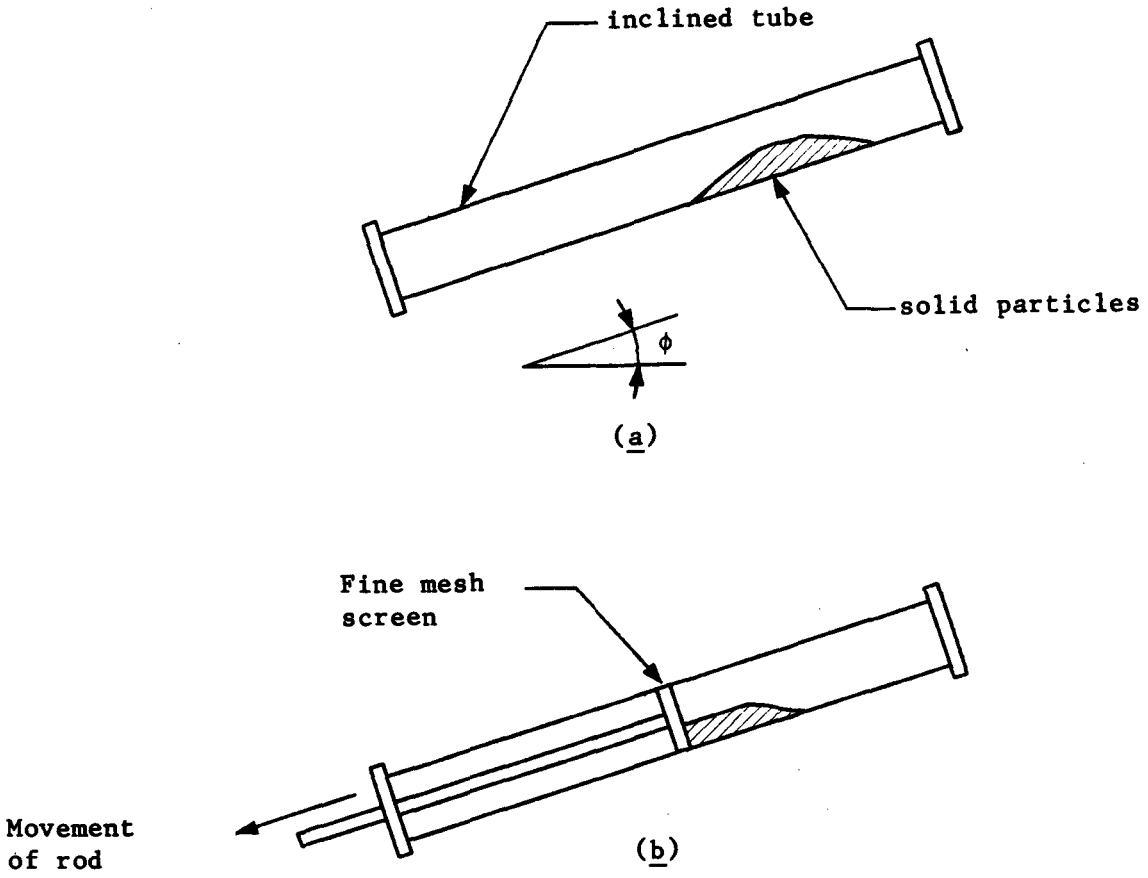

Figure 3.2 : Wilson's tilting tube apparatus

2.2 Shear box

Conventional shear boxes have been used by Butterfield and Andrawes (1972) and Streat *et al* (1976) to measure frictional forces between a solid particle matrix and a solid boundary. The arrangement of a typical shear box apparatus is shown in Figure 3.3. The upper block containing the granular matrix is forced to slide over the block of solid material by applying force F. The coefficient of friction is evaluated from Equation (3.1) using measured values of F and N.

Figure 3.4 shows the results of Streat *et al* (1976) from shear box tests done on the dynamic sliding of a submerged sand matrix over a PVC block. Although there is considerable scatter, the results show a definite increase in μ_d with increased solids packing density. The scatter may be due to difficulty in measuring and maintaining a constant solids packing density during a test.

Butterfield and Andrawes (1972) conducted a series of experiments on the friction between sand and plane surfaces. They found the coefficient of incipient sliding friction and the dynamic coefficient of sliding friction to increase with increased packing density, as shown in Figure 3.5.

Butterfield and Andrawes postulated that the friction mechanism between solid particles sliding over a plane surface is similar to the friction mechanism between granular particles. They considered the ratio of the frictional force for loose sand to that for dense sand, i.e.

$$\frac{\mu \text{ (loose)}}{\mu \text{ (dense)}} = \frac{\text{frictional resistance of loose sand}}{\text{frictional resistance of dense sand}} \quad . \qquad (3.7)$$

Figure 3.6 shows the above ratio plotted for all their tests done with sand sliding against various plane surface materials. It is seen that the data points lie closely on a straight line for all material types. The internal angle of friction δ for the sand tested is 46° and 36° for the dense and loose states respectively. The straight line drawn in Figure 3.6 has a slope of tan (δ loose) / tan (δ dense) calculated using the measured δ values. This implies that the slope of the line

depends only on the properties of the sand and is independent of the solid surface material, and provides strong support for their hypothesis and we may write :

$$\frac{\mu \text{ (loose)}}{\mu \text{ (dense)}} \simeq \frac{\tan (\delta \text{ loose})}{\tan (\delta \text{ dense})} \quad . \tag{3.8}$$

The advantage of the shear box apparatus is that it is generally readily available as it is a standard soil mechanics apparatus. Care must be taken to ensure that the meassuring system is rigid to avoid the stick-slip phenomena during tests (Butterfield and Andrawes (1972)). The disadvantages of the shear box apparatus are :

(i) end effects at the edges of the box

(ii) tests are of a short duration, so it is not possible to measure long term steady state frictional forces.

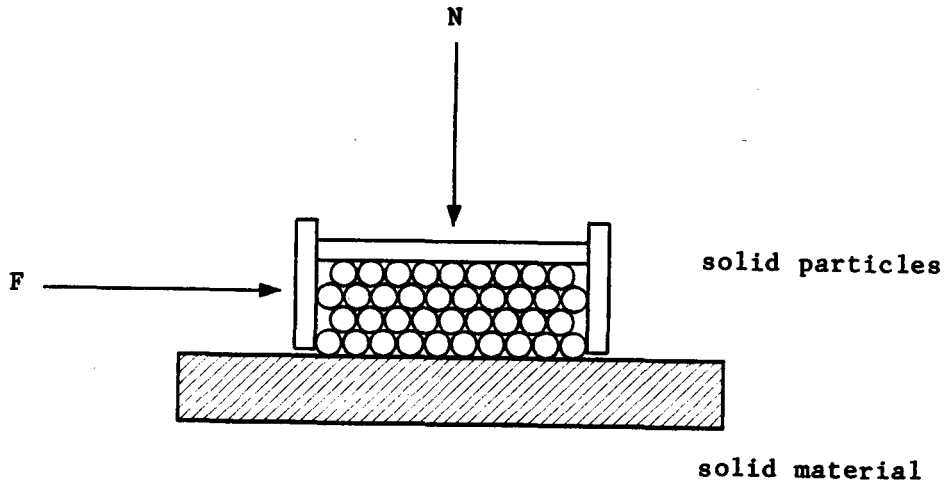

Figure 3.3 : Typical shear box apparatus

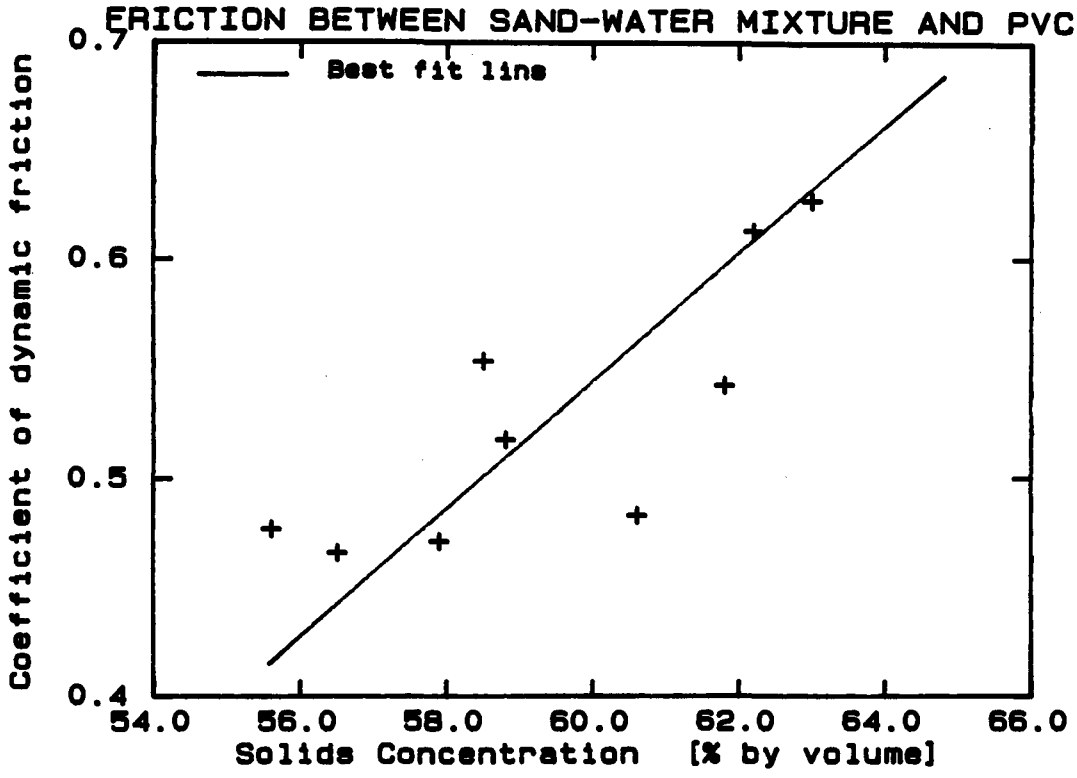

Figure 3.4 : Shear box test results - submerged particles
Streat et al (1976)

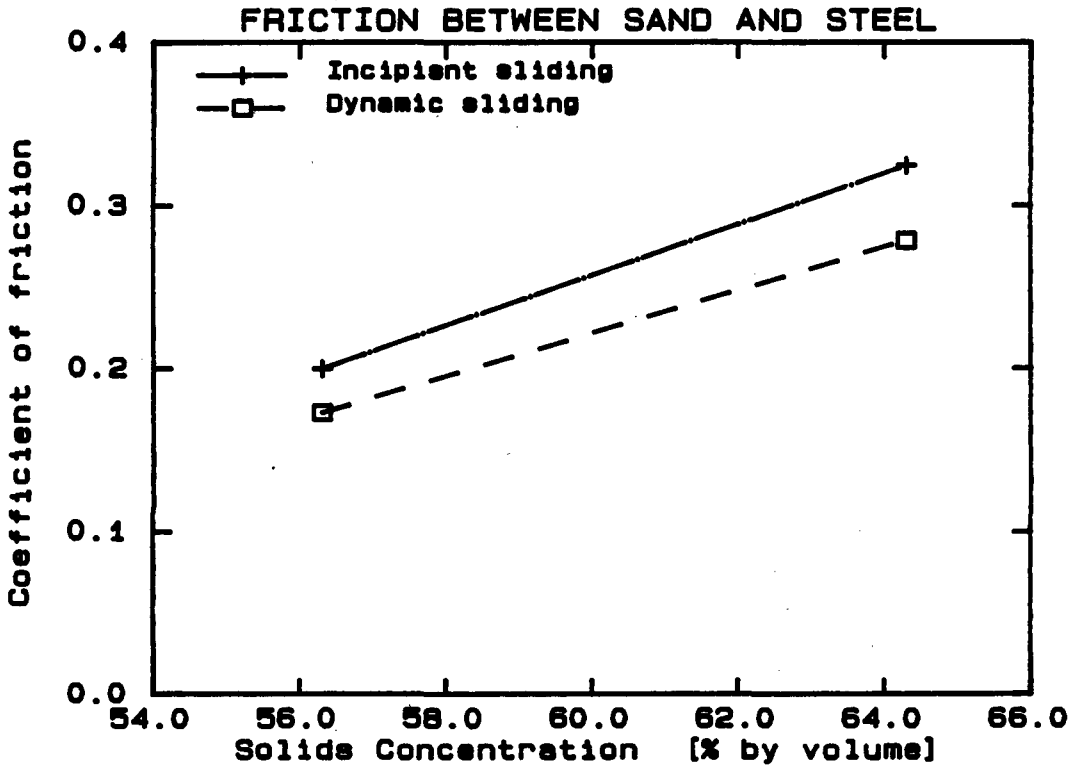

Figure 3.5 : Dry particle shear box tests
Butterfield and Andrawes (1972)

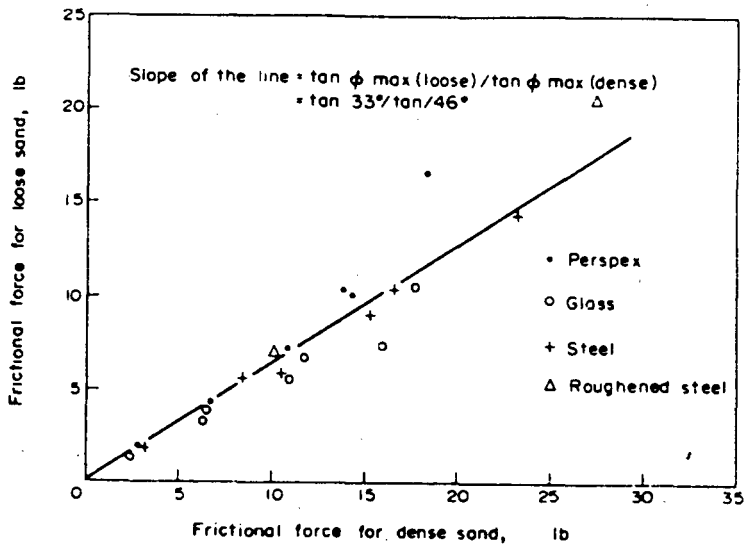

Figure 3.6 : Butterfield and Andrawes (1972)

2.3 Rotating cylinder

Briscoe *et al* (1983) used a rotating cylinder partially filled with sand to investigate the friction mechanism between solid particles and a solid boundary. They used two configurations to measure the incipient coefficient of sliding friction and the dynamic coefficient of sliding friction.

Figure 3.7 shows the apparatus used to determine the incipient coefficient of sliding friction. A quantity of sand to obtain the required bed height is placed in the glass cylinder, and the cylinder filled with water. The cylinder is placed on a plane, the inclination of which is gradually increased until the cylinder is on the point of incipient motion. At this point the slope of the plane ϕ is recorded. Corrections are made for the true slope and rolling resistance. The coefficient of incipient sliding friction is calculated using Wilson's hydrostatic pressure assumption and geometry.

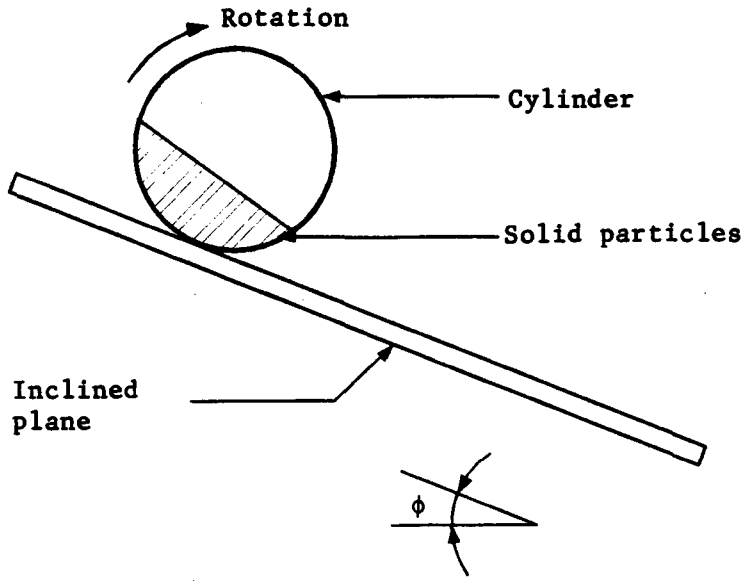

Figure 3.7 : Incipient friction rolling cylinder apparatus
After Briscoe et al (1983)

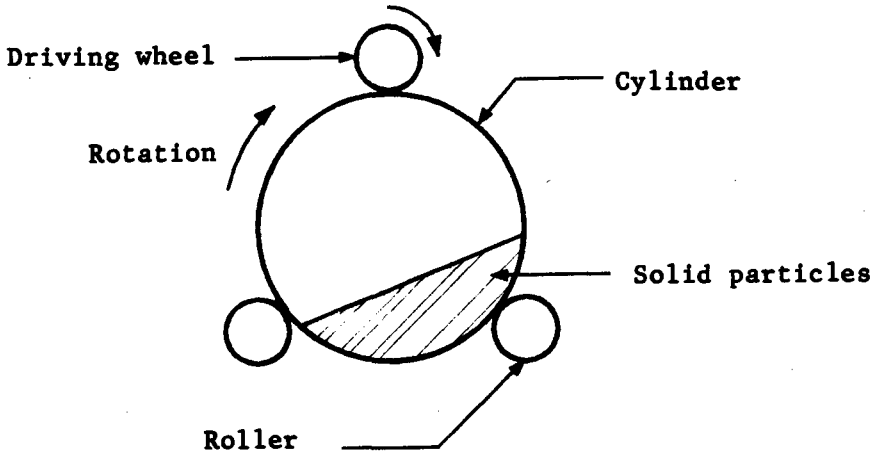

Figure 3.8 : Dynamic friction rolling cylinder apparatus
After Briscoe et al (1983)

The coefficient of dynamic friction was determined by measuring the torque required to continuously rotate a cylinder filled with a sand water mixture. The layout of the apparatus is shown in Figure 3.8. The glass cylinder rests on four rollers and is rotated at different rotational speeds by a variable speed electric motor. The torque delivered by the motor is transmitted to the cylinder via a rubber wheel, and measured using a strain gauge system onto which the motor is mounted.

The strain gauge system is calibrated *in situ* and a correction factor accounted for by rotating empty cylinders. The coefficient of dynamic friction is calculated from the measured torque and the average normal intergranular stress evaluated using the hydrostatic stress distribution.

Sliding and cascading particle behaviour was observed during the dynamic tests. The particle contact density (number of particles per unit surface area of contact) was estimated for the tests by counting the sand particles in contact with the pipe wall from photographs.

Briscoe *et al* report that the dynamic coefficient of friction reduces with mean flow velocity. However they also found that, for their experiments, the contact density decreased with flow velocity. Thus there is no clear indication that for pure sliding friction the coefficient of dynamic friction will reduce with increased velocity.

A disadvantage of the rotating cylinder concept is the difficulty in evaluating one of the two primary parameters - i.e. the mean normal intergranular particle stress against the pipe wall. In the static case the hydrostatic assumption is likely to be closely approximated, but there are great uncertainties during the dynamic test. In addition, the frictional resistance measured during the dynamic test may contain a component due to fluid shear between the particle matrix and pipe wall which complicates interpretation of the results.

2.4 Rotary shear meter

Jacobs and Tatsis (1986) developed a rotary shear meter to investigate the frictional forces between a sliding bed of particles and the pipe wall for high concentration slurries. The device (Figure 3.9) consists of a rotating disc driven by a variable speed motor. The coarse particles are contained in a stationary annular channel which is set at a small clearance above the disc. The coarse particles are restrained from rotating with the disc by flat vertical plates within the channel. An annular loading ring is placed on top of the coarse particles in the channel to enable higher bed heights to be simulated. The rotating disc and channel are immersed in a mixture of water and the fine fraction.

The frictional force is determined by measuring the torque required to prevent the annular channel from rotating with the disc. The rotational speed of the disc is measured using an optical sensor. The vertical load on the channel is measured using strain gauges to correct for any friction between the coarse particles and the vertical sides of the channel.

Results on the variation of the total friction force with rotational speed are presented in Figure 3.10 for a coal slurry (Tatsis and Jacobs (1987)).

The advantages of the shear meter are :

(i) There is no difficulty in interpreting and measuring both the normal and frictional forces.

(ii) The test procedure is objective as no interpretation is required from the operator.

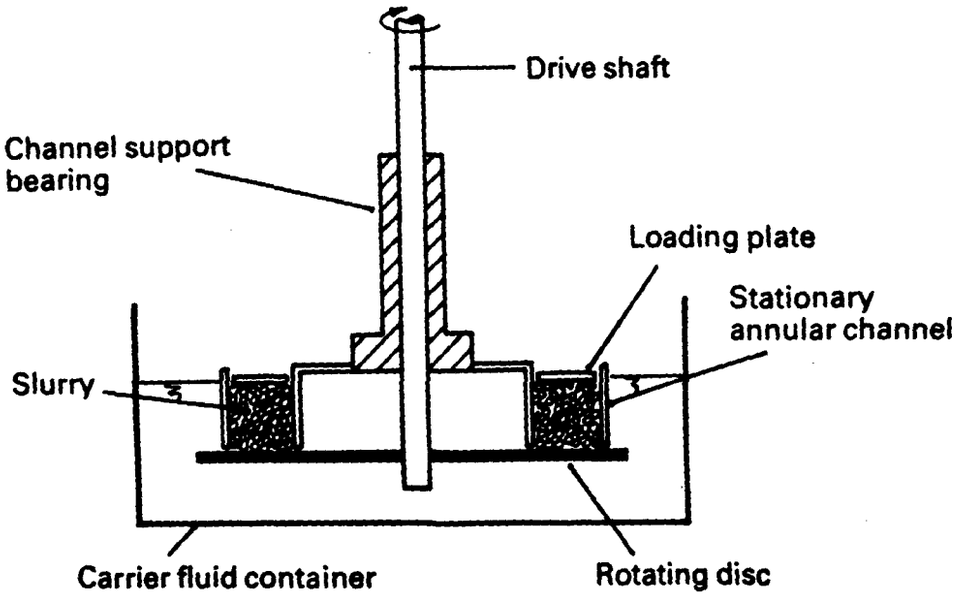

Figure 3.9 : Rotary shear meter - Jacobs and Tatsis (1986)

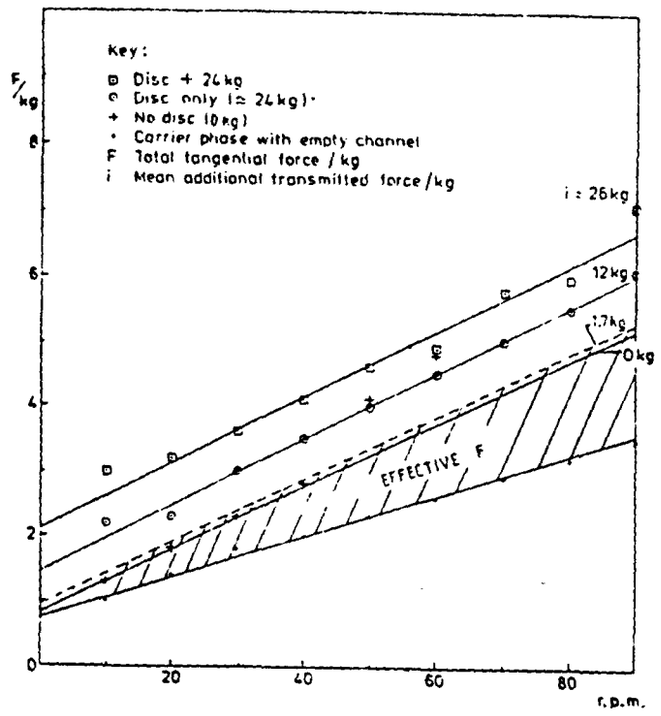

Figure 3.10 : Rotary shear meter results - Tatsis and Jacobs (1987)

3. SOLID PARTICLE SLIDING FRICTION APPARATUS DEVELOPED FOR PRESENT INVESTIGATION

3.1 Measurement concept

In measuring the frictional forces between solid particles and a solid boundary, Briscoe *et al* (1983) attempted to simulate actual pipeline conditions with their rotating cylinder apparatus. However, by simulating actual pipeline conditions further variables are introduced (normal interparticle stress at pipe wall and extent of fluid shear stress in dynamic test) which complicate the interpretation of their results.

The principle adopted in this investigation is to measure frictional forces due to pure mechanical sliding friction. Once the nature of dynamic sliding friction has been established it will be used as input for a mechanistically based model for dense phase flow.

The design of the apparatus selected to determine the coefficient of dynamic sliding friction between a particle matrix and a solid boundary is based on the rotary shear meter (Jacobs and Tatsis (1986)). This design was chosen for the following reasons :

(i) Both the frictional resistance and the normal interparticle stress are easy to measure, thus allowing μ_d to be calculated without making assumptions regarding the stress distribution within the granular matrix.

(ii) The normal interparticle stress may easily be varied using a loading ring.

(iii) There is no time restraint on the test, thus permitting steady state frictional forces to be measured.

(iv) There are minimal end effects compared with the shear box apparatus.

3.2 Description of apparatus

Figure 3.11 shows the layout of the solid particle sliding friction measurement apparatus. The apparatus has the following components :

(i) Rotating disc

The rotating disc is made from 20 mm thick stainless steel and has a diameter of 380 mm. The disc is rotated using a variable speed electric motor. The 40 mm shaft is driven by a belt and pulleys to isolate the apparatus from any vibration from the motor. The speed of the disc at the centre of the channel containing the solid particles may be varied between 1 m/s and 3 m/s.

Various materials may be installed on the disc, enabling the effect of different material types and roughnesses on μ_d to be evaluated. Only stainless steel was used in the present investigation. The surface roughness of the stainless steel was measured using a Taylor-Hobson Surtronic 3P Profilometer. The tangential centre line average roughness was measured as 0,26 µm, and the radial centre line average roughness as 0,38 µm. The differences are due to the lathe machining process.

(ii) Annular channel

Figure 3.12 details the dimensions of the annular channel in which the particles being tested are held. All components of the channel, except the rubber seal, are machined from PVC. The channel is 40 mm wide and 50 mm deep. The mean radius of the channel is 154 mm.

The channel is held in place by a support mechanism as shown in Figure 3.11. The channel is free to rotate about the support shaft on bearings. The channel support mechanism allows the position and height of the channel to be adjusted in relation to the disc. The channel may be raised above the disc using the cable as shown in Figure 3.13 to facilitate removing sample from the apparatus.

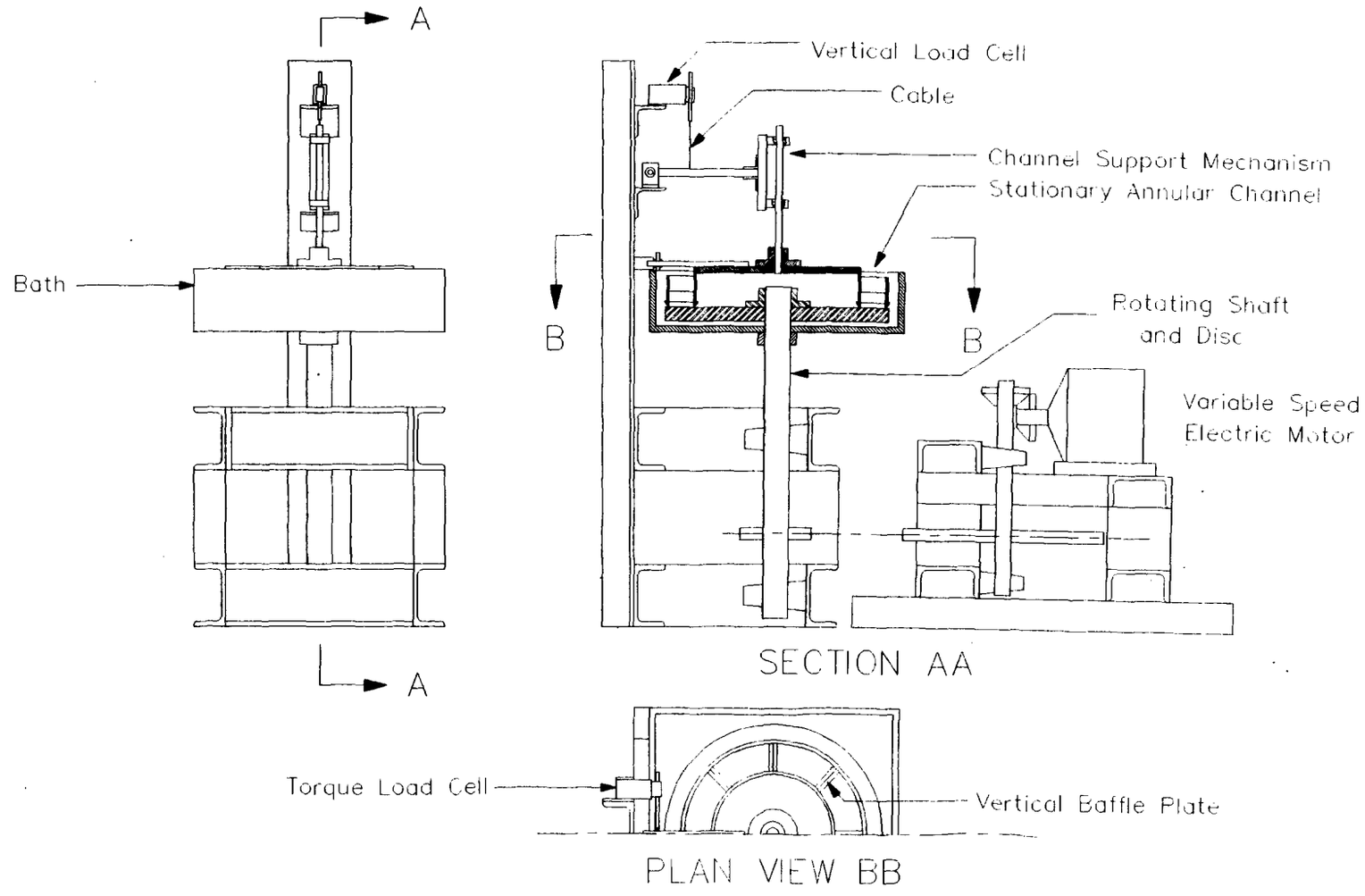

Figure 3.11 : Solid particle sliding friction apparatus

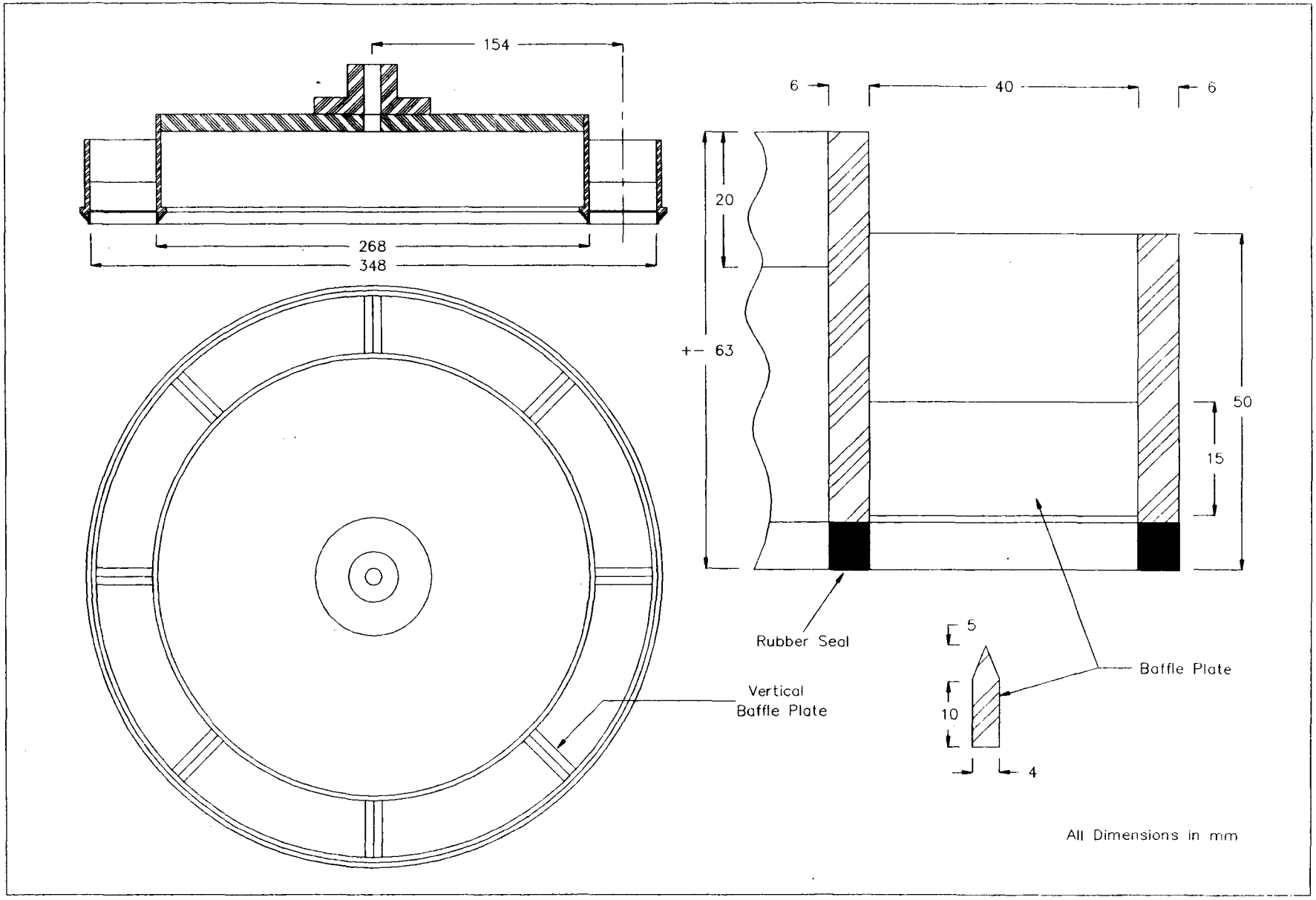

Figure 3.12 : Detail of annular channel

The weight of the channel and the channel support mechanism is measured using the vertical load cell as shown in Figure 3.11. This allows the operator to monitor whether any of the applied normal loading on the sample is being transmitted to the side wall or baffle plates of the channel through friction. If this is the case a correction to the normal loading is made.

(iii) Torque load cell

The annular channel is restrained from moving with the rotating disc by the torque load cell. The load cell thus measured the frictional resistance between the stationary channel filled with solid particles and the rotating disc.

(iv) Loading ring

The normal load on the sample of particles is varied using a loading ring. The ring consists of a PVC frame covered with a fine mesh (apperture size 42 μm). The loading ring is placed on the sample and the load varied using brass weights which are uniformly distributed around the channel as shown in Figure 3.14.

(v) Bath

The rotating disc and annular channel are immersed in water to determine the coefficient of friction for submerged solid particles. The water is contained within a PVC bath as shown in Figure 3.11. The bath is sealed against the rotating shaft using a lip seal. The bath may be lowered and raised to facilitate loading and removing the sample.

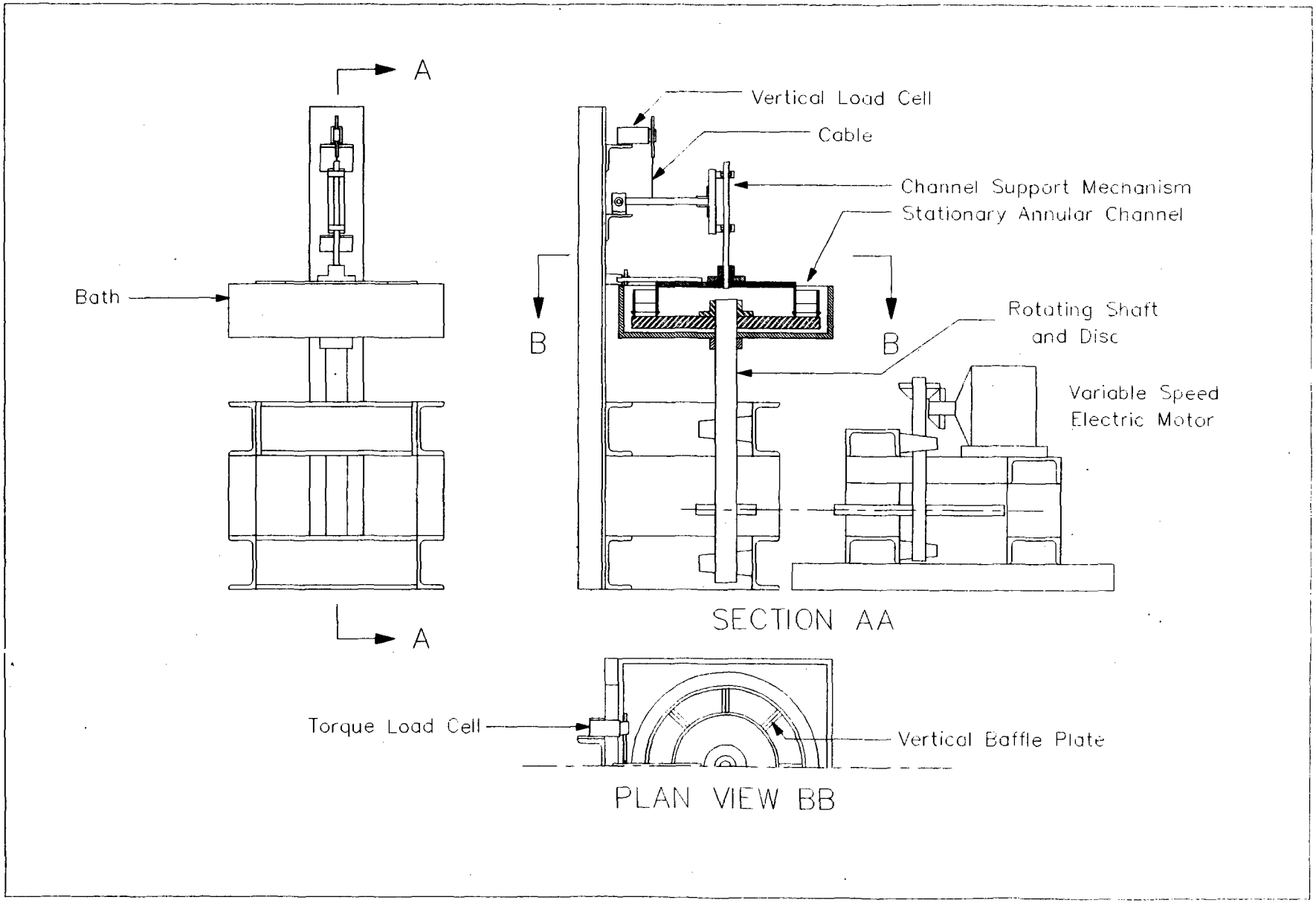

Figure 3.11 : Solid particle sliding friction apparatus

The weight of the channel and the channel support mechanism is measured using the vertical load cell as shown in Figure 3.11. This allows the operator to monitor whether any of the applied normal loading on the sample is being transmitted to the side wall or baffle plates of the channel through friction. If this is the case a correction to the normal loading is made.

(iii) Torque load cell

The annular channel is restrained from moving with the rotating disc by the torque load cell. The load cell thus measured the frictional resistance between the stationary channel filled with solid particles and the rotating disc.

(iv) Loading ring

The normal load on the sample of particles is varied using a loading ring. The ring consists of a PVC frame covered with a fine mesh (apperture size 42 μm). The loading ring is placed on the sample and the load varied using brass weights which are uniformly distributed around the channel as shown in Figure 3.14.

(v) Bath

The rotating disc and annular channel are immersed in water to determine the coefficient of friction for submerged solid particles. The water is contained within a PVC bath as shown in Figure 3.11. The bath is sealed against the rotating shaft using a lip seal. The bath may be lowered and raised to facilitate loading and removing the sample.

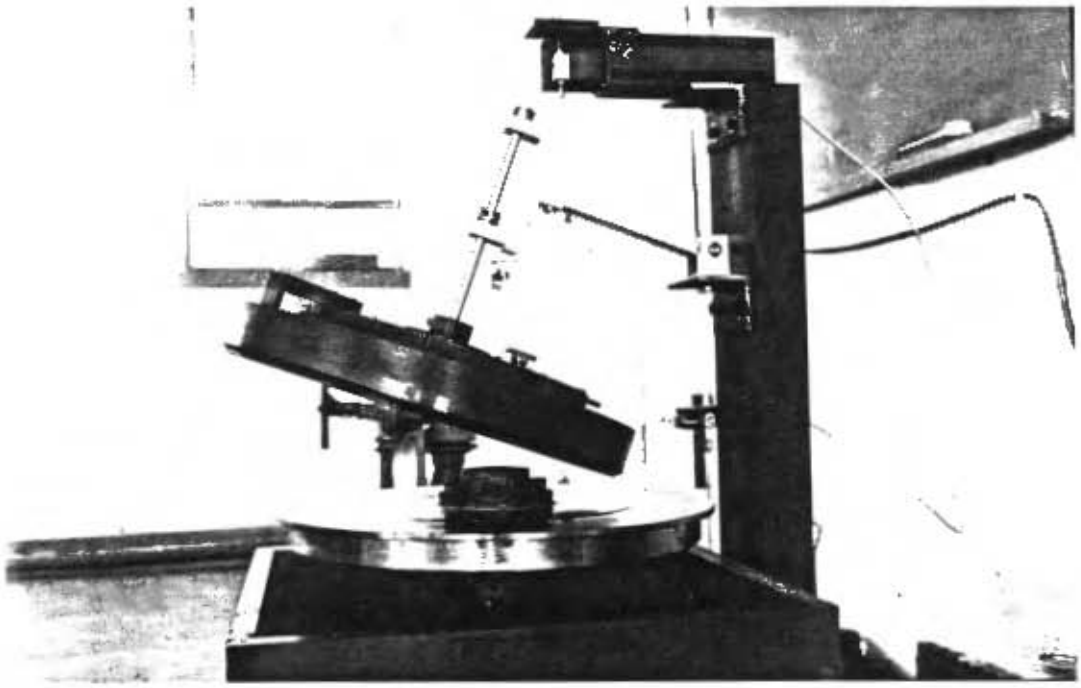

Figure 3.13 : Annular channel in revised position

Figure 3.14 : Brass weights on loading ring

3.3 Measured variables

3.3.1 *Frictional resistance*

The total frictional resistance F of the annular channel filled with solid particles is calculated as

$$F = \frac{F_L\, r}{R} \quad , \tag{3.9}$$

where F_L = force measured using torque load cell
r = mean channel radius = 154 mm
R = distance from centre of disc to load cell = 192 mm.

The load cell's strain gauge bridge has a linear relationship between applied load and the ratio of voltage output to input voltage, i.e.

$$F_L = m_{load}\, \frac{V_{out}}{V_{in}} + c_{load} \quad , \tag{3.10}$$

where V_{out} = strain gauge bridge output voltage
V_{in} = strain gauge bridge supply voltage
m_{load} = slope of calibration line
c_{load} = calibration line constant.

The load cell is calibrated by applying various loads and recording the input and output voltages. The load cell used has a calibration range of 0 to 5 kg. The calibration curve is obtained from a least squares linear regression analysis, and checked using the correlation coefficient R (Equation 2.8).

3.3.2 *Total normal load*

The total normal load N acting on the sample is evaluated as the sum of the applied loading, weight of the loading ring and the submerged weight of the solid particles less any correction required, i.e.

$$N = (M_{weights} + M_{ring} + M_s \left(\frac{S_s - S_\ell}{S_s}\right) - M_{corr})\, g \quad , \qquad (3.11)$$

where M_{weight} = mass of weights placed on loading ring
M_{ring} = mass of loading ring
M_s = dry mass of solid particles
S_s = relative density of solid particles
S_ℓ = relative density of liquid
M_{corr} = possible correction from vertical load cell.

The correction term is evaluated as the difference between the mass measured on the vertical load cell during the test and the mass of the channel support mechanism. The load cell has the same characteristics and calibration procedure as the torque load cell discussed in Section 3.3.1.

3.3.3 *Rotational speed of disc*

The rotational speed of the disc is measured using a digital tachometer. A length of reflective tape is fixed to the shaft of the rotating disc. Each time the reflective tape passes the tachometer it reflects the light beam. The tachometer determines the rotational speed of the shaft from the frequency of the reflected light beams.

Two lengths of reflective tape are placed on opposite sides of the shaft to ensure that the tachometer is used in its optimal accuracy range. The indicated rotational speed on the tachometer obtained this way is twice the actual rotational speed of the shaft.

3.3.4 *Solid particle concentration*

The concentration of solid particles in the channel is calculated as follows :

$$C = \frac{\forall_s}{\forall_{channel}} , \qquad (3.12)$$

where $\forall_s$ = volume of solid particles = $\frac{M_s}{\rho_s}$

$\forall_{channel}$ = volume of channel occupied by solid particles

= $\pi (r_o^2 - r_i^2) d$

r_o = outer radius of channel

r_i = inner radius of channel

d = depth of channel occupied by solid particles.

3.3.5 *Temperature*

The temperature of the liquid in the bath is measured using a mercury thermometer.

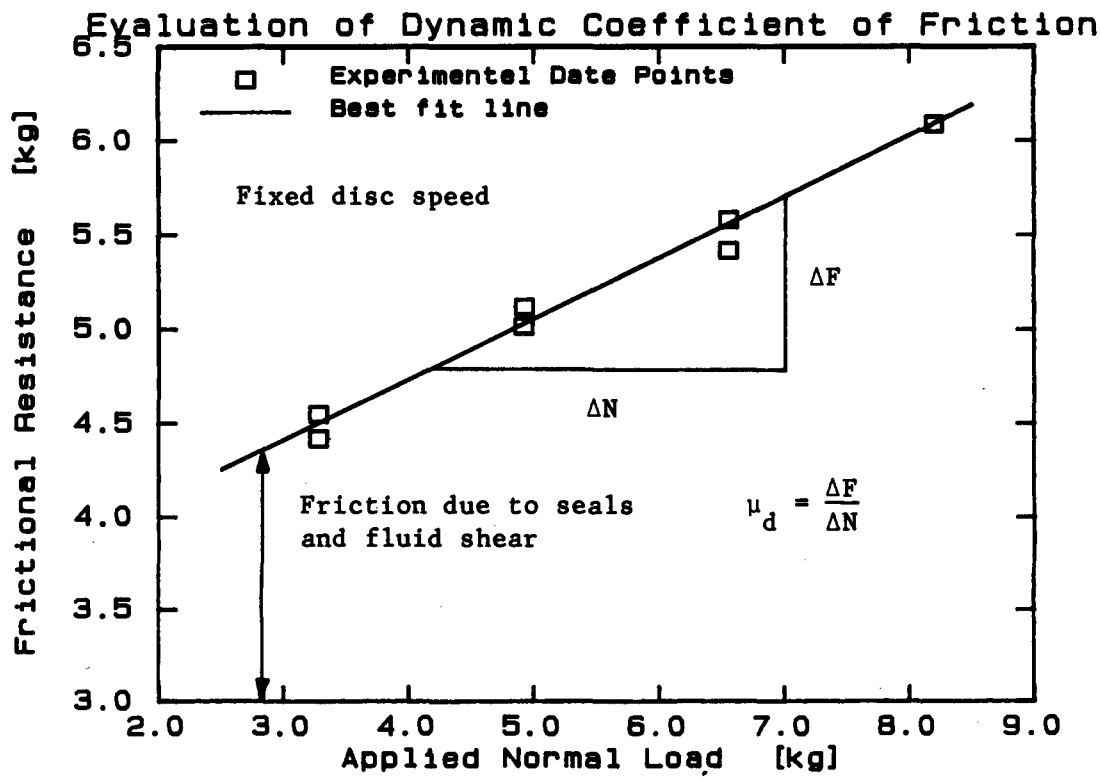

Figure 3.15

3.4 Derived variables

3.4.1 *Dynamic coefficient of sliding friction*

Figure 3.15 shows how the dynamic coefficient of friction is calculated from test data. The frictional resistance is recorded for various normal loadings and plotted as shown in Figure 3.15. The rotational speed of the disc is kept constant during a test, thus the frictional resistance due to fluid shear remains constant. The coefficient of friction is calculated as the slope of the least squares best fit line, i.e.

$$\mu_d = \frac{\Delta \text{ Frictional Resistance}}{\Delta \text{ Normal Loading}} \quad . \tag{3.13}$$

3.4.2 *Relative speed between particles and disc*

The relative speed between the channel and disc is calculated as follows :

$$V = r\,\omega \quad , \tag{3.14}$$

where r = mean channel radius

ω = angular velocity of disc = $\frac{\pi}{30}\,n$

n = shaft rotational speed (rpm).

3.5 Operating procedure

The test apparatus is designed to operate with a small clearance, small enough to prevent particles escaping from the annular channel, between the rubber seals of the annular channel and the rotating disc. Thus if any of the normal loading applied to the solid particles is transferred to the channel walls through friction, this will be detected from the output of the vertical load cell and a correction may be made to the normal loading acting on the solid particles.

This procedure worked when testing sand particles (d_{50} = 2 mm). However, when testing classified tailings it was not possible to set the clearance between the seals and disc small enough to prevent solid particles from escaping from the channel. This problem is resolved by ensuring that the seals are in positive contact with the rotating disc.

The consequence of this operating modification is that it is no longer possible to correct the normal loading for any friction between the wall of the channel and the solid particles. However, in practice it was found that providing sufficient time was allowed for between loading the particles and reading the torque transducer output, the variation of the frictional resistance with normal loading was linear for a fixed disc speed. It was concluded that the effect of wall friction was small.

The dynamic coefficient of sliding friction is thus obtained as the slope of the frictional force versus normal loading curve as shown in Figure 3.15.

A further difficulty experienced during the test work was the method of varying the solids concentration, and ensuring that the concentration remained constant for a particular test. As it was not possible to do this, all tests were conducted at the maximum concentration attainable in the channel. The variation of μ_d with concentration was estimated using relation (3.8) from Butterfield and Andrawes' (1972) work :

$$\frac{\mu_d \text{ (loose)}}{\mu_d \text{ (dense)}} \simeq \frac{\tan (\delta \text{ loose})}{\tan (\delta \text{ dense})} ,$$

where δ = internal angle of friction which is evaluated as discussed in Section 3.6 of Chapter 2.

The experimental test procedure is presented in Figure 3.16. The output of the torque transducer was monitored to determine the effect of the frictional forces between the solid particles and the vertical sides of the annular channel on the normal load acting on the solid particles. After the applied normal loading has been changed the torque transducer output varies with time, and stabilises to a constant value after about 60 seconds. Thus the three minute measurement cycle shown in Figure 3.16 was adopted to minimise the effect of the side wall friction forces. The main test activities are as follows :

(i) Calibration

The torque load cell is calibrated before and verified after each series of tests.

(ii) Test preparation

The rubber seals of the channel are lightly coated with petroleum jelly to minimise the friction between the seals and the rotating disc. The stainless steel disc is cleaned with acetone to remove any contaminants.

(iii) Sample concentration

The volume of solids placed in the channel is determined from the solids relative density and the dry mass of the solids. The solid particles in the channel are vibrated by tapping the disc with a rubber mallet. The volume occupied by the sample is calculated from the depth of the sample and the channel geometry. Hence the solids concentration is calculated as the ratio of the volume of solid particles to the volume occupied by the solid particles.

(iv) Disc speed

The disc speed is set using the variable speed electric motor and measured using a digital tachometer. The disc speed is measured for each normal loading of the test series. It is vital that the disc speed is kept constant for the test series to ensure that the seal friction and fluid shear stress remains constant.

(v) Normal loading

The normal load on the solid particles is varied by changing the number of sets of brass weights on the loading ring. Each set of brass weights comprises 12 weights which are distributed uniformly around the loading ring.

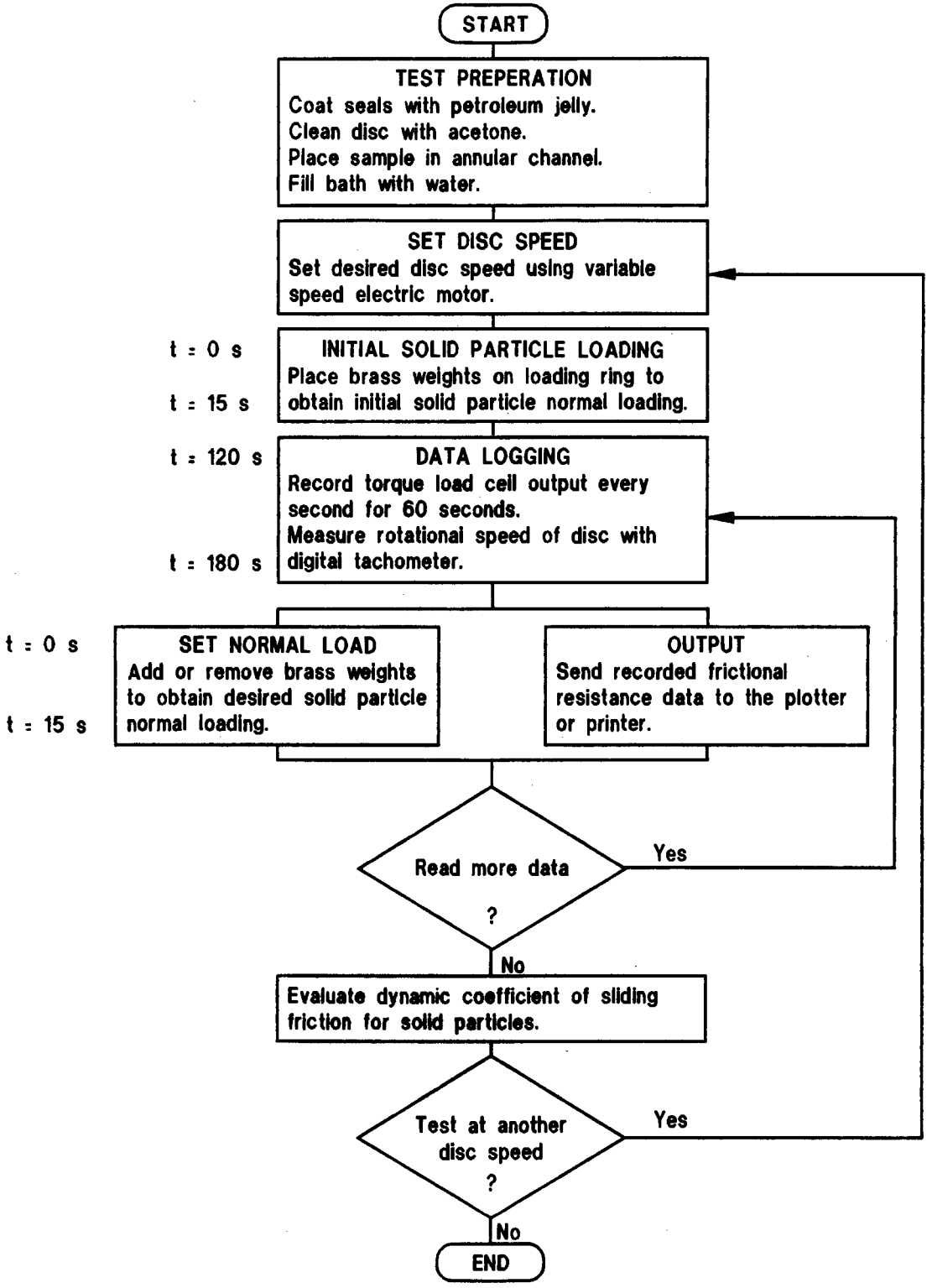
START
TEST PREPERATION
Coat seals with petroleum jelly.
Clean disc with acetone.
Place sample in annular channel.
Fill bath with water.
SET DISC SPEED
Set desired disc speed using variable speed electric motor.
t = 0 s
t = 15 s
INITIAL SOLID PARTICLE LOADING
Place brass weights on loading ring to obtain initial solid particle normal loading.
t = 120 s
t = 180 s
DATA LOGGING
Record torque load cell output every second for 60 seconds.
Measure rotational speed of disc with digital tachometer.
t = 0 s
t = 15 s
SET NORMAL LOAD
Add or remove brass weights to obtain desired solid particle normal loading.
OUTPUT
Send recorded frictional resistance data to the plotter or printer.
Read more data ?
Yes
No
Evaluate dynamic coefficient of sliding friction for solid particles.
Test at another disc speed ?
Yes
No
END

Figure 3.16

(vi) Data logging

The data logging configuration used for recording the test data is shown in Figure 3.17. The data logger converts the load cell output voltages and supply voltages to digital signals which are read by the computer. These readings are converted to engineering units using the calibration constants. Output from the computer may be to the monitor, printer or plotter.

The data logging program takes one set of readings every second for 60 seconds. Figure 3.18 shows the results of a typical test series where the frictional resistance measured using the torque load cell is plotted against time. The frictional resistance for each data point (normal loading and frictional resistance) is calculated as the average of all the readings taken over the 60 second time period.

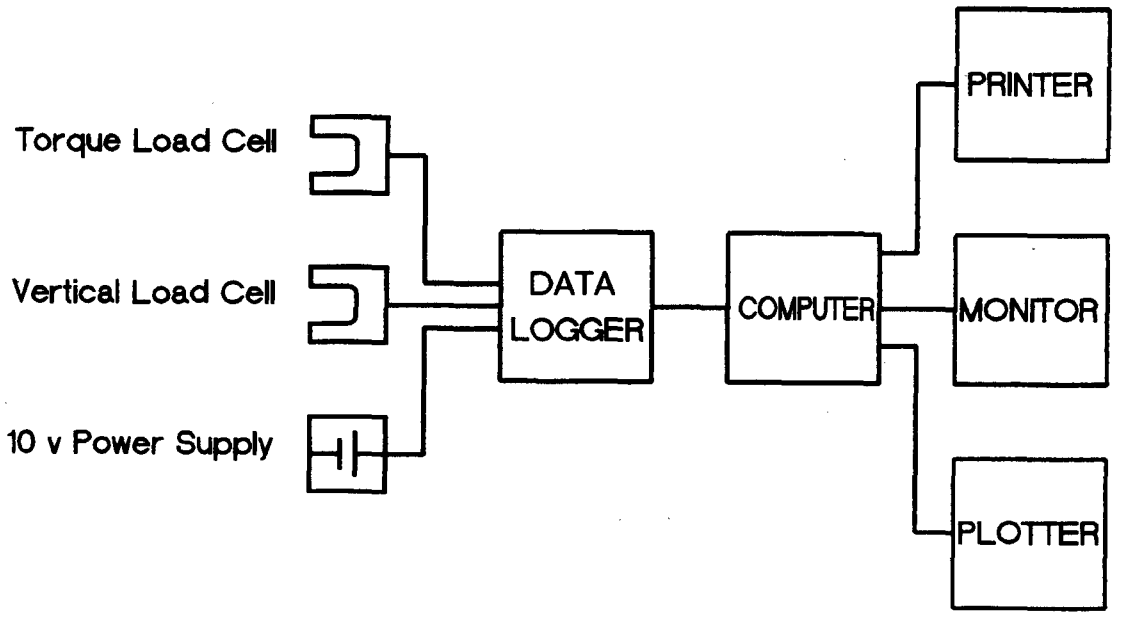

Figure 3.17 : Data logging configuration

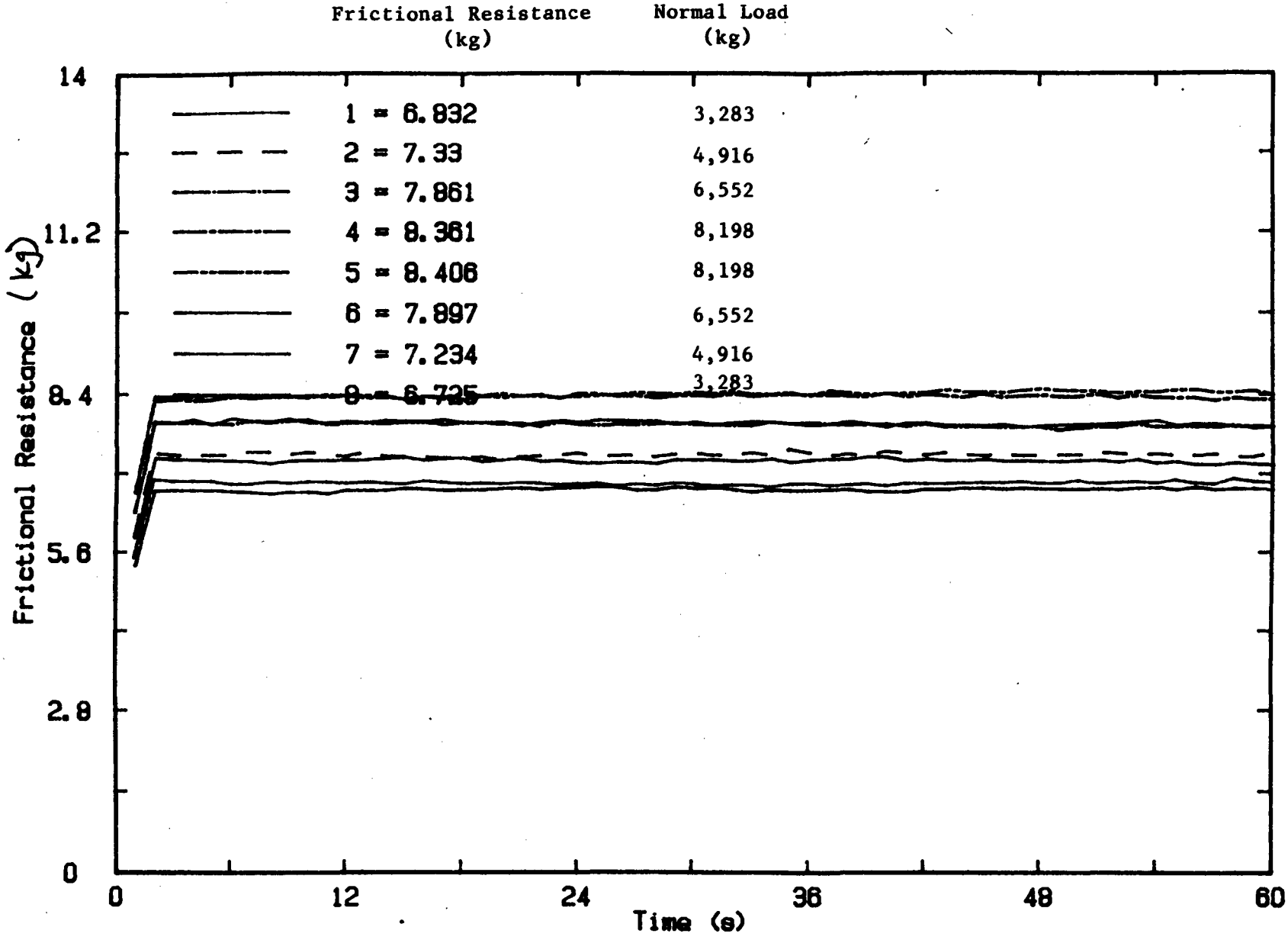

Figure 3.18 : Typical torque load cell output

3.6 Experimental errors

The experimental errors are evaluated using Brinkworth's (1963) relation (2.18) for the highest expected error as discussed in Section 2.5 of Chapter 2 :

$$\left(\frac{\delta x}{x}\right)^2_{exp} = \sum \left(\frac{\delta x}{\partial n}\right)^2 \left(\frac{n}{x}\right)^2 \left(\frac{\delta n}{n}\right)^2 ,$$

where x = value of quality
δx = error in x
n = measured variable value
δn = error in n.

3.6.1 *Frictional resistance*

The frictional resistance between the annular channel and the rotating disc is evaluated from Equation (3.9) :

$$F = \frac{F_L\, r}{\ell} ,$$

where F_L = force measured using torque load cell
r = mean channel radius
R = distance from centre of disc to load cell.

The force F_L measured using the torque load cell will contain a calibration error and a transducer error. The calibration error in the mass of the calibration weights is $\pm$ 0,1 g. The transducer error is 0,1% of the transducer range (5 kg), i.e. $\pm$ 5 g. Thus the total error in measuring F_L is $\pm$ 5,1 g. From Equation (2.18) the highest expected error in F is :

$$\left[\frac{\partial F}{F}\right]^2_{exp} = \left[\frac{\partial F}{\partial F_L}\right]^2 \left[\frac{F_L}{F}\right]^2 \left[\frac{\delta F_L}{F_L}\right]^2 + \left[\frac{\partial F}{\partial r}\right]^2 \left[\frac{r}{F}\right]^2 \left[\frac{\delta r}{r}\right]^2 + \left[\frac{\partial F}{\partial R}\right]^2 \left[\frac{R}{F}\right]^2 \left[\frac{\partial R}{R}\right]^2 , \quad (3.15)$$

where $\frac{\partial F}{\partial F_L} = \frac{r}{R}$

$$\frac{\partial F}{\partial r} = \frac{F_L}{R}$$

$$\frac{\partial F}{\partial R} = -\frac{F_L r}{R^2} .$$

Table 3.1 shows the measurement accuracies, transducer accuracies and the highest expected error in the measurement of the frictional resistance force F = 2,5 kg. Figure 3.19 shows the variation of the highest expected error with frictional resistance.

TABLE 3.1 : Expected highest error - frictional resistance

Variables	Measurements
F (kg)	2,500
F_L (kg)	2,005 ± 0,0051
r (mm)	154 ± 0,1
R (mm)	192 ± 0,1
δF (kg)	0,0043
% Error in F	0,17

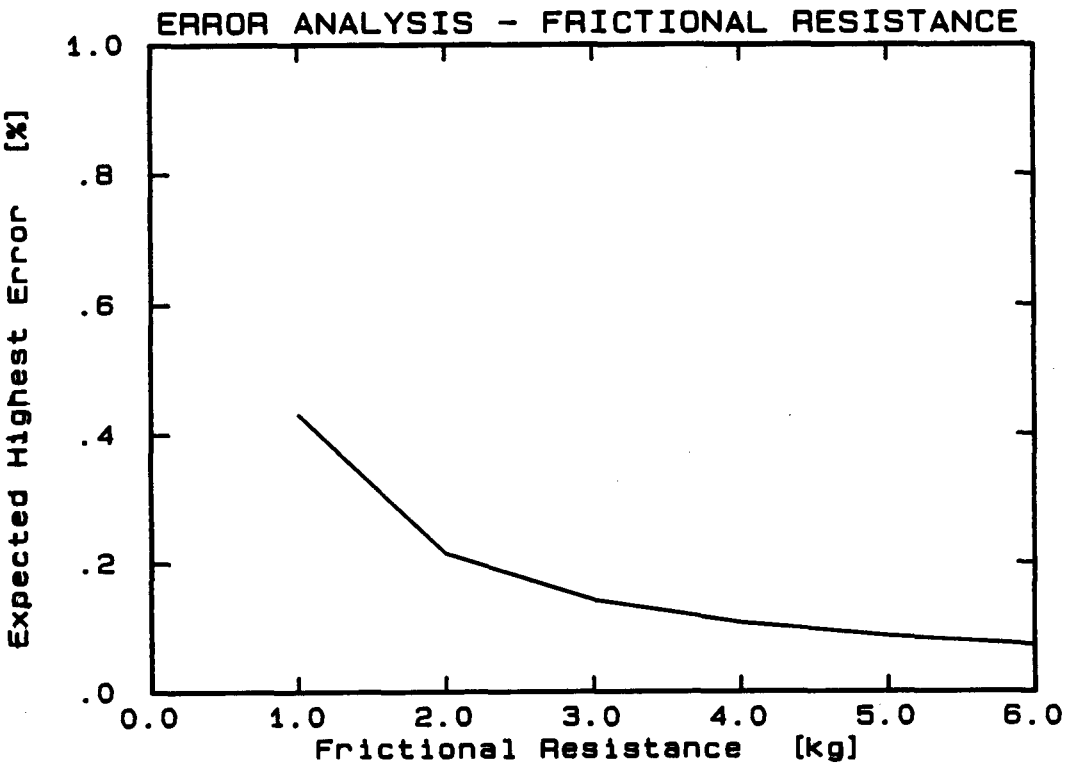

Figure 3.19

3.6.2 *Normal loading*

The normal loading on the sample may be calculated using Equation (3.11) providing the seals of the annular channel are not in contact with the disc. However, to evaluate μ_d for classified tailings the friction apparatus is used with the seals in positive contact with the disc to prevent particles escaping from the annular channel. The coefficient of friction is evaluated from the slope of the frictional resistance - normal loading curve. If the friction between the sample and the vertical walls of the channel may be neglected, ΔN is evaluated as follows :

$$\Delta N = (M_{\text{weights 2}} - M_{\text{weights 1}})\, g \quad , \tag{3.16}$$

where M_{weights} = mass of weights placed on loading ring.

Thus the highest expected error evaluated using Equation (2.18) is

$$\left[\frac{\delta \Delta N}{\Delta N}\right]^2_{exp} = \left[\frac{\delta \Delta N}{\partial M_{\text{weights 1}}}\right]^2 \left[\frac{M_{\text{weights 1}}}{\Delta N}\right]^2 \left[\frac{\delta M_{\text{weights 1}}}{M_{\text{weights 1}}}\right]^2 + \left[\frac{\delta \Delta N}{\partial M_{\text{weights 2}}}\right]^2 \left[\frac{M_{\text{weights 2}}}{\Delta N}\right]^2 \left[\frac{\delta M_{\text{weights 2}}}{M_{\text{weights 2}}}\right]^2 \tag{3.17}$$

where $\dfrac{\partial \Delta N}{\partial M_{\text{weights 1}}} = -g$

$$\frac{\partial \Delta N}{\partial M_{\text{weights 2}}} = g \quad .$$

Table 3.2 shows the measurement accuracies and highest expected error in the measurement of a typical value of ΔN.

TABLE 3.2 : Expected highest error - normal loading

Variables	Measurements
ΔN (kg)	4,920
$M_{weights\ 1}$ (kg)	1,640 ± 0,0001
$M_{weights\ 2}$ (kg)	6,560 ± 0,0001
$\delta\ \Delta N$ (kg)	± 0,0014
% Error in ΔN	0,028

3.6.3 *Relative speed between particles and disc*

The relative speed between the particles and disc is calculated from Equation (3.14) :

$$V = \frac{rn\,\pi}{30} \quad ,$$

where n = shaft rotational speed (rpm)
r = mean channel radius.

The shaft rotational speed is measured using a digital tachometer which has an accuracy of ± 1 rpm. The apparent speed of the shaft is increased by using two reflected strips, thus the accuracy is increased to ± 0,5 rpm. The highest expected error in measuring V is evaluated from Equation (2.18) as

$$\left[\frac{\delta V}{V}\right]^2_{exp} = \left[\frac{\partial V}{\partial r}\right]^2 \left[\frac{r}{V}\right]^2 \left[\frac{\delta r}{r}\right]^2 + \left[\frac{\partial V}{\partial n}\right]^2 \left[\frac{n}{V}\right]^2 \left[\frac{\delta n}{n}\right]^2 \quad , \tag{3.18}$$

where $\frac{\partial V}{\partial r} = \frac{n\,\pi}{30}$

$$\frac{\partial V}{\partial n} = \frac{r\,\pi}{30} \quad .$$

Table 3.3 shows the measurement accuracies, transducer accuracies and the highest expected error in the measurement of the relative speed between the particles and disc for V = 2 m/s. Figure 3.20 shows the variation of the highest expected error with relative velocity.

TABLE 3.3 : Expected highest errors - relative speed between particles and disc

Variables	Measurements
V (m/s)	2,000
r (mm)	154 ± 0,1
n (rpm)	124 ± 0,5
δ V (m/s)	0,008
% Error in V	0,41

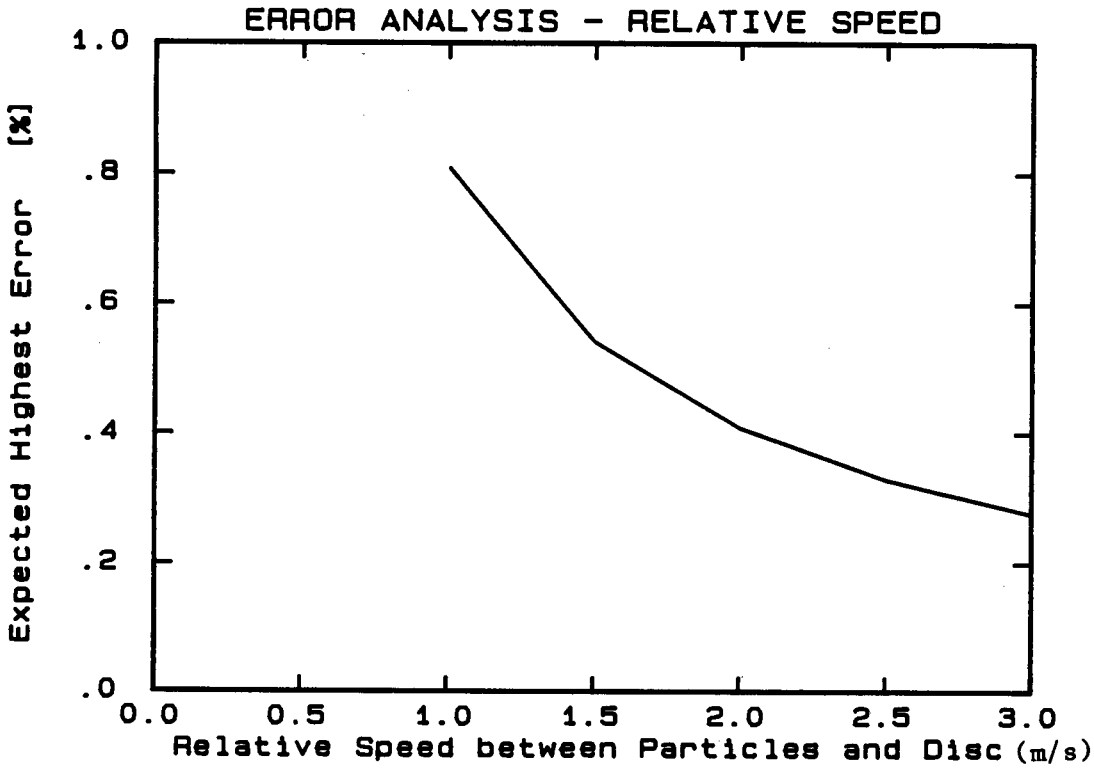

Figure 3.20

(m/s)

3.6.4 *Solid particle concentration*

The concentration of solid particles in the annular channel is calculated from Equation (3.12) :

$$C = \frac{M_s}{\rho_s \pi (r_o^2 - r_i^2) d} ,$$

where M_s = mass of solid particles
ρ_s = density of solid particles
r_o = outer radius of channel
r_i = inner radius of channel
d = depth of channel occupied by solids.

The highest expected error in C is evaluated using Equation (2.18)

$$\left[\frac{\delta C}{C}\right]^2_{exp} = \left[\frac{\partial C}{\partial M_s}\right]^2 \left[\frac{M_s}{C}\right]^2 \left[\frac{\delta M_s}{M_s}\right]^2$$

$$+ \left[\frac{\partial C}{\partial \rho_s}\right]^2 \left[\frac{\rho_s}{C}\right]^2 \left[\frac{\delta \rho_s}{\rho_s}\right]^2$$

$$+ \left[\frac{\partial C}{\partial r_o}\right]^2 \left[\frac{r_o}{C}\right]^2 \left[\frac{\delta r_o}{r_o}\right]^2$$

$$+ \left[\frac{\partial C}{\partial r_i}\right]^2 \left[\frac{r_i}{C}\right]^2 \left[\frac{\delta r_i}{r_i}\right]^2$$

$$+ \left[\frac{\partial C}{\partial d}\right]^2 \left[\frac{d}{C}\right]^2 \left[\frac{\delta d}{d}\right]^2 ,$$

where $\frac{\partial C}{\partial M_s} = \frac{1}{\rho_s \pi (r_o^2 - r_i^2) d}$

$$\frac{\partial C}{\partial \rho_s} = \frac{1}{\rho_s^2 \pi (r_o^2 - r_i^2) d}$$

$$\frac{\partial C}{\partial r_o} = \frac{- M_s 2 r_o}{\rho_s \pi (r_o^2 - r_i^2)^2 d}$$

$$\frac{\partial C}{\partial r_i} = \frac{M_s 2 r_i}{\rho_s \pi (r_o^2 - r_i^2)^2 d}$$

$$\frac{\partial C}{\partial d} = \frac{- M_s}{\rho_s \pi (r_o^2 - r_i^2) d^2} \quad .$$

Table 3.4 shows the measurements accuracies and highest expected error in the measurement of the solid particles concentration in the annular channel for a typical test.

TABLE 3.4 : Expected highest error - solid particle concentration

Variables		Measurements	
C	(%)	52,3	
M_s	(kg)	1,995	± 0,0001
ρ_s	(kg/m³)*	2650	± 10
r_o	(mm)	174	± 0,1
r_i	(mm)	134	± 0,1
d	(mm)	37	± 2
δC	(%)		± 2,8
% Error in C		5,4	

3.6.5 *Temperature*

The water temperature in the bath is measured using a mercury thermometer with a readable accuracy of % 1°C.

4. EXPERIMENTAL RESULTS AND DISCUSSION

4.1 Sliding friction test results

Figure 3.21 shows how the measured frictional resistance varies with the applied normal loading for a typical test series. The coefficient of friction is calculated as the slope of the frictional resistance - normal loading curve.

All tests reported were conducted at a solids concentration of between 56% and 58% by volume.

No repeatable measurements were made using the Western Deeps material. At high solids concentrations the Western Deep slurry has an observable yield stress (i.e. it forms a non-Newtonian mixture). A variable portion of the applied normal loading is transferred to the annular channel via the yield stress of the mixture. This results in a non-linear frictional resistance - normal loading curve, which also displays hysteresis. This presents a dilemma regarding the operation of the sliding friction apparatus - if the device is operated with a small clearance between the disc and channel the actual normal loading on the solid particles may be evaluated, however, if operated in this way the solid particles will escape from the channel. It was thus concluded that the apparatus is not suitable for measuring the sliding frictional forces of fine particles in a non-Newtonian mixture.

4.2 Influence of disc speed on the dynamic coefficient of friction

Figure 3.22 shows the effect of the relative speed between the particles and disc on the dynamic coefficient of sliding friction for the Blyvooruitsig material. The coefficient of friction μ_d is seen to be constant with respect to speed and has an average value of 0,44. This vindicates the contention of Televantos *et al* (1979) that a variation of μ_d with velocity is physically unlikely. The decrease in μ_d with increased speed reported by Briscoe *et al* (1983) is probably due to changes in the flow pattern with increased rotational speed of the cylinder apparatus.

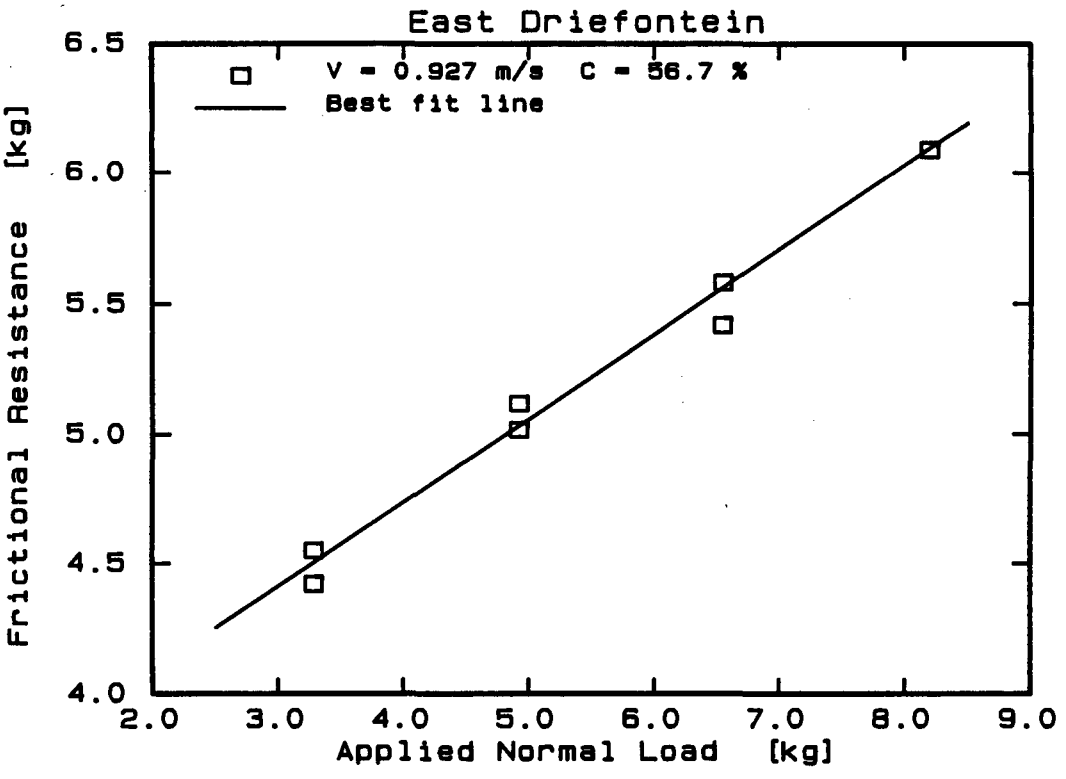

Figure 3.21

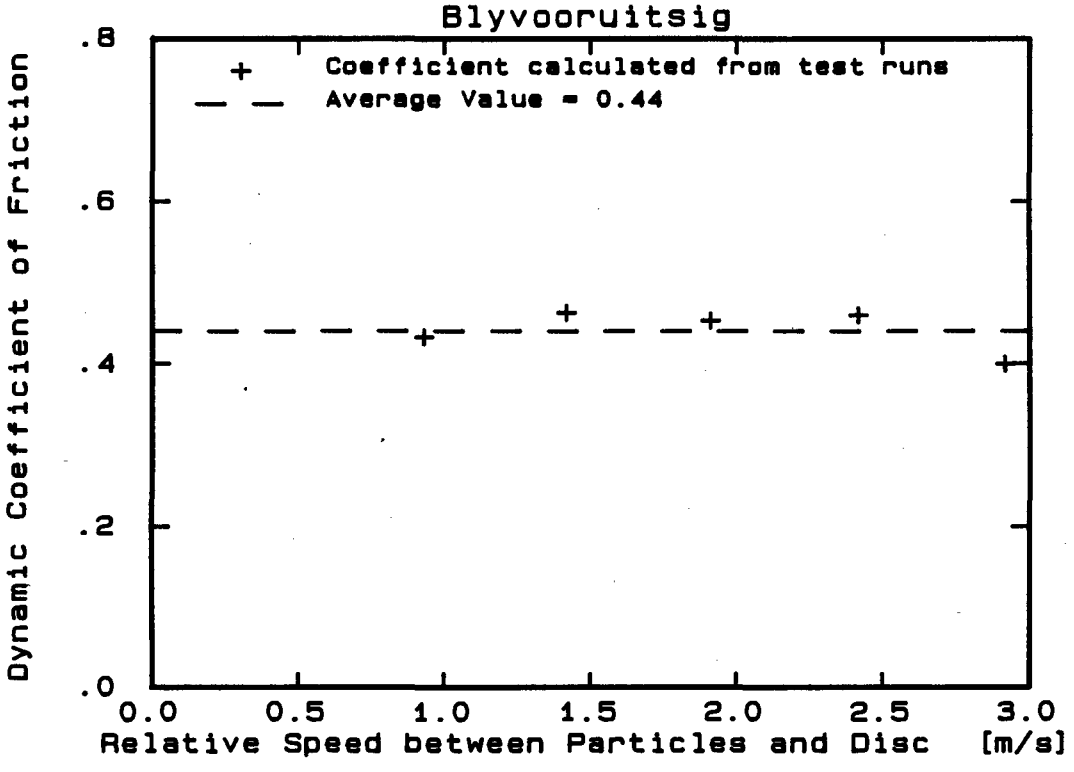

Figure 3.22

Figure 3.23 and 3.24 show a similar trend for the East Driefontein and Vaal Reefs materials respectively. It is surprising that the μ_d value for the East Driefontein material is less than that for the Vaal Reefs material as the East Driefontein material has a larger angle of internal friction (see Figure 2.16). It appears that the fines have a greater lubricating effect on the internal angle of friction of the particles than the sliding friction of the particles.

4.3 Influence of particle size distribution on the dynamic coefficient of friction

Figures 3.25 and 3.26 show the variation of μ_d with the d_{50} and d_{10} particle sizes of the Blyvooruitsig, East Driefontein and Vaal Reefs materials respectively. There appears to be no clear trend regarding the effect of particle size. It is likely that parameters such as angularity and sharpness (which are difficult to evaluate directly) have an important influence on the coefficient of sliding friction.

4.4 Variation of dynamic coefficient of friction with solids concentration

Figure 3.27 shows the variation of the measured angle of internal friction (static test described in Chapter 2, Section 3.6) with solids concentration for the Blyvooruitsig material. The variation of μ_d with concentration shown in Figure 3.27 is estimated using relation (3.8) from Butterfield and Andrawes (1972) work :

$$\frac{\mu_d \text{ (loose)}}{\mu_d \text{ (dense)}} \simeq \frac{\tan (\delta \text{ loose})}{\tan (\delta \text{ dense})} \quad .$$

Figure 3.28 and 3.29 show the estimated variation of μ_d with solids concentration of the East Driefontein and Vaal Reefs materials respectively.

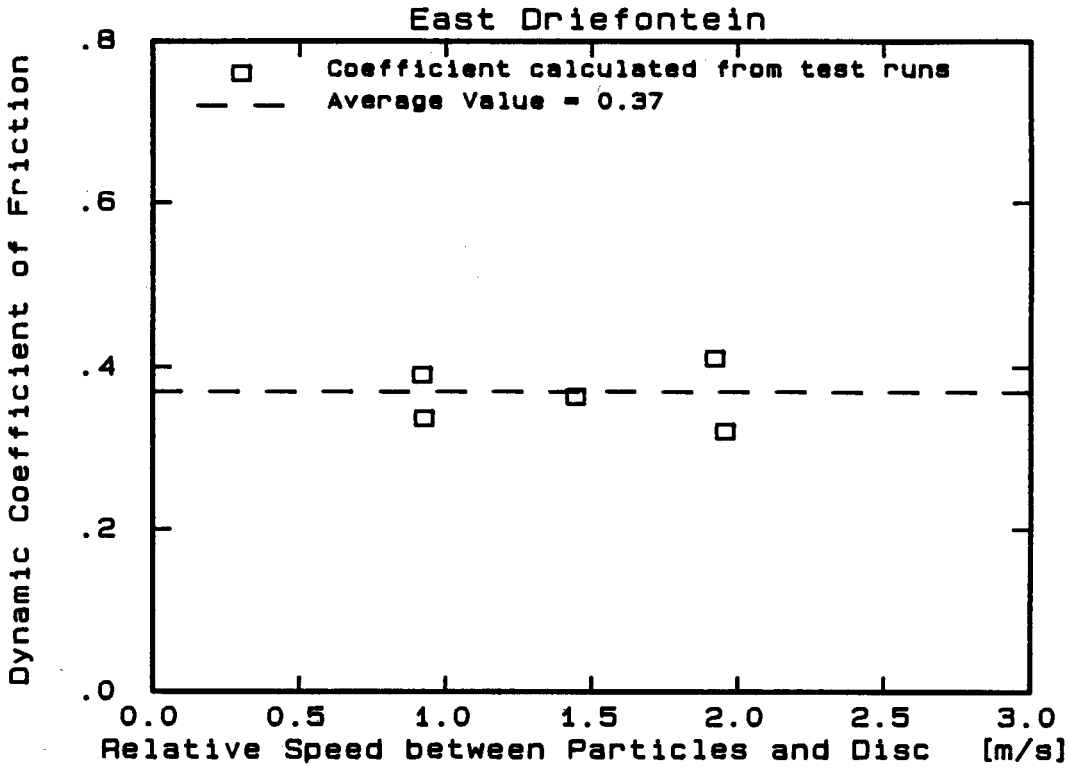

Figure 3.23

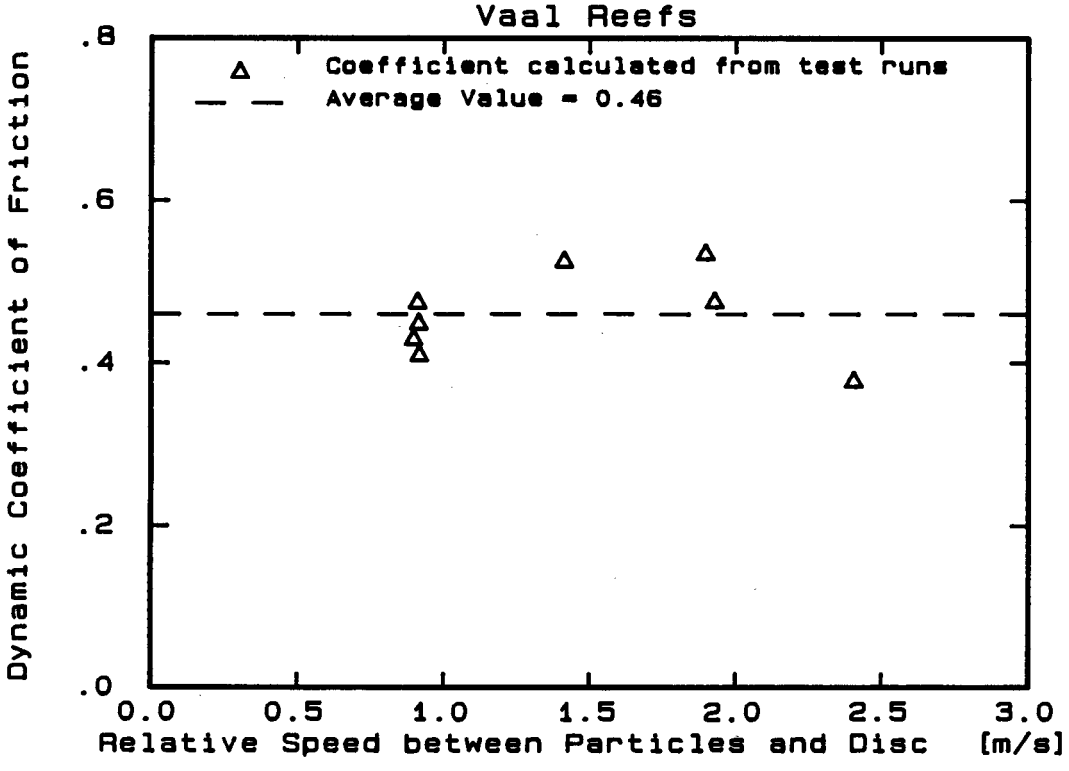

Figure 3.24

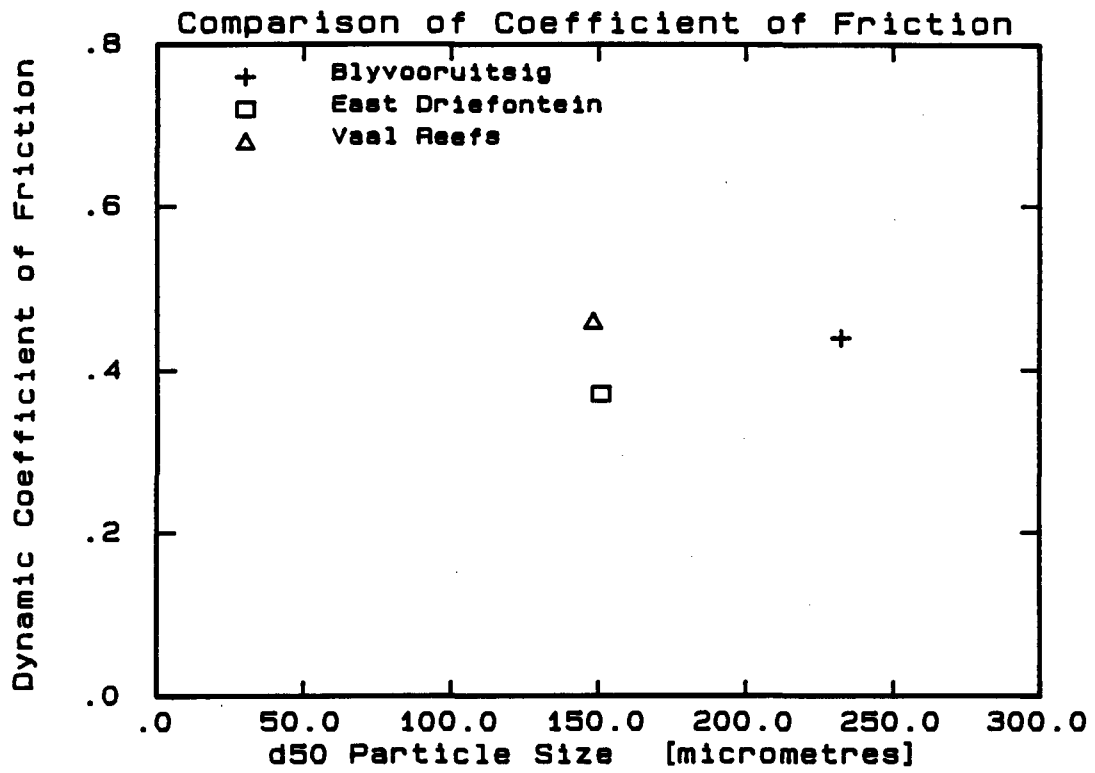

Figure 3.25

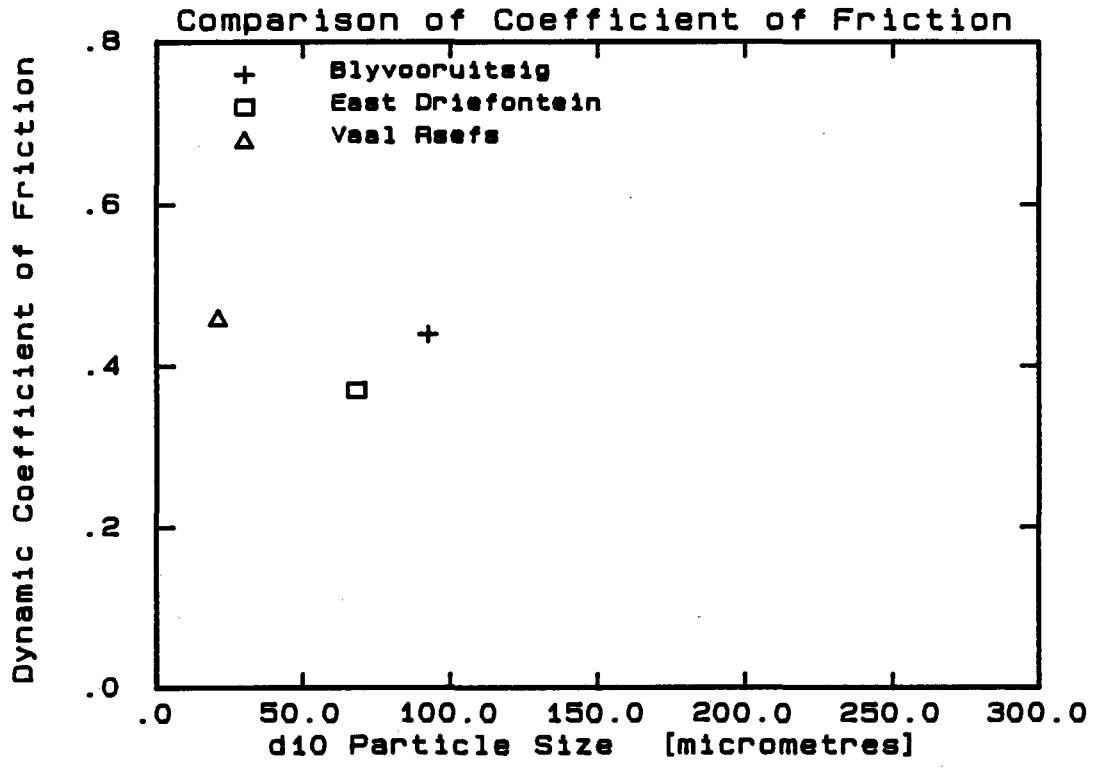

Figure 3.26

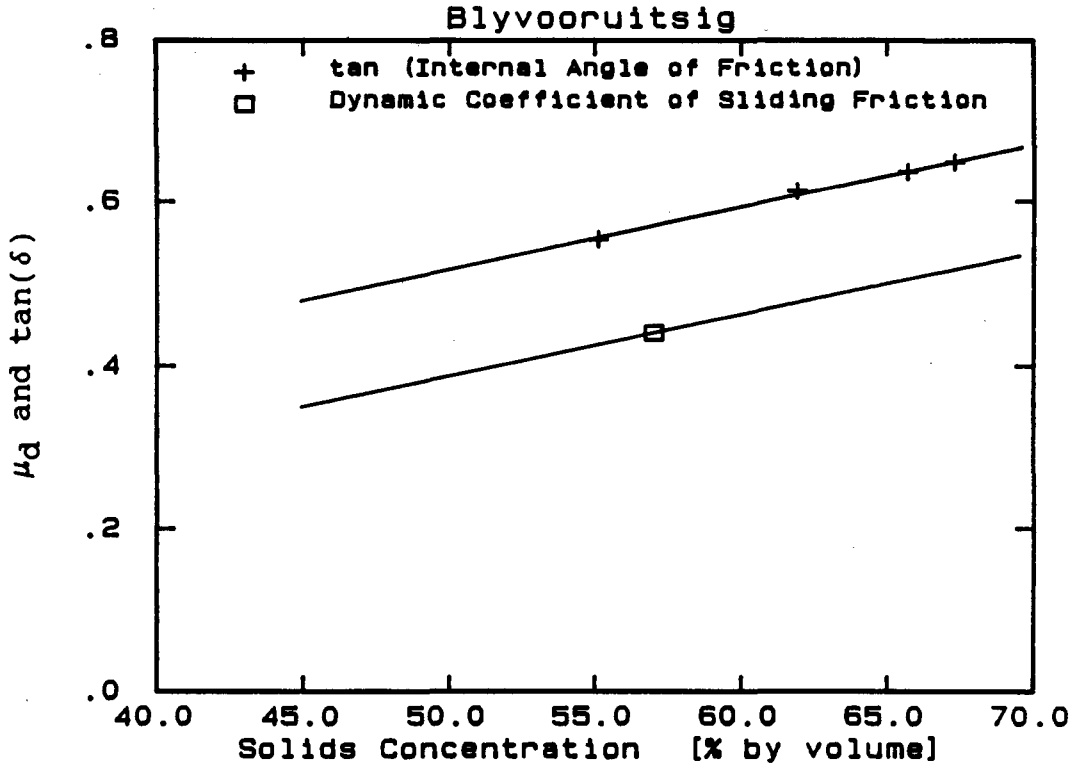

Figure 3.27

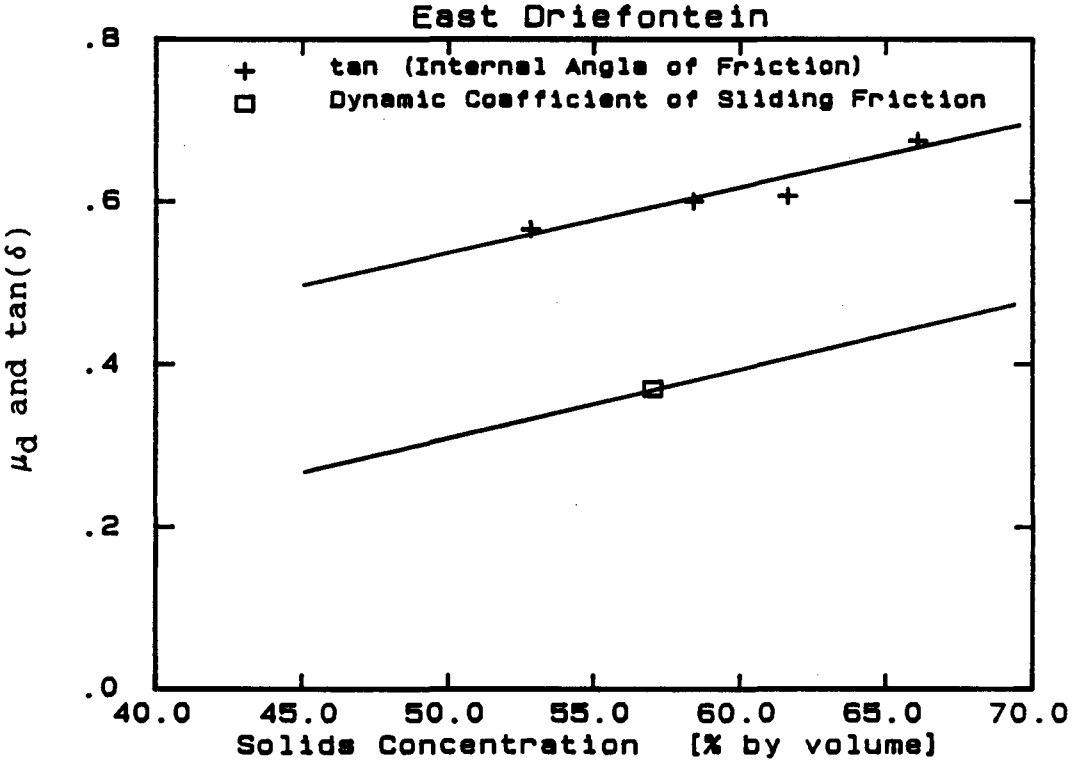

Figure 3.28

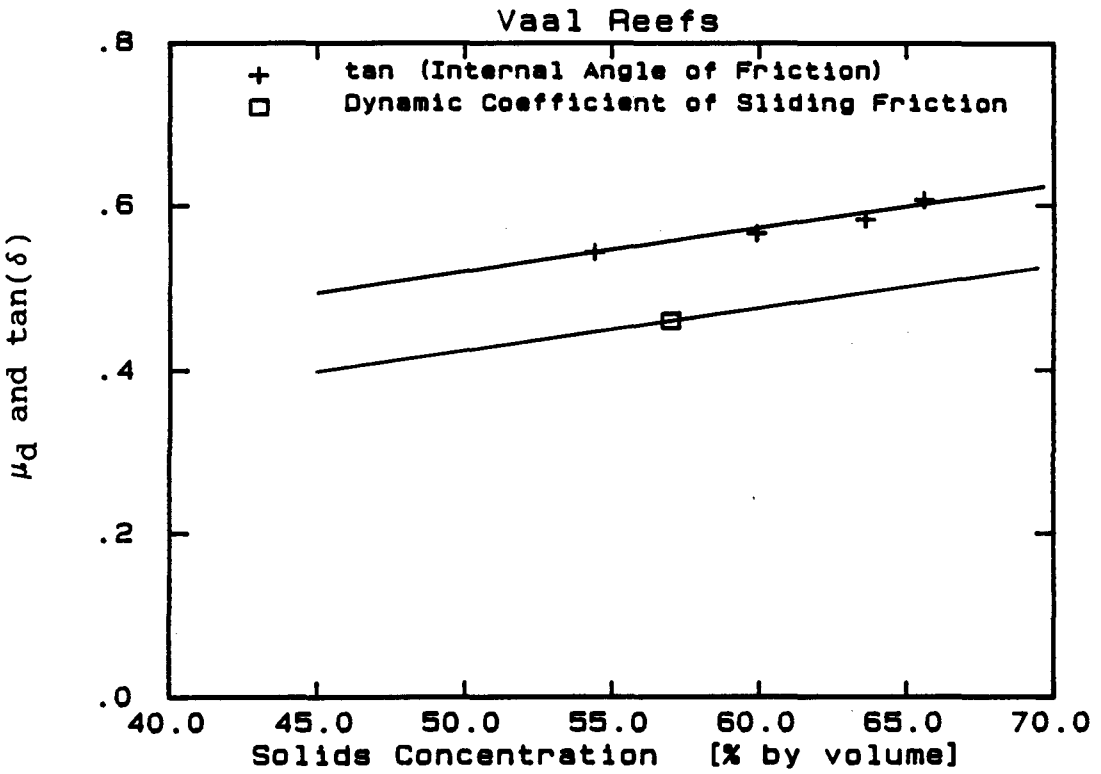
Vaal Reefs
tan (Internal Angle of Friction)
Dynamic Coefficient of Sliding Friction
μ_d and tan(δ)
.8
.6
.4
.2
.0
40.0
45.0
50.0
55.0
60.0
65.0
70.0
Solids Concentration [% by volume]

Figure 3.29

5. CHAPTER SUMMARY AND CONCLUSIONS

Methods that have been used to determine the dynamic coefficient of sliding friction between solid particles and pipe wall are :

- Tilting tube
- Shear box
- Rotating cylinder
- Rotary shear meter.

Of these methods the rotary shear meter is considered the most objective test method, as no interpretation as to the interparticle stress distribution or onset of particle sliding is required. Thus a solid particle sliding friction apparatus has been constructed based on the rotary shear meter. The apparatus and the operating procedure have been described, and experimental errors evaluated for all measurements.

The four materials used in the pipeline tests (Blyvooruitsig, East Driefontein, Vaal Reefs and Western Deeps) have been tested in the friction apparatus. It was not possible to determine the coefficient of friction for the Western Deeps material as it formed a non-Newtonian mixture at high solids concentration. The conclusions from the test work are :

(i) An apparatus has been developed to determine the coefficient of sliding friction for fine grained particles.

(ii) If the solid material forms a non-Newtonian mixture it is not possible to determine the coefficient of friction due to difficulty in evaluating the normal loading on the solid particles.

(iii) The measured dynamic coefficient of sliding friction remains constant with speed for the three settling materials evaluated (Blyvooruitsig, East Driefontein and Vaal Reefs).

(iv) There appears to be no clear trend regarding the effect of particle size distribution on the dynamic coefficient of sliding friction.

(v) The variation of the dynamic coefficient of friction with solids concentration has been assumed to be similar to the variation of the measured angle of internal friction with solids concentration.

CHAPTER 4

DENSE PHASE FLOW - A REVIEW OF ANALYTICAL METHODS

1. INTRODUCTION

Wilson (1982) defines dense phase flow to exist when the concentration of the solid particles approaches that of the loose packed (freely settled) solid particle concentration. Streat (1986) describes dense phase flow as a flow regime in which, most, if not all the solids travelling in horizontal flow are conveyed as contact load, with the submerged weight being transmitted to the pipe invert.

For the purposes of this investigation dense phase flow is defined to exist when :

(i) the concentration of the solid particles equals or exceeds the freely settled particle concentration.

(ii) the dominant mechanism supporting the particles in the mixture is interparticle contact. The mixture is essentially a settling mixture in which the particles are prevented from settling by the high solid particle concentration, as opposed to a stabilised mixture in which particles are supported by a fluid yield stress.

Leung *et al* (1969) in considering vertical hydraulic conveying distinguish between fluidised bed flow and packed bed flow. In fluidised bed flow the solid particles are essentially supported by the liquid through fluid dynamic drag. In packed bed flow the solid particles travel *en bloc* with permanent contact between them and little mixing occurring. Both the solid and liquid phases are continuous and capable of transmitting force. Thus the terms dense phase flow and packed bed flow are considered synonymous for the purposes of this investigation.

This chapter reviews existing techniques for predicting pressure gradients for the hydraulic transport of high concentration slurries. The existing models are compared with experimentally measured pressure gradients.

2. THE STREAT DENSE PHASE SLIDING BED MODEL FOR HORIZONTAL FLOW

2.1 Description of model

The Streat dense phase model has been developed over a number of years - Bantin and Streat (1972), Streat *et al* (1976), Streat (1982) and Streat (1986). This review of Streat's model is primarily based on his 1986 paper - "Dense phase flow of solids-water mixtures in pipelines: a state of the art review".

The dense phase model is a special case of Wilson's (1970) sliding bed model. The pressure gradient required to move a sliding bed through a pipeline at a particular velocity is determined by applying a force balance across a pipe section. Figure 4.1 depicts a schematic view of a sliding bed in a pipeline. The sliding bed occupies a portion of the pipe defined by the deposit angle θ (in dense phase flow θ equals π), and moves with an average velocity V_B. The suspension above the bed occupies a portion of the pipe defined by $\pi - \theta$ and travels at an average speed V_S.

Within the sliding bed the pressure gradient ΔP per unit length of pipe will cause a seepage flow of the liquid between the interstices between the particles. Providing the particles are small (and consequently the interstices between the particles small) the seepage flow through the bed is considered to be sufficiently small to be neglected. However, the pressure force exerted by the seepage flow to the particles in the bed through fluid dynamic drag is significant. This pressure force together with the shear stress τ_{Bi} acting at the interface of the sliding bed constitute the driving forces on the sliding bed. The motion of the bed is resisted by the shear stress τ_{Bw} acting between the sliding bed and pipe wall, thus a force balance per unit length of pipe yields :

$$\frac{\Delta P\ \pi\ D^2}{4}\ (1 - a)\ +\ \tau_{Bi}\ D \sin\theta\ =\ \tau_{Bw}\ D\ \theta\ , \qquad (4.1)$$

where $(1 - a)$ = ratio of area occupied by bed to total area of pipe.

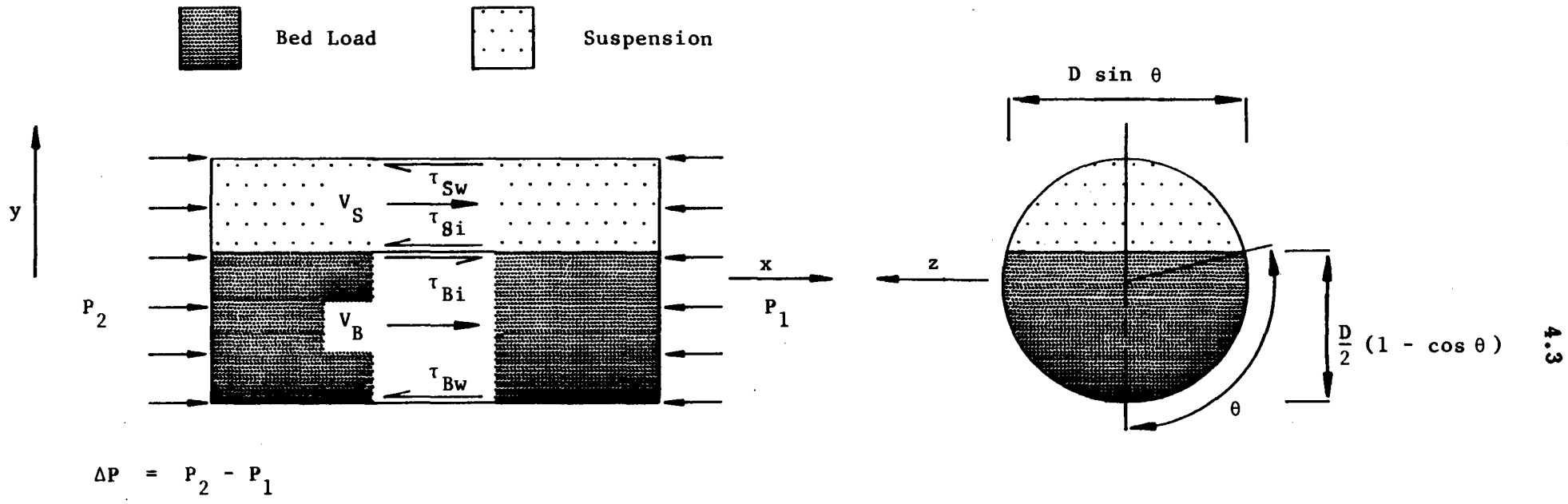

Figure 4.1 : Wilson's bed slip model

The forces acting on the suspension above the sliding bed are due to the pressure gradient ΔP acting on the sectional area occupied by the suspension, the shear stress τ_{Si} acting at the interface between the sliding bed and suspension, and the shear stress τ_{Sw} between the suspension and pipe wall. Applying a force balance on the suspension per unit length we get :

$$\Delta P \frac{\pi D^2}{4} a = \tau_{Si} D \sin\theta + \tau_{Sw} D (\pi - \theta) \quad . \tag{4.2}$$

Adding equations (4.1) and (4.2), and noting that $\tau_{Bi} = \tau_{Si}$, we obtain the total force balance per unit length of pipe for steady flow :

$$\Delta P \frac{\pi D^2}{4} = \tau_{Bw} D \theta + \tau_{Sw} D (\pi - \theta) \tag{4.3}$$

Shear stress acting between pipe wall and sliding bed τ_{Bw}

The bed motion is resisted by the solids-wall and liquid-pipe wall frictional forces. Thus the resisting shear stress acting between the sliding bed and pipe wall is the sum of the shear stress due to the solid and liquid phases, i.e.

$$\tau_{Bw} = \tau_{Bs} + \tau_{B\ell} \quad . \tag{4.4}$$

The liquid phase shear stress $\tau_{B\ell}$ is accounted for by defining a friction factor for the portion of pipe occupied by the sliding bed :

$$\tau_{B\ell} = \tfrac{1}{8} f_B \rho_{mB} V_B^2 \quad , \tag{4.5}$$

where f_B = friction factor

ρ_{mB} = mixture density of the bed.

The slip velocity between the liquid and solid particles is assumed to be negligible, thus the kinetic energy of the bed as a whole is included in expression (4.5). The friction factor f_B is taken to have the same value as for an equal discharge of clear liquid.

The shear stress due to the solids-wall friction is evaluated assuming a linear relationship between the total normal radial stress σ_R and the tangential frictional shear stress τ_{Bs} acting at the sliding bed-pipe wall interface. The coefficient of proportionality being the dynamic coefficient of friction between the pipe wall and sliding bed ($\tau_{Bs} = \mu_d \sigma_R$). The normal stress at any point on the pipewall is evaluated assuming that the granular mass exerts a hydrostatic type of pressure proportional to its own weight, i.e.

$$\frac{d\sigma_R}{dy} = - \rho g (S_s - S_\ell) C_B \quad , \tag{4.6}$$

where S_s = relative density of solid particles
S_ℓ = relative density of liquid
C_B = volumetric concentration.

The hydrostatic interparticle stress distribution (equation 4.6) was developed by Wilson (1970) through a series of tests on the slip points of beds in sloping pipelines. These experiments are discussed in Section 2.1 of Chapter 3.

Streat postulates that the shear stress τ_{Bi} acting on the bed interface has an associated normal interparticle stress equal to $\tau_{Bi}/\tan \Phi$, where Φ is the angle of repose of the granular material. This normal interparticle stress is known as the Bagnold dispersive stress (Govier and Aziz (1972)). Thus the normal pressure acting on the pipe wall at any point defined by angle α is found integrating equation (4.6) and adding the Bagnolds dispersive stress :

$$\sigma_R (\alpha) = \frac{\tau_{Bi}}{\tan \Phi} + \rho g (S_s - S_\ell) C_B \frac{D}{2} (\cos \alpha - \cos \theta) \quad . \tag{4.7}$$

Therefore the local shear stress due to the solid particles at any point on the pipe wall is :

$$\tau_{Bs} (\alpha) = \mu_d \left[\frac{\tau_{Bi}}{\tan \Phi} + \rho g (S_s - S_\ell) C_B \frac{D}{2} (\cos \alpha - \cos \theta) \right] \quad . \tag{4.8}$$

Shear stress acting between suspension and pipewall τ_{Sw}

The shear stress at the pipewall due to the suspension is determined by defining a friction factor for the portion of pipe occupied by the suspension :

$$\tau_{Sw} = \tfrac{1}{2} f_S \rho_{mS} V_S^2 \quad , \tag{4.9}$$

where f_S = friction factor
ρ_{mS} = mixture density of suspension
V_S = mean velocity of suspension.

The friction factor f_S is taken to have the same value as for an equal discharge of clear liquid.

Total force balance

The pipe wall shear stresses due to the suspension (equation (4.9)), the liquid phase of the sliding bed (equation (4.5)) and the solid particle sliding friction of the bed (equation (4.8)) are substituted into the force balance equation (4.3) :

$$\Delta P \frac{\pi D^2}{4} = 2 \int_0^{\theta} \tau_{Bs}(\alpha) \frac{D}{2} d\alpha + \tau_{B\ell} D \theta + \tau_{Sw} D (\pi - \theta) \quad . \tag{4.10}$$

Performing the integration we get :

$$\begin{aligned} \frac{\pi D^2}{4} \rho g i_T = {} & \mu_d \left[\frac{D \theta \tau_{Bi}}{\tan \phi} \right. \\ & \left. + \rho g (S_s - 1) C_B \frac{D^2}{2} (\sin\theta - \theta \cos\theta) \right] \\ & + \tfrac{1}{2} f_B \rho_{mB} V_B^2 D \theta + \tfrac{1}{2} f_S \rho_{mS} V_S^2 D (\pi - \theta) \quad , \end{aligned} \tag{4.11}$$

where i_T = total hydraulic gradient = $\frac{\Delta P}{\rho g}$.

The shear stress acting between the sliding bed and suspension is defined as

$$\tau_{Bi} = \tfrac{1}{2} f_i \rho_{mi} (V_S - V_B)^2 \quad , \tag{4.12}$$

where f_i = interface friction factor
ρ_{mi} = interface mixture density.

Substituting equation (4.12) into expression (4.11) and simplifying we get :

$$i_T = \frac{2 \mu_d f_i S_{mi} (V_S - V_B)^2}{\tan \Phi \; g \; D} \left[\frac{\theta}{\pi}\right] + 2 \mu_d (S_s - S_\ell) C_B \left[\frac{\sin \theta - \theta \cos \theta}{\theta}\right] + \frac{2 f_B S_{mB} V_B^2}{g D} \left[\frac{\theta}{\pi}\right] + \frac{2 f_S S_{mS} V_S^2}{g D} \left[\frac{\pi - \theta}{\pi}\right] \quad , \tag{4.13}$$

where S_{mi} = interface mixture relative density
S_{mB} = relative density of bed
S_{mS} = relative density of suspension.

Thus the total hydraulic gradient is the sum of the contributions due to :

(i) the sliding frictional shear stress between solid particles and pipe wall due to Bagnold's dispersive stress arising from the shear stress at the bed interface.

(ii) the sliding frictional shear stress between solid particles and pipe wall due to hydrostatic pressure distribution exerted by the submerged weight of the sliding bed.

(iii) Fluid shear between the sliding bed and the pipe wall.

(iv) Fluid shear between the suspension and the pipe wall.

For the special case of dense phase flow equation (4.13) may be simplified noting that the interface shear stress term equals zero and the fluid resistance term due to the suspension vanishes as $\theta = \pi$. Thus we get

$$i_T = 2 \mu_d (S_s - S_\ell) C_B + \frac{2 f_B S_{mB} V_B^2}{g D} \quad . \tag{4.14}$$

Observing the following :

(i) As the *insitu* concentration C_t equals the concentration of the bed C_B :

$$S_{mB} = C_t (S_s - S_\ell) + S_\ell \ ,$$

(ii) The mean mixture velocity V_m equals the velocity of the bed V_B ,

(iii) The friction factor for the bed is assumed to equal the value for clear liquid, i.e. $f_B = f_\ell$,

we may simplify equation (4.14) :

$$\boxed{i_T = 2 \mu_d (S_s - S_\ell) C_t + S_m i_\ell \ ,} \tag{4.15}$$

where $i_\ell = 2 f_\ell \frac{V_m^2}{g D}$.

2.2 Discussion

The sliding friction term in Streat's model (first term in equation (4.15)) is independent of pipe diameter and mean mixture velocity. This implies that at low velocities (where the contribution due to fluid shear is small) the pressure gradient is independent of pipe diameter. Figure 4.2 compares the measured pressure gradients and pressure gradients calculated using Streat's model for the Vaal Reefs slurry at a solids concentration of 45,5% by volume in 25 mm, 40 mm and 80 mm NB pipelines. The variation of the dynamic coefficient of

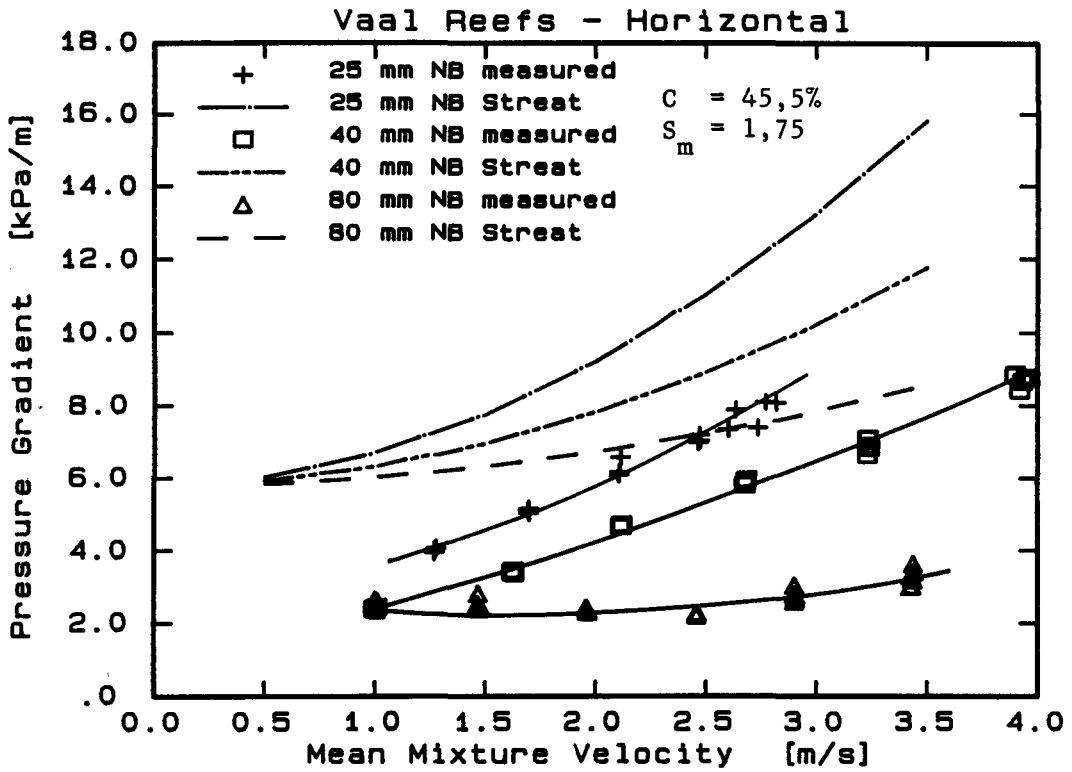

Figure 4.2

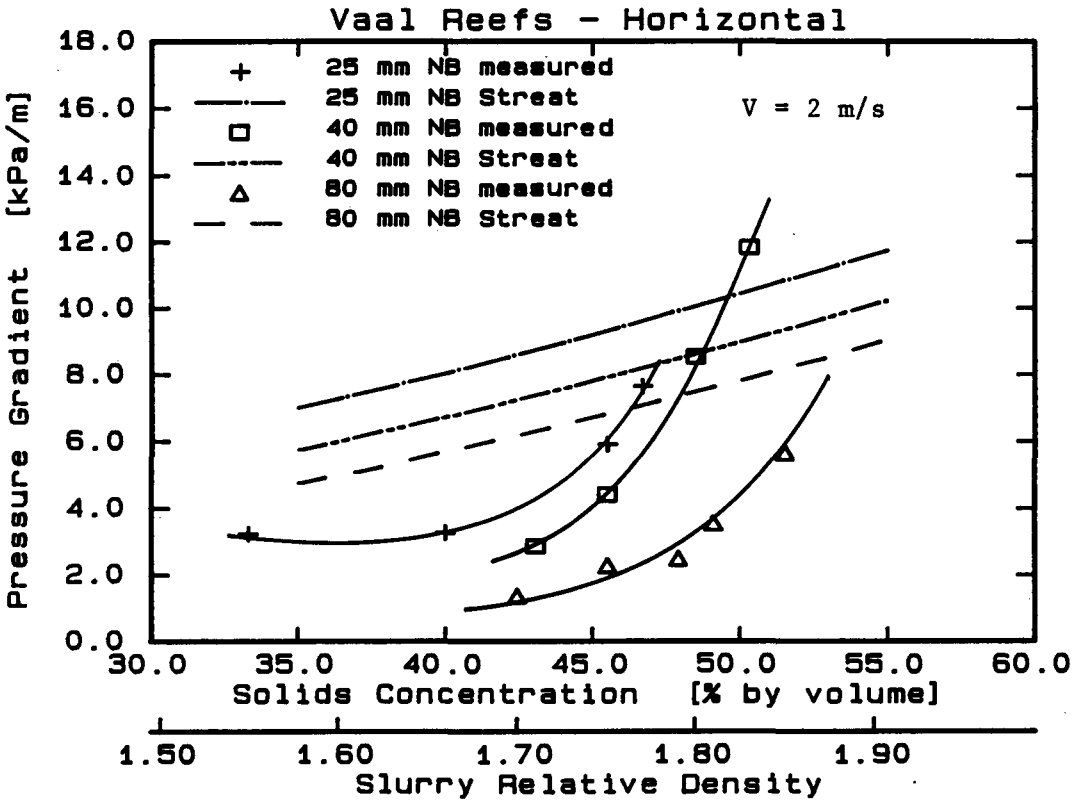

Figure 4.3

friction with concentration shown in Figure 3.29 has been used as input for the model. The Streat model is seen to predict identical pressure gradients for all three pipelines at low velocities, with the pressure gradient in the small diameter pipeline being the highest at higher velocities. Although the shapes of the predicted pressure gradient - mean mixture velocity curves are similar to the measured curves, the Streat model over-predicts the pressure gradient for all three pipelines.

Figure 4.3 shows the variation of the measured pressure gradients and the pressure gradients calculated using Streat's model with solids concentration for the Vaal Reefs slurry at a mean mixture velocity of 2 m/s for the three pipelines. The Streat model predicts a linear increase in pressure gradient with concentration in contrast to the sharp increase in the measured pressure gradient with concentration.

The Streat dense phase model has been developed for one solids concentration - i.e. when the *insitu* concentration C_t equals the freely settled particle concentration C_{min}. The dynamic coefficient of sliding friction is the only parameter used to characterise different solid particle types. The fluid shear term remains constant for a particular pipeline and conveying velocity irrespective of the particle size distribution of the solids in the mixture.

The sliding bed is modelled as an integrated plug moving with a uniform velocity distribution across the pipe section. Flow observations (Chapter 2, Section 4.4) have, however, shown that at solids concentrations corresponding to the freely settled particle concentration asymmetric velocity profiles are evident. This implies that solid particles are shearing relative to each other within the sliding bed.

3. STREAT'S ANALYSIS OF SOLIDS-LIQUID MIXTURES FLOWING IN VERTICAL PIPES

3.1 Analysis

Streat and his co-workers have investigated the vertical flow of solids-liquid mixtures in a number of papers - Cloete *et al* (1967), Bantin and Streat (1970), Bantin and Streat (1972) and Streat (1986). The review of his analysis of the vertical flow of slurries is based on his 1986 paper - "Dense phase flow of solids-water mixtures in pipelines: a state of the art review".

Streat states that the submerged weight of solids in a vertical pipe, acting vertically, does not transmit any stress to the pipe walls. Exceptions are cases where the slurry moves as a packed bed in which solid particle - pipe wall stresses will be significant. Thus the solid particle shear stresses at the pipe wall are likely to be significant for the dense phase flow considered in this investigation. Although Streat ignores these stresses in his analysis it is useful to examine his method as it provides a basis for analysing the vertical flow of solids-liquid mixtures in pipes.

Streat considers the energy losses in the vertical upward transport of a solid-liquid mixture to be the sum of the potential energy changes which are reversible and the irreversible losses due to drag and liquid-wall friction. Thus the total pressure gradient is the sum of the hydrostatic pressure component and the pressure losses due to friction :

$$\Delta P_T = \Delta P_h + \Delta P_f \quad . \tag{4.16}$$

Hydrostatic pressure component

If the energy dissipated in raising the slurry by a unit height per second is E_h , then

$$E_h = A_s V_s \rho_s g + A_\ell V_\ell \rho_\ell g \quad , \tag{4.17}$$

where A_s , A_ℓ = areas occupied by solid and liquid phases respectively.

This energy loss, E_h is equal to the delivered volume per second multiplied by the pressure loss due to the potential energy increase of the slurry, i.e.

$$E_h = A V_m (\Delta P_h) = A V_m i_h g \rho \quad , \tag{4.18}$$

where i_h = hydraulic gradient due to hydrostatic (i.e. reversible) component.

Equating expressions (4.17) and (4.18) :

$$i_h = \frac{A_s V_s}{A V_m} S_s + \frac{A_\ell V_\ell}{A V_m} = \frac{Q_s S_s}{Q_m} + \frac{Q_\ell}{Q_m} \quad . \tag{4.19}$$

Noting that the delivered volumetric concentration of solids,

$$C_d = \frac{A_s V_s}{A V_m} = \frac{Q_s}{Q_m} \quad , \tag{4.20}$$

and substituting into equation (4.19) we obtain :

$$i_h = C_d (S_s - S_\ell) + S_\ell \quad . \tag{4.21}$$

Force balance

The driving force per unit length is due to the total hydraulic gradient

$$F_D = i_T \rho g A \quad . \tag{4.22}$$

The motion of the slurry is resisted by the sum of weight components due to the liquid and solid phases and the shear stress acting at the pipe wall per unit length :

$$F_R = (1 - C_t) \rho_\ell g A + C_t \rho_s g A + \tau_w \pi D \quad , \tag{4.23}$$

where $\tau_w = \frac{1}{2} \rho_m V_m^2 f_\ell$

f_ℓ = friction factor for clear liquid.

Assuming steady flow conditions we can equate expressions (4.22) and (4.23) :

$$i_T = C_t (S_s - S_\ell) + S_\ell + S_m i_\ell \qquad (4.24)$$

where i_ℓ = hydraulic gradient for clear liquid.

Noting equation (4.21) for the reversible hydraulic gradient i_h in expression (4.24) we can write the total hydraulic gradient as :

$$\boxed{i_T = C_d (S_s - S_\ell) + S_\ell + (C_t - C_d) (S_s - S_\ell) + S_m i_\ell} \quad , \qquad (4.25)$$

where $C_d (S_s - S_\ell) + S_\ell$ = reversible hydraulic gradient
$(C_t - C_d) (S_s - S_\ell)$ = friction loss due to slip
$S_m i_\ell$ = wall friction losses.

3.2 Discussion

The friction losses due to slip arise from the drag forces on individual particles caused by the relative velocity of the liquid and solids. For high concentration mixtures this slip velocity is negligible (Appendix B) and the *insitu* concentration will be closely equal to the delivered concentration. Thus for high concentration mixtures equation (4.25) may be simplifed as follows :

$$\begin{aligned} i_T &= C (S_s - S_\ell) + S_\ell + S_m i_\ell \\ &= S_m (1 + i_\ell) \quad . \end{aligned} \qquad (4.26)$$

Note that equation (4.26) has been derived for vertical upward flow; the corresponding equation for vertical downward flow is

$$i_{Tdown} = S_m (i_\ell - 1) \quad . \qquad (4.27)$$

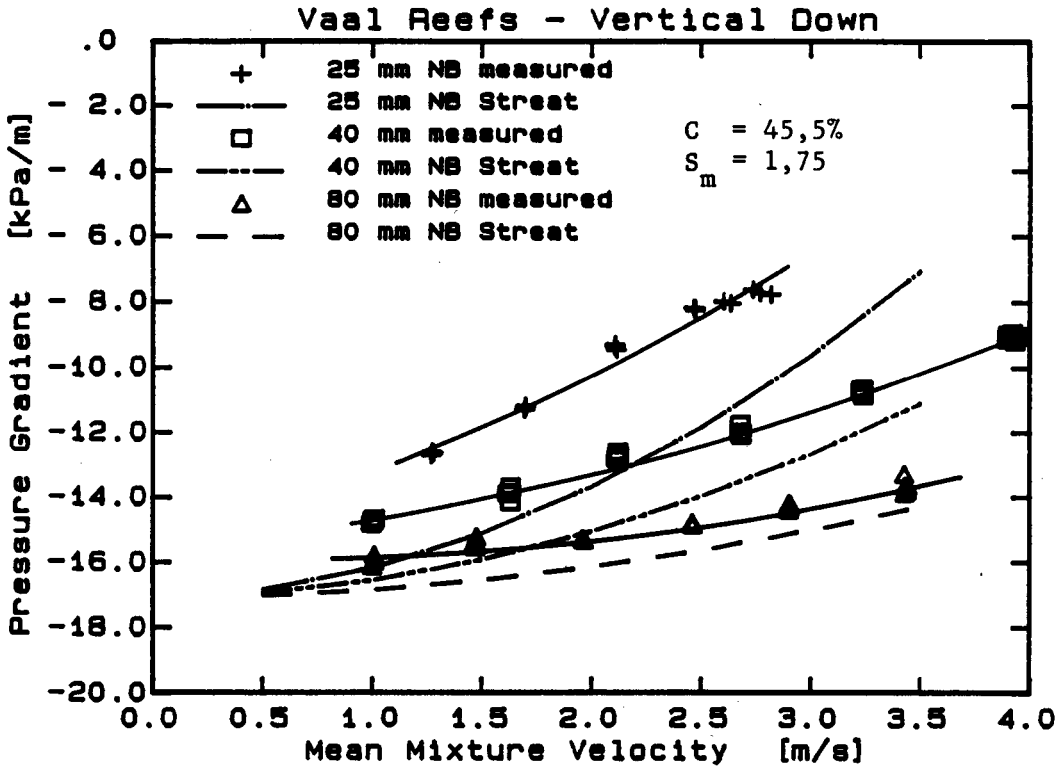

Figure 4.4

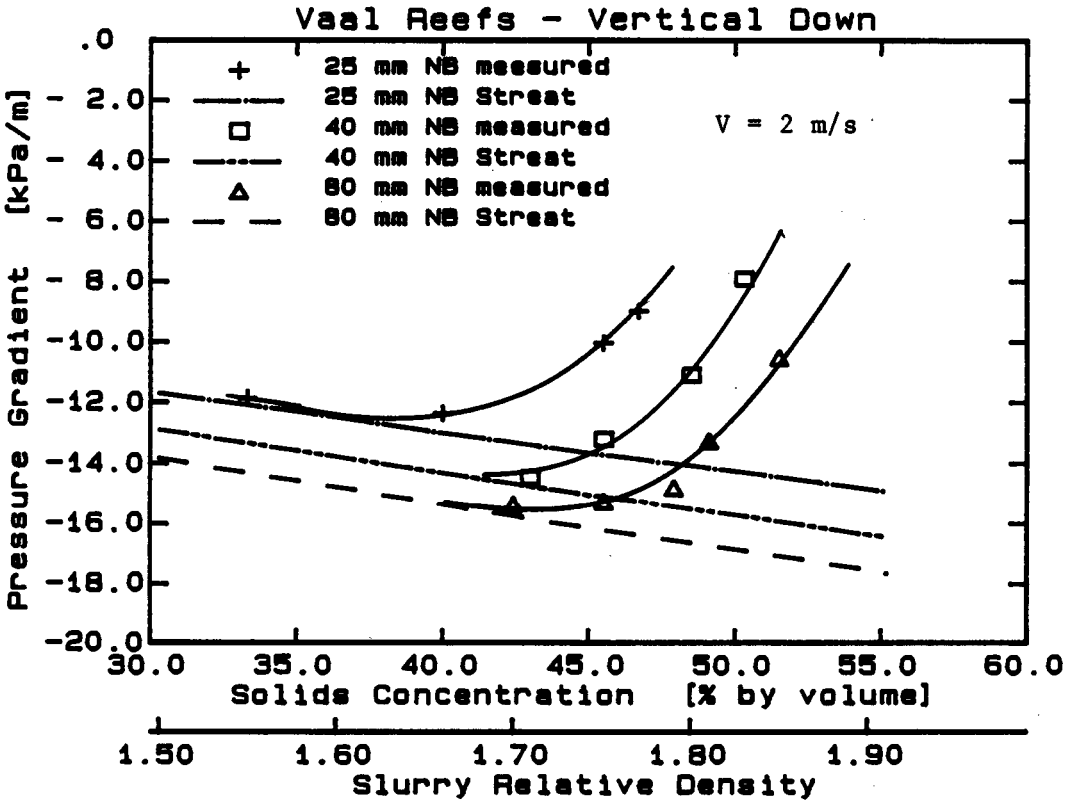

Figure 4.5

Figure 4.4 compares the measured vertical down pressure gradients and calculated pressure gradients using Streat's analysis (equation (4.27)) for the Vaal Reefs slurry at a solids concentration of 45,5% by volume in 25 mm, 40 mm and 80 mm NB pipelines. The shapes of the measured and predicted mean mixture velocity curves are similar, although the Streat analysis under-predicts the pressure gradients for all three pipe diameters. The Streat analysis more closely matches the measured pressure gradients as the pipe diameter is increased. This implies that the Streat analysis does not adequately model the flow mechanisms, and this deficiency is more pronounced in small diameter pipes.

Figure 4.5 shows the variation of the measured pressure gradients and the pressure gradients calculated using Streat's analysis with solids concentration for the Vaal Reefs slurry at a mean mixture velocity of 2 m/s for the three pipelines. The experimental curves are seen to diverge from the Streat analysis as the solids concentration increases. It is apparent that the effect of solid particle - pipe wall frictional forces, which are ignored in Streat's analysis, become significant at high solids concentrations.

4. WILSON, BROWN AND STREAT'S MODEL FOR DENSE PHASE VERTICAL FLOW

4.1 Description of model

Wilson, Brown and Streat (1979) have compared the Streat vertical flow model (described in Section 3 of this chapter) with experimental data obtained on the hydraulic hoisting of granular solids at high concentration in vertical pipes. They have observed that the mixture has a friction gradient (based on the total pressure gradient minus the reversible column effect) which is considerably greater than that for an equal discharge of clear liquid. The authors propose a method of calculating the mixture pressure gradient based on fluid and particulate friction mechanisms. The pipe section is divided into three zones :

(i) A zone of constant concentration (equal to the freely settled particle concentration) with no velocity gradient occupying the central portion of the pipe section termed the *core*.

(ii) An *annulus* surrounding the core in which the solids concentration and mixture velocity vary.

(iii) A *near wall zone* in which the fluid shear and solid particle sliding friction is imparted to the pipe wall.

This review describes the specific case of dense phase flow in which the annulus of varying solids concentration and mixture velocity is absent - i.e. only the core and the near wall zone exist.

The total shear stress τ_T acting in the solid liquid mixture has a maximum value at the pipewall and decreases linearly to zero at the centre line of the pipe, i.e.

$$\tau_T = \rho g i_f \frac{D}{4} \left(\frac{1 - 2\varsigma}{D}\right) , \qquad (4.28)$$

where $i_f = i_T - C_t (S_s - S_\ell)$ = hydraulic friction gradient

ς = distance measured radially inwards from pipe wall.

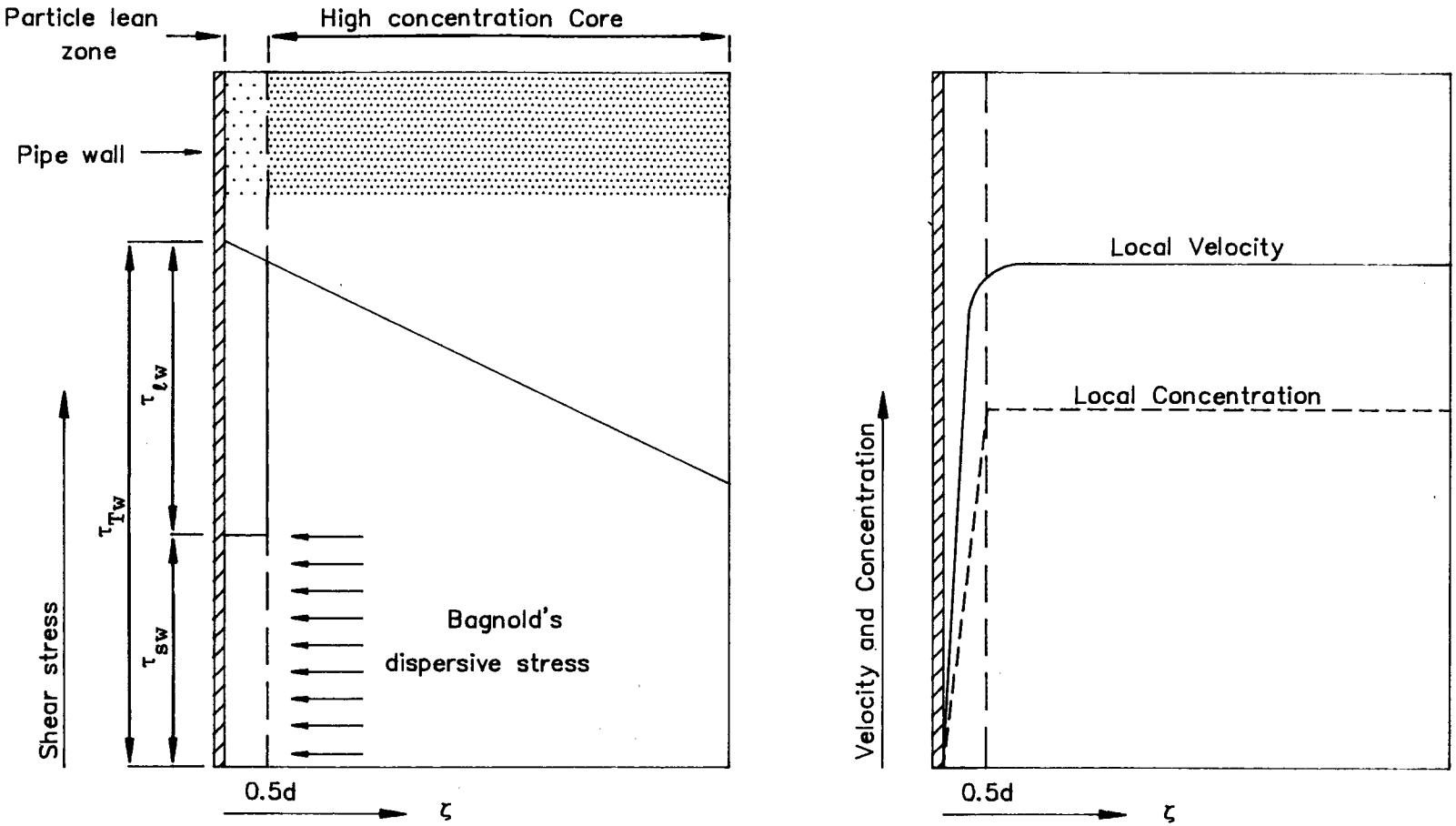

Figure 4.6 : Wilson et al vertical dense phase model

The total shear stress τ_T is the sum of the components due to the liquid phase and the solid particles :

$$\tau_T = \tau_\ell + \tau_s \quad . \tag{4.29}$$

Referring to Figure 4.6, the authors postulate that a core of constant concentration and velocity exists in the centre of the pipe. The closest proximity to the pipe wall that the centre of a particle can achieve is equal to half the particle diameter, thus $\varsigma = d/2$ demarcates the outer layer of particles. Between $\varsigma = d/2$ and the pipe wall there exists an annular region of "particle lean" liquid. It is the limiting case where the core extends to the outer layer of particles at $\varsigma = d/2$ that is of specific interest.

As the liquid phase shear stress at $\varsigma = d/2$ equals zero (no velocity gradient), the solid phase shear stress may be evaluated using equation (4.28) :

$$\tau_s\,(d/2) = \rho\, g\, i_f \frac{D}{4} \left(1 - \frac{d}{D}\right) \quad . \tag{4.30}$$

The dispersive normal stress at $\varsigma = d/2$ is evaluated using the Bagnold relation :

$$\sigma_{sN}\,(d/2) = \frac{\tau_s\,(d/2)}{\tan \Phi} \quad . \tag{4.31}$$

This normal stress is transmitted through the "particle lean" annulus by the particles in direct contact with the wall. The shear stress at the pipe wall due to the sliding particles is obtained by multiplying the normal stress by the dynamic coefficient of friction :

$$\tau_{sw} = \mu_d\, \sigma_{sN}\,(d/2) \quad . \tag{4.32}$$

From equation (4.29) and by substituting relations (4.30) and (4.31) into expression (4.32) we obtain the shear stress at the wall due to the liquid phase :

$$\tau_{\ell w} = \tau_{Tw} \left[1 - \frac{\mu_d}{\tan \Psi} (1 - \frac{d}{D}) \right] . \qquad (4.33)$$

The velocity at $\varsigma = d/2$ is obtained using the logarithmic velocity law

$$v\ (d/2) = V_\ell^* \left[2{,}5\ \ell n\ (\frac{0{,}5\ d\ V_\ell^*}{\nu}) + 5{,}5 \right] , \qquad (4.34)$$

where $V_\ell^* = \sqrt{\frac{\tau_{\ell w}}{\rho}}$ = shear velocity associated with the fluid wall stress.

As the core occupies virtually the whole pipe, the velocity at $\varsigma = d/2$ will correspond to the mean velocity V if the slip between the fluid and solid phases is neglected.

4.2 Evaluation of Bagnold's dispersive stress

To determine the Bagnold dispersive stress normal to the pipe wall (equation (4.31)) a value of the ratio of stresses in a sheared particle matrix is required. Shook and Daniel (1965) have presented a formulation to evaluate $\tan \Psi$ based on Bagnold's (1954) and (1956) work :

$$\tan \Psi = 0{,}32 \qquad \text{for } G^2 > 3\ 700$$
$$\tan \Psi = 0{,}75 \qquad \text{for } G^2 < 28 ,$$

where $G^2 = \frac{\rho_s\ d^2\ \sigma_{sN}}{\mu^2\ \lambda}$

λ = linear concentration = $\left[\frac{1}{\left(\frac{C_{max}}{C}\right)^{-1/3} - 1} \right]$

C_{max} = maximum particle packing concentration.

4.3 Discussion

This description of Wilson, Brown and Streat's model for the vertical flow of high concentration mixtures is a special case of a more complex analysis which includes an annulus of varying velocity and concentration between the near wall particle lean zone and the high concentration constant velocity core.

Figure 4.7 compares the measured vertical down pressure gradients and calculated pressure gradients using the Wilson *et al* model for the Vaal Reefs slurry at a solids concentration of 45,5% by volume in 25 mm, 40 mm and 80 mm NB pipelines. The slopes of the predicted pressure gradient - mean mixture velocity curves are steeper than the experimentally measured curves. The following parameters were used as input for the Wilson *et al* model :

(i) Particle diameter - d

The d_{50} particle size is taken as the representative particle diameter.

(ii) Coefficient of sliding friction - μ_d

The variation of the dynamic coefficient of friction with concentration shown in Figure 3.29 is used as input for the model.

(iii) Bagnold's dispersive stress - σ_{sN}

The value of term Ψ is evaluated as discussed in section 4.2, assuming a linear variation of $\tan \Psi$ with G^2 between the two regions in which $\tan \Psi$ remains constant. The maximum particle packing density is taken to be 70% by volume.

Figure 4.8 shows the variation of the measured pressure gradients and the pressure gradients calculated using the Wilson *et al* model with solids concentration for the Vaal Reefs slurry at a mean mixture velocity of 2 m/s for the three pipelines. The Wilson *et al* model presents a mechanism (absent in Streat's analysis) by which the solid phase shear stress is transferred to the pipe wall (via the Bagnold's dispersive stress). It does not, however, predict the sharp increase in frictional resistance with solids concentration observed in the experimental results.

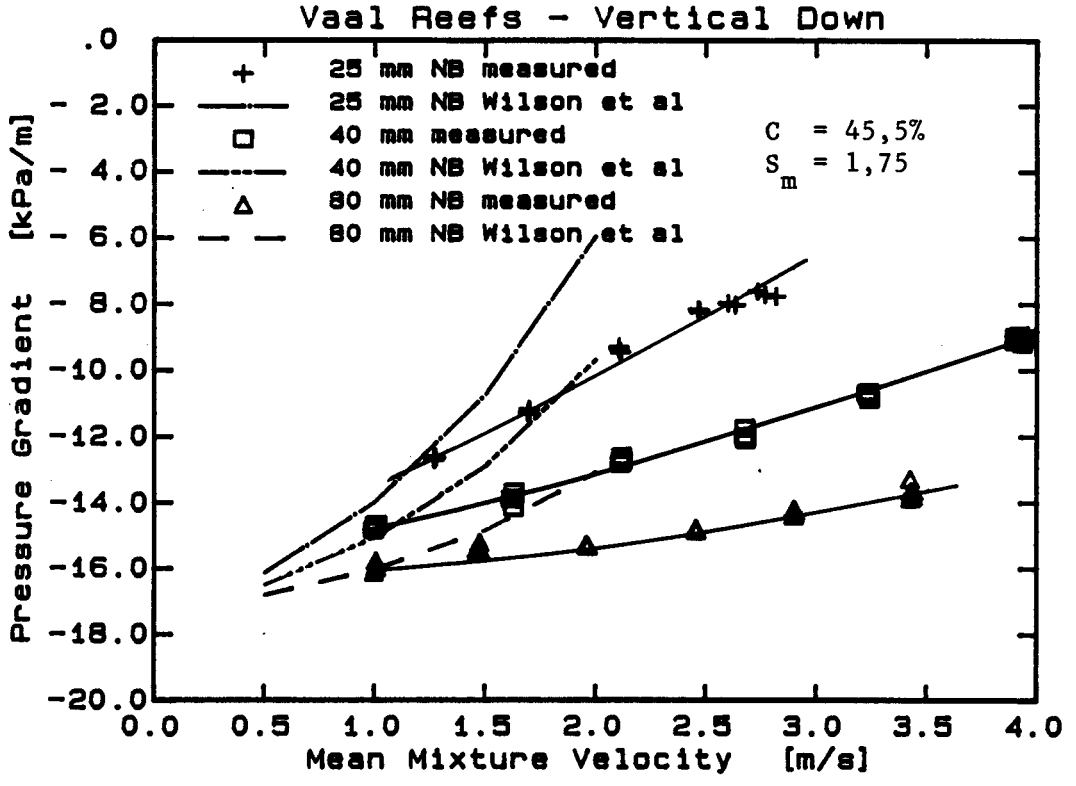

Figure 4.7

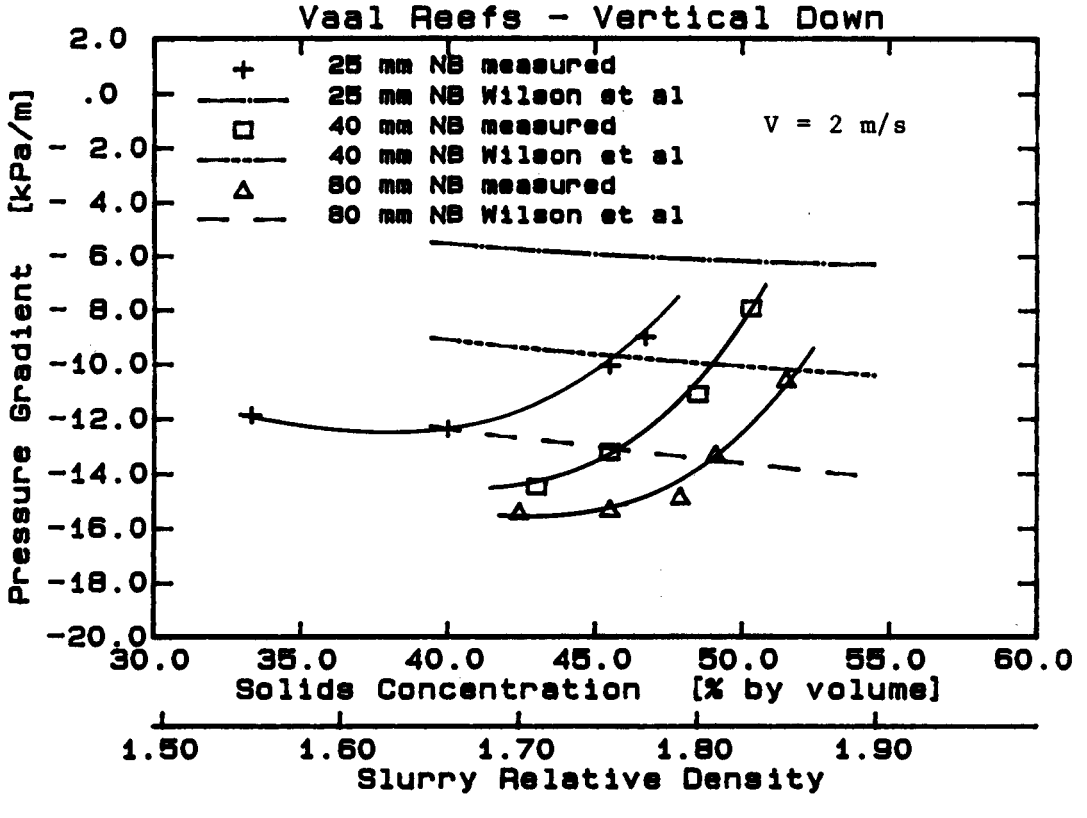

Figure 4.8

5. CHAPTER SUMMARY AND CONCLUSIONS

Dense phase flow is defined to exist when the concentration of solid particles equals or exceeds the freely settled particle concentration, and interparticle contact is the dominant mechanism supporting the particles in the mixture.

The Streat dense phase model has been developed for essentially one concentration - when the concentration of the solids equals the freely settled particle concentration. The model fails to predict the steep increase in pressure gradient with solids concentration observed in experimental measurements.

The Streat analysis of solids-liquid mixtures in vertical pipes does not take into account shear stress at the pipe wall due to the solid phase. The analysis provides a means of separating the hydrostatic and friction components of the total pressure gradient.

The Wilson, Brown and Streat model for high concentration flow in vertical pipes postulates that the solid phase shear stress is transferred to the pipe wall via mechanical sliding friction, with the Bagnold's dispersive stress providing the required normal interparticle stress. The model, however, does not predict the steep increase in pressure gradient with solids concentration.

CHAPTER 5

MECHANISTIC MODEL FOR THE DENSE PHASE FLOW OF CYCLONE CLASSIFIED TAILINGS

1. INTRODUCTION

1.1 Background

In Chapter 4 it was shown that there is no dense phase model available which accurately predicts pressure gradients for the flow of high concentration cyclone classified tailings. The objective is thus to determine the flow mechanisms of dense phase mixtures in pipes, and to develop a model to predict pipeline pressure gradients for high concentration cyclone classified tailings.

1.2 Overview of the dense phase mechanistic model

The basic relations (velocity and stress distributions) required for the dense phase model are described in Section 2. The solid particles are considered to be represented by a single characteristic particle size. The governing differential equation describing the velocity distribution in a pipeline conveying a solids liquid mixture is developed (Roco and Shook 1983) from the Cauchy momentum equations for each phase of the mixture (Section 2.1). The total shear stress distribution in the mixture is shown to be linear for a homogeneous slurry flowing in a circular pipe (Section 2.2). The viscous and turbulent shear stress relations for a Newtonian fluid are presented (Section 2.3). Stress relations within the granular matrix of the solid phase are developed and the coefficient of lateral interparticle stress introduced (Section 2.4). The solid phase shear stress at the pipe wall is examined (Section 2.5). In the light of the shear stress relations developed, the differential equation for the velocity distribution is considered for the sheared and unsheared zones of the solid particle matrix (Section 2.6).

Equation (5.7) states that for steady, uniform, unidirectional flow the mixture shear stresses, body forces and pressure forces acting on an element of slurry are in equilibrium.

2.2 Shear stress distribution

The shear stress distribution may be evaluated by analysing the forces acting on a cylinder of radius r inside a pipe as shown in Figure 5.2. The local mixture density is taken to be a function of both y and z. Wallis (1969 p.111) considers an axially symmetric concentration distribution. The force balance on the cylinder yields :

$$\tau_m = \frac{r}{2}\frac{dp}{dx} - \frac{r}{2}\rho_\ell g \sin\phi - \frac{(\rho_s - \rho_\ell) g \sin\phi}{2\pi r}\int_{-r}^{r}\int_{-f(z)}^{f(z)} c\,(y,z)\,dy\,dz \quad , \tag{5.8}$$

where $f(z) = \sqrt{r^2 - z^2}$.

Equation (5.8) indicates that generally the shear stress distribution within a pipe will not be linear. However, for the particular case of the high concentration flows under consideration the concentration distribution $c\,(y,z)$ may be assumed to be constant across the pipe section, and Equation (5.8) reduces to :

$$\tau_m = \frac{r}{2}\left[\frac{dp}{dx} - \rho_m g \sin\phi\right] \quad , \tag{5.9}$$

where $\rho_m = \rho_\ell + C\,(\rho_s - \rho_\ell)$.

Therefore the shear stress distribution across the pipe section will be linear if the concentration distribution is constant. Note that for the special case of a horizontal pipe the last two terms of equation (5.8) fall away, indicating that for a horizontal pipe the shear stress distribution is linear irrespective of the concentration distribution.

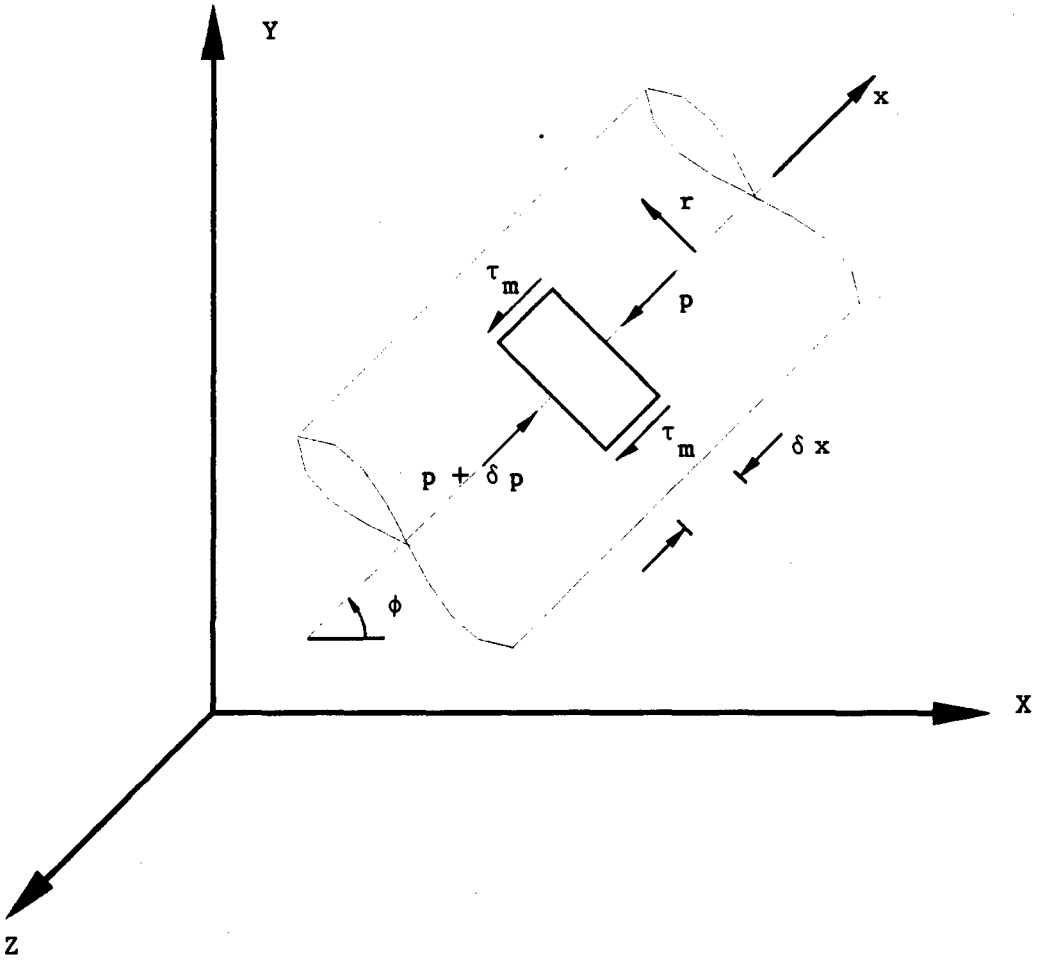

Figure 5.2 : Force balance on a cylinder of slurry

2.3 Shear stresses due to liquid phase

The shear stress due to the liquid phase has components due to the viscosity and turbulence of the mixture, i.e.

$$\tau_\ell = (\tau_\ell)_{\text{viscous}} + (\tau_\ell)_{\text{turbulent}} \quad . \tag{5.10}$$

2.3.1 *Viscous shear stresses*

The rate of strain in the fluid is related to the viscous shearing stress as follows :

$$(\tau_\ell)_{\text{viscous}} = f\left(\frac{\partial v_i}{\partial x_i}\right) \quad . \tag{5.11}$$

Relation (5.11) is known as the constitutive or rheological equation for the fluid. For purely viscous fluids this relation describes the rheological behaviour of the fluid. The constitutive equation for a Newtonian fluid is

$$(\tau_\ell)_{\text{viscous}} = \mu\left(\frac{\partial v_i}{\partial x_i}\right) \quad , \tag{5.12}$$

where μ = dynamic coefficient of viscosity of the fluid.

2.3.2 *Turbulent shear stresses*

Roco and Shook (1984) consider turbulence at a point to be defined by six independent coefficient a_{ij} . Stresses τ_{ij} are then expressed by means of partial derivatives of the time-averaged kinetic energy multiplied by a coefficient α_{ij} :

$$(\tau_\ell)_{\text{turbulent}} = \partial \frac{(\alpha_{ij}\, \rho\, v_j^2)}{\partial x_i} \quad ; \quad i,j = 1,2,3 \quad . \tag{5.13}$$

2.4 Shear stress acting within the solid phase

2.4.1 *Solid phase stress relations*

The analysis of the stress in the mixture due to the solid phase is limited to the special case of dense phase flow, i.e. the concentration of the solid particles is greater than the freely settled (loose poured) concentration. In this case the solid particles are supported via interparticle contact - there are no particles supported by turbulence.

Consider the interparticle normal stress and shear stress acting on face k of the element shown in Figure 5.3. At failure, i.e. when the element slides relative to the adjacent elements, τ_{sk} and τ_{skx} are related as follows :

$$\tau_{skx} = \tau_{sk} \tan \delta \quad ,$$

where k = y or z

δ = internal angle of friction of solid particle matrix.

If the shear stress acting in the mixture is less than the product of the normal stress τ_{sk} and the tangent of the internal angle of friction δ failure will not occur. Thus there will be no relative motion between the elements and they will travel as an integrated plug. Thus the above relation is better expressed as the following inequality (as Wilson *et al* (1979) noted) :

$$\tau_{skx} \leq \tau_{sk} \tan \delta \quad . \tag{5.14}$$

When the solid particle matrix is sheared (particles slide relative to each other) equation (5.14) is expressed as the following equality :

$$(\tau_{skx})_{failure} = \tau_{sk} \tan \delta \quad . \tag{5.15}$$

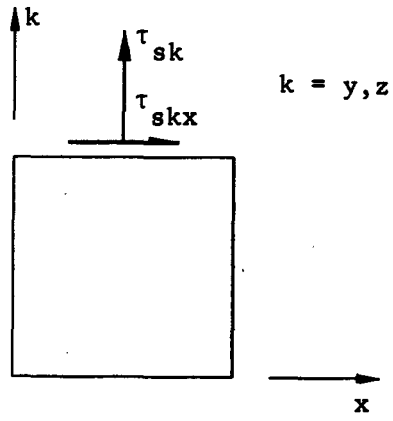

Figure 5.3 : Solid phase normal and shear stresses

The normal interparticle stress τ_{sk} acting in the yz plane has components due to :

(i) the axial normal stress acting in the direction of flow τ_{sx} .

(ii) the submerged weight of the solid particles acting perpendicular to the direction of flow.

Thus we get :

$$\tau_{sk} = (\tau_{sk})_{axial} + (\tau_{sk})_{weight} \quad . \tag{5.16}$$

2.4.2 *Shear stress distribution in dense phase flow*

Figure 5.4 shows the shear stress distribution (Equation 5.9) due to the pressure gradient, and the shear stress τ_{syx} at failure in a horizontal pipe. $(\tau_{syx})_{failure}$ increases towards the bottom of the pipe due to the added contribution of the self-weight of the particles to the normal stress τ_{sy}. In the central portion of the pipe it is seen that the total shear stress imposed is insufficient to cause failure. The two stress distributions intersect at points a and b corresponding to the initiation of failure. In the outer annulus the solid matrix is sheared with the excess shear being accounted for by fluid shear in generating the velocity distribution.

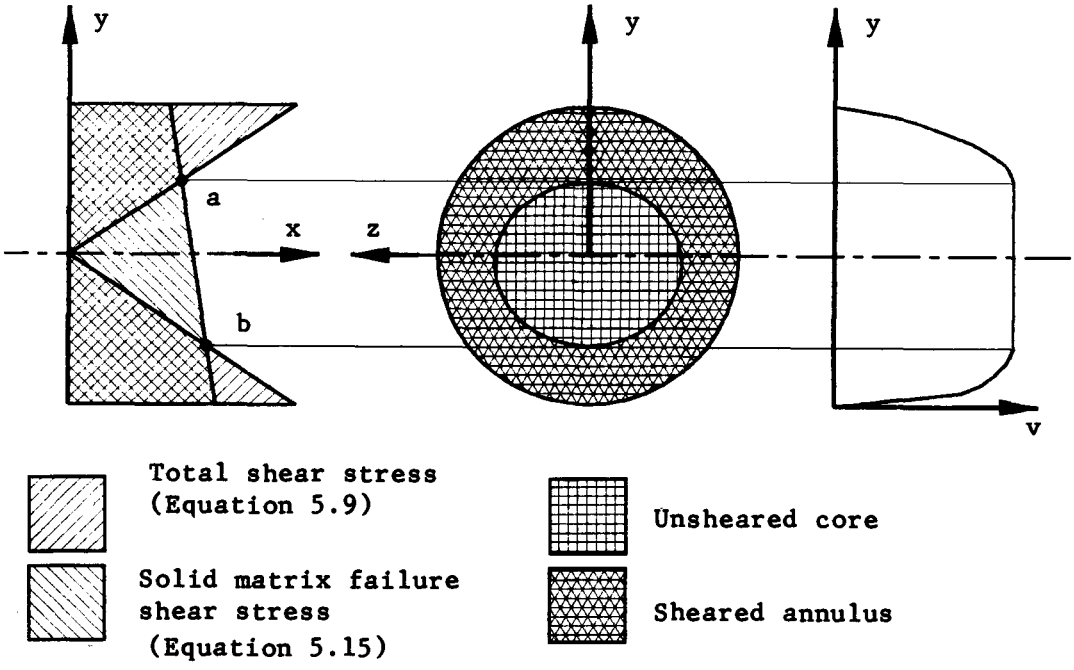

Figure 5.4 : Shear stress distribution in dense phase flow

2.4.3 *Normal stress due to applied axial stress*

Within the array of coarse particles the fluid pressure gradient causes a seepage flow of the fluid between the interstices of the granular matrix. The seepage flow may be considered negligible, providing the interstices between the solid particles are small. Appendix B presents the calculation of interstitial laminar flow and a worked example. This seepage flow exerts a stress on the particles in the direction of flow due to fluid dynamic drag. As the seepage flow is considered negligible, the fluid pressure gradient to overcome friction between the particle matrix and pipe wall is assumed to be entirely transferred to the particles as an interparticle stress.

Considering flow in inclined pipes an additional stress acts in the direction of flow due to the submerged weight of the solid particles acting in the x direction. Figure 5.5 illustrates the two special cases of vertical up flow and vertical down flow. In the case of flow vertically up the submerged weight of each particle acts downwards while the fluid dynamic drag force acting on each particle due to the pressure gradient required to overcome frictional resistance acts upward, thus the net force acting on each particle is the difference between the pressure force and its own submerged weight. For vertically downward flow the net force acting on each particle is the sum of the pressure force and the submerged weight.

The net interparticle axial stress acting on the assembly of particles is assumed to be :

$$\frac{d\,\tau_{sx}}{dx} = \left| \frac{dp}{dx} - (S_m - S_\ell)\,\rho\, g \sin \phi \right| , \qquad (5.17)$$

where τ_{sx} = axial normal interparticle stress

$\frac{dp}{dx}$ = fluid pressure gradient to overcome frictional resistance

S_m = relative density of mixture

S_ℓ = relative density of liquid

ϕ = slope of pipeline.

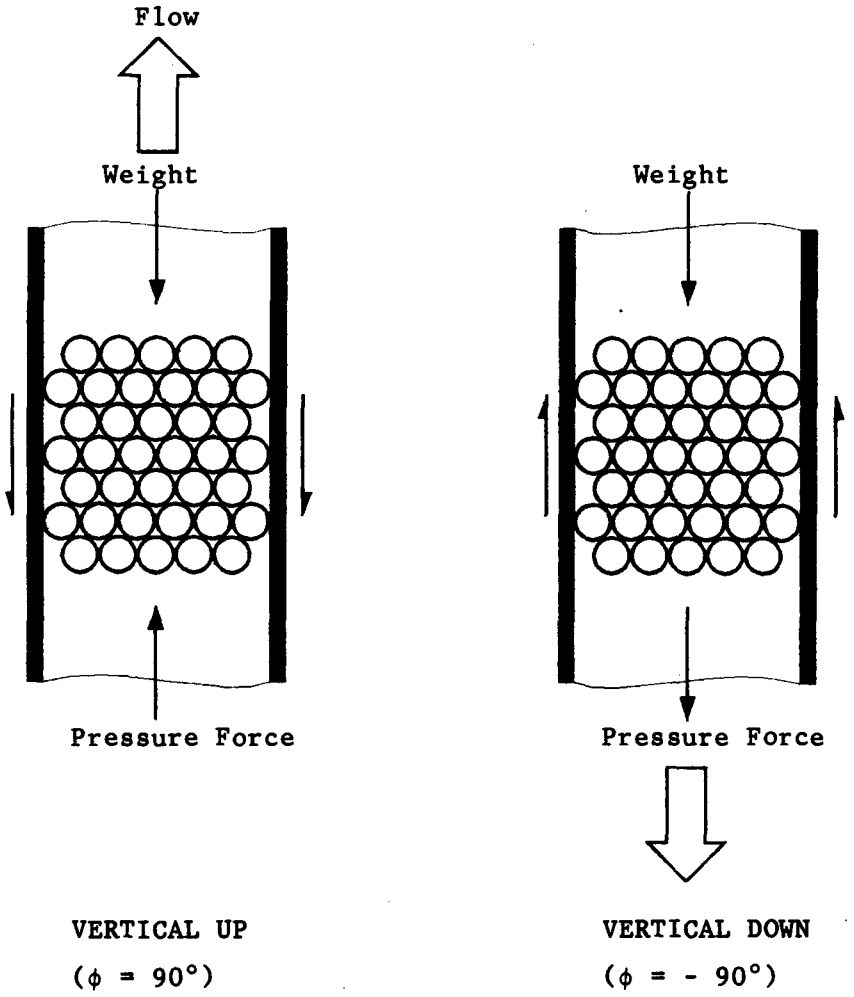

Figure 5.5 : Force acting on particles in vertical flow

The stresses acting on an idealised element in the granular mass are shown in Figure 5.6. From soil mechanics a normal intergranular stress τ_{sk} will act at right angles to the applied normal intergranular stress τ_{sx} (Wilson (1981)). The normal stresses are related as follows :

$$\tau_{sk} = \kappa \tau_{sx} \quad , \tag{5.18}$$

where κ = coefficient of lateral interparticle stress

k = y,z .

The coefficient κ is a function of solids concentration (particle packing density), particle size distribution, particle shape distribution and friction between the solid particles. As the dense phase mixture is assumed to be homogeneous the value of κ is taken as constant across a pipe section. For a unit length of pipe the normal intergranular stress is assumed to be :

$$(\tau_{sk})_{normal} = \kappa \left| \frac{dp}{dx} - (S_m - S_\ell)\, \rho\, g \sin \phi \right| . \tag{5.19}$$

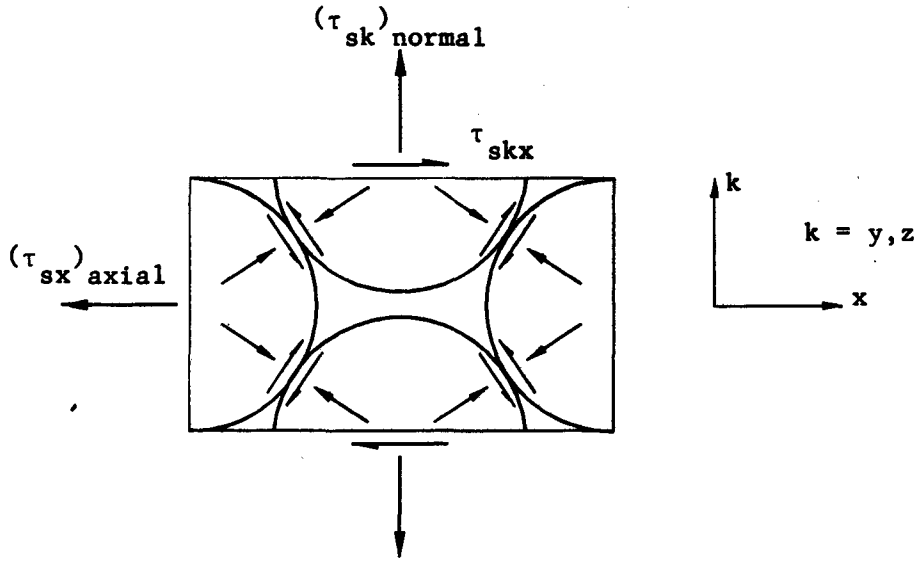

Figure 5.6 : Stresses acting on an idealised element

2.4.4 *Normal stress due to weight of particles*

The normal interparticle stress τ_{sk} has an additional component due to the self-weight of the solid particles acting in the yz plane. The normal stress at a point in the pipe section is evaluated assuming that the granular mass exerts a hydrostatic type of stress distribution proportional to its own weight (after Wilson (1970)). Assuming a homogeneous mixture we get :

$$\frac{d(\tau_{sk})_{weight}}{dy} = -\rho\, g\, (S_s - S_\ell)\, C \cos \phi \quad , \tag{5.20}$$

where τ_{sk} = normal stress due to submerged weight of solid particles

S_s = relative density of solid particles

C = local concentration of solid particles.

Integrating equation (5.20) to obtain the local value $(\tau_{sk})_{weight}$ yields :

$$(\tau_{sk})_{weight} = \rho\, g\, (S_s - S_\ell)\, C\, (\frac{D}{2} - y) \cos \phi \quad . \tag{5.21}$$

2.4.5 *Total normal interparticle stress*

Noting that $\tau_s = \tau_{sy} = \tau_{sz}$ (Wilson's hydrostatic stress distribution), and substituting equations (5.19) and (5.21) into relation (5.16) the total normal interparticle stress is assumed to be :

$$\tau_s = \kappa \left| \frac{dp}{dx} - (S_m - S_\ell)\, \rho\, g \sin \phi \right| + \rho\, g\, (S_s - S_\ell)\, C\, (\frac{D}{2} - y) \cos \phi \quad . \tag{5.22}$$

Thus $(\tau_{sx})_{failure}$ (equation 5.15) may be evaluated at any point within the pipe section using relation (5.22) to evaluate the total normal interparticle stress.

2.5 Shear stress at pipe wall due to solid phase

At the pipe wall the solid phase stress relation (5.14) becomes :

$$\tau_{sx} \leq \mu_d \tau_s \quad , \tag{5.23}$$

where μ_d = dynamic coefficient of sliding friction between the solid particles and pipe wall.

The coefficient of sliding friction is a function of the particle properties (particle size and shape distribution), and the roughness of the pipe wall. Generally μ_d will be less than the tangent of the internal angle of friction δ , as the friction between layers of sliding particles is greater than the friction between sliding particles and a smooth surface.

2.6 Differential equation for velocity distribution in a pipe

Considering the shear stresses acting in the mixture in our case of steady, uniform and unidirectional flow, we get by substituting the liquid phase stress relations ((5.10), (5.12) and (5.13)) and the solid phase stress equation (5.14) into expression (5.6) for the mixture shear stress :

$$\tau_{mkx} = \mu \left(\frac{\partial v}{\partial k}\right) + \frac{\partial (\alpha \rho v^2)}{\partial k} + \tau_{skx} \quad .$$

Thus the total mixture shear stress is the sum of the contributions from viscous shearing, turbulent shear stresses and the solid phase shear stress.

As the mixture is assumed to be homogeneous across the pipe section, μ is taken to be constant and thus we may rewrite the above equation as :

$$\tau_{mkx} = \frac{\partial (\mu v)}{\partial k} + \frac{\partial (\alpha \rho v^2)}{\partial k} + \tau_{skx} \quad . \tag{5.24}$$

Substituting equation (5.24) into the mixture momentum equation (5.7) we get :

$$0 = \frac{\partial^2 (\mu v)}{\partial y^2} + \frac{\partial^2 (\alpha \rho v^2)}{\partial y^2} + \frac{\partial \tau_{syx}}{\partial y}$$

$$+ \frac{\partial^2 (\mu v)}{\partial z^2} + \frac{\partial^2 (\alpha \rho v^2)}{\partial z^2} + \frac{\partial \tau_{szx}}{\partial z}$$

$$+ \rho_m F_x - \frac{dp}{dx} .$$

Simplifying we obtain :

$$0 = \nabla^2 (\mu v + \alpha \rho v^2) + \nabla \tau_{skx} + \rho_m g \sin \phi - \frac{dp}{dx} , \qquad (5.25)$$

where $\rho_m g \sin \phi$ = gravitational body force

∇ = gradient = $(\frac{\partial}{\partial y} + \frac{\partial}{\partial z})$

∇^2 = Laplacian operator = $(\frac{\partial^2}{\partial y^2} + \frac{\partial^2}{\partial z^2})$.

To solve equation (5.25) we consider the two zones shown in Figure 5.4 corresponding to the unsheared granular matrix and the sheared solid-liquid mixture.

2.6.1 *Unsheared solid particle matrix*

In this zone the local failure shear stress of the granular matrix is greater than the local total shear stress τ_m . Thus the shear stress acting in the granular matrix is equal to the local total shear stress and we have :

$$\nabla \tau_{skx} = \frac{dp}{dx} - \rho_m g \sin \phi . \qquad (5.26)$$

Substituting equation (5.26) into the velocity distribution equation (5.25) we get :

$$0 = \nabla^2 (\mu v + \alpha \rho v^2) . \qquad (5.27)$$

Thus the velocity gradient in the unsheared granular matrix is zero as shown in Figure 5.4.

2.6.2 *Sheared solid particle matrix*

In this annular region the local total shear stress in the slurry is greater than the failure shear stress of the granular matrix. Noting that as τ_{szx} is constant with respect to z in this region we get :

$$\frac{\partial \tau_{szx}}{\partial z} = 0 \quad .$$

and we can write the velocity distribution equation (5.25) as :

$$0 = \nabla^2 (\mu v + \alpha \rho v^2) + \frac{\partial \tau_{syx}}{\partial y} + \rho_m g \sin \phi - \frac{dp}{dx} \quad . \quad (5.28)$$

This differential equation is solved using the Finite Element Method as discussed in Section 4 of this chapter.

3. APPLICATION OF DENSE PHASE MODEL TO CYCLONE CLASSIFIED TAILINGS

3.1 Vehicle portion of the slurry

Materials with wide particle size distributions such as cyclone classified tailings contain particles which may be characterised as either "fine" or "coarse". The particles in the fine fraction are small enough to mix with the conveying medium (in our case water), and thus constitute the vehicle portion of the slurry. The coarse fraction is transported as a heterogeneous suspension, contact load or a combination of both. In this case dense phase flow is defined to exist when the concentration of the coarse fraction exceeds the freely settled packing concentration of the coarse particles, thus the coarse fraction forms a granular matrix filling the pipe section with particles supported by interparticle contact. The vehicle portion fills the interstices between the matrix of coarse particles.

In order to find the vehicle portion of the slurry a particle diameter d_t is defined as the particle size below which all particles in the particle size distribution, together with the water, form the vehicle. Govier and Charles (1961), from experience and laboratory tests, consider a mixture with a particle settling velocity of less than 1,5 to 0,6 mm/s to be non-settling, and treat such a mixture as pseudo-homogeneous fluid. Lazarus (1986) has characterised a non-settling mixture as one in which the settling velocities of the particles are less than 0,1 mm/s, and a slow settling slurry is considered to have a particle settling velocity of less than 1 mm/s. Although these classifications are arbitrary, they present a useful method for dividing the slurry in fine and coarse fractions. For our purposes we define the vehicle portion of the slurry to contain that fraction of solid particles which have a settling velocity of less than 1 mm/s.

Considering the fall of a particle of diameter d, we assume the particle to be falling through a homogeneous mixture comprising the conveying liquid (water) and all other particles of size less than d. Stokes' law for laminar settling in a homogeneous fluid is :

$$V_{set} = (S_s - S_{mF}) \frac{g\, d^2}{18\, \nu_{mF}} , \qquad (5.29)$$

where V_{set} = particle settling velocity
S_{mF} = relative density of mixture of water and solid particles of size less than d.
ν_{mF} = kinematic coefficient of viscosity of the mixture of water and solid particles of size less than d.

Defining a particle settling shape factor S_f as the ratio of the terminal settling velocity of the particle to the terminal settling velocity of a sphere with an equivalent volume and density, and solving for d we get :

$$d = \sqrt{\frac{18\, v_{set}\, \nu_{mF}}{g\, S_f\, (S_s - S_{mF})}} .$$

Evaluating the above expression with the settling velocity equal to 1 mm/s we obtain the transition particle diameter :

$$d_t = \sqrt{\frac{0{,}018\, \nu_{mF}}{g\, S_f\, (S_s - S_{mF})}} . \qquad (5.30)$$

Note all particles smaller than d_t form the vehicle portion of the slurry.

3.2 Definition of dense phase flow for slurries with wide particle size distributions

Referring to Figure 5.7 dense phase flow is defined to exist when

$$C_C = P_C C_m \geq C_{C\,min} \quad , \tag{5.31}$$

where C_C = concentration of coarse fraction
C_m = concentration of mixture
$C_{C\,min}$ = minimum packing concentration of coarse fraction
P_C = percentage of coarse particles in mixture as defined in Figure 5.7.

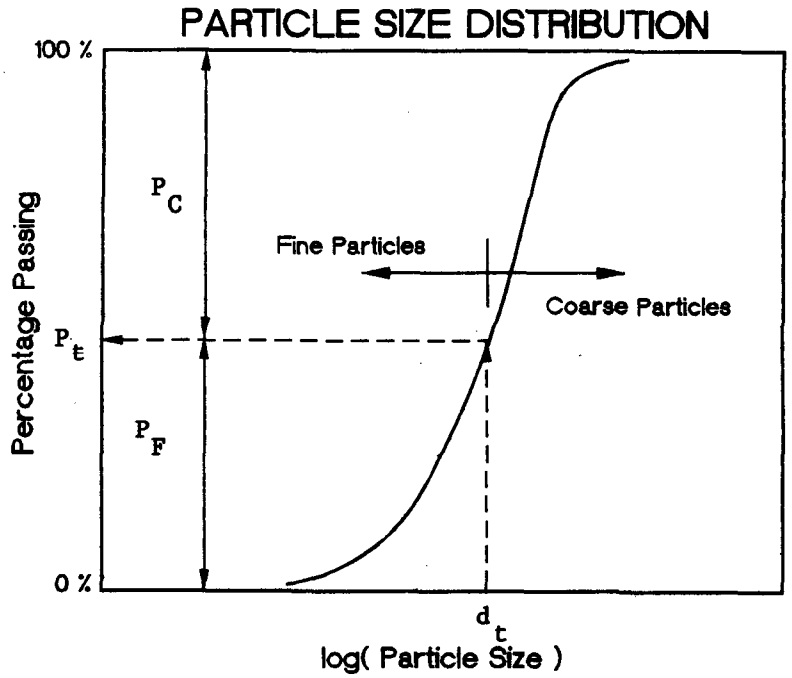

Figure 5.7 : Particle size distribution split into fine and coarse fractions

3.3 Fluid shear stress in mixture

The fluid shear stress at any point consists of components of viscous and turbulent origin. In the dense phase mixtures considered in this investigation it is assumed that the turbulent shear stresses are negligible as the high concentration solid particle matrix almost completely damps the turbulence. Thus the liquid phase shear stress equation (5.10) becomes :

$$\tau_\ell = (\tau_\ell)_{viscous} \quad . \tag{5.32}$$

The Newtonian viscosity of a pseudo-homogeneous suspension of particles is determined by the viscosity of the carrier liquid, solids concentration, particle size distribution and particle shape distribution. The correlation of Landel *et al* (Govier and Aziz (1972)) is widely used to evaluate μ_m :

$$\frac{\mu_m}{\mu} = (1 - \frac{C}{C_{max}})^m \quad , \tag{5.33}$$

where μ = dynamic coefficient of viscosity for water

C = concentration of solids in mixture

C_{max} = maximum attainable concentration of the solid particles

m = experimental coefficient, Landel *et al* found that with $m = -2,5$ they obtained a good correlation to their measurements carried out on water suspensions of particles of various densities in the size range of 10 μm to over 100 μm (Govier and Aziz (1972)).

The viscosity of the *vehicle portion* of the slurry may be obtained from the following relation :

$$\frac{\mu_{mV}}{\mu} = \left(1 - \frac{C_F}{C_{Fmax}}\right)^m , \qquad (5.34)$$

where C_F = concentration of fine fraction in mixture
C_{Fmax} = maximum attainable concentration of the fine fraction.

The concentration of fines may be calculated using

$$C_F = \frac{P_F\, C_m}{1 - P_C\, C_m} , \qquad (5.35)$$

where P_F = percentage of fine particles in mixture as defined in Figure 5.7.

3.4 Shear stress due to coarse solid particles

The stress relations developed in sections 2.4 and 2.5 of this chapter are applicable, although the normal stress relation (5.22) must be modified to account for the presence of the vehicle :

$$\tau_s = \kappa \left| \frac{dp}{dx} - (S_m - S_{mV})\, \rho\, g \sin \phi \right| + \rho\, g\, (S_S - S_{mV})\, C_C \left(\frac{D}{2} - y\right) \cos \phi \quad . \qquad (5.36)$$

3.5 Differential equation for velocity distribution in a pipe

As the degree of turbulence in the mixture is assumed negligible, the shear stress due to turbulence may be neglected (equation (5.32)), and thus we may write the velocity distribution equation (5.28) for the sheared zone as :

$$0 = \nabla^2 (\mu\, v) + \frac{\partial\, \tau_{syx}}{\partial y} + \rho_m\, g \sin \phi - \frac{dp}{dx} \quad . \qquad (5.37)$$

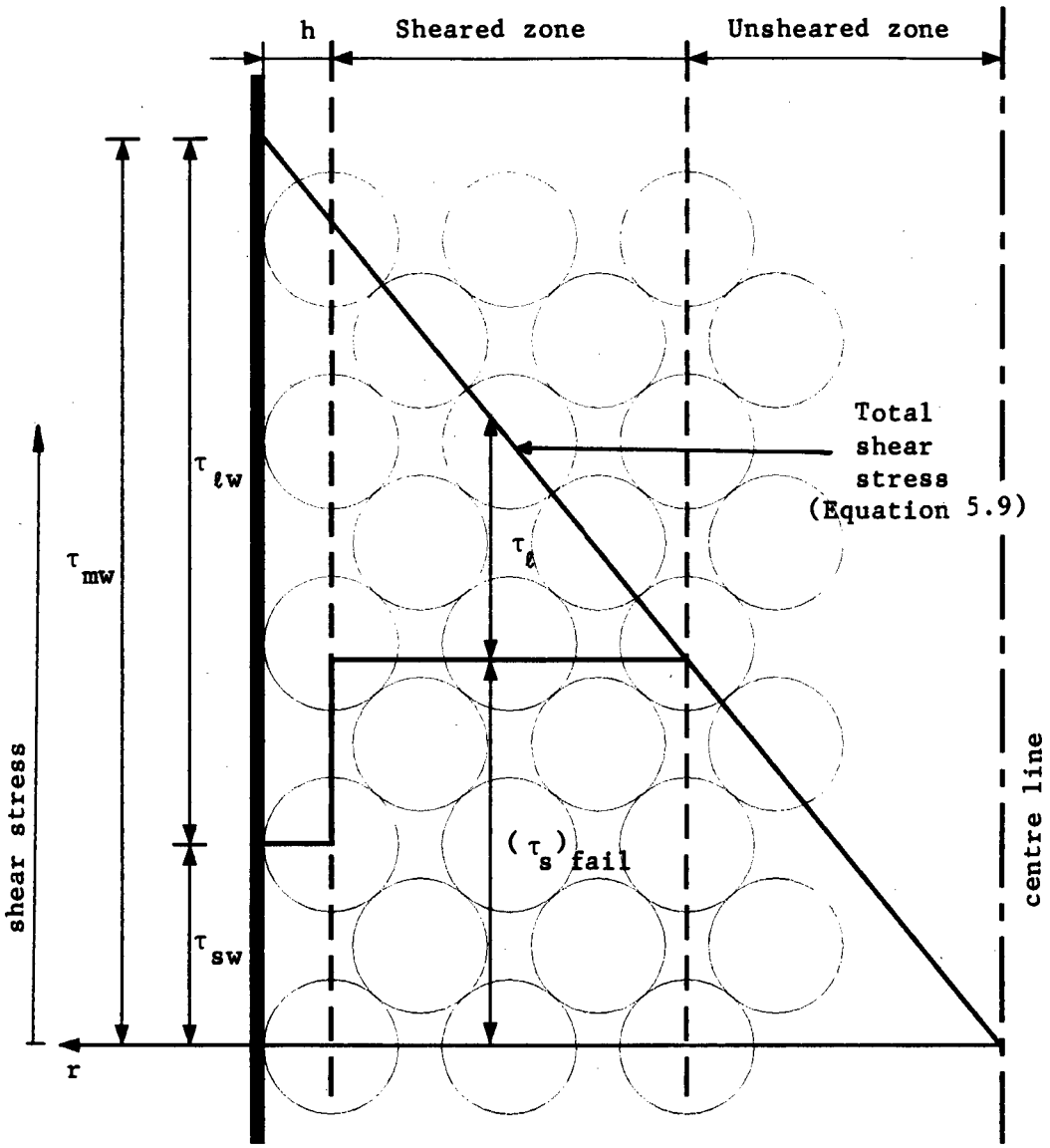

Figure 5.8 : Shear stress distribution

3.6 Boundary conditions at pipe wall

At the pipe wall the granular matrix of coarse particles is treated as a rough boundary moving at velocity v with a fluid shear layer of thickness h between the pipe wall and the granular matrix. The asperities of the coarse particles penetrate through the fluid shear layer, thereby transferring the solid phase shear stress τ_{ws} to the pipe wall via mechanical sliding friction. The fluid shear stress at the pipe wall is obtained from :

$$\tau_{w\ell} = \tau_w - \tau_{ws} \quad , \tag{5.38}$$

where τ_w = total shear stress at pipe wall = $\frac{D}{4}\frac{dp}{dx}$

τ_{ws} = solid phase shear stress at pipe wall = $\mu_d \tau_s$.

Figure 5.8 shows the solid and liquid phase shear stress distributions in the zone near the pipe wall. The evaluation of the thickness of the fluid shear layer is discussed in detail in Section 3.6.4.

3.6.1 *Solid phase shear stress at pipe wall*

Figure 5.9 shows the possible flow regimes which may occur in dense phase flow.

Unsheared core surrounded by sheared annulus

The failure stress of the coarse particles matrix is exceeded by the applied shear stress along the whole circumference of the pipe diameter as shown in Figure 5.9(a). The local solid shear stress at the pipe wall may be evaluated using equation (5.23), i.e.

$$\tau_{ws} = \mu_d \tau_s$$

where τ_s = local normal solid stress - equation 5.22

μ_d = dynamic coefficient of friction between the solid particles and pipe wall.

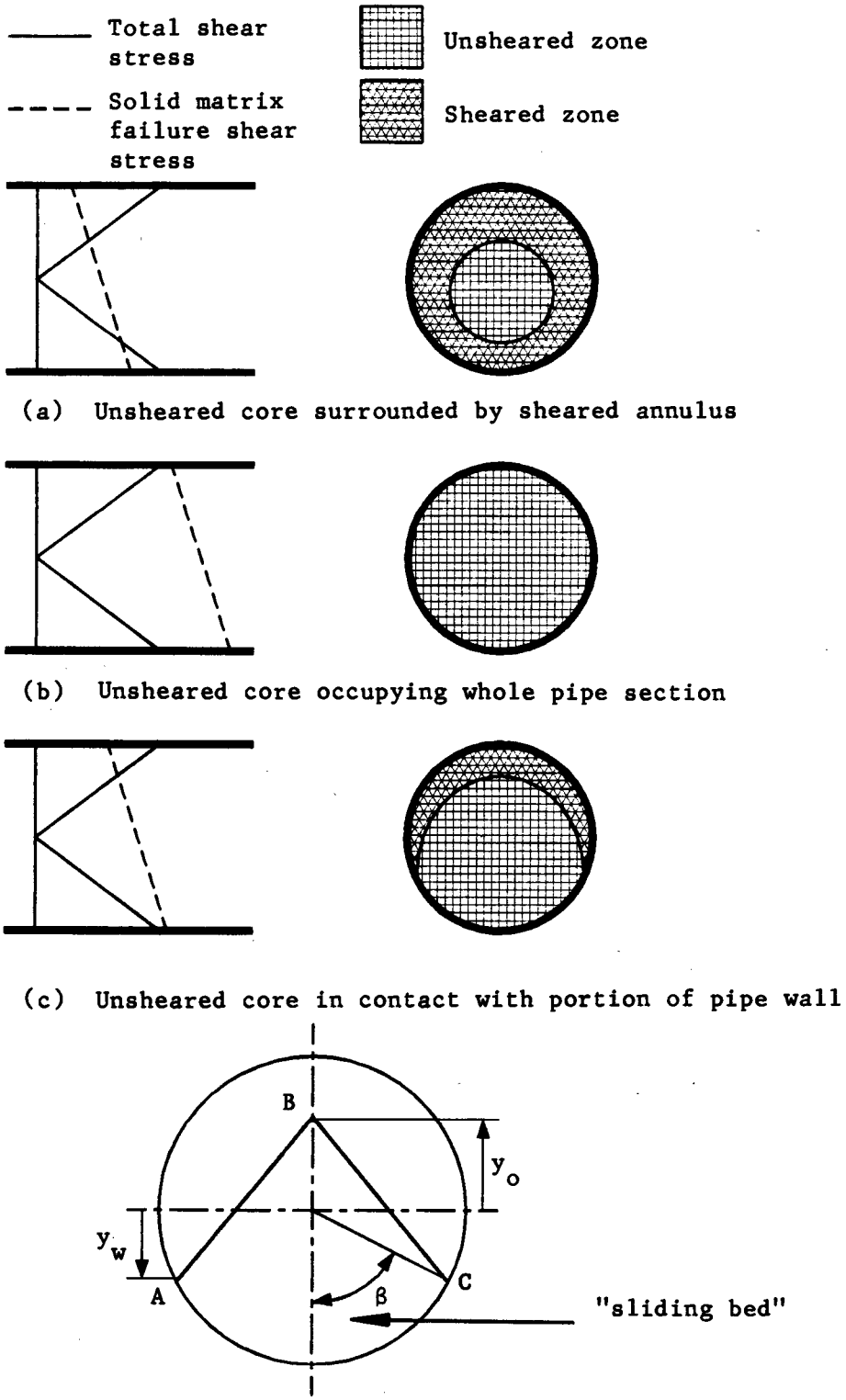

(a) Unsheared core surrounded by sheared annulus

(b) Unsheared core occupying whole pipe section

(c) Unsheared core in contact with portion of pipe wall

(d) Modelled "sliding bed" geometry

Figure 5.9 : Dense phase flow regimes

Unsheared core in contact with pipe wall

The failure shear stress of the coarse particle matrix is greater than the applied shear stress along a portion of the whole of the pipe circumference. Thus the flow regime may be a sliding "bed" of the unsheared coarse particle matrix with the sheared zone above (Figure 5.9(c)), or an unsheared plug occupying the whole pipe section (Figure 5.9(b)).

For the portion of the pipe wall in contact with the sheared zone the solid phase shear stress equation (5.23) may be used to determine the local solid shear stress at the pipe wall.

Within the unsheared zone of the coarse particle the local shear stress does not necessarily obey the linear stress distribution (equation (5.9)), consequently we treat the unsheared zone as a rigid body and consider the average shear stress between the solid phase and pipe wall. The unsheared zone is approximated by assuming that the transition between the two zones occurs along a straight line ABC from the intersection at the pipe wall and the intersection point on the y axis (Figure 5.9(d)). The intersection points are as follows :

$$x_w = \sqrt{(D/2)^2 - y_w} \quad , \quad y_w = \frac{D}{2} - \frac{(\frac{A.D}{4} - B)}{E} \quad ; \qquad (5.39)$$

and

$$x_o = 0 \quad , \quad y_o = \frac{B + \frac{ED}{2}}{E + \frac{A}{2}} \quad , \qquad (5.40)$$

where $A = \frac{dp}{dx}$

$$B = \kappa \left| \frac{dp}{dx} - (S_m - S_{mV}) \rho g \sin \phi \right| \tan \delta$$

$$E = \rho g (S_s - S_{mV}) C_c \cos \phi \tan \delta \quad .$$

To obtain the average solid shear stress acting on the unsheared zone at the pipe wall, the local shear stresses are integrated over the portion of the pipe wall in contact with the unsheared zone and divided by the contact length :

$$\bar{\tau}_{ws} = \frac{\int_0^{\beta} \tau_{ws}(\alpha)\, D\, d\alpha}{\beta D}$$

$$= \left[\rho g (S_s - S_{mV}) C_c \frac{D}{2} \left(\frac{(\beta - \sin\beta)}{\beta}\right) + \kappa \left| \frac{dp}{dx} - (S_m S_{mV}) \rho g \sin\phi \right| \right] \mu_d \quad , \qquad (5.41)$$

where $\tau_{ws}(\alpha)$ is evaluated from the solid phase shear stress equations (5.22) and (5.23).

For the limiting case of the unsheared zone filling the whole pipe section (i.e. $\beta = \pi$) we get :

$$\bar{\tau}_{ws} = \left[\rho g (S_s - S_{mV}) C_c \frac{D}{2} + \kappa \left| \frac{dp}{dx} - (S_m S_{mV}) \rho g \sin\phi \right| \right] \mu_d \quad .$$

3.6.2 *Vehicle shear stress at pipe wall*

The flow between the rough boundary (coarse particle matrix) and the pipe wall may be treated as parallel Couette flow. Reichardt has shown that for parallel Couette flow of a Newtonian fluid the flow remains laminar for Reynolds numbers below 1 500 (Schlichting (1968) p.557-558). The Couette flow Reynolds number is defined as :

$$Re_{CF} = \frac{\bar{v}\, h}{\nu} \quad , \qquad (5.42)$$

where ν = kinematic coefficient of viscosity for the fluid

$\bar{v}$ = mean velocity of fluid = ½ v.

As the particles in a suspension would tend to suppress the onset of turbulence, the above criteria may be applied as a lower bound value of the transition from laminar to turbulent flow. For typical values of h and $\bar{v}$ for the dense phase flow of classified tailings the value of Re_{CF} will generally be less than 400, and consequently we treat the flow in layer h as laminar.

The rate of strain in the fluid ($\frac{dv}{dy}$, i.e. velocity gradient) is related to the shear stress as follows :

$$\tau = f\left(\frac{dv}{dy}\right) \quad . \tag{5.43}$$

As the shearing stress imposed on the fluid remains constant in Couette flow, we can write relation (5.43) as :

$$\tau_{w\ell} = f\left(\frac{v}{h}\right) \quad , \tag{5.44}$$

where v = local velocity of granular matrix at distance h radially inwards from pipe wall.

3.6.3 *Boundary velocity of coarse particle matrix*

From the constitutive equation (5.12) for a Newtonian fluid and the fluid wall shear stress - velocity gradient relation (5.44), the local boundary velocity of the *sheared* coarse particle matrix is

$$v = \frac{\tau_{w\ell}\, h}{\mu_{mV}} \quad , \tag{5.45}$$

where $\tau_{w\ell} = \tau_w - \tau_{ws}$ (equation 5.38)
μ_{mV} = viscosity of vehicle equation 5.34).

Note the viscosity of the vehicle is used at the pipe wall, while the viscosity of the total mixture (equation 5.33) is used over the pipe section. If $\tau_{w\ell}$ is less than or equal to zero the coarse particle matrix is stationary at that point.

Considering the *unsheared* coarse particle matrix in contact with the pipe wall we get :

$$v_{bed} = \frac{\bar{\tau}_{w\ell}\, h}{\mu_{mV}} \quad , \tag{5.46}$$

where v_{bed} = velocity of unsheared "bed" of coarse particles

$\bar{\tau}_{w\ell} = \tau_w - \bar{\tau}_{ws}$ = average fluid shear stress at pipe wall

$\bar{\tau}_{ws}$ = average solid phase shear stress at pipe wall (equation 5.41).

3.6.4 *Evaluation of boundary fluid shear layer thickness*

As the solids concentration in the mixture increases, the thickness of the fluid shear layer at the pipe wall boundary h decreases due to a change in the packing configuration of the coarse particles. This effect is illustrated in Figure 5.10.

The thickness of the fluid shear layer h is taken to equal half the diameter of a representative particle size of the coarse fraction d_{Crep} when the concentration of the coarse particles equals the freely settled concentration C_{Cmin} . The representative particle size of the coarse fraction is assumed to equal the d_{50} particle size of the coarse fraction.

The case with the coarse particle concentration equal to C_{Cmin} and the thickness of the fluid shear layer equal to half the representative diameter of the coarse fraction is used as a basis of comparison to evaluate the variation of the thickness of the fluid shear layer with solids concentration. The volume of the coarse particles in the annulus between the pipe wall and layer h is used as a reference volume V_{sref} .

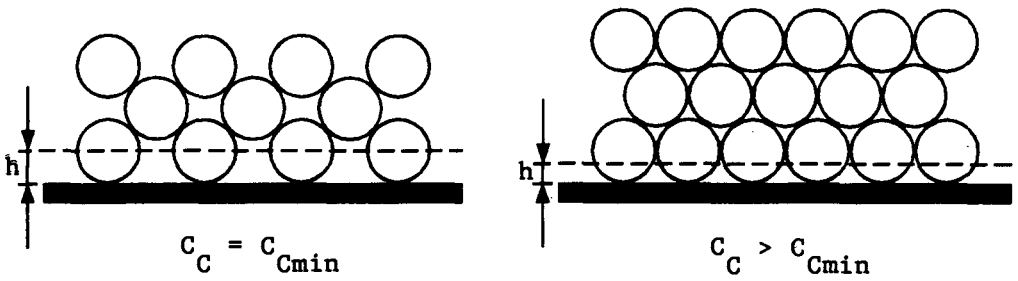

Figure 5.10 : Variation in thickness of fluid shear layer with solids concentration

In cases where the concentration of the coarse particles exceeds C_{Cmin} the thickness of the fluid shear layer is determined by choosing h such that the volume of coarse particles in the annulus of sheared fluid equals the reference volume $\forall_{sref}$.

The volume of coarse particles $\forall_s$ in the sheared fluid annulus is determined as follows :

Assuming that all the particles of the coarse fraction have diameter d_{Crep} and are spherical we get for a unit length of pipe :

$$\text{Total number of particles} = \frac{\text{Total volume of solids}}{\text{Volume of one particle}} \qquad (5.47)$$

$$= \frac{3}{2} C_c \frac{1}{d_{Crep}} \left(\frac{D}{d_{Crep}}\right)^2 .$$

Assuming that no particle further than d_{Crep} from the pipe wall can touch the pipe wall (after Liu and Schmidt (1985)) the fraction of solids which can be in contact with the wall is

$$\frac{4\, d_{Crep}\,(D-1)}{D^2} ,$$

thus the number of particles contacting wall

$$= 6\, C_c \frac{1}{d_{Crep}} \left(\frac{D}{d_{Crep}} - 1\right) . \qquad (5.48)$$

The volume of a single spherical particle (touching the pipe wall) in fluid shear layer h is :

$$\forall_{particle} = \int_{o}^{h} \pi \left(\frac{d_{Crep}^2}{4} - \left(\varsigma - \frac{d_{Crep}}{2}\right)^2 \right) d\varsigma$$

$$= \pi \left[\frac{h^2 \, d_{Crep}}{2} - \frac{h^3}{3} \right] , \qquad (5.49)$$

where ς is measured radially inwards from the pipe wall.

The total volume of coarse particles in the sheared layer is

$$\forall_s = 6 \, C_c \, \frac{1}{d_{Crep}} \left(\frac{D}{d_{Crep}} - 1\right) \pi \left[\frac{h^2 d_{Crep}}{2} - \frac{h^3}{3} \right] \qquad (5.50)$$

For the reference case ($C_C = C_{Cmin}$, $h = d_{Crep}/2$), we obtain the volume of solid particles in the fluid shear layer as :

$$\forall_{sref} = \frac{\pi}{2} \, C_{Cmin} \, d_{Crep}^2 \left(\frac{D}{d_{Crep}} - 1\right) . \qquad (5.51)$$

Thus the thickness of the fluid shear layer h may be evaluated by matching the volume of coarse particles in the fluid sheared layer $\forall_s$ (equation 5.50) to the reference volume $\forall_{sref}$ (equation 5.51).

3.7 Solution procedure

The required input values for the model and the solution algorithm are shown in Figure 5.11.

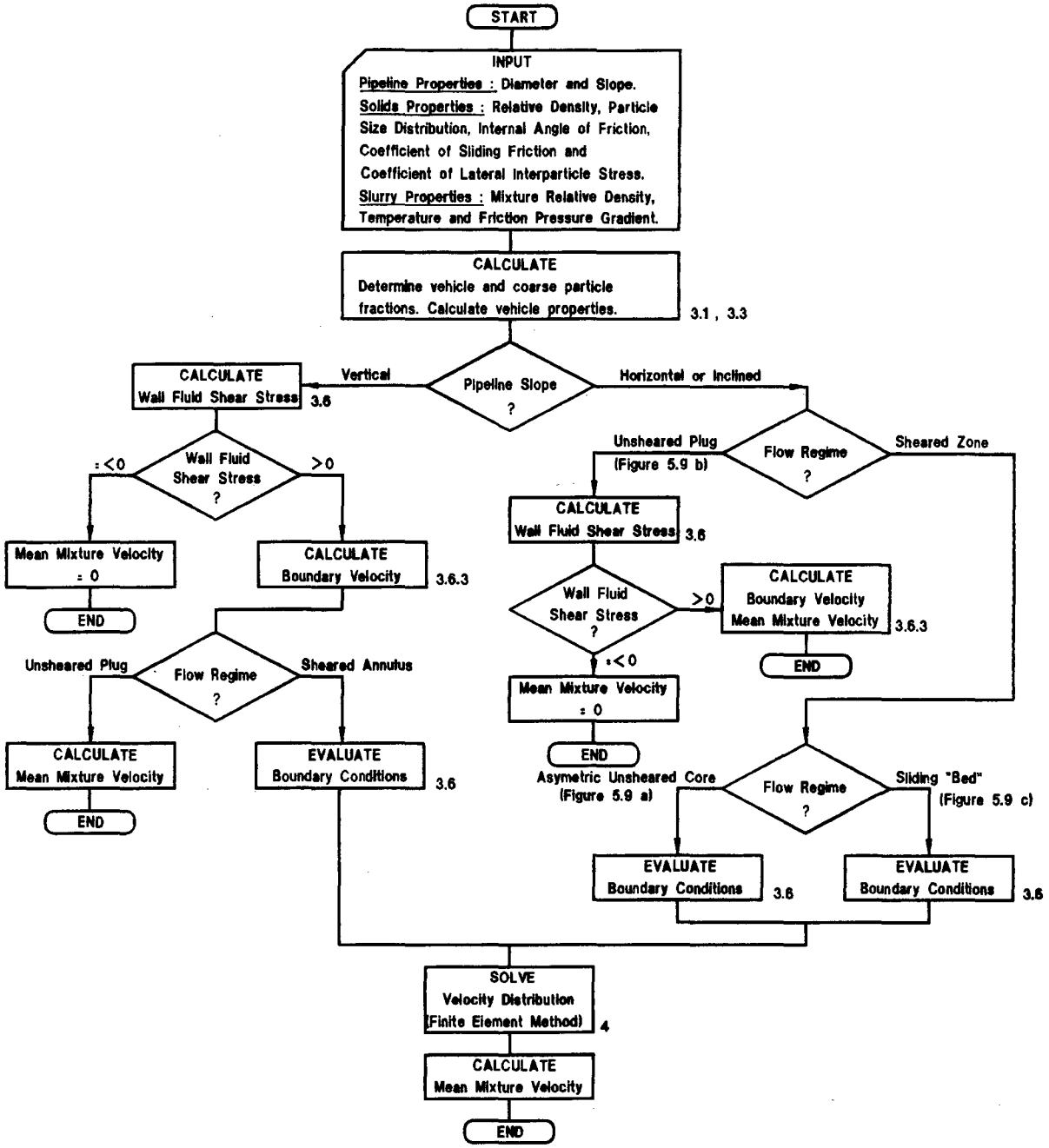

NOTE : Numbers to the bottom right of processing blocks indicate relevant sections in this chapter.

Figure 5.11 : Solution algorithm

4. SOLUTION OF DIFFERENTIAL EQUATION DESCRIBING THE VELOCITY DISTRIBUTION BY THE FINITE ELEMENT METHOD

4.1 Problem definition

The velocity distribution equation (5.37) may be expressed as :

$$0 = v^2 \epsilon + \gamma(y) \quad , \tag{5.52}$$

where $\epsilon = \mu_m v$

$$\gamma(y) = \frac{\partial \tau_{syx}}{\partial y} + \rho_m g \sin\phi - \frac{dp}{dx} \quad .$$

Equation (5.52) has the same form as the steady state heat conduction problem which has been described by Owen and Hinton (1979) and Owen and Hinton (1980). The method described herein is based on the solution procedure outlined by the above authors. The differential equation is solved to obtain local values of ϵ (and thus v).

4.2 Boundary conditions

The finite element method is used to solve the velocity distribution in the region of the pipe section bounded by the fluid shear layer at the pipe wall, i.e. over the area $\pi (D-2h)^2/4$. The following boundary conditions are applied to the differential equation describing the velocity distribution (5.52) :

(i) Boundary velocity

The local boundary velocities are evaluated using equation (5.45) and (5.46) as discussed in Section 3.6.3.

(ii) Unsheared zone

In the zone of the pipe section where the failure shear stress of the granular matrix is greater than the applied shear stress we get from equation (5.27) of Section 2.6.1 :

$$v^2 \epsilon = 0 \quad . \tag{5.53}$$

Thus in this zone the velocity gradient will be zero as shown in Figure 5.4.

(iii) Sheared zone

Throughout the sheared zone of the pipe section the applied shear stress exceeds the failure stress of the granular matrix. Considering a vertical pipe (τ_{sfail} constant across the whole pipe section) we get for the sheared zone :

$$\nabla \tau_{skx} = 0 \quad . \tag{5.54}$$

Substituting equation (5.54) into the differential equation (5.52) we get :

$$\nabla^2 \epsilon = \frac{dp}{dx} - \rho_m g \sin \phi \quad . \tag{5.55}$$

Equation (5.55) implies that all the applied loading (due to the pressure gradient required to overcome friction and weight) is used to generate the velocity distribution, i.e. the viscous shearing stress of the mixture must equal the applied shear stress. Figure 5.12 shows a cross-section of dense phase flow with sheared and unsheared zones. We know that the solid shear stress at the periphery of the unsheared core and at the boundary of the fluid shear layer equal the failure shear stress of the granular matrix τ_{sfail} . It is clear that the integrated solid shear stress along the outer boundary of the sheared annulus is greater than the integrated solid shear stress along the inner boundary of the sheared annulus. Thus some of the applied loading is used to generate this "extra" solid shear, and clearly equation (5.55) is not applicable in our case.

To evaluate the velocity distribution in the sheared zone we need to establish the pressure gradient acting on the mixture producing the velocity distribution, i.e. the difference between the applied pressure gradient and the pressure

gradient used to shear the granular matrix and overcome the friction at the pipe wall. This is done by determining an average fluid shear pressure gradient $(\overline{\frac{dp}{dx}})_\ell$ by applying a force balance to the sheared zone. We consider the following cases :

(i) the unsheared cone forms a symmetric or symmetric core surrounded by the sheared annulus.

(ii) the unsheared zone is in contact with the pipe wall.

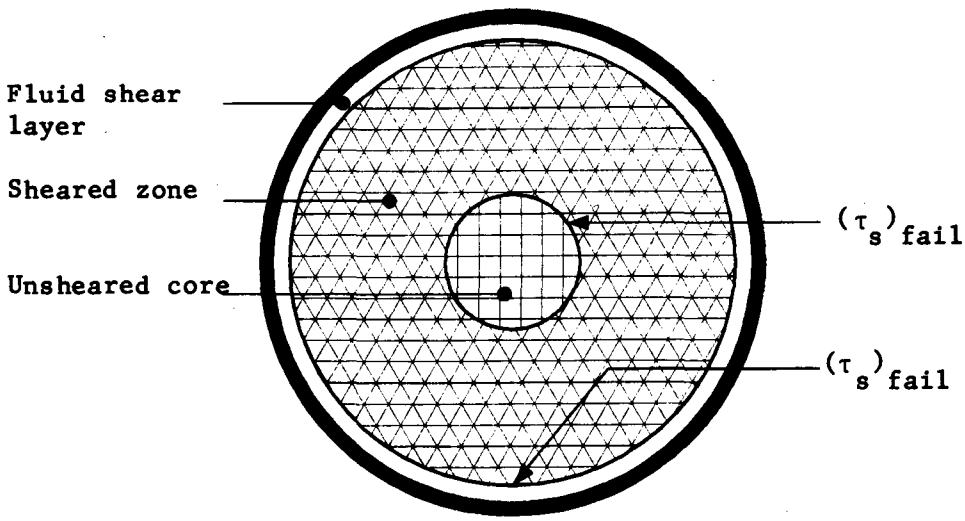

Figure 5.12 : Solid phase stresses acting on sheared zone

4.2.1 *Annular sheared zone*

This case is illustrated in Figure 5.13(a). The liquid shear stress at the outer periphery of the core equals zero. The liquid shear stress at the outer boundary of the sheared zone is found from :

$$\tau_\ell = \tau_m - \tau_{sfail} \quad . \tag{5.56}$$

The intersection points of the boundary of the unsheared core with y axis are :

$$x = 0 \ , \qquad y_{ot} = \frac{B + \frac{ED}{2}}{E + \frac{A}{2}} \tag{5.57}$$

$$x = 0 \ , \qquad y_{ob} = \frac{B + \frac{ED}{2}}{E + \frac{A}{2}} \ , \tag{5.58}$$

where $A = \frac{dp}{dx}$

$$B = \kappa \left| \frac{dp}{dx} - (S_m - S_{mV}) \rho g \sin \phi \right| \tan \delta$$

$$E = \rho g (S_m - S_{mV}) C_c \cos \phi \tan \delta \quad .$$

The area of the unsheared core is approximated by the area of a circle with diameter equal to $y_{ot} - y_{ob}$. Applying the force balance to the sheared zone we get :

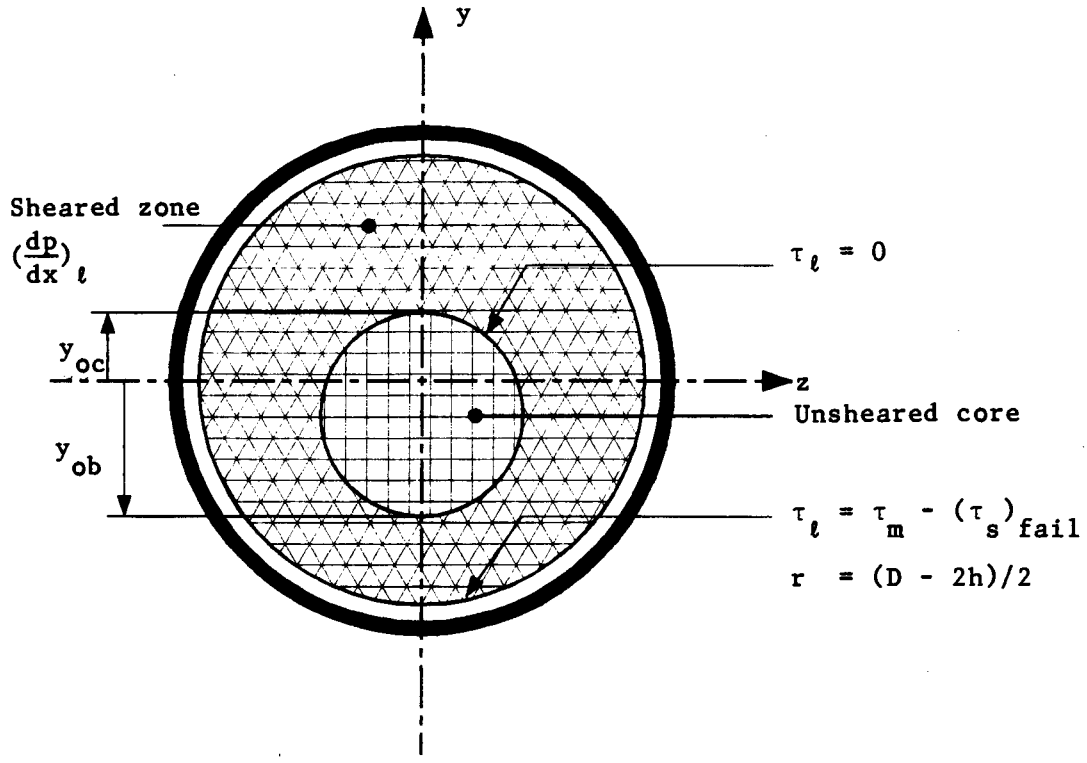

(a) Asymmetric core

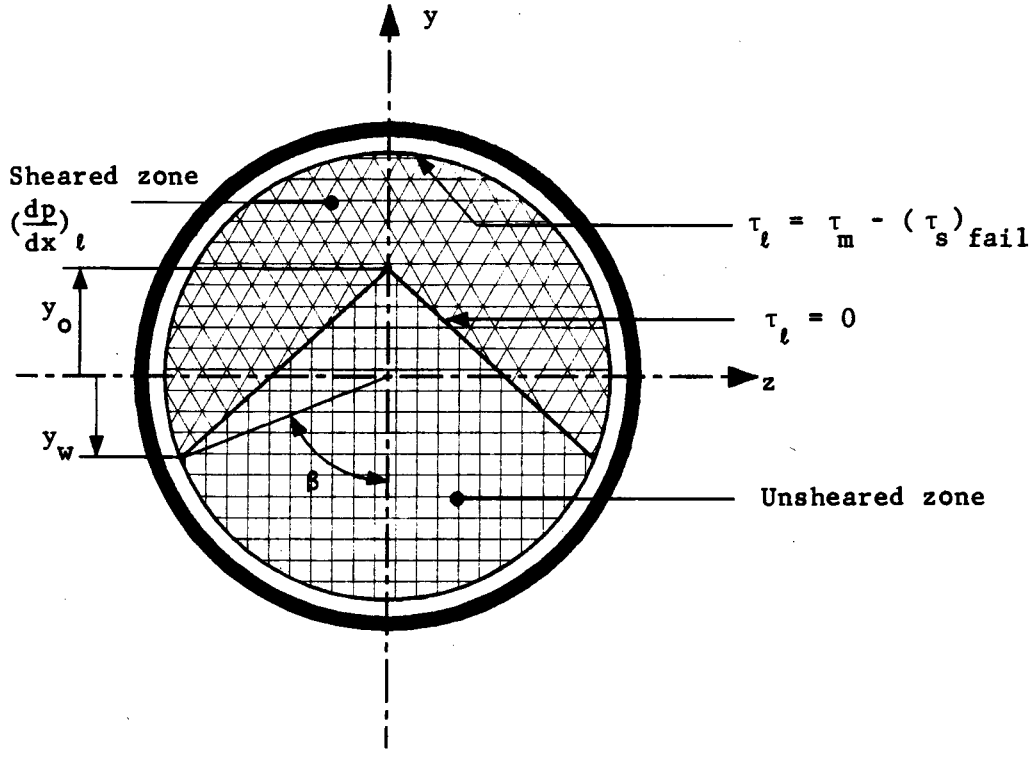

(b) Unsheared zone in contact with pipe wall

Figure 5.13 : Fluid shear stresses

$$\left(\overline{\frac{dp}{dx}}\right)_\ell = \frac{2\int_0^{\pi} R_h\,\tau_\ell\,(h)\,d\alpha}{\left[\pi R_h^2 - \pi\,\frac{(y_{ot} - y_{ob})^2}{4}\right]}\,, \qquad (5.59)$$

where $R_h = \frac{D}{2} - h$.

The integral is numerically solved by evaluating the local values of the liquid shear stress at the outer boundary of the sheared zone.

4.2.2 *Unsheared core in contact with pipe wall*

Figure 5.13(b) shows the case with the unsheared zone in contact with pipe wall. The boundary of the unsheared zone is taken as a straight line between the intersection points on the y axis and pipe wall as discussed in Section 3.6.1. The liquid shear stress along this straight line is zero. The liquid shear stress acting along r = D/2 - h on the sheared zone is evaluated using equation (5.56). The intersection point with the y axis is found from equation (5.57), and the wall intersection from

$$x_w = \sqrt{(D/2)^2 - y_w}\,, \quad y_w = \frac{D}{2} - \frac{(\frac{A\,D}{4} - B)}{E}\,. \qquad (5.60)$$

The force balance on the sheared zone yields :

$$\left(\overline{\frac{dp}{dx}}\right)_\ell = \frac{2\int_\beta^{\pi} R_h\,\tau_\ell\,(h)\,d\alpha}{\left[\pi R_h^2 - [(y_o - y_w)R_h \sin\beta + \beta R_h^2 - y_w R_h \sin\beta]\right]}\,. \qquad (5.61)$$

4.3 Galerkin weighted residual method

The Galerkin method seeks to minimise the error, e in satisfying equation (5.52) by an approximate solution. In this case it is required that

$$\int_A e\, w\, dA = 0 \quad , \tag{5.62}$$

where $e = \frac{\partial^2 \epsilon}{\partial y^2} + \frac{\partial^2 \epsilon}{\partial z^2} + \gamma$ (5.63)

A = pipe cross-sectional area

w = weighting function.

Substituting (5.63) into (5.62) we get :

$$\int_A \left[\frac{\partial^2 \epsilon}{\partial y^2} + \frac{\partial^2 \epsilon}{\partial z^2} + \gamma \right] w\, dA = 0 \quad . \tag{5.64}$$

The Green-Gauss theorem relates the integrals of quantities over a region A and over its boundary S as follows :

$$\int_A \left[\frac{\partial C}{\partial x} \frac{\partial D}{\partial x} + C \frac{\partial D^2}{\partial x^2} \right] dA = \int_S C \frac{\partial D}{\partial x} n_x\, dS \quad , \tag{5.65}$$

where C,D = arbitrary scaler functions.

Applying (5.65) to (5.64) we get :

$$\int_S \left[\frac{\partial \epsilon}{\partial y} n_y + \frac{\partial \epsilon}{\partial z} n_z \right] w \, dS$$

$$- \int_A \left[\frac{\partial w}{\partial y} \frac{\partial \epsilon}{\partial y} + \frac{\partial w}{\partial z} \frac{\partial \epsilon}{\partial z} - \gamma w \right] dA = 0 . \qquad (5.66)$$

According to the finite element method the unknown function ϵ is approximated throughout the domain, A as

$$\epsilon = \sum_{i=1}^{n} N_i a_i , \qquad (5.67)$$

where n_i = total number of nodes in the finite element mesh

N_i = global shape functions

a_i = nodal values of ϵ .

In the Galerkin process the number of weighting functions must equal the total number of unknown nodal values. The weighting function w_i corresponding to node i is chosen to equal the shape function N_i . At all nodes where the value of ϵ is prescribed (i.e. boundary condition imposed) there is no unknown associated with the point and consequently the weighting function is zero at the point. Thus the first integral in equation (5.66) is zero as ϵ is specified along S by boundary condition (i) of Section 4.2. Substituting expression (5.67) into equation (5.66) and noting above we get :

$$\int_A \left[\sum_{i=1}^{n} \left(\frac{\partial N_i}{\partial y} \frac{\partial N_j}{\partial y} + \frac{\partial N_i}{\partial z} \frac{\partial N_j}{\partial z} \right) aj - N_i \gamma \right] dA = 0 . \qquad (5.68)$$

Expression (5.68) represents a system of $i = 1, n$ equations in which the equations corresponding to nodal points at which ϵ is prescribed are deleted. The expression may be rewritten as :

$$\sum_{j=1}^{n} \left[\int_A \left(\frac{\partial N_i}{\partial y} \frac{\partial N_j}{\partial y} + \frac{\partial N_i}{\partial z} \frac{\partial N_j}{\partial z} \right) dA \right] aj = \int_A \gamma N_i \, dA \, , \quad (5.69)$$

or in matrix form as

$$\tilde{K} \, \tilde{a} = \tilde{f} \, ,$$

where $\tilde{K}_{ij}$ = "stiffness matrix"

$$= \int_A \left(\frac{\partial N_i}{\partial y} \frac{\partial N_j}{\partial y} + \frac{\partial N_i}{\partial z} \frac{\partial N_j}{\partial z} \right) dA \quad (5.70)$$

and $\tilde{f}$ = "force vector" $= \int_A \gamma N_i \, dA$. (5.71)

4.4 Element stiffness matrix and force vector

The type of element chosen for the finite element analysis is the linear triangular element shown in Figure 5.14. The element has three nodes, each of which has one degree of freedom correspondiong to the unknown value of ϵ at that node. As a linear variation of ϵ is assumed throughout the element the value of ϵ at any point within the element can be expressed as :

$$\epsilon^{(e)} = \alpha_1 + \alpha_2 x + \alpha_3 y \, , \quad (5.72)$$

where α_1 , α_2 and α_3 are constants which are obtained by substituting the nodal values of ϵ into (5.72) in turn :

$$a_i^{(e)} = \alpha_1 + \alpha_2 y_i^{(e)} + \alpha_3 z_i^{(e)} \, , \; i = 1,3 \, . \quad (5.73)$$

Solving (5.73) for α_i and substituting in (5.72) results in :

$$\epsilon^{(e)} = \sum_{i=1}^{3} \frac{1}{2A^{(e)}} (b_i + c_i y + d_i z) \, a_i^{(e)} \, , \quad (5.74)$$

where $b_i = y_2^{(e)} z_3^{(e)} - y_3^{(e)} z_2^{(e)}$

$c_i = z_2^{(e)} - z_3^{(e)}$

$d_i = y_3^{(e)} - y_2^{(e)}$,

with the other values being given by cyclic permutation of the subscripts in the order 1, 2, 3. The area $A^{(e)}$ of the element is given by

$$2\,A^{(e)} = \text{Det} \begin{bmatrix} 1 & y_1^{(e)} & z_1^{(e)} \\ 1 & y_2^{(e)} & z_2^{(e)} \\ 1 & y_3^{(e)} & z_3^{(e)} \end{bmatrix} .$$

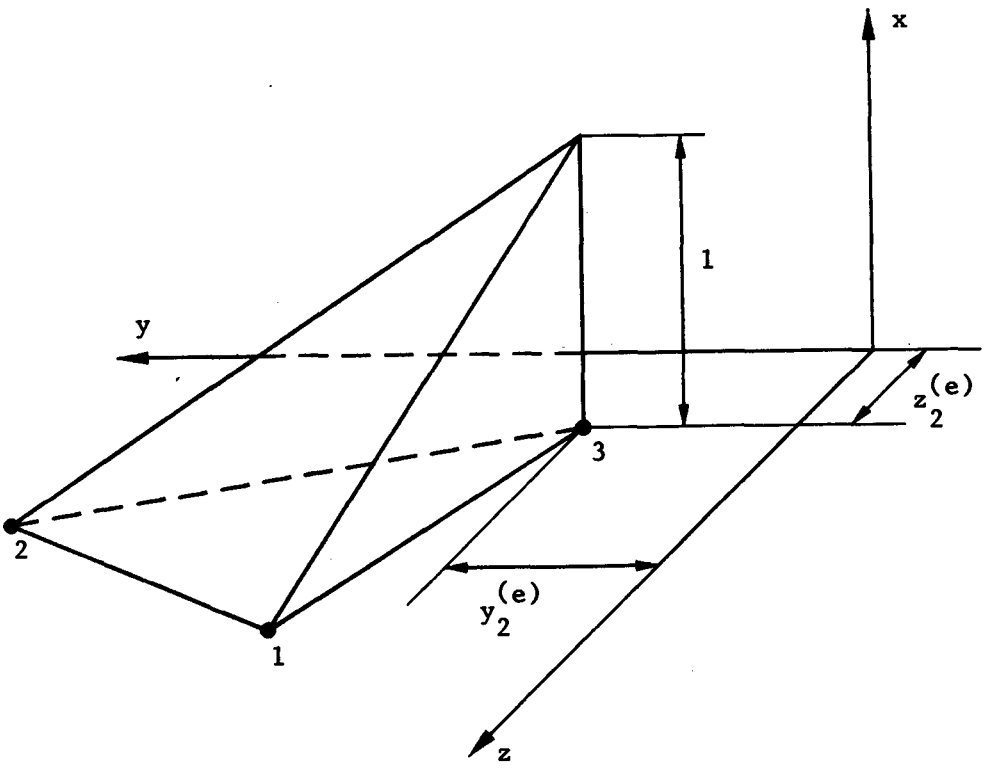

Figure 5.14 : Element shape function

Expression (5.74) may be written as

$$\epsilon^{(e)} = \sum_{i=1}^{3} N_i^{(e)} a_i^{(e)} \quad , \tag{5.75}$$

where N_i = element shape functions

$$= \frac{1}{2\,A^{(e)}} (b_i + c_i\, y + d_i\, z) \quad . \tag{5.76}$$

Expressions (67) and (68) can be used to evaluate the element stiffness matrix and force vector by assuming that the global shape functions N_i and the element shape functions $N_i^{(e)}$ are identical. The evaluation of the element stiffness matrix and load vector is made simpler by the use of area coordinates, which are described in Appendix C.

The element stiffness matrix is obtained by substituting (5.76) into (5.71) and noting $N_i^{(e)} = N_i$:

$$K_{ij}^{(e)} = \int_{A^{(e)}} \frac{1}{4\,(A^{(e)})^2} \left[c_i\, c_y + d_i\, d_y \right] dA \quad ; \tag{5.77}$$

$$i,j = 1, 2, 3 \; .$$

Integrating we get :

$$\boxed{K_{ij}^{(e)} = \frac{1}{4\,A^{(e)}} (c_i\, c_j + d_i\, d_j) \; ; \; i,j = 1, 2, 3 \; .} \tag{5.78}$$

The element force vector can be found by rewriting equation (5.71) as

$$\tilde{f}^{(e)} = \gamma \int_A \begin{bmatrix} N_1^{(e)} \\ N_2^{(e)} \\ N_3^{(e)} \end{bmatrix} dA \, . \qquad (5.79)$$

Noting that $L_i = N_i^{(e)}$ from Appendix C, and assuming ϵ to be constant over the element we get :

$$\tilde{f}^{(e)} = \gamma \int_{A^{(e)}} \begin{bmatrix} L_1^1 & L_2^0 & L_3^0 \\ L_1^0 & L_2^1 & L_3^0 \\ L_1^0 & L_2^0 & L_3^1 \end{bmatrix} dA = \frac{\gamma A^{(e)}}{3} \begin{bmatrix} 1 \\ 1 \\ 1 \end{bmatrix} \qquad (5.80)$$

using integration formula (C.4) from Appendix C.

4.5 Finite element mesh

Figure 5.15 illustrates the two finite element mesh geometries used in the analysis. The mesh shown in Figure 5.15(a) is used where symmetry about the y axis may be assumed, i.e. the velocity distribution is asymmetric about the z axis. The mesh shown in Figure 5.15(b) is used when radial symmetry may be assumed (in our case vertical up or down flow).

4.6 Computational algorithm

The computer program, written using the True Basic programming language, is presented in Appendix E. The finite element method subroutines are based on the FORTRAN code presented by Owen and Hinton (1979) and (1980).

The sequence of the main subroutines in the finite element method are shown in Figure 5.16. The following is a description of each subroutine in the order executed by the program.

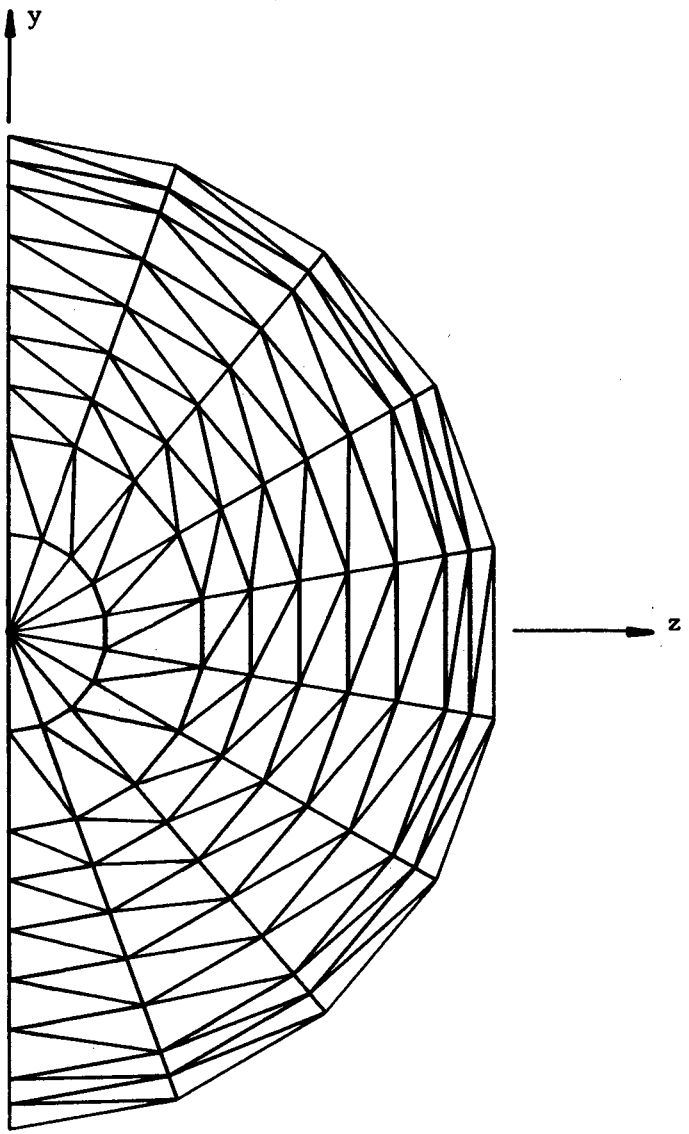

(a)

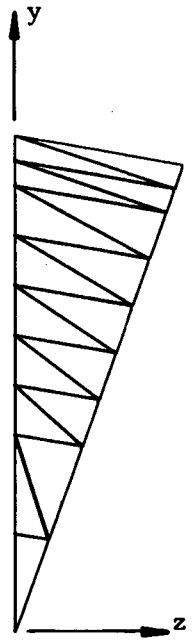

(b)

Figure 5.15 : Typical finite element mesh geometries

Subroutine MESHREAD

The nodal coordinates, nodal connectivity and number of boundary nodes are read from the data file containing the finite element mesh.

Subroutine MESHPLOT

This is an optional routine used to verify visually that the mesh input data is correct. The elements from the finite element mesh are plotted at their nodal coordinates.

Subroutine BOUNDARY-VALUES

The velocity of each boundary node is evaluated as discussed in Section 3.6.

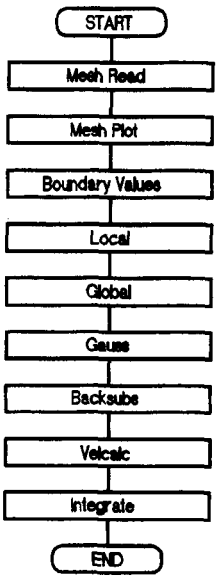

Figure 5.16 : Finite element method algorithm

Subroutine LOCAL

The stiffness matrix and force vector for each element is calculated using expressions (5.78) and (5.80).

Subroutine GLOBAL

The local stiffness matrices and force vectors are assembled to form the global stiffness matrix and force vector. To optimise the solution procedure the symmetric and banded nature of the stiffness matrix is utilised, and the stiffness matrix elements stored in a one-dimensional array.

Subroutine GAUSS

The routine performs Gauss reduction on the global force vector and the one-dimensional stiffness matrix.

Subroutine BACKSUBS

The nodal values of ϕ are evaluated from the reduced stiffness matrix and force vector using a back substitution procedure.

Subroutine VELCALC

The local velocity values at each node are evaluated from the nodal values of ϕ using equation (5.52).

Subroutine INTEGRATE

The velocity at the centroid of each element is evaluated using linear interpolation, and the mixture flow rate calculated as follows :

$$Q = \sum_{e=1}^{n} v^{(e)} A^{(e)} \quad , \tag{5.81}$$

where $v^{(e)}$ = velocity at centroid of element.

5. CHAPTER SUMMARY

5.1 Mechanistic model

A mechanistic model for the dense phase flow of classified tailings has been developed. The primary features of the model are :

(i) The particle size distribution of the solid particles in the mixture is divided into two fractions which are characterised as "fine" and "coarse". The division of the particle size distribution is based on a minimum settling velocity calculated using Stoke's law for laminar settling.

(ii) The model has specifically been developed for dense phase mixtures which are defined to exist when the concentration of the coarse fraction exceeds the freely settled (loose poured) concentration of the coarse fraction and the predominant mechanism supporting the particles is interparticle contact.

(iii) A differential equation describing the velocity distribution within the pipe has been formulated from the Cauchy momentum equations applied to the solid liquid mixture.

(iv) The shear stress distribution due to the applied pressure gradient is shown to be linear provided the concentration distribution may be taken as constant across the pipe section.

(v) The concept of lateral interparticle stress, arising from the stress on particles due to fluid dynamic drag exerted on the particles by the seepage flow of the vehicle, is presented.

(vi) The solid phase shear stress within the pipe section is evaluated using the internal angle of friction between the solid particles. At the pipe wall the coefficient of sliding friction is used to calculate the wall shear stress due to the solid phase.

(vii) The concept of sheared and unsheared zones within the pipe section based on the applied shear stress distribution and the failure shear stress of the granular matrix is introduced. In the unsheared zone the fluid shear is zero and consequently there is no velocity gradient. It is shown that three possible flow regimes are possible :

a) unsheared zone occupying the whole pipe section - plug flow.

b) unsheared core surrounded by annular region of sheared granular matrix.

c) unsheared zone in contact with a portion of the pipe wall forming a "sliding bed" of unsheared particles.

(viii) The viscosity of the mixture and the vehicle are evaluated using the correlation ascribed to Landel *et al*.

(ix) The differential equation describing the velocity distribution is solved using the finite element method with boundary conditions specific to the problem imposed.

(x) The boundary velocity of the mixture is evaluated by considering the local applied stress and solid phase shear stress at the pipe wall.

5.2 Input required for model

The input required for the model to solve the mean mixture velocity (slurry flow rate) for a given friction pressure gradient is as follows :

(i) Pipeline properties :
- Internal pipe diameter
- Pipeline slope

(ii) Solids properties :
- Solids relative density
- Particle size distribution
- Internal angle of friction
- Coefficient of sliding friction
- Coefficient of lateral interparticle stress

(iii) Slurry properties :
- Mixture relative density
- Slurry temperature
- Friction pressure gradient.

Note that the roughness of the pipe is not required as only viscous (laminar) shearing stresses are considered. The pipe roughness is however indirectly included in the dynamic coefficient of sliding friction between the particles and pipe wall.

CHAPTER 6

EVALUATION OF DENSE PHASE MODEL

1. INTRODUCTION

This chapter evaluates the dense phase mechanistic model developed in Chapter 5. The experimentally determined solid particle properties described and presented in Chapters 2 and 3 are used as input for the model. The experimentally measured pressure gradients discussed in Chapter 2 and presented in the Cyclone Classified Tailings data base (Appendix A) are used to compare predicted pressure gradients calculated using the model with actual pressure gradients.

The computational results of the model are evaluated as follows :

(i) Dense phase flow regimes

Computational results are presented showing velocity profiles and isovels (lines of equal velocity) for various dense phase flow regimes - stationary bed, "sliding" bed, asymmetric core and symmetric core.

(ii) Velocity profiles

The influence of mean mixture velocity, concentration and pipe diameter on the computed velocity profiles is examined.

(iii) Transition velocity between stationary bed and "sliding" bed flow regimes

The calculated transition mean mixture velocity between the stationary bed and "sliding" bed flow regimes are compared to observed flow regimes in 40 mm NB and 80 mm NB pipelines.

(iv) Pressure gradients

Graphs showing the variation of the predicted and experimentally measured pressure gradients with mean mixture velocity and solids concentration are presented to provide a visual evaluation of the model.

(v) Log standard error analysis

The model is numerically evaluated by comparing the log standard error between the predicted pressure gradients and the experimentally measured pressure gradients.

2. INPUT PARAMETERS REQUIRED BY MODEL

2.1 Pipeline properties

The internal pipe diameter (D) and the slope of the pipeline (ϕ) are required by the model. The roughness of the pipeline is not required as only viscous (laminar) fluid shearing stresses are considered. The pipe roughness is however indirectly included in the dynamic coefficient of sliding friction between the particles and pipe wall.

2.2 Solid particle properties

2.2.1 *Solid particle relative density*

The relative density of the solid particles (S_s) is evaluated as discussed in Section 3.1 of Chapter 2. Table 6.1 shows the values used for the evaluation of the model.

2.2.2 *Particle size distribution*

The measurement of the particle size distribution of the solid particles is described in Section 3.2 of Chapter 2. The particle size distribution is treated as a continuous curve with linear interpolation used to find values between sieve sizes. Referring to Figure 6.1 the percentage of solid particles P less than size d is :

$$P = P_i + m \left[\log (d) - \log (d_i) \right] , \qquad (6.1)$$

where $$m = \frac{P_{i+1} - P_i}{\log (d_{i+1}) - \log (d_i)}$$

P_i = percentage of particles less than size d_i .

Similarly, the particle size d corresponding to a percentage of solids passing P is found from :

$$\log (d) = \frac{(P - P_i)}{m} + \log (d_i) \quad . \qquad (6.2)$$

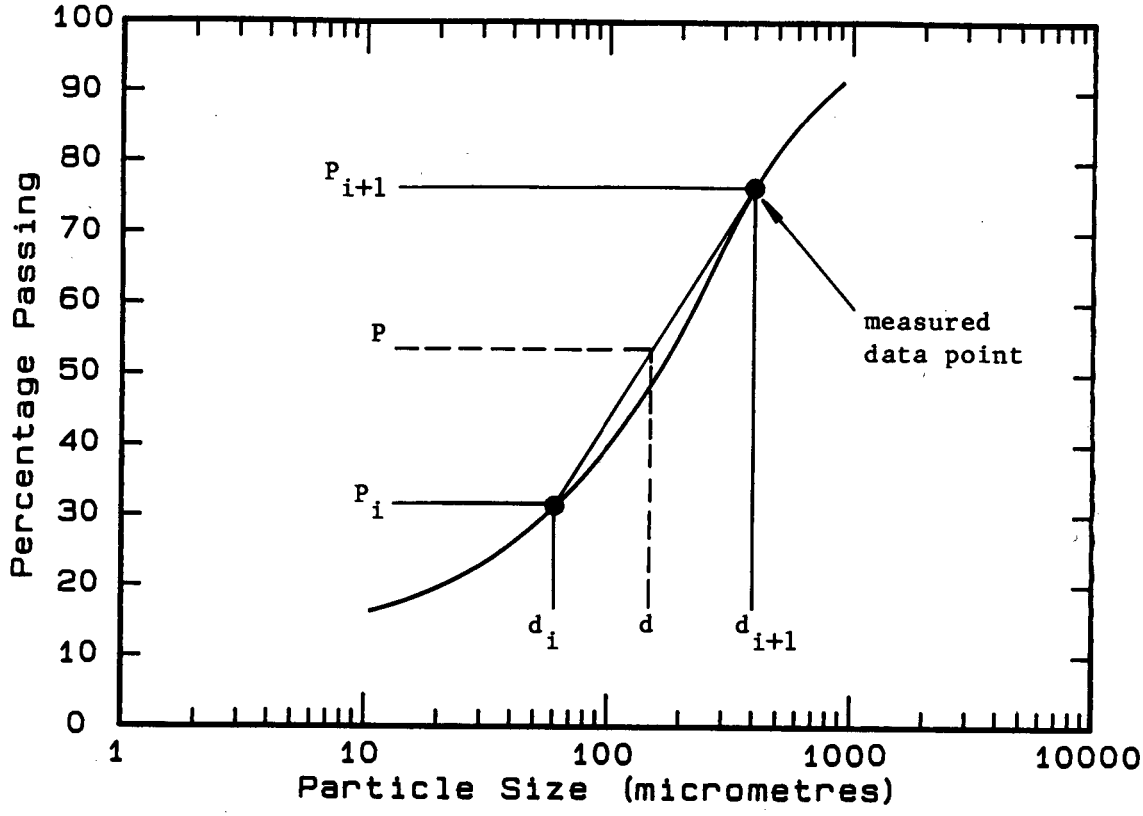

Figure 6.1

2.2.3 *Particle shape factor*

The particle shape factor (S_f) is measured as discussed in Section 3.3 of Chapter 2. As the particle shape factor is used to determine the vehicle portion of the mixture, the shape factors measured for the smallest particle size range (211 μm to 300 μm) are used as input for the model. Table 6.1 shows the values used for the evaluation of the model.

2.2.4 *Freely settled particle concentration*

The freely settled concentration (C_{min}) of the solid particles is measured as discussed in Section 3.5 of Chapter 2. Table 6.1 shows the values used for the evaluation of the model.

2.2.5 *Internal angle of friction of solid particles*

The submerged internal angle of friction of the solid particles (δ) is measured as described in Section 3.6 of Chapter 2. The variation of tan (δ) with solids concentration is taken to be linear as shown in

Figures 3.27, 3.28 and 3.29 for the Blyvooruitsig, East Driefontein and Vaal Reefs materials respectively. The internal angle of friction is determined as follows :

$$\tan \delta = m_\delta C + c_\delta \quad , \qquad (6.3)$$

where m_δ = slope of experimental curve
c_δ = experimental constant
C = solids concentration.

The values of m_δ and c_δ are determined from the experimental curves, (Figures 3,27, 3.28 and 3.29) and Table 6.1 presents the values used for the four materials.

It was felt that the high percentage of fines in the Western Deeps material (possibly forming a mixture with a yield stress) contributed to the high observed angle of internal friction compared with the other materials (Figure 2.16). Consequently, as the Vaal Reefs material is closest to the Western Deeps material in terms of particle size distribution, the Vaal Reefs experimental values were used for the Western Deeps model evaluation as shown in Table 6.1.

Brandt and Johnson (1963) have noted that the fluid flowing through the particle matrix alters the internal friction of the particles. However, in the absence of any other measurements, the static test without interstitial flow is considered adequate to establish the magnitude of the internal frictional forces.

2.2.6 *Coefficient of sliding friction*

The coefficient of sliding friction (μ_d) between the solid particles and pipe wall is evaluated using the apparatus described in Sections 3 and 4 of Chapter 3. As the friction mechanism between layers of sliding particles and particles against a solid boundary are considered similar, the variation of the dynamic coefficient of friction with solids concentration is assumed to have the same slope as the variation of tan (δ) with solids concentration as shown in Figures 3.27, 3.28 and 3.29 for the Blyvooruitsig, East Driefontein and Vaal Reefs materials

TABLE 6.1 : Solid Particle Properties used in Model Evaluation

Material :	Blyvooruitsig	East Driefontein	Vaal Reefs	Western Deeps
Ss	2.66	2.65	2.65	2.65
S_f	0.88	0.80	0.79	0.71
C_{min} (% by vol)	48.0	45.6	46.0	49.0
m_δ (equ. 6.3)	0.76	0.80	0.54	0.54
c_δ (equ. 6.3)	0.14	0.14	0.25	0.25
m_μ (equ. 6.4)	0.76	0.80	0.54	0.54
c_μ (equ. 6.4)	0.01	-0.08	0.15	0.15
a_κ (equ. 6.5)	0.004	0.004	0.004	0.002
b_κ (equ. 6.5)	3.69	2.70	2.75	6.45

Ss = Relative density of solid particles
Sf = Particle shape factor
C_{min} = Freely settled particle concentration

respectively. The coefficient of sliding friction is evaluated as follows :

$$\mu_d = m_\mu C + c_\mu \quad , \tag{6.4}$$

where $m_\mu = m_\delta$ (equation 6.3)
c_μ = experimental constant (from Figures 3.27, 3.28 and 3.29).

The values of m_μ and c_μ used for the model evaluation are shown in Table 6.1. As with the angle of internal friction the values for the Western Deeps material have been assumed to equal those for the Vaal Reefs material.

2.2.7 *Coefficient of lateral interparticle stress*

The coefficient of lateral interparticle stress κ was evaluated by comparing the output of the model to the experimental pressure gradient test results. Figure 6.2 shows the variation of κ with solids concentration used for the evaluation of the model for the four materials tested. The value of the coefficient of lateral interparticle stress used for the model evaluation is calculated from :

$$\kappa = a_\kappa \left(\frac{C - 0,35}{C_{min} - 0,35}\right)^{b_\kappa} \qquad C \geq 0,35$$

$$\kappa = 0 \qquad C < 0,35 \quad , \tag{6.5}$$

where a_κ , b_κ = experimental coefficients
C_{min} = freely settled concentration.

Table 6.1 shows the values of a_κ and b_κ used for the model evaluation. From equation (6.5) it is seen that κ is considered negligible for solids concentrations less than 35% by volume.

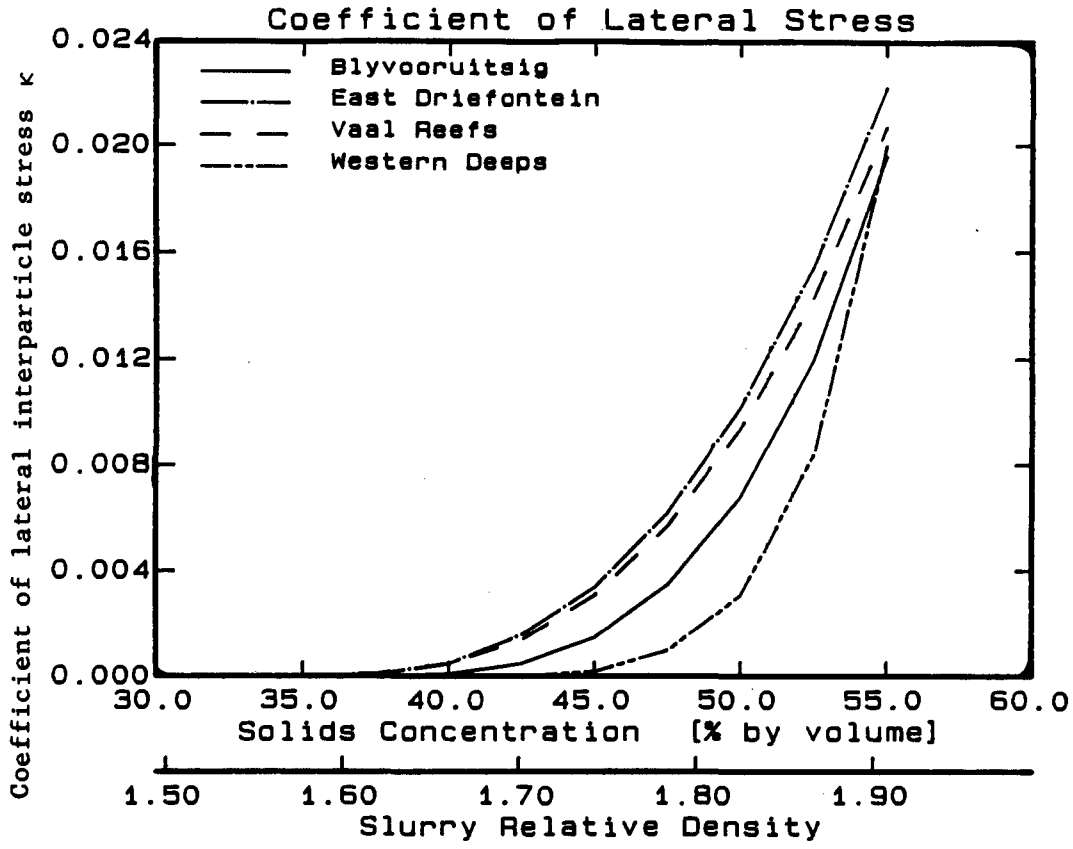

Figure 6.2

2.3 Slurry properties

2.3.1 *Solids concentration*

The solids concentration is required as input for the model. The values of the internal angle of friction, coefficient of sliding friction and coefficient of lateral interparticle stress, depend on the solids concentration as well as other constants.

2.3.2 *Slurry temperature*

The slurry temperature is used to determine the density and viscosity of clear water, which is used as a basis for evaluating the vehicle density and viscosity. The water density is calculated using (Sive 1988) :

$$\rho_w = 1004{,}166\ e^{-0{,}0002958T} \quad , \qquad (6.6)$$

where T = temperature (°C) .

The dynamic coefficient of viscosity for the water is calculated from (Sive 1988) :

$$\mu_w = \frac{1{,}732\ e^{-0{,}028T}}{1000} \qquad T < 23°C$$

$$\mu_w = \frac{2{,}516 - 0{,}505\ \ell n\ (T)}{1000} \qquad 23°C \leq T < 43°C \qquad (6.7)$$

$$\mu_w = \frac{15{,}971\ T^{-0{,}863}}{1000} \qquad T \geq 43°C\ .$$

2.3.3 *Viscosity of mixture and vehicle*

The viscosity of the mixture and vehicle is calculated using the Landel *et al* correlation (equations (5.33) and (5.34) respectively). The correlation requires an experimental coefficient m . Landel *et al* found a good correlation with $m = -2{,}5$ for particles in the size range 10 μm to 100 μm (Govier and Aziz (1972)) and this value has been used for calculating the viscosity of the vehicle. For calculating the mixture viscosity a value of $m = -4{,}0$ was used, as this provided better fit to the experimental data for the computational results.

The maximum attainable concentration of the solid particles C_{max} was taken to be 70% by volume.

2.3.4 *Friction pressure gradient*

The friction pressure gradient is required as input by the model, which is solved to obtain the corresponding mean mixture velocity.

3. CALCULATED PARAMETERS USED BY MODEL

3.1 Vehicle portion of the slurry

The vehicle portion of the slurry is defined to comprise the conveying liquid (water) and that fraction of solid particles which have a settling velocity of less than 1 mm/s (Section 3.1, Chapter 5). The maximum particle size in the vehicle portion (i.e. that particle size having a settling velocity of 1 mm/s) is termed d_t - the transition particle diameter between the fine and coarse fractions of the particle size distribution. The transition particle diameter is determined by solving equation (5.30) using an iterative solution procedure. Note that the evaluation of d_t is dependent on the particle size distribution as the particles are considered to be falling through a homogeneous mixture comprising the conveying liquid and all other particles of size less than d_t .

Figure 6.3 shows the variation of the transition particle diameter d_t with solids concentration for the four cyclone classified tailings materials. The transition particle diameter is seen to increase with increasing solids concentration. The rapid increase of d_t for the Western Deeps material is due to the high percentage of fines in the mixture.

Figure 6.4 depicts the variation of the vehicle solids concentration with the total solids concentration for the four materials. The vehicle concentration of the Western Deeps slurry is seen to increase very steeply and is almost equal to the solids concentration at $C = 55\%$ by volume - i.e. virtually the whole mixture is the vehicle portion of the slurry with a very small coarse fraction. It is clear that the Western Deeps material does not form a true dense phase mixture with interparticle contact as the predominant particle support mechanism.

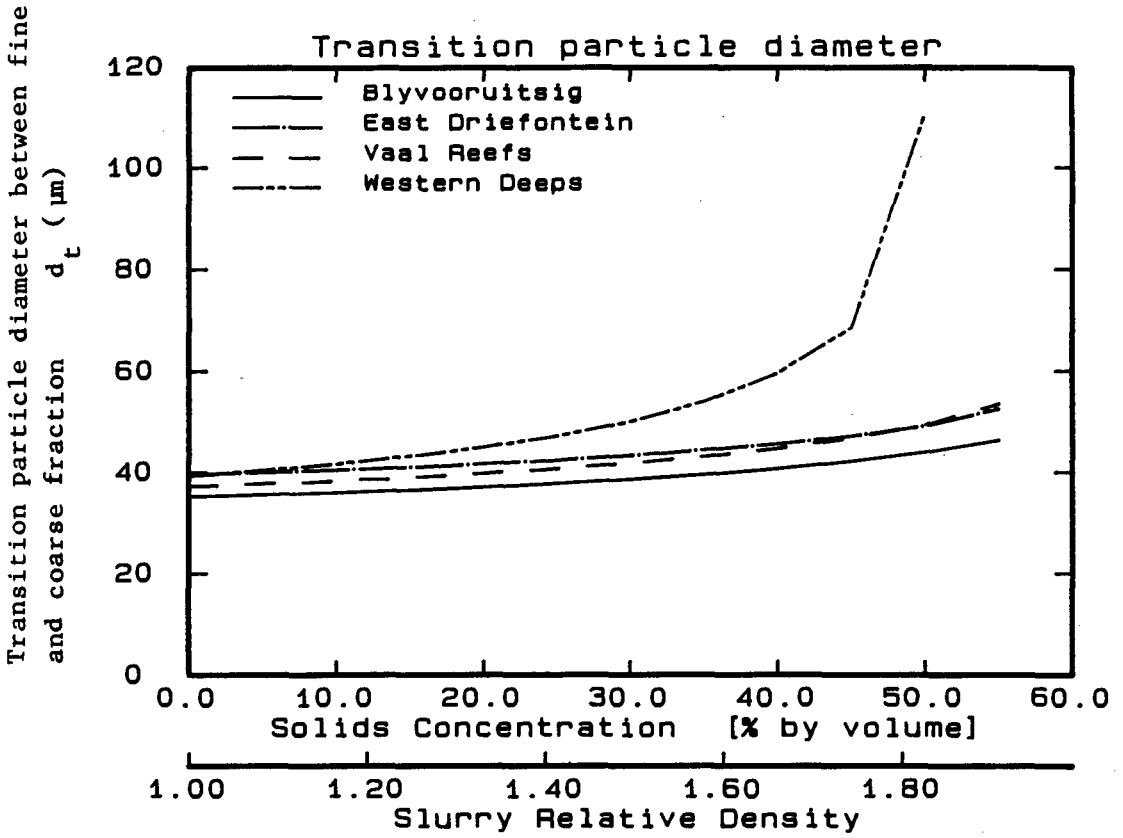

Figure 6.3

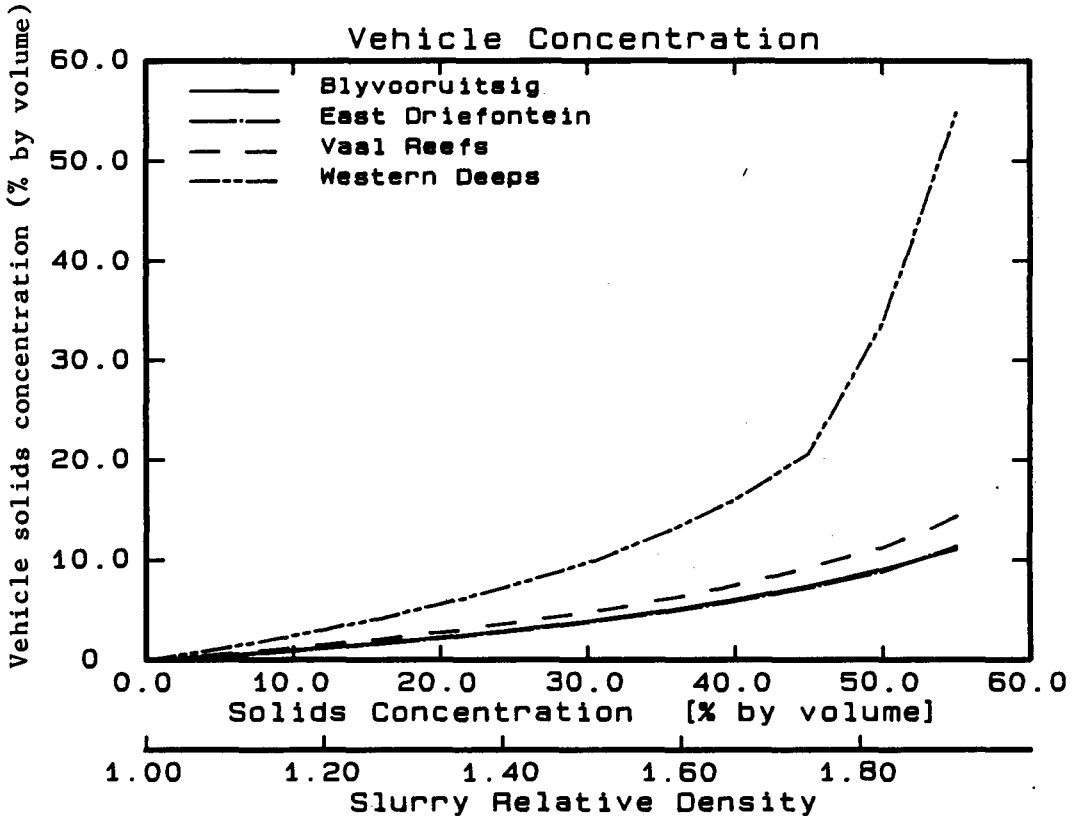

Figure 6.4

3.2 Boundary fluid shear layer thickness

Figure 6.5 shows the variation of the thickness of the fluid shear layer (h) with solids concentration for the four materials tested. The evaluation of the fluid shear layer thickness is discussed in Section 3.6.4 of Chapter 5. Apart from the Western Deeps mixture, the other materials show the expected decrease in h with increased solids concentration. The increase in the fluid shear layer thickness for the Western Deeps material is due to virtually the whole mixture forming the vehicle portion at high concentration.

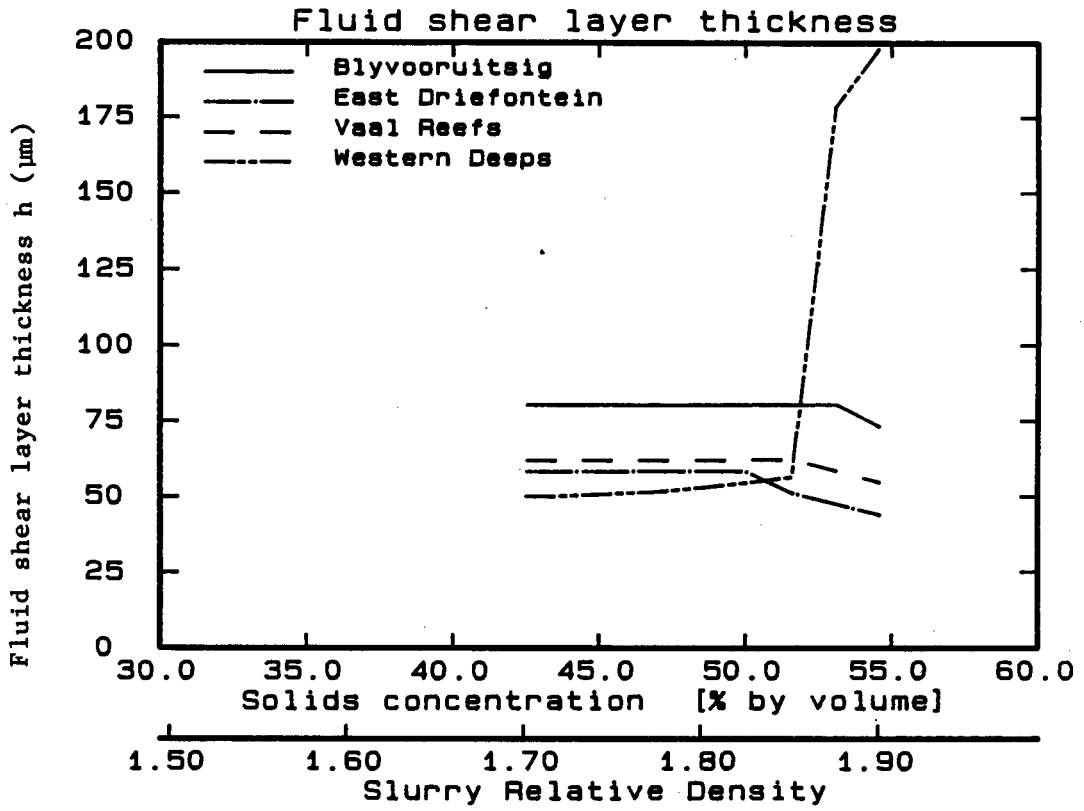

Figure 6.5

4. COMPUTATIONAL RESULTS

The computational results are illustrated by presenting the trends for the Vaal Reefs slurry which are typical for all the cyclone classified tailings (Sections 4.1 to 4.4). The model is numerically evaluated by analysing the log standard error for each set of test results of the data base (Section 4.5).

4.1 Dense phase flow regimes

There are five possible dense phase flow regimes, all of which are examined here except for the plug flow regime. The plug flow regime which generally occurs at high solids concentration in vertical pipes (although it may also occur in horizontal pipes) has a uniform velocity distribution across the whole pipe section with all the shear taking place at the pipe wall.

4.1.1 *Stationary bed flow regime*

Figure 6.6 shows the velocity profile along the y axis ($z = 0$) and the shear stress distribution for a typical flow case with a stationary bed. The applied shear stress τ_m is greater than the solid particle matrix failure stress τ_{sfail} over all but the top portion of the pipe section. Note that we would expect the velocity gradient to be zero over the region of the pipe section where τ_{sfail} exceeds τ_m from the discussion in Section 2.6.1 of Chapter 5. However, the finite element method provides an approximate solution (to the differential equation describing the velocity distribution) which results in a velocity gradient over this region.

Figure 6.7 shows the isovels (lines of equal mixture velocity) over the pipe section for the stationary bed flow regime. The isovels are obtained by linear interpolation between the nodal solution values (velocities) of the finite element mesh.

4.1.2 *"Sliding" bed flow regime*

The velocity profile and shear stress distribution for a typical "sliding" bed flow regime are shown in Figure 6.8. In this case, although the solid particle matrix failure shear stress exceeds the applied shear stress at the pipe invert, the solid phase shear stress is

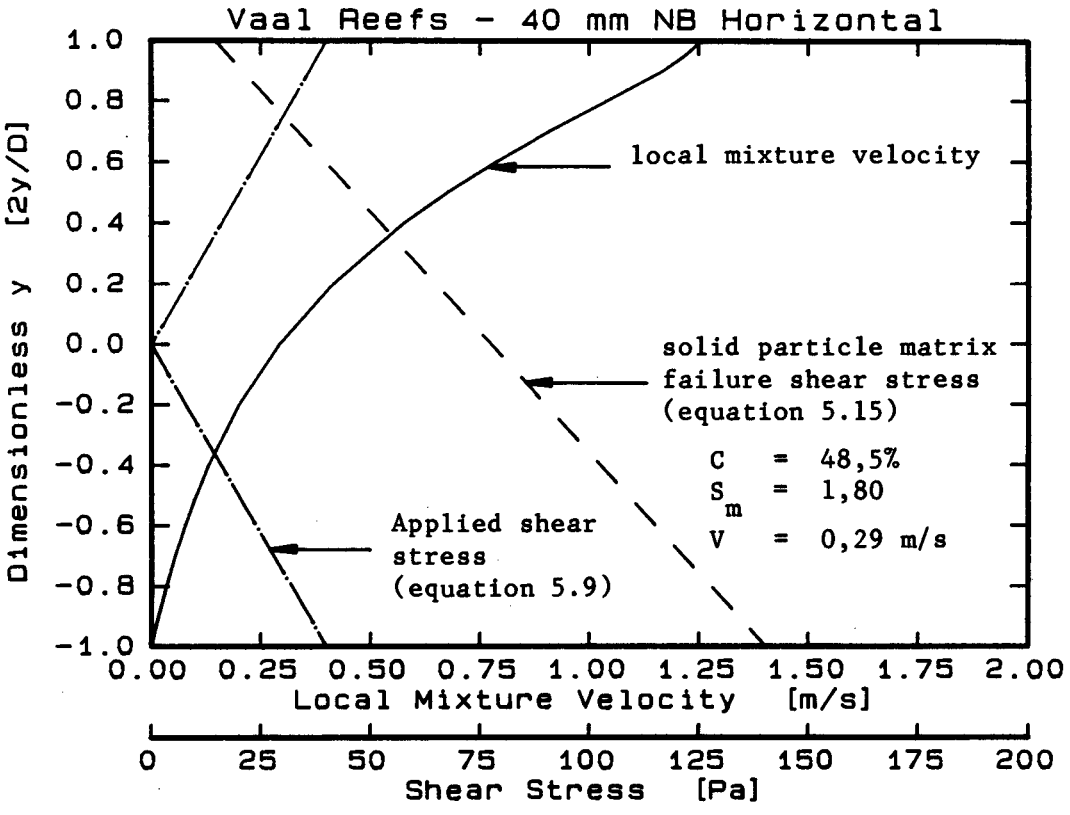

Figure 6.6 : Stationary bed flow regime: Velocity profile and shear stress distribution

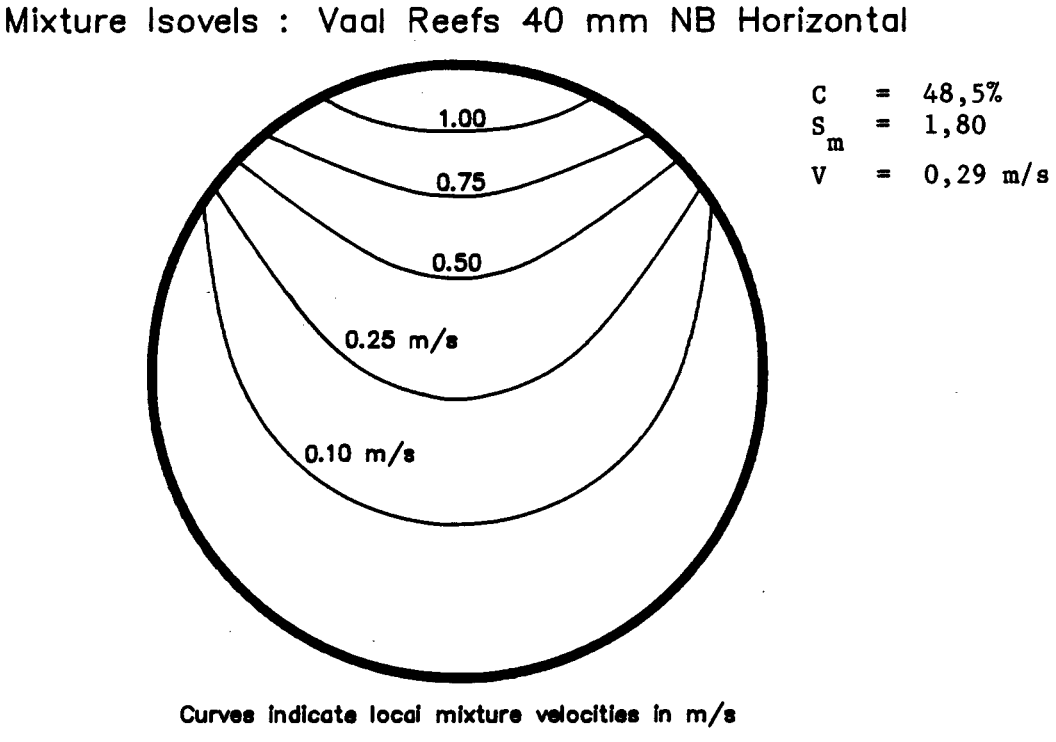

Figure 6.7 : Stationary bed flow regime: Isovels

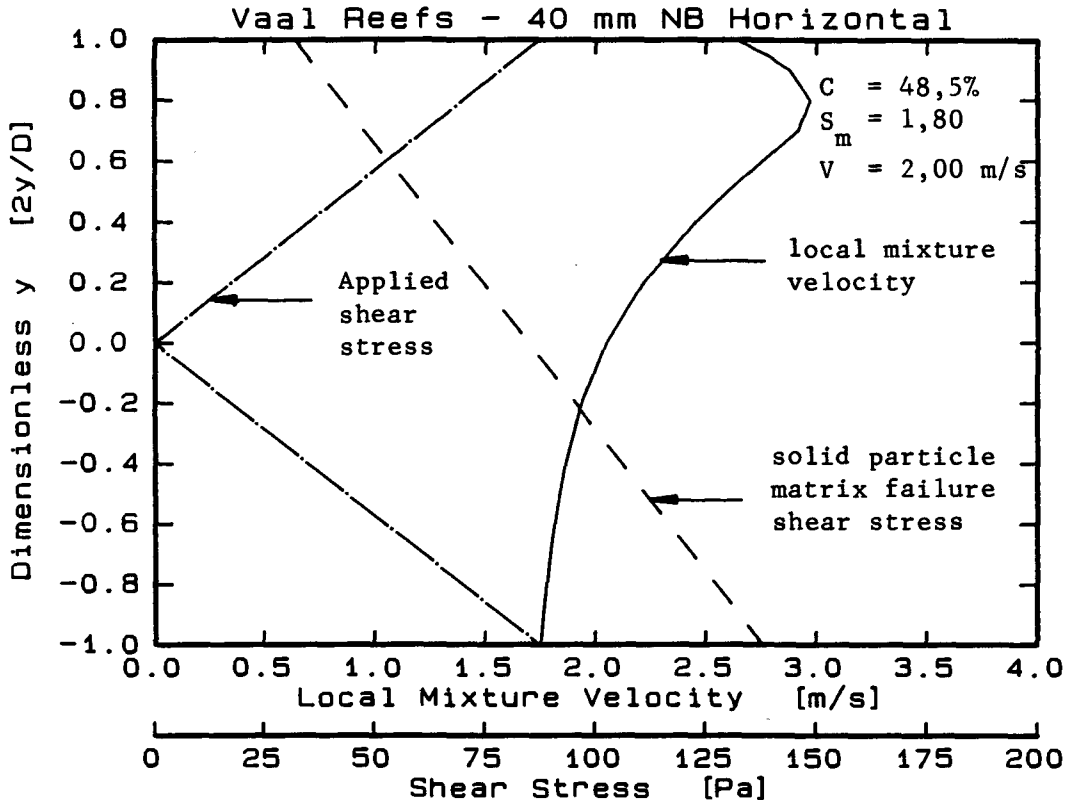

Figure 6.8 : "Sliding" bed flow regime: Velocity profile and shear stress distribution

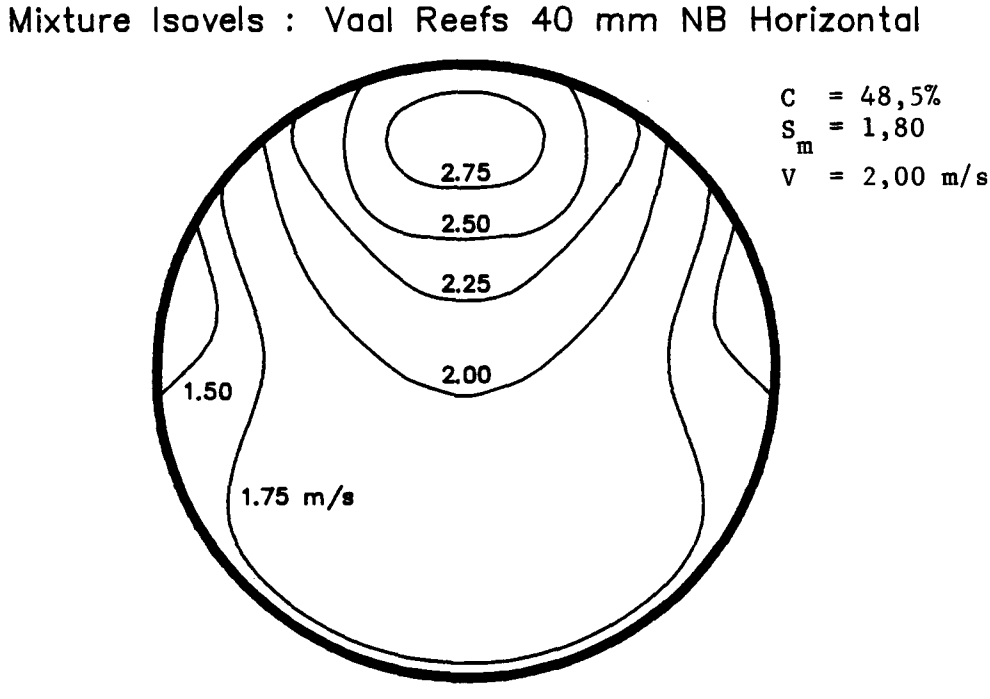

Figure 6.9 : "Sliding" bed flow regime: Isovels

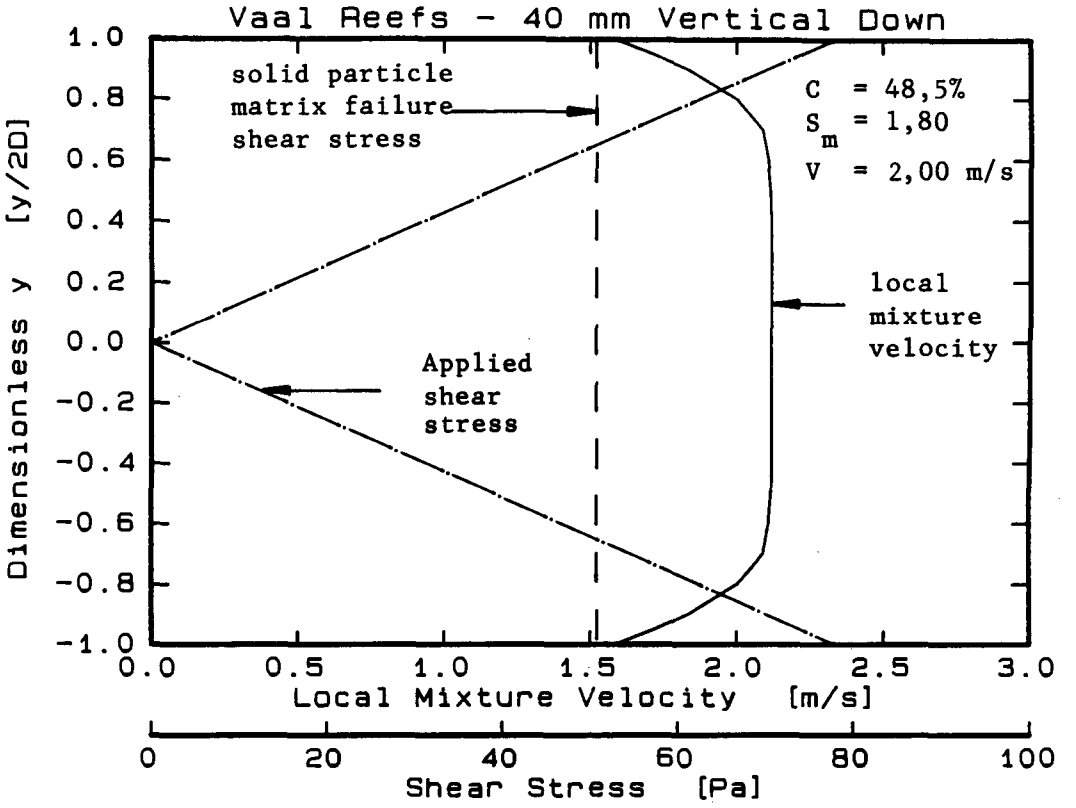

Figure 6.12 : Symmetric core flow regime: Velocity profile and shear stress distribution

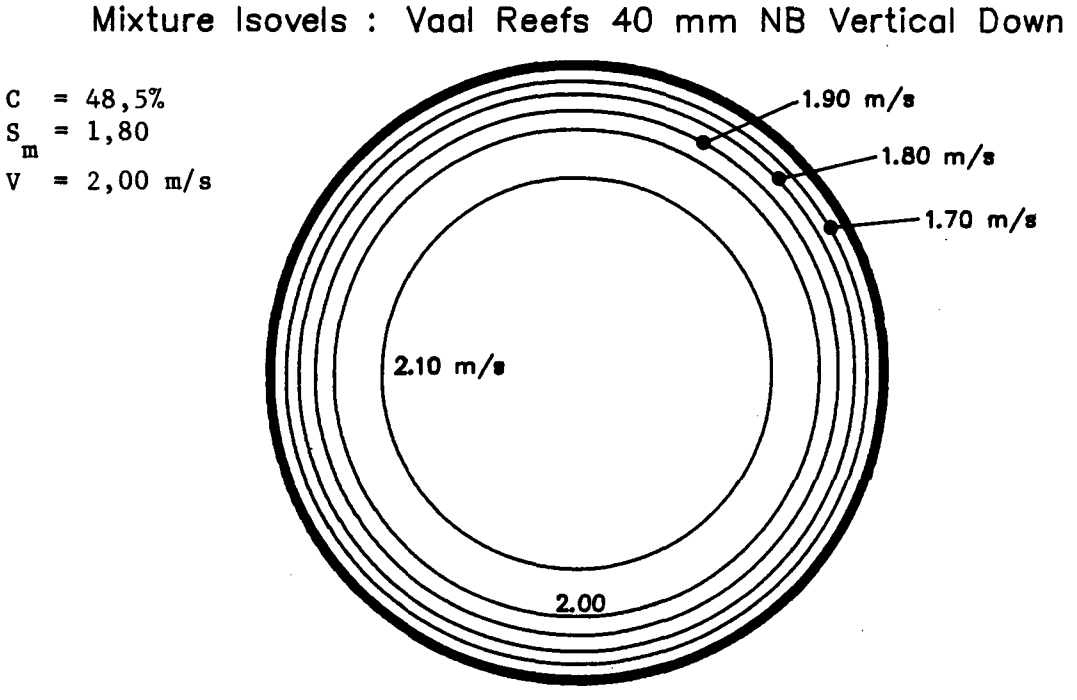

Figure 6.13 : Symmetric core flow regime: Isovels

4.2.2 *Influence of solids concentration on the velocity profile*

Figure 6.16 shows the "sliding" bed flow regime profiles in a horizontal pipe at a mean mixture velocity of 2,0 m/s for solids concentrations of 45,5%, 48,5% and 51,5% by volume respectively. The asymmetry of the velocity profile is reduced as the solids concentration is increased, due to the increase of the internal friction within the mixture.

Comparing the velocity profiles at solids concentrations of 48,5% and 51,5%, it is seen that the profiles are similar in the bottom half of the pipe while the local velocities for the 48,5% are greater in the top portion of the pipe. From these velocity profiles it seems unlikely that they are both for mean mixture velocities of 2 m/s. However, if the isovels for the 48,5% and 51,5% mixtures are plotted as shown in Figures 6.18 and 6.19 respectively, it is seen that the zone between 1,75 m/s and 2,00 m/s for the 51,5% mixture occupies a much larger portion of the pipe cross section than for the 48,5% mixture.

4.2.3 *Influence of pipe diameter on the velocity profile*

Figure 6.17 shows the "sliding" bed flow regime profiles in a horizontal pipe at a mean mixture velocity of 2,0 m/s for internal pipe diameters of 26,6 mm, 40,0 mm and 73,4 mm. The asymmetry of the velocity profiles increase with increasing pipe diameter.

4.3 Transition velocity between stationary bed and "sliding" bed flow regimes

Figures 6.20 and 6.21 show the variation of the calculated transition mean mixture velocity of the stationary bed and "sliding" bed flow regimes compared with the flow observations in the 40 mm NB and 80 mm NB pipelines respectively. The model under predicts the transition velocity at low concentrations, while predicting stationary bed at high concentrations where symmetric flow was observed.

Figure 6.22 shows the variation of the calculated transition velocity between the stationary bed and sliding bed flow regimes for solids concentrations of 42,4%, 48,5% and 54,5% by volume. The model predicts an increasing transition velocity with increasing pipe diameter, and that the rate of increase is greater for the lower concentration mixtures.

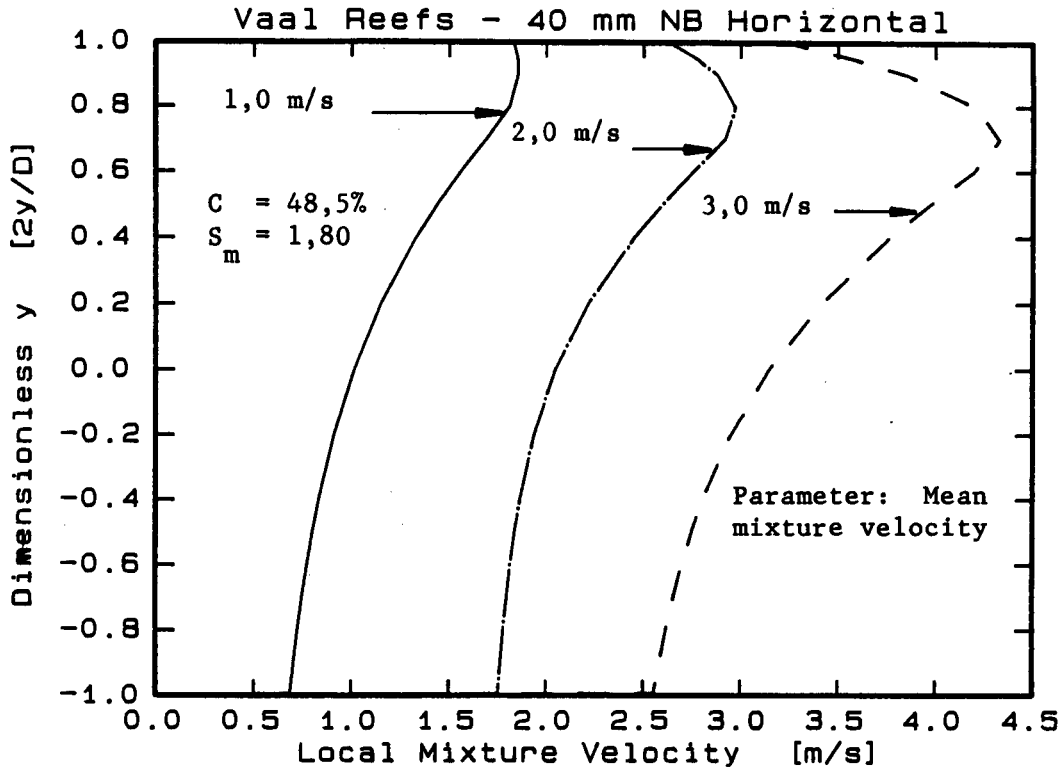

Figure 6.14 : Velocity profiles: Horizontal pipe

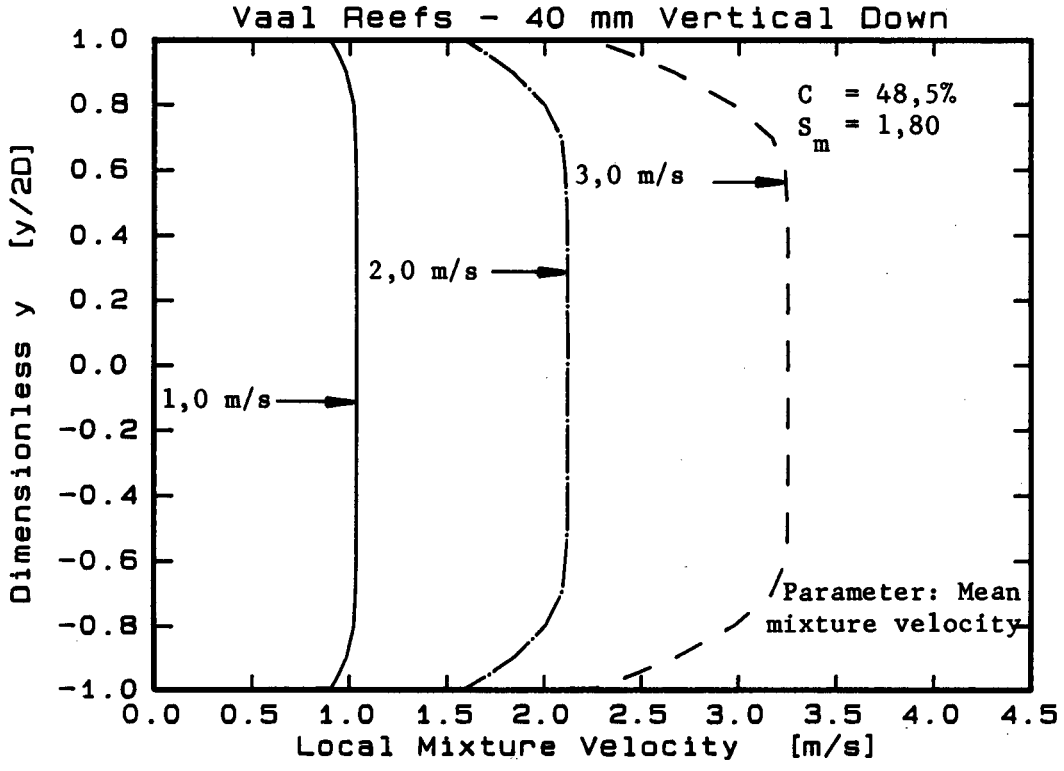

Figure 6.15 : Velocity profiles: Vertical down pipe

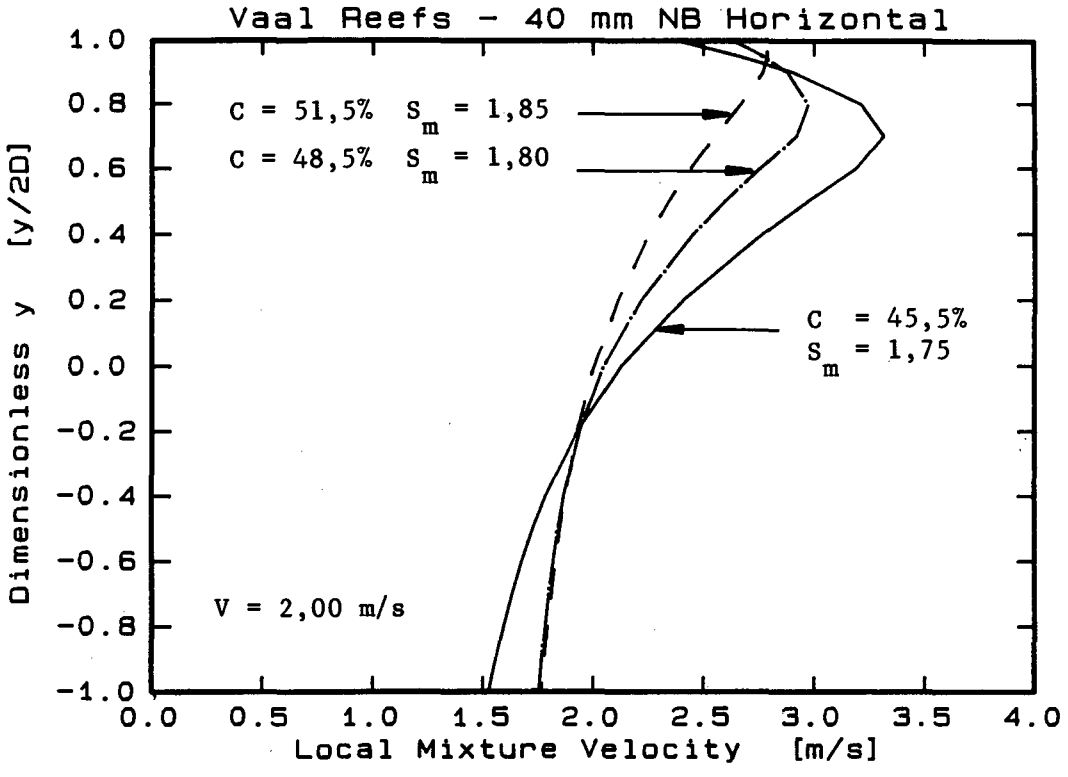

Figure 6.16 : Velocity profiles: Horizontal pipe

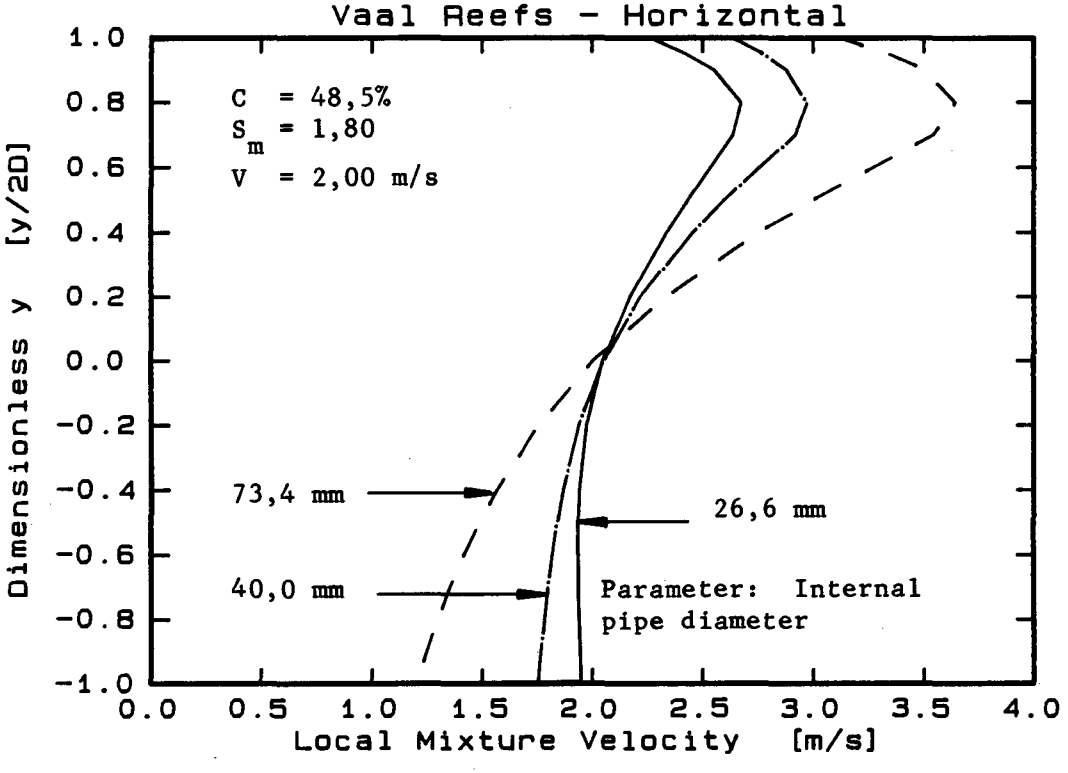

Figure 6.17 : Velocity profiles: Horizontal pipe

Mixture Isovels : Vaal Reefs 40 mm NB Horizontal

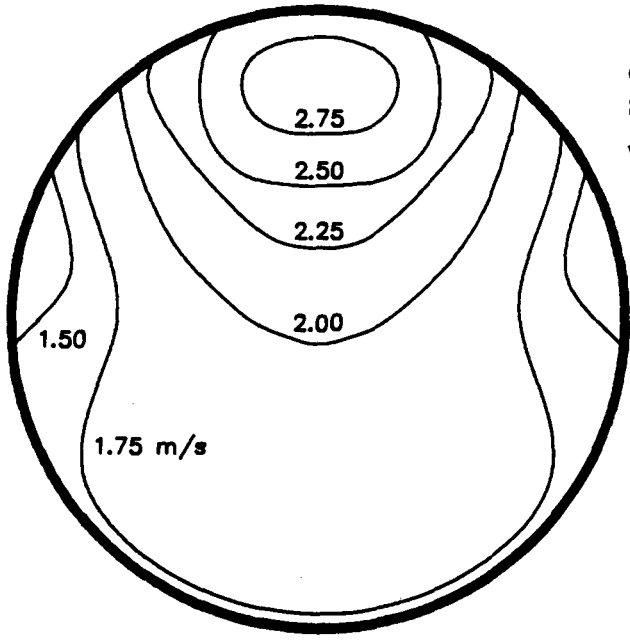

C = 48,5%
S_m = 1,80
V = 2,00 m/s

Curves indicate local mixture velocities in m/s

Figure 6.18

Mixture Isovels : Vaal Reefs 40 mm NB Horizontal

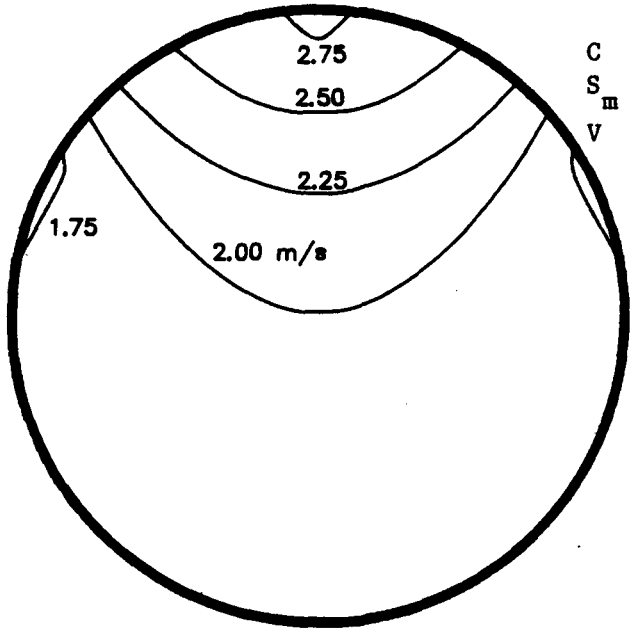

C = 51,5%
S_m = 1,85
V = 2,00 m/s

Curves indicate local mixture velocities in m/s

Figure 6.19

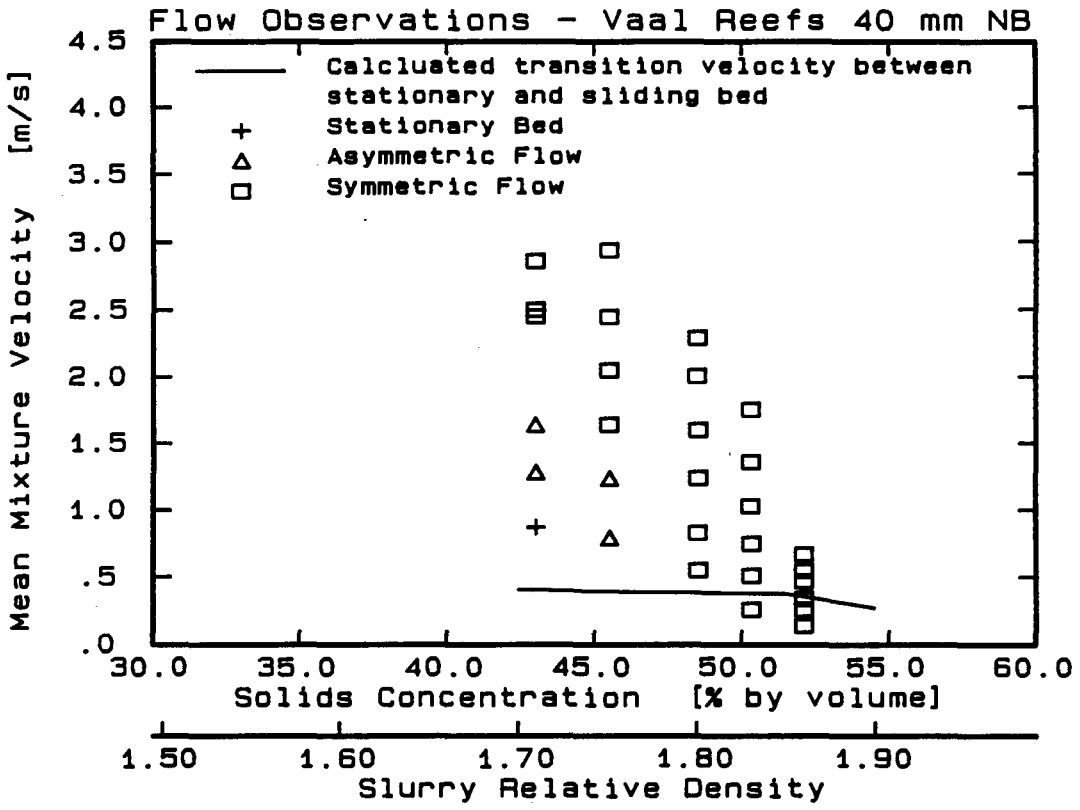

Figure 6.20

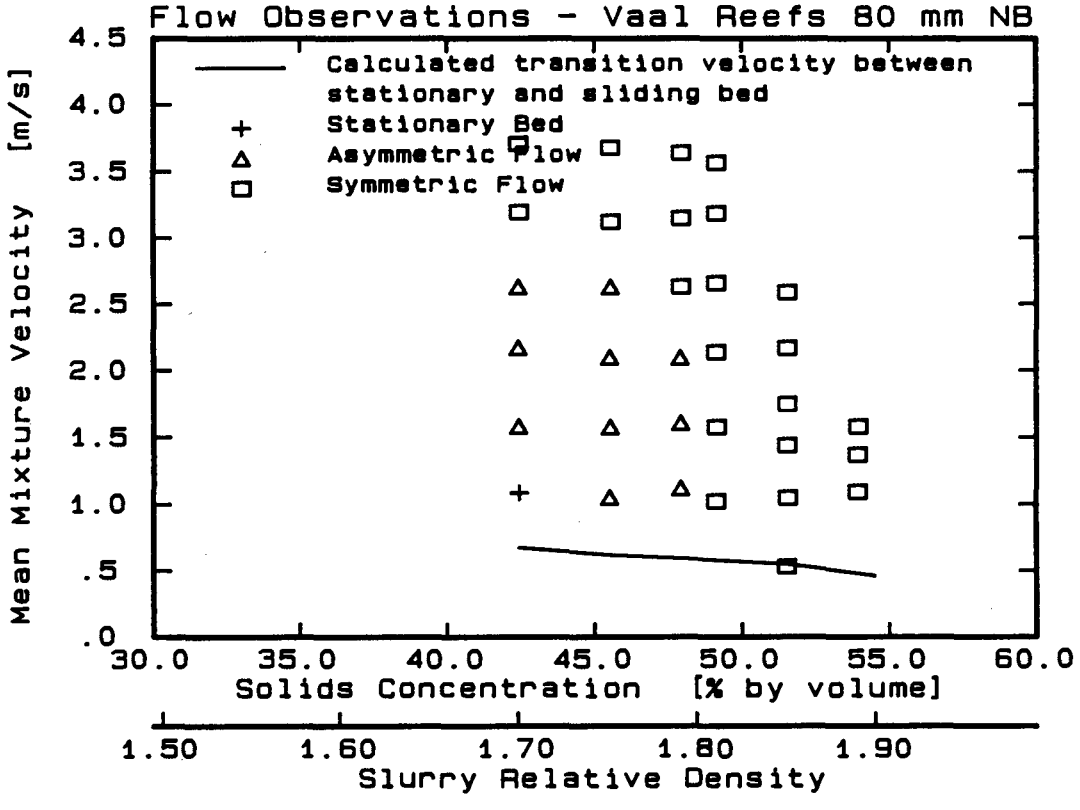

Figure 6.21

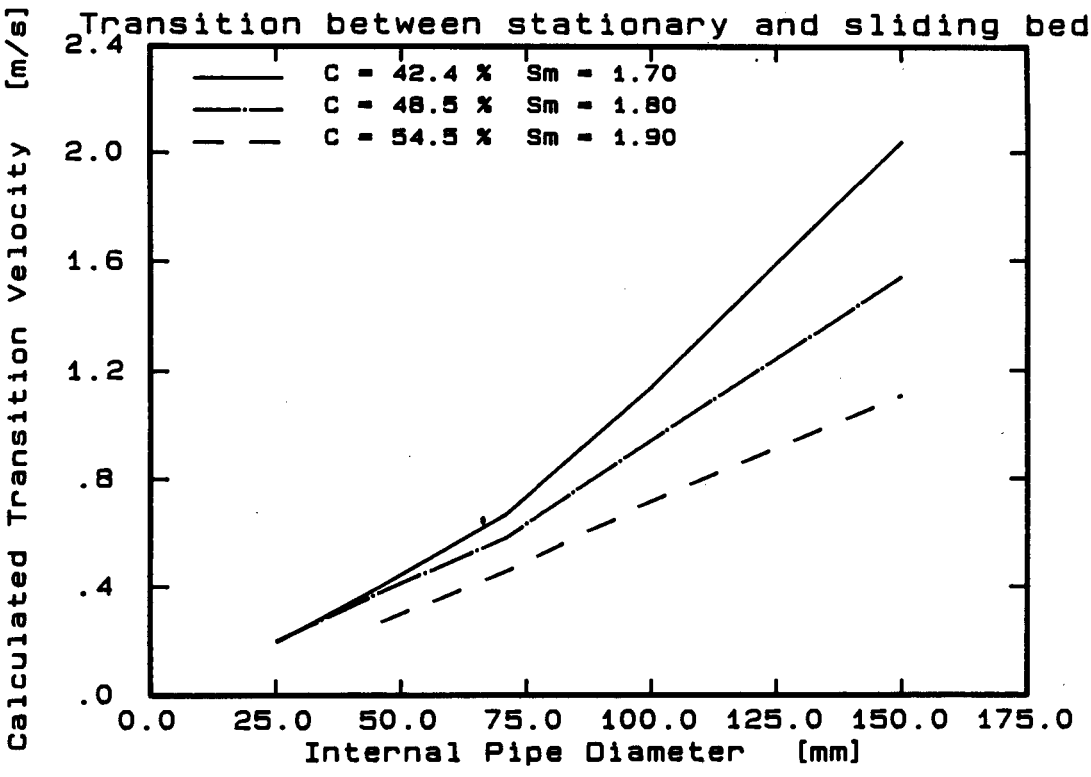
Transition between stationary and sliding bed
C = 42.4 % Sm = 1.70
C = 48.5 % Sm = 1.80
C = 54.5 % Sm = 1.90
Calculated Transition Velocity [m/s]
2.4
2.0
1.6
1.2
.8
.4
.0
0.0
25.0
50.0
75.0
100.0
125.0
150.0
175.0
Internal Pipe Diameter [mm]

Figure 6.22

4.4 Pressure gradients

4.4.1 *Influence of mean mixture velocity on pressure gradient*

Table 6.2 shows the key to the figures comparing the calculated and measured pressure gradient versus mean mixture velocity curves for the Vaal Reefs slurry in 25 mm, 40 mm and 80 mm NB pipelines.

Table 6.2 : Key to pressure gradient versus mean mixture velocity figures

Pipeline	25 mm NB	40 mm NB	80 mm NB
Horizontal	6.23	6.26	6.28
Vertical Down	6.24	6.27	6.29
Vertical Up	6.25	-	-

The predicted pressure gradients for the horizontal pipeline are greater than the measured values for solids concentrations less than 48% by volume (note that the dense phase model is only applicable for C > 46% for the Vaal Reefs slurry). The horizontal pressure gradient curves are linear and generally have a slope similar to the measured pressure gradient curves.

The vertical down calculated pressure gradients have similar slopes to the measured pressure gradients although they are slightly greater than the measured curves. For solids concentrations greater than 51% by volume the predicted curves are greater than the measured curves.

The calculated vertical up pressure gradients have similar slopes to the measured pressure gradients, although they under predict the pressure gradients.

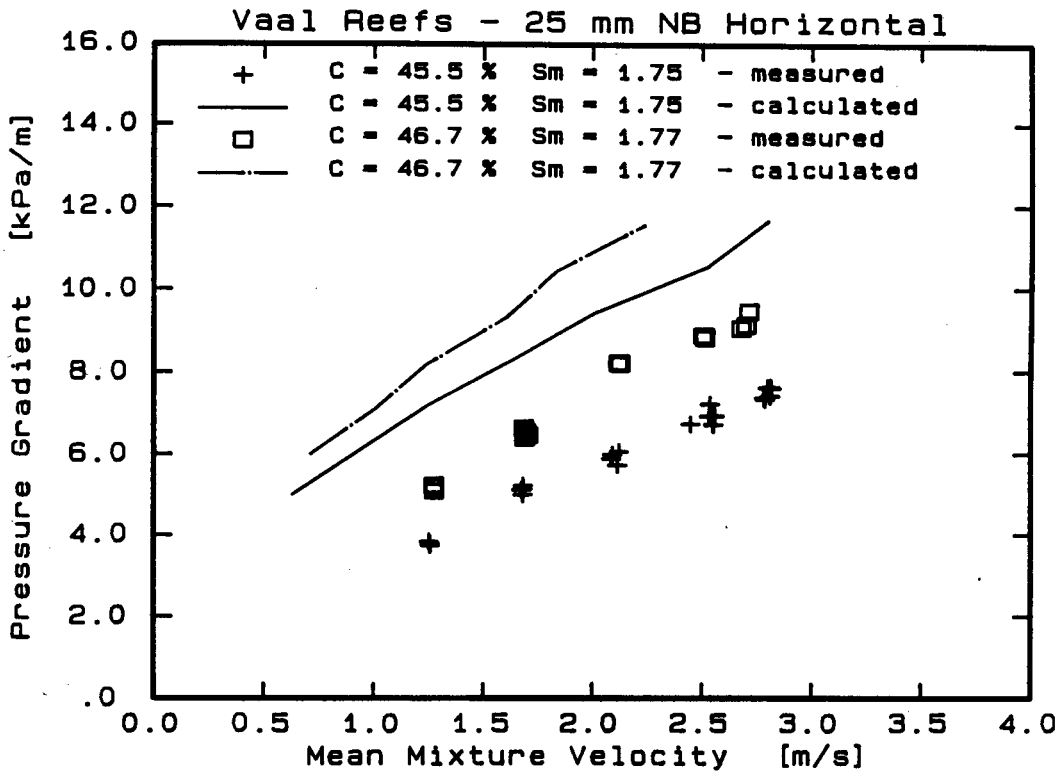

Figure 6.23

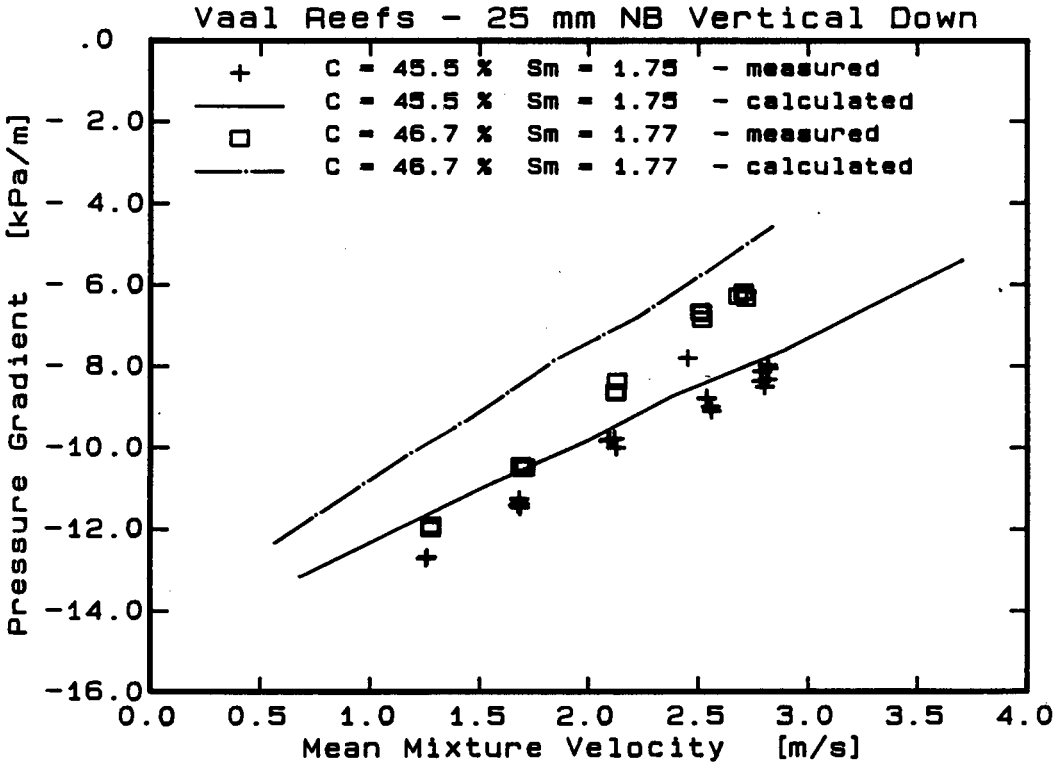

Figure 6.24

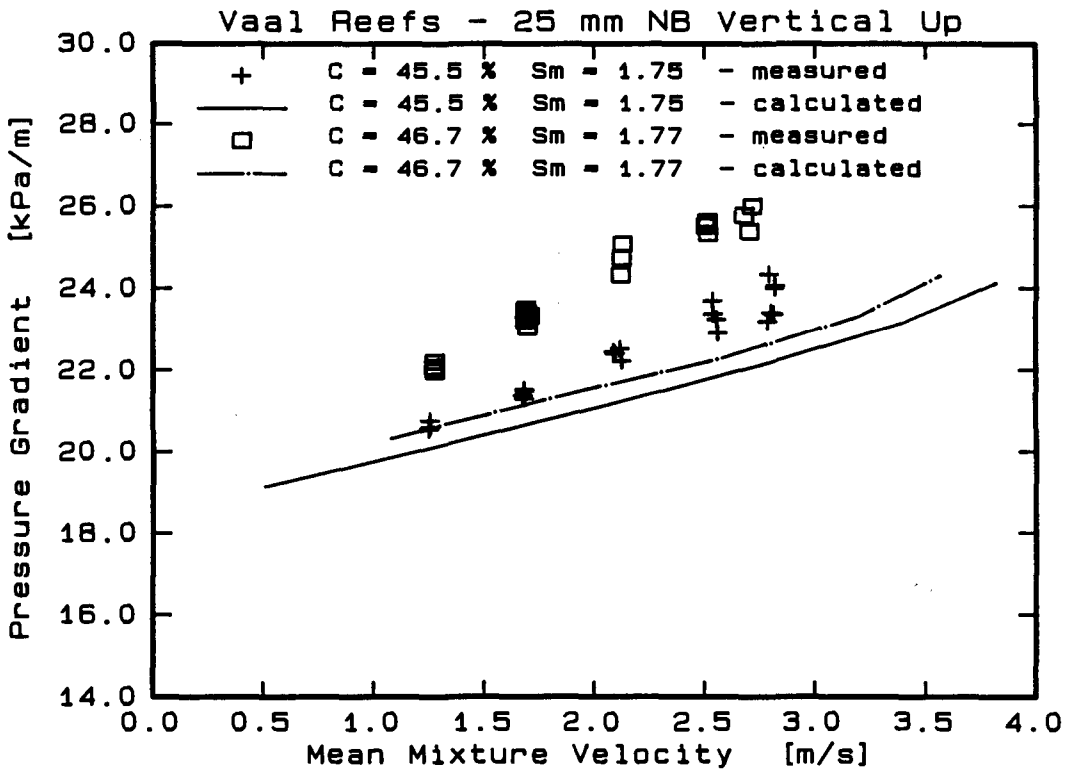
Vaal Reefs - 25 mm NB Vertical Up
C = 45.5 % Sm = 1.75 - measured
C = 45.5 % Sm = 1.75 - calculated
C = 46.7 % Sm = 1.77 - measured
C = 46.7 % Sm = 1.77 - calculated
Pressure Gradient [kPa/m]
30.0
28.0
26.0
24.0
22.0
20.0
18.0
16.0
14.0
0.0
0.5
1.0
1.5
2.0
2.5
3.0
3.5
4.0
Mean Mixture Velocity [m/s]

Figure 6.25

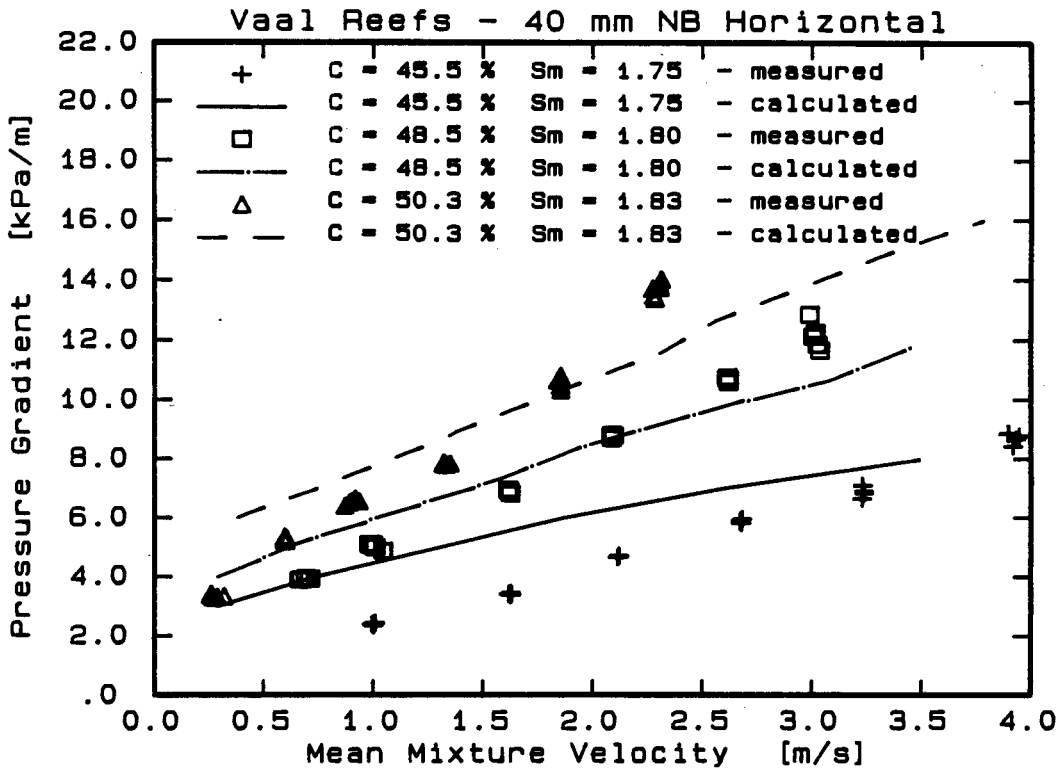

Figure 6.26

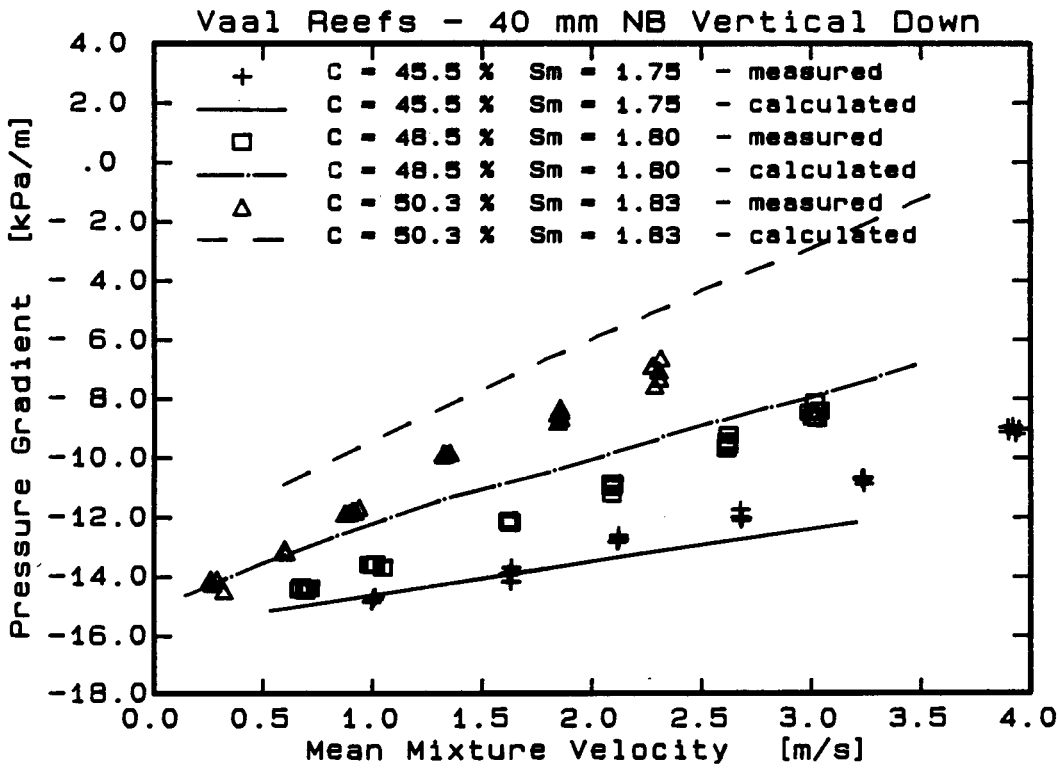

Figure 6.27

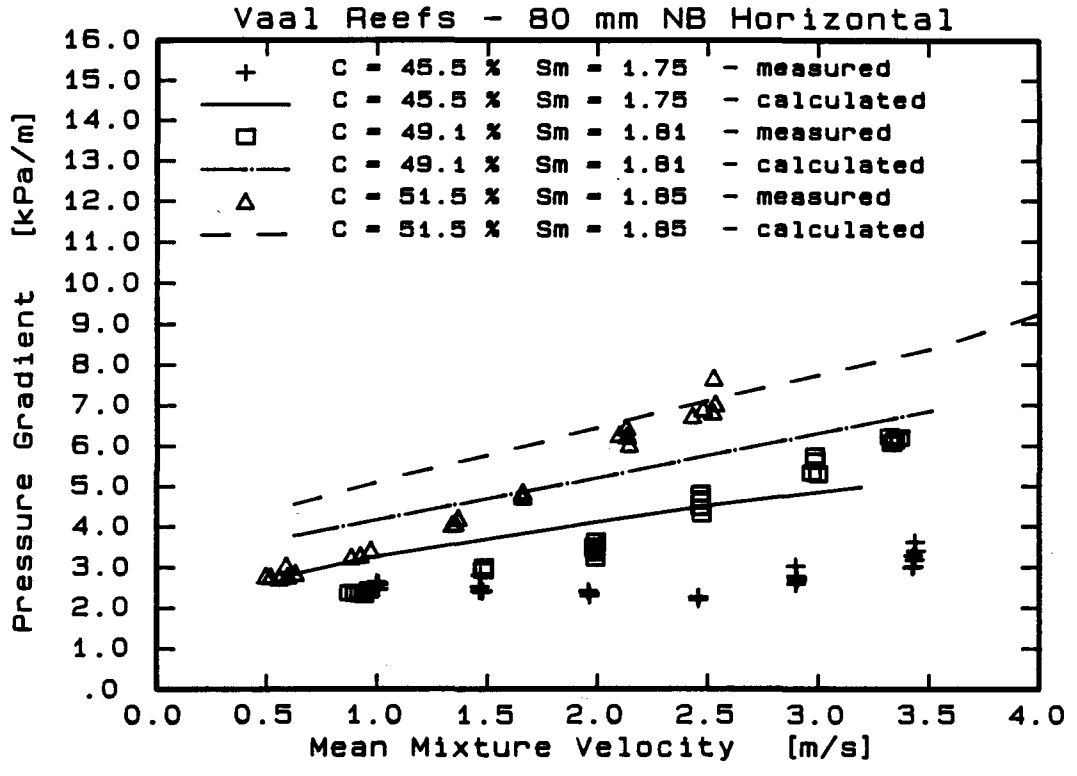

Figure 6.28

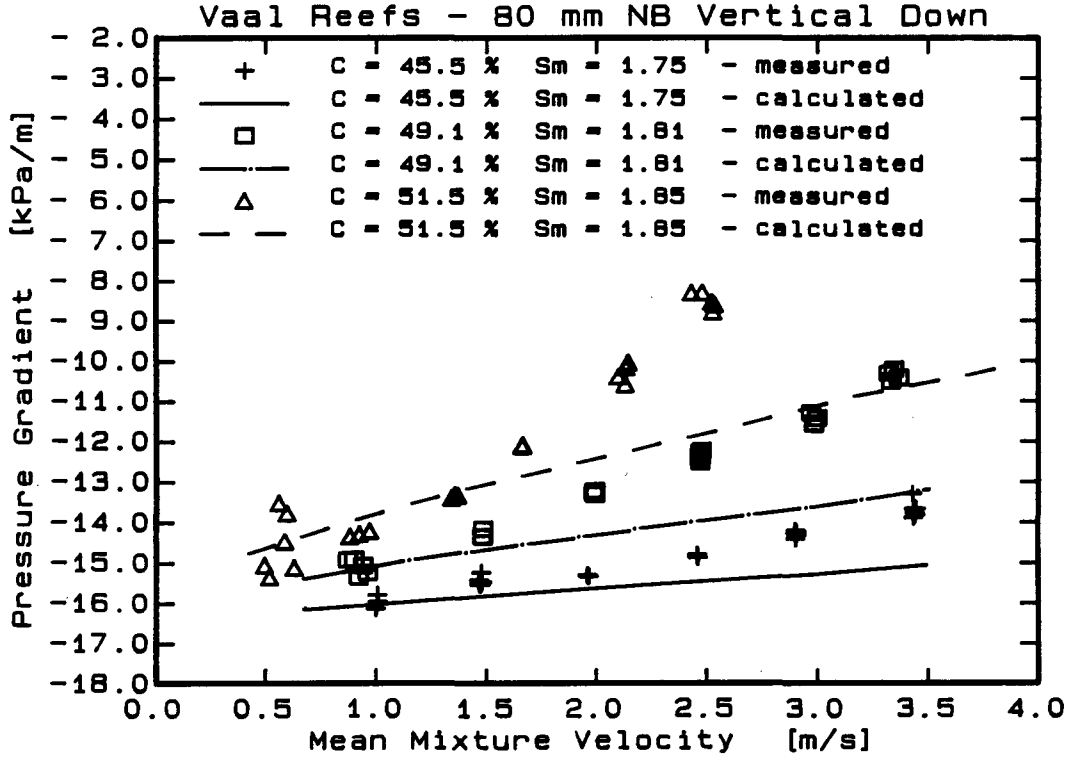

Figure 6.29

4.4.2 *Influence of solids concentration on pressure gradient*

Table 6.3 shows the key to the figures comparing the variation of the calculated and measured pressure gradients with solids concentration for the Vaal Reefs slurry in 25 mm, 40 mm and 80 mm NB pipelines.

Table 6.3 : Key to pressure gradient versus solids concentration figures

Pipeline	25 mm NB	40 mm NB	80 mm NB
Horizontal	6.30	6.32	6.34
Vertical Down	6.31	6.33	6.35

The variation of the calculated horizontal pressure gradients versus solids concentration curves are similar to the measured curves, although for solids concentrations below 48% by volume the predicted curves are higher than the measured curves. The model appears to over predict the pressure gradient for the 80 mm NB pipeline (i.e. the friction due to the sliding bed may be overestimated).

The variation of the predicted vertical down friction pressure gradient shows good agreement with the measured friction pressure gradients.

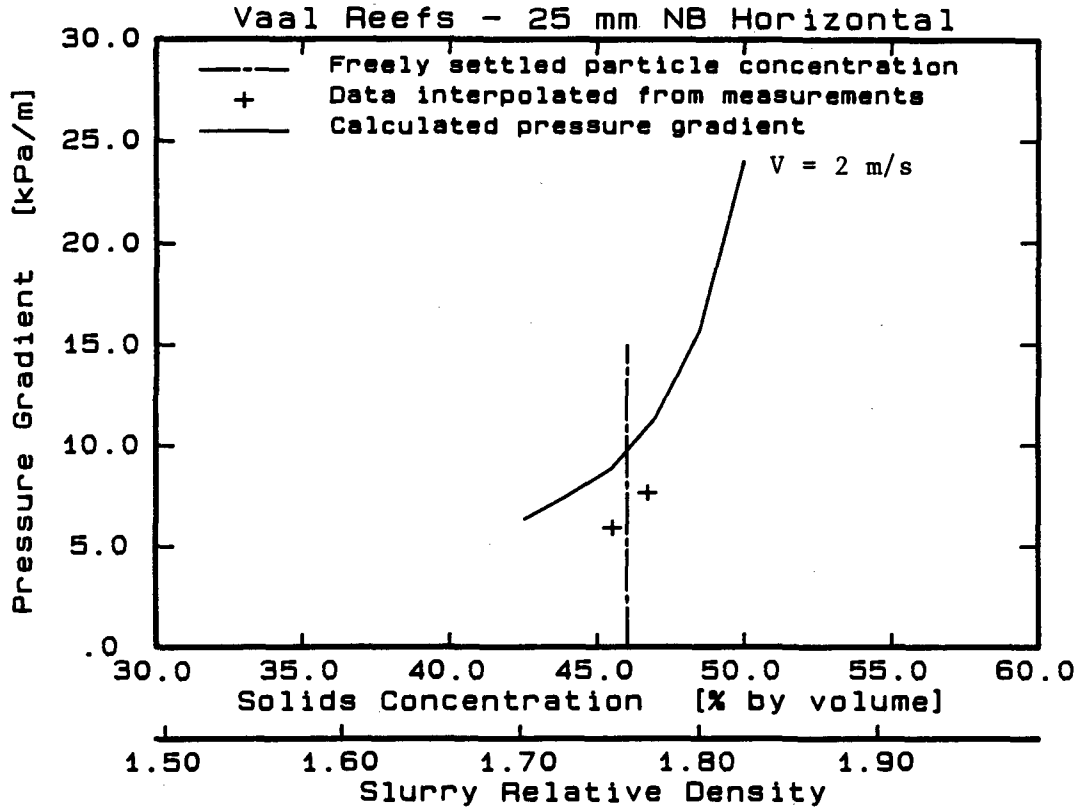

Figure 6.30

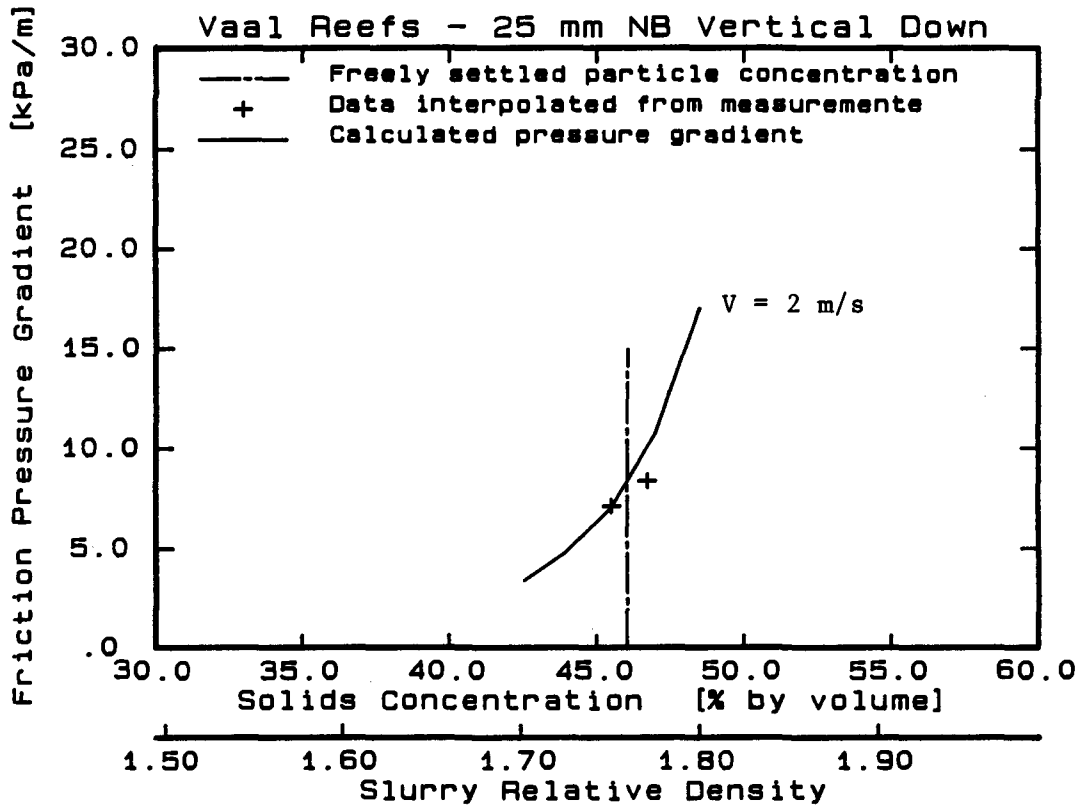

Figure 6.31

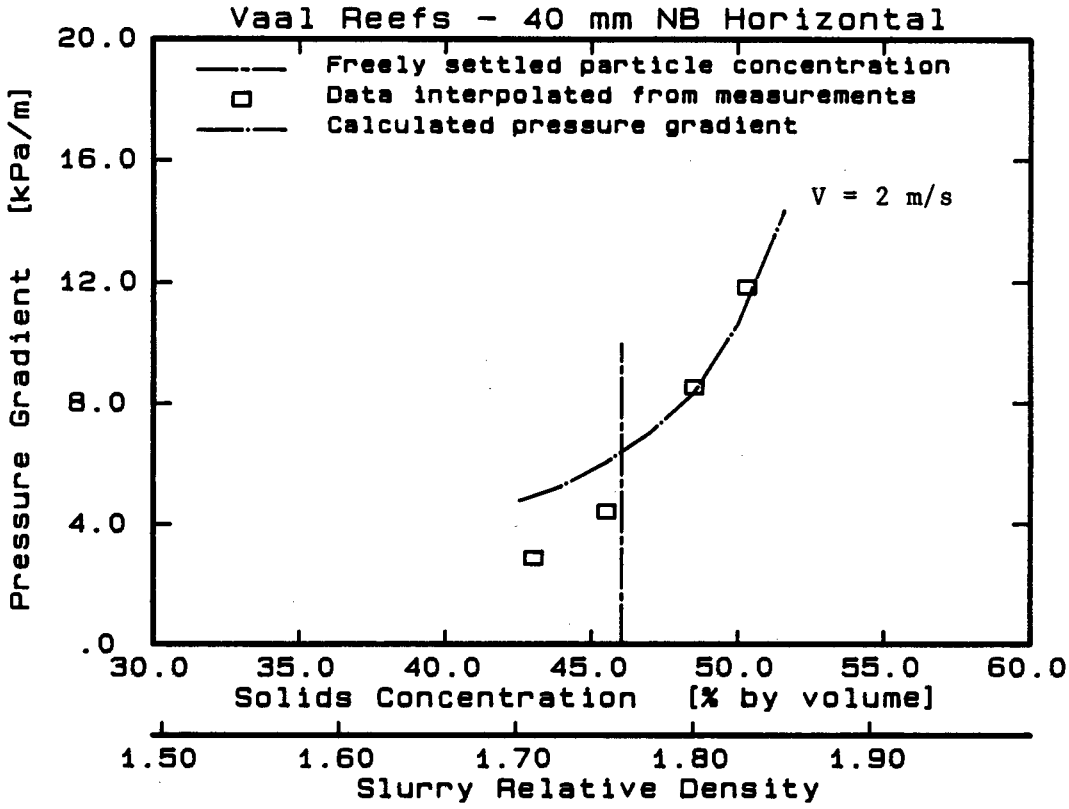

Figure 6.32

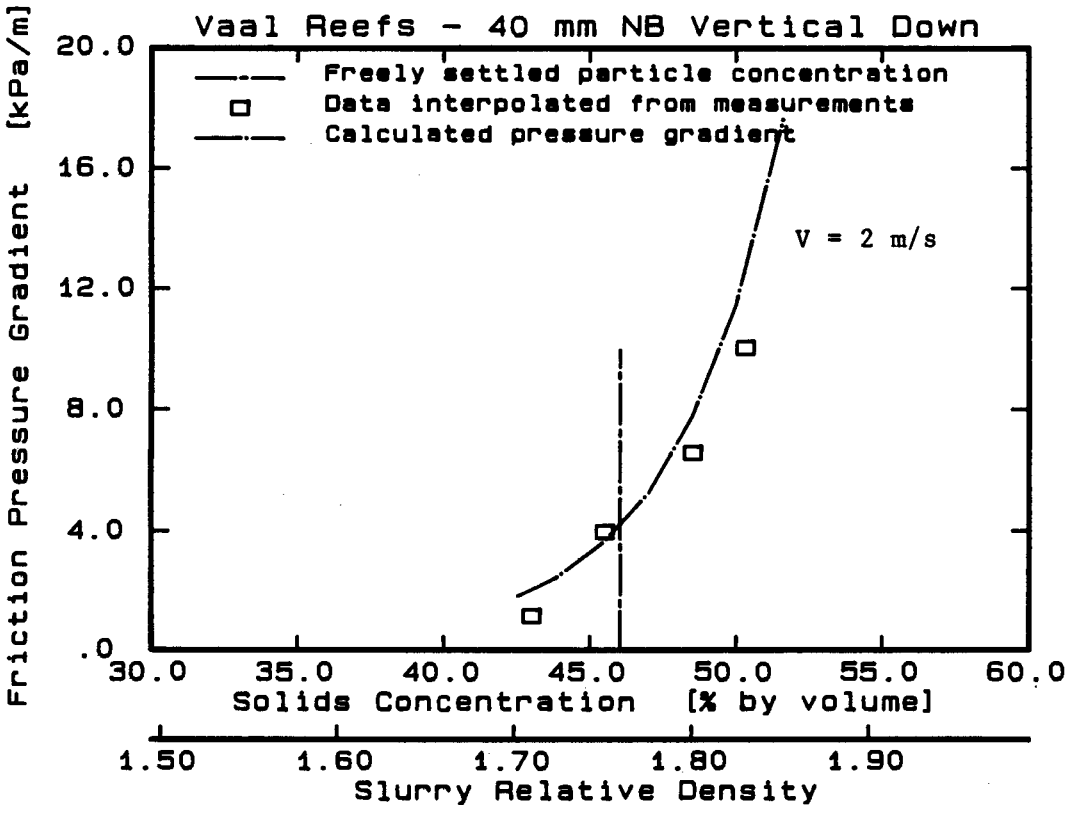

Figure 6.33

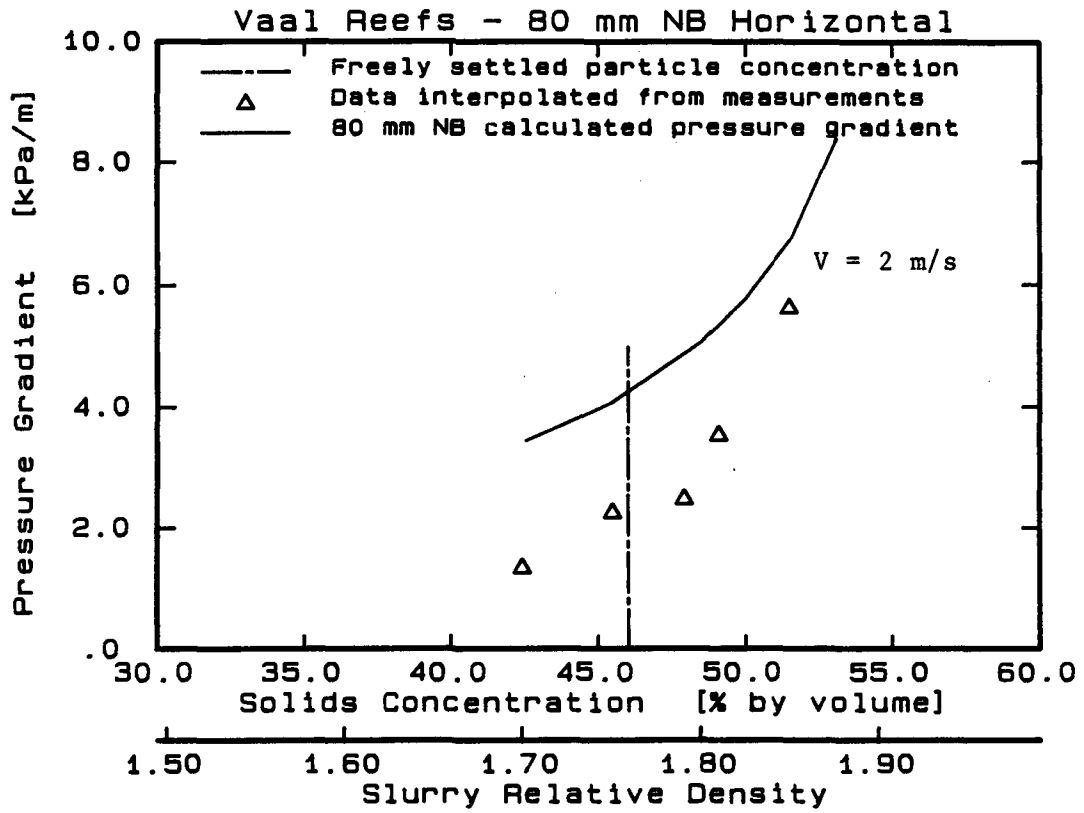

Figure 6.34

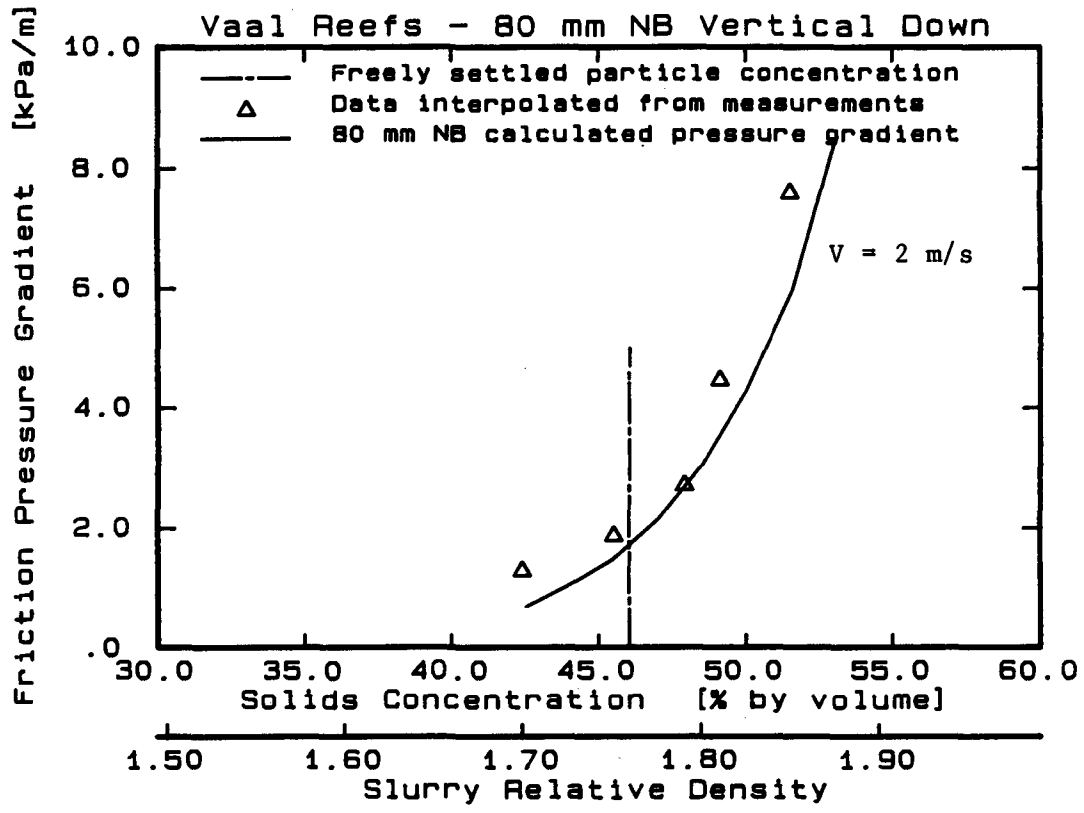

Figure 6.35

4.5 Log standard error analysis

Lazarus and Nielson (1978) considered the log standard error to be the most meaningful technique for numerically comparing the accuracy of pressure gradient correlations with experimental data. The log standard error is defined as

$$S = \sqrt{\frac{\sum_{i=1}^{n} \left[\log (\text{observed}) - \log (\text{calculated}) \right]^2}{(n-1)}} \quad , \qquad (6.8)$$

where S = log standard error

n = number of data points.

Sive (1988) suggests that care should be taken as the log standard error gives an indication of the average error values and not the maximum expected error. The log standard error is related to the average error e as follows :

$$\text{average percentage error above, } +e = 100\,(10^{S} - 1) \quad , \qquad (6.9)$$

$$\text{average percentage error below, } -e = 100\,(1 - 10^{-S}) \quad .$$

Figure 6.36 shows the variation of the average errors with the log standard error. Table 6.4 shows the average error values corresponding to log standard error values of 0,02 and 0,04. A log standard error of 0,02 indicates an average error of less than 5%, while a log standard error of 0,04 indicates an average error of less than 10%.

Table 6.4 : Log standard error and average errors

Log standard error	Percentage error	
	Above	Below
0,02	4,71	4,50
0,04	9,65	8,80

Figures 6.37 to 6.40 show the variation of the log standard error between the measured pressure gradients and the pressure gradients calculated using the model with solids concentration for the four cyclone classified tailings - Blyvooruitsig, East Driefontein, Vaal Reefs and Western Deeps. The log standard error is generally less than 0,04 (average error less than 10%) for all the test results above the freely settled particle concentration.

Figure 6.36 :

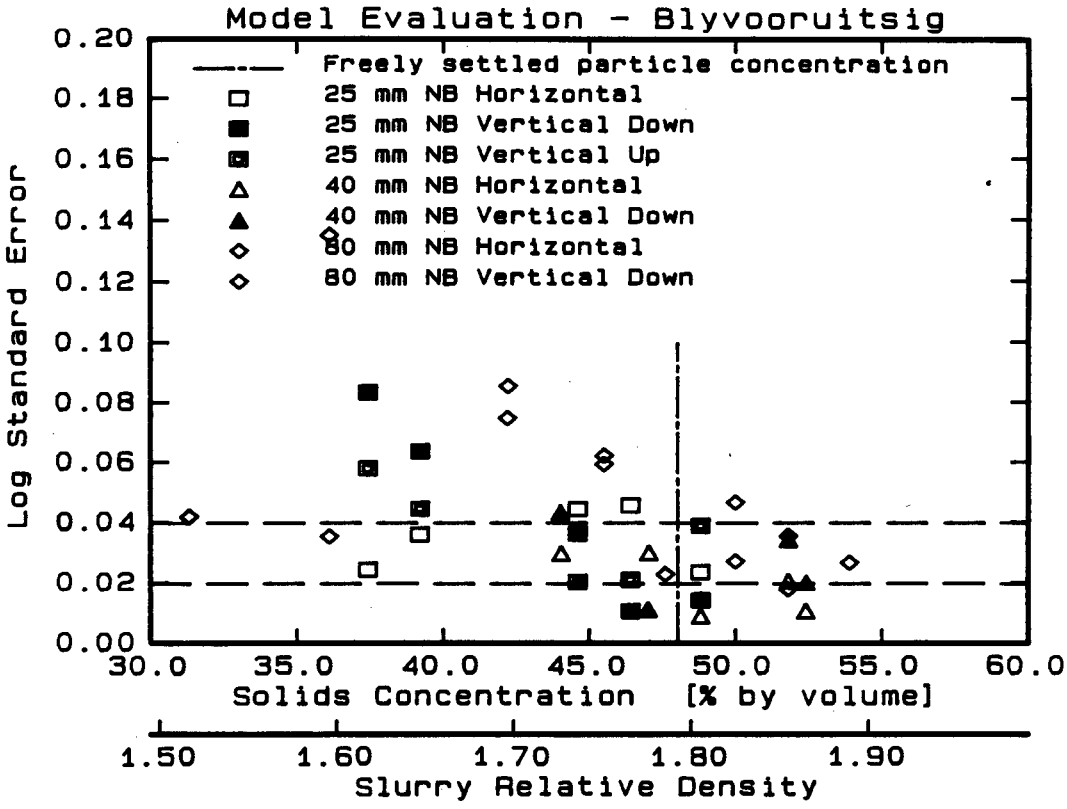

Figure 6.37

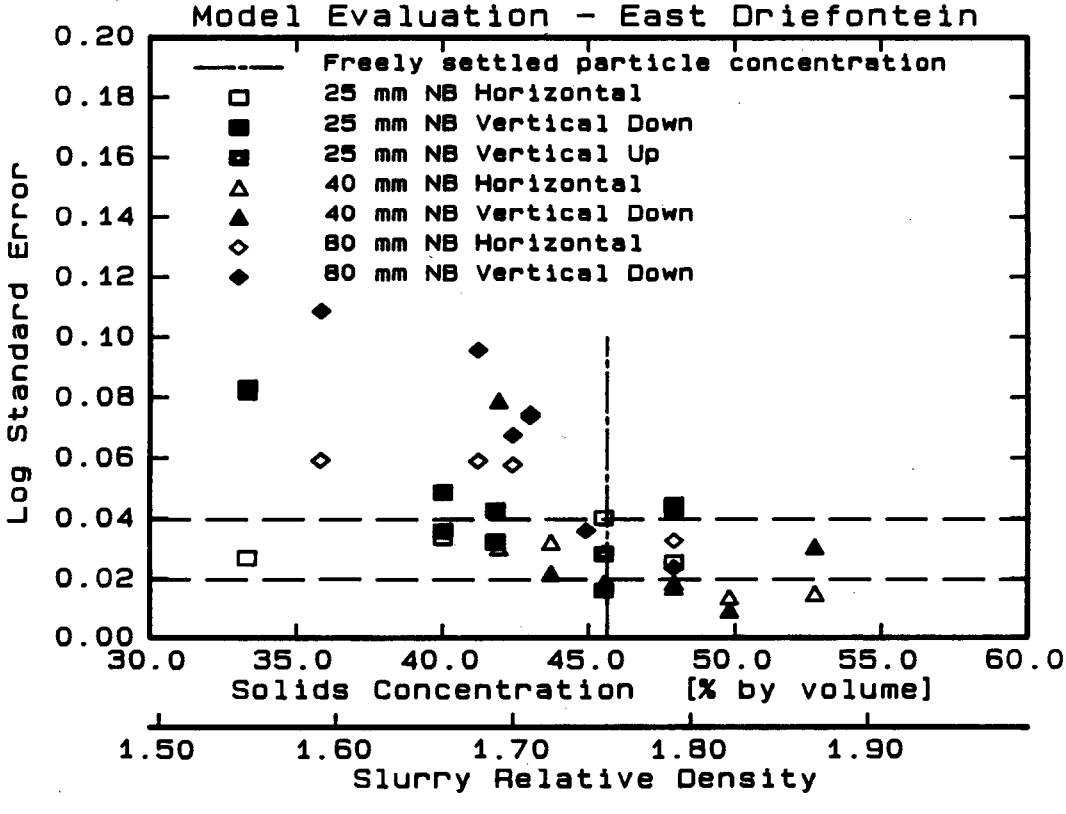

Figure 6.38

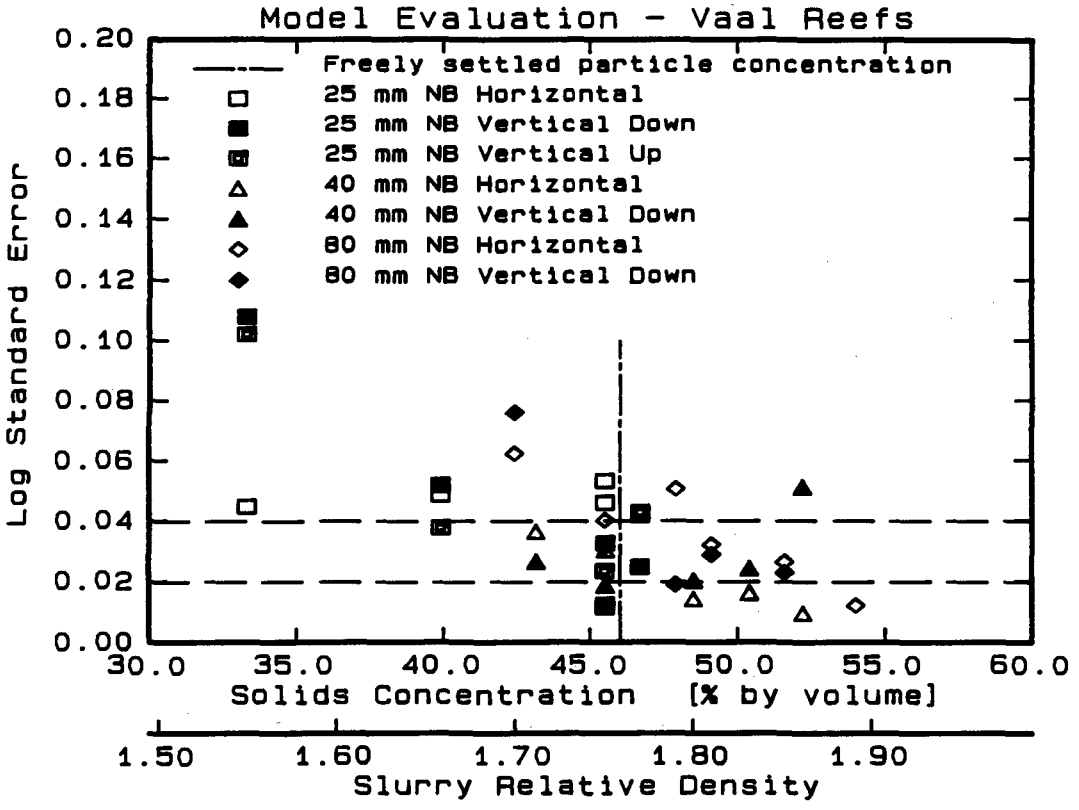

Figure 6.39

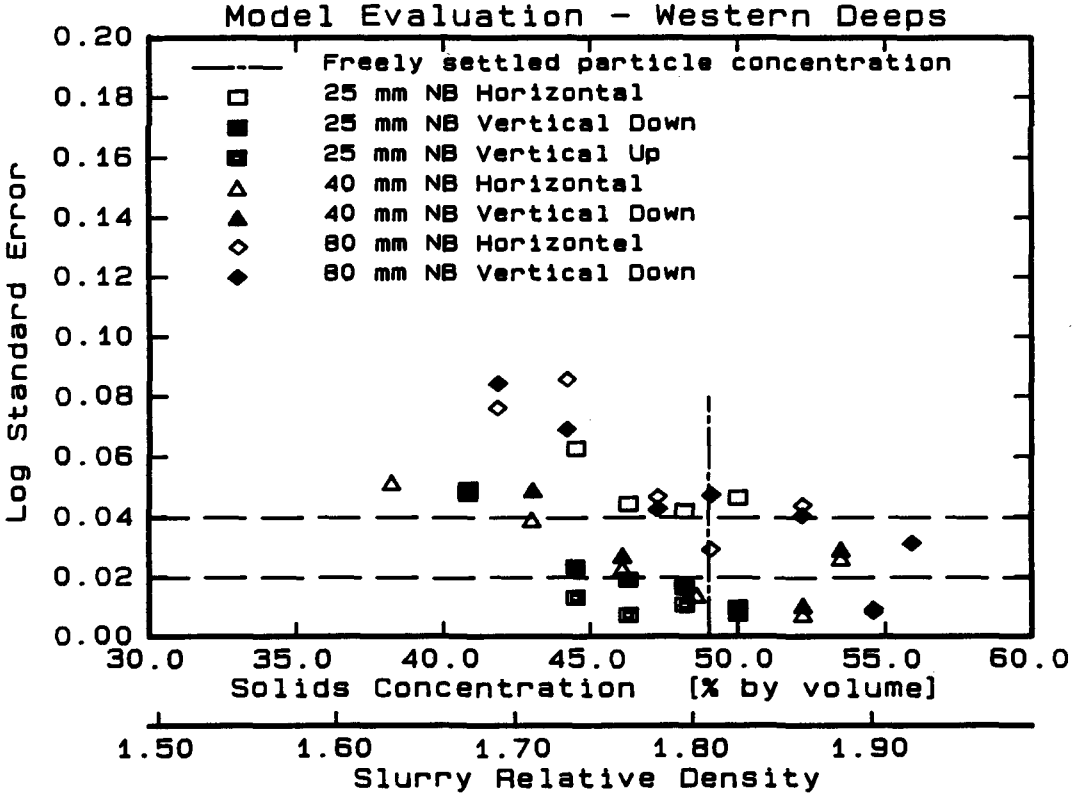

Figure 6.40

5. CHAPTER SUMMARY AND CONCLUSIONS

The dense phase flow mechanistic model has been evaluated using the experimentally determined solid particle properties discussed in Chapters 2 and 3 as input for the model. The comparitive results may be summarised as follows :

(i) The calculated velocity profiles and mixture isovels of the various dense phase flow regimes have been examined. The asymmetry of the velocity profile in a horizontal pipe becomes more pronounced with increasing mean mixture velocity and pipe diameter, and decreasing solids concentration.

(ii) The calculated transition velocity between the stationary bed and "sliding" bed flow regimes under predicts the transition at low solids concentrations (less than the freely settled particle concentration). For high concentration mixtures the model appears to over predict the transition velocity. The model predicts an increasing transition velocity with increasing pipe diameter, and that the rate of increase is greater for lower concentration mixtures.

(iii) The calculated horizontal pressure gradient versus mean mixture velocity are linear and have a similar slope to the measured curves. The variation of the calculated horizontal pressure gradient with solids concentration is similar to the measured curves, although the model over predicts the pressure gradient for solids concentrations less than 48% by volume.

(iv) The vertical down calculated pressure gradients have similar slopes to the measured curves. The variation of the predicted vertical down pressure gradient with solids concentration shows good agreement with the measured curves.

(v) The log standard error between the calculated pressure gradients and the measured pressure gradients are generally less than 0,04 (average error less than 10%) for all the tests above the freely settled particle concentration.

CHAPTER 7

CONCLUSIONS

This thesis is an analytical and experimental investigation of the hydraulic transport of high concentration cyclone classified tailings by pipeline with particular reference to backfilling in gold mines.

Two pipeline test facilities (comprising 25 mm, 40 mm and 80 mm NB pipelines) have been constructed to experimentally investigate the hydraulic transport characteristics of high concentration slurries. A data base (Appendix A) of pipeline test results has been established from tests conducted using cyclone classified tailings materials from four gold mines (Blyvooruitsig, East Driefontein, Vaal Reefs and Western Deeps).

As mechanical sliding friction makes an important contribution to the pressure gradient of pipelines transporting high concentration slurries, a rotating disc apparatus has been built to investigate the dynamic coefficient of sliding friction for fine grained particles.

A mechanistically based model has been developed to analyse the flow of high concentration settling mixtures. The model is based on the governing differential equation describing the velocity distribution in a pipeline conveying a solids liquid mixture. The differential equation is derived by applying the Cauchy momentum equations to the solid and liquid phases of the flow. Boundary conditions particular to high concentration slurries are applied to the differential equation which is solved using the finite element method.

1. EXPERIMENTAL OBSERVATIONS

1.1 The mean mixture velocity versus pressure gradient curves becomes linear at high concentrations indicating that turbulence may be negligible due to dampening by the solid particle matrix. Thus at high solids concentration the pipe wall shear stress consists primarily of viscous fluid shear stresses and mechanical sliding friction between the solid particles and pipe wall.

1.2 The pressure gradient increases sharply with solids concentration for solids concentrations greater than 45% by volume (corresponding closely to the freely settled particle concentration) for both horizontal and vertical flow.

1.3 No stationary bed was observed for the Western Deeps slurry, which has a higher percentage of fine particles than the other materials, and appears to form a semi-stabilised mixture. The other materials (Blyvooruitsig, East Driefontein and Vaal Reefs) form settling mixtures.

1.4 The transition solids concentration between observed heterogeneous flow and observed homogeneous flow increases with increasing pipe diameter. The ratio of the transition solids concentration to the freely settled particle concentration is similar for the three settling slurries (Blyvooruitsig, East Driefontein and Vaal Reefs).

1.5 The pressure gradient versus solid concentration curves for all the backfill materials have a similar shape. The pressure gradient data points for the three settling slurries lie on a single line when plotted against the ratio of solids concentration to the freely settled concentration of the solid particles.

1.6 The ratio of the solids concentration to the freely settled concentration is identified as an important parameter, and may be interpreted as an indication of the mobility of a particle within the mixture.

1.7 The horizontal and vertical down friction gradients have similar values.

1.8 The vertical down friction pressure gradient is slightly greater than the vertical up friction loss.

1.9 The Western Deeps slurry appears to form a non-Newtonian mixture at high concentration, which prevented the determination of the dynamic coefficient of friction for the Western Deeps particles due to difficulty in evaluating the normal loading on the solid particles.

1.10 The dynamic coefficient of sliding friction, measured using the rotating disc apparatus, remains constant with rotational speed for the three settling materials evaluated (Blyvooruitsig, East Driefontein and Vaal Reefs).

1.11 There appears to be no discernible trend regarding the effect of particle size distribution on the dynamic coefficient of sliding friction.

1.12 As the mechanism of solid particles sliding relative to each other is similar to solid particles sliding against a solid boundary, the variation of the dynamic coefficient of friction with solids concentration has been estimated as being the same as the variation of the measured angle of internal friction with solids concentration.

2. MECHANISTIC MODEL

2.1 The particle size distribution of the solid particles in the mixture is divided into "fine" and "coarse" fractions. The division of the particle size distribution is based on a particle settling velocity of 1 mm/s calculated using Stoke's law for laminar settling.

2.2 The model has been specifically been developed for dense phase mixtures which are defined to exist when the concentration of the coarse fraction exceeds the freely settled (submerged loose poured) concentration of the coarse fraction and the predominant mechanism supporting the particles is interparticle contact.

2.3 The differential equation describing the velocity distribution within the pipe has been formulated by applying the Cauchy momentum equations to the solid and liquid phases of the mixture.

2.4 The shear stress distribution due to the applied pressure gradient is linear for homogeneous mixtures.

2.5 The concept of lateral interparticle stress, arising from the stress on particles due to fluid dynamic drag exerted on the particles by the seepage flow of the vehicle, is presented.

2.6 The solid phase shear stress within the pipe section is evaluated using the internal angle of friction between the solid particles. At the pipe wall the coefficient of sliding friction is used to calculate the wall shear stress due to the solid phase.

2.7 The concept of sheared and unsheared zones within the pipe section based on the applied shear stress distribution and the failure shear stress of the granular matrix is introduced. In the unsheared zone the fluid shear is zero and consequently there is no velocity gradient. It is shown that three possible flow regimes are possible :

a) unsheared zone occupying the whole pipe section - plug flow.

b) unsheared core surrounded by annular region of sheared granular matrix.

c) unsheared zone in contact with a portion of the pipe wall forming a "sliding bed" of unsheared particles.

2.8 The viscosity of the mixture and the vehicle are evaluated using the correlation ascribed to Landel *et al*.

2.9 The differential equation describing the velocity distribution is solved using the finite element method with boundary conditions specific to the problem imposed.

2.10 The boundary velocity of the mixture is evaluated by considering the local applied stress and solid phase shear stress at the pipe wall.

3. EVALUATION OF MECHANISTIC MODEL

3.1 The asymmetry of the velocity profile calculated using the mechanistic model becomes more pronounced with increasing mean mixture velocity and pipe diameter, and decreasing concentration.

3.2 The calculated transition velocity between the stationary bed and "sliding" bed flow regimes under predicts the transition at low solids concentrations (less than the freely settled particle concentration). For high concentration mixtures the model appears to over predict the transition velocity. The model predicts an increasing transition velocity with increasing pipe diameter, and that the rate of increase is greater for lower concentration mixtures.

3.3 The calculated horizontal pressure gradient versus mean mixture velocity curves are linear and have a similar slope to the measured curves. The curve of the calculated horizontal pressure gradient versus solids concentration is similar to the measured curves, although the model over predicts the pressure gradient for solids concentrations less than 48% by volume (i.e. the freely settled concentration).

3.4 The vertical down calculated pressure gradients have similar slopes to the measured curves. The curve of the predicted vertical down pressure gradient versus solids concentration shows good agreement with the measured curves.

3.5 The log standard error between the predicted pressure gradients and the measured pressure gradients are generally less than 0,04 (average error less than 10%) for all the tests above the freely settled particle concentration.

4. CONTRIBUTIONS MADE BY THIS THESIS

The major contributions made to the field of *Hydraulic Transport of Solids in Pipelines* are as follows :

4.1 A data base of measured pressure gradients for the high concentration flow of cyclone classified tailings has been established.

4.2 A standardised procedure for determining the submerged internal angle of friction for solid particles has been presented.

4.3 A rotating disc apparatus has been developed to determine the dynamic coefficient of friction for fine grained solid particles.

4.4 A mechanistic analytical model for the dense phase flow of cyclone classified tailings has been developed, which is an advancement on previous dense models as :

(i) the model is applicable for solids with wide particle size distributions

(ii) detailed solid particle and fluid friction mechanisms have been considered

(iii) the concept of sheared and unsheared zones within the pipe is introduced, and various flow regimes are shown to exist.

CHAPTER 8

FUTURE RESEARCH

1. INTRODUCTION

The objective of this chapter is to highlight and discuss possible future research topics that may arise as an extension of the work presented in this thesis. The following research topics are discussed :

(a) Solid particle sliding friction

The range of the experimentally measured values of the dynamic coefficient of friction may be extended by testing different types of solid particles sliding over various surface materials of varying roughness. A method of measuring the incipient coefficient of friction using the existing rotating disc apparatus is suggested.

(b) Normal interparticle stress at pipe wall

Knowledge of the interparticle stress acting against the pipe wall is of prime importance for the correct evaluation of the solid particle pipe wall frictional forces. The design of an apparatus is proposed which will allow for the normal interparticle stress at the pipe wall to be measured experimentally.

(c) Velocity and concentration distribution in pipeline

The velocity distribution predicted by the mechanistic model, and the assumption of a uniform concentration distribution, should be verified by experimentally measuring the local mixture velocities and solids concentrations.

(d) Further development of mechanistic model

It is envisaged that the mechanistic model developed in this thesis will form part of an ongoing investigation of solids liquid flows. The model may be used as a basis for analysing

other types of slurry flow such as heterogeneous turbulent mixtures, and non-Newtonian mixtures.

(e) Distribution of wear around the pipe circumference

As a hydraulic transport pipeline will fail at that point of its cross section that has the least pipe wall thickness, the operating life of the pipeline is determined by the *local* wear rates around the pipe circumference opposed to the *global* wear rate. It is proposed that the dense phase mechanistic model be used to determine local pipeline wear rates.

2. SOLID PARTICLE SLIDING FRICTION

2.1 Dynamic coefficient of sliding friction

This thesis examined the dynamic frictional forces between a smooth stainless steel surface and typical cyclone classified tailings solid particles. It would be of interest to examine the influence of different surface roughnesses and solid particle types (i.e. various particle size distributions, shape factors and mineral compositions) on the dynamic coefficient of friction.

Backfill pipelines are being lined with various polymethanes and high density polyethylenes to provide greater pipeline wear resistance and hence increased pipeline life. As these materials have a very wide range of hardnesses, the nature of the frictional forces between these polymeric materials and solid particles should be investigated.

2.2 Incipient coefficient of sliding friction

The incipient coefficient of friction between the solid particles and the pipe wall (expected to be greater than the dynamic coefficient of friction) is important when analysing problems such as the restart of a pipeline filled with slurry. Figure 8.1 shows an arrangement by which the existing rotating disc apparatus (used to measure the dynamic coefficient of friction) could be used to determine the incipient coefficient of friction.

Referring to Figure 8.1, torque is transmitted to the shaft of the rotating disc by a suspended weight attached to a cable. Provided that the frictional resistance between the annular channel filled with solid particle is greater than the applied torque the disc will not rotate. As the mass of the weight is gradually increased the torque applied to the rotating disc is increased until the applied torque exceeds the frictional resistance causing the disc to rotate. The peak force measured on the load cell restraining the annular channel from rotating will correspond to the incipient frictional resistance.

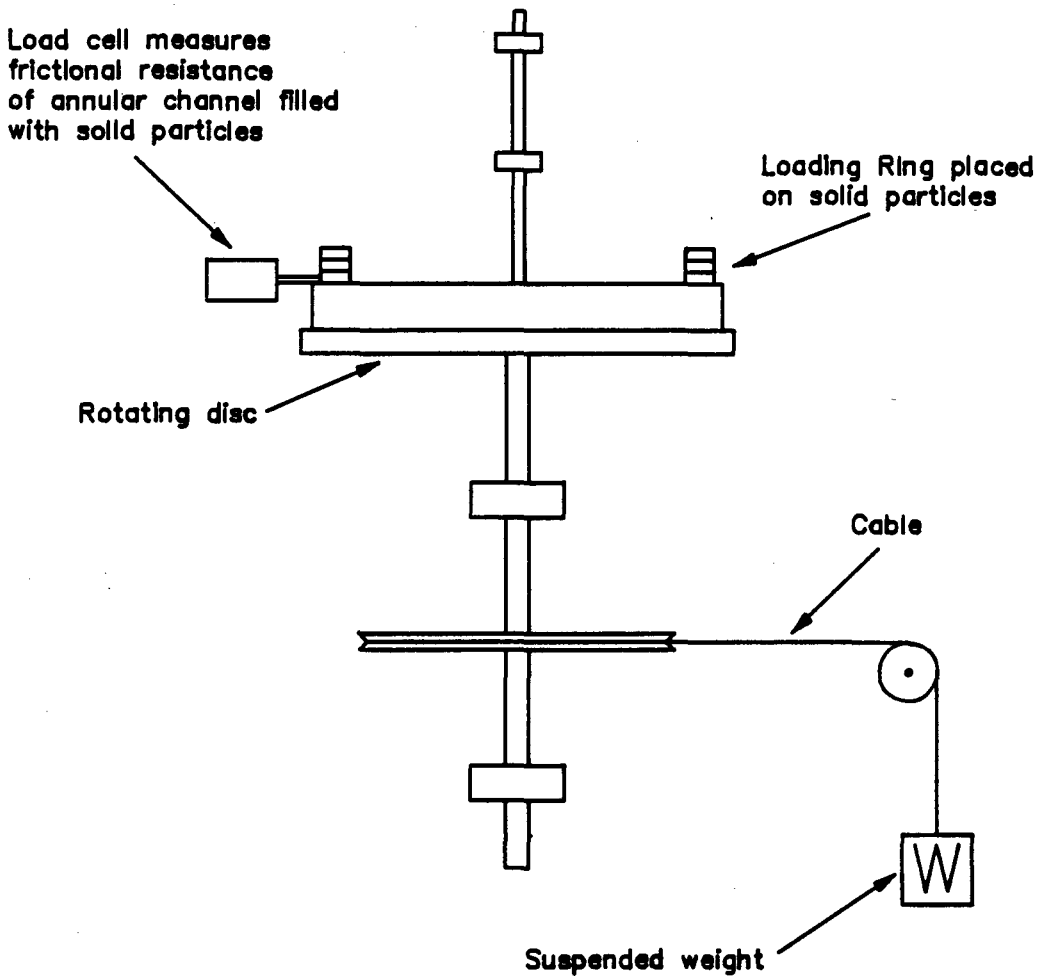

Figure 8.1 : Proposed arrangement of rotating disc apparatus to measure incipient friction

3. NORMAL INTERPARTICLE STRESS AT PIPE WALL

The solid phase shear stress at the pipe wall is the product of the normal interparticle stress acting against the pipe wall and the dynamic coefficient of friction between the solid particles and pipe wall. In this thesis the dynamic coefficient of friction has been measured independently of the pipeline using the rotating disc apparatus, while the normal interparticle stress has been estimated using assumed stress relations (coefficient of lateral interparticle stress and Wilson's hydrostatic assumption). A direct measurement of the normal interparticle stress will yield valuable information on the solid phase shear stress at the pipe wall, solid particle stress relations and dense phase flow mechanisms.

Figure 8.2 illustrates the proposed design of a device to measure the normal interparticle stress at the pipe wall. The principle of the method is to compare the total stress (fluid pressure plus normal interparticle stress) and the pore water pressure (fluid pressure) acting at two points at the same level on the pipe cross section. The difference between the two measurements will be the normal interparticle stress (effective stress in soil mechanics).

The fluid pressure is measured using a static wall tapping, while the total stress is measured by placing a flexible rubber membrane over a hole in the pipe wall as shown in Figure 8.2. Both the fluid pressure and the normal interparticle stress will be transmitted through the membrane. There are various techniques by which the pressures may be compared - the primary requirement being that the deflection of the membrane is either nulled or kept to a minimum by using a small volumetric displacement system. The simplest method is probably to use an electronic pressure transducer as shown in Figure 8.2.

Figure 8.3 shows an arrangement whereby the device could be used to verify Wilson's hydrostatic interparticle stress distribution for stationary and sliding bed flow regimes. The variation of the normal interparticle stress with height above the pipe invert could be determined (by comparing pressures at different levels in the pipe section) and compared to the hydrostatic pressure distribution.

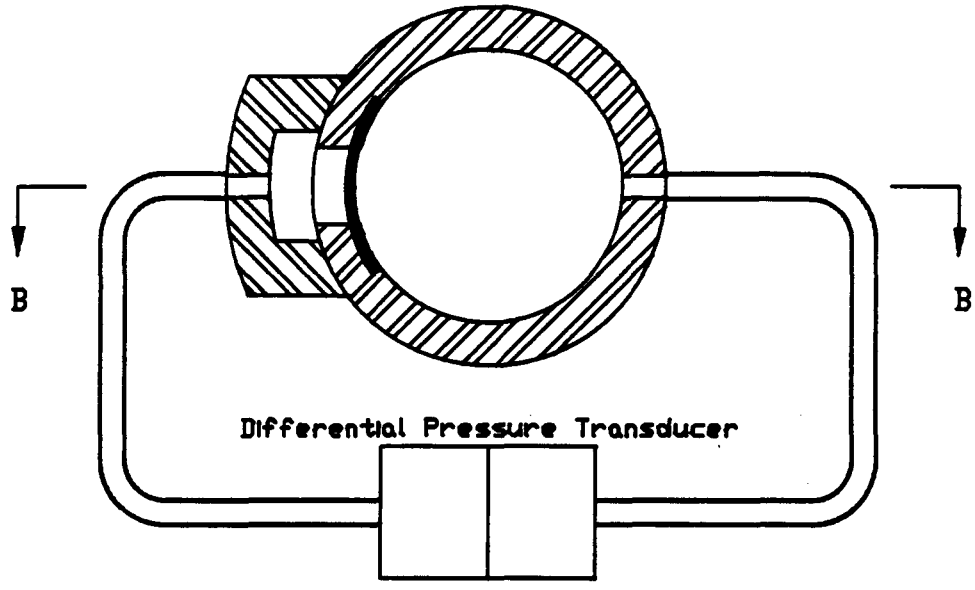

PLAN VIEW AA

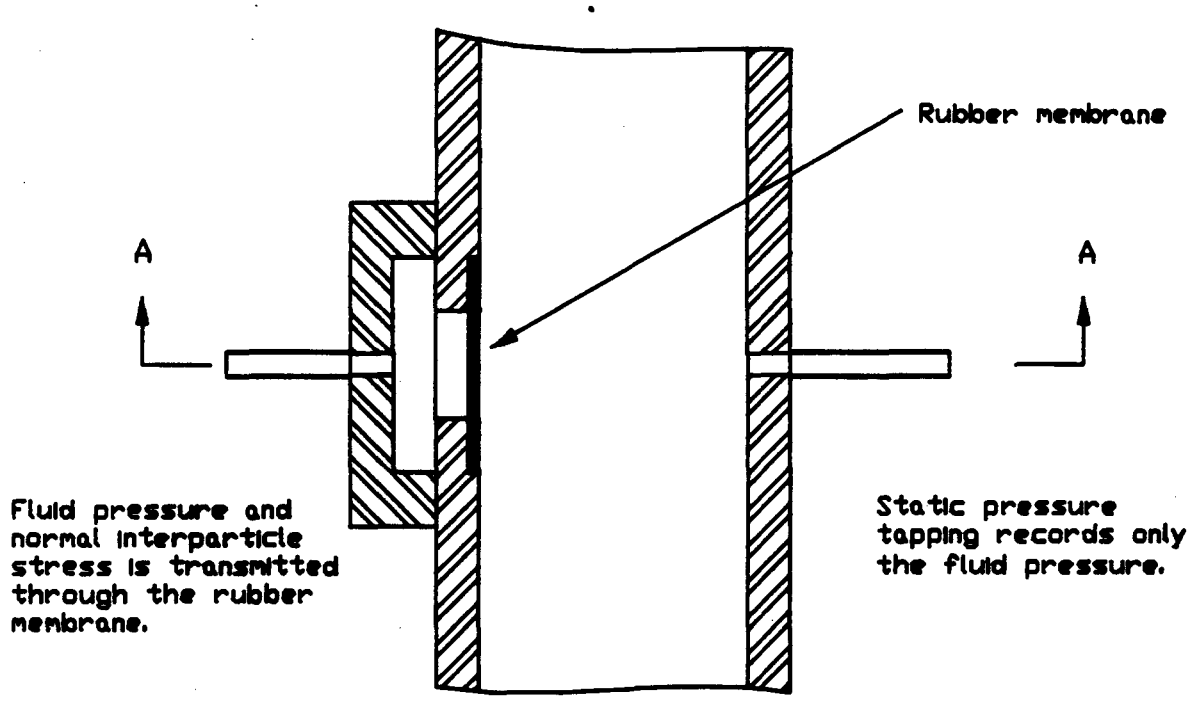

SECTION BB

Figure 8.2 : Proposed design for device to measure normal interparticle stress at pipe wall

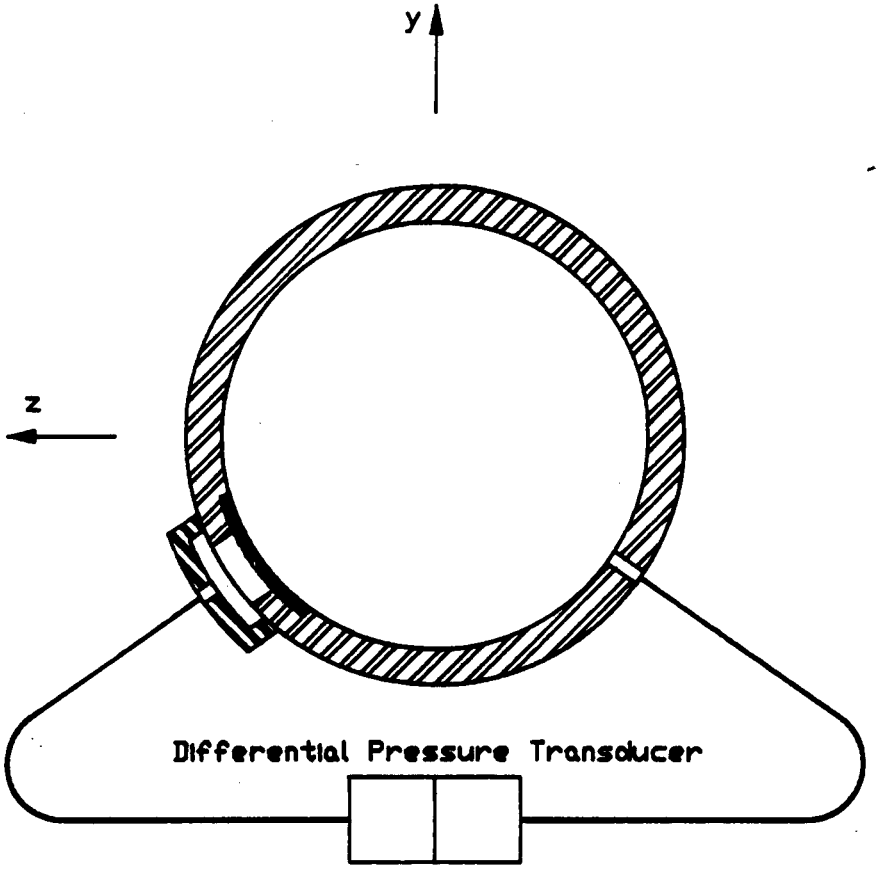

Figure 8.3 : Arrangement of normal interparticle stress device to verify Wilson's hydrostatic stress assumption in a horizontal pipe

4. VELOCITY AND CONCENTRATION DISTRIBUTION

As part of the early investigations conducted for this thesis into the nature of the flow of solids liquid mixtures in pipelines an isokinetic sampling probe was developed (Cooke and Lazarus (1988)). The probe samples slurry flows isokinetically without requiring a separate measurement of the local velocity, by using the stagnation pressure in the sampling tube as a reference. The isokinetic probe is described in Appendix D.

When using the probe to sample high concentration mixtures such as typical backfill slurries, the integrated local mixture velocities do not equal the measured mixture flow rate. Thus it is concluded that the probe is not suitable for sampling high concentration mixtures.

Brown *et al* (1983) developed a probe to measure point velocities in slurry flows using a cross-correlation technique. Nasr-el-Din (1986) used this probe to measure local mixture concentrations based on the mixture resistivity. It is suggested that these methods be used to determine local mixture velocities and solids concentrations for dense phase mixtures.

5. FURTHER DEVELOPMENT OF MECHANISTIC MODEL

5.1 Turbulent heterogeneous slurry flow

The mechanistic model may be extended to deal with heterogeneous mixtures in which particles are partially or completely suspended through turbulent diffusion. The work of Roco and Shook ((1982), (1983), (1984), (1985a), (1985b), (1987)), Roco and Balakrishnam (1985) and Roco and Mahadevan ((1986a) and (1986b)) provides the foundation for the analysis of turbulent slurry flows.

5.2 Non-Newtonian slurry flow

The mechanistic model may be adapted to deal with non-Newtonian mixtures by incorporating the appropriate constitutive relations for the fluid shearing stress. To illustrate the analysis of a non-Newtonian mixture, the analysis of a slurry which is considered to be a combination of a dense phase mixture and a stabilised mixture (all particles supported by the yield stress of the mixture) is examined below.

Figure 8.4 shows the distribution of shear stresses acting within a non-Newtonian dense phase mixture, i.e. a slurry in which the particles are supported by a combination of interparticle contact and the yield stress of the mixture. For relative motion between adjacent elements of the mixture to occur (i.e. $dv/dy \neq 0$) the applied shear stress must exceed the sum of the solid particle matrix failure shear stress and the yield stress of the mixture. Referring to Figure 8.4 this is seen to occur at points a b resulting in an unsheared core of slurry surrounded by a sheared annulus of mixture with the slurry velocity distribution as shown. This flow case may be solved using the methods presented in Chapter 5.

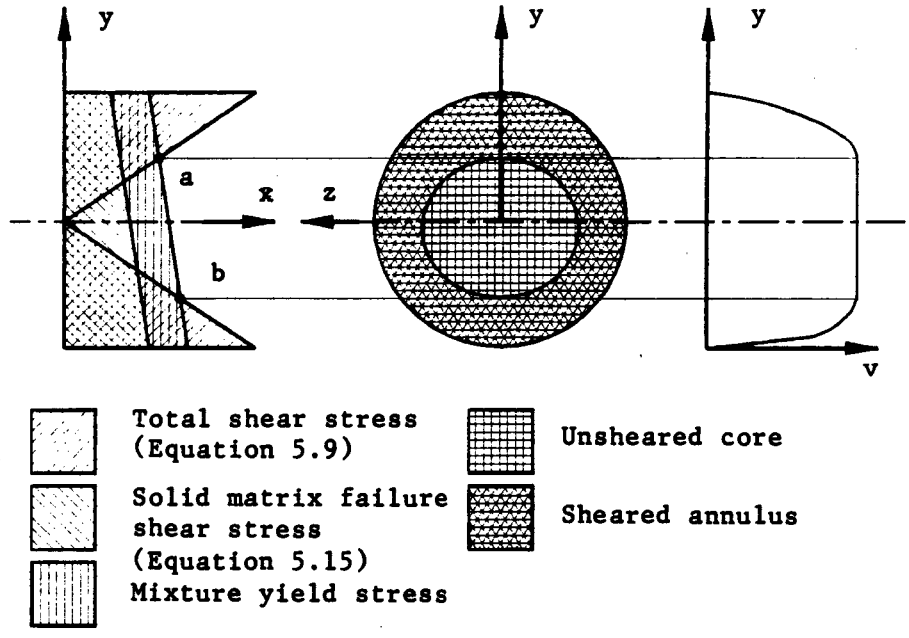

Figure 8.4 : Shear stress distribution in a non-Newtonian dense phase mixture

6. DISTRIBUTION OF WEAR AROUND THE PIPE CIRCUMFERENCE

Roco and Cader (1985) have outlined a computational approach to predicting wear distribution in slurry pipelines. They postulate that wear occurs through a combination of three wear mechanisms :

(i) random impact of particles having fluctuating velocities,

(ii) directional impact of particles with a predominant convective velocity toward the wall, and

(iii) friction.

Sliding friction is likely to be the dominant mechanism by which material is removed from pipelines conveying the dense phase mixtures considered in this investigation. The material loss due to friction should be directly related to the interparticle normal stress at the pipe wall and the particle velocity. As the dense phase mechanistic model may be used to calculate the local interparticle normal stress and particle velocity, the use of the model for predicting local wear rates should be investigated.

APPENDIX A

CYCLONE CLASSIFIED TAILINGS PIPELINE TEST DATA BASE

DATA FILE : BV25H62U

Test Facility	UCT 25 mm NB
Test Date	June 1990
Material Description	Blyvooruitsig CCT
Material Relative Density	2.66
Slurry Relative Density	1.62
Solids Volumetric Concentration (%)	37.35
Solids Mass Concentration (%)	61.33
Mean Slurry Temperature (°C)	16.9
Pipe Internal Diameter (mm)	26.60
Pipe Roughness (μm)	21.0
Pipeline Slope	Horizontal

Mixture Velocity (m/s)	Pressure Gradient (kPa/m)	Slurry Temp. (°C)
3.794	7.399	16.1
3.812	7.331	16.1
3.810	7.232	16.2
3.834	7.315	16.3
3.345	5.979	16.5
3.367	6.224	16.6
3.362	6.267	16.6
3.183	5.568	16.7
3.084	5.365	16.9
3.093	5.422	17.0
3.099	5.540	17.0
2.757	4.886	17.1
2.753	4.493	17.1
2.748	4.404	17.1
2.375	3.713	17.1
2.386	3.558	17.1
2.384	3.713	17.1
2.075	2.962	17.1
2.077	3.018	17.1
2.073	2.993	17.1
1.680	2.405	17.1
1.678	2.433	17.1
1.675	2.410	17.1
1.253	2.432	17.1
1.251	2.468	17.1
1.254	2.386	17.1

Particle Size Distribution
Sieve and Malvern Size Analysis *

Size (μm)	% Passing	% Retained
2360.0	100.0	.0
1180.0	99.7	.3
600.0	96.2	3.5
425.0	87.8	8.4
261.6	58.5	29.3
160.4	23.7	34.8
112.8	14.8	8.9
84.3	7.9	6.9
64.6	6.9	1.0
50.2	6.5	.4
39.0	5.5	1.0
30.3	5.1	.4
23.7	4.8	.3
18.5	4.4	.4
14.5	4.0	.4
11.4	3.6	.4
9.1	3.0	.6
7.2	2.5	.5
5.8	1.6	.9
Pan	.1	1.5

OBSERVED FLOW BEHAVIOUR

Velocity (m/s)	Observation (D = .0 mm)

* --425 μm Malvern Particle Size Analyser

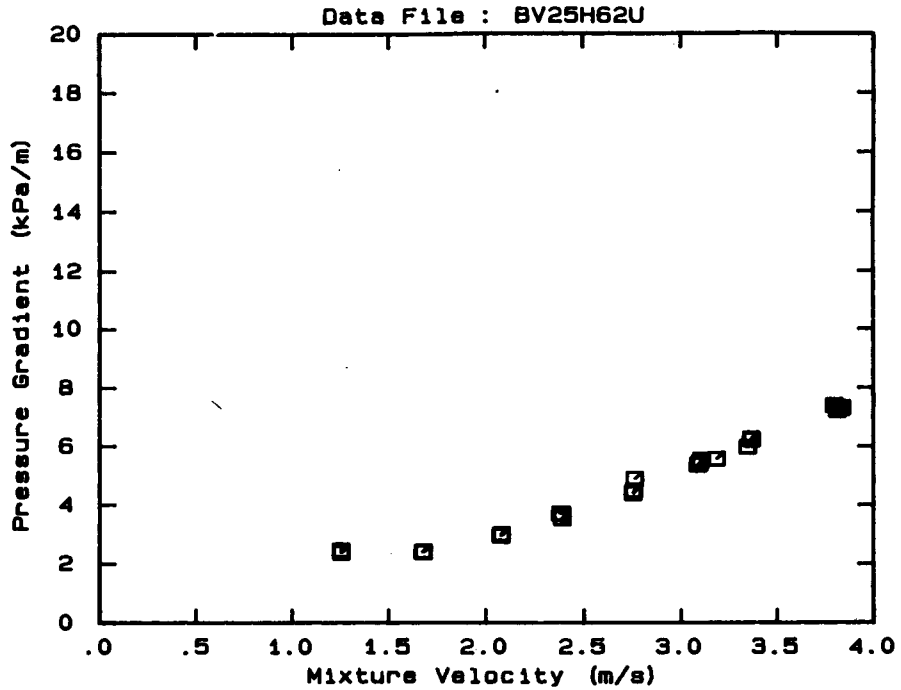

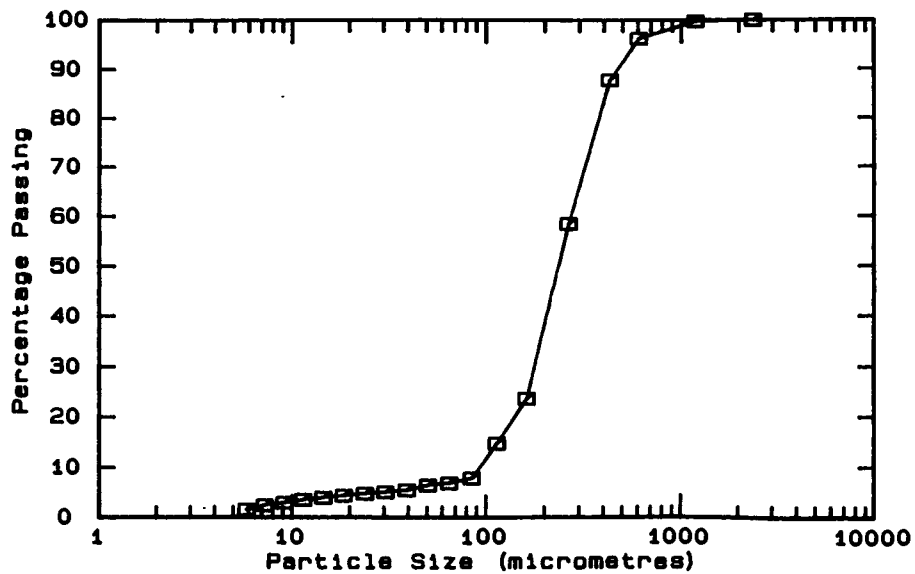

DATA FILE : BV25H65U

Test Facility	UCT 25 mm NB
Test Date	June 1990
Material Description	Blyvooruitsig CCT
Material Relative Density	2.66
Slurry Relative Density	1.65
Solids Volumetric Concentration (%)	39.16
Solids Mass Concentration (%)	63.13
Mean Slurry Temperature (°C)	17.4
Pipe Internal Diameter (mm)	26.60
Pipe Roughness (μm)	21.0
Pipeline Slope	Horizontal

Mixture Velocity (m/s)	Pressure Gradient (kPa/m)	Slurry Temp. (°C)
3.458	6.793	16.9
3.467	7.334	17.0
3.473	6.961	17.0
3.465	7.039	17.1
2.929	5.523	17.3
2.933	5.524	17.3
2.932	5.731	17.3
2.941	5.502	17.4
2.551	4.373	17.4
2.561	4.623	17.4
2.557	4.585	17.5
2.562	4.357	17.5
2.106	3.190	17.5
2.103	3.207	17.5
2.079	3.150	17.5
2.066	3.188	17.5
1.698	2.434	17.5
1.691	2.445	17.5
1.695	2.527	17.5
1.243	2.186	17.5
1.240	2.185	17.4
1.236	2.164	17.4

Particle Size Distribution
Sieve and Malvern Size Analysis *

Size (μm)	% Passing	% Retained
2360.0	100.0	.0
1180.0	99.9	.1
600.0	99.5	.4
425.0	96.3	3.2
261.6	73.6	22.7
160.4	37.5	36.1
112.8	23.4	14.1
84.3	16.1	7.3
64.6	14.0	2.1
50.2	12.7	1.3
39.0	11.3	1.4
30.3	10.4	.9
23.7	9.7	.7
18.5	8.8	.9
14.5	7.9	.9
11.4	6.9	1.0
9.1	5.7	1.2
7.2	4.5	1.2
5.8	2.8	1.7
Pan	- .2	3.0

OBSERVED FLOW BEHAVIOUR

* -425 μm Malvern Particle Size Analyser

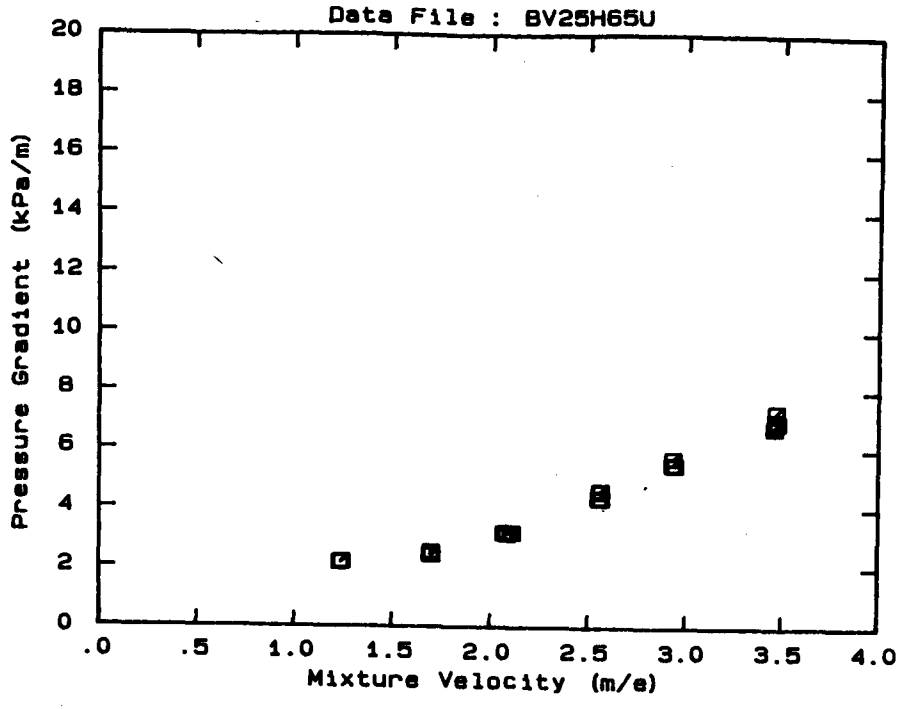

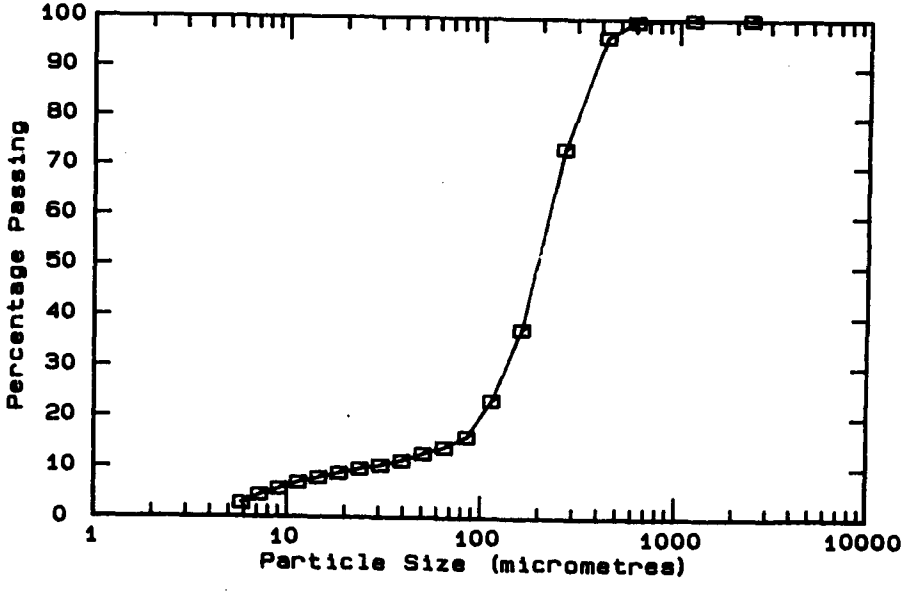

DATA FILE : BV25H74U

Test Facility	UCT 25 mm NB
Test Date	June 1990
Material Description	Blyvooruitsig CCT
Material Relative Density	2.66
Slurry Relative Density	1.74
Solids Volumetric Concentration (%)	44.58
Solids Mass Concentration (%)	68.15
Mean Slurry Temperature (°C)	17.8
Pipe Internal Diameter (mm)	26.60
Pipe Roughness (μm)	21.0
Pipeline Slope	Horizontal

Mixture Velocity (m/s)	Pressure Gradient (kPa/m)	Slurry Temp. (°C)
3.484	7.091	17.1
3.477	7.497	17.2
3.501	7.245	17.3
2.933	6.186	17.6
2.922	5.900	17.7
2.929	5.860	17.7
2.519	5.090	17.8
2.513	5.299	17.9
2.518	4.996	17.9
2.103	4.233	17.9
2.107	4.470	17.9
2.109	4.436	17.9
1.691	3.597	18.0
1.691	3.497	18.0
1.690	3.593	18.0
1.277	2.663	18.0
1.270	2.671	18.0
1.273	2.956	18.0

Particle Size Distribution
Sieve and Malvern Size Analysis *

Size (μm)	% Passing	% Retained
2360.0	100.0	.0
1180.0	99.9	.1
600.0	99.4	.5
425.0	92.9	6.5
261.6	68.4	24.5
160.4	33.6	34.8
112.8	19.8	13.8
84.3	12.8	7.0
64.6	11.1	1.7
50.2	9.8	1.3
39.0	8.5	1.3
30.3	7.9	.6
23.7	7.3	.6
18.5	6.5	.8
14.5	5.9	.6
11.4	5.2	.7
9.1	4.3	.9
7.2	3.5	.8
5.8	2.2	1.3
Pan	.0	2.2

* -425 μm Malvern Particle Size Analyser

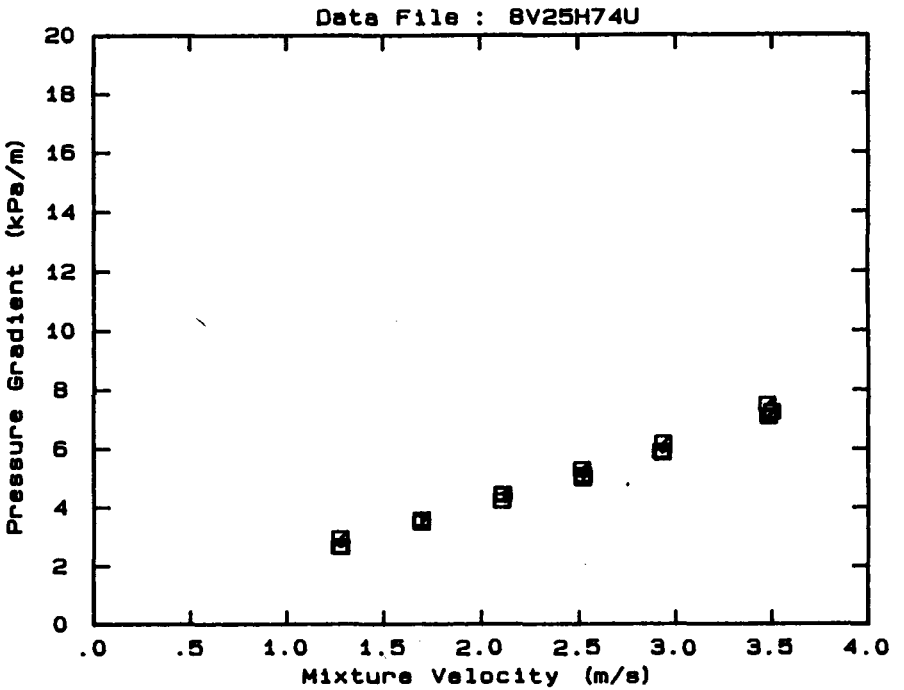

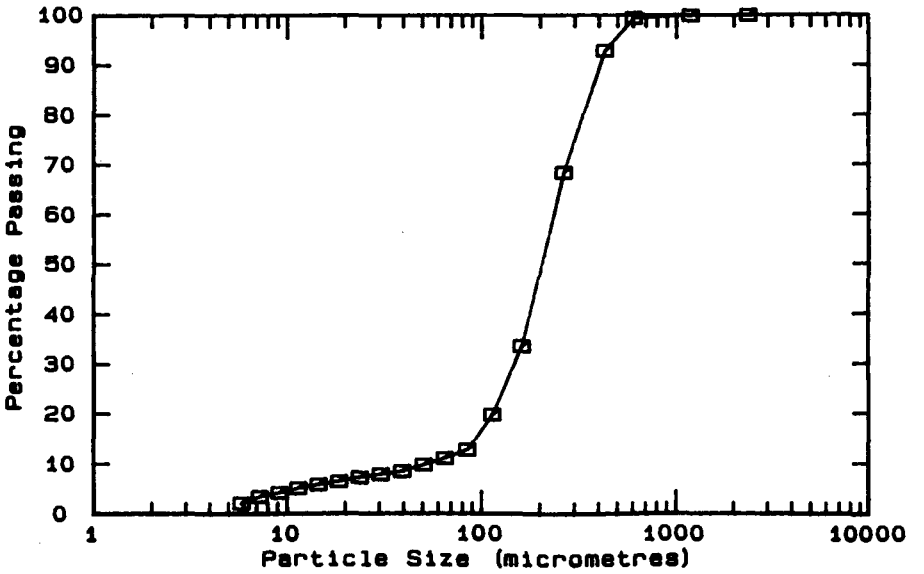

DATA FILE : BV25H77U

Test Facility	UCT 25 mm NB
Test Date	June 1990
Material Description	Blyvooruitsig CCT
Material Relative Density	2.66
Slurry Relative Density	1.77
Solids Volumetric Concentration (%)	46.39
Solids Mass Concentration (%)	69.71
Mean Slurry Temperature (°C)	18.8
Pipe Internal Diameter (mm)	26.60
Pipe Roughness (μm)	21.0
Pipeline Slope	Horizontal

Mixture Velocity (m/s)	Pressure Gradient (kPa/m)	Slurry Temp. (°C)
1.949	4.756	17.8
2.374	5.539	17.9
2.405	5.147	17.9
2.459	6.668	18.2
2.486	7.327	18.3
2.505	6.271	18.4
2.103	5.773	18.8
2.033	4.985	18.9
2.042	4.978	18.9
2.085	5.471	19.0
1.728	4.763	19.1
1.719	4.616	19.2
1.738	4.672	19.2
1.381	3.794	19.3
1.378	3.663	19.3
1.377	3.755	19.4
1.240	3.595	19.4
1.242	3.477	19.5
1.240	3.553	19.5

Particle Size Distribution
Sieve and Malvern Size Analysis *

Size (μm)	% Passing	% Retained
2360.0	100.0	.0
1180.0	100.0	.0
600.0	99.2	.8
425.0	94.7	4.5
261.6	77.3	17.4
160.4	37.4	39.9
112.8	23.6	13.8
84.3	14.7	8.9
64.6	13.2	1.5
50.2	12.2	1.0
39.0	10.8	1.4
30.3	10.0	.8
23.7	9.3	.7
18.5	8.4	.9
14.5	7.7	.7
11.4	6.8	.9
9.1	5.6	1.2
7.2	4.6	1.0
5.8	3.0	1.6
Pan	.1	2.9

* -425 μm Malvern Particle Size Analyser

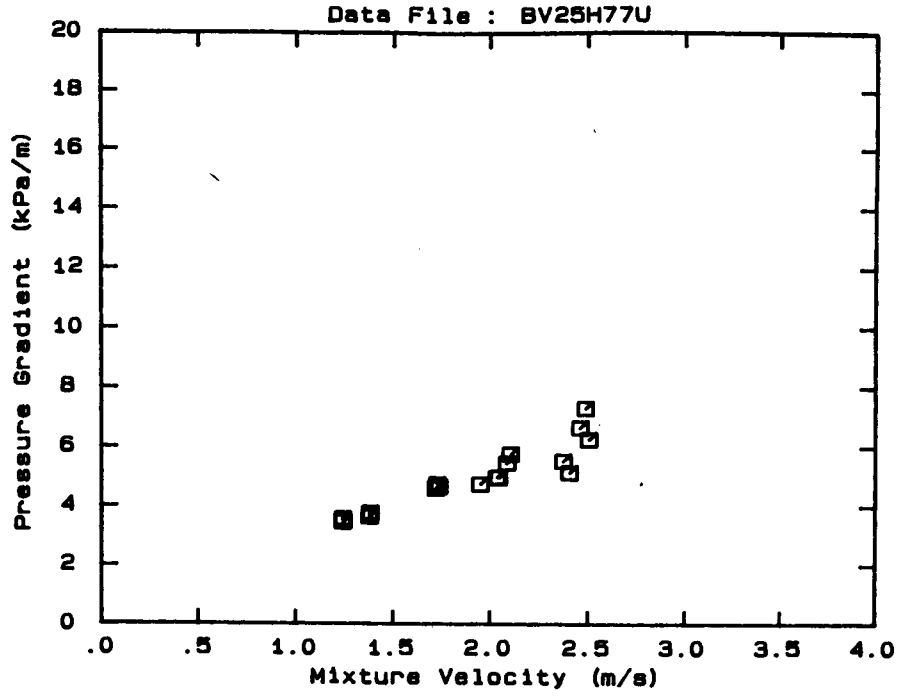

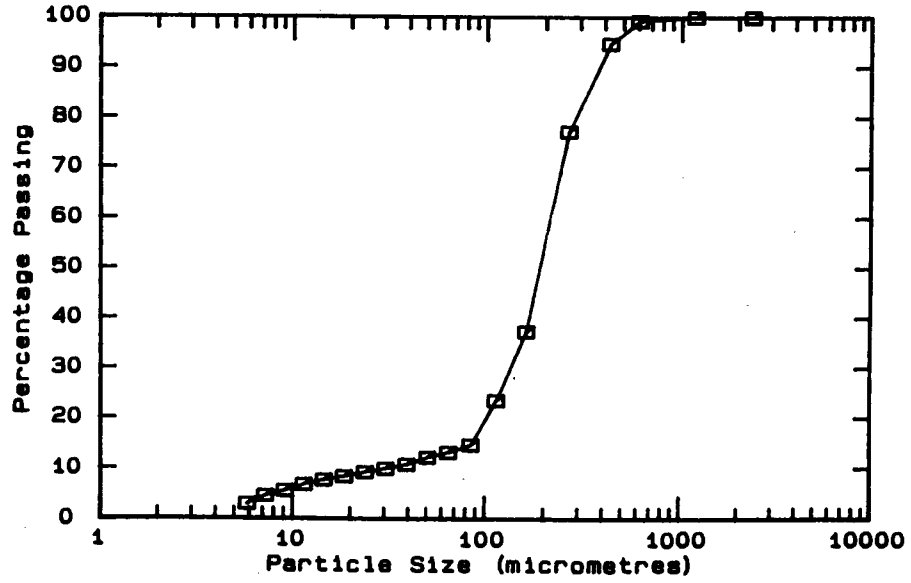

DATA FILE : BV25H81U

Test Facility	UCT 25 mm NB
Test Date	June 1990
Material Description	Blyvooruitsig CCT
Material Relative Density	2.66
Slurry Relative Density	1.81
Solids Volumetric Concentration (%)	48.80
Solids Mass Concentration (%)	71.71
Mean Slurry Temperature (°C)	20.1
Pipe Internal Diameter (mm)	26.60
Pipe Roughness (μm)	21.0
Pipeline Slope	Horizontal

Mixture Velocity (m/s)	Pressure Gradient (kPa/m)	Slurry Temp. (°C)
2.140	7.862	19.4
2.129	8.471	19.5
2.146	8.083	19.6
2.142	8.387	19.7
1.783	7.183	19.8
1.768	7.637	19.9
1.773	7.716	19.9
1.454	6.602	20.1
1.439	6.556	20.2
1.430	6.297	20.2
1.197	5.870	20.4
1.177	5.923	20.4
1.177	5.998	20.4
1.186	5.510	20.5
1.203	6.010	20.5
1.234	5.750	20.5
1.245	5.587	20.5

Particle Size Distribution
Sieve and Malvern Size Analysis *

Size (μm)	% Passing	% Retained
2360.0	100.0	.0
1180.0	99.9	.1
600.0	99.1	.8
425.0	95.6	3.5
261.6	70.5	25.1
160.4	34.5	36.0
112.8	21.8	12.7
84.3	13.1	8.7
64.6	11.4	1.7
50.2	10.4	1.0
39.0	9.0	1.4
30.3	8.4	.6
23.7	7.9	.5
18.5	7.1	.8
14.5	6.5	.6
11.4	5.7	.8
9.1	4.6	1.1
7.2	3.6	1.0
5.8	2.2	1.4
Pan	- .3	2.5

* -425 μm Malvern Particle Size Analyser

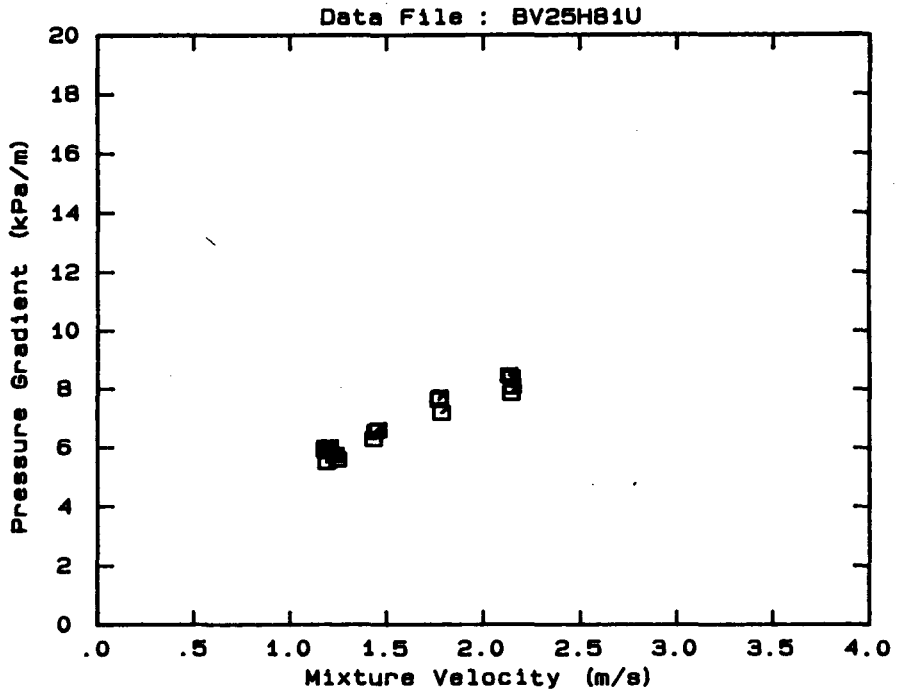

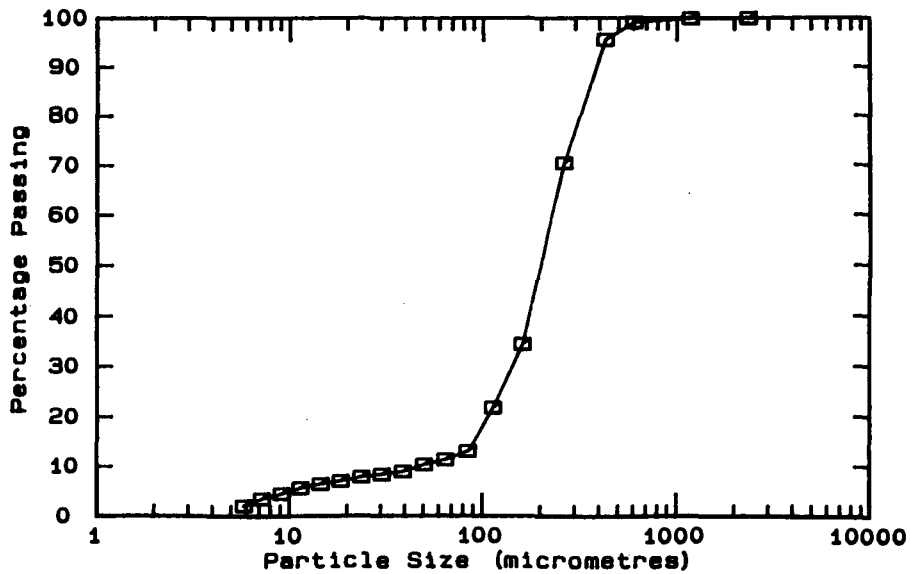

DATA FILE : BV25D62U

Test Facility	UCT 25 mm NB
Test Date	June 1990
Material Description	Blyvooruitsig CCT
Material Relative Density	2.66
Slurry Relative Density	1.62
Solids Volumetric Concentration (%)	37.35
Solids Mass Concentration (%)	61.33
Mean Slurry Temperature (°C)	16.9
Pipe Internal Diameter (mm)	26.60
Pipe Roughness (μm)	21.0
Pipeline Slope	Vertical Down

Mixture Velocity (m/s)	Pressure Gradient (kPa/m)	Slurry Temp. (°C)
3.794	- 6.607	16.1
3.812	- 6.703	16.1
3.810	- 6.595	16.2
3.834	- 6.520	16.3
3.345	- 8.471	16.5
3.367	- 8.376	16.6
3.362	- 8.587	16.6
3.183	- 8.579	16.7
3.084	- 9.575	16.9
3.093	- 9.277	17.0
3.099	- 9.571	17.0
2.757	-10.837	17.1
2.753	-10.529	17.1
2.748	-10.672	17.1
2.375	-11.592	17.1
2.386	-11.640	17.1
2.384	-11.734	17.1
2.075	-12.277	17.1
2.077	-12.454	17.1
2.073	-12.205	17.1
1.680	-13.538	17.1
1.678	-13.439	17.1
1.675	-13.396	17.1
1.253	-14.437	17.1
1.251	-14.478	17.1
1.254	-14.407	17.1

Particle Size Distribution
Sieve and Malvern Size Analysis *

Size (μm)	% Passing	% Retained
2360.0	100.0	.0
1180.0	99.7	.3
600.0	96.2	3.5
425.0	87.8	8.4
261.6	58.5	29.3
160.4	23.7	34.8
112.8	14.8	8.9
84.3	7.9	6.9
64.6	6.9	1.0
50.2	6.5	.4
39.0	5.5	1.0
30.3	5.1	.4
23.7	4.8	.3
18.5	4.4	.4
14.5	4.0	.4
11.4	3.6	.4
9.1	3.0	.6
7.2	2.5	.5
5.8	1.6	.9
Pan	.1	1.5

OBSERVED FLOW BEHAVIOUR

Velocity (m/s)	Observation (D = .0 mm)

* -425 μm Malvern Particle Size Analyser

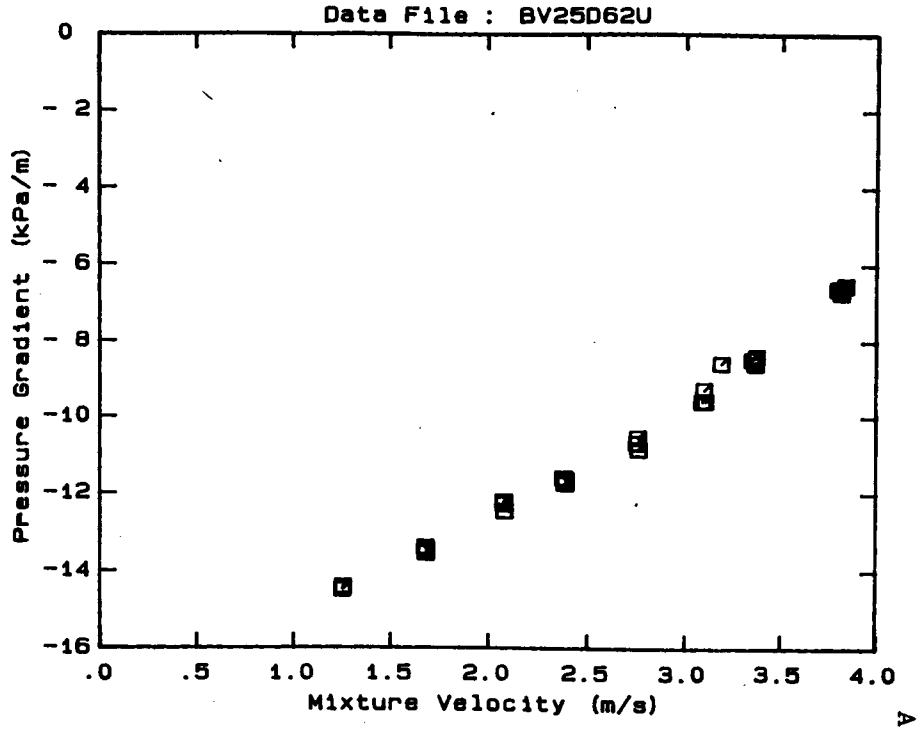

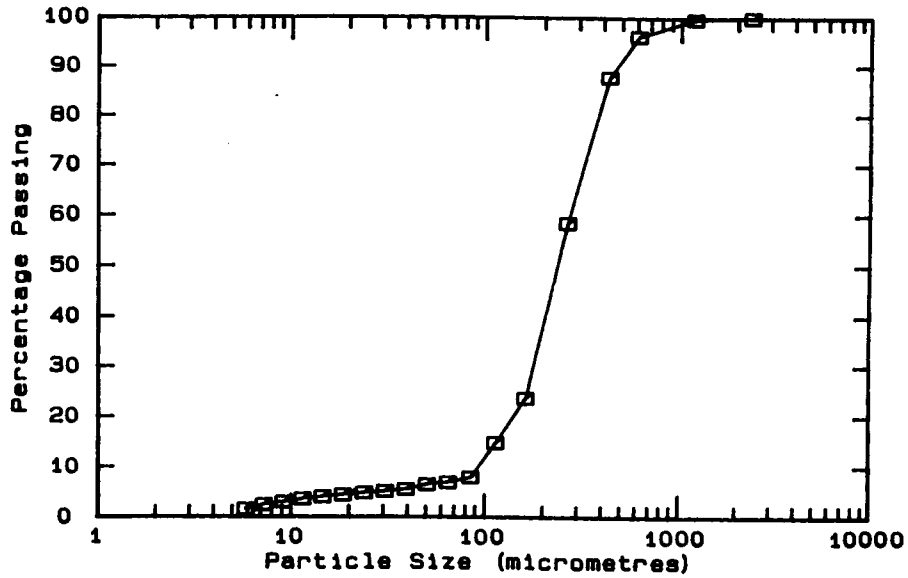

DATA FILE : BV25D65U

Test Facility	UCT 25 mm NB
Test Date	June 1990
Material Description	Blyvooruitsig CCT
Material Relative Density	2.66
Slurry Relative Density	1.65
Solids Volumetric Concentration (%)	39.16
Solids Mass Concentration (%)	63.13
Mean Slurry Temperature (°C)	17.4
Pipe Internal Diameter (mm)	26.60
Pipe Roughness (μm)	21.0
Pipeline Slope	Vertical Down

Mixture Velocity (m/s)	Pressure Gradient (kPa/m)	Slurry Temp. (°C)
3.458	- 8.935	16.9
3.467	- 8.708	17.0
3.473	- 8.410	17.0
3.465	- 8.672	17.1
2.929	-10.646	17.3
2.933	-10.382	17.3
2.932	-10.631	17.3
2.941	-10.833	17.4
2.551	-11.483	17.4
2.561	-11.411	17.4
2.557	-11.566	17.5
2.562	-11.258	17.5
2.106	-12.760	17.5
2.103	-12.280	17.5
2.079	-12.341	17.5
2.066	-12.521	17.5
1.698	-13.450	17.5
1.691	-13.584	17.5
1.695	-13.294	17.5
1.243	-14.552	17.5
1.240	-14.535	17.4
1.236	-14.513	17.4

Particle Size Distribution
Sieve and Malvern Size Analysis *

Size (μm)	% Passing	% Retained
2360.0	100.0	.0
1180.0	99.9	.1
600.0	99.5	.4
425.0	96.3	3.2
261.6	73.6	22.7
160.4	37.5	36.1
112.8	23.4	14.1
84.3	16.1	7.3
64.6	14.0	2.1
50.2	12.7	1.3
39.0	11.3	1.4
30.3	10.4	.9
23.7	9.7	.7
18.5	8.8	.9
14.5	7.9	.9
11.4	6.9	1.0
9.1	5.7	1.2
7.2	4.5	1.2
5.8	2.8	1.7
Pan	- .2	3.0

OBSERVED FLOW BEHAVIOUR

* -425 μm Malvern Particle Size Analyser

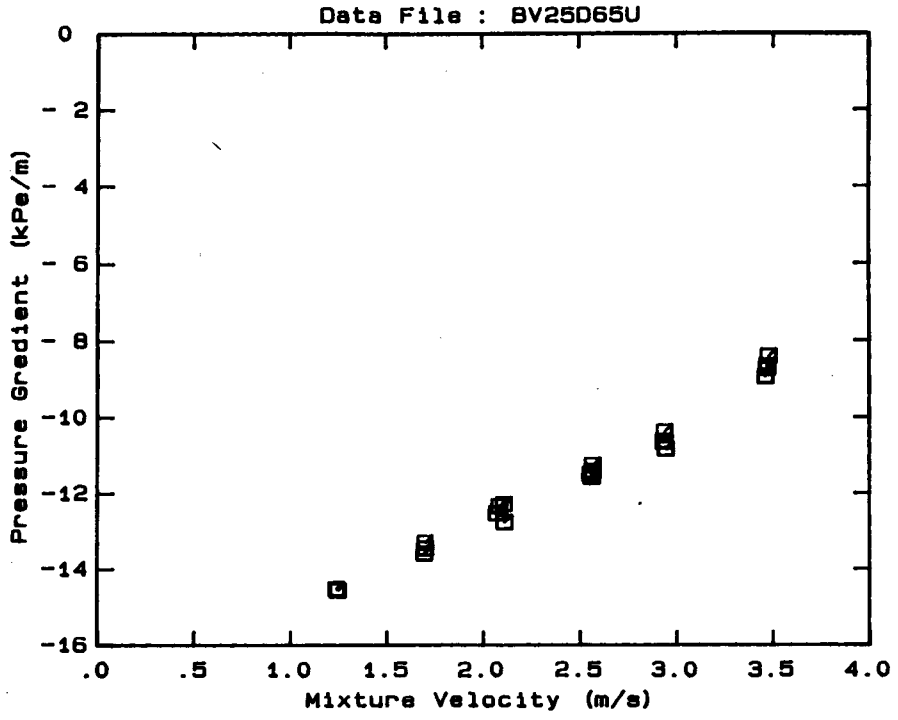

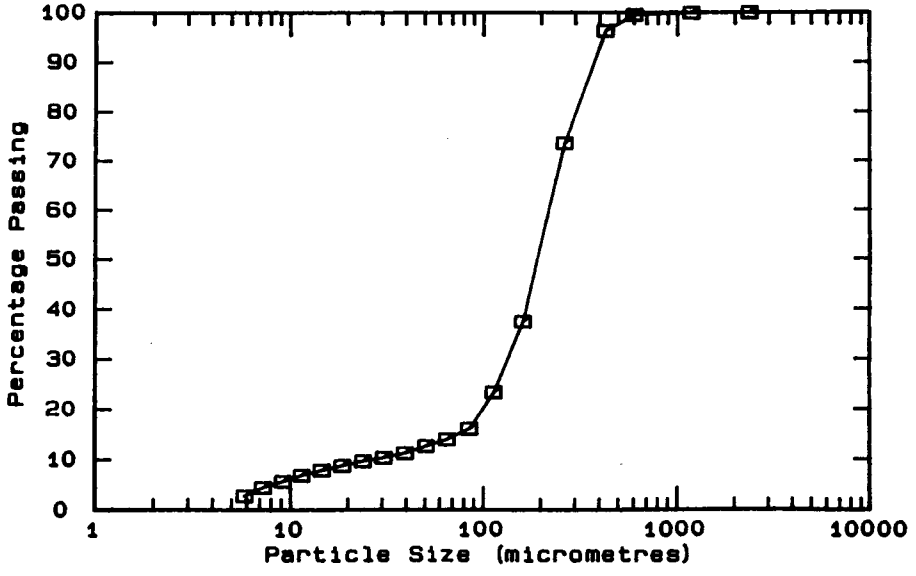

DATA FILE : BV25D74U

Test Facility	UCT 25 mm NB
Test Date	June 1990
Material Description	Blyvooruitsig CCT
Material Relative Density	2.66
Slurry Relative Density	1.74
Solids Volumetric Concentration (%)	44.58
Solids Mass Concentration (%)	68.15
Mean Slurry Temperature (°C)	17.8
Pipe Internal Diameter (mm)	26.60
Pipe Roughness (μm)	21.0
Pipeline Slope	Vertical Down

Mixture Velocity (m/s)	Pressure Gradient (kPa/m)	Slurry Temp. (°C)	Particle Size Distribution Sieve and Malvern Size Analysis * Size (μm)	% Passing	% Retained
3.484	- 7.900	17.1	2360.0	100.0	.0
3.477	- 7.548	17.2	1180.0	99.9	.1
3.501	- 7.306	17.3	600.0	99.4	.5
2.933	- 9.280	17.6	425.0	92.9	6.5
2.922	- 9.515	17.7	261.6	68.4	24.5
2.929	- 9.285	17.7	160.4	33.6	34.8
2.519	-10.572	17.8	112.8	19.8	13.8
2.513	-10.672	17.9	84.3	12.8	7.0
2.518	-10.466	17.9	64.6	11.1	1.7
2.103	-11.763	17.9	50.2	9.8	1.3
2.107	-11.810	17.9	39.0	8.5	1.3
2.109	-11.816	17.9	30.3	7.9	.6
1.691	-13.010	18.0	23.7	7.3	.6
1.691	-12.882	18.0	18.5	6.5	.8
1.690	-12.943	18.0	14.5	5.9	.6
1.277	-13.925	18.0	11.4	5.2	.7
1.270	-13.935	18.0	9.1	4.3	.9
1.273	-13.955	18.0	7.2	3.5	.8
			5.8	2.2	1.3
			Pan	.0	2.2

* -425 μm Malvern Particle Size Analyser

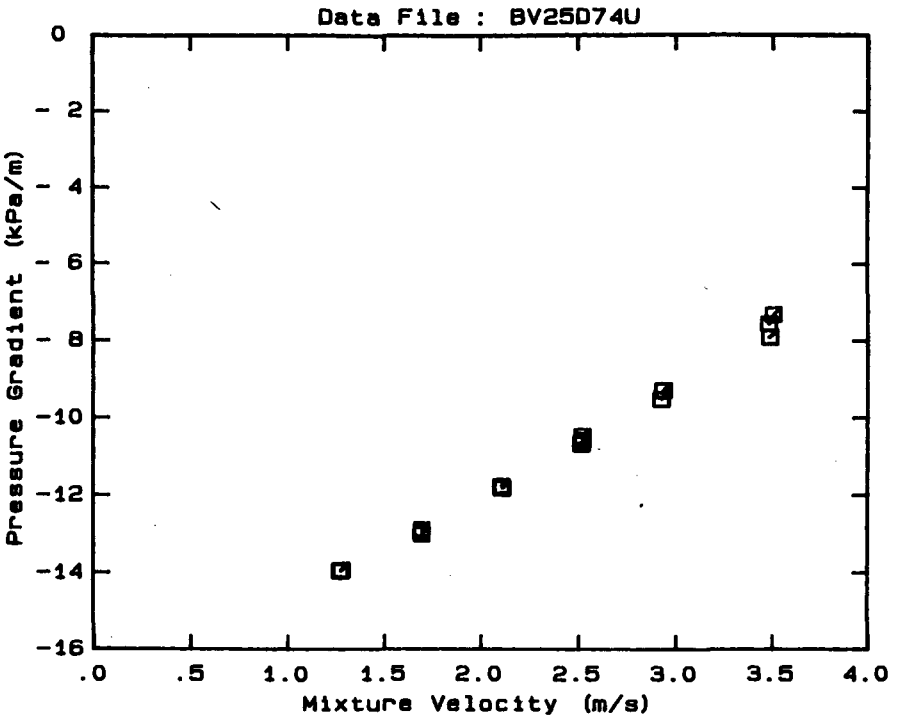

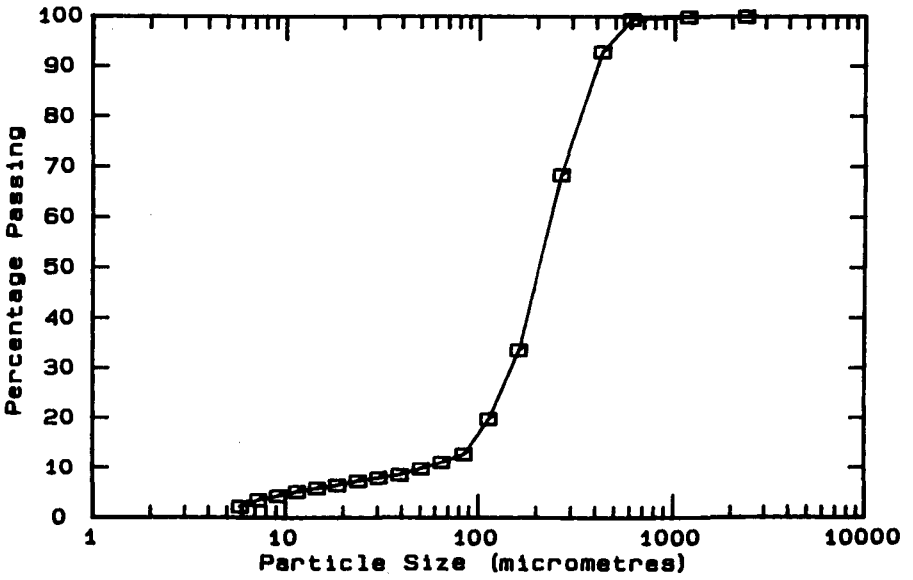

DATA FILE : BV25D77U

Test Facility	UCT 25 mm NB
Test Date	June 1990
Material Description	Blyvooruitsig CCT
Material Relative Density	2.66
Slurry Relative Density	1.77
Solids Volumetric Concentration (%)	46.39
Solids Mass Concentration (%)	69.71
Mean Slurry Temperature (°C)	18.8
Pipe Internal Diameter (mm)	26.60
Pipe Roughness (μm)	21.0
Pipeline Slope	Vertical Down

Mixture Velocity (m/s)	Pressure Gradient (kPa/m)	Slurry Temp. (°C)	Particle Size Distribution Sieve and Malvern Size Analysis * Size (μm)	% Passing	% Retained
1.949	-11.196	17.8	2360.0	100.0	.0
2.374	-10.043	17.9	1180.0	100.0	.0
2.405	-10.217	17.9	600.0	99.2	.8
2.459	- 9.611	18.2	425.0	94.7	4.5
2.486	- 9.633	18.3	261.6	77.3	17.4
2.505	- 9.496	18.4	160.4	37.4	39.9
2.103	-10.852	18.8	112.8	23.6	13.8
2.033	-11.262	18.9	84.3	14.7	8.9
2.042	-10.837	18.9	64.6	13.2	1.5
2.085	-10.742	19.0	50.2	12.2	1.0
1.728	-11.924	19.1	39.0	10.8	1.4
1.719	-12.029	19.2	30.3	10.0	.8
1.738	-11.972	19.2	23.7	9.3	.7
1.381	-13.019	19.3	18.5	8.4	.9
1.378	-12.884	19.3	14.5	7.7	.7
1.377	-12.951	19.4	11.4	6.8	.9
1.240	-13.275	19.4	9.1	5.6	1.2
1.242	-13.169	19.5	7.2	4.6	1.0
1.240	-13.139	19.5	5.8	3.0	1.6
			Pan	.1	2.9

* -425 μm Malvern Particle Size Analyser

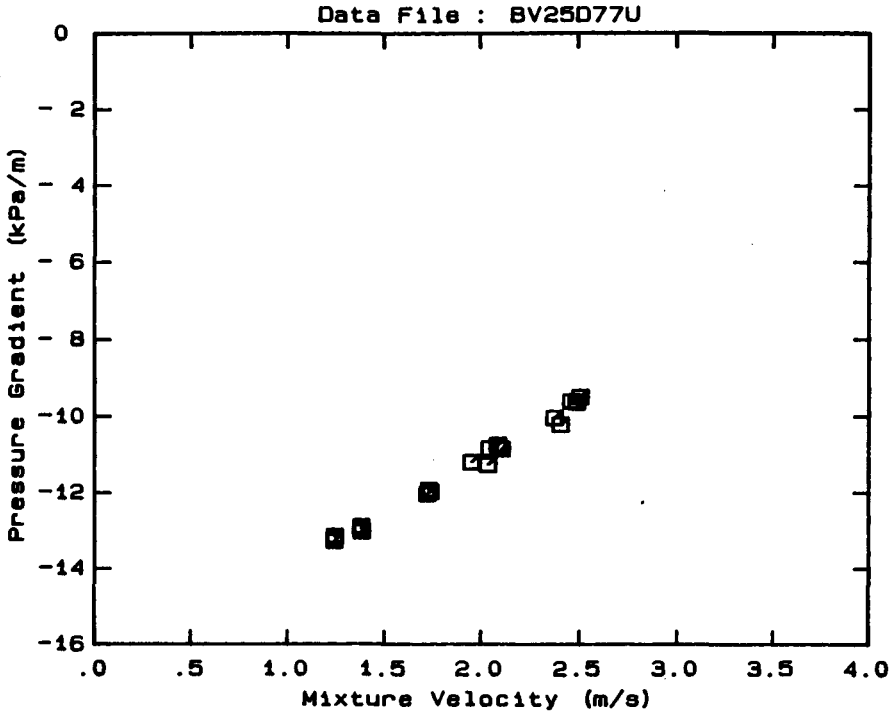

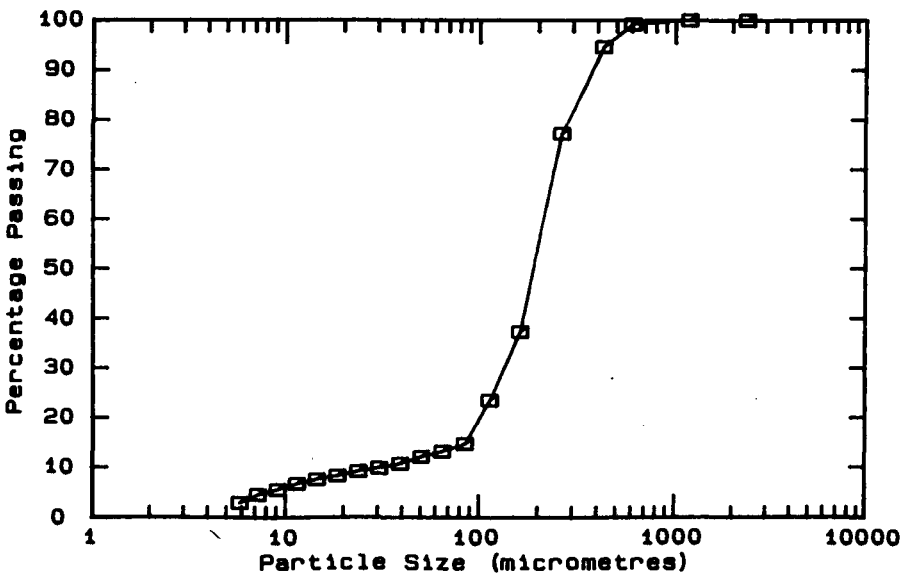

DATA FILE : BV25D81U

Test Facility	UCT 25 mm NB
Test Date	June 1990
Material Description	Blyvooruitsig CCT
Material Relative Density	2.66
Slurry Relative Density	1.81
Solids Volumetric Concentration (%)	48.80
Solids Mass Concentration (%)	71.71
Mean Slurry Temperature (°C)	20.1
Pipe Internal Diameter (mm)	26.60
Pipe Roughness (μm)	21.0
Pipeline Slope	Vertical Down

Mixture Velocity (m/s)	Pressure Gradient (kPa/m)	Slurry Temp. (°C)
2.140	- 8.307	19.4
2.129	- 8.172	19.5
2.146	- 7.988	19.6
2.142	- 7.902	19.7
1.783	- 9.893	19.8
1.768	- 9.821	19.9
1.773	- 9.843	19.9
1.454	-11.279	20.1
1.439	-11.096	20.2
1.430	-11.039	20.2
1.197	-11.521	20.4
1.177	-10.792	20.4
1.177	-11.125	20.4
1.186	-11.182	20.5
1.203	-11.637	20.5
1.234	-12.176	20.5
1.245	-12.057	20.5

Particle Size Distribution
Sieve and Malvern Size Analysis *

Size (μm)	% Passing	% Retained
2360.0	100.0	.0
1180.0	99.9	.1
600.0	99.1	.8
425.0	95.6	3.5
261.6	70.5	25.1
160.4	34.5	36.0
112.8	21.8	12.7
84.3	13.1	8.7
64.6	11.4	1.7
50.2	10.4	1.0
39.0	9.0	1.4
30.3	8.4	.6
23.7	7.9	.5
18.5	7.1	.8
14.5	6.5	.6
11.4	5.7	.8
9.1	4.6	1.1
7.2	3.6	1.0
5.8	2.2	1.4
Pan	- .3	2.5

* -425 μm Malvern Particle Size Analyser

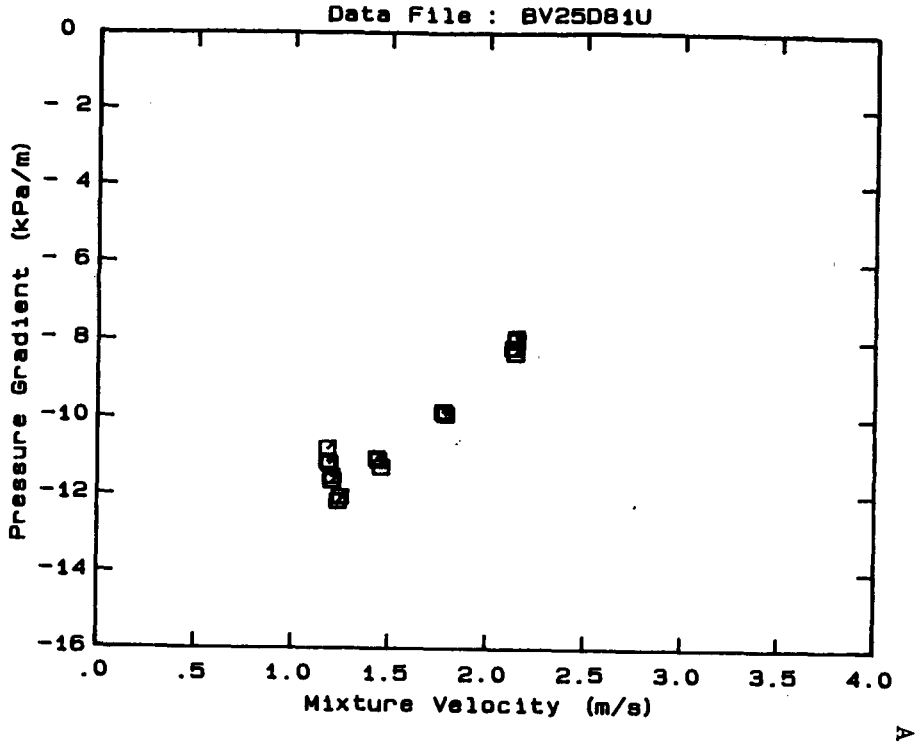

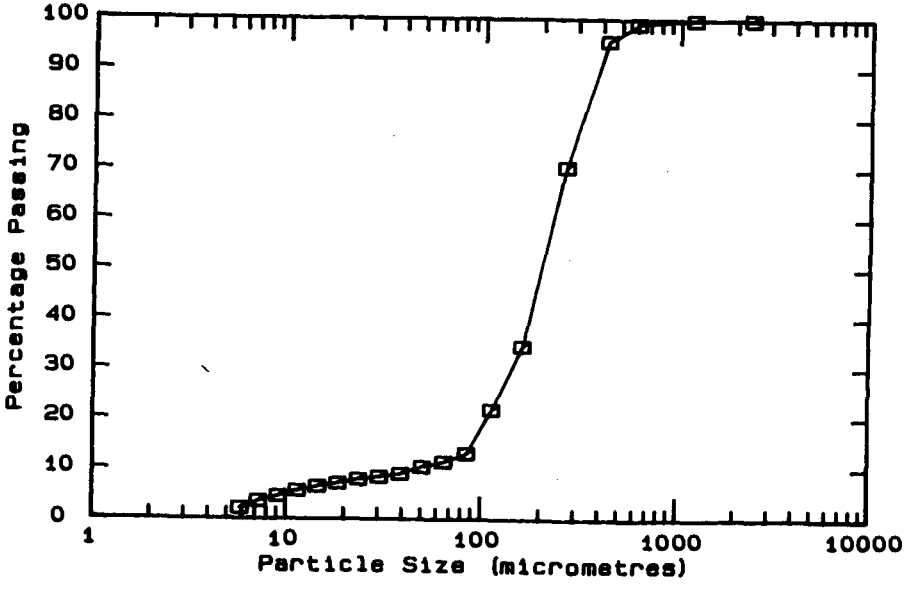

DATA FILE : BV25U62U

Test Facility	UCT 25 mm NB
Test Date	June 1990
Material Description	Blyvooruitsig CCT
Material Relative Density	2.66
Slurry Relative Density	1.62
Solids Volumetric Concentration (%)	37.35
Solids Mass Concentration (%)	61.33
Mean Slurry Temperature (°C)	16.9
Pipe Internal Diameter (mm)	26.60
Pipe Roughness (μm)	21.0
Pipeline Slope	Vertical Up

Mixture Velocity (m/s)	Pressure Gradient (kPa/m)	Slurry Temp. (°C)
3.794	23.110	16.1
3.812	23.223	16.1
3.810	23.214	16.2
3.834	23.371	16.3
3.345	21.217	16.5
3.367	21.748	16.6
3.362	21.649	16.6
3.183	22.569	16.7
3.084	20.577	16.9
3.093	20.805	17.0
3.099	20.133	17.0
2.757	19.005	17.1
2.753	19.436	17.1
2.748	19.424	17.1
2.375	18.373	17.1
2.386	18.867	17.1
2.384	18.564	17.1
2.075	18.237	17.1
2.077	17.900	17.1
2.073	18.220	17.1
1.680	17.386	17.1
1.678	17.337	17.1
1.675	17.351	17.1
1.253	17.251	17.1
1.251	17.170	17.1
1.254	17.216	17.1

Particle Size Distribution
Sieve and Malvern Size Analysis *

Size (μm)	% Passing	% Retained
2360.0	100.0	.0
1180.0	99.7	.3
600.0	96.2	3.5
425.0	87.8	8.4
261.6	58.5	29.3
160.4	23.7	34.8
112.8	14.8	8.9
84.3	7.9	6.9
64.6	6.9	1.0
50.2	6.5	.4
39.0	5.5	1.0
30.3	5.1	.4
23.7	4.8	.3
18.5	4.4	.4
14.5	4.0	.4
11.4	3.6	.4
9.1	3.0	.6
7.2	2.5	.5
5.8	1.6	.9
Pan	.1	1.5

OBSERVED FLOW BEHAVIOUR

Velocity (m/s)	Observation (D = .0 mm)

* -425 μm Malvern Particle Size Analyser

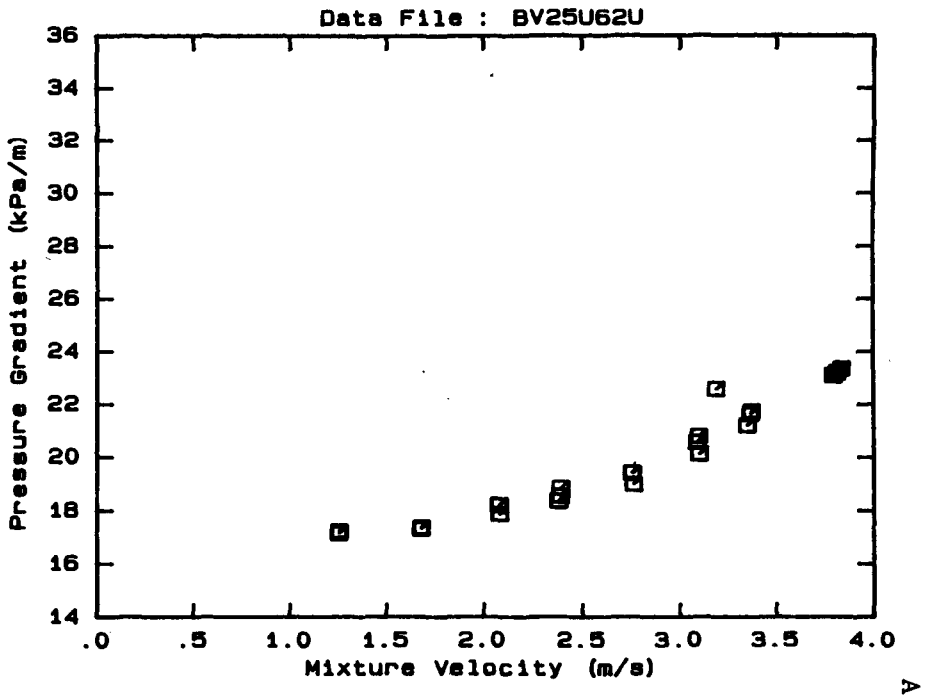

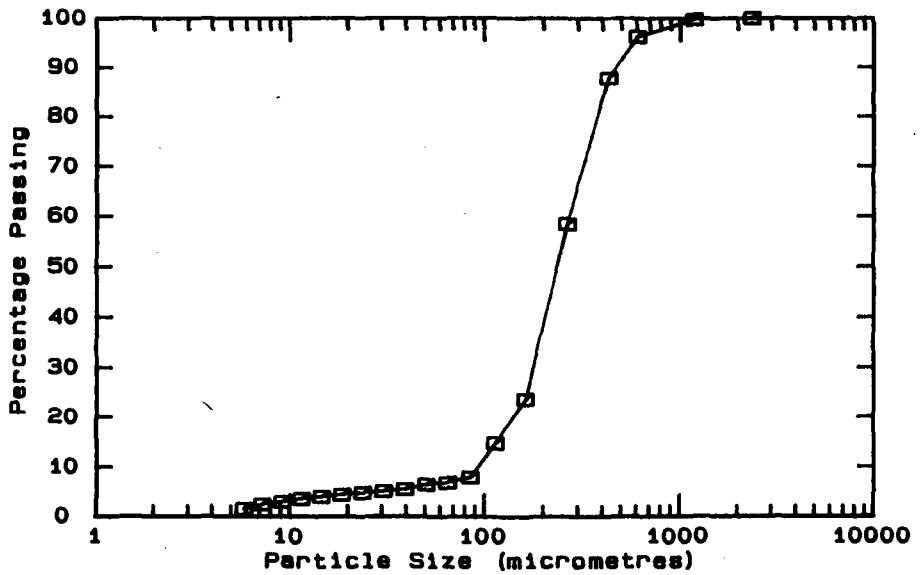

DATA FILE : BV25U65U

Test Facility	UCT 25 mm NB
Test Date	June 1990
Material Description	Blyvooruitsig CCT
Material Relative Density	2.66
Slurry Relative Density	1.65
Solids Volumetric Concentration (%)	39.16
Solids Mass Concentration (%)	63.13
Mean Slurry Temperature (°C)	17.4
Pipe Internal Diameter (mm)	26.60
Pipe Roughness (μm)	21.0
Pipeline Slope	Vertical Up

Mixture Velocity (m/s)	Pressure Gradient (kPa/m)	Slurry Temp. (°C)
3.458	22.976	16.9
3.467	22.551	17.0
3.473	22.481	17.0
3.465	22.711	17.1
2.929	20.817	17.3
2.933	21.044	17.3
2.932	20.708	17.3
2.941	20.799	17.4
2.551	20.126	17.4
2.561	19.908	17.4
2.557	19.831	17.5
2.562	19.984	17.5
2.106	18.701	17.5
2.103	18.878	17.5
2.079	18.725	17.5
2.066	18.724	17.5
1.698	17.759	17.5
1.691	17.694	17.5
1.695	17.834	17.5
1.243	17.209	17.5
1.240	17.291	17.4
1.236	17.300	17.4

Particle Size Distribution
Sieve and Malvern Size Analysis *

Size (μm)	% Passing	% Retained
2360.0	100.0	.0
1180.0	99.9	.1
600.0	99.5	.4
425.0	96.3	3.2
261.6	73.6	22.7
160.4	37.5	36.1
112.8	23.4	14.1
84.3	16.1	7.3
64.6	14.0	2.1
50.2	12.7	1.3
39.0	11.3	1.4
30.3	10.4	.9
23.7	9.7	.7
18.5	8.8	.9
14.5	7.9	.9
11.4	6.9	1.0
9.1	5.7	1.2
7.2	4.5	1.2
5.8	2.8	1.7
Pan	- .2	3.0

OBSERVED FLOW BEHAVIOUR

* -425 μm Malvern Particle Size Analyser

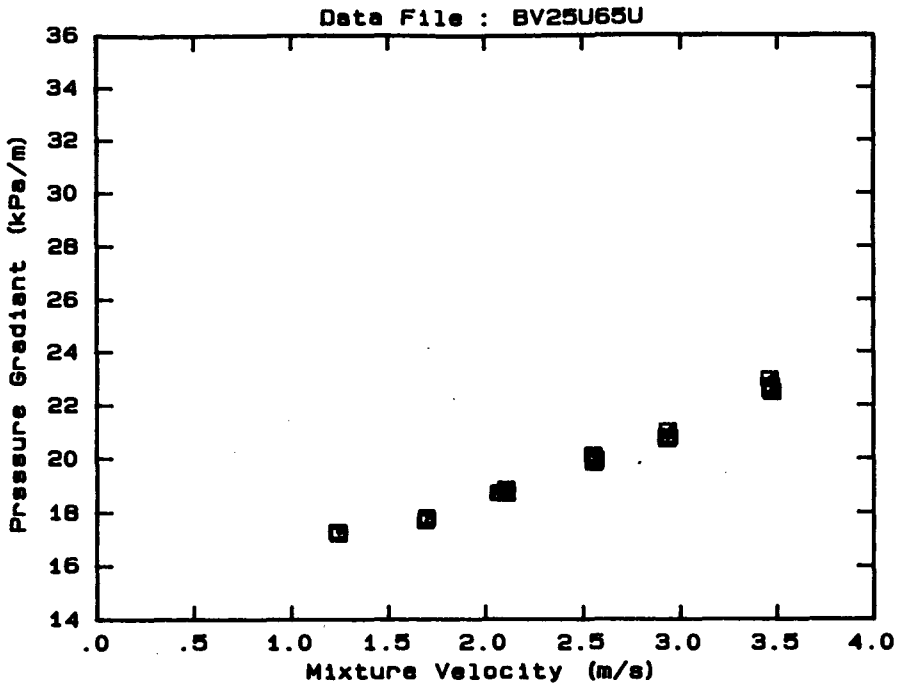

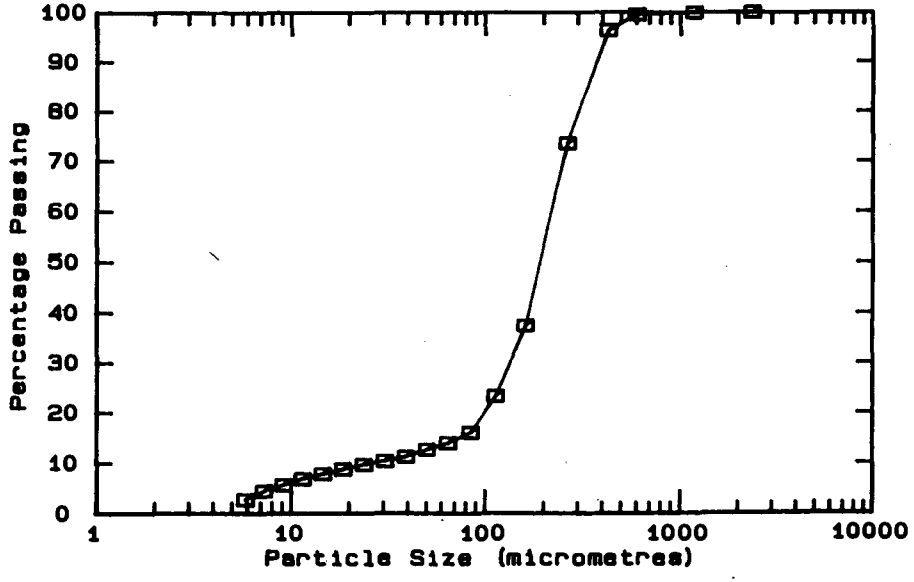

DATA FILE : BV25U74U

Test Facility	UCT 25 mm NB
Test Date	June 1990
Material Description	Blyvooruitsig CCT
Material Relative Density	2.66
Slurry Relative Density	1.74
Solids Volumetric Concentration (%)	44.58
Solids Mass Concentration (%)	68.15
Mean Slurry Temperature (°C)	17.8
Pipe Internal Diameter (mm)	26.60
Pipe Roughness (μm)	21.0
Pipeline Slope	Vertical Up

Mixture Velocity (m/s)	Pressure Gradient (kPa/m)	Slurry Temp. (°C)
3.484	23.855	17.1
3.477	23.610	17.2
3.501	23.921	17.3
2.933	22.294	17.6
2.922	21.835	17.7
2.929	22.746	17.7
2.519	21.394	17.8
2.513	21.160	17.9
2.518	21.626	17.9
2.103	20.745	17.9
2.107	20.622	17.9
2.109	20.680	17.9
1.691	19.599	18.0
1.691	19.881	18.0
1.690	19.689	18.0
1.277	19.084	18.0
1.270	19.037	18.0
1.273	18.959	18.0

Particle Size Distribution
Sieve and Malvern Size Analysis *

Size (μm)	% Passing	% Retained
2360.0	100.0	.0
1180.0	99.9	.1
600.0	99.4	.5
425.0	92.9	6.5
261.6	68.4	24.5
160.4	33.6	34.8
112.8	19.8	13.8
84.3	12.8	7.0
64.6	11.1	1.7
50.2	9.8	1.3
39.0	8.5	1.3
30.3	7.9	.6
23.7	7.3	.6
18.5	6.5	.8
14.5	5.9	.6
11.4	5.2	.7
9.1	4.3	.9
7.2	3.5	.8
5.8	2.2	1.3
Pan	.0	2.2

* -425 μm Malvern Particle Size Analyser

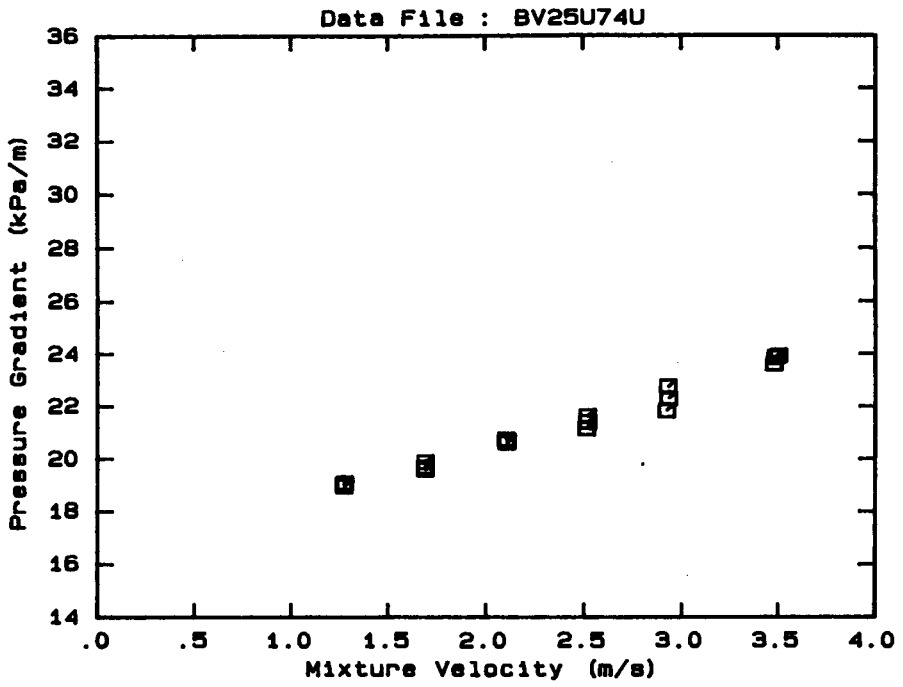

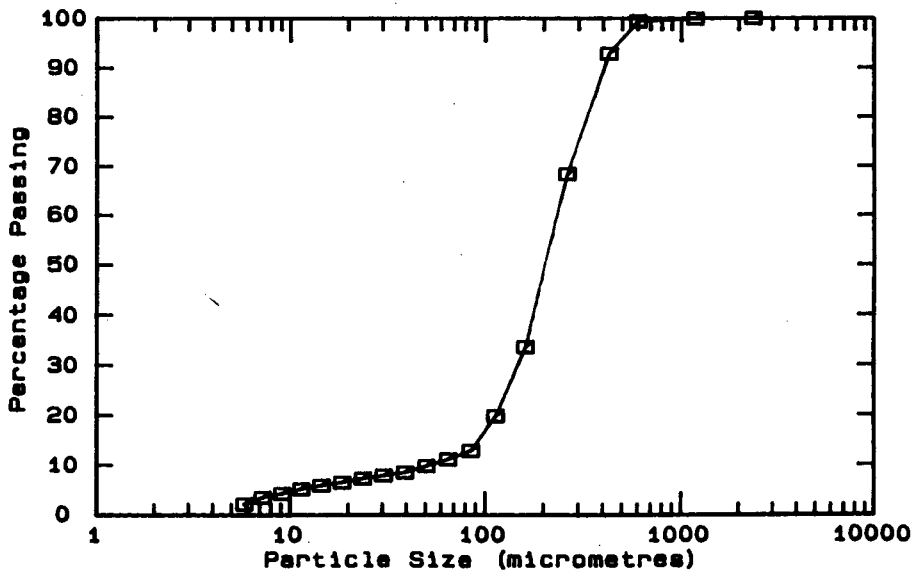

DATA FILE : BV25U77U

Test Facility	UCT 25 mm NB
Test Date	June 1990
Material Description	Blyvooruitsig CCT
Material Relative Density	2.66
Slurry Relative Density	1.77
Solids Volumetric Concentration (%)	46.39
Solids Mass Concentration (%)	69.71
Mean Slurry Temperature (°C)	18.8
Pipe Internal Diameter (mm)	26.60
Pipe Roughness (μm)	21.0
Pipeline Slope	Vertical Up

Mixture Velocity (m/s)	Pressure Gradient (kPa/m)	Slurry Temp. (°C)
1.949	22.953	17.8
2.374	23.315	17.9
2.405	22.383	17.9
2.459	23.009	18.2
2.486	22.291	18.3
2.505	22.693	18.4
2.103	21.964	18.8
2.033	21.667	18.9
2.042	22.454	18.9
2.085	22.163	19.0
1.728	21.413	19.1
1.719	20.966	19.2
1.738	21.277	19.2
1.381	20.281	19.3
1.378	20.603	19.3
1.377	20.545	19.4
1.240	20.401	19.4
1.242	20.392	19.5
1.240	20.555	19.5

Particle Size Distribution
Sieve and Malvern Size Analysis *

Size (μm)	% Passing	% Retained
2360.0	100.0	.0
1180.0	100.0	.0
600.0	99.2	.8
425.0	94.7	4.5
261.6	77.3	17.4
160.4	37.4	39.9
112.8	23.6	13.8
84.3	14.7	8.9
64.6	13.2	1.5
50.2	12.2	1.0
39.0	10.8	1.4
30.3	10.0	.8
23.7	9.3	.7
18.5	8.4	.9
14.5	7.7	.7
11.4	6.8	.9
9.1	5.6	1.2
7.2	4.6	1.0
5.8	3.0	1.6
Pan	.1	2.9

* -425 μm Malvern Particle Size Analyser

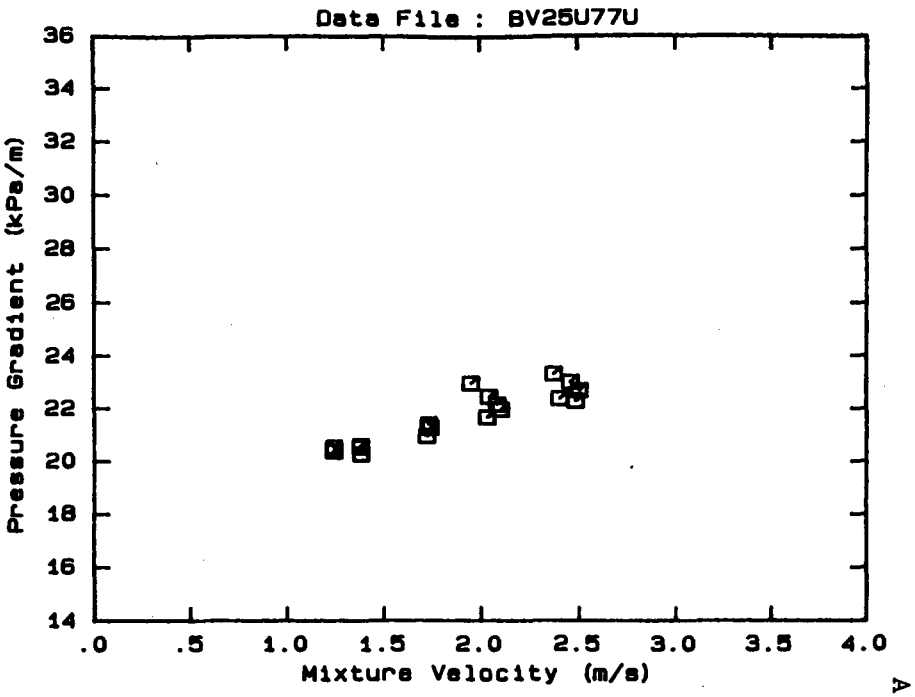

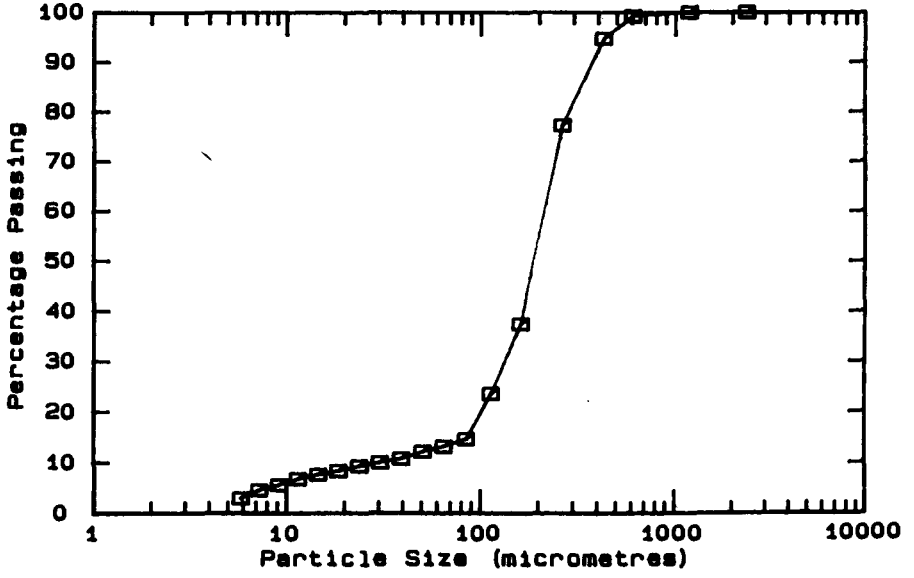

DATA FILE : BV25U81U

Test Facility	UCT 25 mm NB
Test Date	June 1990
Material Description	Blyvooruitsig CCT
Material Relative Density	2.66
Slurry Relative Density	1.81
Solids Volumetric Concentration (%)	48.80
Solids Mass Concentration (%)	71.71
Mean Slurry Temperature (°C)	20.1
Pipe Internal Diameter (mm)	26.60
Pipe Roughness (μm)	21.0
Pipeline Slope	Vertical Up

Mixture Velocity (m/s)	Pressure Gradient (kPa/m)	Slurry Temp. (°C)
2.140	26.331	19.4
2.129	25.995	19.5
2.146	26.719	19.6
2.142	26.653	19.7
1.783	24.999	19.8
1.768	25.480	19.9
1.773	24.773	19.9
1.454	23.816	20.1
1.439	23.482	20.2
1.430	23.874	20.2
1.197	22.574	20.4
1.177	23.141	20.4
1.177	23.029	20.4
1.186	23.088	20.5
1.203	22.950	20.5
1.234	22.715	20.5
1.245	22.661	20.5

Particle Size Distribution
Sieve and Malvern Size Analysis *

Size (μm)	% Passing	% Retained
2360.0	100.0	.0
1180.0	99.9	.1
600.0	99.1	.8
425.0	95.6	3.5
261.6	70.5	25.1
160.4	34.5	36.0
112.8	21.8	12.7
84.3	13.1	8.7
64.6	11.4	1.7
50.2	10.4	1.0
39.0	9.0	1.4
30.3	8.4	.6
23.7	7.9	.5
18.5	7.1	.8
14.5	6.5	.6
11.4	5.7	.8
9.1	4.6	1.1
7.2	3.6	1.0
5.8	2.2	1.4
Pan	- .3	2.5

* -425 μm Malvern Particle Size Analyser

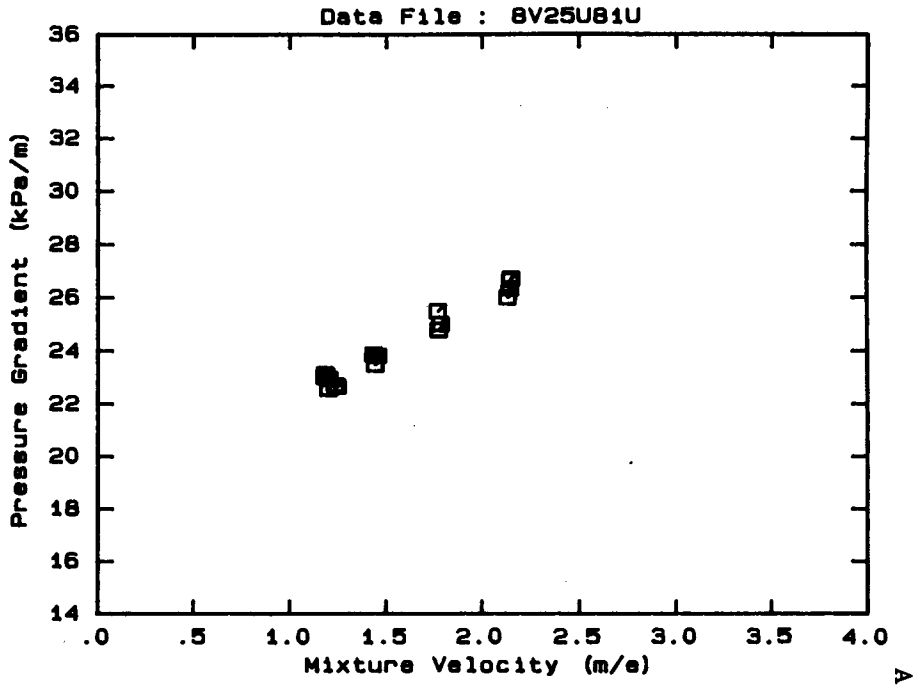

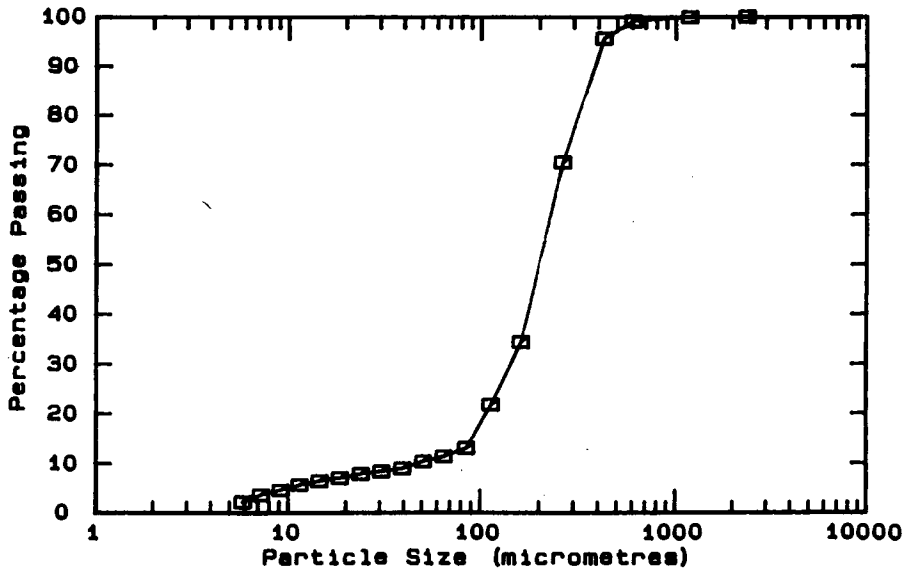

DATA FILE : BV40H73U

Test Facility	UCT 40 mm NB
Test Date	August 1990
Material Description	Blyvooruitsig CCT
Material Relative Density	2.66
Slurry Relative Density	1.73
Solids Volumetric Concentration (%)	43.98
Solids Mass Concentration (%)	67.62
Mean Slurry Temperature (°C)	18.7
Pipe Internal Diameter (mm)	40.00
Pipe Roughness (μm)	52.0
Pipeline Slope	Horizontal

Mixture Velocity (m/s)	Pressure Gradient (kPa/m)	Slurry Temp. (°C)
3.847	6.685	18.3
3.861	6.341	18.4
3.854	6.409	18.5
3.844	6.725	18.6
3.843	6.473	18.7
3.223	5.034	18.8
3.232	4.950	18.8
3.233	4.819	18.8
3.231	4.904	18.8
3.233	4.881	18.8
2.705	3.823	18.9
2.707	4.117	18.9
2.692	3.956	18.9
2.706	4.026	18.8
2.146	3.116	18.8
2.145	3.024	18.8
2.136	3.157	18.8
2.143	3.120	18.7
1.660	2.487	18.7
1.656	2.616	18.6
1.650	2.557	18.6
1.650	2.530	18.6
.993	2.561	18.5
.964	3.488	18.5
.951	3.187	18.5
.942	3.095	18.5
.959	2.413	18.4
.953	3.146	18.4

Particle Size Distribution
Sieve and Malvern Size Analysis *

Size (μm)	% Passing	% Retained
3350.0	100.0	.0
2000.0	100.0	.0
1180.0	99.9	.1
600.0	99.0	.9
425.0	95.3	3.7
261.6	74.7	20.6
160.4	40.6	34.1
112.8	25.5	15.1
84.3	16.3	9.2
64.6	13.2	3.1
50.2	11.2	2.0
39.0	9.9	1.3
30.3	9.0	.9
23.7	8.1	.9
18.5	7.3	.8
14.5	6.6	.7
11.4	5.7	.9
9.1	4.7	1.0
7.2	3.7	1.0
5.8	2.3	1.4
Pan	- .2	2.5

OBSERVED FLOW BEHAVIOUR

Velocity (m/s)	Observation (D = 46.0 mm)
.79	35% sliding bed
1.28	Asymmetric - sliding part.
1.64	Asymmetric - sliding part.
2.09	Asymmetric
2.45	Appears homogeneous
2.94	Appears homogeneous

* -425 μm Malvern Particle Size Analyser

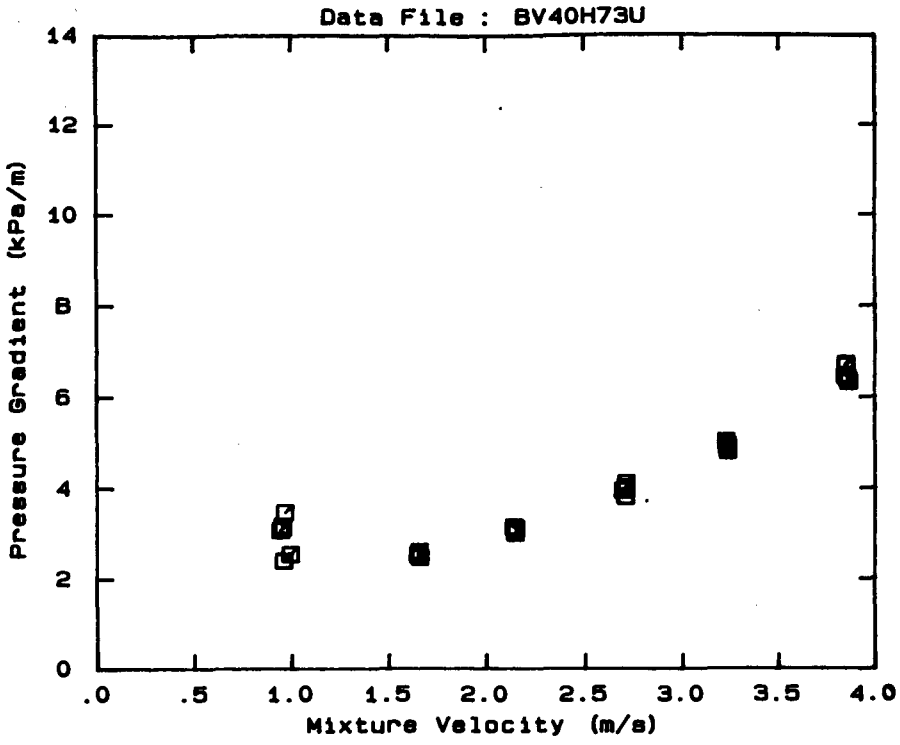

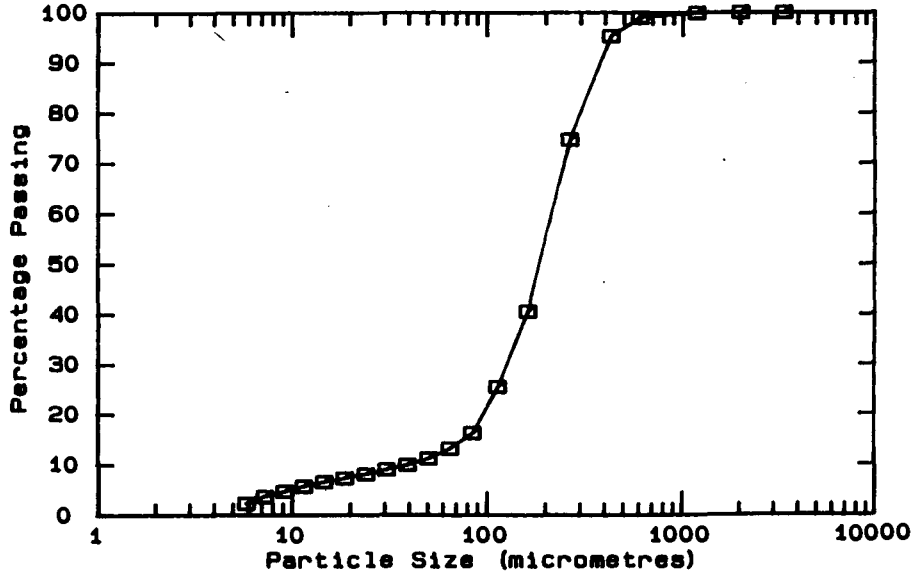

DATA FILE : BV40H78U

Test Facility	UCT 40 mm NB
Test Date	August 1990
Material Description	Blyvooruitsig CCT
Material Relative Density	2.66
Slurry Relative Density	1.78
Solids Volumetric Concentration (%)	46.99
Solids Mass Concentration (%)	70.22
Mean Slurry Temperature (°C)	19.6
Pipe Internal Diameter (mm)	40.00
Pipe Roughness (μm)	52.0
Pipeline Slope	Horizontal

Mixture Velocity (m/s)	Pressure Gradient (kPa/m)	Slurry Temp. (°C)
4.055	8.235	18.9
4.061	7.789	19.1
4.086	7.900	19.2
4.095	7.865	19.3
4.097	8.030	19.4
3.170	5.899	19.6
3.173	6.143	19.7
3.167	6.018	19.7
3.159	6.184	19.7
2.684	5.323	19.8
2.685	5.372	19.8
2.681	5.420	19.9
2.683	5.087	19.9
2.151	4.262	19.9
2.147	4.342	19.8
2.160	4.276	19.8
2.145	4.378	19.8
2.153	4.428	19.8
1.593	3.094	19.7
1.594	3.062	19.7
1.599	3.001	19.7
1.594	3.555	19.7
1.593	3.042	19.6
1.589	3.069	19.6
1.156	2.448	19.5
1.129	2.445	19.5
1.175	2.447	19.5
1.166	2.420	19.4

Particle Size Distribution
Sieve and Malvern Size Analysis *

Size (μm)	% Passing	% Retained
3350.0	100.0	.0
2000.0	100.0	.0
1180.0	99.9	.1
600.0	99.1	.8
425.0	95.4	3.7
261.6	70.7	24.7
160.4	34.9	35.8
112.8	23.2	11.7
84.3	15.1	8.1
64.6	12.9	2.2
50.2	11.8	1.1
39.0	10.7	1.1
30.3	9.8	.9
23.7	9.0	.8
18.5	8.3	.7
14.5	7.6	.7
11.4	6.6	1.0
9.1	5.4	1.2
7.2	4.4	1.0
5.8	2.8	1.6
Pan	- .2	3.0

OBSERVED FLOW BEHAVIOUR

Velocity (m/s)	Observation (D = 46.0 mm)
.87	Asymmetric - sliding part.
1.24	Asymmetric - sliding part.
1.64	Asymmetric - sliding part.
2.05	Asymmetric
2.45	Appears homogeneous
3.06	Appears homogeneous

* -425 μm Malvern Particle Size Analyser

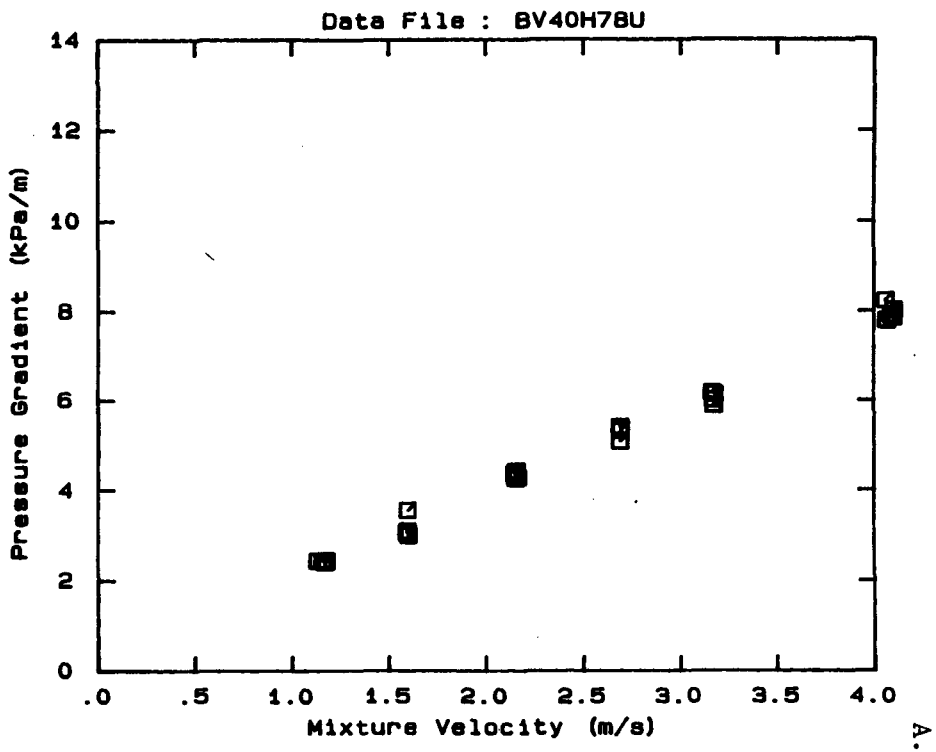

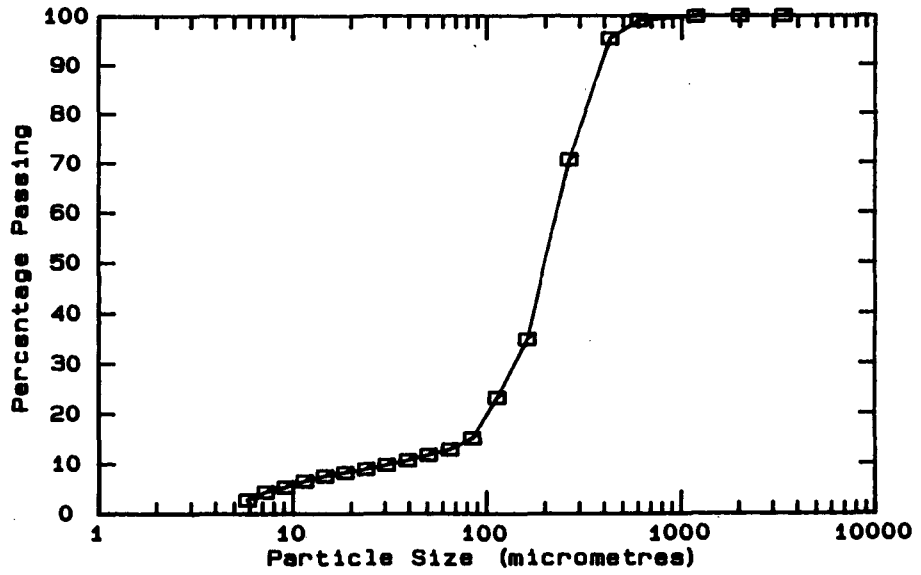

DATA FILE : BV40H81U

Test Facility	UCT 40 mm NB
Test Date	August 1990
Material Description	Blyvooruitsig CCT
Material Relative Density	2.66
Slurry Relative Density	1.81
Solids Volumetric Concentration (%)	48.80
Solids Mass Concentration (%)	71.71
Mean Slurry Temperature (°C)	20.6
Pipe Internal Diameter (mm)	40.00
Pipe Roughness (μm)	52.0
Pipeline Slope	Horizontal

Mixture Velocity (m/s)	Pressure Gradient (kPa/m)	Slurry Temp. (°C)
3.458	9.638	19.2
3.458	9.337	19.4
3.478	9.433	19.5
3.487	9.661	19.7
3.499	9.523	19.9
3.175	8.691	20.2
3.180	8.485	20.3
3.178	8.783	20.4
3.178	8.658	20.5
3.187	8.496	20.6
2.615	7.318	20.8
2.592	7.388	20.9
2.616	7.262	20.9
2.612	7.495	21.0
2.086	6.080	21.0
2.091	6.389	21.1
2.101	6.278	21.1
2.084	6.265	21.1
1.594	5.031	21.1
1.578	5.267	21.1
1.575	5.144	21.1
1.568	5.256	21.1
1.573	5.303	21.1
1.025	3.397	21.0
.925	3.633	21.0
.890	3.931	21.0
.861	3.973	21.0
.865	3.962	21.0

Particle Size Distribution
Sieve and Malvern Size Analysis *

Size (μm)	% Passing	% Retained
3350.0	100.0	.0
2000.0	100.0	.0
1180.0	100.0	.0
600.0	99.2	.8
425.0	95.2	4.0
261.6	68.3	26.9
160.4	32.2	36.1
112.8	21.0	11.2
84.3	13.1	7.9
64.6	11.6	1.5
50.2	10.6	1.0
39.0	9.6	1.0
30.3	9.0	.6
23.7	8.4	.6
18.5	7.8	.6
14.5	7.2	.6
11.4	6.3	.9
9.1	5.3	1.0
7.2	4.4	.9
5.8	2.9	1.5
Pan	.1	2.8

OBSERVED FLOW BEHAVIOUR

Velocity (m/s)	Observation (D = 46.0 mm)
.83	Asymmetric - sliding part.
1.24	Slight asymmetry
1.64	Slight asymmetry
2.01	Appears homogeneous
2.05	Appears homogeneous
2.62	Appears homogeneous

* -425 μm Malvern Particle Size Analyser

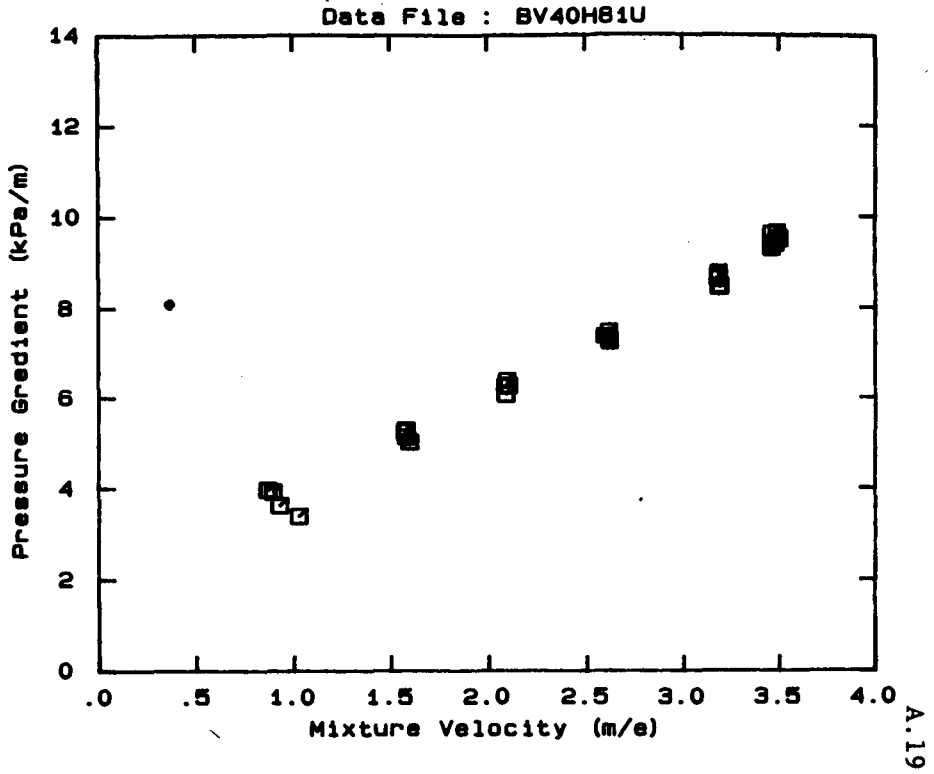

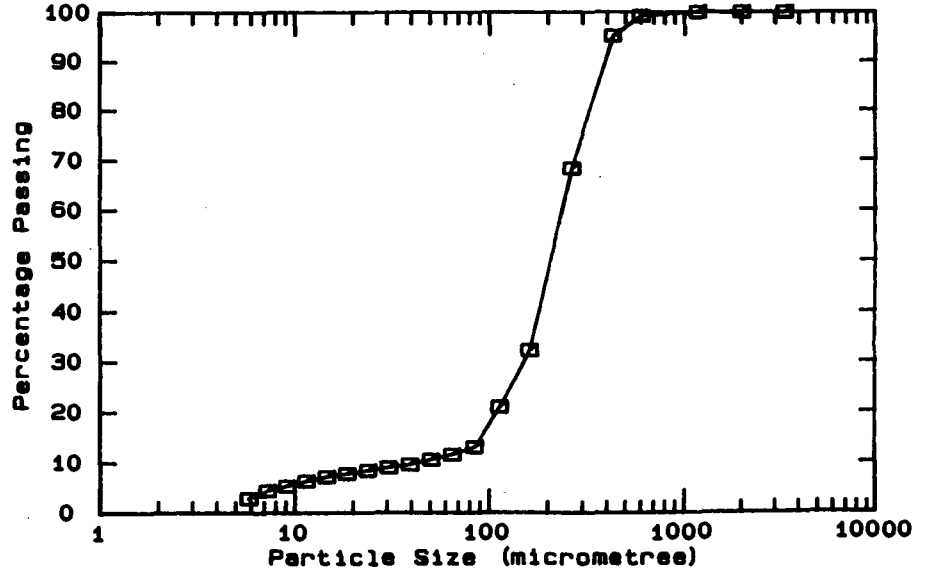

DATA FILE : BV40H86U

Test Facility	UCT 40 mm NB
Test Date	August 1990
Material Description	Blyvooruitsig CCT
Material Relative Density	2.66
Slurry Relative Density	1.86
Solids Volumetric Concentration (%)	51.81
Solids Mass Concentration (%)	74.09
Mean Slurry Temperature (°C)	18.7
Pipe Internal Diameter (mm)	40.00
Pipe Roughness (μm)	52.0
Pipeline Slope	Horizontal

Mixture Velocity (m/s)	Pressure Gradient (kPa/m)	Slurry Temp. (°C)
2.705	13.597	18.3
2.731	13.419	18.4
2.724	13.499	18.8
2.739	12.808	18.8
2.728	13.177	18.8
2.126	10.259	18.8
2.119	10.070	18.8
2.121	10.244	18.9
2.123	10.207	18.9
2.125	10.287	18.9
1.504	7.518	18.8
1.481	7.801	18.8
1.492	7.744	18.8
1.516	7.781	18.8
1.536	7.832	18.7
.992	5.735	18.7
.906	5.644	18.6
.834	5.894	18.6
.790	5.988	18.6
.770	6.012	18.5
.495	4.748	18.5
.475	4.573	18.5
.380	4.486	18.5
.376	4.509	18.4
.347	4.555	18.4

Particle Size Distribution
Sieve and Malvern Size Analysis *

Size (μm)	% Passing	% Retained
3350.0	100.0	.0
2000.0	100.0	.0
1180.0	99.9	.1
600.0	99.2	.7
425.0	95.1	4.1
261.6	76.0	19.1
160.4	43.6	32.4
112.8	27.7	15.9
84.3	17.9	9.8
64.6	15.0	2.9
50.2	13.3	1.7
39.0	12.1	1.2
30.3	11.1	1.0
23.7	10.3	.8
18.5	9.6	.7
14.5	8.8	.8
11.4	7.7	1.1
9.1	6.5	1.2
7.2	5.5	1.0
5.8	3.7	1.8
Pan	.3	3.4

OBSERVED FLOW BEHAVIOUR

Velocity (m/s)	Observation (D = 46.0 mm)
.42	Appears homogeneous
.67	Appears homogeneous
1.24	Appears homogeneous
1.64	Appears homogeneous
2.05	Appears homogeneous

* -425 μm Malvern Particle Size Analyser

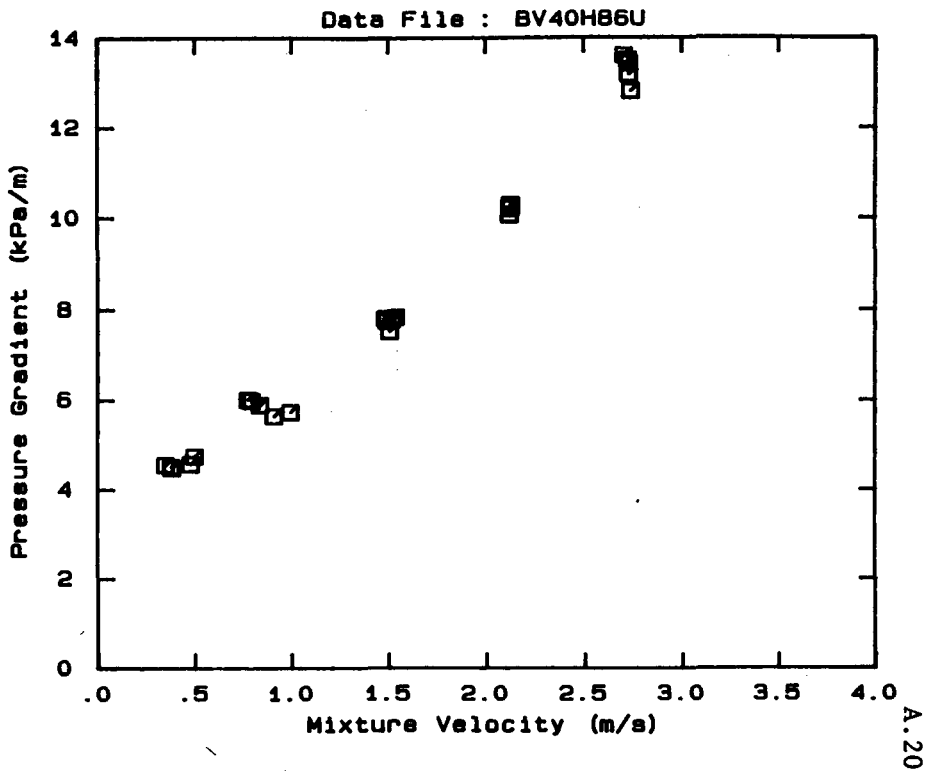

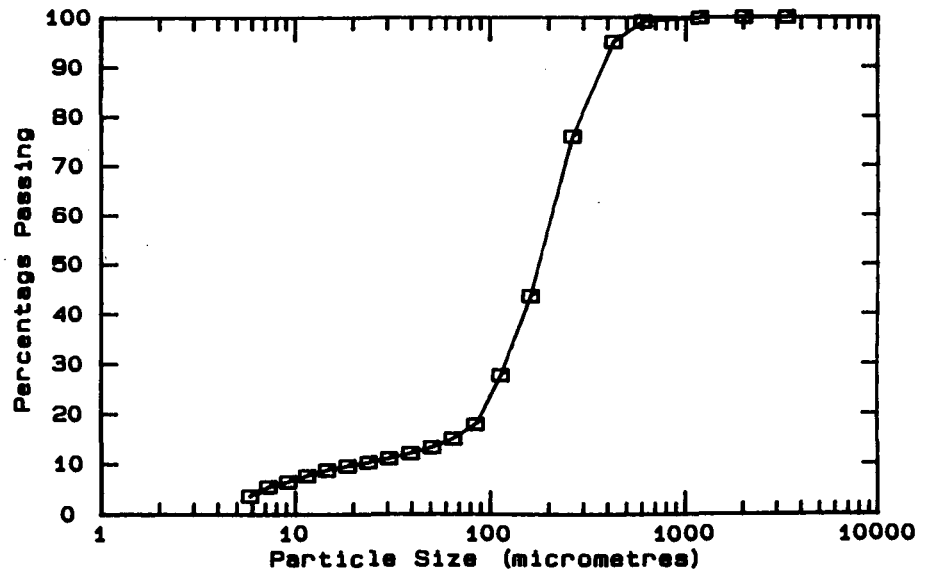

DATA FILE : BV40H87U

Test Facility	UCT 40 mm NB
Test Date	August 1990
Material Description	Blyvooruitsig CCT
Material Relative Density	2.66
Slurry Relative Density	1.87
Solids Volumetric Concentration (%)	52.41
Solids Mass Concentration (%)	74.55
Mean Slurry Temperature (°C)	29.2
Pipe Internal Diameter (mm)	40.00
Pipe Roughness (μm)	52.0
Pipeline Slope	Horizontal

Mixture Velocity (m/s)	Pressure Gradient (kPa/m)	Slurry Temp. (°C)
1.640	11.050	25.8
1.754	11.324	26.0
2.038	12.127	27.4
2.039	12.263	27.7
2.067	12.498	27.9
2.088	12.480	28.1
1.773	10.620	28.7
1.741	10.646	29.0
1.747	11.041	29.3
1.755	10.784	29.5
1.424	9.168	30.0
1.403	9.329	30.2
1.390	9.361	30.2
1.376	9.174	30.2
1.384	9.344	30.1
1.109	8.130	30.0
1.106	8.269	30.0
1.113	8.150	30.0
1.111	8.157	30.0
.771	6.607	30.0
.737	6.550	29.9
.733	6.557	29.9
.743	6.632	29.9
.509	5.155	29.8
.485	5.175	29.7
.454	5.079	29.7
.448	5.024	29.6
.360	4.336	29.6
.318	4.264	29.5
.339	4.274	29.5
.323	4.105	29.4
.309	4.121	29.3

Particle Size Distribution
Sieve and Malvern Size Analysis *

Size (μm)	% Passing	% Retained
3350.0	100.0	.0
2000.0	100.0	.0
1180.0	100.0	.0
600.0	99.4	.6
425.0	95.5	3.9
261.6	68.7	26.8
160.4	32.2	36.5
112.8	22.9	9.3
84.3	15.6	7.3
64.6	13.9	1.7
50.2	13.1	.8
39.0	12.2	.9
30.3	11.5	.7
23.7	10.8	.7
18.5	10.1	.7
14.5	9.4	.7
11.4	8.4	1.0
9.1	7.1	1.3
7.2	6.0	1.1
5.8	4.0	2.0
Pan	.2	3.8

OBSERVED FLOW BEHAVIOUR

Velocity (m/s)	Observation (D = 46.0 mm)
.30	Appears homogeneous
.42	Appears homogeneous
.63	Appears homogeneous
.87	Appears homogeneous
1.12	Appears homogeneous
1.36	Appears homogeneous
1.52	Appears homogeneous

* -425 μm Malvern Particle Size Analyser

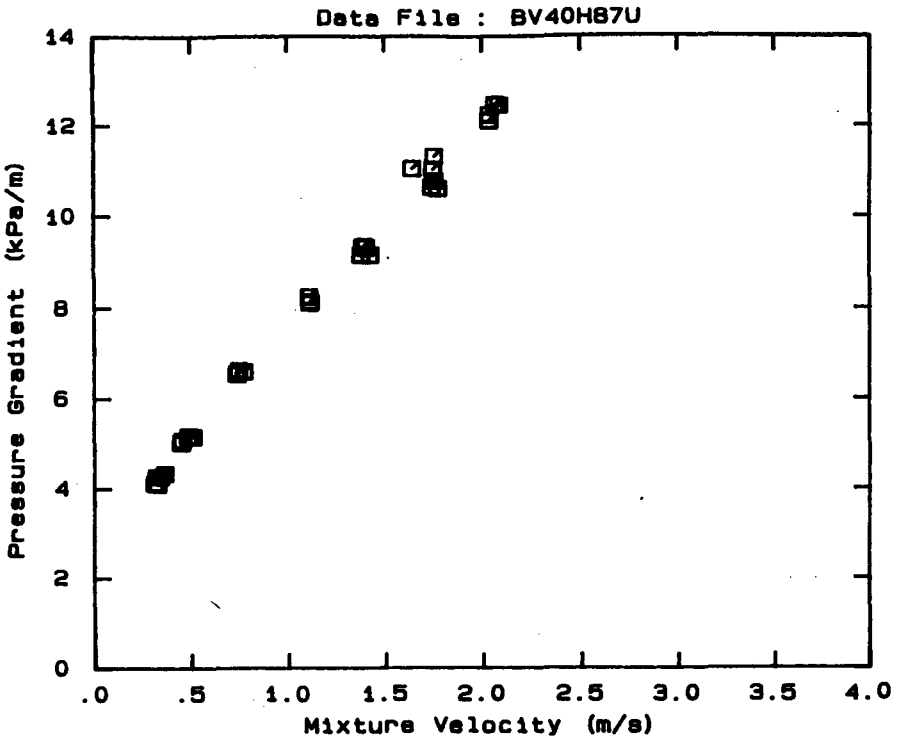

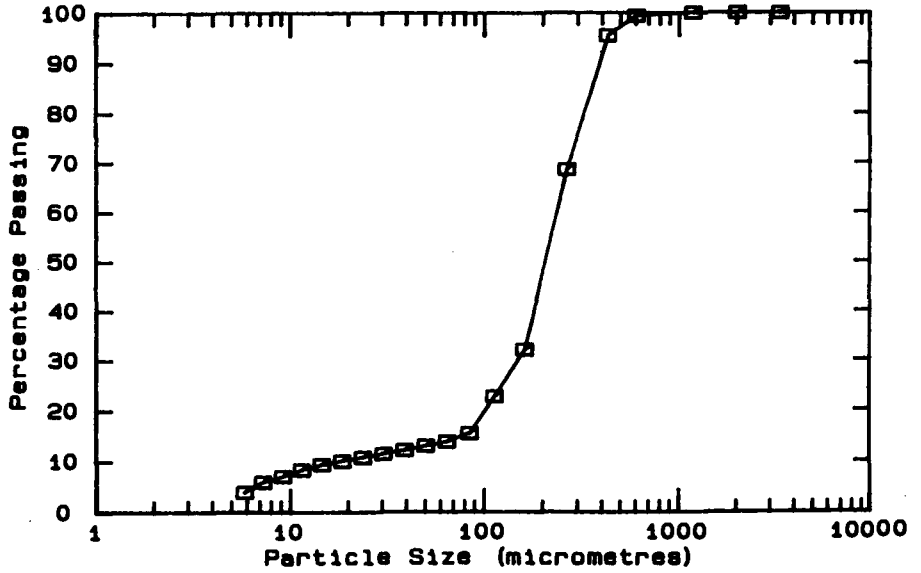

DATA FILE : BV40D73U

Test Facility	UCT 40 mm NB
Test Date	August 1990
Material Description	Blyvooruitsig CCT
Material Relative Density	2.66
Slurry Relative Density	1.73
Solids Volumetric Concentration (%)	43.98
Solids Mass Concentration (%)	67.62
Mean Slurry Temperature (°C)	18.7
Pipe Internal Diameter (mm)	40.00
Pipe Roughness (μm)	52.0
Pipeline Slope	Vertical Down

Mixture Velocity (m/s)	Pressure Gradient (kPa/m)	Slurry Temp. (°C)
3.847	- 9.203	18.3
3.861	- 9.075	18.4
3.854	- 9.090	18.5
3.844	- 9.492	18.6
3.843	- 9.622	18.7
3.223	-11.477	18.8
3.232	-11.736	18.8
3.233	-11.418	18.8
3.231	-11.406	18.8
3.233	-11.369	18.8
2.705	-13.448	18.9
2.707	-13.939	18.9
2.692	-13.393	18.9
2.706	-13.514	18.8
2.146	-14.466	18.8
2.145	-14.422	18.8
2.136	-14.579	18.8
2.143	-14.447	18.7
1.660	-14.960	18.7
1.656	-14.982	18.6
1.650	-15.012	18.6
1.650	-14.980	18.6
.993	-15.184	18.5
.964	-15.388	18.5
.951	-15.192	18.5
.942	-15.071	18.5
.959	-14.730	18.4
.953	-15.322	18.4

Particle Size Distribution
Sieve and Malvern Size Analysis *

Size (μm)	% Passing	% Retained
3350.0	100.0	.0
2000.0	100.0	.0
1180.0	99.9	.1
600.0	99.0	.9
425.0	95.3	3.7
261.6	74.7	20.6
160.4	40.6	34.1
112.8	25.5	15.1
84.3	16.3	9.2
64.6	13.2	3.1
50.2	11.2	2.0
39.0	9.9	1.3
30.3	9.0	.9
23.7	8.1	.9
18.5	7.3	.8
14.5	6.6	.7
11.4	5.7	.9
9.1	4.7	1.0
7.2	3.7	1.0
5.8	2.3	1.4
Pan	- .2	2.5

OBSERVED FLOW BEHAVIOUR

Velocity (m/s)	Observation (D = 46.0 mm)

* -425 μm Malvern Particle Size Analyser

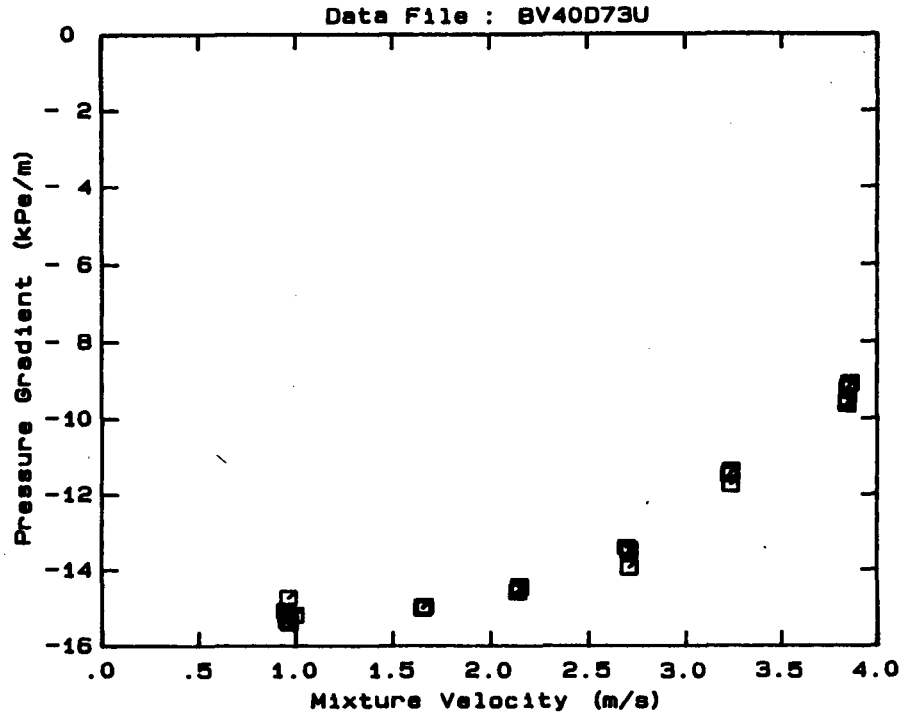

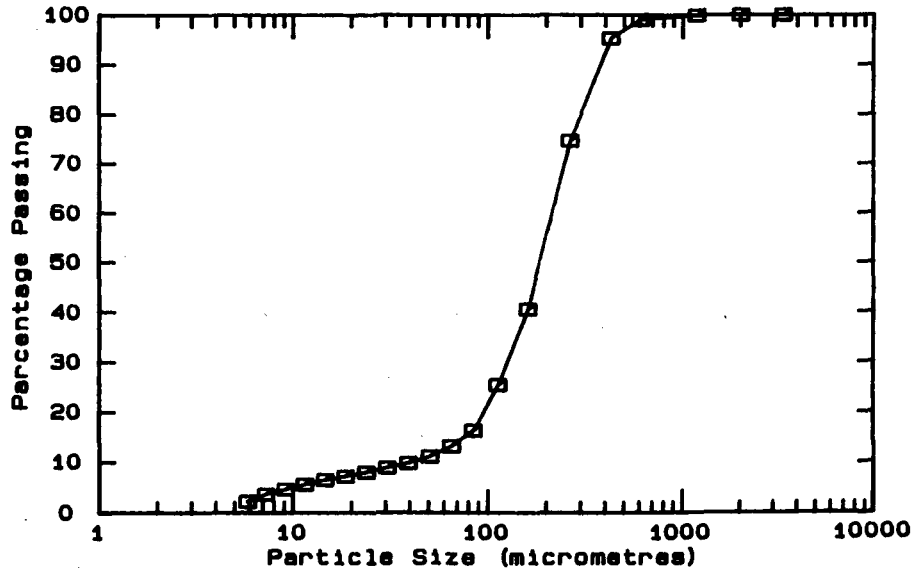

DATA FILE : BV40D78U

Test Facility	UCT 40 mm NB
Test Date	August 1990
Material Description	Blyvooruitsig CCT
Material Relative Density	2.66
Slurry Relative Density	1.78
Solids Volumetric Concentration (%)	46.99
Solids Mass Concentration (%)	70.22
Mean Slurry Temperature (°C)	19.6
Pipe Internal Diameter (mm)	40.00
Pipe Roughness (μm)	52.0
Pipeline Slope	Vertical Down

Mixture Velocity (m/s)	Pressure Gradient (kPa/m)	Slurry Temp. (°C)
4.055	-10.128	18.9
4.061	-10.327	19.1
4.086	-10.502	19.2
4.095	-10.286	19.3
4.097	-10.468	19.4
3.170	-12.350	19.6
3.173	-12.006	19.7
3.167	-12.040	19.7
3.159	-11.903	19.7
2.684	-12.891	19.8
2.685	-12.754	19.8
2.681	-12.811	19.9
2.683	-12.981	19.9
2.151	-13.826	19.9
2.147	-13.817	19.8
2.160	-13.815	19.8
2.145	-13.769	19.8
2.153	-13.692	19.8
1.593	-14.572	19.7
1.594	-14.726	19.7
1.599	-14.205	19.7
1.594	-14.701	19.7
1.593	-14.723	19.6
1.589	-14.692	19.6
1.156	-15.050	19.5
1.129	-15.033	19.5
1.175	-15.013	19.5
1.166	-15.038	19.4

Particle Size Distribution
Sieve and Malvern Size Analysis *

Size (μm)	% Passing	% Retained
3350.0	100.0	.0
2000.0	100.0	.0
1180.0	99.9	.1
600.0	99.1	.8
425.0	95.4	3.7
261.6	70.7	24.7
160.4	34.9	35.8
112.8	23.2	11.7
84.3	15.1	8.1
64.6	12.9	2.2
50.2	11.8	1.1
39.0	10.7	1.1
30.3	9.8	.9
23.7	9.0	.8
18.5	8.3	.7
14.5	7.6	.7
11.4	6.6	1.0
9.1	5.4	1.2
7.2	4.4	1.0
5.8	2.8	1.6
Pan	- .2	3.0

OBSERVED FLOW BEHAVIOUR

Velocity (m/s)	Observation (D = 46.0 mm)

* -425 μm Malvern Particle Size Analyser

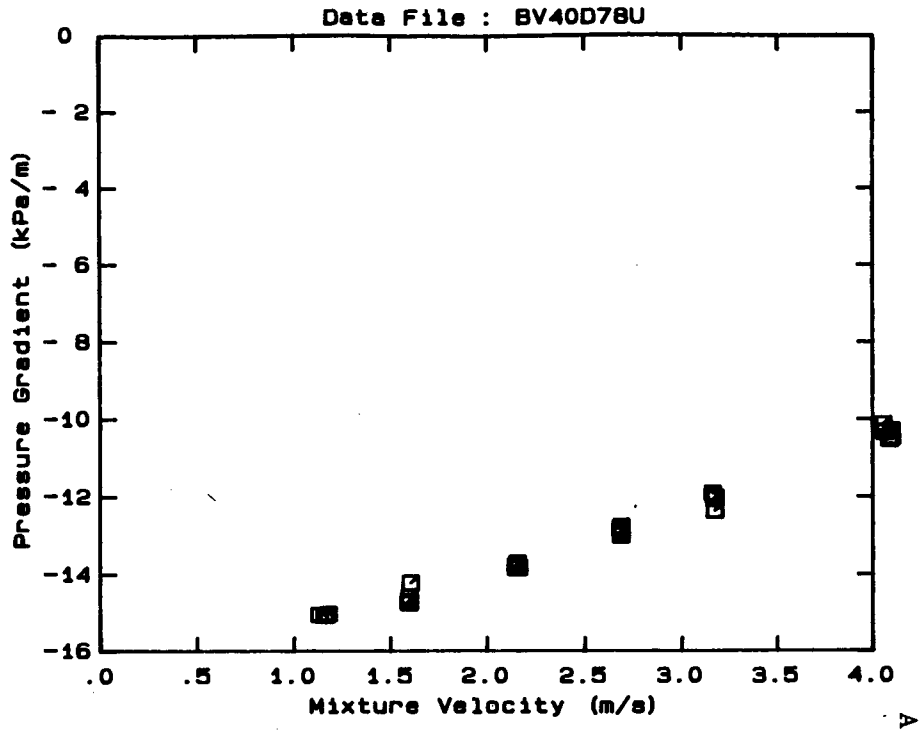

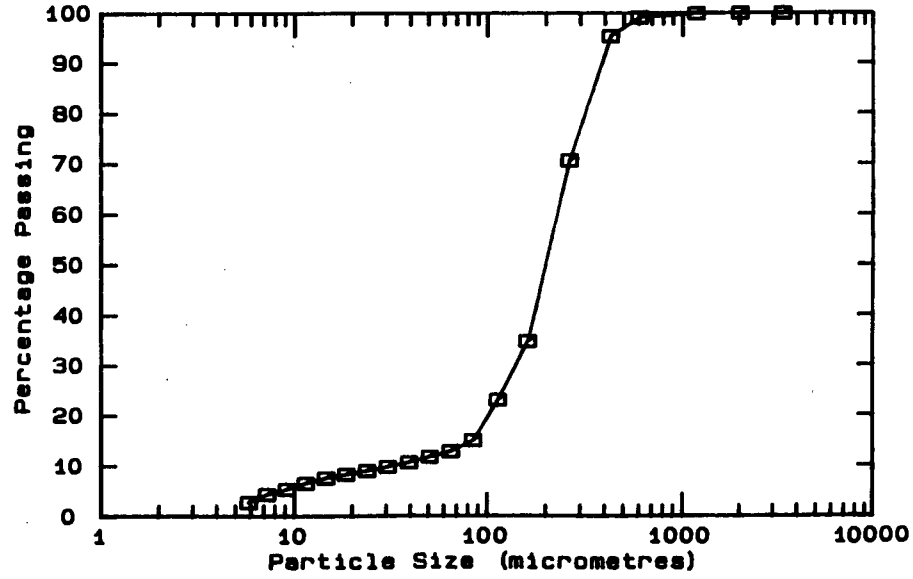

DATA FILE : BV40D81U

Test Facility	UCT 40 mm NB
Test Date	August 1990
Material Description	Blyvooruitsig CCT
Material Relative Density	2.66
Slurry Relative Density	1.81
Solids Volumetric Concentration (%)	48.80
Solids Mass Concentration (%)	71.71
Mean Slurry Temperature (°C)	20.6
Pipe Internal Diameter (mm)	40.00
Pipe Roughness (μm)	52.0
Pipeline Slope	Vertical Down

Mixture Velocity (m/s)	Pressure Gradient (kPa/m)	Slurry Temp. (°C)
3.458	- 8.505	19.2
3.458	- 8.712	19.4
3.478	- 8.441	19.5
3.487	- 8.722	19.7
3.499	- 8.394	19.9
3.175	- 9.452	20.2
3.180	- 9.066	20.3
3.178	- 9.435	20.4
3.178	- 9.423	20.5
3.187	- 9.018	20.6
2.615	-10.896	20.8
2.592	-11.118	20.9
2.616	-10.980	20.9
2.612	-10.919	21.0
2.086	-12.105	21.0
2.091	-12.020	21.1
2.101	-12.129	21.1
2.084	-12.315	21.1
1.594	-13.407	21.1
1.578	-13.300	21.1
1.575	-13.436	21.1
1.568	-13.370	21.1
1.573	-13.375	21.1
1.025	-14.599	21.0
.925	-14.520	21.0
.890	-14.572	21.0
.861	-14.596	21.0
.865	-14.567	21.0

Particle Size Distribution
Sieve and Malvern Size Analysis *

Size (μm)	% Passing	% Retained
3350.0	100.0	.0
2000.0	100.0	.0
1180.0	100.0	.0
600.0	99.2	.8
425.0	95.2	4.0
261.6	68.3	26.9
160.4	32.2	36.1
112.8	21.0	11.2
84.3	13.1	7.9
64.6	11.6	1.5
50.2	10.6	1.0
39.0	9.6	1.0
30.3	9.0	.6
23.7	8.4	.6
18.5	7.8	.6
14.5	7.2	.6
11.4	6.3	.9
9.1	5.3	1.0
7.2	4.4	.9
5.8	2.9	1.5
Pan	.1	2.8

OBSERVED FLOW BEHAVIOUR

Velocity (m/s)	Observation (D = 46.0 mm)

* -425 μm Malvern Particle Size Analyser

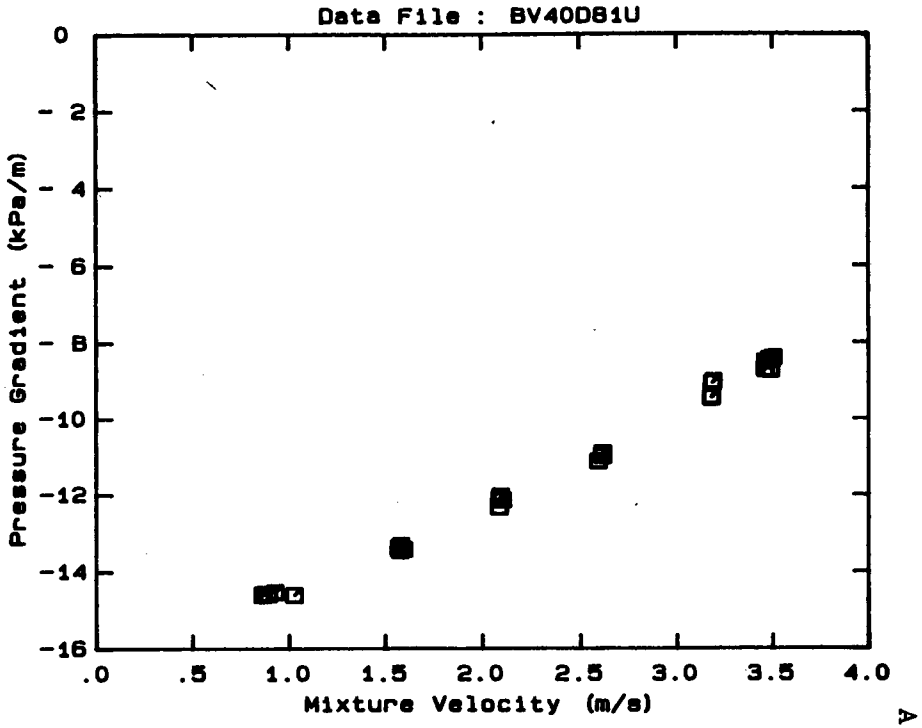

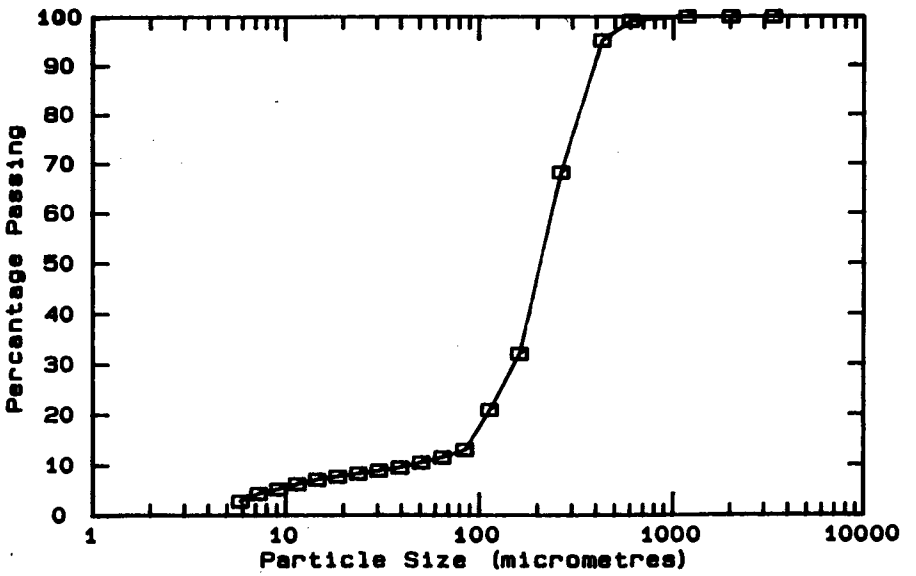

DATA FILE : BV40D86U

Test Facility	UCT 40 mm NB
Test Date	August 1990
Material Description	Blyvooruitsig CCT
Material Relative Density	2.66
Slurry Relative Density	1.86
Solids Volumetric Concentration (%)	51.81
Solids Mass Concentration (%)	74.09
Mean Slurry Temperature (°C)	23.0
Pipe Internal Diameter (mm)	40.00
Pipe Roughness (μm)	52.0
Pipeline Slope	Vertical Down

Mixture Velocity (m/s)	Pressure Gradient (kPa/m)	Slurry Temp. (°C)
2.705	- 7.970	21.5
2.731	- 7.400	21.8
2.724	- 7.833	22.1
2.739	- 8.103	22.3
2.728	- 7.686	22.5
2.126	- 9.229	23.0
2.119	- 9.255	23.1
2.121	- 9.423	23.1
2.123	- 9.482	23.2
2.125	- 9.670	23.3
1.504	-11.108	23.4
1.481	-10.992	23.4
1.492	-10.989	23.4
1.516	-11.087	23.3
1.536	-11.058	23.3
.992	-12.816	23.4
.906	-12.523	23.4
.834	-12.580	23.3
.790	-12.702	23.3
.770	-12.713	23.3
.495	-13.899	23.2
.475	-13.902	23.3
.380	-13.850	23.2
.376	-13.759	23.2
.347	-13.872	23.2

Particle Size Distribution
Sieve and Malvern Size Analysis *

Size (μm)	% Passing	% Retained
3350.0	100.0	.0
2000.0	100.0	.0
1180.0	99.9	.1
600.0	99.2	.7
425.0	95.1	4.1
261.6	76.0	19.1
160.4	43.6	32.4
112.8	27.7	15.9
84.3	17.9	9.8
64.6	15.0	2.9
50.2	13.3	1.7
39.0	12.1	1.2
30.3	11.1	1.0
23.7	10.3	.8
18.5	9.6	.7
14.5	8.8	.8
11.4	7.7	1.1
9.1	6.5	1.2
7.2	5.5	1.0
5.8	3.7	1.8
Pan	.3	3.4

OBSERVED FLOW BEHAVIOUR

Velocity (m/s)	Observation (D = 46.0 mm)

*. -425 μm Malvern Particle Size Analyser

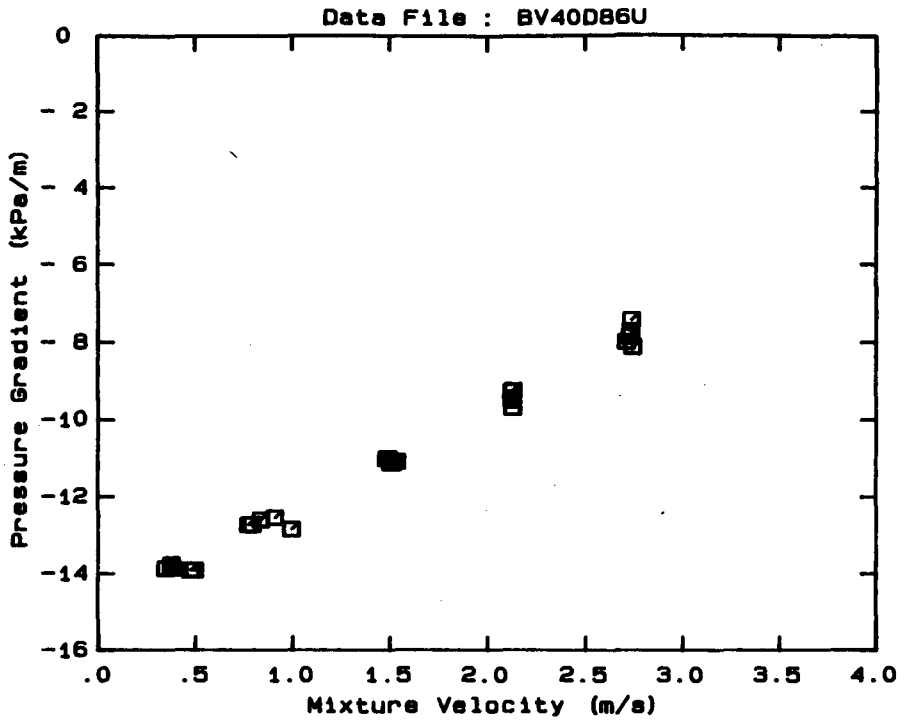

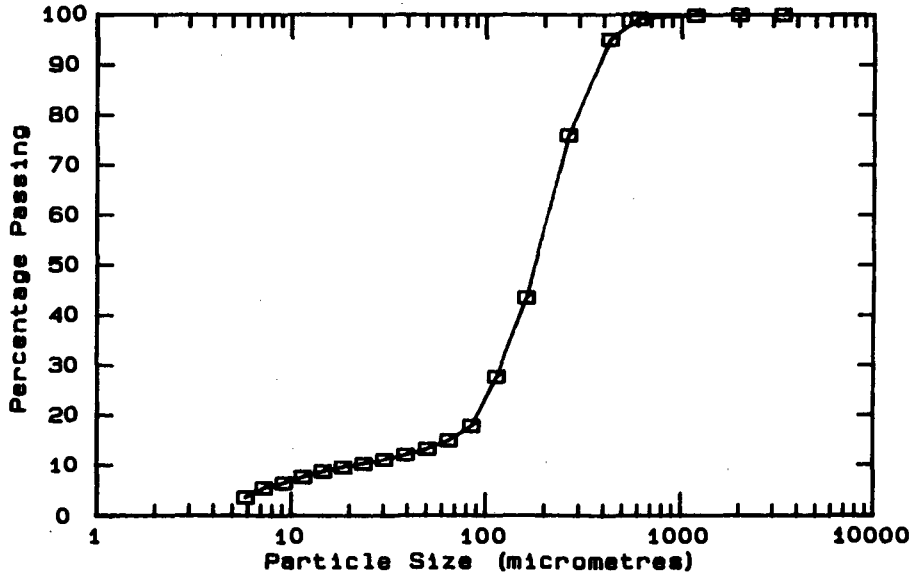

DATA FILE : BV40D87U

Test Facility	UCT 40 mm NB
Test Date	August 1990
Material Description	Blyvooruitsig CCT
Material Relative Density	2.66
Slurry Relative Density	1.87
Solids Volumetric Concentration (%)	52.41
Solids Mass Concentration (%)	74.55
Mean Slurry Temperature (°C)	29.4
Pipe Internal Diameter (mm)	40.00
Pipe Roughness (μm)	52.0
Pipeline Slope	Vertical Down

Mixture Velocity (m/s)	Pressure Gradient (kPa/m)	Slurry Temp. (°C)
1.754	- 7.291	26.0
2.038	- 6.550	27.4
2.039	- 6.488	27.7
2.067	- 6.332	27.9
2.088	- 6.213	28.1
1.773	- 7.898	28.7
1.741	- 7.755	29.0
1.747	- 7.499	29.3
1.755	- 7.631	29.5
1.424	- 8.460	30.0
1.403	- 8.692	30.2
1.390	- 8.613	30.2
1.376	- 8.766	30.2
1.384	- 8.897	30.1
1.109	-10.248	30.0
1.106	-10.179	30.0
1.113	-10.094	30.0
1.111	-10.136	30.0
.771	-11.727	30.0
.737	-11.632	29.9
.733	-11.766	29.9
.743	-11.737	29.9
.509	-12.767	29.8
.485	-12.743	29.7
.454	-12.966	29.7
.448	-12.983	29.6
.360	-13.363	29.6
.318	-13.572	29.5
.339	-13.453	29.5
.323	-13.441	29.4
.309	-13.553	29.3

Particle Size Distribution
Sieve and Malvern Size Analysis *

Size (μm)	% Passing	% Retained
3350.0	100.0	.0
2000.0	100.0	.0
1180.0	100.0	.0
600.0	99.4	.6
425.0	95.5	3.9
261.6	68.7	26.8
160.4	32.2	36.5
112.8	22.9	9.3
84.3	15.6	7.3
64.6	13.9	1.7
50.2	13.1	.8
39.0	12.2	.9
30.3	11.5	.7
23.7	10.8	.7
18.5	10.1	.7
14.5	9.4	.7
11.4	8.4	1.0
9.1	7.1	1.3
7.2	6.0	1.1
5.8	4.0	2.0
Pan	.2	3.8

OBSERVED FLOW BEHAVIOUR

Velocity (m/s)	Observation (D = .0 mm)

* -425 μm Malvern Particle Size Analyser

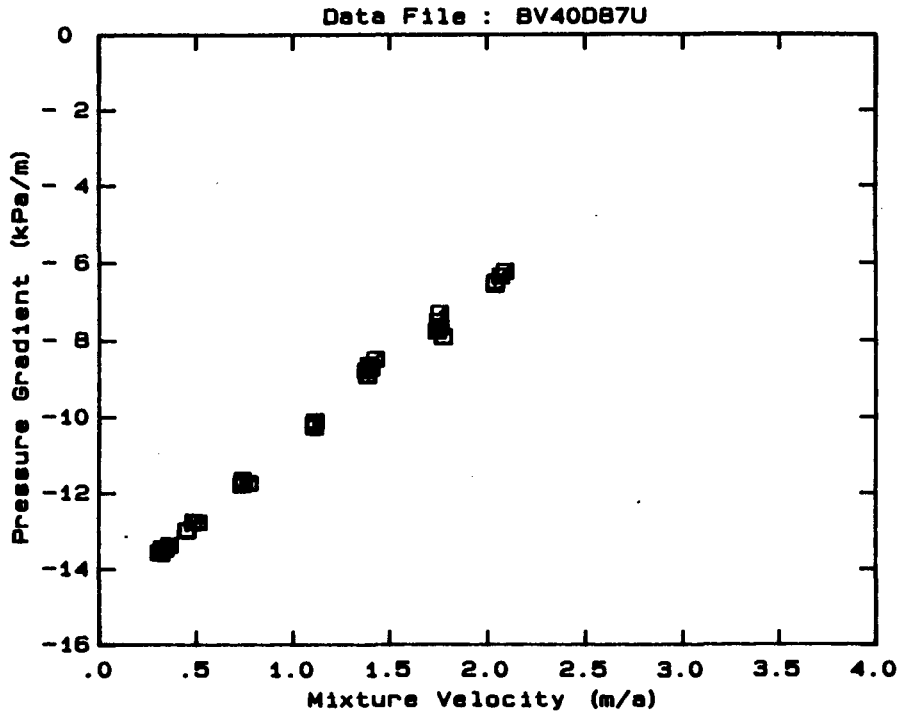

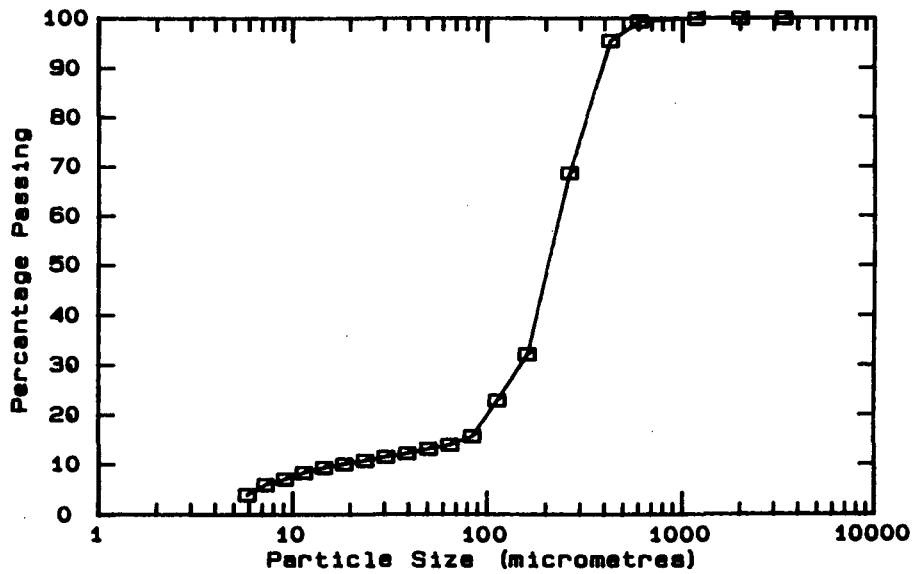

DATA FILE : BV80H52U

Test Facility	UCT 80 mm NB
Test Date	June 1990
Material Description	Blyvooruitsig CCT
Material Relative Density	2.66
Slurry Relative Density	1.52
Solids Volumetric Concentration (%)	31.33
Solids Mass Concentration (%)	54.82
Mean Slurry Temperature (°C)	16.1
Pipe Internal Diameter (mm)	73.40
Pipe Roughness (μm)	87.0
Pipeline Slope	Horizontal

Mixture Velocity (m/s)	Pressure Gradient (kPa/m)	Slurry Temp. (°C)
3.426	2.465	15.4
3.419	2.252	15.4
3.425	2.511	15.5
3.446	2.330	15.6
2.953	1.869	15.8
2.953	1.724	15.8
2.951	1.791	15.9
2.958	1.723	15.9
2.489	1.376	16.0
2.491	1.390	16.1
2.484	1.439	16.1
1.987	1.110	16.2
1.997	.942	16.2
1.988	.909	16.2
1.991	.865	16.2
1.985	.830	16.2
1.988	.964	16.2
1.992	.975	16.3
1.452	.785	16.3
1.455	.910	16.3
1.454	.922	16.3
1.458	.767	16.3
1.469	.875	16.3
1.088	1.153	16.4
1.108	.860	16.4
1.115	1.221	16.4
1.114	1.361	16.4
1.106	1.380	16.4
1.117	1.364	16.4

Particle Size Distribution
Sieve and Malvern Size Analysis *

Size (μm)	% Passing	% Retained
2360.0	100.0	.0
1180.0	99.7	.3
600.0	97.6	2.1
425.0	92.8	4.8
261.6	66.7	26.1
160.4	29.2	37.5
112.8	17.0	12.2
84.3	8.5	8.5
64.6	7.1	1.4
50.2	6.3	.8
39.0	5.0	1.3
30.3	4.6	.4
23.7	4.3	.3
18.5	3.8	.5
14.5	3.5	.3
11.4	3.1	.4
9.1	2.5	.6
7.2	2.0	.5
5.8	1.3	.7
Pan	.0	1.3

OBSERVED FLOW BEHAVIOUR

Velocity (m/s)	Observation (D = 71.0 mm)
1.16	45% stationary bed
1.54	Asym. - sliding particles
2.14	Asymmetric
2.66	Appears homogeneous
3.19	Appears homogeneous
3.68	Appears homogeneous

* -425 μm Malvern Particle Size Analyser

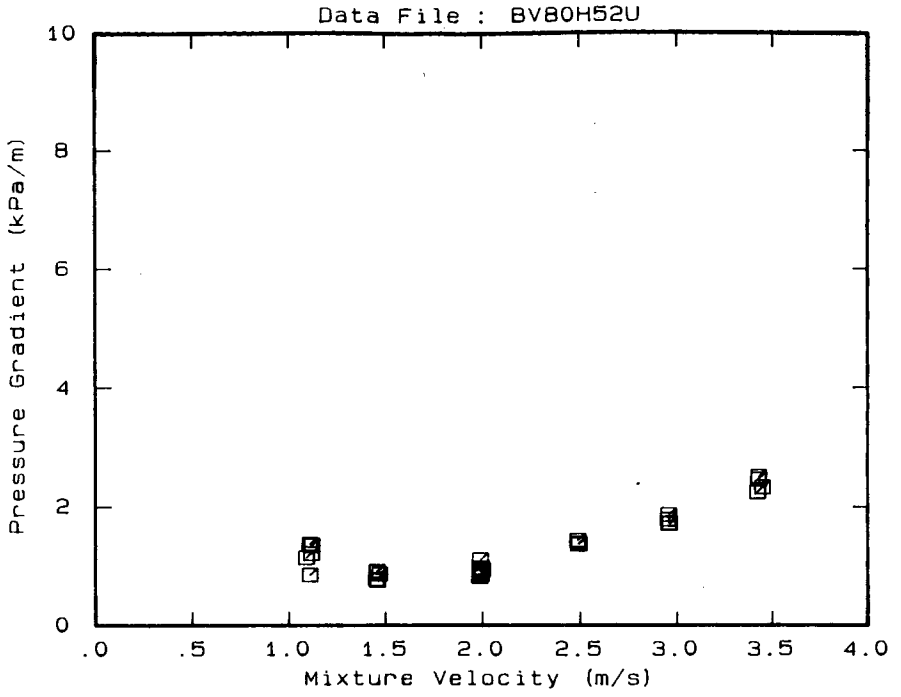

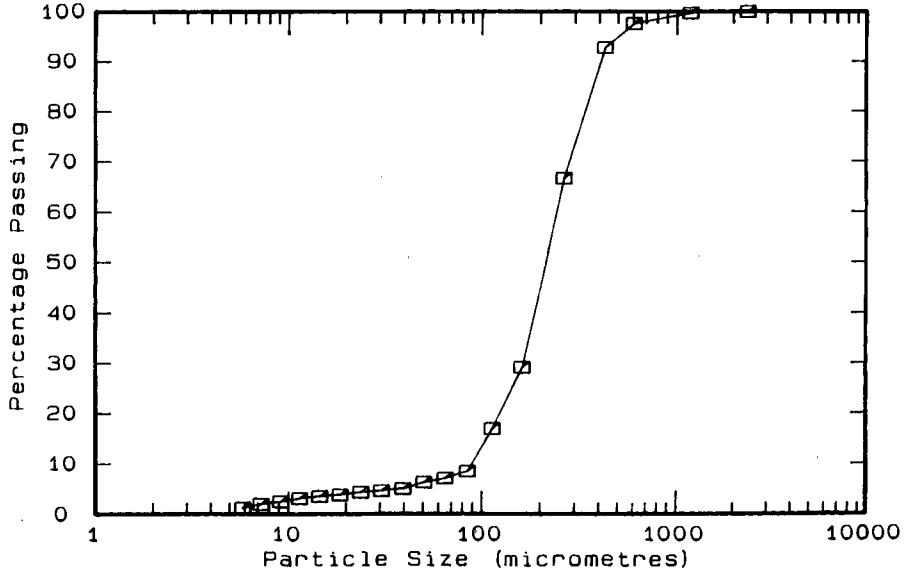

DATA FILE : BV80H60U

Test Facility	UCT 80 mm NB
Test Date	June 1990
Material Description	Blyvooruitsig CCT
Material Relative Density	2.66
Slurry Relative Density	1.60
Solids Volumetric Concentration (%)	36.14
Solids Mass Concentration (%)	60.09
Mean Slurry Temperature (°C)	16.3
Pipe Internal Diameter (mm)	73.40
Pipe Roughness (μm)	87.0
Pipeline Slope	Horizontal

Mixture Velocity (m/s)	Pressure Gradient (kPa/m)	Slurry Temp. (°C)
3.424	2.575	15.9
3.431	2.781	16.0
3.424	2.548	16.1
3.411	2.722	16.1
3.414	2.559	16.2
2.917	1.973	16.3
2.926	2.021	16.3
2.927	1.988	16.3
2.446	1.516	16.4
2.451	1.519	16.4
2.451	1.470	16.4
1.981	1.232	16.4
1.980	.991	16.4
1.973	1.279	16.4
1.976	1.368	16.3
1.984	1.258	16.3
1.476	.748	16.3
1.474	.577	16.3
1.477	.489	16.3
1.474	.928	16.3
1.470	.645	16.3
1.474	.538	16.3
1.024	.873	16.2
1.032	1.250	16.2
1.032	1.028	16.2
1.030	1.028	16.2
1.027	1.409	16.2
1.028	1.361	16.2
1.024	1.625	16.2
1.020	1.531	16.2
1.013	1.668	16.2
1.016	1.413	16.2

Particle Size Distribution
Sieve and Malvern Size Analysis *

Size (μm)	% Passing	% Retained
2360.0	100.0	.0
1180.0	99.9	.1
600.0	98.8	1.1
425.0	90.7	8.1
261.6	67.9	22.8
160.4	33.1	34.8
112.8	20.2	12.9
84.3	12.7	7.5
64.6	11.0	1.7
50.2	9.7	1.3
39.0	8.3	1.4
30.3	7.7	.6
23.7	7.2	.5
18.5	6.5	.7
14.5	5.9	.6
11.4	5.2	.7
9.1	4.3	.9
7.2	3.6	.7
5.8	2.4	1.2
Pan	.2	2.2

OBSERVED FLOW BEHAVIOUR

Velocity (m/s)	Observation ('D = 71.0 mm)
1.09	25% Stationary bed
1.58	Asym. - sliding particles
2.14	Asymmetric
2.63	Asymmetric
3.15	Appears homogeneous
3.68	Appears homogeneous

* -425 μm Malvern Particle Size Analyser

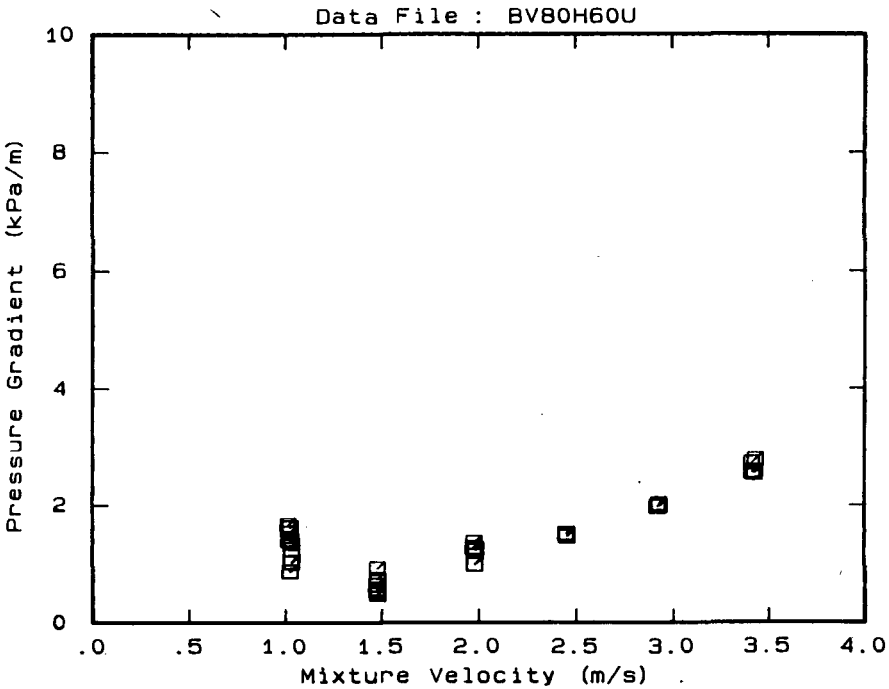

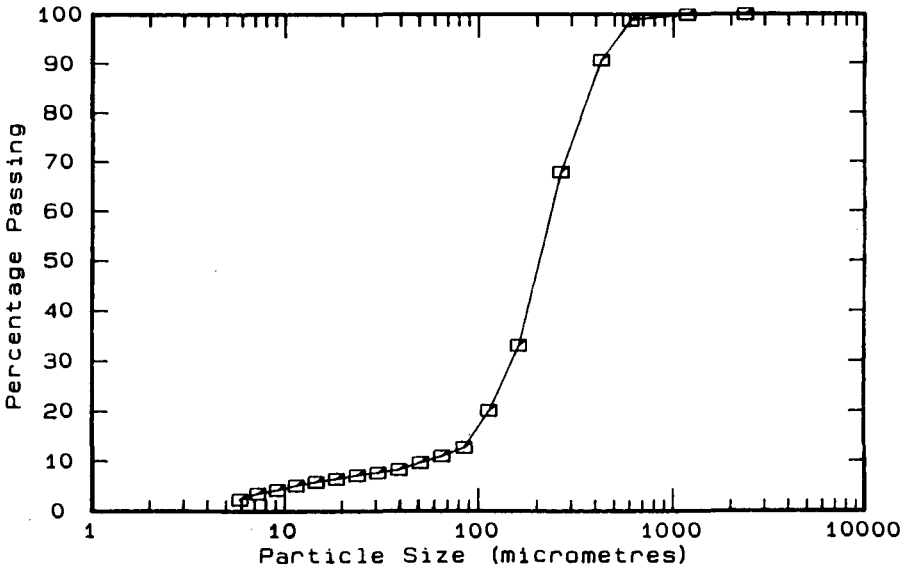

DATA FILE : BV80H70U

Test Facility	UCT 80 mm NB
Test Date	June 1990
Material Description	Blyvooruitsig CCT
Material Relative Density	2.66
Slurry Relative Density	1.70
Solids Volumetric Concentration (%)	42.17
Solids Mass Concentration (%)	65.98
Mean Slurry Temperature (°C)	16.7
Pipe Internal Diameter (mm)	73.40
Pipe Roughness (μm)	87.0
Pipeline Slope	Horizontal

Mixture Velocity (m/s)	Pressure Gradient (kPa/m)	Slurry Temp. (°C)
3.424	3.020	16.1
3.414	3.063	16.2
3.421	3.085	16.2
3.424	2.954	16.3
3.419	3.193	16.4
2.975	2.467	16.6
2.978	2.391	16.7
2.978	2.322	16.7
2.988	2.470	16.7
2.420	1.832	16.8
2.426	1.798	16.8
2.420	1.834	16.9
1.970	1.408	16.9
1.971	1.577	16.9
1.970	1.381	16.9
1.965	1.146	16.9
1.964	1.790	16.9
1.965	1.504	16.9
1.968	1.703	16.9
1.966	1.399	16.9
1.475	1.181	16.9
1.476	.908	16.9
1.474	.771	16.9
1.475	.933	16.8
1.476	.724	16.8
1.477	.475	16.8
1.477	.574	16.8
1.038	.516	16.8
1.058	.649	16.8
1.054	.933	16.8
1.064	.701	16.8

Particle Size Distribution
Sieve and Malvern Size Analysis *

Size (μm)	% Passing	% Retained
2360.0	100.0	.0
1180.0	99.9	.1
600.0	99.0	.9
425.0	93.6	5.4
261.6	74.3	19.3
160.4	33.9	40.4
112.8	21.7	12.2
84.3	12.3	9.4
64.6	10.7	1.6
50.2	9.9	.8
39.0	8.5	1.4
30.3	7.8	.7
23.7	7.3	.5
18.5	6.6	.7
14.5	5.9	.7
11.4	5.2	.7
9.1	4.3	.9
7.2	3.6	.7
5.8	2.3	1.3
Pan	.1	2.2

OBSERVED FLOW BEHAVIOUR

Velocity (m/s)	Observation (D = 71.0 mm)
1.09	35% Stationary bed
1.58	Asymmetric sliding bed
2.10	Asymmetric sliding bed
2.59	Asymmetric
3.19	Appears homogeneous
3.68	Appears homogeneous

* -425 μm Malvern Particle Size Analyser

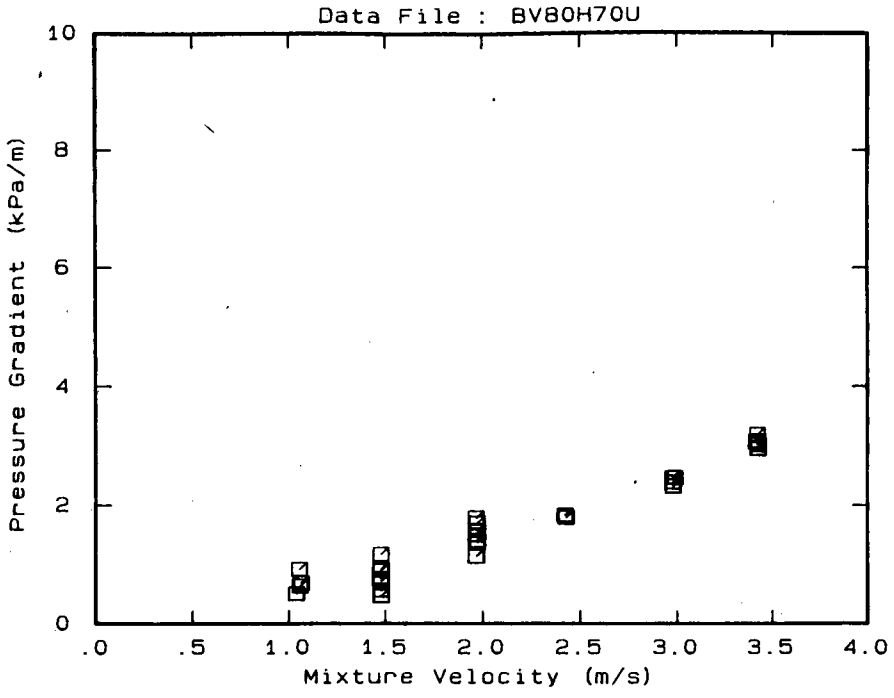

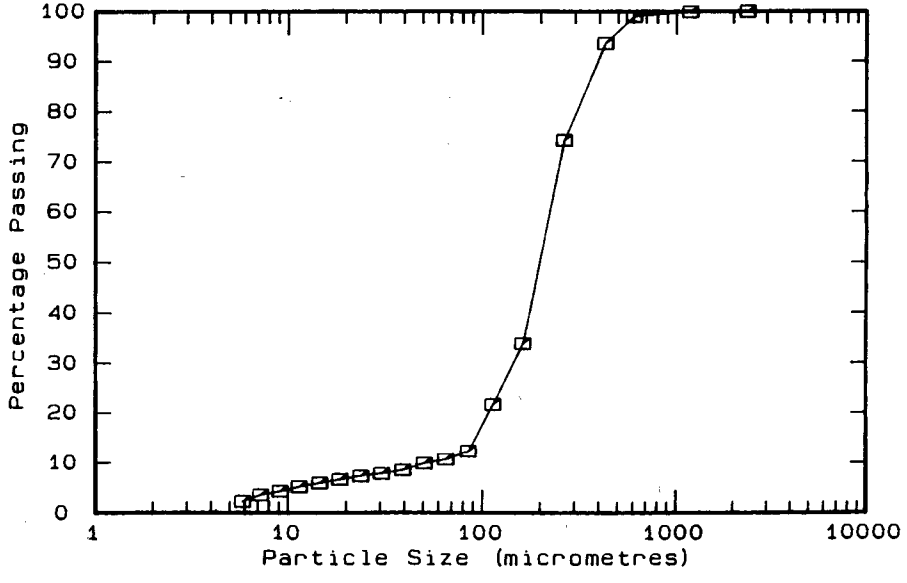

DATA FILE : BV80H75U

Test Facility	UCT 80 mm NB
Test Date	June 1990
Material Description	Blyvooruitsig CCT
Material Relative Density	2.66
Slurry Relative Density	1.75
Solids Volumetric Concentration (%)	45.18
Solids Mass Concentration (%)	68.67
Mean Slurry Temperature (°C)	17.9
Pipe Internal Diameter (mm)	73.40
Pipe Roughness (μm)	87.0
Pipeline Slope	Horizontal

Mixture Velocity (m/s)	Pressure Gradient (kPa/m)	Slurry Temp. (°C)
3.402	3.033	17.3
3.403	2.686	17.4
3.412	2.894	17.4
3.409	3.236	17.5
3.412	3.052	17.6
2.941	2.420	17.8
2.947	2.327	17.9
2.945	2.348	17.9
2.442	1.774	18.1
2.437	1.894	18.1
2.451	1.680	18.1
2.444	1.856	18.1
1.971	1.231	18.1
1.975	1.306	18.1
1.976	1.348	18.1
1.512	1.067	18.1
1.538	1.767	18.1
1.500	2.079	18.1
1.497	2.115	18.1
1.499	2.006	18.1
.996	2.292	18.0
1.004	2.309	18.0
1.002	2.529	18.0
1.006	2.242	17.9

Particle Size Distribution
Sieve and Malvern Size Analysis *

Size (μm)	% Passing	% Retained
2360.0	100.0	.0
1180.0	99.9	.1
600.0	99.0	.9
425.0	92.3	6.7
261.6	74.0	18.3
160.4	35.3	38.7
112.8	22.2	13.1
84.3	12.8	9.4
64.6	11.0	1.8
50.2	9.9	1.1
39.0	8.5	1.4
30.3	7.9	.6
23.7	7.3	.6
18.5	6.6	.7
14.5	6.1	.5
11.4	5.4	.7
9.1	4.4	1.0
7.2	3.6	.8
5.8	2.3	1.3
Pan	.0	2.3

OBSERVED FLOW BEHAVIOUR

Velocity (m/s)	Observation (D = 71.0 mm)
1.05	15% stationary bed
1.61	Asym. - sliding particles
2.10	Asym - slid part + pulses
2.63	Asym. - sliding particles
3.19	Asymmetric with pulses
3.68	Appears homogeneous

* ∟425 μm Malvern Particle Size Analyser

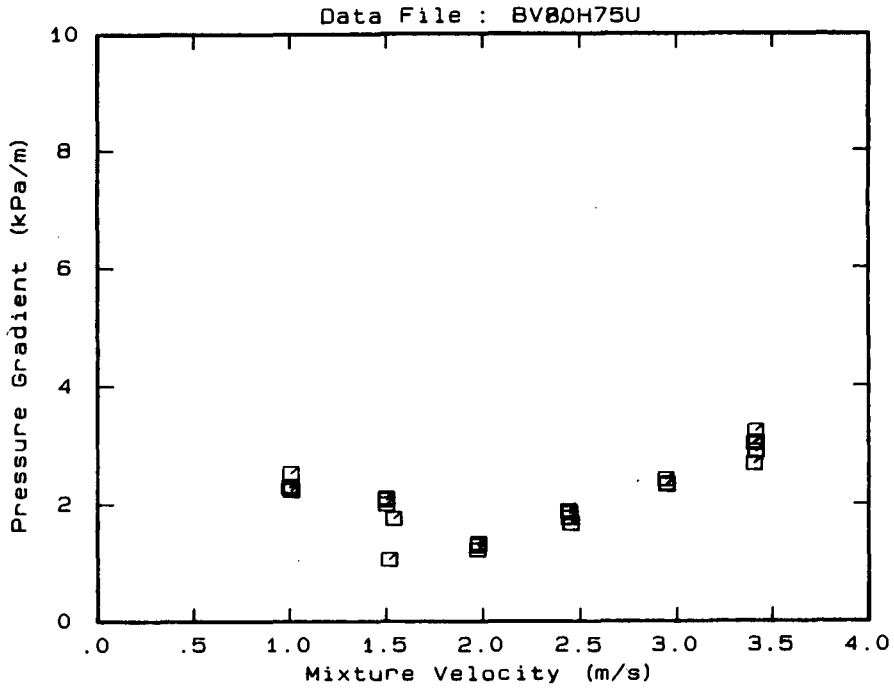

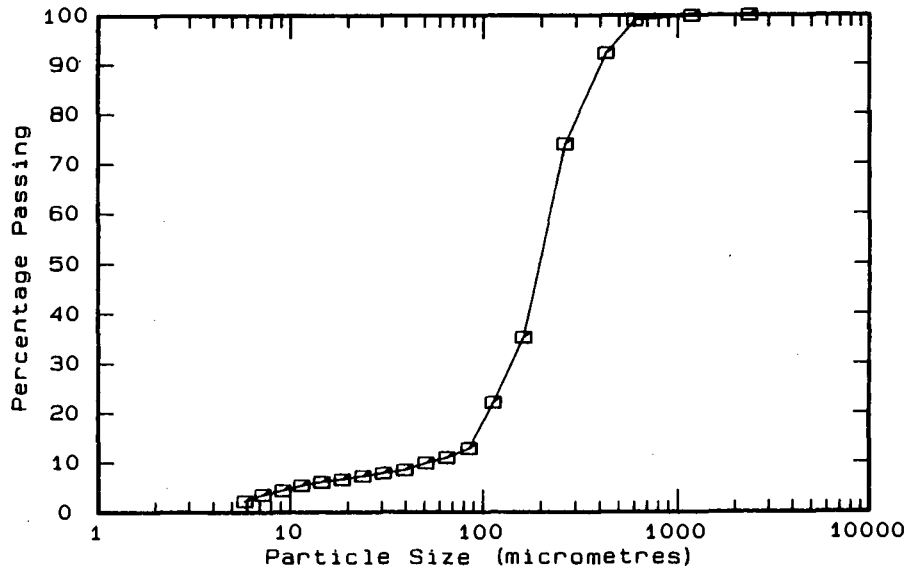

DATA FILE : BV80H83U

Test Facility	UCT 80 mm NB
Test Date	June 1990
Material Description	Blyvooruitsig CCT
Material Relative Density	2.66
Slurry Relative Density	1.83
Solids Volumetric Concentration (%)	50.00
Solids Mass Concentration (%)	72.68
Mean Slurry Temperature (°C)	20.2
Pipe Internal Diameter (mm)	73.40
Pipe Roughness (μm)	87.0
Pipeline Slope	Horizontal

Mixture Velocity (m/s)	Pressure Gradient (kPa/m)	Slurry Temp. (°C)
3.425	4.575	18.9
3.435	4.939	19.1
3.436	4.159	19.2
3.447	4.734	19.4
3.451	4.272	19.5
2.916	3.762	20.1
2.923	4.016	20.2
2.925	3.744	20.2
2.932	3.639	20.3
2.433	3.124	20.5
2.437	2.916	20.5
2.439	3.302	20.6
1.955	2.769	20.6
1.948	2.725	20.6
1.945	2.511	20.6
1.950	2.627	20.6
1.503	2.240	20.6
1.507	2.130	20.5
1.504	2.206	20.5
1.008	1.811	20.4
.991	2.446	20.3
.997	1.974	20.3
.998	1.901	20.3
1.001	1.993	20.3
1.011	1.972	20.2
1.020	2.011	20.2
1.018	1.939	20.2
1.017	1.970	20.1
1.011	1.945	20.1
1.012	2.044	20.1
1.024	1.924	20.1

Particle Size Distribution
Sieve and Malvern Size Analysis *

Size (μm)	% Passing	% Retained
2360.0	100.0	.0
1180.0	99.9	.1
600.0	99.2	.7
425.0	95.1	4.1
261.6	73.5	21.6
160.4	35.4	38.1
112.8	22.7	12.7
84.3	14.1	8.6
64.6	12.3	1.8
50.2	11.1	1.2
39.0	9.8	1.3
30.3	9.2	.6
23.7	8.5	.7
18.5	7.7	.8
14.5	7.1	.6
11.4	6.3	.8
9.1	5.2	1.1
7.2	4.2	1.0
5.8	2.7	1.5
Pan	.0	2.7

OBSERVED FLOW BEHAVIOUR

Velocity (m/s)	Observation (D = 71.0 mm)
1.05	Asymmetric slid particles
1.61	Asymmetric slid particles
2.10	Appears homogeneous
2.63	Appears homogeneous
3.15	Appears homogeneous
3.71	Appears homogeneous

* -425 μm Malvern Particle Size Analyser

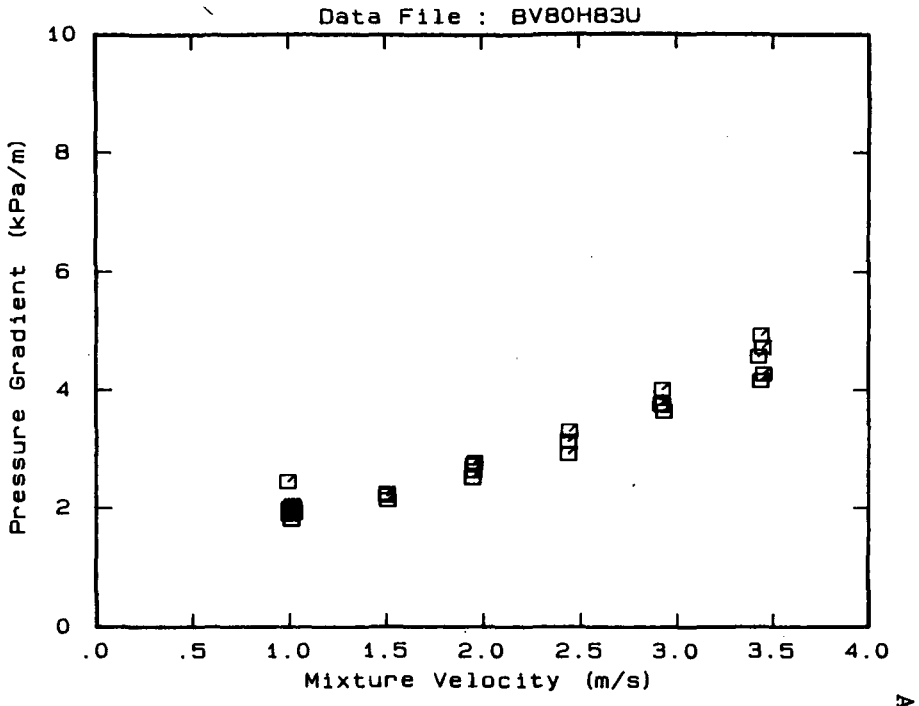

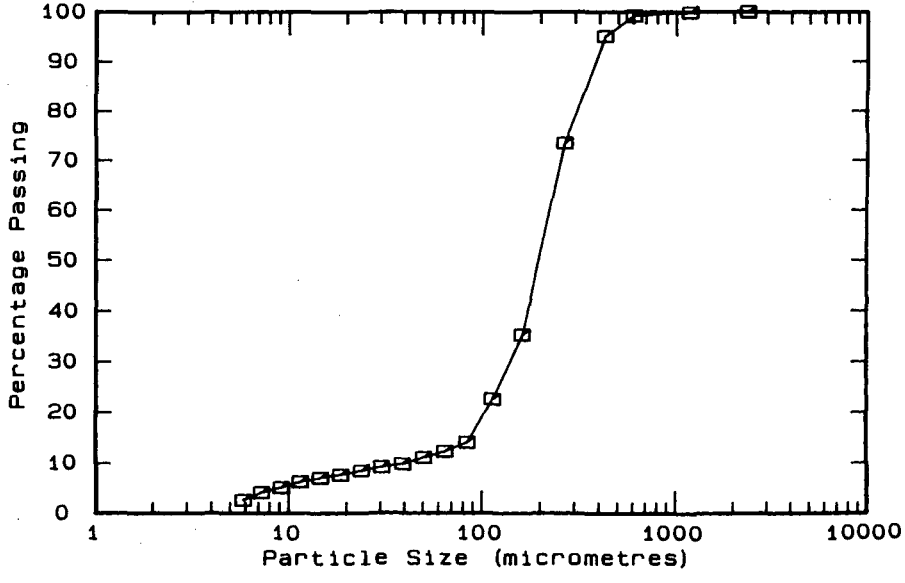

DATA FILE : BV80H86U

Test Facility	UCT 80 mm NB
Test Date	June 1990
Material Description	Blyvooruitsig CCT
Material Relative Density	2.66
Slurry Relative Density	1.86
Solids Volumetric Concentration (%)	51.81
Solids Mass Concentration (%)	74.09
Mean Slurry Temperature (°C)	21.8
Pipe Internal Diameter (mm)	73.40
Pipe Roughness (μm)	87.0
Pipeline Slope	Horizontal

Mixture Velocity (m/s)	Pressure Gradient (kPa/m)	Slurry Temp. (°C)
3.080	5.898	20.4
3.096	6.335	20.6
3.108	6.107	20.6
3.119	5.942	21.0
2.581	5.366	21.4
2.597	5.325	21.5
2.596	5.188	21.6
2.606	5.113	21.7
2.244	4.540	22.0
2.252	4.280	22.0
2.250	4.692	22.1
2.251	4.780	22.1
1.928	3.974	22.2
1.928	3.886	22.2
1.929	3.841	22.3
1.614	3.466	22.3
1.610	3.386	22.3
1.611	3.386	22.3
1.292	2.956	22.2
1.291	2.973	22.2
1.283	2.910	22.2
.967	2.569	22.1
.955	2.556	22.0
.934	2.622	22.0

Particle Size Distribution
Sieve and Malvern Size Analysis *

Size (μm)	% Passing	% Retained
2360.0	100.0	.0
1180.0	99.9	.1
600.0	99.0	.9
425.0	89.7	9.3
261.6	72.5	17.2
160.4	36.3	36.2
112.8	22.9	13.4
84.3	14.4	8.5
64.6	12.2	2.2
50.2	11.0	1.2
39.0	9.7	1.3
30.3	9.0	.7
23.7	8.5	.5
18.5	7.8	.7
14.5	7.2	.6
11.4	6.4	.8
9.1	5.3	1.1
7.2	4.2	1.1
5.8	2.6	1.6
Pan	- .3	2.9

OBSERVED FLOW BEHAVIOUR

Velocity (m/s)	Observation (D = 71.0 mm)
1.02	Appears homogeneous
1.37	Appears homogeneous
1.72	Appears homogeneous
2.07	Appears homogeneous
2.42	Appears homogeneous
2.77	Appears homogeneous
3.36	Appears homogeneous

* -425 μm Malvern Particle Size Analyser

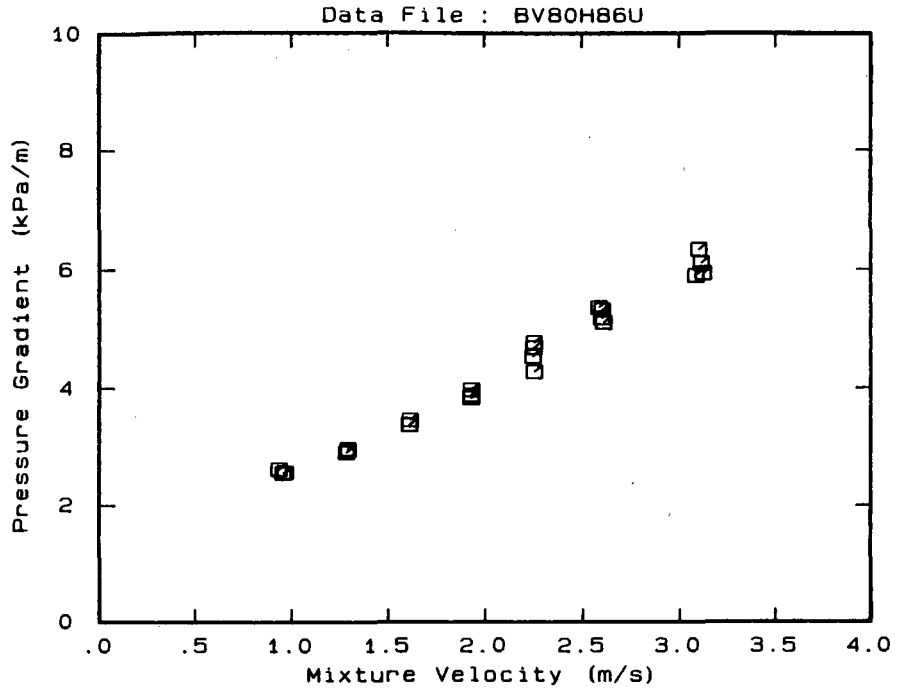

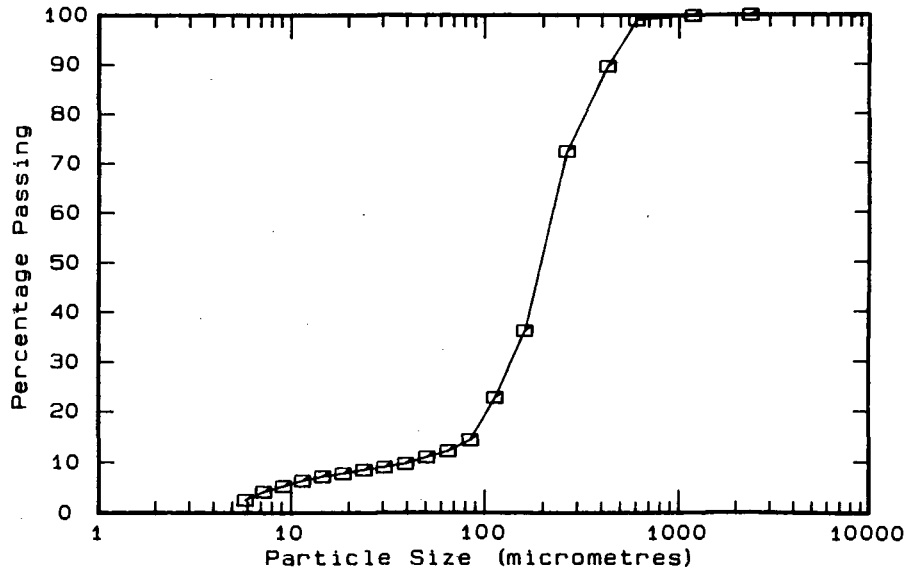

DATA FILE : BV80H89U

Test Facility	UCT 80 mm NB
Test Date	June 1990
Material Description	Blyvooruitsig CCT
Material Relative Density	2.66
Slurry Relative Density	1.89
Solids Volumetric Concentration (%)	53.61
Solids Mass Concentration (%)	75.46
Mean Slurry Temperature (°C)	24.4
Pipe Internal Diameter (mm)	73.40
Pipe Roughness (μm)	87.0
Pipeline Slope	Horizontal

Mixture Velocity (m/s)	Pressure Gradient (kPa/m)	Slurry Temp. (°C)
2.112	8.620	23.1
2.135	8.262	23.4
2.158	8.925	23.6
1.804	6.538	24.3
1.808	7.310	24.4
1.799	7.758	24.5
1.793	6.849	24.5
1.468	4.847	24.7
1.395	5.359	24.8
1.364	5.264	24.9
1.017	4.374	25.0
.965	4.130	25.1
.930	4.174	25.1

Particle Size Distribution
Sieve and Malvern Size Analysis *

Size (μm)	% Passing	% Retained
2360.0	100.0	.0
1180.0	99.9	.1
600.0	99.3	.6
425.0	92.4	6.9
261.6	72.4	20.0
160.4	39.0	33.4
112.8	24.5	14.5
84.3	15.4	9.1
64.6	13.8	1.6
50.2	12.4	1.4
39.0	10.9	1.5
30.3	10.3	.6
23.7	9.7	.6
18.5	9.0	.7
14.5	8.4	.6
11.4	7.5	.9
9.1	6.2	1.3
7.2	5.1	1.1
5.8	3.3	1.8
Pan	- .1	3.4

OBSERVED FLOW BEHAVIOUR

Velocity (m/s)	Observation (D = 71.0 mm)
1.09	Appears homogeneous
1.61	Appears homogeneous
1.96	Appears homogeneous
2.28	Appears homogeneous

* -425 μm Malvern Particle Size Analyser

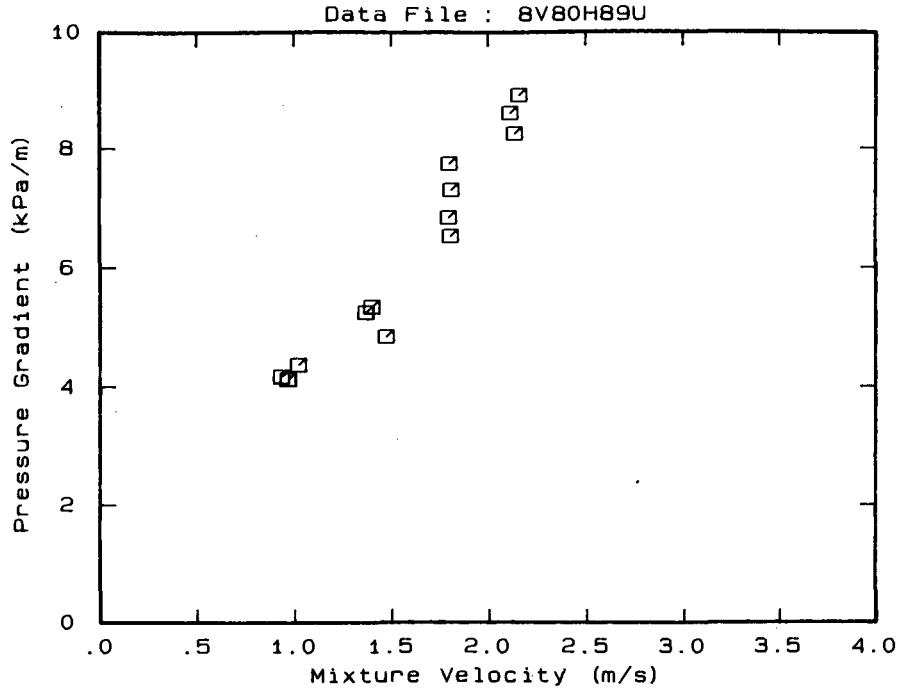

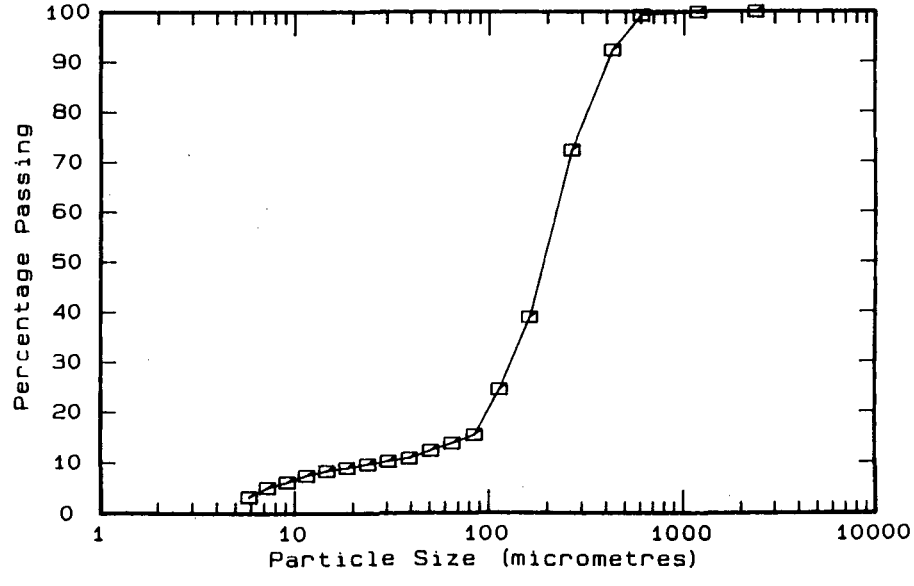

DATA FILE : BV80D52U

Test Facility	UCT 80 mm NB
Test Date	June 1990
Material Description	Blyvooruitsig CCT
Material Relative Density	2.66
Slurry Relative Density	1.52
Solids Volumetric Concentration (%)	31.33
Solids Mass Concentration (%)	54.82
Mean Slurry Temperature (°C)	16.1
Pipe Internal Diameter (mm)	73.40
Pipe Roughness (μm)	84.0
Pipeline Slope	Vertical Down

Mixture Velocity (m/s)	Pressure Gradient (kPa/m)	Slurry Temp. (°C)
3.426	-12.114	15.4
3.419	-12.029	15.4
3.425	-12.181	15.5
3.446	-12.058	15.6
2.953	-12.747	15.8
2.953	-12.595	15.8
2.951	-12.652	15.9
2.958	-12.664	15.9
2.489	-13.227	16.0
2.491	-13.221	16.1
2.484	-13.207	16.1
1.987	-13.809	16.2
1.997	-13.868	16.2
1.988	-13.840	16.2
1.991	-13.734	16.2
1.985	-13.785	16.2
1.988	-13.855	16.2
1.992	-13.823	16.3
1.452	-14.452	16.3
1.455	-14.387	16.3
1.454	-14.434	16.3
1.458	-14.415	16.3
1.469	-14.417	16.3
1.088	-15.061	16.4
1.108	-14.964	16.4
1.115	-14.929	16.4
1.114	-14.959	16.4
1.106	-14.946	16.4
1.117	-14.910	16.4

Particle Size Distribution
Sieve and Malvern Size Analysis *

Size (μm)	% Passing	% Retained
2360.0	100.0	.0
1180.0	99.7	.3
600.0	97.6	2.1
425.0	92.8	4.8
261.6	66.7	26.1
160.4	29.2	37.5
112.8	17.0	12.2
84.3	8.5	8.5
64.6	7.1	1.4
50.2	6.3	.8
39.0	5.0	1.3
30.3	4.6	.4
23.7	4.3	.3
18.5	3.8	.5
14.5	3.5	.3
11.4	3.1	.4
9.1	2.5	.6
7.2	2.0	.5
5.8	1.3	.7
Pan	.0	1.3

OBSERVED FLOW BEHAVIOUR

Velocity (m/s)	Observation (D = .0 mm)

* -425 μm Malvern Particle Size Analyser

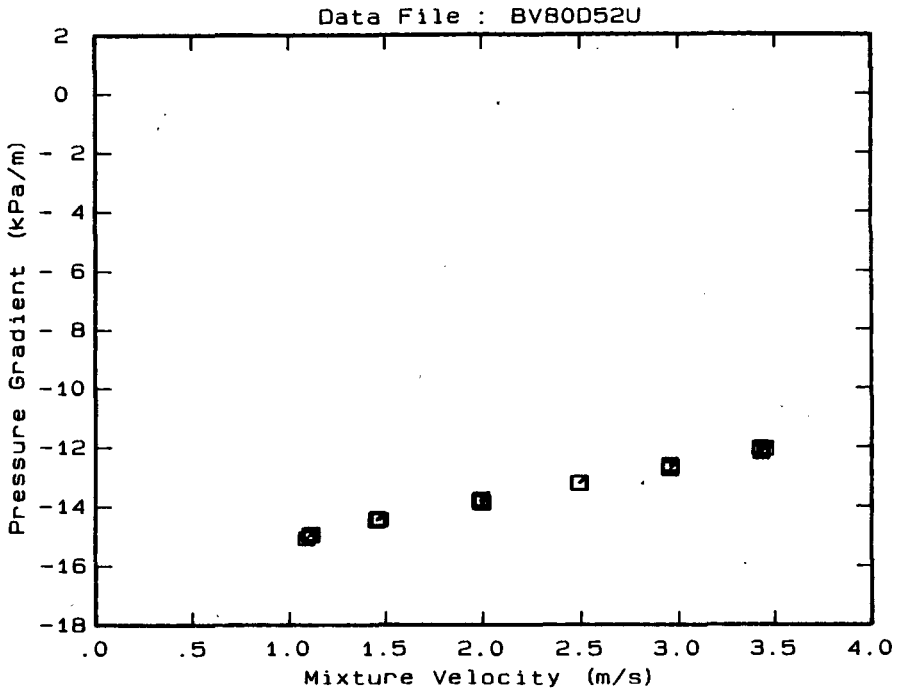

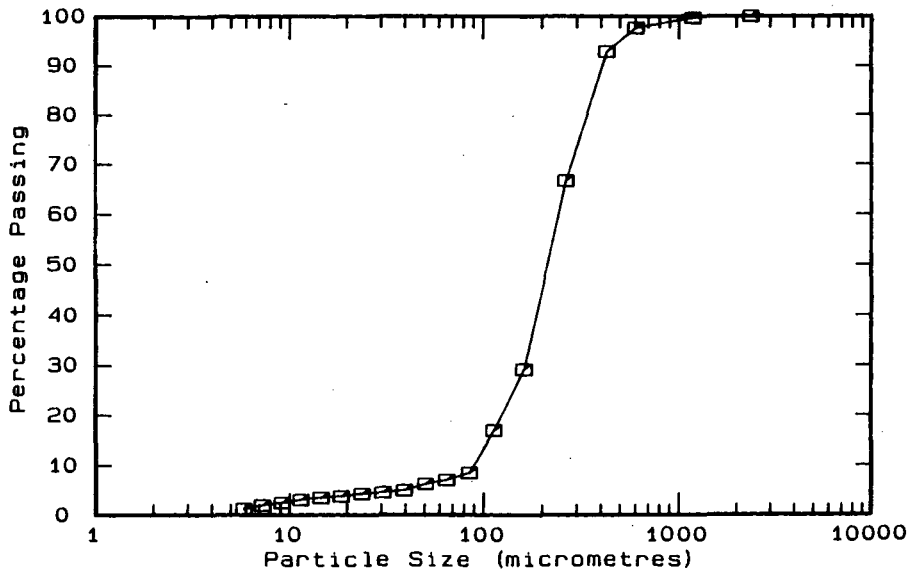

DATA FILE : BV80D60U

Test Facility	UCT 80 mm NB
Test Date	June 1990
Material Description	Blyvooruitsig CCT
Material Relative Density	2.66
Slurry Relative Density	1.60
Solids Volumetric Concentration (%)	36.14
Solids Mass Concentration (%)	60.09
Mean Slurry Temperature (°C)	16.3
Pipe Internal Diameter (mm)	73.40
Pipe Roughness (μm)	84.0
Pipeline Slope	Vertical Down

Mixture Velocity (m/s)	Pressure Gradient (kPa/m)	Slurry Temp. (°C)
3.424	-12.658	15.9
3.431	-12.733	16.0
3.424	-12.523	16.1
3.411	-12.620	16.1
3.414	-12.598	16.2
2.917	-13.368	16.3
2.926	-13.292	16.3
2.927	-13.393	16.3
2.446	-13.975	16.4
2.451	-14.000	16.4
2.451	-13.923	16.4
1.981	-14.515	16.4
1.980	-14.485	16.4
1.973	-14.592	16.4
1.976	-14.607	16.3
1.984	-14.485	16.3
1.476	-15.161	16.3
1.474	-15.092	16.3
1.477	-15.206	16.3
1.474	-15.115	16.3
1.470	-15.211	16.3
1.474	-14.962	16.3
1.024	-15.740	16.2
1.032	-15.563	16.2
1.032	-15.688	16.2
1.030	-15.705	16.2
1.027	-15.609	16.2
1.028	-15.401	16.2
1.024	-15.672	16.2
1.020	-15.600	16.2
1.013	-15.448	16.2
1.016	-15.576	16.2

Particle Size Distribution
Sieve and Malvern Size Analysis *

Size (μm)	% Passing	% Retained
2360.0	100.0	.0
1180.0	99.9	.1
600.0	98.8	1.1
425.0	90.7	8.1
261.6	67.9	22.8
160.4	33.1	34.8
112.8	20.2	12.9
84.3	12.7	7.5
64.6	11.0	1.7
50.2	9.7	1.3
39.0	8.3	1.4
30.3	7.7	.6
23.7	7.2	.5
18.5	6.5	.7
14.5	5.9	.6
11.4	5.2	.7
9.1	4.3	.9
7.2	3.6	.7
5.8	2.4	1.2
Pan	.2	2.2

OBSERVED FLOW BEHAVIOUR

Velocity (m/s)	Observation (D = 71.0 mm)

* -425 μm Malvern Particle Size Analyser

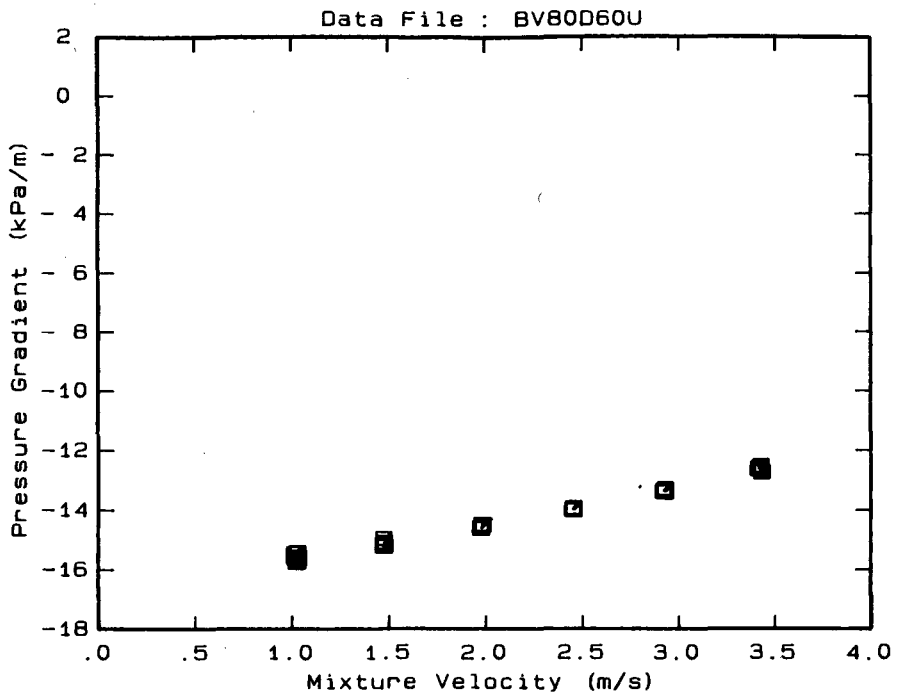

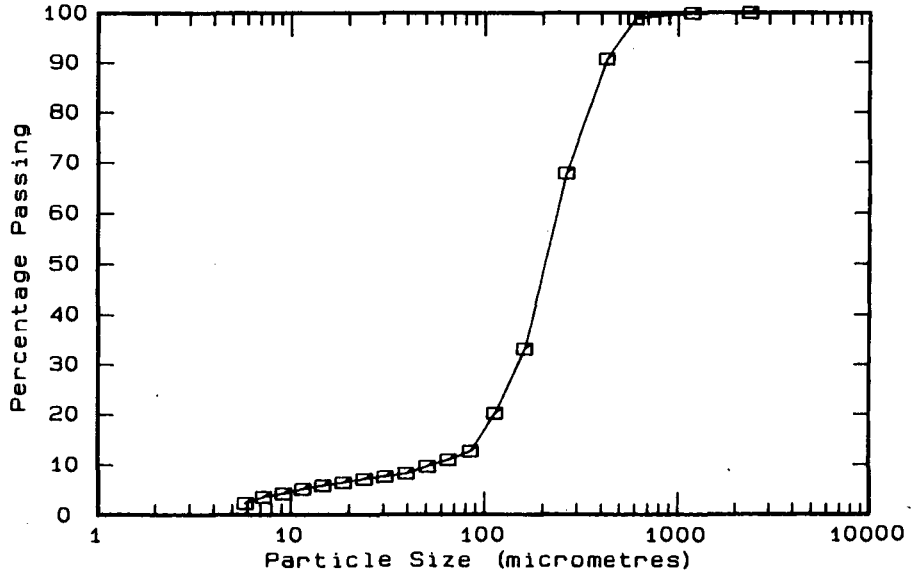

DATA FILE : BV80D70U

Test Facility	UCT 80 mm NB
Test Date	June 1990
Material Description	Blyvooruitsig CCT
Material Relative Density	2.66
Slurry Relative Density	1.70
Solids Volumetric Concentration (%)	42.17
Solids Mass Concentration (%)	65.98
Mean Slurry Temperature (°C)	16.7
Pipe Internal Diameter (mm)	73.40
Pipe Roughness (μm)	84.0
Pipeline Slope	Vertical Down

Mixture Velocity (m/s)	Pressure Gradient (kPa/m)	Slurry Temp. (°C)
3.424	-12.999	16.1
3.414	-13.094	16.2
3.421	-12.954	16.2
3.424	-12.741	16.3
3.419	-13.000	16.4
2.975	-13.665	16.6
2.978	-13.694	16.7
2.978	-13.795	16.7
2.988	-13.727	16.7
2.420	-14.422	16.8
2.426	-14.451	16.8
2.420	-14.393	16.9
1.970	-15.238	16.9
1.971	-15.129	16.9
1.970	-15.156	16.9
1.965	-15.325	16.9
1.964	-15.252	16.9
1.965	-15.244	16.9
1.968	-15.503	16.9
1.966	-15.119	16.9
1.475	-15.771	16.9
1.476	-15.631	16.9
1.474	-15.635	16.9
1.475	-15.417	16.8
1.476	-15.724	16.8
1.477	-15.852	16.8
1.477	-15.912	16.8
1.038	-16.116	16.8
1.058	-15.919	16.8
1.054	-16.013	16.8
1.064	-15.780	16.8

Particle Size Distribution
Sieve and Malvern Size Analysis *

Size (μm)	% Passing	% Retained
2360.0	100.0	.0
1180.0	99.9	.1
600.0	99.0	.9
425.0	93.6	5.4
261.6	74.3	19.3
160.4	33.9	40.4
112.8	21.7	12.2
84.3	12.3	9.4
64.6	10.7	1.6
50.2	9.9	.8
39.0	8.5	1.4
30.3	7.8	.7
23.7	7.3	.5
18.5	6.6	.7
14.5	5.9	.7
11.4	5.2	.7
9.1	4.3	.9
7.2	3.6	.7
5.8	2.3	1.3
Pan	.1	2.2

OBSERVED FLOW BEHAVIOUR

Velocity (m/s)	Observation (D = 71.0 mm)

* -425 μm Malvern Particle Size Analyser

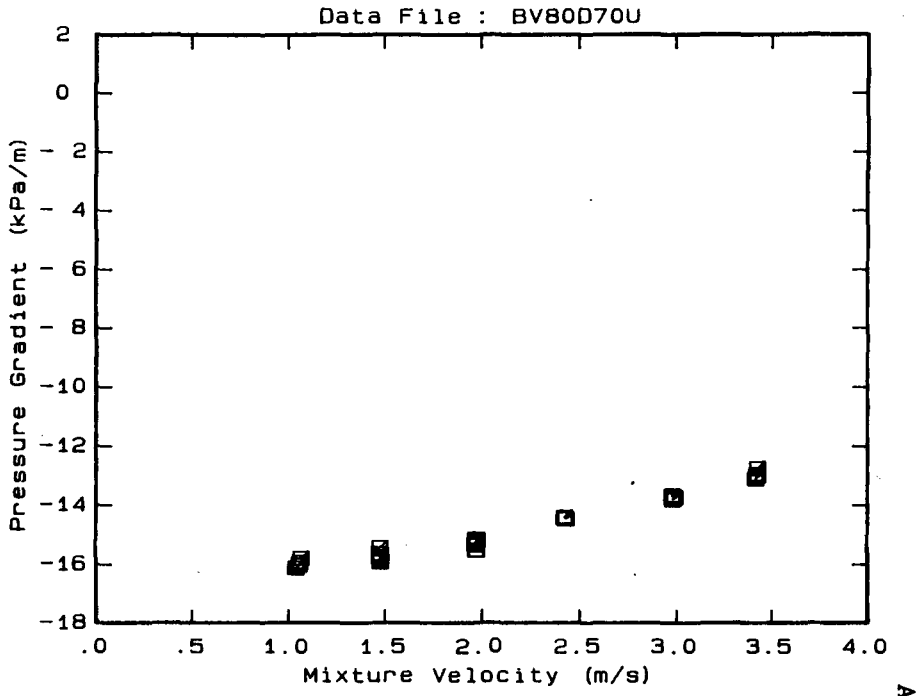

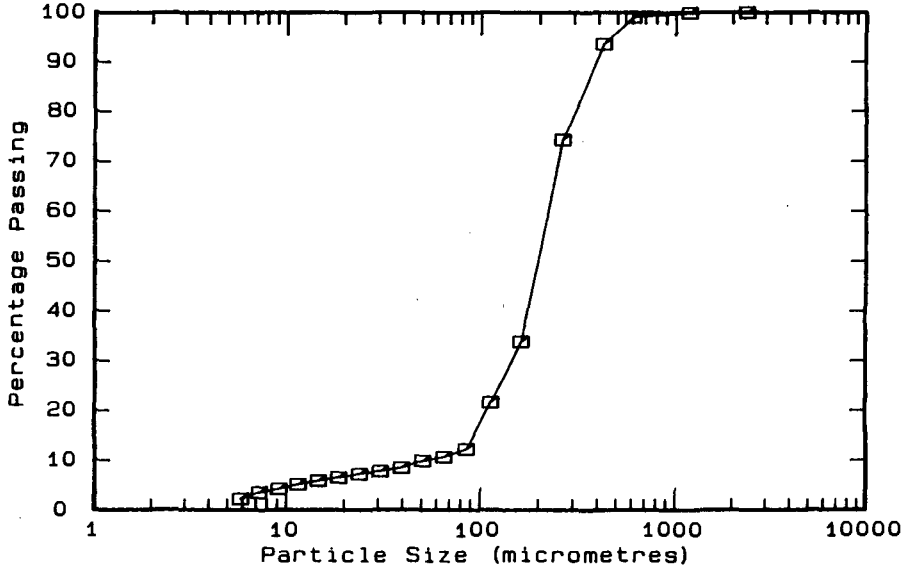

DATA FILE : BV80D75U

Test Facility	UCT 80 mm NB
Test Date	June 1990
Material Description	Blyvooruitsig CCT
Material Relative Density	2.66
Slurry Relative Density	1.75
Solids Volumetric Concentration (%)	45.18
Solids Mass Concentration (%)	68.67
Mean Slurry Temperature (°C)	17.9
Pipe Internal Diameter (mm)	73.40
Pipe Roughness (μm)	84.0
Pipeline Slope	Vertical Down

Mixture Velocity (m/s)	Pressure Gradient (kPa/m)	Slurry Temp. (°C)
3.402	-13.177	17.3
3.403	-13.153	17.4
3.412	-13.166	17.4
3.409	-13.265	17.5
3.412	-13.130	17.6
2.941	-14.085	17.8
2.947	-14.050	17.9
2.945	-13.946	17.9
2.442	-15.092	18.1
2.437	-15.065	18.1
2.451	-15.223	18.1
2.444	-15.053	18.1
1.971	-15.559	18.1
1.975	-15.672	18.1
1.976	-15.633	18.1
1.512	-15.857	18.1
1.538	-15.800	18.1
1.500	-15.914	18.1
1.497	-15.862	18.1
1.499	-15.739	18.1
.996	-15.980	18.0
1.004	-16.077	18.0
1.002	-16.115	18.0
1.006	-16.083	17.9

Particle Size Distribution
Sieve and Malvern Size Analysis *

Size (μm)	% Passing	% Retained
2360.0	100.0	.0
1180.0	99.9	.1
600.0	99.0	.9
425.0	92.3	6.7
261.6	74.0	18.3
160.4	35.3	38.7
112.8	22.2	13.1
84.3	12.8	9.4
64.6	11.0	1.8
50.2	9.9	1.1
39.0	8.5	1.4
30.3	7.9	.6
23.7	7.3	.6
18.5	6.6	.7
14.5	6.1	.5
11.4	5.4	.7
9.1	4.4	1.0
7.2	3.6	.8
5.8	2.3	1.3
Pan	.0	2.3

OBSERVED FLOW BEHAVIOUR

Velocity (m/s)	Observation (D = 71.0 mm)

* -425 μm Malvern Particle Size Analyser

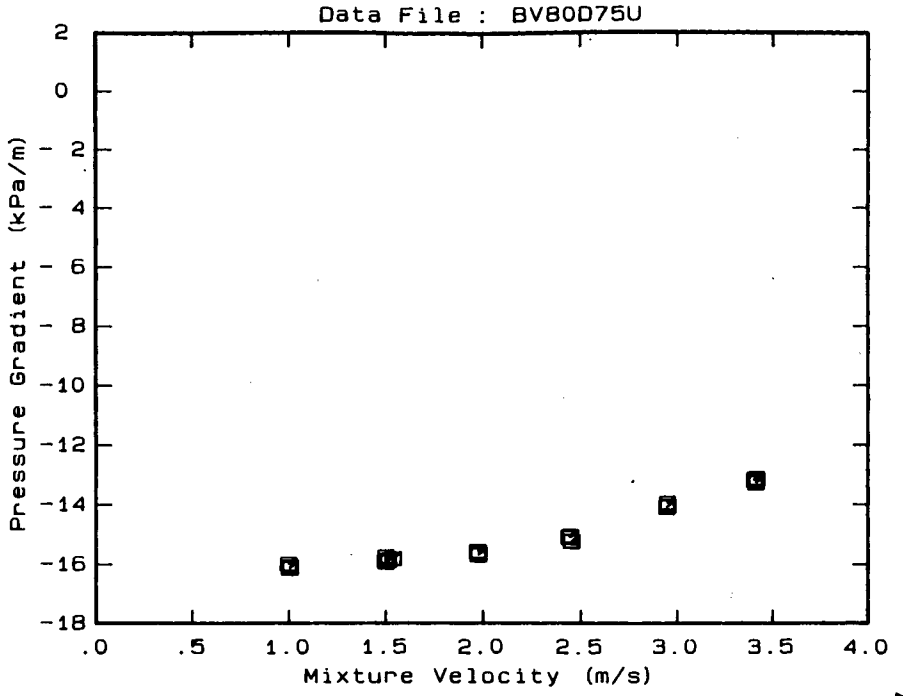

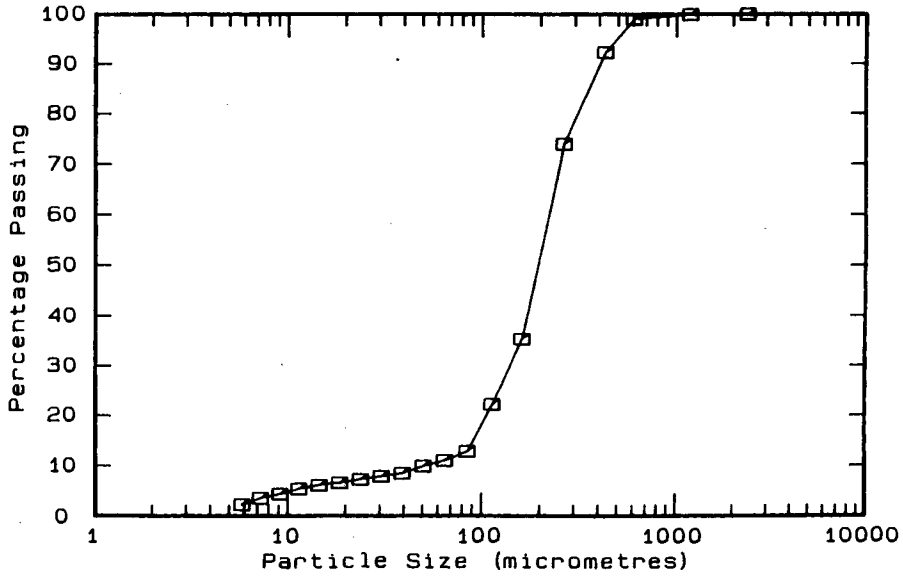

DATA FILE : BV80D79U

Test Facility	UCT 80 mm NB
Test Date	June 1990
Material Description	Blyvooruitsig CCT
Material Relative Density	2.66
Slurry Relative Density	1.79
Solids Volumetric Concentration (%)	47.59
Solids Mass Concentration (%)	70.72
Mean Slurry Temperature (°C)	18.9
Pipe Internal Diameter (mm)	73.40
Pipe Roughness (μm)	84.0
Pipeline Slope	Vertical Down

Mixture Velocity (m/s)	Pressure Gradient (kPa/m)	Slurry Temp. (°C)
3.398	-13.919	18.1
3.398	-13.694	18.3
3.412	-13.814	18.4
3.407	-13.887	18.5
2.952	-14.446	18.7
2.920	-14.452	18.8
2.928	-14.359	18.9
2.949	-14.561	18.9
2.406	-15.049	19.0
2.403	-15.240	19.1
2.411	-15.405	19.1
2.410	-15.320	19.1
2.412	-15.161	19.1
1.935	-15.652	19.1
1.936	-15.618	19.1
1.928	-15.694	19.1
1.538	-16.019	19.1
1.529	-16.001	19.1
1.533	-15.984	19.1
1.537	-15.972	19.0
1.008	-15.706	19.0
1.017	-15.973	19.0
1.021	-15.980	18.9
1.021	-16.019	18.9
1.012	-15.862	18.9
1.023	-15.961	18.9
1.026	-15.981	18.9

Particle Size Distribution
Sieve and Malvern Size Analysis *

Size (μm)	% Passing	% Retained
2360.0	100.0	.0
1180.0	99.9	.1
600.0	99.0	.9
425.0	92.2	6.8
261.6	70.2	22.0
160.4	34.1	36.1
112.8	20.9	13.2
84.3	12.9	8.0
64.6	11.0	1.9
50.2	9.7	1.3
39.0	8.5	1.2
30.3	7.9	.6
23.7	7.3	.6
18.5	6.6	.7
14.5	6.1	.5
11.4	5.5	.6
9.1	4.5	1.0
7.2	3.7	.8
5.8	2.4	1.3
Pan	.1	2.3

OBSERVED FLOW BEHAVIOUR

Velocity (m/s)	Observation (D = 71.0 mm)

* -425 μm Malvern Particle Size Analyser

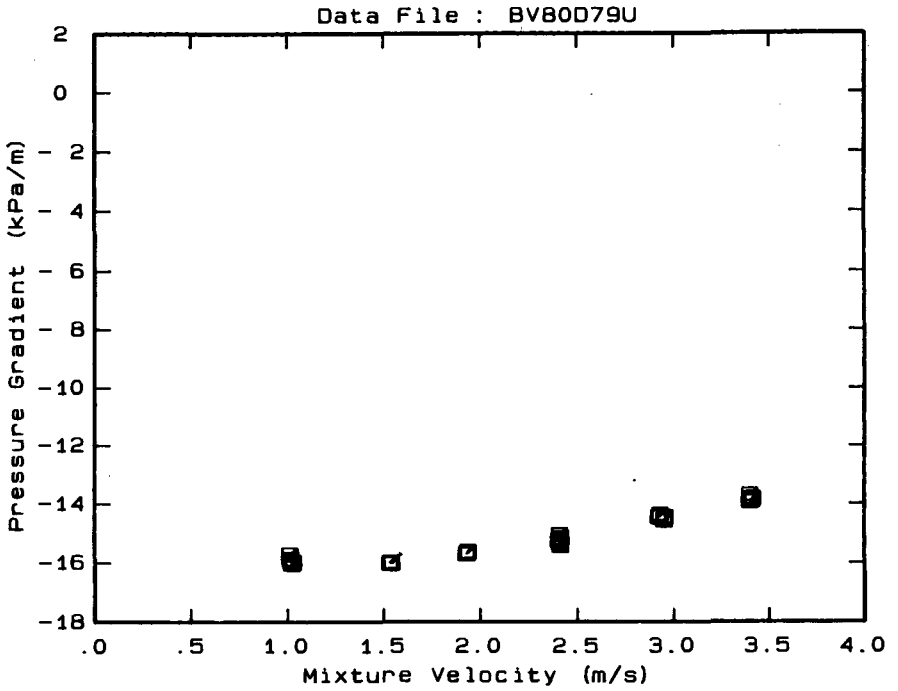

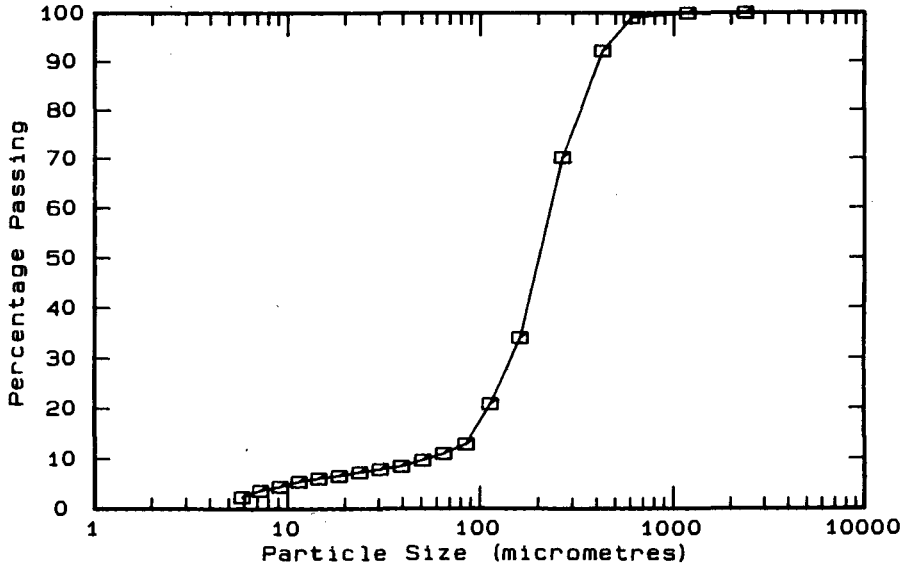

DATA FILE : BV80D83U

Test Facility	UCT 80 mm NB
Test Date	June 1990
Material Description	Blyvooruitsig CCT
Material Relative Density	2.66
Slurry Relative Density	1.83
Solids Volumetric Concentration (%)	50.00
Solids Mass Concentration (%)	72.68
Mean Slurry Temperature (°C)	20.2
Pipe Internal Diameter (mm)	73.40
Pipe Roughness (μm)	84.0
Pipeline Slope	Vertical Down

Mixture Velocity (m/s)	Pressure Gradient (kPa/m)	Slurry Temp. (°C)
3.425	-12.640	18.9
3.435	-12.505	19.1
3.436	-12.534	19.2
3.447	-12.482	19.4
3.451	-12.498	19.5
2.916	-13.642	20.1
2.923	-13.433	20.2
2.925	-13.439	20.2
2.932	-13.526	20.3
2.433	-14.192	20.5
2.437	-14.174	20.5
2.439	-14.204	20.6
1.955	-15.115	20.6
1.948	-14.967	20.6
1.945	-14.996	20.6
1.950	-14.958	20.6
1.503	-15.389	20.6
1.507	-15.316	20.5
1.504	-15.327	20.5
1.008	-15.665	20.4
.991	-15.698	20.3
.997	-15.655	20.3
.998	-16.451	20.3
1.001	-15.804	20.3
1.011	-13.596	20.2
1.020	-13.689	20.2
1.018	-14.280	20.2
1.017	-14.075	20.1
1.011	-13.572	20.1
1.012	-16.932	20.1
1.024	-15.797	20.1

Particle Size Distribution
Sieve and Malvern Size Analysis *

Size (μm)	% Passing	% Retained
2360.0	100.0	.0
1180.0	99.9	.1
600.0	99.2	.7
425.0	95.1	4.1
261.6	73.5	21.6
160.4	35.4	38.1
112.8	22.7	12.7
84.3	14.1	8.6
64.6	12.3	1.8
50.2	11.1	1.2
39.0	9.8	1.3
30.3	9.2	.6
23.7	8.5	.7
18.5	7.7	.8
14.5	7.1	.6
11.4	6.3	.8
9.1	5.2	1.1
7.2	4.2	1.0
5.8	2.7	1.5
Pan	.0	2.7

OBSERVED FLOW BEHAVIOUR

Velocity (m/s)	Observation (D = 71.0 mm)

* -425 μm Malvern Particle Size Analyser

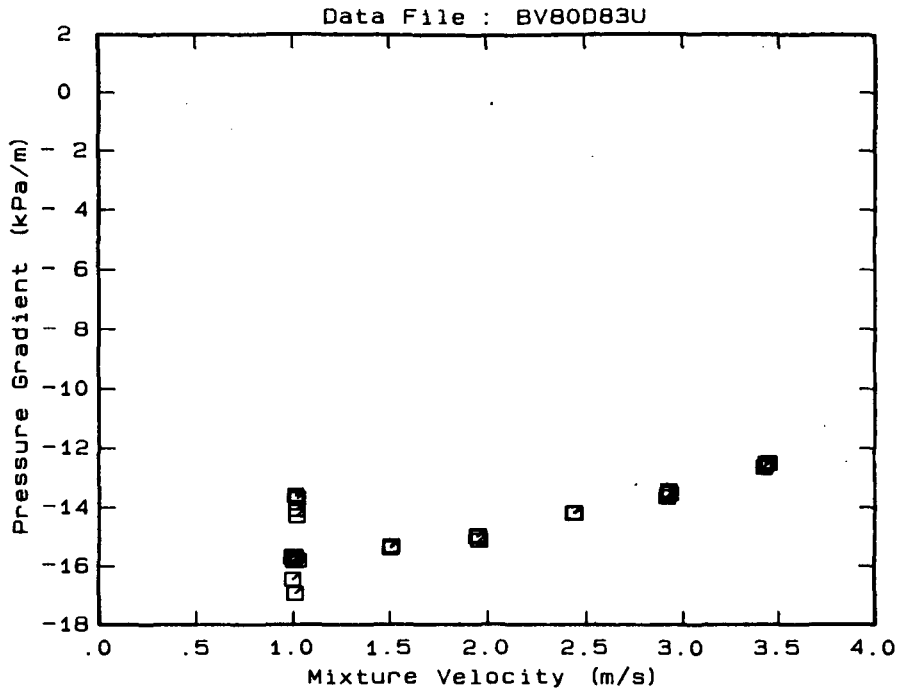

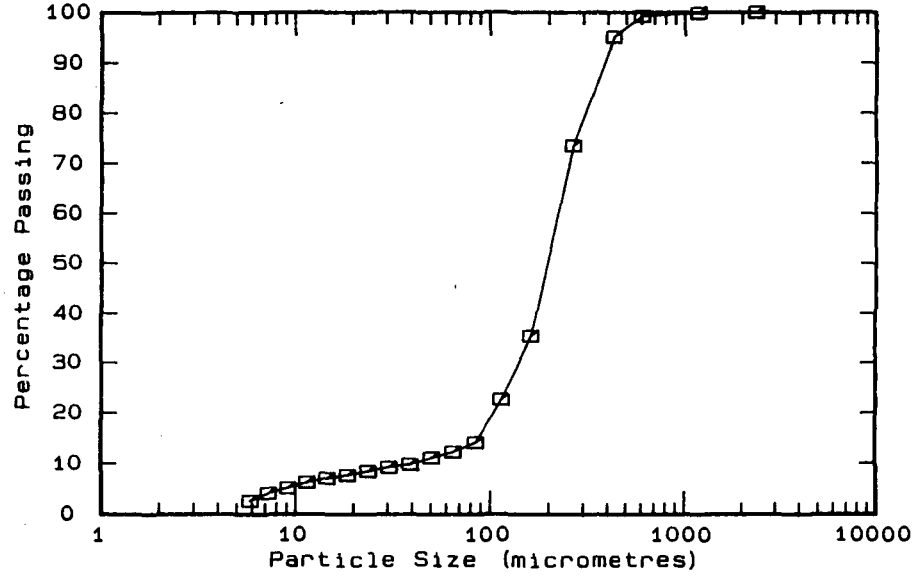

DATA FILE : BV80D86U

Test Facility	UCT 80 mm NB
Test Date	June 1990
Material Description	Blyvooruitsig CCT
Material Relative Density	2.66
Slurry Relative Density	1.86
Solids Volumetric Concentration (%)	51.81
Solids Mass Concentration (%)	74.09
Mean Slurry Temperature (°C)	21.8
Pipe Internal Diameter (mm)	73.40
Pipe Roughness (μm)	84.0
Pipeline Slope	Vertical Down

Mixture Velocity (m/s)	Pressure Gradient (kPa/m)	Slurry Temp. (°C)
3.080	-10.386	20.4
3.096	-10.555	20.6
3.108	-10.495	20.6
3.119	-10.535	21.0
2.581	-11.931	21.4
2.597	-11.445	21.5
2.596	-11.847	21.6
2.606	-11.454	21.7
2.244	-12.513	22.0
2.252	-12.400	22.0
2.250	-12.605	22.1
2.251	-12.539	22.1
1.928	-13.381	22.2
1.928	-13.234	22.2
1.929	-13.180	22.3
1.614	-14.159	22.3
1.610	-14.099	22.3
1.611	-14.157	22.3
1.292	-14.693	22.2
1.291	-14.721	22.2
1.283	-14.775	22.2
.967	-15.261	22.1
.955	-15.341	22.0
.934	-15.270	22.0

Particle Size Distribution
Sieve and Malvern Size Analysis *

Size (μm)	% Passing	% Retained
2360.0	100.0	.0
1180.0	99.9	.1
600.0	99.0	.9
425.0	89.7	9.3
261.6	72.5	17.2
160.4	36.3	36.2
112.8	22.9	13.4
84.3	14.4	8.5
64.6	12.2	2.2
50.2	11.0	1.2
39.0	9.7	1.3
30.3	9.0	.7
23.7	8.5	.5
18.5	7.8	.7
14.5	7.2	.6
11.4	6.4	.8
9.1	5.3	1.1
7.2	4.2	1.1
5.8	2.6	1.6
Pan	- .3	2.9

OBSERVED FLOW BEHAVIOUR

Velocity (m/s)	Observation (D = 71.0 mm)

* -425 μm Malvern Particle Size Analyser

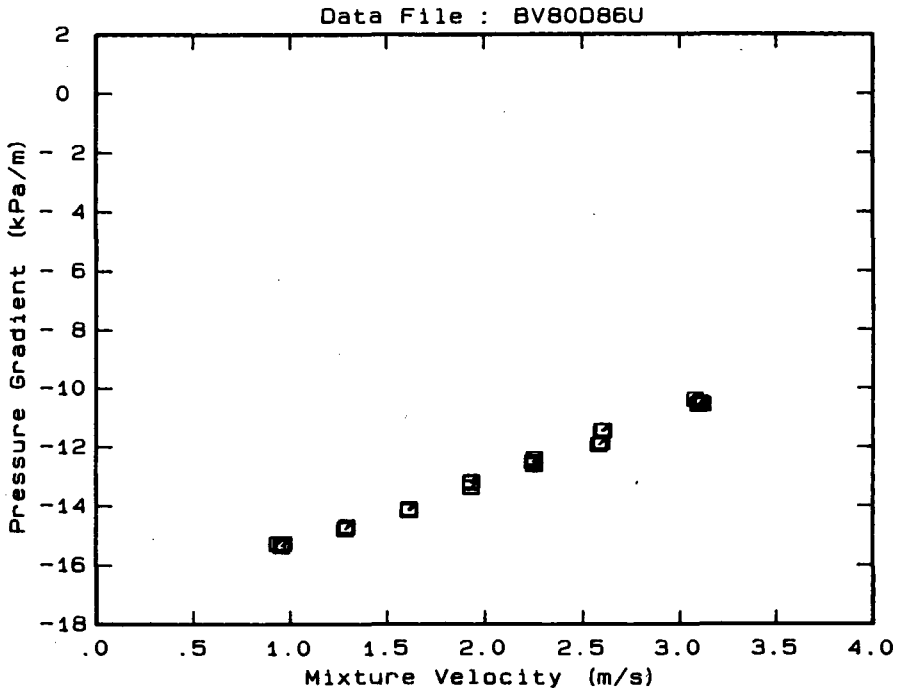

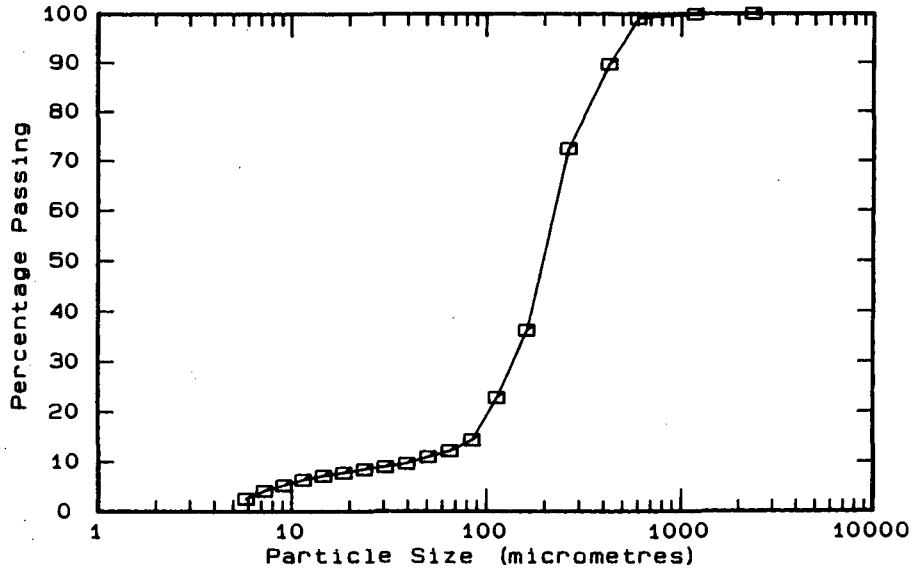

DATA FILE : BV80D89U

Test Facility	UCT 80 mm NB
Test Date	June 1990
Material Description	Blyvooruitsig CCT
Material Relative Density	2.66
Slurry Relative Density	1.89
Solids Volumetric Concentration (%)	53.61
Solids Mass Concentration (%)	75.46
Mean Slurry Temperature (°C)	24.4
Pipe Internal Diameter (mm)	73.40
Pipe Roughness (μm)	84.0
Pipeline Slope	Vertical Down

Mixture Velocity (m/s)	Pressure Gradient (kPa/m)	Slurry Temp. (°C)
2.112	- 8.644	23.1
2.135	- 8.667	23.4
2.158	- 8.636	23.6
1.804	-10.901	24.3
1.808	-10.630	24.4
1.799	-10.832	24.5
1.793	-10.791	24.5
1.468	-12.419	24.7
1.395	-12.615	24.8
1.364	-12.589	24.9
1.017	-13.751	25.0
.965	-13.752	25.1
.930	-13.644	25.1

Particle Size Distribution
Sieve and Malvern Size Analysis *

Size (μm)	% Passing	% Retained
2360.0	100.0	.0
1180.0	99.9	.1
600.0	99.3	.6
425.0	92.4	6.9
261.6	72.4	20.0
160.4	39.0	33.4
112.8	24.5	14.5
84.3	15.4	9.1
64.6	13.8	1.6
50.2	12.4	1.4
39.0	10.9	1.5
30.3	10.3	.6
23.7	9.7	.6
18.5	9.0	.7
14.5	8.4	.6
11.4	7.5	.9
9.1	6.2	1.3
7.2	5.1	1.1
5.8	3.3	1.8
Pan	- .1	3.4

* -425 μm Malvern Particle Size Analyser

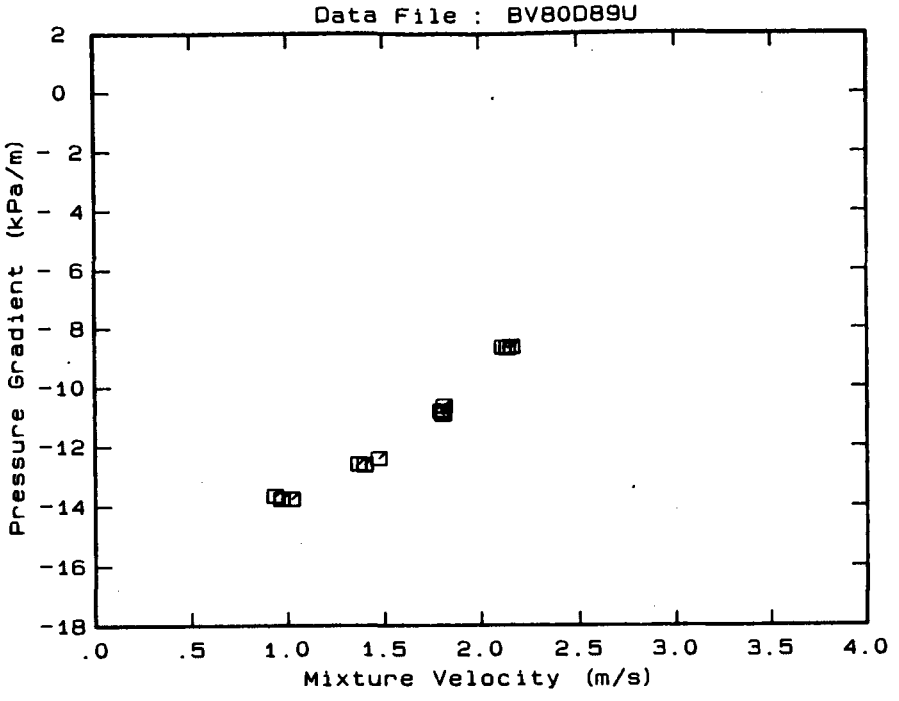

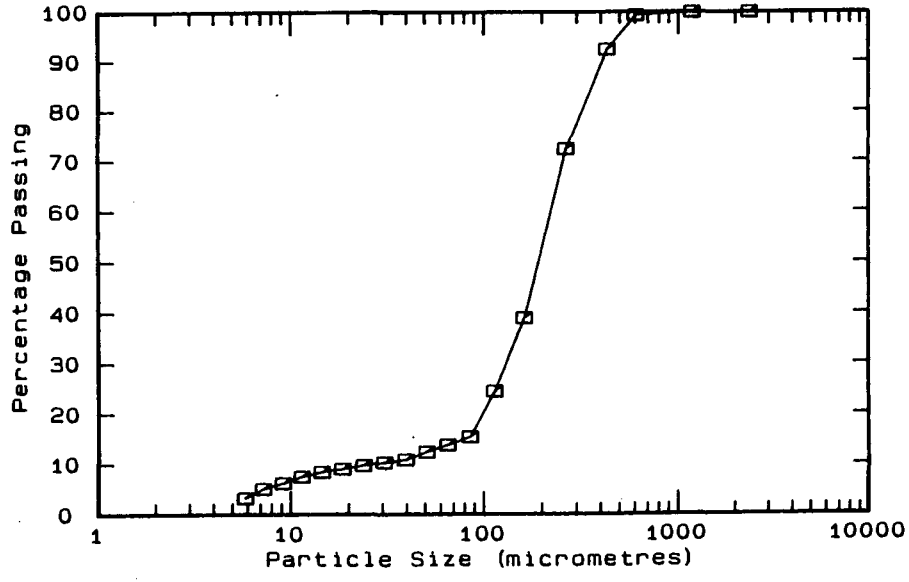

DATA FILE : ED25H55U

Test Facility	UCT 25 mm NB
Test Date	June 1990
Material Description	East Driefontein CCT
Material Relative Density	2.65
Slurry Relative Density	1.55
Solids Volumetric Concentration (%)	33.33
Solids Mass Concentration (%)	56.99
Mean Slurry Temperature (°C)	18.1
Pipe Internal Diameter (mm)	26.60
Pipe Roughness (μm)	21.0
Pipeline Slope	Horizontal

Mixture Velocity (m/s)	Pressure Gradient (kPa/m)	Slurry Temp. (°C)
2.483	4.458	16.1
2.448	4.340	17.4
2.462	4.356	17.4
2.464	4.387	17.4
3.063	6.095	17.6
3.068	6.140	17.6
3.079	6.148	17.7
3.455	7.331	17.9
3.451	7.307	17.9
3.319	6.879	17.9
3.265	6.694	18.0
3.375	7.051	18.0
3.951	9.061	18.2
3.937	9.012	18.2
3.944	8.958	18.3
1.555	2.138	18.5
1.557	2.145	18.5
1.544	2.125	18.5
1.879	2.764	18.4
1.875	2.780	18.4
1.901	2.804	18.4
2.199	3.454	18.4
2.200	3.520	18.4
2.193	3.542	18.4
2.542	4.420	18.4
2.545	4.452	18.4
2.548	4.388	18.4
2.866	5.286	18.4
2.864	5.299	18.4
2.871	5.292	18.4

Particle Size Distribution
Malvern Particle Size Analyser

Size (μm)	% Passing	% Retained
564.0	100.0	.0
261.6	94.4	5.6
160.4	55.5	38.9
112.8	23.3	32.2
84.3	12.6	10.7
64.6	9.4	3.2
50.2	6.2	3.2
39.0	4.8	1.4
30.3	4.4	.4
23.7	4.0	.4
18.5	3.6	.4
14.5	3.3	.3
11.4	3.0	.3
9.1	2.5	.5
7.2	2.0	.5
5.8	1.3	.7
Pan	- .0	1.3

OBSERVED FLOW BEHAVIOUR

Velocity (m/s)	Observation (D = .0 mm)

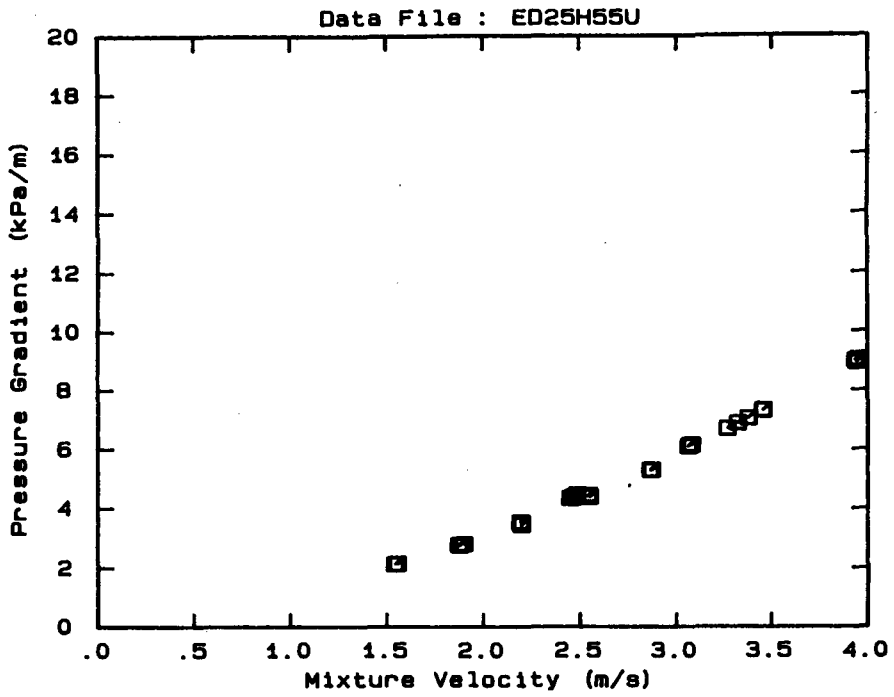

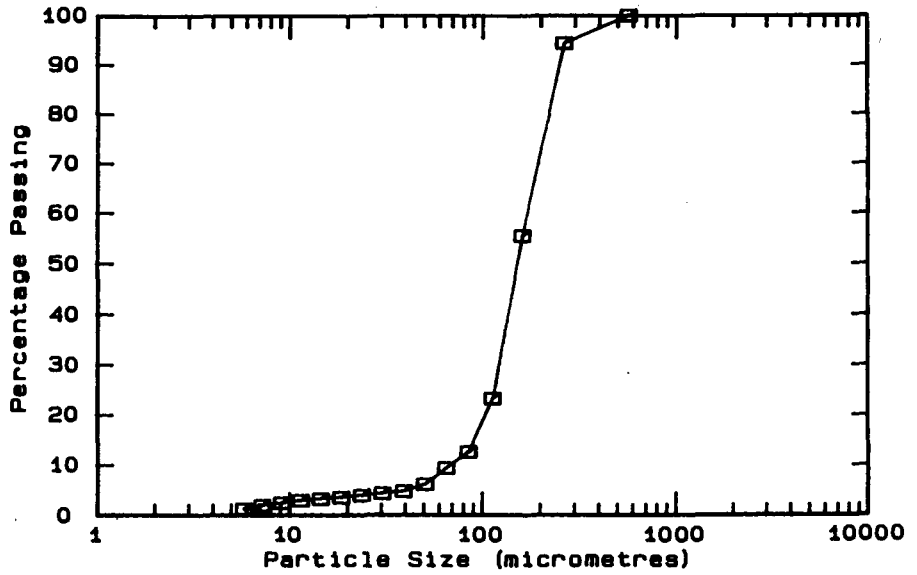

DATA FILE : ED25H66U

Test Facility	UCT 25 mm NB
Test Date	June 1990
Material Description	East Driefontein CCT
Material Relative Density	2.65
Slurry Relative Density	1.66
Solids Volumetric Concentration (%)	40.00
Solids Mass Concentration (%)	63.86
Mean Slurry Temperature (°C)	18.6
Pipe Internal Diameter (mm)	26.60
Pipe Roughness (μm)	21.0
Pipeline Slope	Horizontal

Mixture Velocity (m/s)	Pressure Gradient (kPa/m)	Slurry Temp. (°C)
2.743	4.546	18.0
2.721	4.571	18.0
2.705	4.610	18.1
3.016	5.172	18.2
3.022	5.242	18.2
3.013	5.327	18.3
3.177	5.796	18.4
3.182	5.702	18.4
3.194	5.934	18.5
3.344	6.726	18.7
3.354	6.743	18.8
3.374	6.864	18.8
1.139	2.260	18.8
1.152	2.275	18.8
1.161	2.265	18.8
1.496	2.416	18.8
1.501	2.427	18.8
1.502	2.441	18.8
1.786	2.722	18.8
1.784	2.764	18.8
1.784	2.803	18.8
2.096	3.374	18.7
2.095	3.368	18.7
2.092	3.391	18.7
2.398	3.831	18.7
2.391	3.815	18.7
2.397	3.823	18.7
2.453	3.891	18.7
2.448	3.864	18.7
2.446	3.875	18.7
2.778	4.525	18.7
2.772	4.555	18.7
2.774	4.643	18.7

Particle Size Distribution
Malvern Particle Size Analyser

Size (μm)	% Passing	% Retained
564.0	100.0	.0
261.6	91.9	8.1
160.4	55.2	36.7
112.8	25.8	29.4
84.3	13.5	12.3
64.6	10.0	3.5
50.2	6.9	3.1
39.0	5.8	1.1
30.3	5.3	.5
23.7	4.7	.6
18.5	4.4	.3
14.5	4.1	.3
11.4	3.6	.5
9.1	3.1	.5
7.2	2.6	.5
5.8	1.7	.9
Pan	.0	1.7

OBSERVED FLOW BEHAVIOUR

Velocity (m/s)	Observation (D = .0 mm)

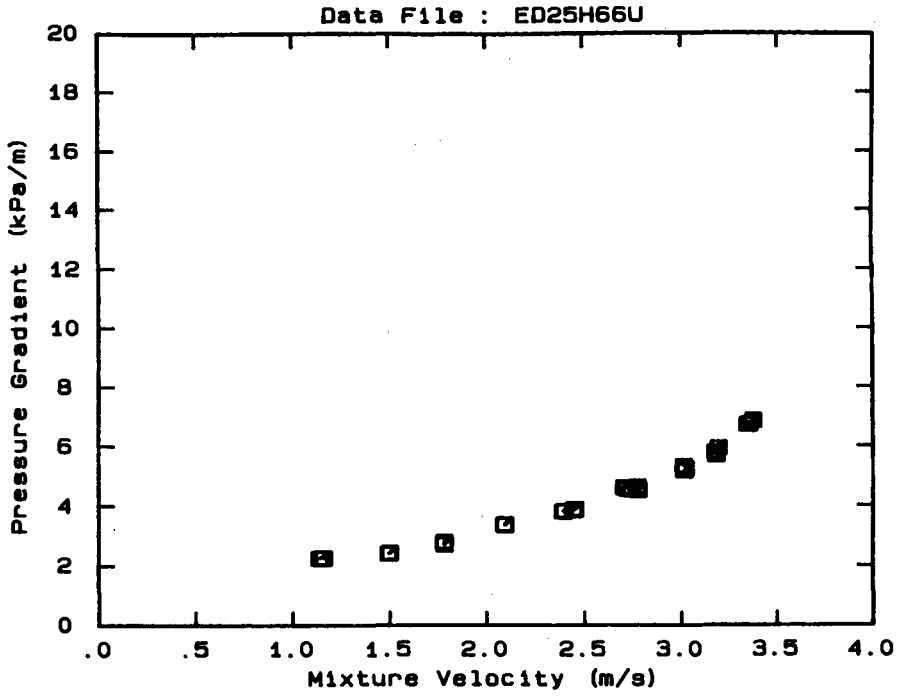

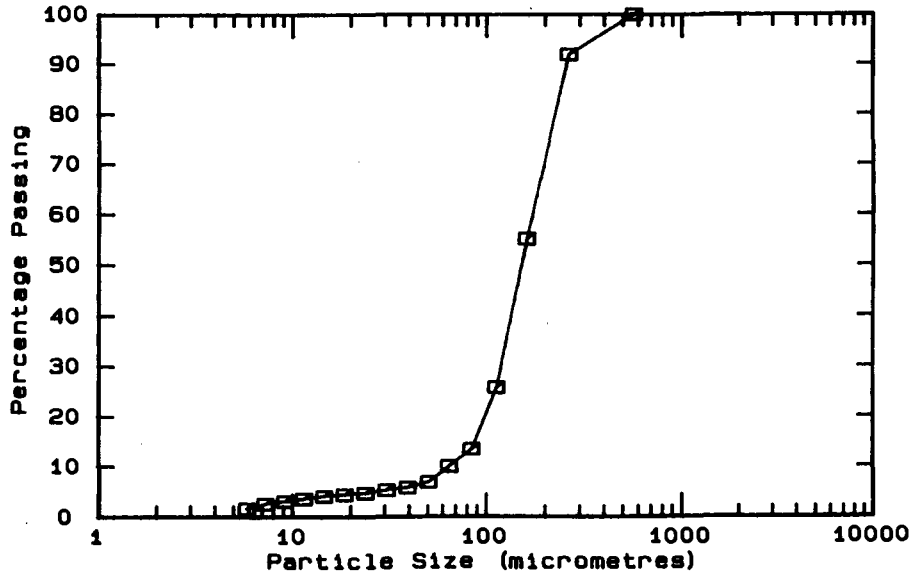

DATA FILE : ED25H69U

Test Facility	UCT 25 mm NB
Test Date	June 1990
Material Description	East Driefontein CCT
Material Relative Density	2.65
Slurry Relative Density	1.69
Solids Volumetric Concentration (%)	41.82
Solids Mass Concentration (%)	65.57
Mean Slurry Temperature (°C)	19.0
Pipe Internal Diameter (mm)	26.60
Pipe Roughness (μm)	21.0
Pipeline Slope	Horizontal

Mixture Velocity (m/s)	Pressure Gradient (kPa/m)	Slurry Temp. (°C)
3.744	7.628	17.7
3.737	7.507	17.9
3.763	7.562	18.0
3.787	7.709	18.1
3.807	7.664	18.2
3.361	6.685	18.5
3.336	6.724	18.5
3.336	6.719	18.6
2.984	6.067	19.0
2.962	5.964	19.0
2.976	5.912	19.0
2.507	4.845	19.2
2.503	4.777	19.2
2.505	4.893	19.3
2.520	4.816	19.3
2.528	4.949	19.3
2.086	4.030	19.4
2.081	4.090	19.4
2.077	4.266	19.5
2.077	4.162	19.5
1.664	3.212	19.6
1.663	3.219	19.6
1.660	3.319	19.5
1.232	2.674	19.5
1.212	2.604	19.5
1.208	2.631	19.5
1.208	2.680	19.5

Particle Size Distribution
Malvern Particle Size Analyser

Size (μm)	% Passing	% Retained
564.0	100.0	.0
261.6	93.6	6.4
160.4	58.1	35.5
112.8	27.6	30.5
84.3	15.2	12.4
64.6	12.1	3.1
50.2	8.7	3.4
39.0	7.2	1.5
30.3	6.8	.4
23.7	6.3	.5
18.5	5.6	.7
14.5	5.2	.4
11.4	4.7	.5
9.1	3.9	.8
7.2	3.2	.7
5.8	2.0	1.2
Pan	- .1	2.1

OBSERVED FLOW BEHAVIOUR

Velocity (m/s)	Observation (D = .0 mm)

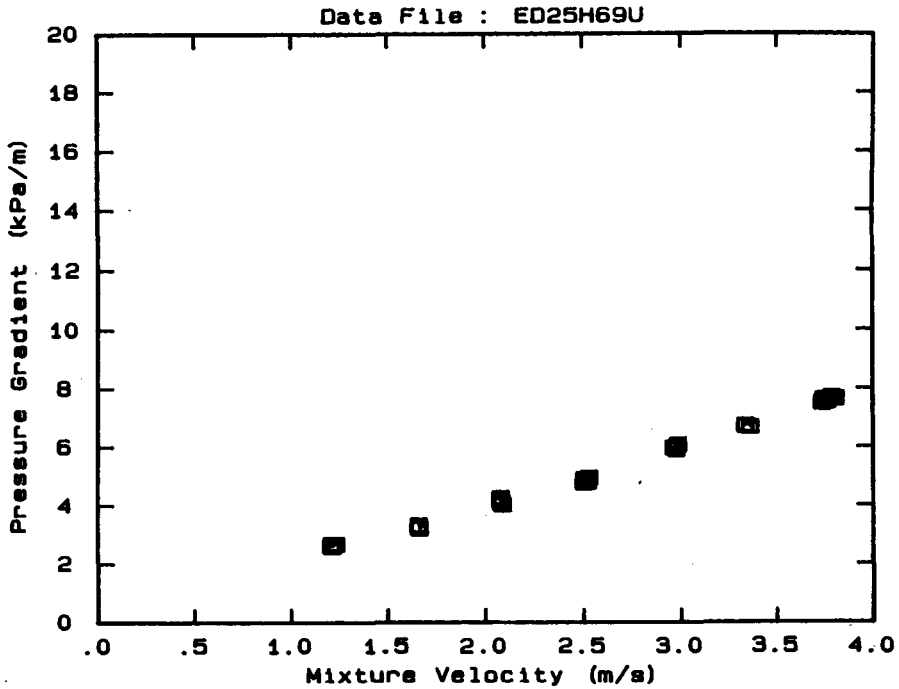

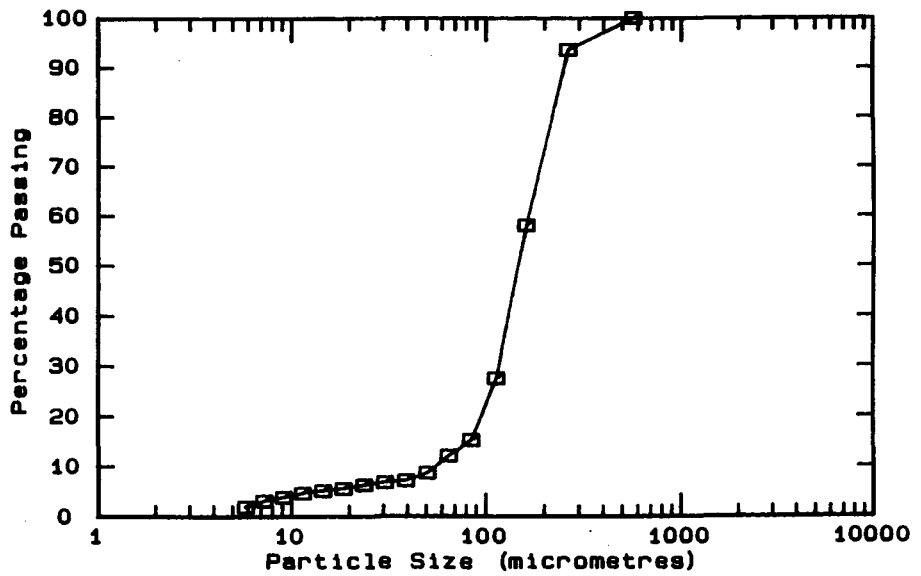

DATA FILE : ED25H75U

Test Facility	UCT 25 mm NB
Test Date	June 1990
Material Description	East Driefontein CCT
Material Relative Density	2.65
Slurry Relative Density	1.75
Solids Volumetric Concentration (%)	45.45
Solids Mass Concentration (%)	68.83
Mean Slurry Temperature (°C)	24.2
Pipe Internal Diameter (mm)	26.60
Pipe Roughness (μm)	21.0
Pipeline Slope	Horizontal

Mixture Velocity (m/s)	Pressure Gradient (kPa/m)	Slurry Temp. (°C)
3.321	9.061	23.4
3.323	8.792	23.4
3.336	9.019	23.5
3.337	9.031	23.5
2.931	7.847	23.8
2.919	7.853	23.9
2.923	7.879	24.0
2.930	7.928	24.0
2.523	6.551	24.3
2.520	6.606	24.3
2.521	6.462	24.4
2.066	5.330	24.5
2.072	5.396	24.5
2.080	5.225	24.6
2.091	5.357	24.6
1.679	4.189	24.6
1.655	4.180	24.7
1.639	4.224	24.7
1.352	3.540	24.7
1.345	3.600	24.7
1.354	3.614	24.7

Particle Size Distribution
Malvern Particle Size Analyser

Size (μm)	% Passing	% Retained
564.0	100.0	.0
261.6	92.2	7.8
160.4	55.4	36.8
112.8	28.7	26.7
84.3	16.9	11.8
64.6	14.8	2.1
50.2	11.4	3.4
39.0	9.7	1.7
30.3	9.4	.3
23.7	8.8	.6
18.5	7.9	.9
14.5	7.4	.5
11.4	6.7	.7
9.1	5.7	1.0
7.2	4.7	1.0
5.8	3.0	1.7
Pan	- .1	3.1

OBSERVED FLOW BEHAVIOUR

Velocity (m/s)	Observation (D = .0 mm)

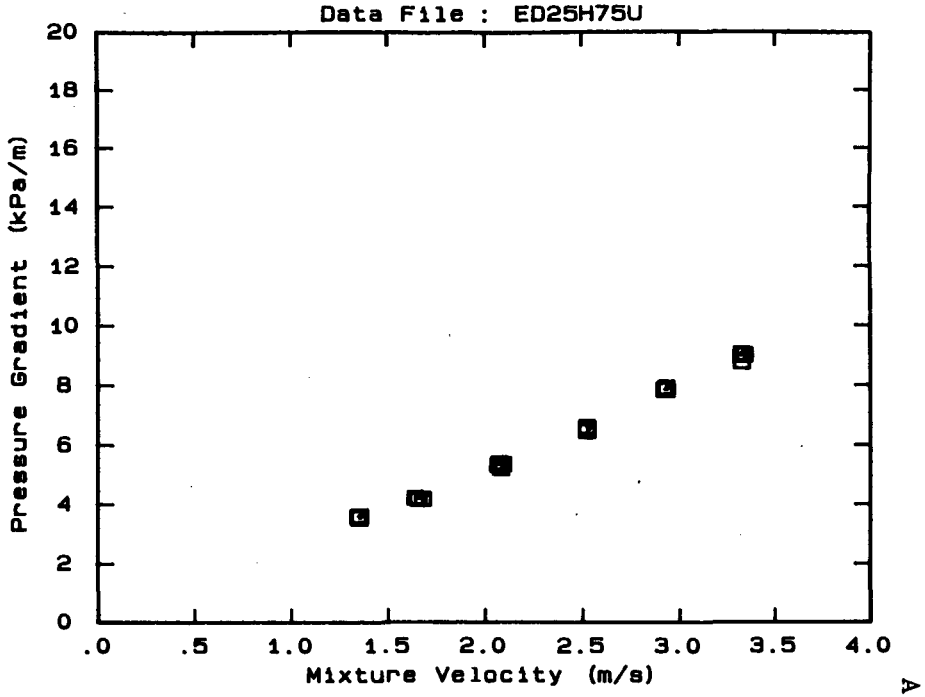

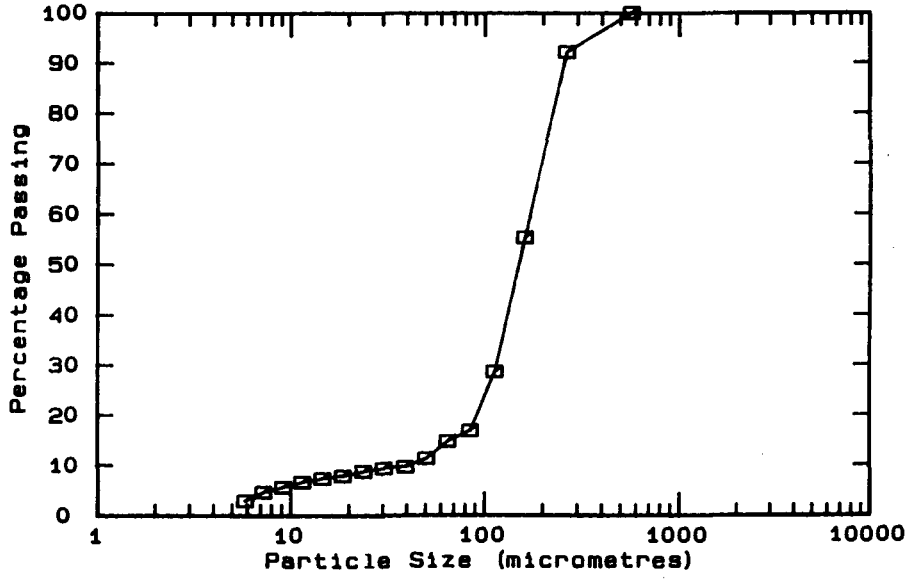

DATA FILE : ED25H79U

Test Facility	UCT 25 mm NB
Test Date	June 1990
Material Description	East Driefontein CCT
Material Relative Density	2.65
Slurry Relative Density	1.79
Solids Volumetric Concentration (%)	47.88
Solids Mass Concentration (%)	70.88
Mean Slurry Temperature (°C)	24.6
Pipe Internal Diameter (mm)	26.60
Pipe Roughness (μm)	21.0
Pipeline Slope	Horizontal

Mixture Velocity (m/s)	Pressure Gradient (kPa/m)	Slurry Temp. (°C)
2.950	14.064	24.4
2.952	13.753	24.4
2.966	13.626	24.4
2.978	13.332	24.4
2.547	11.472	24.4
2.549	10.996	24.4
2.544	11.270	24.4
2.091	8.742	24.6
2.099	8.823	24.6
2.113	8.833	24.6
2.123	8.546	24.6
1.615	6.985	24.7
1.605	6.944	24.7
1.591	7.074	24.8
1.612	6.917	24.8
1.353	6.236	24.8
1.316	6.452	24.8
1.303	6.360	24.8
1.298	6.623	24.8

Particle Size Distribution
Malvern Particle Size Analyser

Size (μm)	% Passing	% Retained
564.0	100.0	.0
261.6	93.0	7.0
160.4	57.0	36.0
112.8	29.0	28.0
84.3	18.4	10.6
64.6	15.5	2.9
50.2	12.1	3.4
39.0	10.6	1.5
30.3	10.2	.4
23.7	9.6	.6
18.5	8.8	.8
14.5	8.2	.6
11.4	7.5	.7
9.1	6.4	1.1
7.2	5.4	1.0
5.8	3.5	1.9
Pan	.0	3.5

OBSERVED FLOW BEHAVIOUR

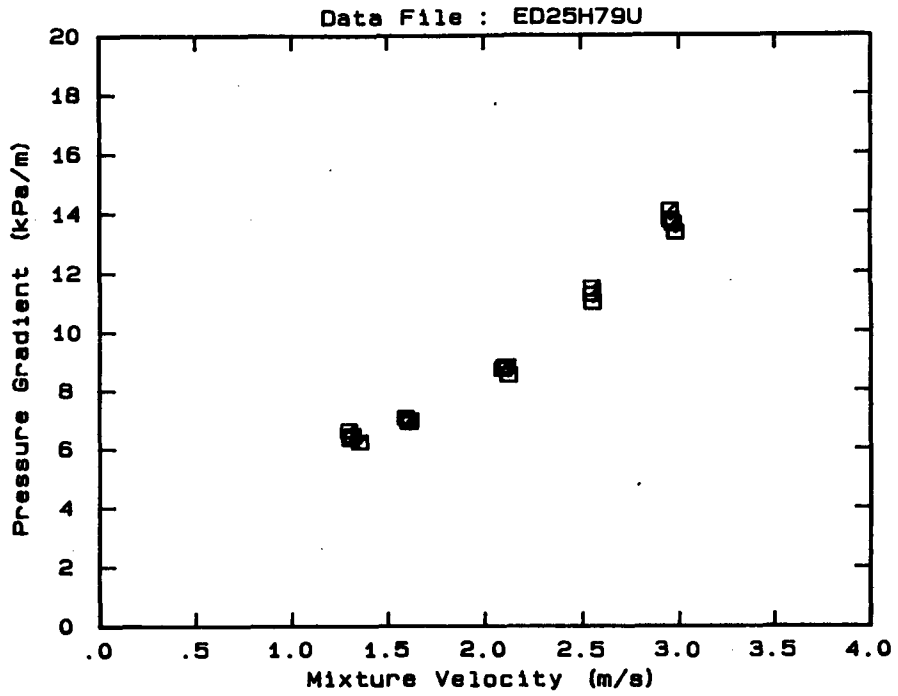

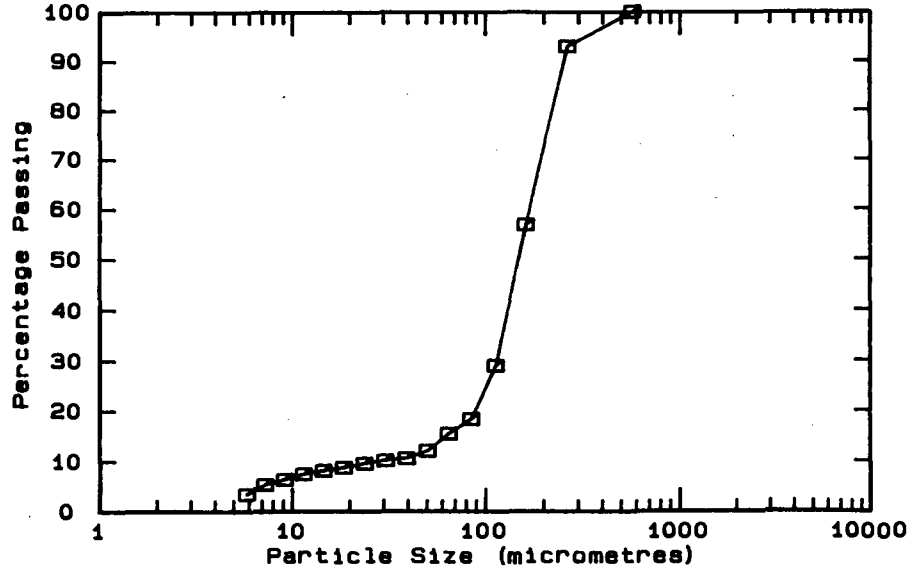

DATA FILE : ED25D55U

Test Facility	UCT 25 mm NB
Test Date	June 1990
Material Description	East Driefontein CCT
Material Relative Density	2.65
Slurry Relative Density	1.55
Solids Volumetric Concentration (%)	33.33
Solids Mass Concentration (%)	56.99
Mean Slurry Temperature (°C)	18.1
Pipe Internal Diameter (mm)	26.60
Pipe Roughness (μm)	21.0
Pipeline Slope	Vertical Down

Mixture Velocity (m/s)	Pressure Gradient (kPa/m)	Slurry Temp. (°C)
2.483	-10.675	16.1
2.448	-10.711	17.4
2.462	-10.673	17.4
2.464	-10.704	17.4
3.063	- 8.850	17.6
3.068	- 8.711	17.6
3.079	- 8.748	17.7
3.455	- 7.251	17.9
3.451	- 7.363	17.9
3.319	- 7.875	17.9
3.265	- 8.054	18.0
3.375	- 7.709	18.0
3.951	- 5.331	18.2
3.937	- 5.415	18.2
3.944	- 5.409	18.3
1.555	-13.240	18.5
1.557	-13.187	18.5
1.544	-13.222	18.5
1.879	-12.336	18.4
1.875	-12.314	18.4
1.901	-12.291	18.4
2.199	-11.357	18.4
2.200	-11.365	18.4
2.193	-11.382	18.4
2.542	-10.400	18.4
2.545	-10.390	18.4
2.548	-10.429	18.4
2.866	- 9.631	18.4
2.864	- 9.686	18.4
2.871	- 9.597	18.4

Particle Size Distribution
Malvern Particle Size Analyser

Size (μm)	% Passing	% Retained
564.0	100.0	.0
261.6	94.4	5.6
160.4	55.5	38.9
112.8	23.3	32.2
84.3	12.6	10.7
64.6	9.4	3.2
50.2	6.2	3.2
39.0	4.8	1.4
30.3	4.4	.4
23.7	4.0	.4
18.5	3.6	.4
14.5	3.3	.3
11.4	3.0	.3
9.1	2.5	.5
7.2	2.0	.5
5.8	1.3	.7
Pan	- .0	1.3

OBSERVED FLOW BEHAVIOUR

Velocity (m/s)	Observation (D = .0 mm)

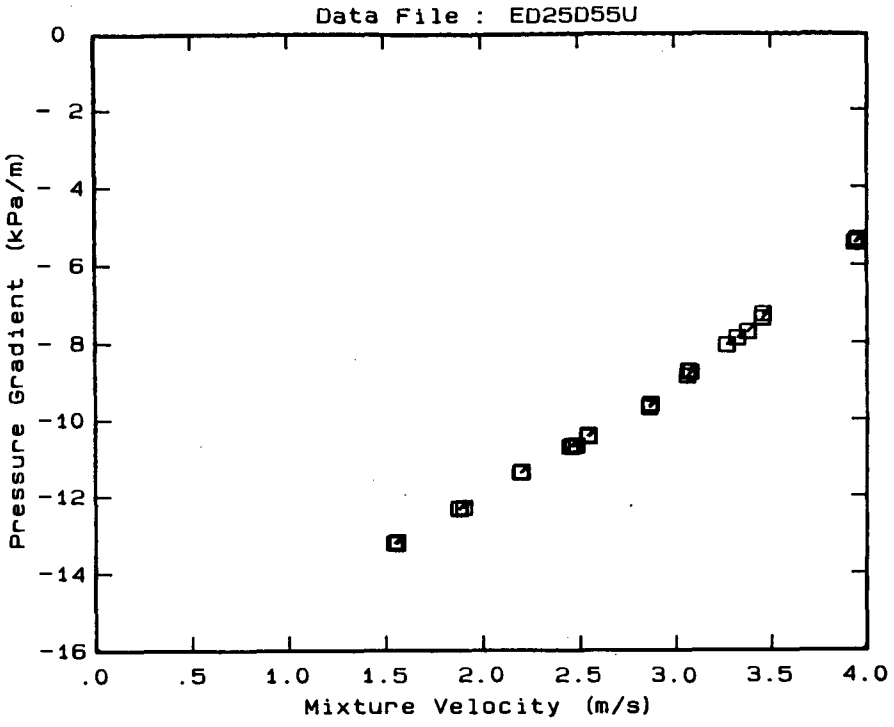

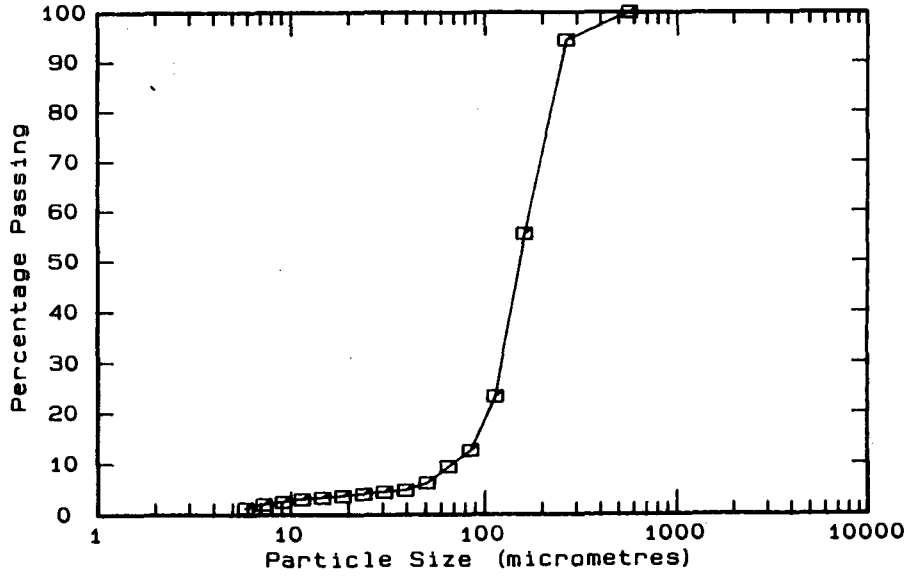

DATA FILE : ED25D66U

Test Facility	UCT 25 mm NB
Test Date	June 1990
Material Description	East Driefontein CCT
Material Relative Density	2.65
Slurry Relative Density	1.66
Solids Volumetric Concentration (%)	40.00
Solids Mass Concentration (%)	63.86
Mean Slurry Temperature (°C)	18.7
Pipe Internal Diameter (mm)	26.60
Pipe Roughness (μm)	21.0
Pipeline Slope	Vertical Down

Mixture Velocity (m/s)	Pressure Gradient (kPa/m)	Slurry Temp. (°C)
3.016	- 9.682	18.2
3.022	- 9.730	18.2
3.013	- 9.685	18.3
3.177	- 9.269	18.4
3.182	- 9.235	18.4
3.194	- 9.237	18.5
3.344	- 8.705	18.7
3.354	- 8.804	18.8
3.374	- 8.843	18.8
1.139	-14.415	18.8
1.152	-14.404	18.8
1.161	-14.385	18.8
1.496	-13.692	18.8
1.501	-13.708	18.8
1.502	-13.716	18.8
1.786	-13.022	18.8
1.784	-13.040	18.8
1.784	-13.054	18.8
2.096	-12.292	18.7
2.095	-12.270	18.7
2.092	-12.282	18.7
2.398	-11.292	18.7
2.391	-11.288	18.7
2.397	-11.288	18.7
2.453	-11.107	18.7
2.448	-11.097	18.7
2.446	-11.104	18.7
2.778	-10.364	18.7
2.772	-10.412	18.7
2.774	-10.400	18.7

Particle Size Distribution
Malvern Particle Size Analyser

Size (μm)	% Passing	% Retained
564.0	100.0	.0
261.6	91.9	8.1
160.4	55.2	36.7
112.8	25.8	29.4
84.3	13.5	12.3
64.6	10.0	3.5
50.2	6.9	3.1
39.0	5.8	1.1
30.3	5.3	.5
23.7	4.7	.6
18.5	4.4	.3
14.5	4.1	.3
11.4	3.6	.5
9.1	3.1	.5
7.2	2.6	.5
5.8	1.7	.9
Pan	.0	1.7

OBSERVED FLOW BEHAVIOUR

Velocity (m/s)	Observation (D = .0 mm)

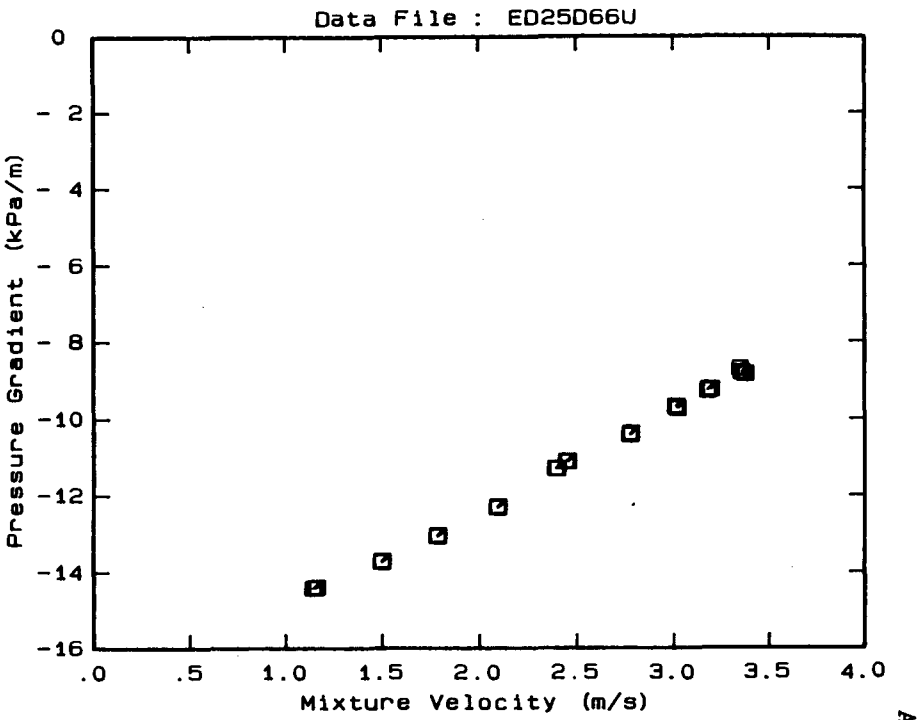

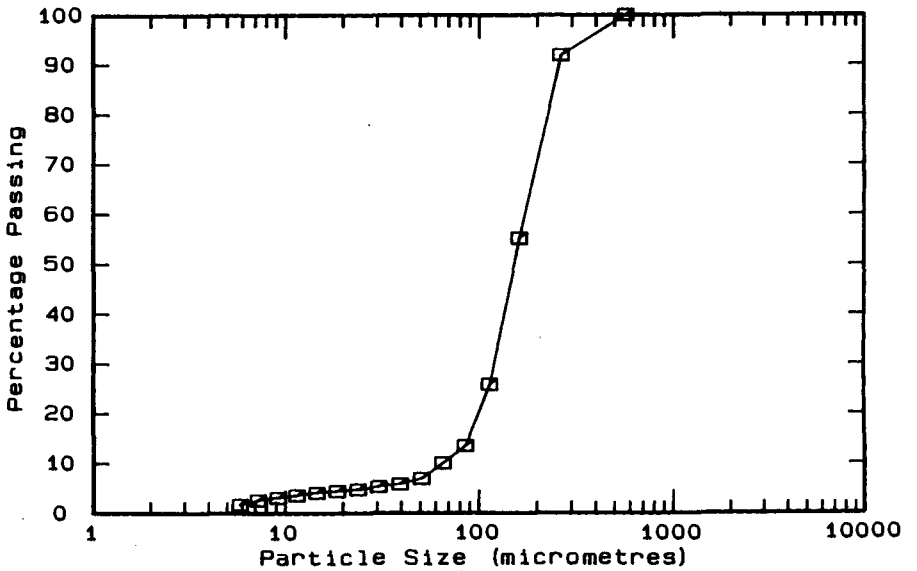

DATA FILE : ED25D69U

Test Facility	UCT 25 mm NB
Test Date	June 1990
Material Description	East Driefontein CCT
Material Relative Density	2.65
Slurry Relative Density	1.69
Solids Volumetric Concentration (%)	41.82
Solids Mass Concentration (%)	65.57
Mean Slurry Temperature (°C)	19.0
Pipe Internal Diameter (mm)	26.60
Pipe Roughness (μm)	21.0
Pipeline Slope	Vertical Down

Mixture Velocity (m/s)	Pressure Gradient (kPa/m)	Slurry Temp. (°C)
3.744	- 5.925	17.7
3.737	- 5.821	17.9
3.763	- 6.385	18.0
3.787	- 6.130	18.1
3.807	- 5.975	18.2
3.361	- 7.551	18.5
3.336	- 7.497	18.5
3.336	- 7.474	18.6
2.984	- 9.082	19.0
2.962	- 8.865	19.0
2.976	- 8.904	19.0
2.507	-10.263	19.2
2.503	-10.473	19.2
2.505	-10.262	19.3
2.520	-10.421	19.3
2.528	-10.294	19.3
2.086	-11.647	19.4
2.081	-11.786	19.4
2.077	-11.725	19.5
2.077	-11.657	19.5
1.664	-12.815	19.6
1.663	-12.788	19.6
1.660	-12.799	19.5
1.232	-13.973	19.5
1.212	-13.929	19.5
1.208	-13.945	19.5
1.208	-13.811	19.5

Particle Size Distribution
Malvern Particle Size Analyser

Size (μm)	% Passing	% Retained
564.0	100.0	.0
261.6	93.6	6.4
160.4	58.1	35.5
112.8	27.6	30.5
84.3	15.2	12.4
64.6	12.1	3.1
50.2	8.7	3.4
39.0	7.2	1.5
30.3	6.8	.4
23.7	6.3	.5
18.5	5.6	.7
14.5	5.2	.4
11.4	4.7	.5
9.1	3.9	.8
7.2	3.2	.7
5.8	2.0	1.2
Pan	- .1	2.1

OBSERVED FLOW BEHAVIOUR

Velocity (m/s)	Observation (D = .0 mm)

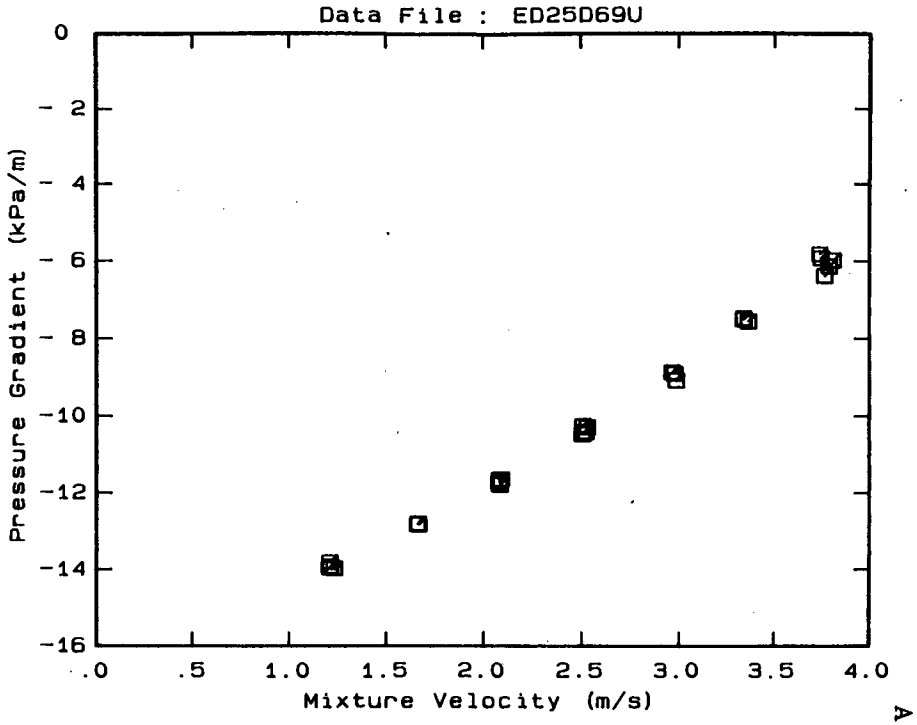

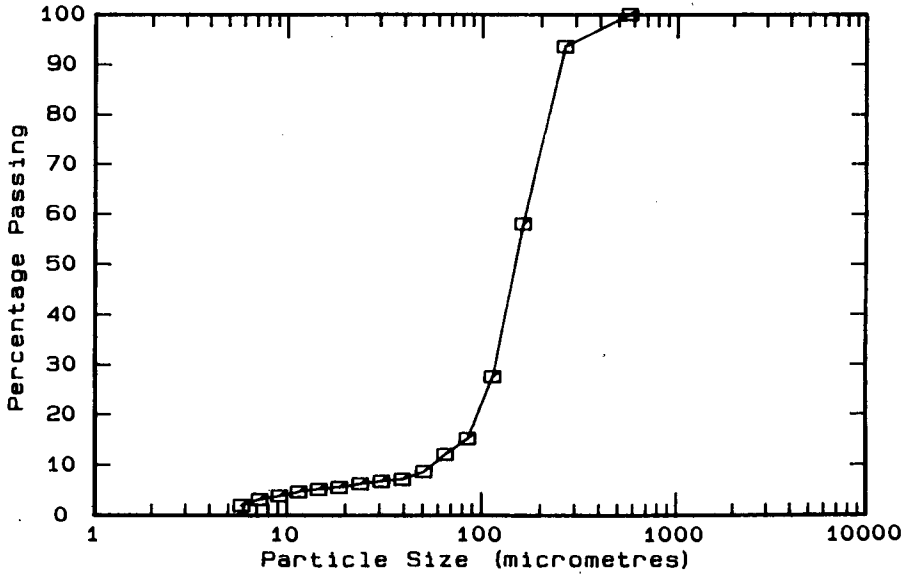

DATA FILE : ED25D75U

Test Facility	UCT 25 mm NB
Test Date	June 1990
Material Description	East Driefontein CCT
Material Relative Density	2.65
Slurry Relative Density	1.75
Solids Volumetric Concentration (%)	45.45
Solids Mass Concentration (%)	68.83
Mean Slurry Temperature (°C)	24.2
Pipe Internal Diameter (mm)	26.60
Pipe Roughness (μm)	21.0
Pipeline Slope	Vertical Down

Mixture Velocity (m/s)	Pressure Gradient (kPa/m)	Slurry Temp. (°C)
3.321	- 6.641	23.4
3.323	- 6.522	23.4
3.336	- 6.391	23.5
3.337	- 6.471	23.5
2.931	- 8.230	23.8
2.919	- 8.174	23.9
2.923	- 8.097	24.0
2.930	- 7.952	24.0
2.523	- 9.675	24.3
2.520	- 9.655	24.3
2.521	- 9.712	24.4
2.066	-10.978	24.5
2.072	-11.102	24.5
2.080	-11.154	24.6
2.091	-11.128	24.6
1.679	-12.328	24.6
1.655	-12.443	24.7
1.639	-12.190	24.7
1.352	-13.134	24.7
1.345	-13.065	24.7
1.354	-13.174	24.7

Particle Size Distribution
Malvern Particle Size Analyser

Size (μm)	% Passing	% Retained
564.0	100.0	.0
261.6	92.2	7.8
160.4	55.4	36.8
112.8	28.7	26.7
84.3	16.9	11.8
64.6	14.8	2.1
50.2	11.4	3.4
39.0	9.7	1.7
30.3	9.4	.3
23.7	8.8	.6
18.5	7.9	.9
14.5	7.4	.5
11.4	6.7	.7
9.1	5.7	1.0
7.2	4.7	1.0
5.8	3.0	1.7
Pan	- .1	3.1

OBSERVED FLOW BEHAVIOUR

Velocity (m/s)	Observation (D = .0 mm)

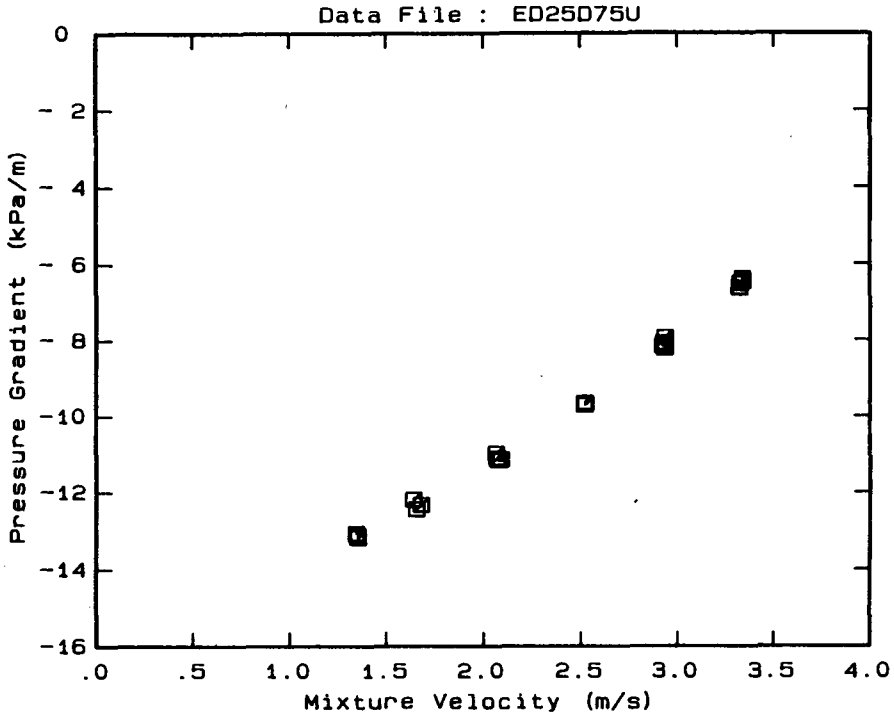

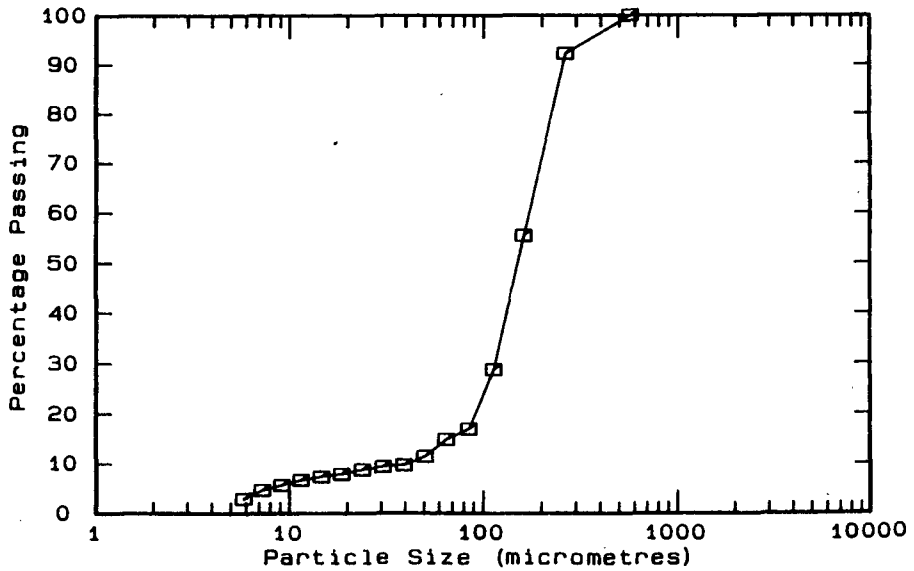

A.50

DATA FILE : ED25D79U

Test Facility	UCT 25 mm NB
Test Date	June 1990
Material Description	East Driefontein CCT
Material Relative Density	2.65
Slurry Relative Density	1.79
Solids Volumetric Concentration (%)	47.88
Solids Mass Concentration (%)	70.88
Mean Slurry Temperature (°C)	24.6
Pipe Internal Diameter (mm)	26.60
Pipe Roughness (μm)	21.0
Pipeline Slope	Vertical Down

Mixture Velocity (m/s)	Pressure Gradient (kPa/m)	Slurry Temp. (°C)
2.950	- 4.518	24.4
2.952	- 4.562	24.4
2.966	- 5.131	24.4
2.978	- 4.902	24.4
2.547	- 6.639	24.4
2.549	- 6.529	24.4
2.544	- 6.754	24.4
2.091	- 9.268	24.6
2.099	- 9.239	24.6
2.113	- 9.123	24.6
2.123	- 9.157	24.6
1.615	-11.211	24.7
1.605	-11.269	24.7
1.591	-11.360	24.8
1.612	-11.468	24.8
1.353	-12.236	24.8
1.316	-12.362	24.8
1.303	-12.152	24.8
1.298	-12.325	24.8

Particle Size Distribution
Malvern Particle Size Analyser

Size (μm)	% Passing	% Retained
564.0	100.0	.0
261.6	93.0	7.0
160.4	57.0	36.0
112.8	29.0	28.0
84.3	18.4	10.6
64.6	15.5	2.9
50.2	12.1	3.4
39.0	10.6	1.5
30.3	10.2	.4
23.7	9.6	.6
18.5	8.8	.8
14.5	8.2	.6
11.4	7.5	.7
9.1	6.4	1.1
7.2	5.4	1.0
5.8	3.5	1.9
Pan	.0	3.5

OBSERVED FLOW BEHAVIOUR

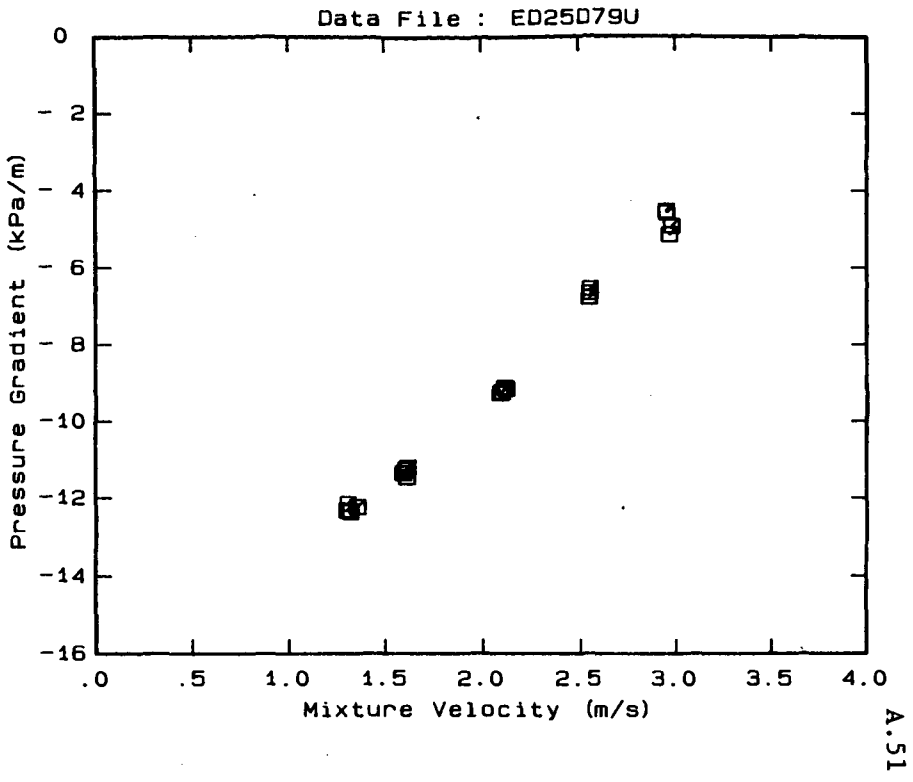

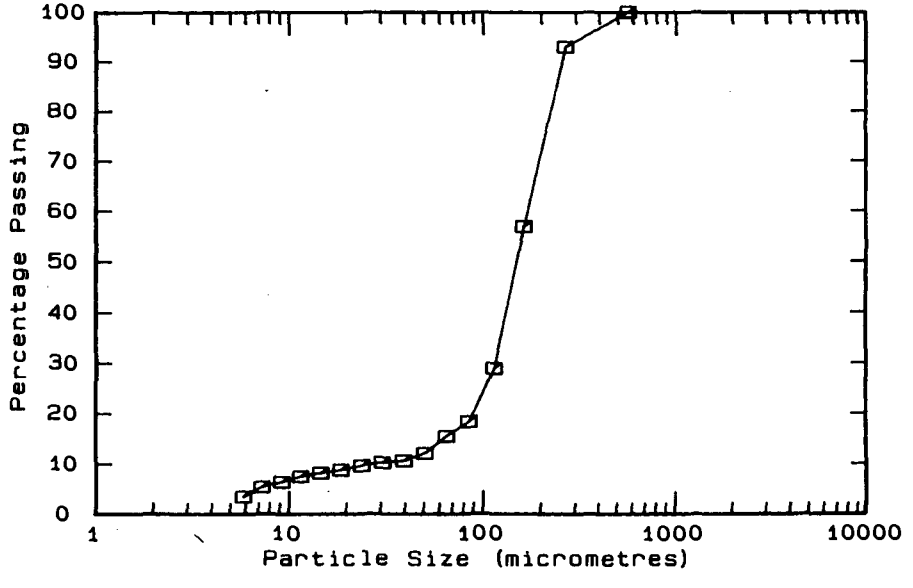

DATA FILE : ED25U55U

Test Facility	UCT 25 mm NB
Test Date	June 1990
Material Description	East Driefontein CCT
Material Relative Density	2.65
Slurry Relative Density	1.55
Solids Volumetric Concentration (%)	33.33
Solids Mass Concentration (%)	56.99
Mean Slurry Temperature (°C)	18.1
Pipe Internal Diameter (mm)	26.60
Pipe Roughness (μm)	21.0
Pipeline Slope	Vertical Up

Mixture Velocity (m/s)	Pressure Gradient (kPa/m)	Slurry Temp. (°C)
2.483	19.676	16.1
2.448	19.642	17.4
2.462	19.637	17.4
2.464	19.650	17.4
3.063	21.610	17.6
3.068	21.667	17.6
3.079	21.671	17.7
3.455	23.168	17.9
3.451	23.003	17.9
3.319	22.521	17.9
3.265	22.365	18.0
3.375	22.692	18.0
3.951	25.136	18.2
3.937	24.952	18.2
3.944	25.096	18.3
1.555	17.139	18.5
1.557	17.140	18.5
1.544	17.149	18.5
1.879	17.806	18.4
1.875	17.820	18.4
1.901	17.800	18.4
2.199	18.615	18.4
2.200	18.615	18.4
2.193	18.620	18.4
2.542	19.633	18.4
2.545	19.618	18.4
2.548	19.640	18.4
2.866	20.638	18.4
2.864	20.606	18.4
2.871	20.591	18.4

Particle Size Distribution
Malvern Particle Size Analyser

Size (μm)	% Passing	% Retained
564.0	100.0	.0
261.6	94.4	5.6
160.4	55.5	38.9
112.8	23.3	32.2
84.3	12.6	10.7
64.6	9.4	3.2
50.2	6.2	3.2
39.0	4.8	1.4
30.3	4.4	.4
23.7	4.0	.4
18.5	3.6	.4
14.5	3.3	.3
11.4	3.0	.3
9.1	2.5	.5
7.2	2.0	.5
5.8	1.3	.7
Pan	- .0	1.3

OBSERVED FLOW BEHAVIOUR

Velocity (m/s)	Observation (D = .0 mm)

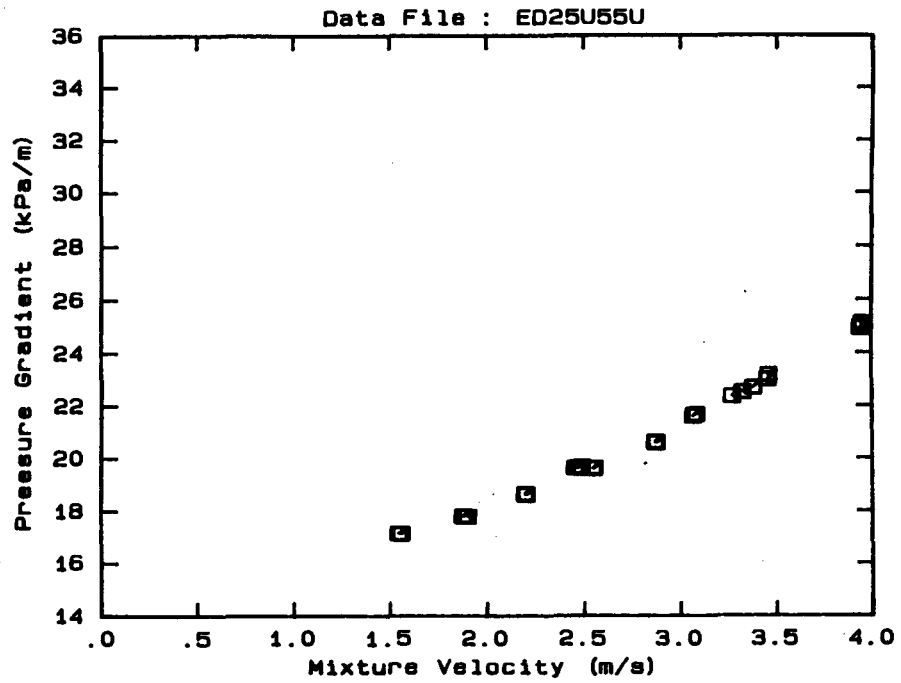

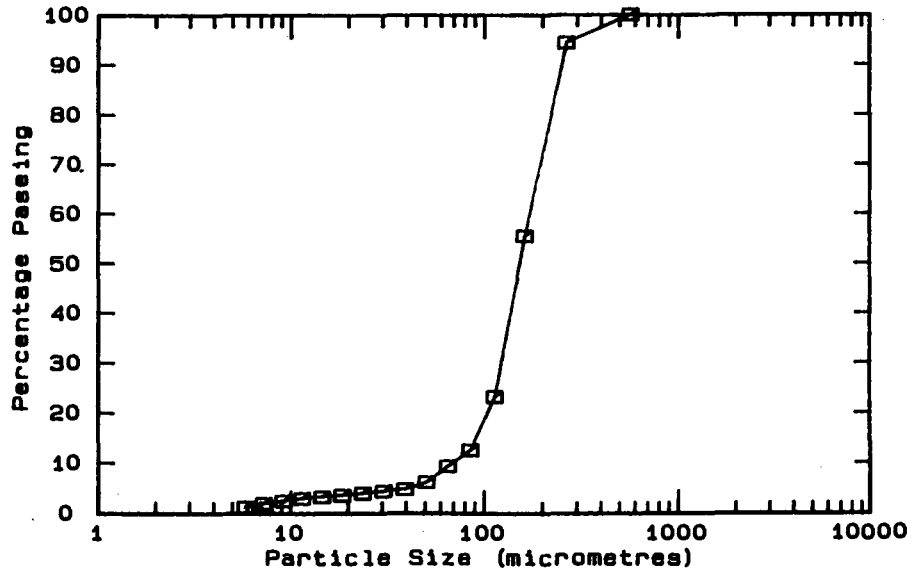

DATA FILE : ED25U66U

Test Facility	UCT 25 mm NB
Test Date	June 1990
Material Description	East Driefontein CCT
Material Relative Density	2.65
Slurry Relative Density	1.66
Solids Volumetric Concentration (%)	40.00
Solids Mass Concentration (%)	63.86
Mean Slurry Temperature (°C)	18.6
Pipe Internal Diameter (mm)	26.60
Pipe Roughness (μm)	21.0
Pipeline Slope	Vertical Up

Mixture Velocity (m/s)	Pressure Gradient (kPa/m)	Slurry Temp. (°C)
2.743	20.628	18.0
2.721	20.606	18.0
2.705	20.652	18.1
3.016	21.437	18.2
3.022	21.503	18.2
3.013	21.516	18.3
3.177	22.205	18.4
3.182	22.109	18.4
3.194	22.175	18.5
3.344	22.997	18.7
3.354	22.943	18.8
3.374	22.865	18.8
1.139	17.868	18.8
1.152	17.872	18.8
1.161	17.897	18.8
1.496	18.159	18.8
1.501	18.125	18.8
1.502	18.134	18.8
2.096	19.229	18.7
2.095	19.179	18.7
2.092	19.251	18.7
2.398	19.720	18.7
2.391	19.734	18.7
2.397	19.740	18.7
2.453	19.650	18.7
2.448	19.648	18.7
2.446	19.657	18.7
2.778	20.779	18.7
2.772	20.684	18.7
2.774	20.617	18.7

Particle Size Distribution
Malvern Particle Size Analyser

Size (μm)	% Passing	% Retained
564.0	100.0	.0
261.6	91.9	8.1
160.4	55.2	36.7
112.8	25.8	29.4
84.3	13.5	12.3
64.6	10.0	3.5
50.2	6.9	3.1
39.0	5.8	1.1
30.3	5.3	.5
23.7	4.7	.6
18.5	4.4	.3
14.5	4.1	.3
11.4	3.6	.5
9.1	3.1	.5
7.2	2.6	.5
5.8	1.7	.9
Pan	.0	1.7

OBSERVED FLOW BEHAVIOUR

Velocity (m/s)	Observation (D = .0 mm)

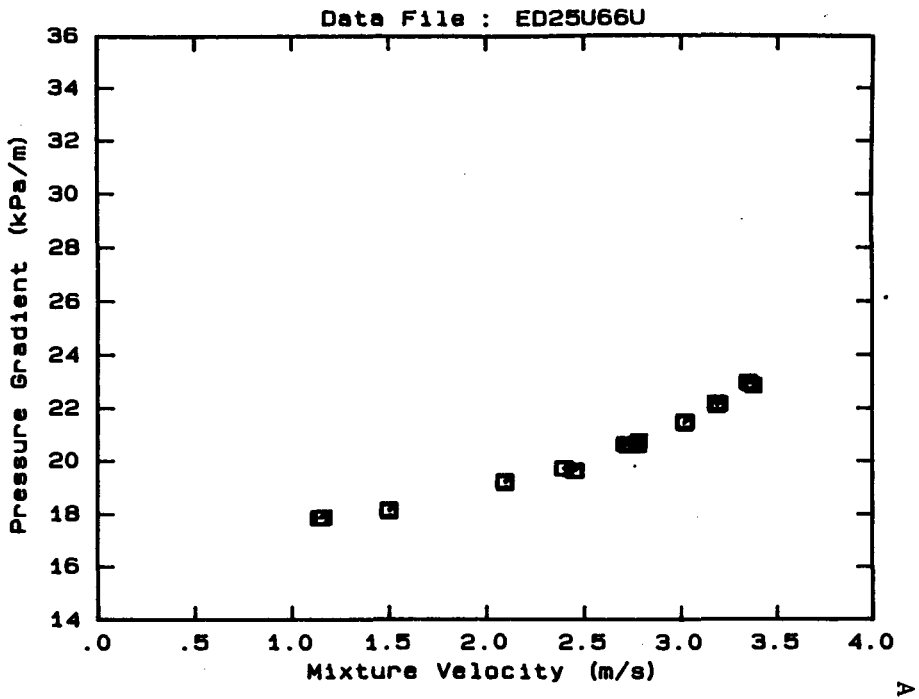

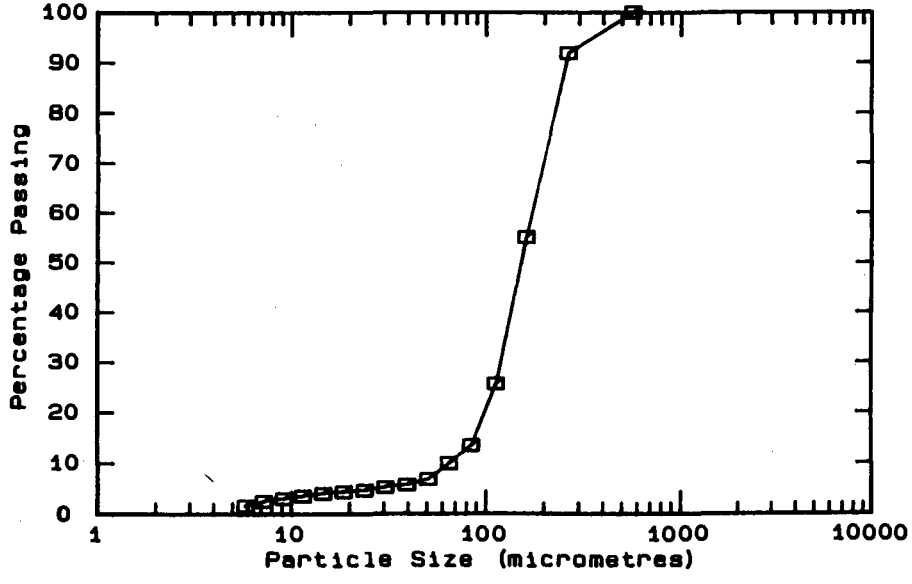

DATA FILE : ED25U69U

Test Facility	UCT 25 mm NB
Test Date	June 1990
Material Description	East Driefontein CCT
Material Relative Density	2.65
Slurry Relative Density	1.69
Solids Volumetric Concentration (%)	41.82
Solids Mass Concentration (%)	65.57
Mean Slurry Temperature (°C)	19.0
Pipe Internal Diameter (mm)	26.60
Pipe Roughness (μm)	21.0
Pipeline Slope	Vertical Up

Mixture Velocity (m/s)	Pressure Gradient (kPa/m)	Slurry Temp. (°C)
3.744	24.345	17.7
3.737	23.983	17.9
3.763	23.919	18.0
3.787	24.755	18.1
3.807	23.799	18.2
3.361	23.284	18.5
3.336	22.919	18.5
3.336	22.817	18.6
2.984	22.020	19.0
2.962	22.053	19.0
2.976	22.149	19.0
2.507	21.234	19.2
2.503	21.073	19.2
2.505	21.269	19.3
2.520	20.821	19.3
2.528	21.046	19.3
2.086	20.014	19.4
2.081	20.067	19.4
2.077	20.014	19.5
2.077	19.964	19.5
1.664	19.051	19.6
1.663	19.232	19.6
1.660	19.048	19.5
1.232	18.350	19.5
1.212	18.524	19.5
1.208	18.493	19.5
1.208	18.342	19.5

Particle Size Distribution
Malvern Particle Size Analyser

Size (μm)	% Passing	% Retained
564.0	100.0	.0
261.6	93.6	6.4
160.4	58.1	35.5
112.8	27.6	30.5
84.3	15.2	12.4
64.6	12.1	3.1
50.2	8.7	3.4
39.0	7.2	1.5
30.3	6.8	.4
23.7	6.3	.5
18.5	5.6	.7
14.5	5.2	.4
11.4	4.7	.5
9.1	3.9	.8
7.2	3.2	.7
5.8	2.0	1.2
Pan	- .1	2.1

OBSERVED FLOW BEHAVIOUR

Velocity (m/s)	Observation (D = .0 mm)

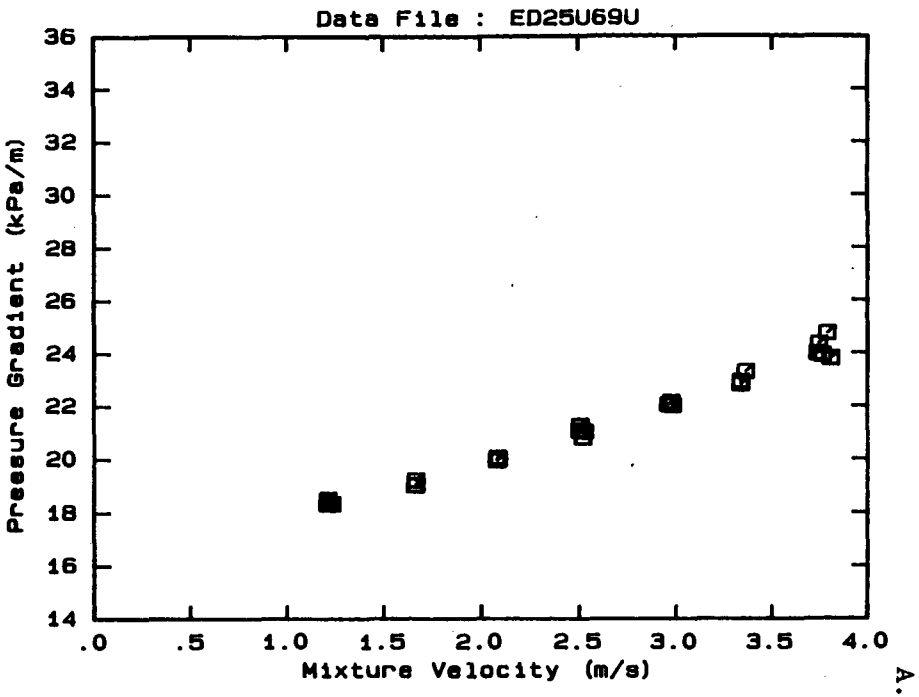

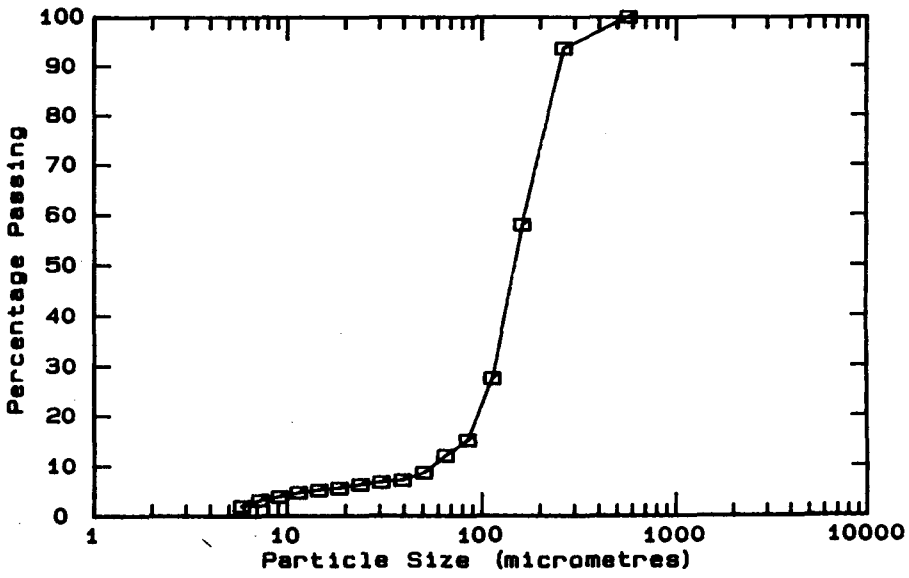

DATA FILE : ED25U75U

Test Facility	UCT 25 mm NB
Test Date	June 1990
Material Description	East Driefontein CCT
Material Relative Density	2.65
Slurry Relative Density	1.75
Solids Volumetric Concentration (%)	45.45
Solids Mass Concentration (%)	68.83
Mean Slurry Temperature (°C)	24.2
Pipe Internal Diameter (mm)	26.60
Pipe Roughness (μm)	21.0
Pipeline Slope	Vertical Up

Mixture Velocity (m/s)	Pressure Gradient (kPa/m)	Slurry Temp. (°C)
3.321	25.385	23.4
3.323	24.978	23.4
3.336	25.440	23.5
3.337	25.387	23.5
2.931	23.714	23.8
2.919	23.943	23.9
2.923	23.965	24.0
2.930	23.918	24.0
2.523	22.472	24.3
2.520	22.423	24.3
2.521	22.378	24.4
2.066	21.580	24.5
2.072	21.222	24.5
2.080	21.594	24.6
2.091	21.655	24.6
1.679	20.155	24.6
1.655	20.198	24.7
1.639	20.558	24.7
1.352	19.893	24.7
1.345	20.002	24.7
1.354	19.771	24.7

Particle Size Distribution
Malvern Particle Size Analyser

Size (μm)	% Passing	% Retained
564.0	100.0	.0
261.6	92.2	7.8
160.4	55.4	36.8
112.8	28.7	26.7
84.3	16.9	11.8
64.6	14.8	2.1
50.2	11.4	3.4
39.0	9.7	1.7
30.3	9.4	.3
23.7	8.8	.6
18.5	7.9	.9
14.5	7.4	.5
11.4	6.7	.7
9.1	5.7	1.0
7.2	4.7	1.0
5.8	3.0	1.7
Pan	- .1	3.1

OBSERVED FLOW BEHAVIOUR

Velocity (m/s)	Observation (D = .0 mm)

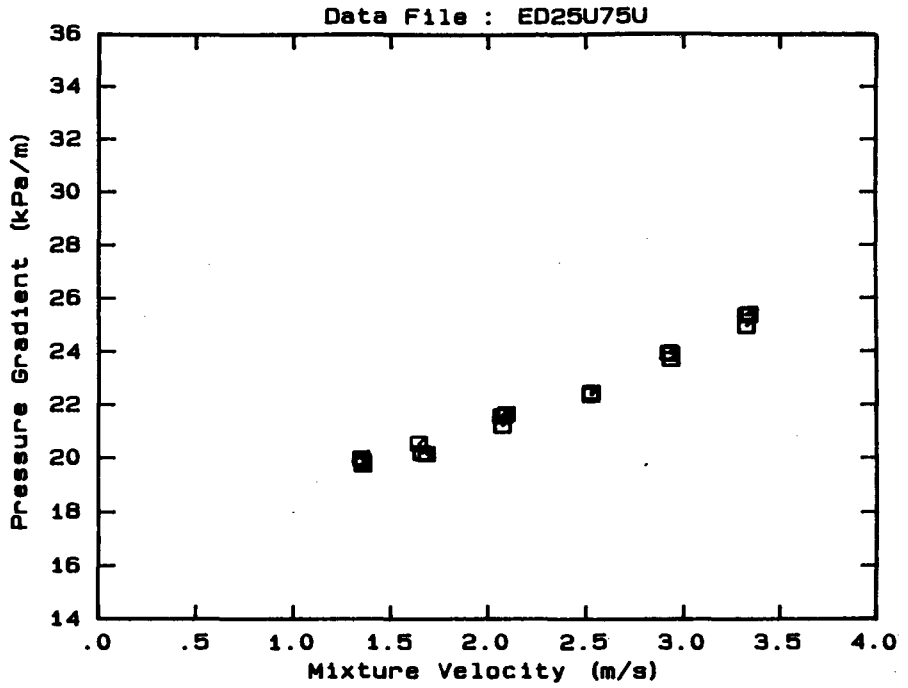

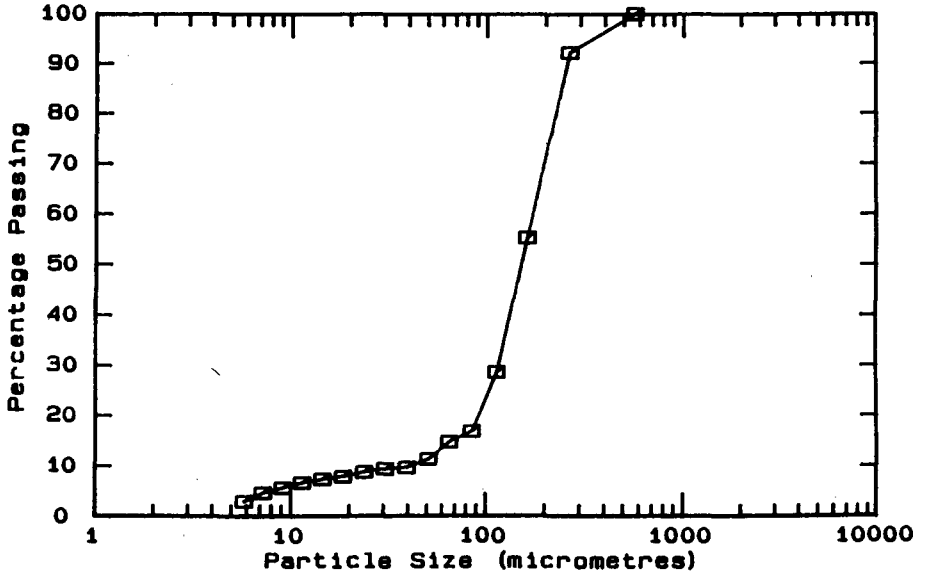

DATA FILE : ED25U79U

Test Facility	UCT 25 mm NB
Test Date	June 1990
Material Description	East Driefontein CCT
Material Relative Density	2.65
Slurry Relative Density	1.79
Solids Volumetric Concentration (%)	47.88
Solids Mass Concentration (%)	70.88
Mean Slurry Temperature (°C)	24.6
Pipe Internal Diameter (mm)	26.60
Pipe Roughness (μm)	21.0
Pipeline Slope	Vertical Up

Mixture Velocity (m/s)	Pressure Gradient (kPa/m)	Slurry Temp. (°C)
2.950	28.236	24.4
2.952	28.526	24.4
2.966	28.222	24.4
2.978	27.582	24.4
2.547	26.807	24.4
2.549	26.901	24.4
2.544	27.047	24.4
2.091	24.911	24.6
2.099	24.863	24.6
2.113	24.725	24.6
2.123	24.819	24.6
1.615	22.950	24.7
1.605	23.011	24.7
1.591	22.894	24.8
1.612	22.870	24.8
1.353	22.316	24.8
1.316	22.358	24.8
1.303	22.547	24.8
1.298	22.279	24.8

Particle Size Distribution
Malvern Particle Size Analyser

Size (μm)	% Passing	% Retained
564.0	100.0	.0
261.6	93.0	7.0
160.4	57.0	36.0
112.8	29.0	28.0
84.3	18.4	10.6
64.6	15.5	2.9
50.2	12.1	3.4
39.0	10.6	1.5
30.3	10.2	.4
23.7	9.6	.6
18.5	8.8	.8
14.5	8.2	.6
11.4	7.5	.7
9.1	6.4	1.1
7.2	5.4	1.0
5.8	3.5	1.9
Pan	.0	3.5

OBSERVED FLOW BEHAVIOUR

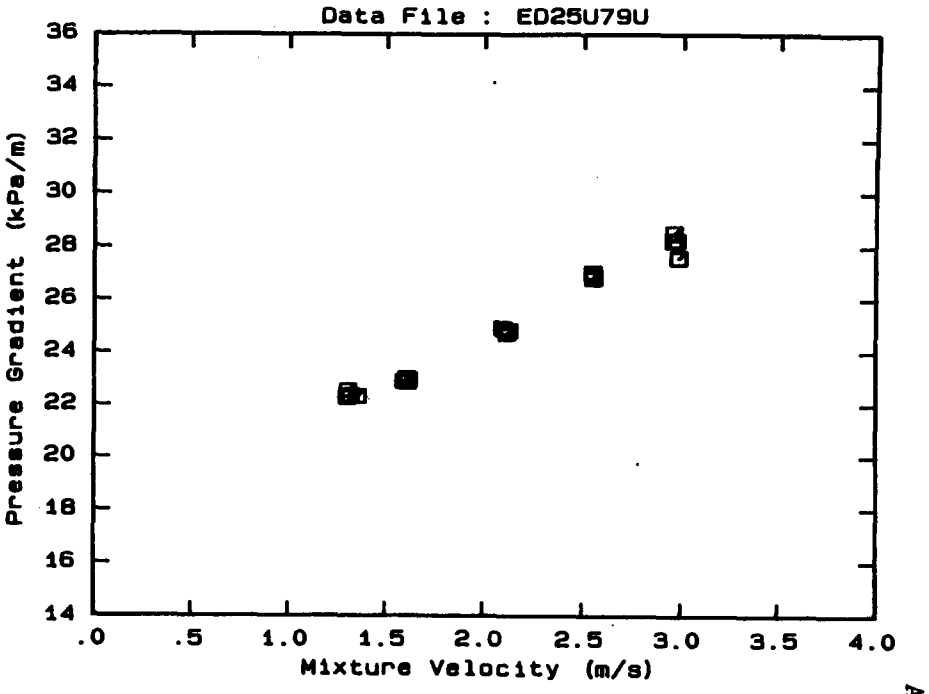

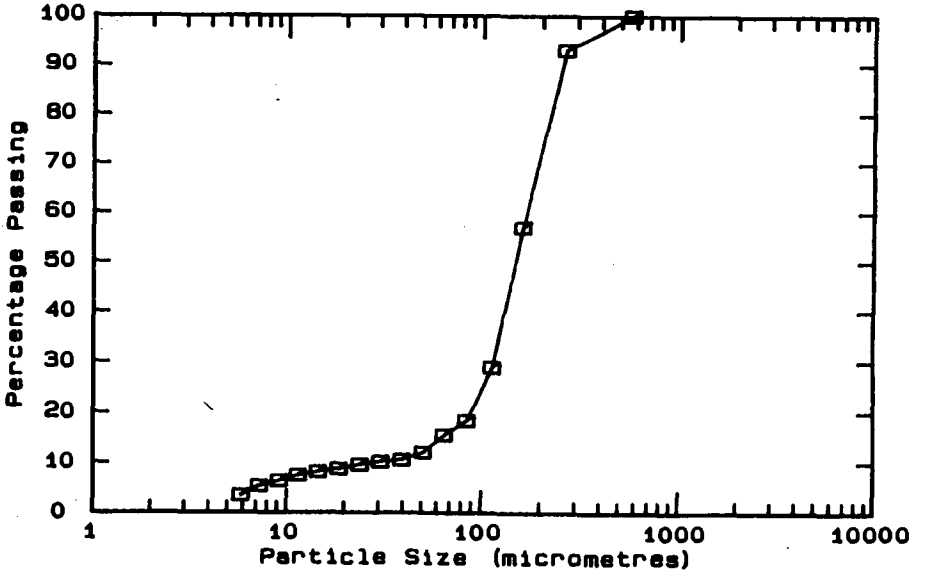

DATA FILE : ED40H69U

Test Facility	UCT 40 mm NB
Test Date	August 1990
Material Description	East Driefontein CCT
Material Relative Density	2.65
Slurry Relative Density	1.69
Solids Volumetric Concentration (%)	41.82
Solids Mass Concentration (%)	65.57
Mean Slurry Temperature (°C)	23.3
Pipe Internal Diameter (mm)	40.00
Pipe Roughness (μm)	52.0
Pipeline Slope	Horizontal

Mixture Velocity (m/s)	Pressure Gradient (kPa/m)	Slurry Temp. (°C)
3.942	7.535	23.5
3.646	6.743	23.5
3.957	7.383	23.5
3.963	7.947	23.5
3.961	8.058	23.6
3.251	5.459	23.6
3.233	5.120	23.6
3.252	5.019	23.5
3.221	5.323	23.5
2.479	3.671	23.3
2.452	3.456	23.2
2.942	4.463	23.2
2.953	4.497	23.2
2.951	4.722	23.1
2.175	2.803	23.0
2.112	3.016	23.0
2.115	2.866	22.9
2.107	2.605	22.9

Particle Size Distribution
Malvern Particle Size Analyser

Size (μm)	% Passing	% Retained
564.0	100.0	.0
261.6	91.8	8.2
160.4	57.6	34.2
112.8	27.1	30.5
84.3	15.9	11.2
64.6	12.0	3.9
50.2	8.1	3.9
39.0	7.0	1.1
30.3	6.5	.5
23.7	5.8	.7
18.5	5.3	.5
14.5	4.9	.4
11.4	4.3	.6
9.1	3.6	.7
7.2	3.0	.6
5.8	1.9	1.1
Pan	- .0	1.9

OBSERVED FLOW BEHAVIOUR

Velocity (m/s)	Observation (D = 46.0 mm)
1.64	Asymmetric - slid particles
1.89	Asymmetric
2.45	Appears homogeneous
3.02	Appears homogeneous

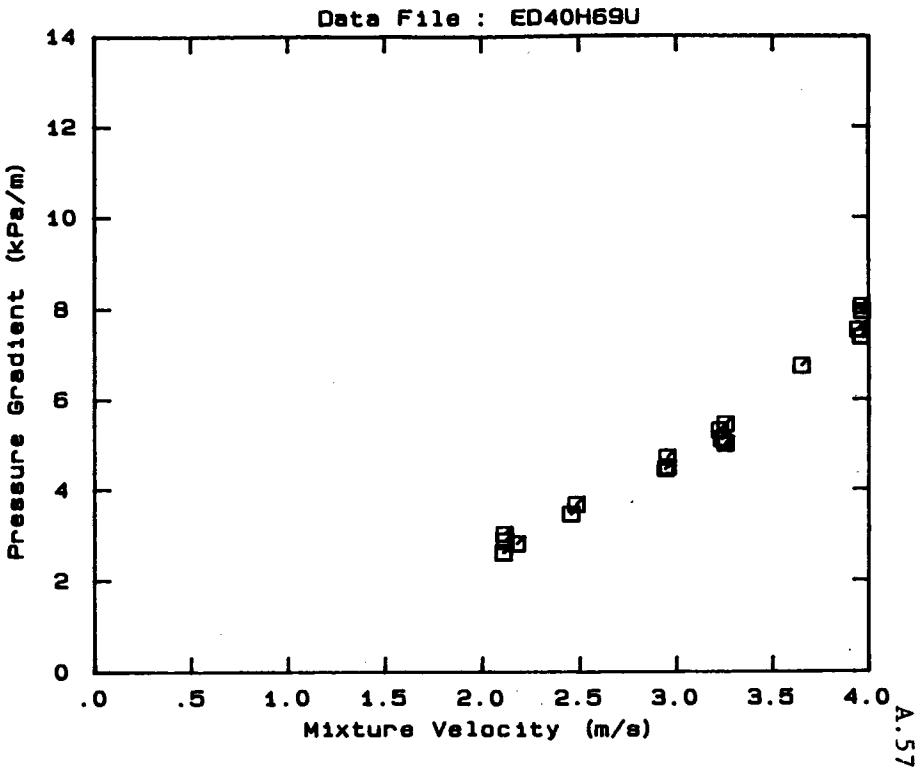

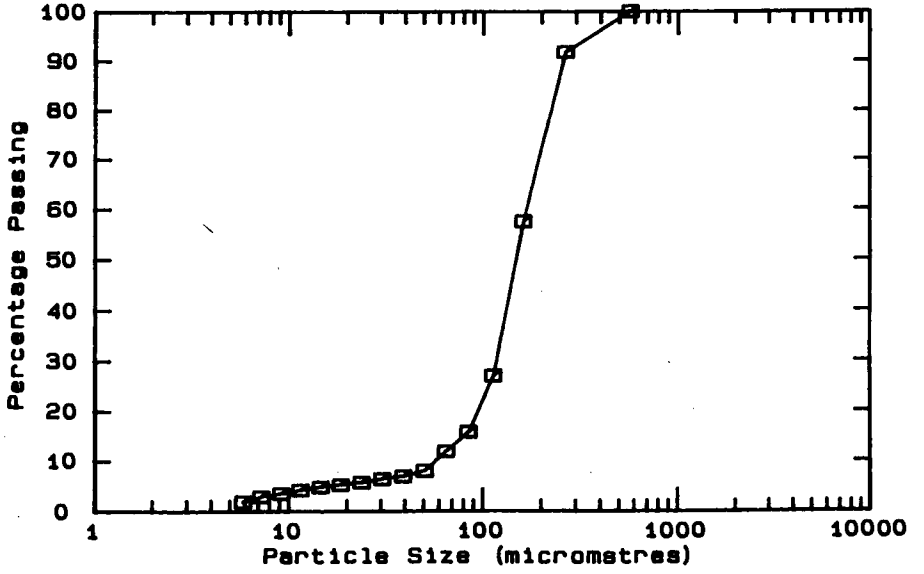

DATA FILE : ED40H72U

Test Facility	UCT 40 mm NB
Test Date	August 1990
Material Description	East Driefontein CCT
Material Relative Density	2.65
Slurry Relative Density	1.72
Solids Volumetric Concentration (%)	43.64
Solids Mass Concentration (%)	67.23
Mean Slurry Temperature (°C)	23.8
Pipe Internal Diameter (mm)	40.00
Pipe Roughness (μm)	52.0
Pipeline Slope	Horizontal

Mixture Velocity (m/s)	Pressure Gradient (kPa/m)	Slurry Temp. (°C)
3.733	6.354	23.6
3.736	6.351	23.6
3.772	6.361	23.7
3.784	6.591	23.8
3.211	5.399	24.1
3.204	5.387	24.1
3.208	5.161	24.1
3.213	5.212	24.1
2.667	4.249	24.1
2.654	4.621	24.1
2.653	4.418	24.1
2.660	4.387	24.1
2.168	3.347	23.9
2.174	3.452	23.9
2.124	3.488	23.9
2.138	3.530	23.8
1.603	2.658	23.7
1.601	2.606	23.6
1.534	2.487	23.6
1.048	2.083	23.4
1.022	2.386	23.4
1.014	2.447	23.3
.993	2.458	23.2

Particle Size Distribution
Malvern Particle Size Analyser

Size (μm)	% Passing	% Retained
564.0	100.0	.0
261.6	92.9	7.1
160.4	59.7	33.2
112.8	32.0	27.7
84.3	18.3	13.7
64.6	15.0	3.3
50.2	11.5	3.5
39.0	10.0	1.5
30.3	9.5	.5
23.7	8.7	.8
18.5	8.1	.6
14.5	7.6	.5
11.4	6.8	.8
9.1	5.7	1.1
7.2	4.7	1.0
5.8	3.0	1.7
Pan	- .1	3.1

OBSERVED FLOW BEHAVIOUR

Velocity (m/s)	Observation (D = 46.0 mm)
.83	35% sliding bed
1.24	Asymmetric-slid particles
1.68	Asymmetric-slid particles
2.05	Asymmetric
2.45	Appears homogeneous
2.86	Appears homogeneous

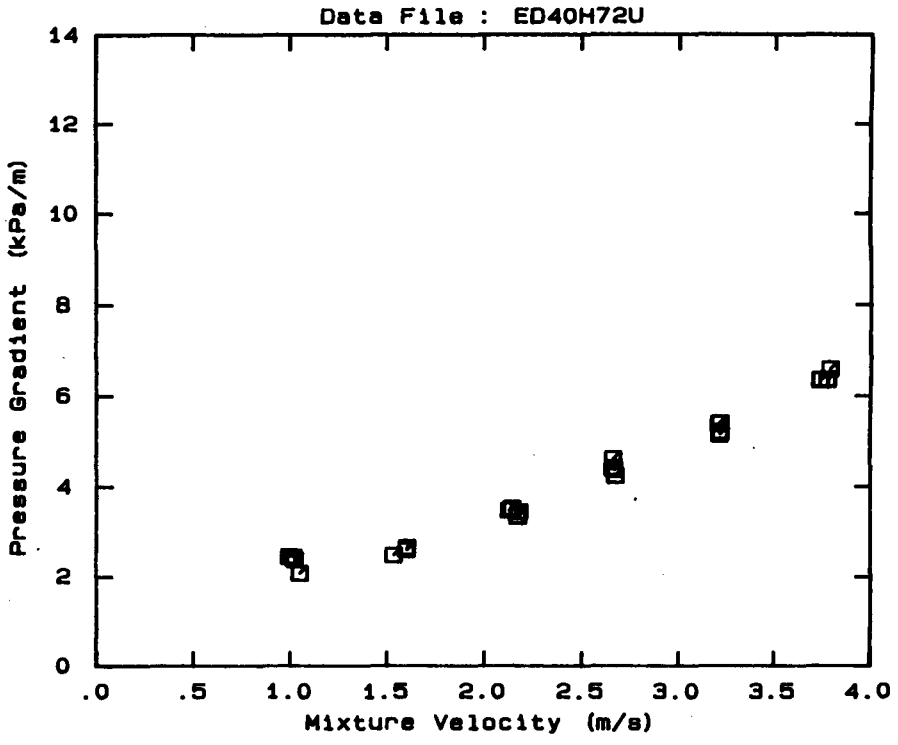

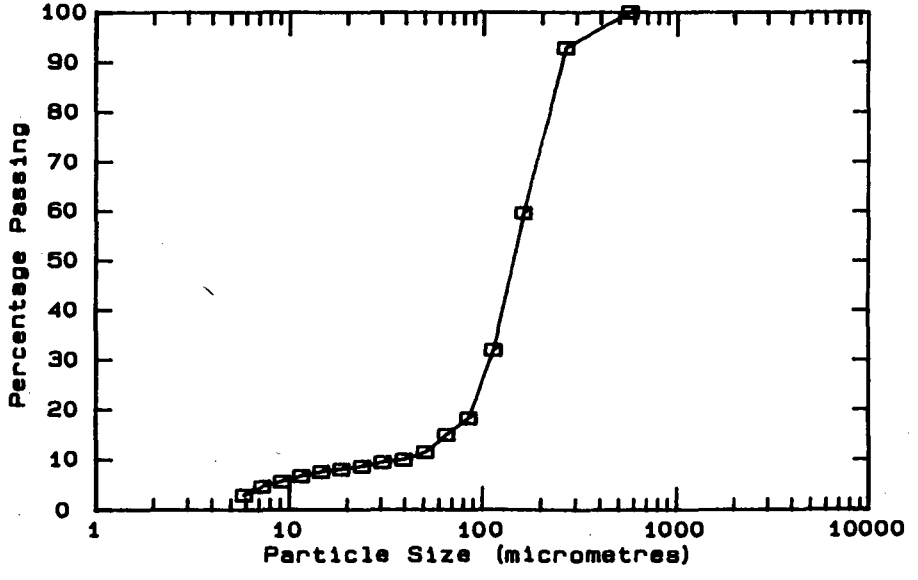

DATA FILE : ED40H75U

Test Facility	UCT 40 mm NB
Test Date	August 1990
Material Description	East Driefontein CCT
Material Relative Density	2.65
Slurry Relative Density	1.75
Solids Volumetric Concentration (%)	45.45
Solids Mass Concentration (%)	68.83
Mean Slurry Temperature (°C)	23.2
Pipe Internal Diameter (mm)	40.00
Pipe Roughness (μm)	52.0
Pipeline Slope	Horizontal

Mixture Velocity (m/s)	Pressure Gradient (kPa/m)	Slurry Temp. (°C)
3.291	7.370	22.4
3.298	7.827	22.6
3.312	7.735	22.7
3.313	7.514	22.8
3.334	7.555	23.0
2.711	6.111	23.3
2.704	6.237	23.3
2.697	5.977	23.4
2.704	6.078	23.4
2.132	4.956	23.5
2.120	4.895	23.5
2.148	4.914	23.5
2.148	4.934	23.5
1.615	3.391	23.4
1.604	3.391	23.4
1.613	3.460	23.4
1.614	3.235	23.3
1.031	2.472	23.2
1.021	2.429	23.2
1.016	2.401	23.1
.969	2.401	23.1

Particle Size Distribution
Malvern Particle Size Analyser

Size (μm)	% Passing	% Retained
564.0	100.0	.0
261.6	93.1	6.9
160.4	59.1	34.0
112.8	29.2	29.9
84.3	17.6	11.6
64.6	14.2	3.4
50.2	10.3	3.9
39.0	9.1	1.2
30.3	8.7	.4
23.7	7.9	.8
18.5	7.3	.6
14.5	6.9	.4
11.4	6.2	.7
9.1	5.3	.9
7.2	4.5	.8
5.8	3.0	1.5
Pan	.2	2.8

OBSERVED FLOW BEHAVIOUR

Velocity (m/s)	Observation (D = 46.0 mm)
.79	Asymmetric-slid particles
1.24	Asymmetric-slid particles
1.64	Asymmetric-slid particles
2.09	Appears homogeneous
2.50	Appears homogeneous

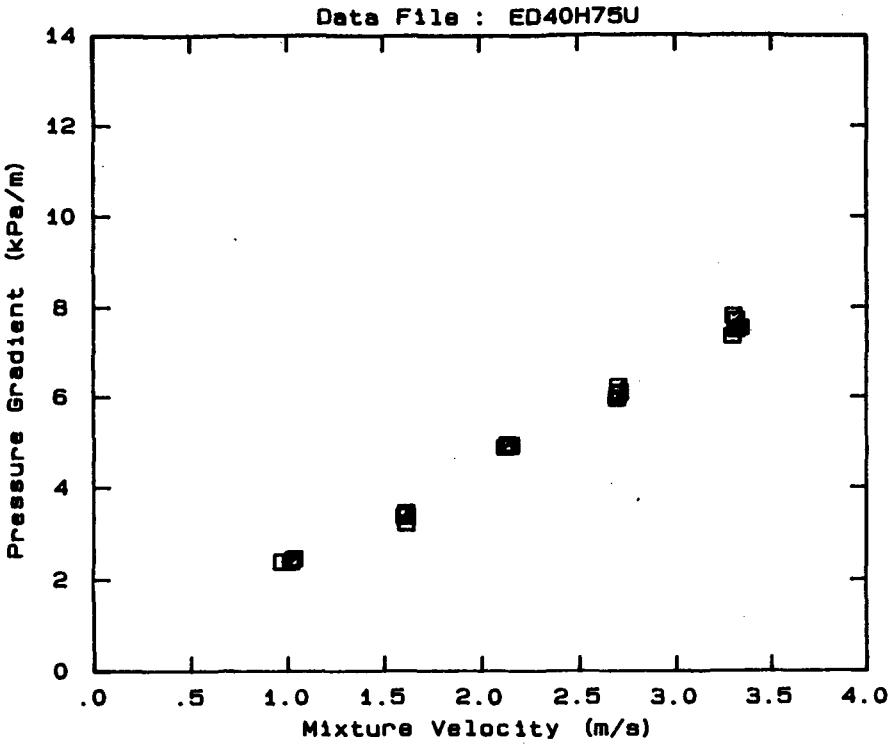

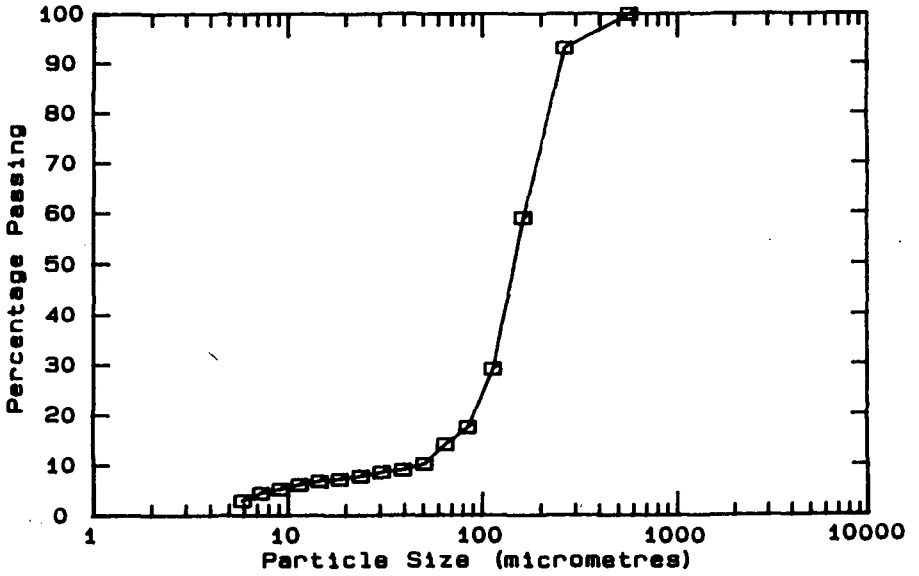

DATA FILE : ED40H79U

Test Facility	UCT 40 mm NB
Test Date	August 1990
Material Description	East Driefontein CCT
Material Relative Density	2.65
Slurry Relative Density	1.79
Solids Volumetric Concentration (%)	47.88
Solids Mass Concentration (%)	70.88
Mean Slurry Temperature (°C)	23.7
Pipe Internal Diameter (mm)	40.00
Pipe Roughness (μm)	52.0
Pipeline Slope	Horizontal

Mixture Velocity (m/s)	Pressure Gradient (kPa/m)	Slurry Temp. (°C)
2.691	10.893	22.6
2.718	10.712	22.9
2.720	10.834	23.1
2.726	10.512	23.3
2.720	10.736	23.4
2.136	8.169	23.9
2.147	8.111	23.9
2.155	8.120	24.0
2.148	8.025	24.0
1.585	6.031	24.1
1.589	6.018	24.1
1.725	6.029	24.1
1.601	6.087	24.1
1.591	5.814	24.0
1.076	4.174	24.0
1.056	4.296	24.0
1.048	4.255	23.9
1.037	4.207	23.9
.593	4.215	23.8
.604	3.279	23.7
.596	3.043	23.7
.595	3.006	23.7
.565	2.917	23.6
.529	2.931	23.6
.520	2.816	23.5
.507	2.798	23.5

Particle Size Distribution
Malvern Particle Size Analyser

Size (μm)	% Passing	% Retained
564.0	100.0	.0
261.6	94.2	5.8
160.4	59.1	35.1
112.8	29.2	29.9
84.3	17.2	12.0
64.6	13.5	3.7
50.2	9.9	3.6
39.0	8.9	1.0
30.3	8.4	.5
23.7	7.6	.8
18.5	7.1	.5
14.5	6.7	.4
11.4	6.0	.7
9.1	5.1	.9
7.2	4.3	.8
5.8	2.8	1.5
Pan	.0	2.8

OBSERVED FLOW BEHAVIOUR

Velocity (m/s)	Observation (D = 46.0 mm)
.42	Appears homogeneous
.83	Appears homogeneous
1.24	Appears homogeneous
1.64	Appears homogeneous
2.05	Appears homogeneous

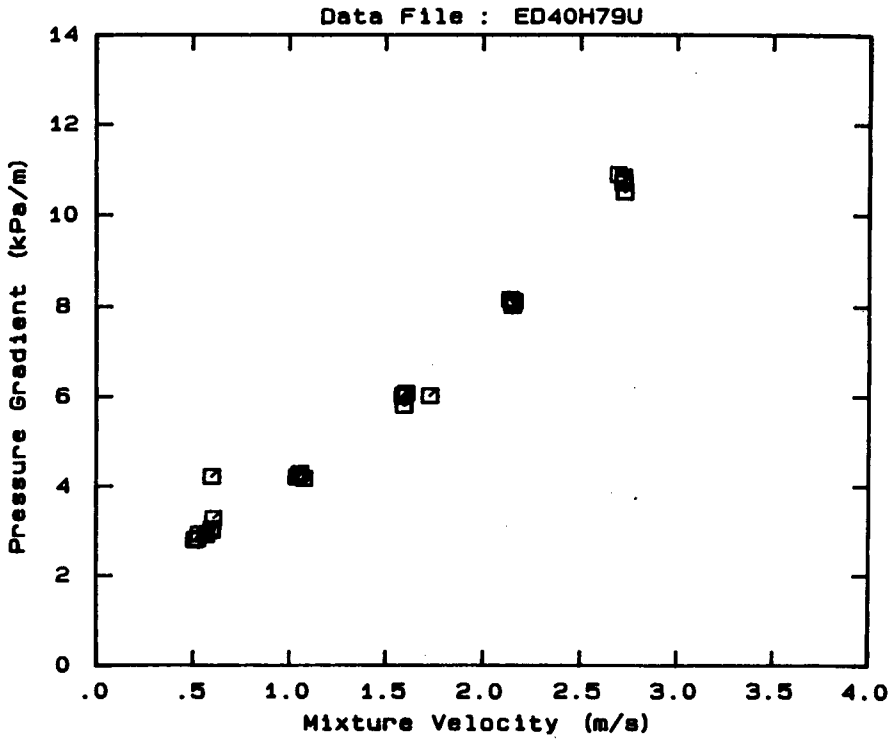

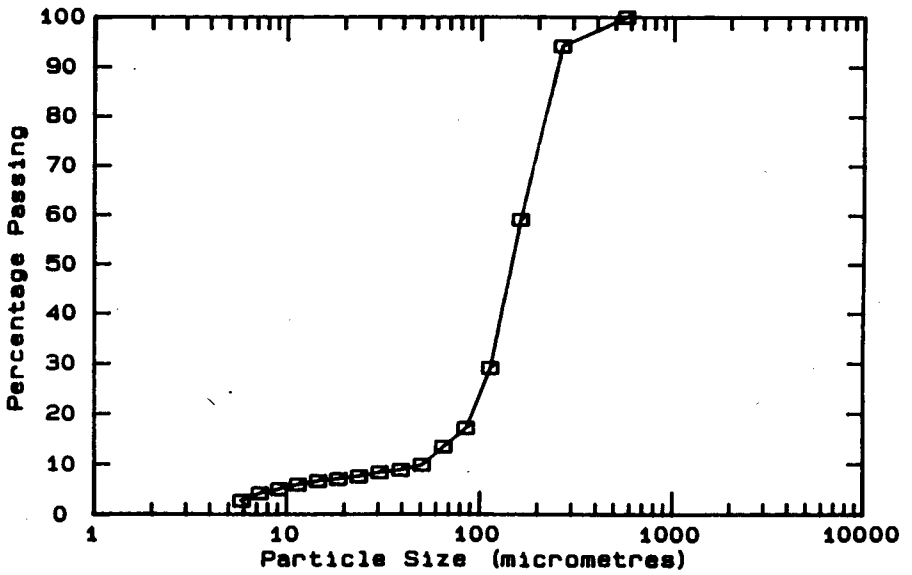

A.60

DATA FILE : ED40H82U

Test Facility	UCT 40 mm NB
Test Date	August 1990
Material Description	East Driefontein CCT
Material Relative Density	2.65
Slurry Relative Density	1.82
Solids Volumetric Concentration (%)	49.70
Solids Mass Concentration (%)	72.36
Mean Slurry Temperature (°C)	26.7
Pipe Internal Diameter (mm)	40.00
Pipe Roughness (μm)	52.0
Pipeline Slope	Horizontal

Mixture Velocity (m/s)	Pressure Gradient (kPa/m)	Slurry Temp. (°C)
2.205	11.577	25.7
2.208	11.804	25.9
2.209	11.694	26.0
2.205	11.594	26.2
2.206	11.797	26.3
1.723	8.555	26.6
1.708	8.649	26.8
1.706	8.670	26.8
1.702	8.596	26.8
1.704	8.660	26.9
1.708	8.542	26.9
1.256	6.643	26.9
1.243	6.748	27.0
1.218	6.624	27.0
1.211	6.669	26.9
1.202	6.618	26.9
.828	5.328	26.9
.809	5.331	26.8
.811	5.367	26.8
.798	5.266	26.8
.396	3.645	26.7
.364	3.565	26.7
.345	3.662	26.7
.305	3.769	26.7

Particle Size Distribution
Malvern Particle Size Analyser

Size (μm)	% Passing	% Retained
564.0	100.0	.0
261.6	92.2	7.8
160.4	59.0	33.2
112.8	29.4	29.6
84.3	17.3	12.1
64.6	13.7	3.6
50.2	10.0	3.7
39.0	9.0	1.0
30.3	8.6	.4
23.7	7.8	.8
18.5	7.3	.5
14.5	6.9	.4
11.4	6.2	.7
9.1	5.3	.9
7.2	4.5	.8
5.8	3.0	1.5
Pan	.1	2.9

OBSERVED FLOW BEHAVIOUR

Velocity (m/s)	Observation (D = 46.0 mm)
.67	Appears homogeneous
.99	Appears homogeneous
1.32	Appears homogeneous
1.68	Appears homogeneous

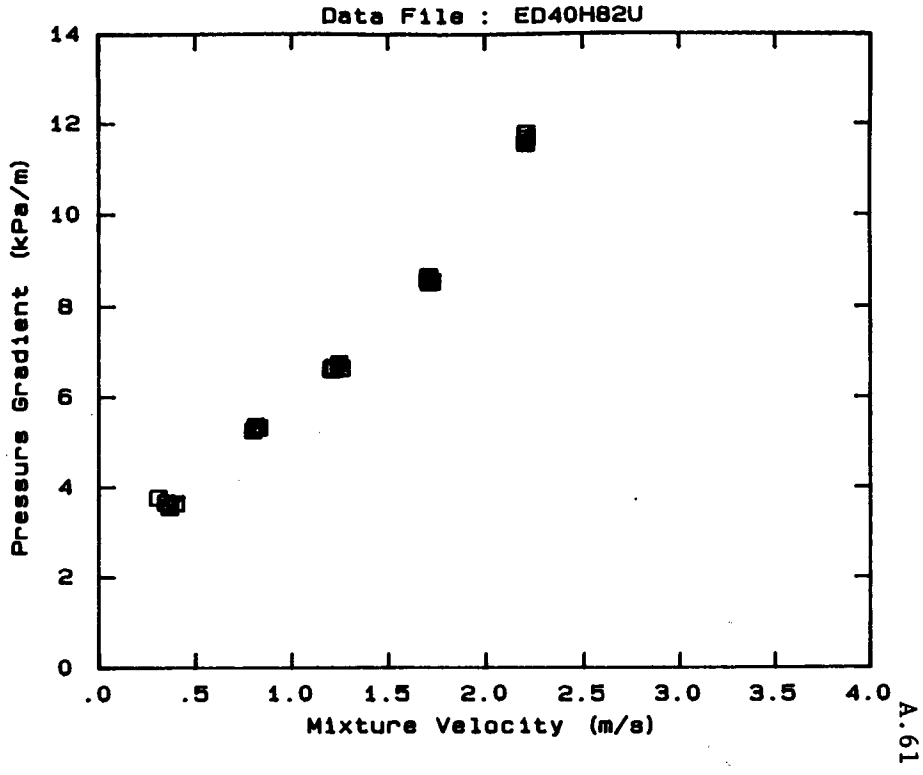

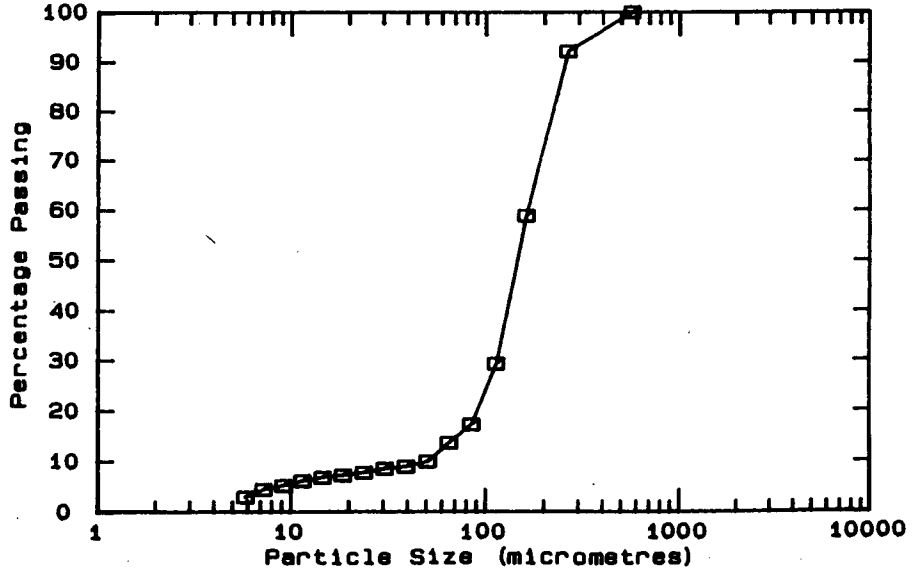

DATA FILE : ED40H87U

Test Facility	UCT 40 mm NB
Test Date	August 1990
Material Description	East Driefontein CCT
Material Relative Density	2.65
Slurry Relative Density	1.87
Solids Volumetric Concentration (%)	52.73
Solids Mass Concentration (%)	74.72
Mean Slurry Temperature (°C)	30.0
Pipe Internal Diameter (mm)	40.00
Pipe Roughness (μm)	52.0
Pipeline Slope	Horizontal

Mixture Velocity (m/s)	Pressure Gradient (kPa/m)	Slurry Temp. (°C)
.856	10.665	27.6
.994	13.393	27.6
1.263	11.516	27.6
1.254	11.420	27.7
1.226	11.031	27.9
1.233	12.337	28.1
1.227	11.619	28.4
1.217	11.601	28.6
1.196	11.424	28.9
.838	9.364	29.4
.822	10.271	29.7
.828	10.073	29.9
.792	9.704	30.2
.762	9.581	30.3
.774	10.242	30.7
.766	10.630	30.8
.757	9.376	30.9
.747	10.387	31.0
.518	7.905	31.2
.512	7.806	31.3
.505	8.523	31.4
.500	8.493	31.5
.286	6.556	31.9
.272	6.574	32.0
.266	6.424	32.0
.273	6.439	32.1
.274	6.663	32.2

Particle Size Distribution
Malvern Particle Size Analyser

Size (μm)	% Passing	% Retained
564.0	100.0	.0
261.6	92.9	7.1
160.4	59.1	33.8
112.8	31.7	27.4
84.3	17.9	13.8
64.6	14.7	3.2
50.2	11.7	3.0
39.0	10.2	1.5
30.3	9.6	.6
23.7	8.9	.7
18.5	8.3	.6
14.5	7.8	.5
11.4	7.1	.7
9.1	6.1	1.0
7.2	5.1	1.0
5.8	3.3	1.8
Pan	- .1	3.4

OBSERVED FLOW BEHAVIOUR

Velocity (m/s)	Observation (D = 46.0 mm)
.22	Appears homogeneous
.42	Appears homogeneous
.71	Appears homogeneous
.99	Appears homogeneous

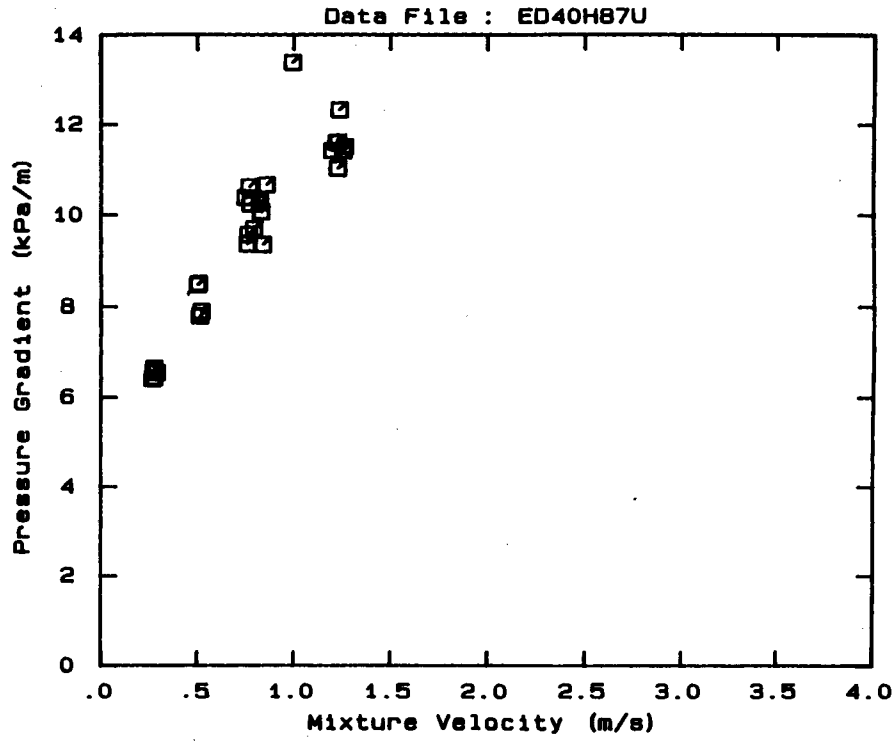

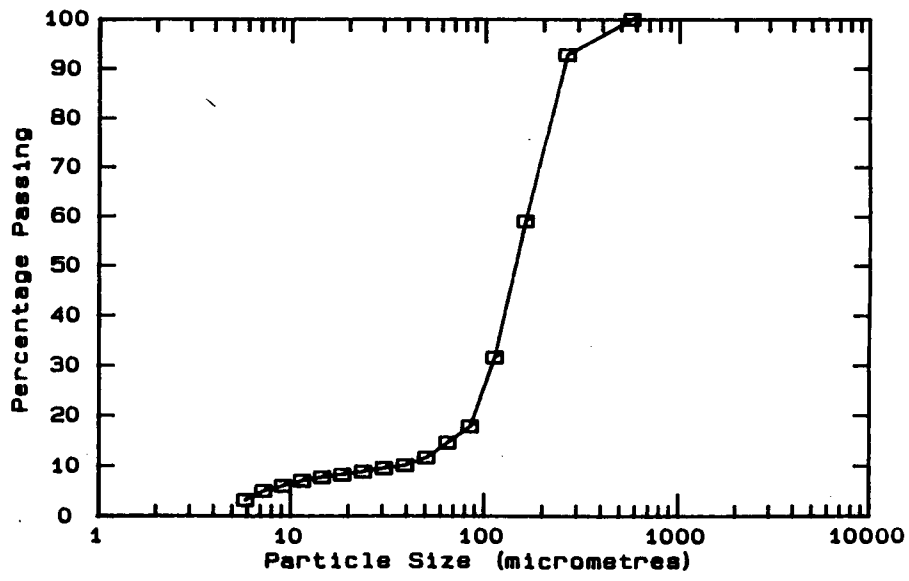

DATA FILE : ED40D69U

Test Facility	UCT 40 mm NB
Test Date	August 1990
Material Description	East Driefontein CCT
Material Relative Density	2.65
Slurry Relative Density	1.69
Solids Volumetric Concentration (%)	41.82
Solids Mass Concentration (%)	65.57
Mean Slurry Temperature (°C)	23.3
Pipe Internal Diameter (mm)	40.00
Pipe Roughness (μm)	52.0
Pipeline Slope	Vertical Down

Mixture Velocity (m/s)	Pressure Gradient (kPa/m)	Slurry Temp. (°C)
3.942	- 8.904	23.5
3.646	- 9.479	23.5
3.957	- 8.505	23.5
3.963	- 8.501	23.5
3.961	- 8.522	23.6
3.251	-11.376	23.6
3.233	-10.958	23.6
3.252	-11.339	23.5
3.221	-11.204	23.5
2.479	-14.033	23.3
2.452	-13.670	23.2
2.295	-14.502	23.2
2.942	-11.915	23.2
2.953	-12.169	23.2
2.951	-12.087	23.1
2.175	-14.673	23.0
2.112	-14.719	23.0
2.115	-14.558	22.9
2.107	-14.667	22.9

Particle Size Distribution
Malvern Particle Size Analyser

Size (μm)	% Passing	% Retained
564.0	100.0	.0
261.6	91.8	8.2
160.4	57.6	34.2
112.8	27.1	30.5
84.3	15.9	11.2
64.6	12.0	3.9
50.2	8.1	3.9
39.0	7.0	1.1
30.3	6.5	.5
23.7	5.8	.7
18.5	5.3	.5
14.5	4.9	.4
11.4	4.3	.6
9.1	3.6	.7
7.2	3.0	.6
5.8	1.9	1.1
Pan	- .0	1.9

OBSERVED FLOW BEHAVIOUR

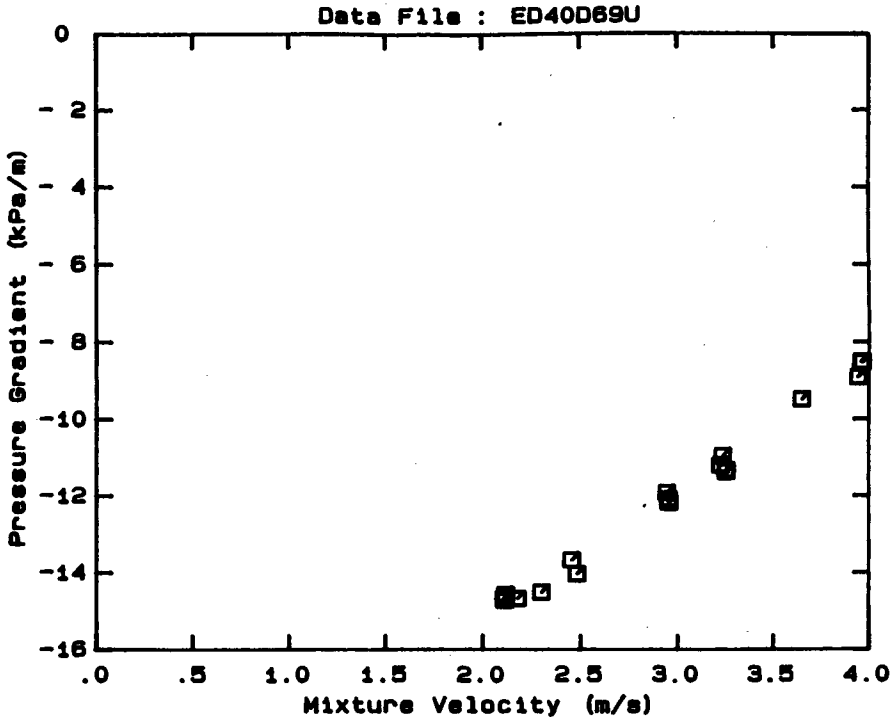

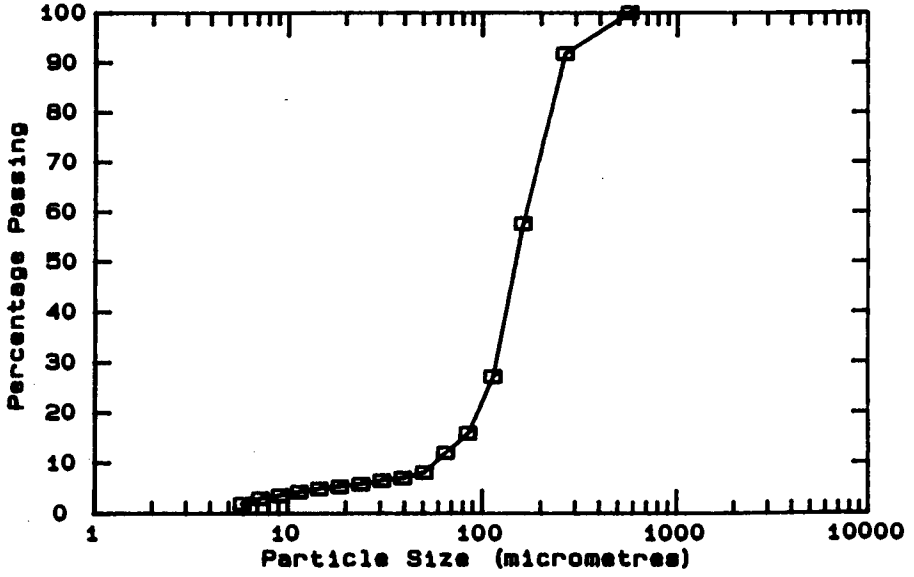

DATA FILE : ED40D72U

Test Facility	UCT 40 mm NB
Test Date	August 1990
Material Description	East Driefontein CCT
Material Relative Density	2.65
Slurry Relative Density	1.72
Solids Volumetric Concentration (%)	43.64
Solids Mass Concentration (%)	67.23
Mean Slurry Temperature (°C)	23.8
Pipe Internal Diameter (mm)	40.00
Pipe Roughness (μm)	52.0
Pipeline Slope	Vertical Down

Mixture Velocity (m/s)	Pressure Gradient (kPa/m)	Slurry Temp. (°C)
3.733	-11.242	23.6
3.736	-11.337	23.6
3.772	-11.047	23.7
3.784	-11.453	23.8
3.211	-12.489	24.1
3.204	-12.488	24.1
3.208	-12.176	24.1
3.213	-12.551	24.1
2.667	-13.237	24.1
2.654	-13.295	24.1
2.653	-13.428	24.1
2.660	-13.330	24.1
2.168	-14.262	23.9
2.174	-14.012	23.9
2.124	-14.216	23.9
2.138	-14.004	23.8
1.603	-14.773	23.7
1.601	-14.886	23.6
1.534	-14.969	23.6
1.048	-15.393	23.4
1.022	-15.323	23.4
1.014	-15.306	23.3
.993	-15.319	23.2

Particle Size Distribution
Malvern Particle Size Analyser

Size (μm)	% Passing	% Retained
564.0	100.0	.0
261.6	92.9	7.1
160.4	59.7	33.2
112.8	32.0	27.7
84.3	18.3	13.7
64.6	15.0	3.3
50.2	11.5	3.5
39.0	10.0	1.5
30.3	9.5	.5
23.7	8.7	.8
18.5	8.1	.6
14.5	7.6	.5
11.4	6.8	.8
9.1	5.7	1.1
7.2	4.7	1.0
5.8	3.0	1.7
Pan	- .1	3.1

OBSERVED FLOW BEHAVIOUR

Velocity (m/s)	Observation (D = 46.0 mm)

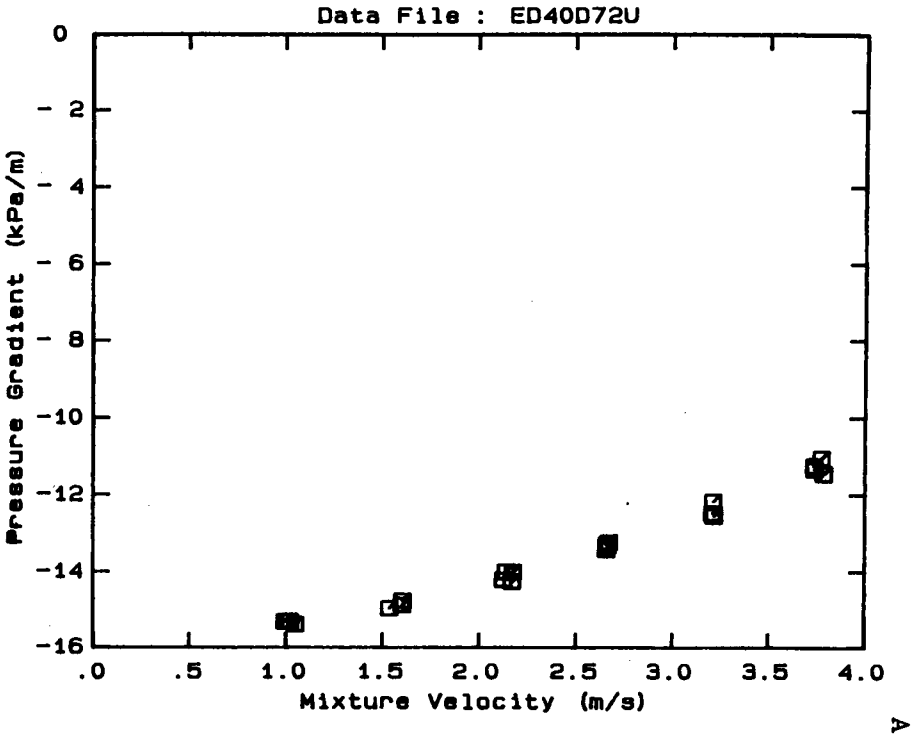

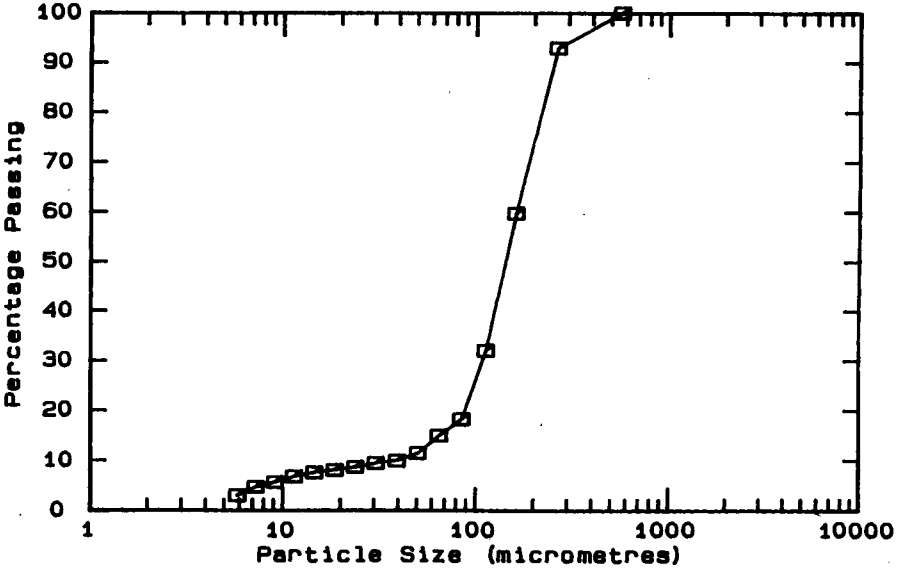

DATA FILE : ED40D75U

Test Facility	UCT 40 mm NB
Test Date	August 1990
Material Description	East Driefontein CCT
Material Relative Density	2.65
Slurry Relative Density	1.75
Solids Volumetric Concentration (%)	45.45
Solids Mass Concentration (%)	68.83
Mean Slurry Temperature (°C)	23.2
Pipe Internal Diameter (mm)	40.00
Pipe Roughness (μm)	52.0
Pipeline Slope	Vertical Down

Mixture Velocity (m/s)	Pressure Gradient (kPa/m)	Slurry Temp. (°C)
3.291	-10.135	22.4
3.298	-10.404	22.6
3.312	-10.212	22.7
3.313	-10.658	22.8
3.334	-10.426	23.0
2.711	-11.775	23.3
2.704	-11.675	23.3
2.697	-11.442	23.4
2.704	-11.692	23.4
2.132	-12.695	23.5
2.120	-12.566	23.5
2.148	-12.519	23.5
2.148	-12.632	23.5
1.615	-14.081	23.4
1.604	-13.999	23.4
1.613	-13.875	23.4
1.614	-13.999	23.3
1.031	-14.858	23.2
1.021	-14.883	23.2
1.016	-14.881	23.1
.969	-14.958	23.1

Particle Size Distribution
Malvern Particle Size Analyser

Size (μm)	% Passing	% Retained
564.0	100.0	.0
261.6	93.1	6.9
160.4	59.1	34.0
112.8	29.2	29.9
84.3	17.6	11.6
64.6	14.2	3.4
50.2	10.3	3.9
39.0	9.1	1.2
30.3	8.7	.4
23.7	7.9	.8
18.5	7.3	.6
14.5	6.9	.4
11.4	6.2	.7
9.1	5.3	.9
7.2	4.5	.8
5.8	3.0	1.5
Pan	.2	2.8

OBSERVED FLOW BEHAVIOUR

Velocity (m/s)	Observation (D = 46.0 mm)

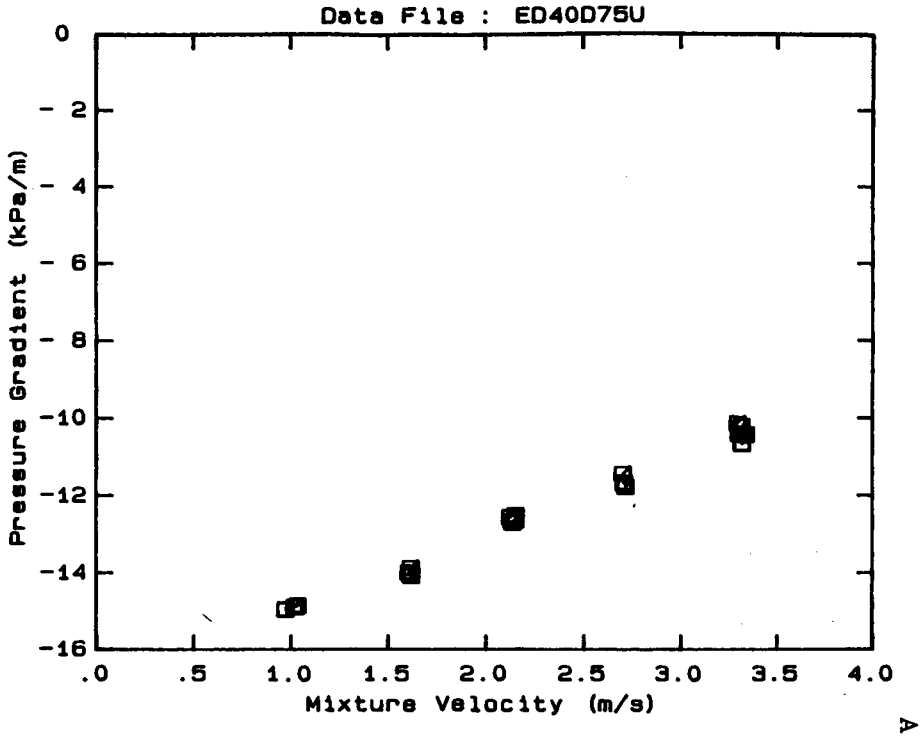

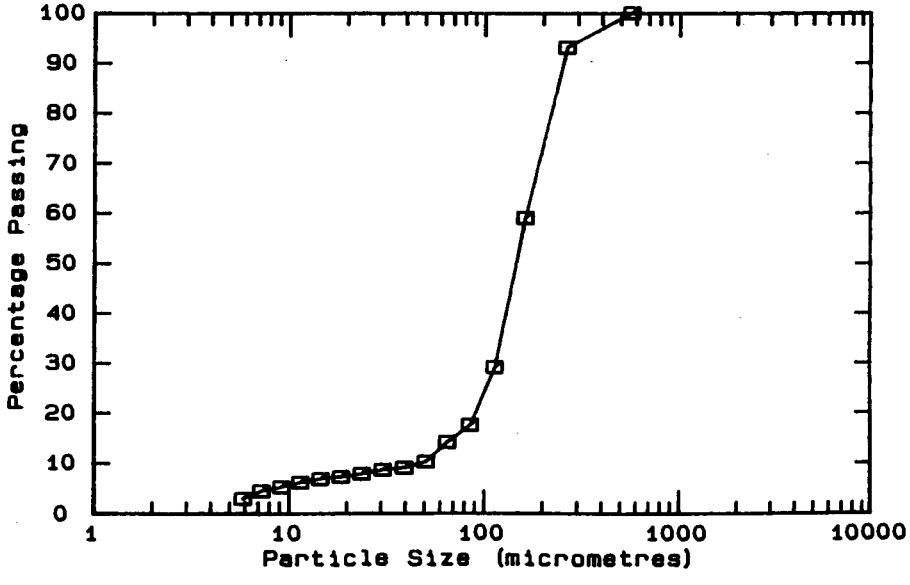

DATA FILE : ED40D79U

Test Facility	UCT 40 mm NB
Test Date	August 1990
Material Description	East Driefontein CCT
Material Relative Density	2.65
Slurry Relative Density	1.79
Solids Volumetric Concentration (%)	47.88
Solids Mass Concentration (%)	70.88
Mean Slurry Temperature (°C)	23.7
Pipe Internal Diameter (mm)	40.00
Pipe Roughness (μm)	52.0
Pipeline Slope	Vertical Down

Mixture Velocity (m/s)	Pressure Gradient (kPa/m)	Slurry Temp. (°C)
2.691	- 9.949	22.6
2.718	-10.220	22.9
2.720	-10.083	23.1
2.726	-10.240	23.3
2.720	- 9.965	23.4
2.136	-11.371	23.9
2.147	-11.431	23.9
2.155	-11.466	24.0
2.148	-11.707	24.0
1.585	-12.710	24.1
1.589	-12.736	24.1
1.725	-12.600	24.1
1.601	-12.646	24.1
1.591	-12.802	24.0
1.076	-13.969	24.0
1.056	-13.956	24.0
1.048	-13.995	23.9
1.037	-13.933	23.9
.593	-12.029	23.8
.604	-15.421	23.7
.596	-14.434	23.7
.595	-13.782	23.7
.565	-13.719	23.6
.529	-13.551	23.6
.520	-13.568	23.5
.507	-13.398	23.5

Particle Size Distribution
Malvern Particle Size Analyser

Size (μm)	% Passing	% Retained
564.0	100.0	.0
261.6	94.2	5.8
160.4	59.1	35.1
112.8	29.2	29.9
84.3	17.2	12.0
64.6	13.5	3.7
50.2	9.9	3.6
39.0	8.9	1.0
30.3	8.4	.5
23.7	7.6	.8
18.5	7.1	.5
14.5	6.7	.4
11.4	6.0	.7
9.1	5.1	.9
7.2	4.3	.8
5.8	2.8	1.5
Pan	.0	2.8

OBSERVED FLOW BEHAVIOUR

Velocity (m/s)	Observation (D = 46.0 mm)

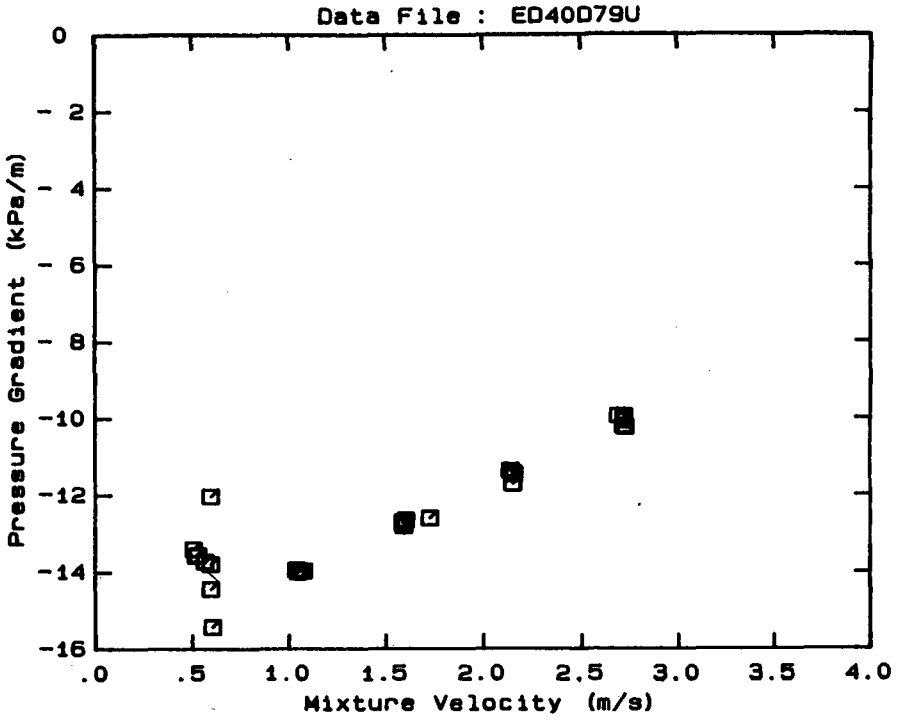

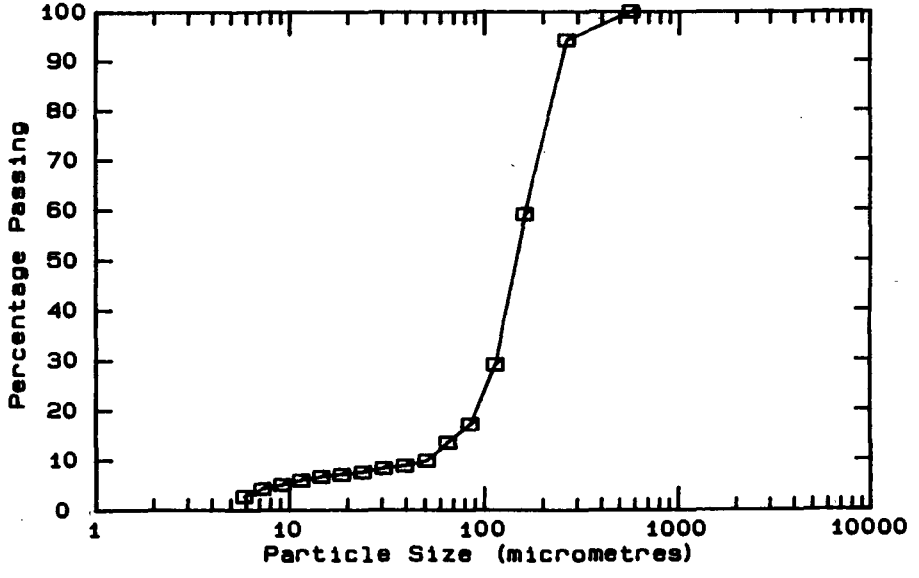

DATA FILE : ED40D82U

Test Facility	UCT 40 mm NB
Test Date	August 1990
Material Description	East Driefontein CCT
Material Relative Density	2.65
Slurry Relative Density	1.82
Solids Volumetric Concentration (%)	49.70
Solids Mass Concentration (%)	72.36
Mean Slurry Temperature (°C)	26.7
Pipe Internal Diameter (mm)	40.00
Pipe Roughness (μm)	52.0
Pipeline Slope	Vertical Down

Mixture Velocity (m/s)	Pressure Gradient (kPa/m)	Slurry Temp. (°C)
2.205	- 8.485	25.7
2.208	- 8.385	25.9
2.209	- 8.677	26.0
2.205	- 8.621	26.2
2.206	- 8.551	26.3
1.723	- 9.698	26.6
1.708	-10.101	26.8
1.706	-10.212	26.8
1.702	-10.115	26.8
1.704	-10.112	26.9
1.708	-10.073	26.9
1.256	-11.480	26.9
1.243	-11.418	27.0
1.218	-11.352	27.0
1.211	-11.588	26.9
1.202	-11.653	26.9
.828	-13.021	26.9
.809	-13.007	26.8
.811	-13.013	26.8
.798	-13.108	26.8
.396	-14.609	26.7
.364	-14.543	26.7
.345	-14.461	26.7
.305	-14.319	26.7

Particle Size Distribution
Malvern Particle Size Analyser

Size (μm)	% Passing	% Retained
564.0	100.0	.0
261.6	92.2	7.8
160.4	59.0	33.2
112.8	29.4	29.6
84.3	17.3	12.1
64.6	13.7	3.6
50.2	10.0	3.7
39.0	9.0	1.0
30.3	8.6	.4
23.7	7.8	.8
18.5	7.3	.5
14.5	6.9	.4
11.4	6.2	.7
9.1	5.3	.9
7.2	4.5	.8
5.8	3.0	1.5
Pan	.1	2.9

OBSERVED FLOW BEHAVIOUR

Velocity (m/s)	Observation (D = 46.0 mm)

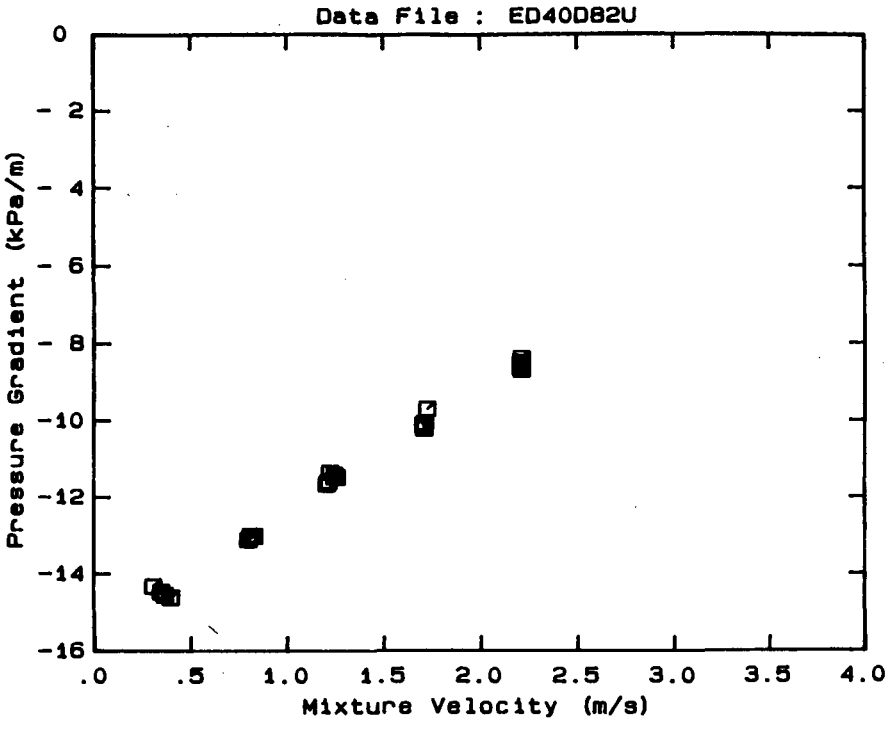

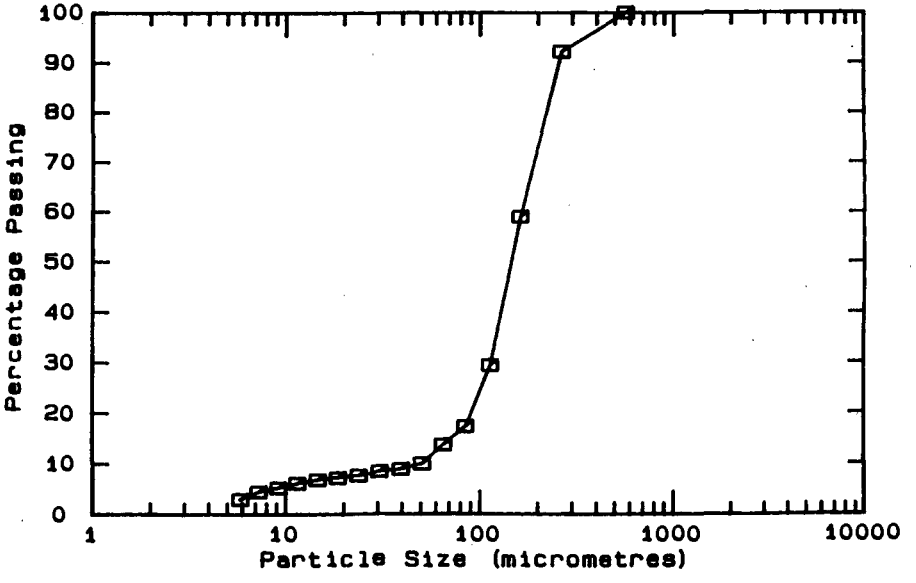

DATA FILE : ED80H59A

Test Facility	UCT 80 mm NB
Test Date	June 1990
Material Description	East Driefontein CCT
Material Relative Density	2.65
Slurry Relative Density	1.59
Solids Volumetric Concentration (%)	35.76
Solids Mass Concentration (%)	59.60
Mean Slurry Temperature (°C)	17.3
Pipe Internal Diameter (mm)	73.40
Pipe Roughness (μm)	84.0
Pipeline Slope	Horizontal

Mixture Velocity (m/s)	Pressure Gradient (kPa/m)	Slurry Temp. (°C)
3.447	2.603	17.0
3.475	2.862	17.1
3.478	2.730	17.3
3.500	2.741	17.3
3.491	2.717	17.4
2.951	1.965	17.5
2.951	2.129	17.5
2.952	2.169	17.5
2.959	2.089	17.5
2.486	1.629	17.5
2.491	1.589	17.5
2.485	1.537	17.5
2.001	1.549	17.4
2.000	1.477	17.4
2.001	1.254	17.4
1.465	.998	17.3
1.464	.966	17.3
1.462	.790	17.3
.994	.589	17.2
.990	.460	17.2
.999	.866	17.2
1.003	.969	17.2

Particle Size Distribution
Malvern Particle Size Analyser

Size (μm)	% Passing	% Retained
564.0	100.0	.0
261.6	93.1	6.9
160.4	57.8	35.3
112.8	25.8	32.0
84.3	13.4	12.4
64.6	10.0	3.4
50.2	6.9	3.1
39.0	5.4	1.5
30.3	4.8	.6
23.7	4.3	.5
18.5	3.9	.4
14.5	3.5	.4
11.4	3.1	.4
9.1	2.6	.5
7.2	2.1	.5
5.8	1.6	.5
Pan	.8	.8

OBSERVED FLOW BEHAVIOUR

Velocity (m/s)	Observation (D = 71.0 mm)
1.05	30% Stationary Bed
1.58	Pulses travelling thru.
2.14	Sliding particles - invert
2.66	Asymmetric
3.19	Appears homgeneous
3.75	Appears homogeneous

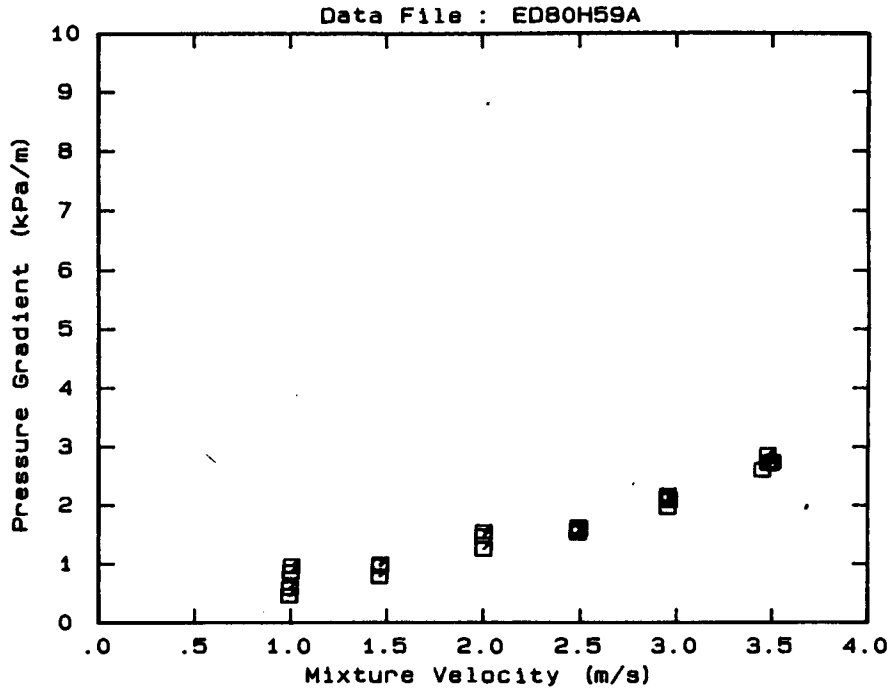

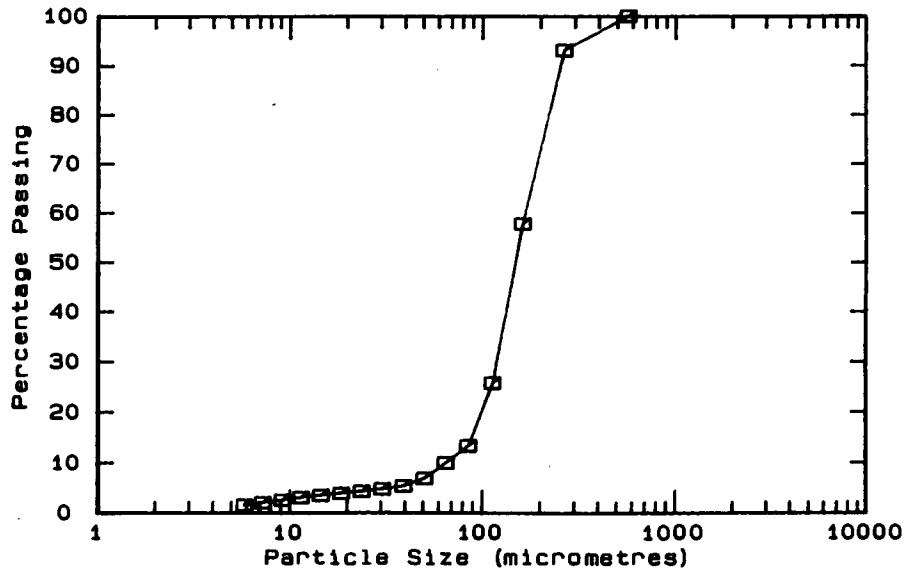

DATA FILE : ED80H59B

Test Facility	UCT 80 mm NB
Test Date	June 1990
Material Description	East Driefontein CCT
Material Relative Density	2.65
Slurry Relative Density	1.59
Solids Volumetric Concentration (%)	35.76
Solids Mass Concentration (%)	59.60
Mean Slurry Temperature (°C)	16.4
Pipe Internal Diameter (mm)	73.40
Pipe Roughness (μm)	84.0
Pipeline Slope	Horizontal

Mixture Velocity (m/s)	Pressure Gradient (kPa/m)	Slurry Temp. (°C)
3.406	2.866	15.9
3.414	2.998	16.0
3.425	2.269	16.1
3.413	3.028	16.1
3.414	2.817	16.2
2.937	2.160	16.3
2.933	2.183	16.4
2.939	2.295	16.4
2.622	2.303	16.5
2.623	2.092	16.5
2.623	1.790	16.5
2.304	1.448	16.5
2.303	1.525	16.5
2.303	1.454	16.5
1.992	1.537	16.6
1.997	1.046	16.5
1.995	1.090	16.5
1.501	1.007	16.5
1.507	.598	16.5
1.502	1.183	16.5
1.501	.589	16.5
1.048	.702	16.5
1.056	.653	16.5
1.051	.690	16.5

Particle Size Distribution
Malvern Particle Size Analyser

Size (μm)	% Passing	% Retained
564.0	100.0	.0
261.6	91.6	8.4
160.4	56.6	35.0
112.8	25.1	31.5
84.3	14.0	11.1
64.6	10.7	3.3
50.2	7.5	3.2
39.0	6.2	1.3
30.3	5.8	.4
23.7	5.4	.4
18.5	4.9	.5
14.5	4.5	.4
11.4	4.1	.4
9.1	3.5	.6
7.2	2.9	.6
5.8	1.9	1.0
Pan	.1	1.8

OBSERVED FLOW BEHAVIOUR

Velocity (m/s)	Observation (D = 71.0 mm)
1.12	20% Stationary Bed
1.61	Pulses, no clear bed
2.14	Sliding particles
2.45	Heter. and some slid. part
2.80	Asymmetric

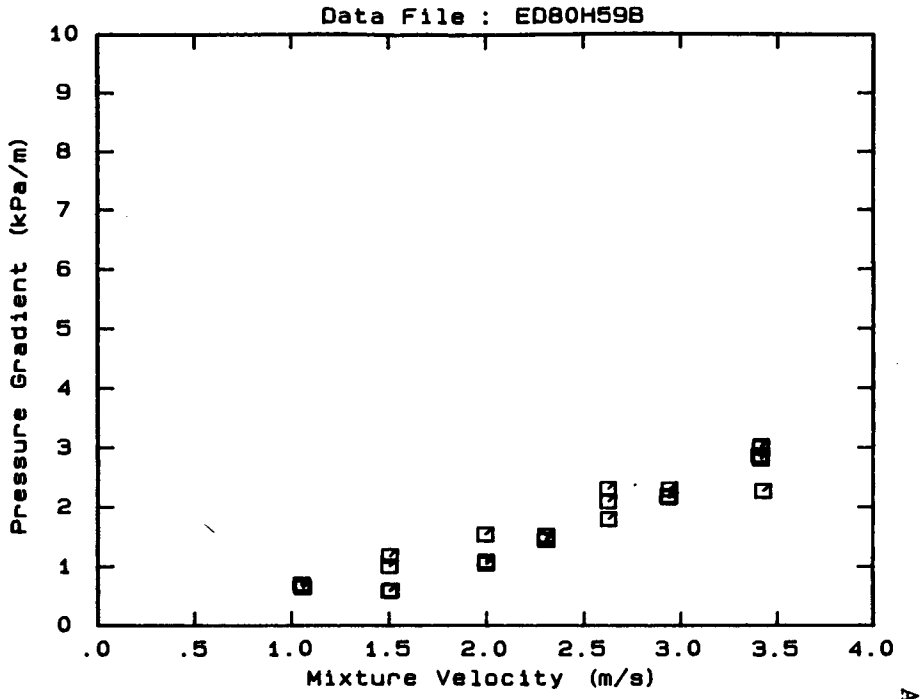

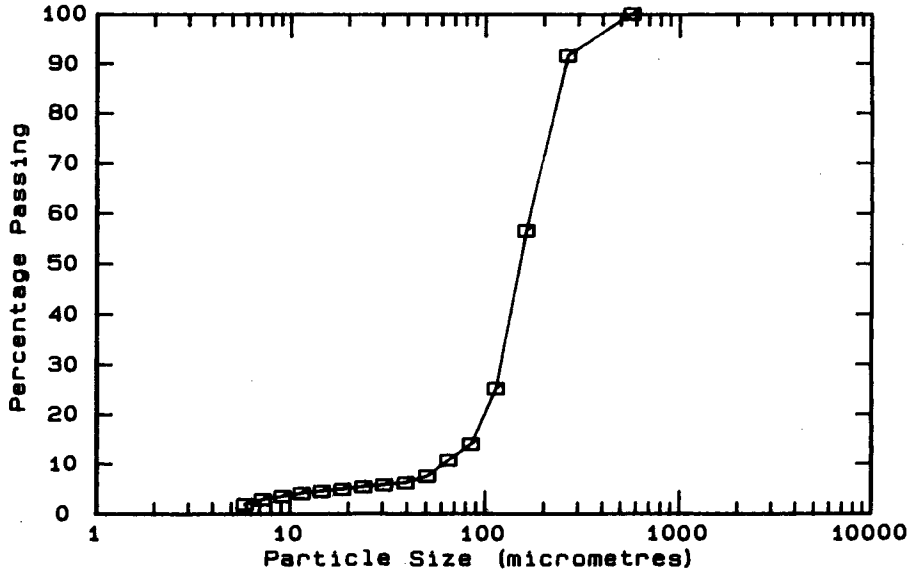

DATA FILE : ED80H68U

Test Facility	UCT 80 mm NB
Test Date	June 1990
Material Description	East Driefontein CCT
Material Relative Density	2.65
Slurry Relative Density	1.68
Solids Volumetric Concentration (%)	41.21
Solids Mass Concentration (%)	65.01
Mean Slurry Temperature (°C)	19.5
Pipe Internal Diameter (mm)	73.40
Pipe Roughness (μm)	84.0
Pipeline Slope	Horizontal

Mixture Velocity (m/s)	Pressure Gradient (kPa/m)	Slurry Temp. (°C)
3.415	3.060	19.2
3.420	3.147	19.3
3.416	3.230	19.4
2.969	3.212	19.6
2.972	2.438	19.7
2.962	2.671	19.8
2.959	2.350	19.8
2.465	1.835	19.9
2.467	1.820	19.9
2.466	1.894	19.8
2.012	1.365	19.7
2.007	1.544	19.7
2.006	1.248	19.7
2.005	1.700	19.6
1.494	.978	19.5
1.488	1.077	19.5
1.496	.861	19.5
1.494	1.087	19.4
1.025	.983	19.3
1.024	1.368	19.3
1.025	1.666	19.3
1.030	1.830	19.3
1.030	1.650	19.2

Particle Size Distribution
Malvern Particle Size Analyser

Size (μm)	% Passing	% Retained
564.0	100.0	.0
261.6	92.0	8.0
160.4	56.5	35.5
112.8	26.1	30.4
84.3	15.4	10.7
64.6	12.0	3.4
50.2	8.2	3.8
39.0	7.1	1.1
30.3	6.8	.3
23.7	6.0	.8
18.5	5.4	.6
14.5	5.1	.3
11.4	4.6	.5
9.1	3.8	.8
7.2	3.1	.7
5.8	2.0	1.1
Pan	.0	2.0

OBSERVED FLOW BEHAVIOUR

Velocity (m/s)	Observation (D = 71.0 mm)
1.09	30% Stationary Bed
1.58	Pulses travelling thru.
2.17	Asymmetric - slid.part.
2.63	Asymmetric
3.19	Appears homgeneous
3.68	Appears homogeneous

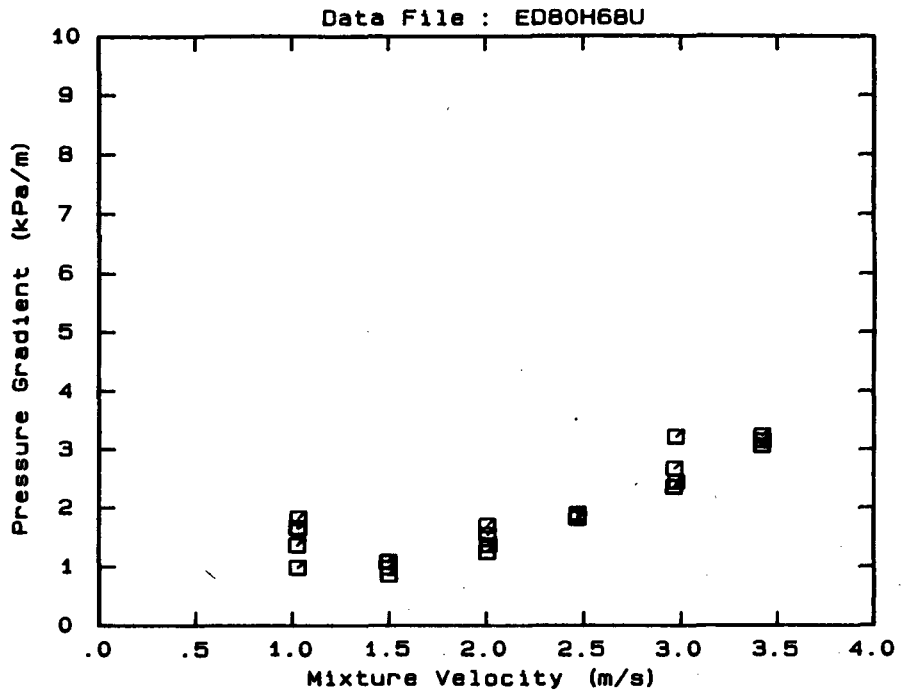

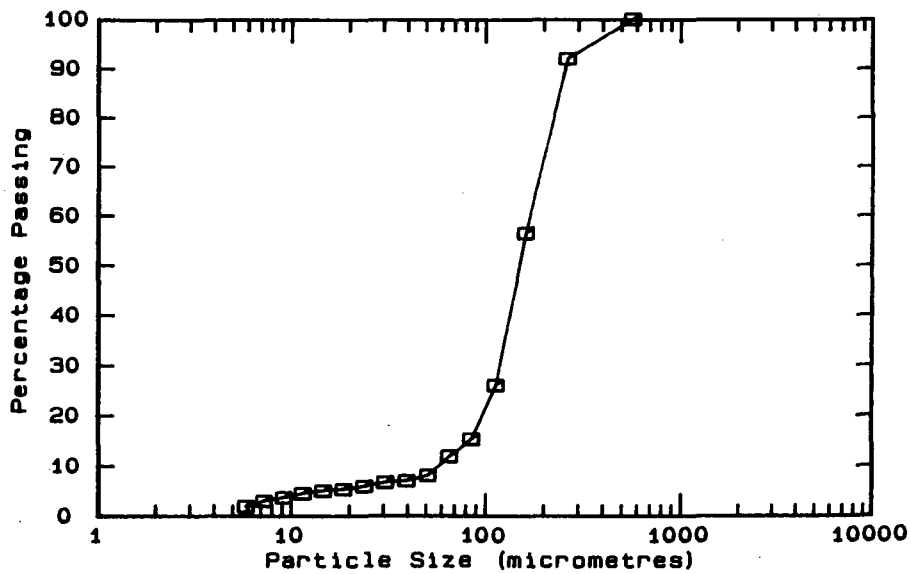

DATA FILE : ED80H70U

Test Facility	UCT 80 mm NB
Test Date	June 1990
Material Description	East Driefontein CCT
Material Relative Density	2.65
Slurry Relative Density	1.70
Solids Volumetric Concentration (%)	42.42
Solids Mass Concentration (%)	66.13
Mean Slurry Temperature (°C)	18.9
Pipe Internal Diameter (mm)	73.40
Pipe Roughness (μm)	84.0
Pipeline Slope	Horizontal

Mixture Velocity (m/s)	Pressure Gradient (kPa/m)	Slurry Temp. (°C)
3.447	3.145	18.4
3.447	3.188	18.5
3.457	3.531	18.6
3.461	3.563	18.7
3.456	3.461	18.8
2.931	2.431	18.9
2.931	2.402	19.0
2.935	2.565	19.0
2.933	2.191	19.0
2.478	2.028	19.1
2.487	2.019	19.1
2.481	2.210	19.1
1.951	1.474	19.1
1.956	.800	19.1
1.956	.919	19.1
1.958	1.166	19.1
1.954	1.105	19.0
1.513	.716	19.0
1.538	1.312	19.0
1.537	1.289	19.0
1.537	1.742	19.0
1.535	1.635	18.9
1.543	2.233	18.9
1.534	2.038	18.9
1.011	2.401	18.9
1.000	2.419	18.9
1.002	2.852	18.8

Particle Size Distribution
Malvern Particle Size Analyser

Size (μm)	% Passing	% Retained
564.0	100.0	.0
261.6	91.4	8.6
160.4	56.5	34.9
112.8	26.8	29.7
84.3	14.9	11.9
64.6	12.0	2.9
50.2	8.7	3.3
39.0	7.3	1.4
30.3	6.9	.4
23.7	6.4	.5
18.5	5.8	.6
14.5	5.4	.4
11.4	4.9	.5
9.1	4.1	.8
7.2	3.4	.7
5.8	2.2	1.2
Pan	- .0	2.2

OBSERVED FLOW BEHAVIOUR

Velocity (m/s)	Observation (D = 71.0 mm)
1.61	10% stationary bed-pulses
2.10	Asymetric - slid. part.
2.66	Asymmetric - pulses
3.15	Asymmetric
3.71	Appears homogeneous

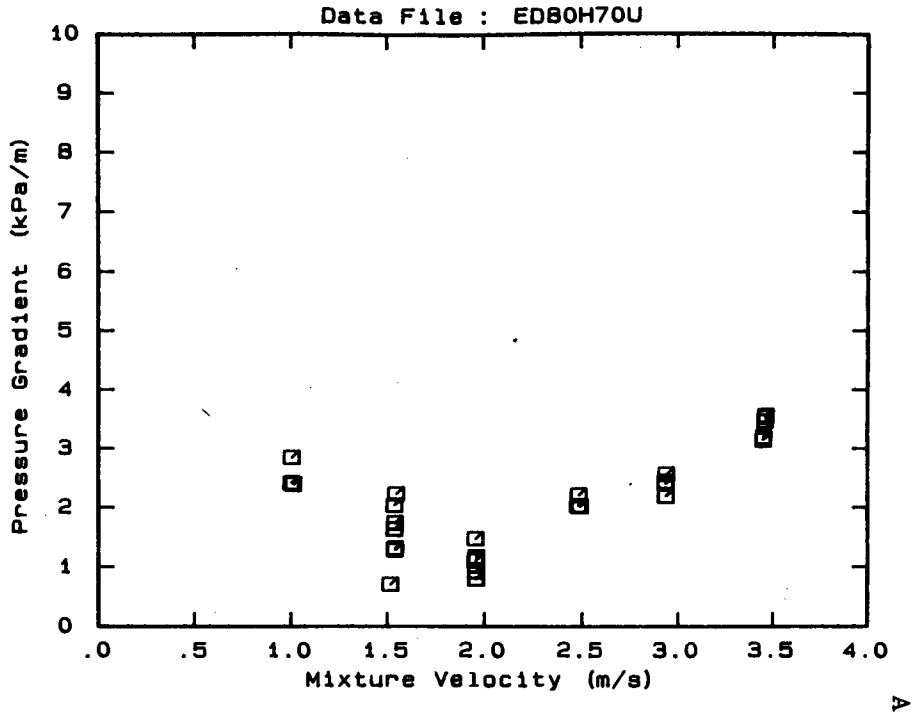

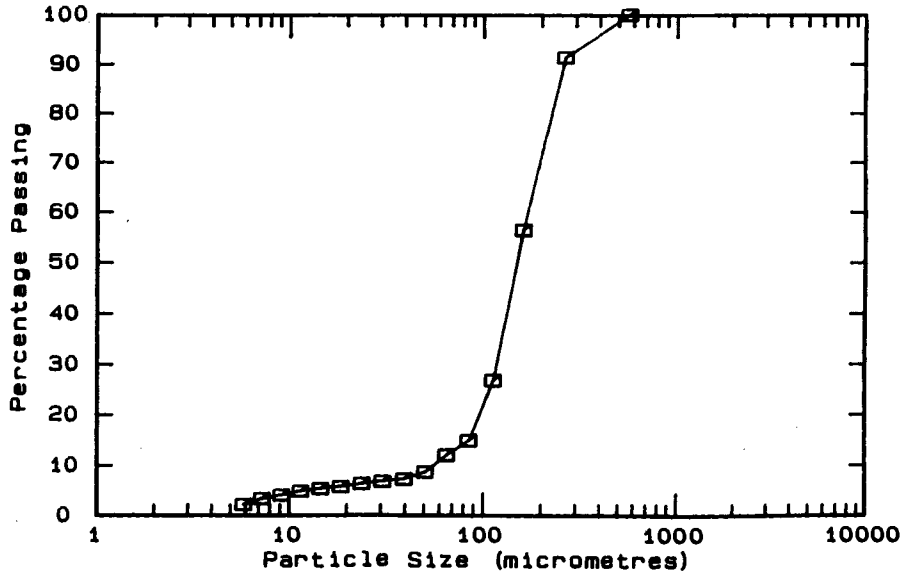

DATA FILE : ED80H71U

Test Facility	UCT 80 mm NB
Test Date	June 1990
Material Description	East Driefontein CCT
Material Relative Density	2.65
Slurry Relative Density	1.71
Solids Volumetric Concentration (%)	43.03
Solids Mass Concentration (%)	66.68
Mean Slurry Temperature (°C)	17.8
Pipe Internal Diameter (mm)	73.40
Pipe Roughness (μm)	84.0
Pipeline Slope	Horizontal

Mixture Velocity (m/s)	Pressure Gradient (kPa/m)	Slurry Temp. (°C)
3.425	3.417	16.9
3.440	3.337	17.0
3.465	3.690	17.1
3.472	3.319	17.2
2.918	2.561	17.7
2.915	2.383	17.8
2.913	2.374	17.8
2.924	2.305	17.8
2.436	1.923	17.9
2.432	1.733	17.9
2.439	1.951	18.0
2.438	1.826	18.0
1.987	1.692	18.0
2.000	1.379	18.0
1.998	1.732	18.0
1.993	1.695	18.0
1.489	.909	18.0
1.518	.296	17.9
1.510	.904	17.9
1.527	.735	17.9
1.106	2.074	17.9
1.113	2.385	17.9
1.102	2.556	17.9
1.114	2.186	17.9

Particle Size Distribution
Malvern Particle Size Analyser

Size (μm)	% Passing	% Retained
564.0	100.0	.0
261.6	93.6	6.4
160.4	58.7	34.9
112.8	27.1	31.6
84.3	15.9	11.2
64.6	12.8	3.1
50.2	8.9	3.9
39.0	7.7	1.2
30.3	7.3	.4
23.7	6.5	.8
18.5	5.9	.6
14.5	5.5	.4
11.4	4.9	.6
9.1	4.1	.8
7.2	3.4	.7
5.8	2.2	1.2
Pan	- .0	2.2

OBSERVED FLOW BEHAVIOUR

Velocity (m/s)	Observation (D = 71.0 mm)
1.58	Stat bed moves with pulses
2.14	Slid particles - pulses
2.63	Asymmetric - pulses
3.15	Appears homogeneous
3.71	Appears homogeneous

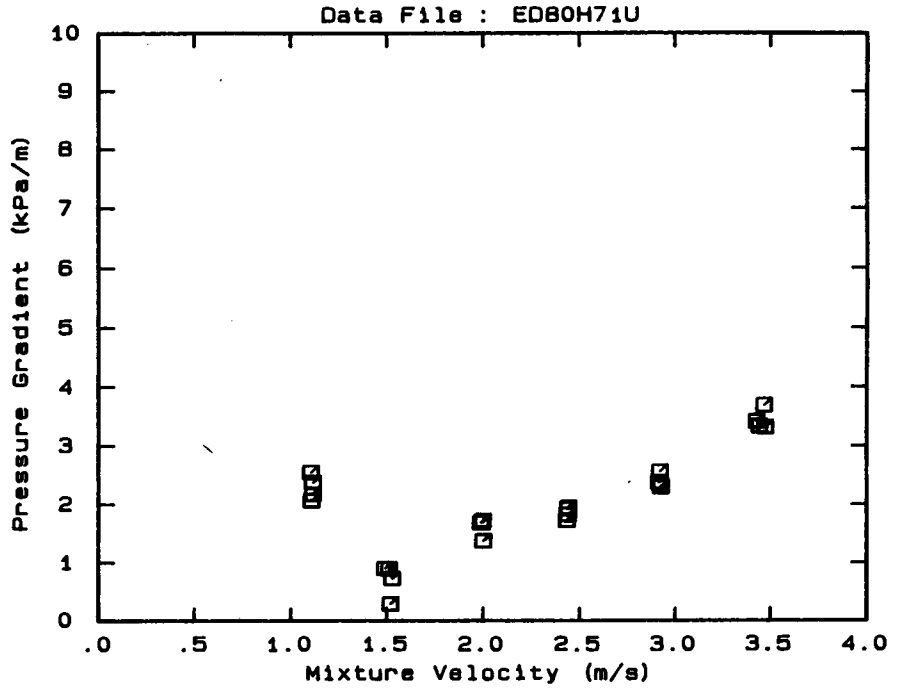

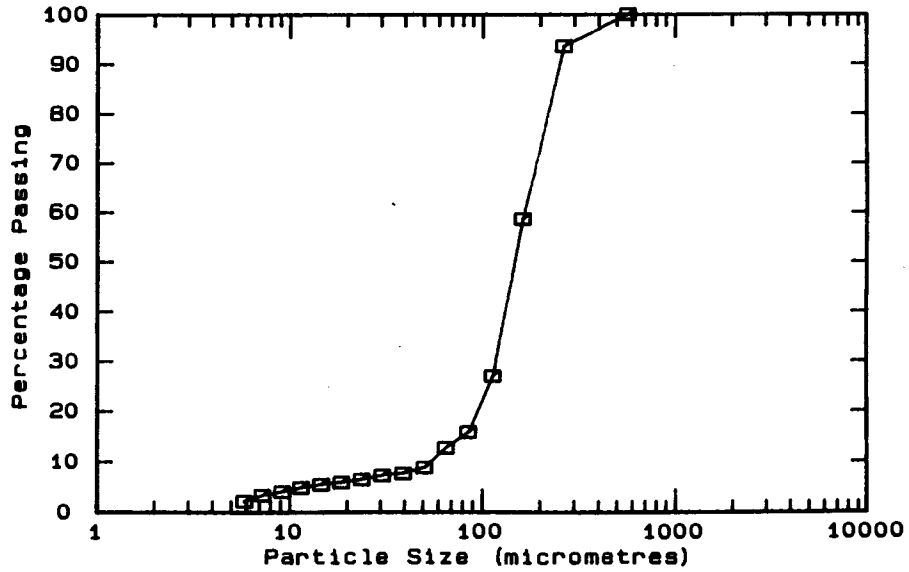

DATA FILE : ED80H79U

Test Facility	UCT 80 mm NB
Test Date	June 1990
Material Description	East Driefontein CCT
Material Relative Density	2.65
Slurry Relative Density	1.79
Solids Volumetric Concentration (%)	47.88
Solids Mass Concentration (%)	70.88
Mean Slurry Temperature (°C)	21.7
Pipe Internal Diameter (mm)	73.40
Pipe Roughness (μm)	84.0
Pipeline Slope	Horizontal

Mixture Velocity (m/s)	Pressure Gradient (kPa/m)	Slurry Temp. (°C)
3.374	3.809	20.0
3.346	3.755	20.2
3.315	3.839	20.4
3.287	3.994	20.6
3.280	3.791	20.7
3.247	3.603	20.9
3.208	3.701	21.0
3.128	3.814	21.1
3.048	3.279	21.8
3.052	3.310	21.9
3.062	3.228	21.9
2.539	3.752	22.0
2.546	3.287	22.2
2.548	3.028	22.2
2.553	2.784	22.3
2.556	2.700	22.3
2.087	2.627	22.3
2.084	2.496	22.3
2.091	2.471	22.3
1.547	3.225	22.2
1.563	2.139	22.2
1.536	2.966	22.1
1.550	2.612	22.1
1.547	2.512	22.1
1.546	2.464	22.0
1.031	2.682	21.9
1.068	2.785	21.9
1.065	2.566	21.9
1.055	2.832	21.8
1.074	2.745	21.8
1.068	2.876	21.8
1.079	2.703	21.7

Particle Size Distribution
Malvern Particle Size Analyser

Size (μm)	% Passing	% Retained
564.0	100.0	.0
261.6	92.3	7.7
160.4	58.3	34.0
112.8	28.4	29.9
84.3	16.9	11.5
64.6	13.8	3.1
50.2	10.3	3.5
39.0	9.0	1.3
30.3	8.6	.4
23.7	7.8	.8
18.5	7.1	.7
14.5	6.7	.4
11.4	6.0	.7
9.1	5.0	1.0
7.2	4.1	.9
5.8	2.6	1.5
Pan	- .2	2.8

OBSERVED FLOW BEHAVIOUR

Velocity (m/s)	Observation (D = 71.0 mm)
1.09	45% Stationary bed
1.61	Asymmetric
2.24	Appears homogeneous
2.73	Appears homogeneous
3.22	Appears homogeneous
3.54	Appears homogeneous

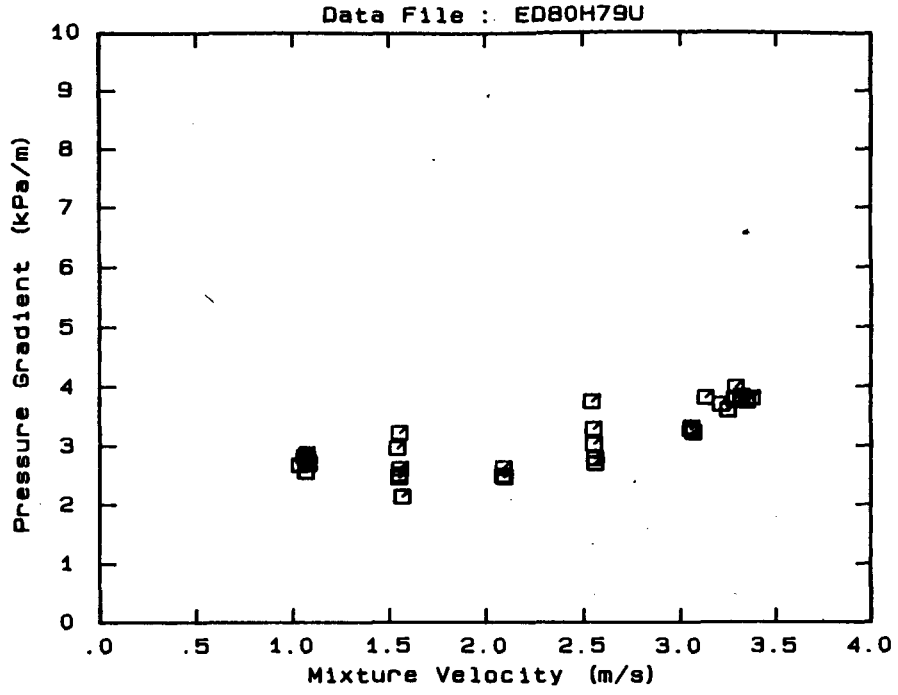

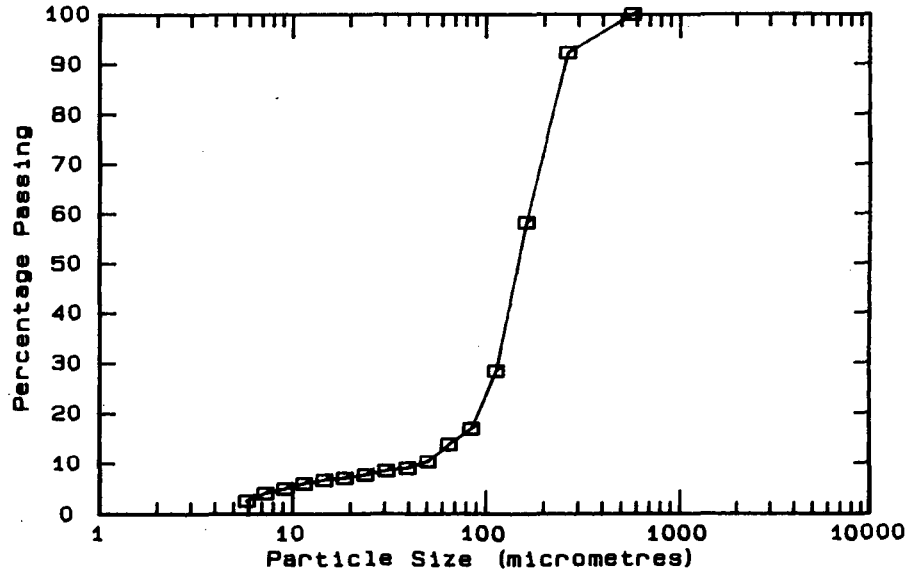

DATA FILE : ED80D59A

Test Facility	UCT 80 mm NB
Test Date	June 1990
Material Description	East Driefontein CCT
Material Relative Density	2.65
Slurry Relative Density	1.59
Solids Volumetric Concentration (%)	35.76
Solids Mass Concentration (%)	59.60
Mean Slurry Temperature (°C)	17.3
Pipe Internal Diameter (mm)	73.40
Pipe Roughness (μm)	84.0
Pipeline Slope	Vertical Down

Mixture Velocity (m/s)	Pressure Gradient (kPa/m)	Slurry Temp. (°C)
3.447	-12.443	17.0
3.475	-12.474	17.1
3.478	-12.362	17.3
3.500	-12.422	17.3
3.491	-12.485	17.4
2.951	-13.236	17.5
2.951	-13.079	17.5
2.952	-13.134	17.5
2.959	-12.876	17.5
2.486	-13.727	17.5
2.491	-13.735	17.5
2.485	-13.750	17.5
2.001	-14.119	17.4
2.000	-14.117	17.4
2.001	-14.122	17.4
1.465	-14.576	17.3
1.464	-14.582	17.3
1.462	-14.589	17.3
.994	-14.755	17.2
.990	-14.955	17.2
.999	-14.964	17.2
1.003	-14.902	17.2

Particle Size Distribution
Malvern Particle Size Analyser

Size (μm)	% Passing	% Retained
564.0	100.0	.0
261.6	93.1	6.9
160.4	57.8	35.3
112.8	25.8	32.0
84.3	13.4	12.4
64.6	10.0	3.4
50.2	6.9	3.1
39.0	5.4	1.5
30.3	4.8	.6
23.7	4.3	.5
18.5	3.9	.4
14.5	3.5	.4
11.4	3.1	.4
9.1	2.6	.5
7.2	2.1	.5
5.8	1.6	.5
Pan	.8	.8

OBSERVED FLOW BEHAVIOUR

Velocity (m/s)	Observation (D = 71.0 mm)

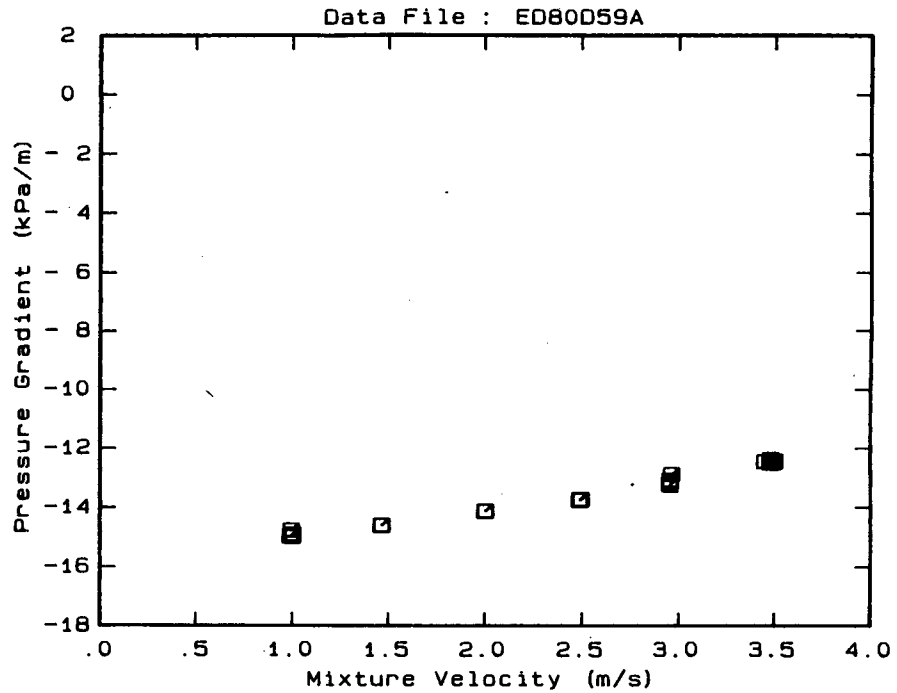

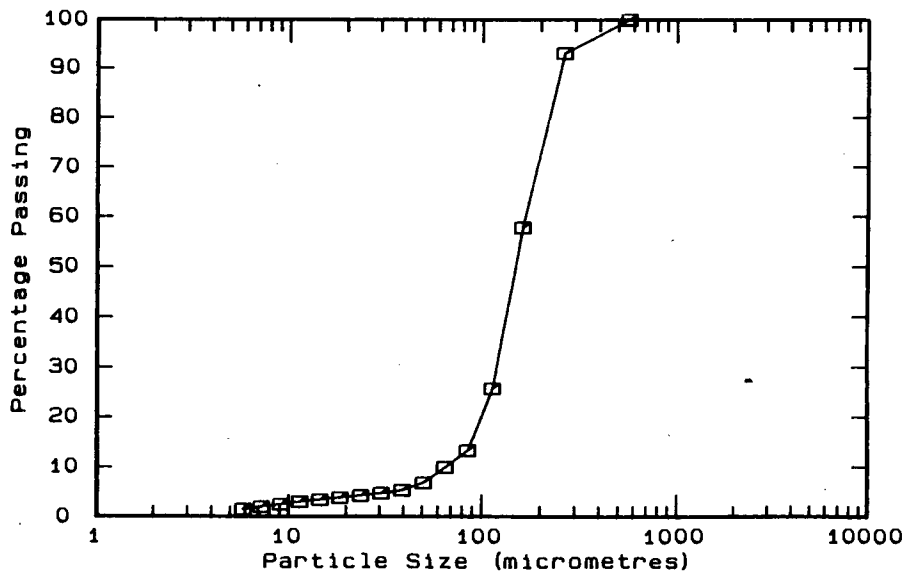

DATA FILE : ED80D59B

Test Facility	UCT 80 mm NB
Test Date	June 1990
Material Description	East Driefontein CCT
Material Relative Density	2.65
Slurry Relative Density	1.59
Solids Volumetric Concentration (%)	35.76
Solids Mass Concentration (%)	59.60
Mean Slurry Temperature (°C)	16.4
Pipe Internal Diameter (mm)	73.40
Pipe Roughness (μm)	84.0
Pipeline Slope	Vertical Down

Mixture Velocity (m/s)	Pressure Gradient (kPa/m)	Slurry Temp. (°C)
3.406	-12.483	15.9
3.414	-12.686	16.0
3.425	-12.291	16.1
3.413	-12.321	16.1
3.414	-12.572	16.2
2.937	-13.241	16.3
2.933	-13.207	16.4
2.939	-13.245	16.4
2.622	-13.786	16.5
2.623	-13.800	16.5
2.623	-13.508	16.5
2.304	-14.089	16.5
2.303	-14.072	16.5
2.303	-14.051	16.5
1.992	-14.379	16.6
1.997	-14.307	16.5
1.995	-14.371	16.5
1.501	-14.883	16.5
1.507	-14.747	16.5
1.502	-14.560	16.5
1.501	-14.717	16.5
1.048	-15.245	16.5
1.056	-15.127	16.5
1.051	-15.149	16.5

Particle Size Distribution
Malvern Particle Size Analyser

Size (μm)	% Passing	% Retained
564.0	100.0	.0
261.6	91.6	8.4
160.4	56.6	35.0
112.8	25.1	31.5
84.3	14.0	11.1
64.6	10.7	3.3
50.2	7.5	3.2
39.0	6.2	1.3
30.3	5.8	.4
23.7	5.4	.4
18.5	4.9	.5
14.5	4.5	.4
11.4	4.1	.4
9.1	3.5	.6
7.2	2.9	.6
5.8	1.9	1.0
Pan	.1	1.8

OBSERVED FLOW BEHAVIOUR

Velocity (m/s)	Observation (D = 71.0 mm)

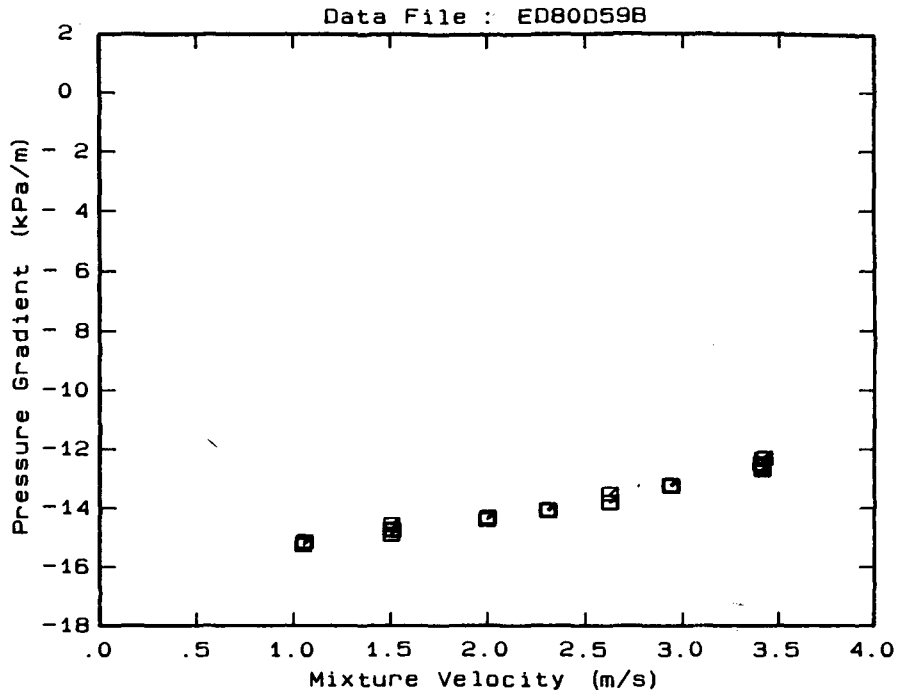

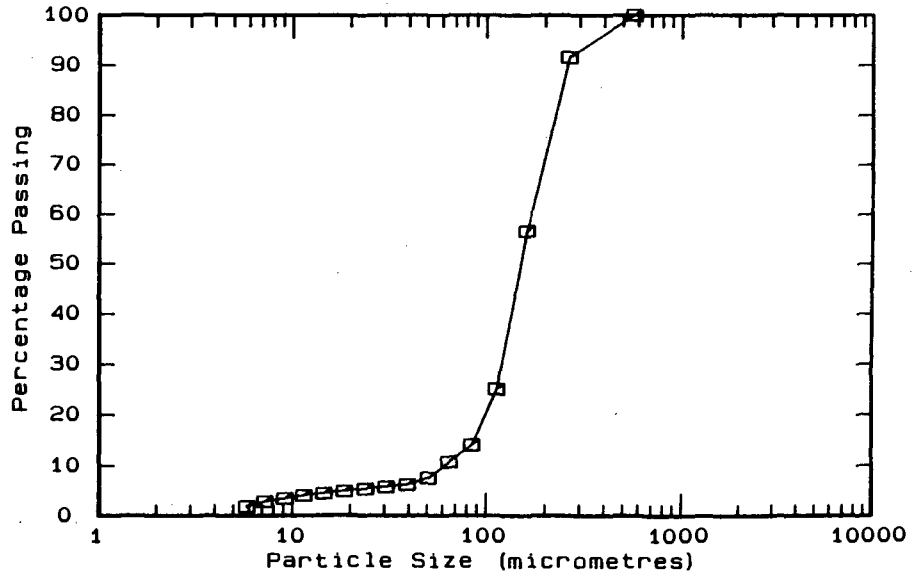

DATA FILE : ED80D68U

Test Facility	UCT 80 mm NB
Test Date	June 1990
Material Description	East Driefontein CCT
Material Relative Density	2.65
Slurry Relative Density	1.68
Solids Volumetric Concentration (%)	41.21
Solids Mass Concentration (%)	65.01
Mean Slurry Temperature (°C)	19.5
Pipe Internal Diameter (mm)	73.40
Pipe Roughness (μm)	84.0
Pipeline Slope	Vertical Down

Mixture Velocity (m/s)	Pressure Gradient (kPa/m)	Slurry Temp. (°C)
3.415	-12.805	19.2
3.420	-12.783	19.3
3.416	-12.835	19.4
2.969	-13.534	19.6
2.972	-13.403	19.7
2.962	-13.420	19.8
2.959	-13.366	19.8
2.465	-14.261	19.9
2.467	-14.243	19.9
2.466	-14.256	19.8
2.012	-14.999	19.7
2.007	-14.799	19.7
2.006	-14.952	19.7
2.005	-15.001	19.6
1.494	-15.470	19.5
1.488	-15.363	19.5
1.496	-15.560	19.5
1.494	-15.552	19.4
1.025	-15.764	19.3
1.024	-15.753	19.3
1.025	-15.718	19.3
1.030	-15.855	19.3
1.030	-15.832	19.2

Particle Size Distribution
Malvern Particle Size Analyser

Size (μm)	% Passing	% Retained
564.0	100.0	.0
261.6	92.0	8.0
160.4	56.5	35.5
112.8	26.1	30.4
84.3	15.4	10.7
64.6	12.0	3.4
50.2	8.2	3.8
39.0	7.1	1.1
30.3	6.8	.3
23.7	6.0	.8
18.5	5.4	.6
14.5	5.1	.3
11.4	4.6	.5
9.1	3.8	.8
7.2	3.1	.7
5.8	2.0	1.1
Pan	.0	2.0

OBSERVED FLOW BEHAVIOUR

Velocity (m/s)	Observation (D = 71.0 mm)

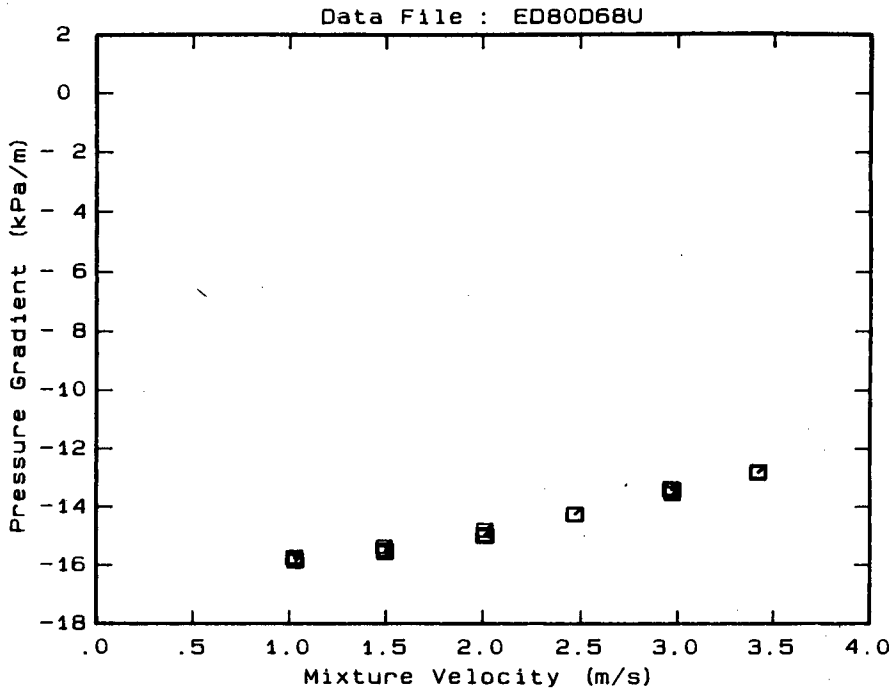

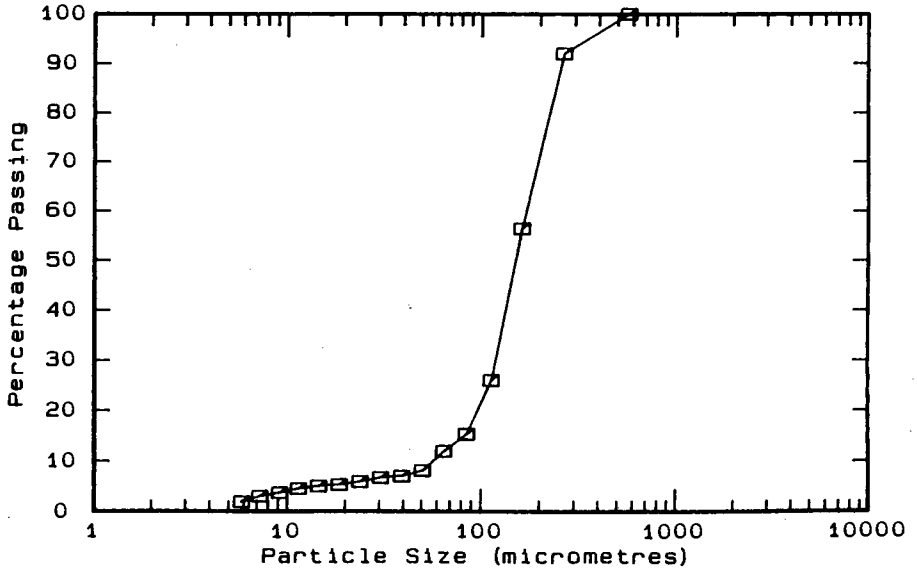

DATA FILE : ED80D70U

Test Facility	UCT 80 mm NB
Test Date	June 1990
Material Description	East Driefontein CCT
Material Relative Density	2.65
Slurry Relative Density	1.70
Solids Volumetric Concentration (%)	42.42
Solids Mass Concentration (%)	66.13
Mean Slurry Temperature (°C)	18.9
Pipe Internal Diameter (mm)	73.40
Pipe Roughness (μm)	84.0
Pipeline Slope	Vertical Down

Mixture Velocity (m/s)	Pressure Gradient (kPa/m)	Slurry Temp. (°C)
3.447	-12.648	18.4
3.447	-12.755	18.5
3.457	-12.900	18.6
3.461	-12.932	18.7
3.456	-12.725	18.8
2.931	-13.789	18.9
2.931	-13.820	19.0
2.935	-13.851	19.0
2.933	-13.775	19.0
2.478	-14.595	19.1
2.487	-14.689	19.1
2.481	-14.640	19.1
1.951	-15.561	19.1
1.956	-15.539	19.1
1.956	-15.481	19.1
1.958	-15.409	19.1
1.954	-15.410	19.0
1.513	-15.670	19.0
1.538	-15.691	19.0
1.537	-15.773	19.0
1.537	-15.753	19.0
1.535	-15.702	18.9
1.543	-15.752	18.9
1.534	-15.625	18.9
1.011	-15.965	18.9
1.000	-15.833	18.9
1.002	-15.797	18.8

Particle Size Distribution
Malvern Particle Size Analyser

Size (μm)	% Passing	% Retained
564.0	100.0	.0
261.6	91.4	8.6
160.4	56.5	34.9
112.8	26.8	29.7
84.3	14.9	11.9
64.6	12.0	2.9
50.2	8.7	3.3
39.0	7.3	1.4
30.3	6.9	.4
23.7	6.4	.5
18.5	5.8	.6
14.5	5.4	.4
11.4	4.9	.5
9.1	4.1	.8
7.2	3.4	.7
5.8	2.2	1.2
Pan	- .0	2.2

OBSERVED FLOW BEHAVIOUR

Velocity (m/s)	Observation (D = 71.0 mm)

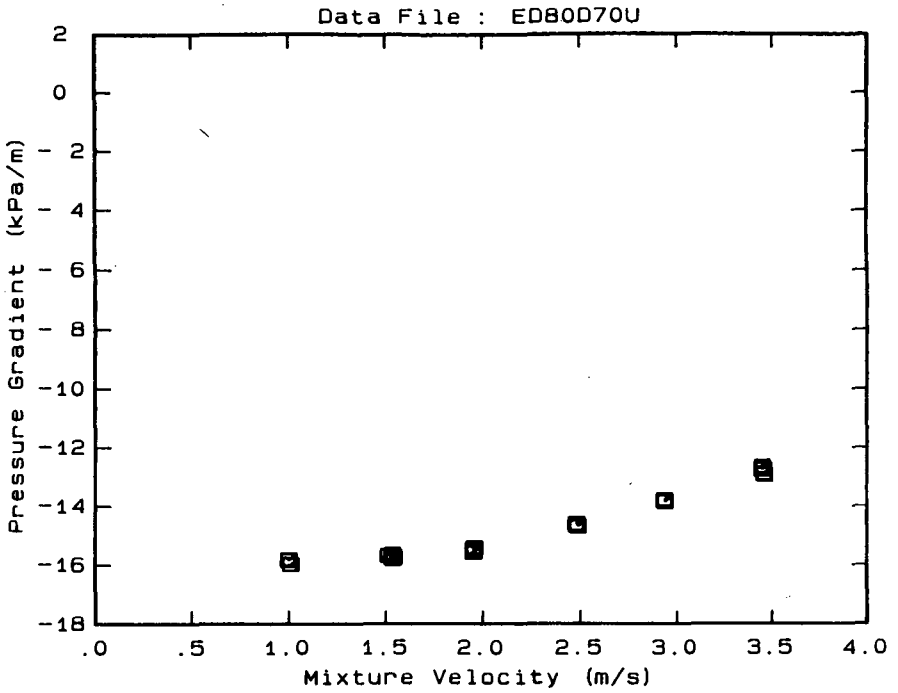

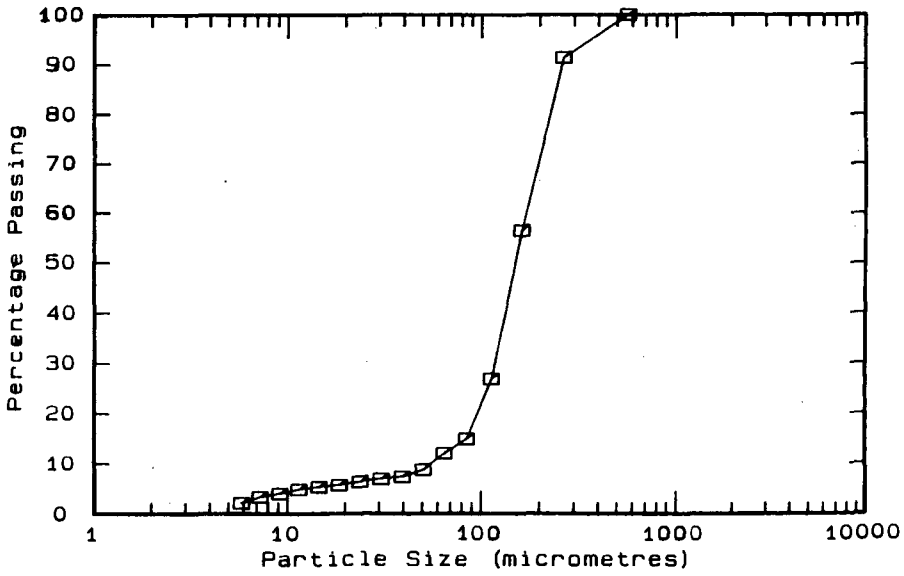

DATA FILE : ED80D71U

Test Facility	UCT 80 mm NB
Test Date	June 1990
Material Description	East Driefontein CCT
Material Relative Density	2.65
Slurry Relative Density	1.71
Solids Volumetric Concentration (%)	43.03
Solids Mass Concentration (%)	66.68
Mean Slurry Temperature (°C)	17.8
Pipe Internal Diameter (mm)	73.40
Pipe Roughness (μm)	84.0
Pipeline Slope	Vertical Down

Mixture Velocity (m/s)	Pressure Gradient (kPa/m)	Slurry Temp. (°C)
3.425	-12.803	16.9
3.440	-12.776	17.0
3.465	-12.676	17.1
3.472	-12.801	17.2
2.918	-13.696	17.7
2.915	-13.650	17.8
2.913	-13.758	17.8
2.924	-13.673	17.8
2.436	-14.271	17.9
2.432	-14.223	17.9
2.439	-14.344	18.0
2.438	-14.236	18.0
1.987	-15.256	18.0
2.000	-14.766	18.0
1.998	-14.971	18.0
1.993	-15.259	18.0
1.489	-15.880	18.0
1.518	-15.519	17.9
1.510	-15.586	17.9
1.527	-15.683	17.9
1.106	-16.041	17.9
1.113	-15.864	17.9
1.102	-15.879	17.9
1.114	-15.911	17.9

Particle Size Distribution
Malvern Particle Size Analyser

Size (μm)	% Passing	% Retained
564.0	100.0	.0
261.6	93.6	6.4
160.4	58.7	34.9
112.8	27.1	31.6
84.3	15.9	11.2
64.6	12.8	3.1
50.2	8.9	3.9
39.0	7.7	1.2
30.3	7.3	.4
23.7	6.5	.8
18.5	5.9	.6
14.5	5.5	.4
11.4	4.9	.6
9.1	4.1	.8
7.2	3.4	.7
5.8	2.2	1.2
Pan	- .0	2.2

OBSERVED FLOW BEHAVIOUR

Velocity (m/s)	Observation (D = 71.0 mm)

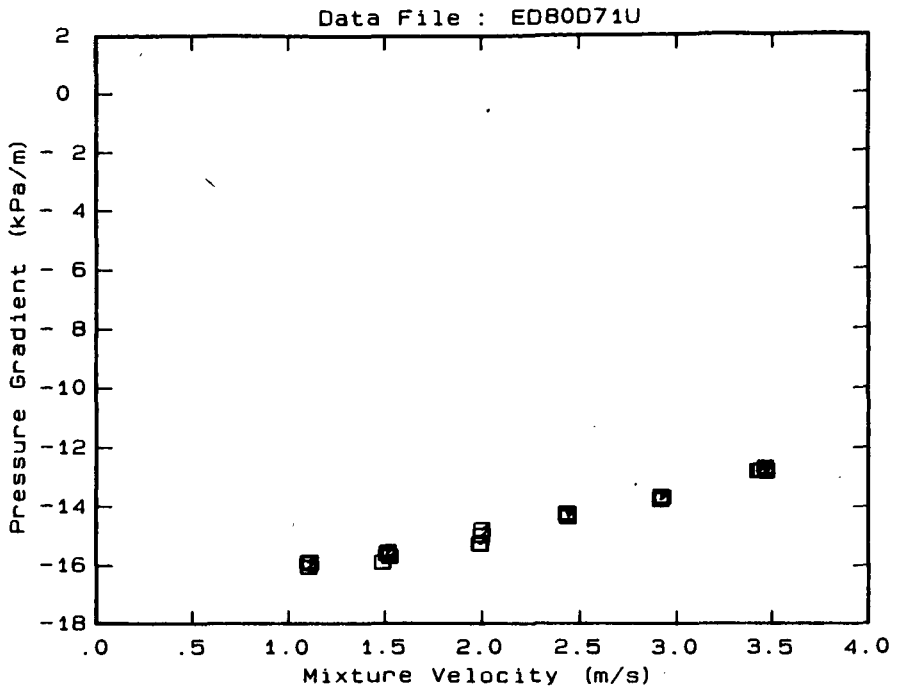

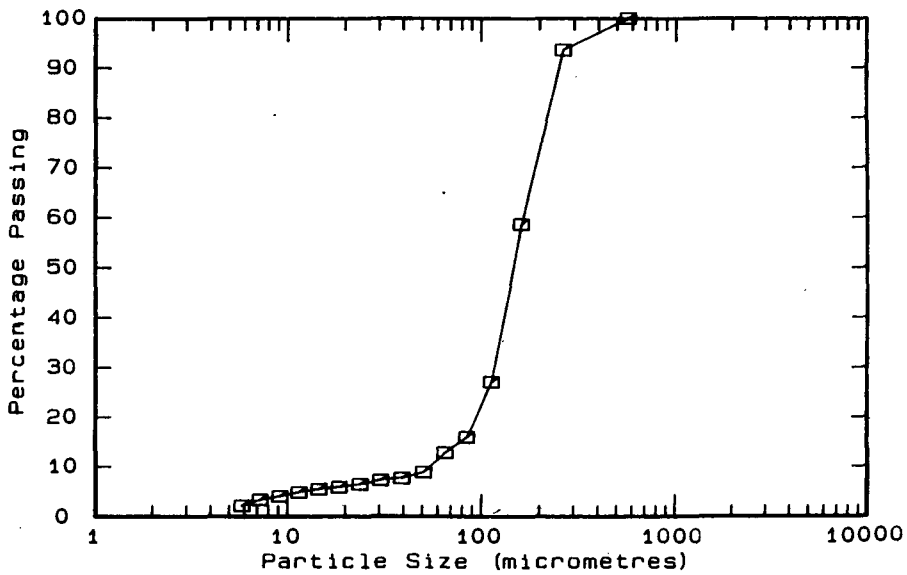

DATA FILE : ED80D74U

Test Facility	UCT 80 mm NB
Test Date	June 1990
Material Description	East Driefontein CCT
Material Relative Density	2.65
Slurry Relative Density	1.74
Solids Volumetric Concentration (%)	44.85
Solids Mass Concentration (%)	68.30
Mean Slurry Temperature (°C)	19.9
Pipe Internal Diameter (mm)	73.40
Pipe Roughness (μm)	84.0
Pipeline Slope	Vertical Down

Mixture Velocity (m/s)	Pressure Gradient (kPa/m)	Slurry Temp. (°C)
3.425	-13.710	18.9
3.439	-13.857	19.0
3.448	-13.469	19.1
3.447	-13.799	19.2
3.458	-13.553	19.3
3.477	-13.186	19.4
3.459	-13.537	19.6
3.476	-13.616	19.7
2.969	-14.259	19.9
2.966	-14.359	20.0
2.960	-14.205	20.0
2.978	-14.177	20.1
2.419	-15.119	20.2
2.422	-15.054	20.2
2.422	-15.051	20.2
2.429	-14.997	20.2
1.973	-15.260	20.2
1.966	-15.434	20.2
1.973	-15.452	20.2
1.979	-15.437	20.2
1.519	-15.601	20.1
1.540	-15.589	20.1
1.522	-15.371	20.1
1.514	-15.459	20.1
1.514	-15.651	20.1
1.536	-15.424	20.0

Particle Size Distribution
Malvern Particle Size Analyser

Size (μm)	% Passing	% Retained
564.0	100.0	.0
261.6	92.7	7.3
160.4	58.0	34.7
112.8	27.7	30.3
84.3	16.6	11.1
64.6	13.5	3.1
50.2	9.9	3.6
39.0	8.6	1.3
30.3	8.2	.4
23.7	7.5	.7
18.5	6.8	.7
14.5	6.4	.4
11.4	5.8	.6
9.1	4.9	.9
7.2	4.1	.8
5.8	2.7	1.4
Pan	.1	2.6

OBSERVED FLOW BEHAVIOUR

Velocity (m/s)	Observation (D = 71.0 mm)

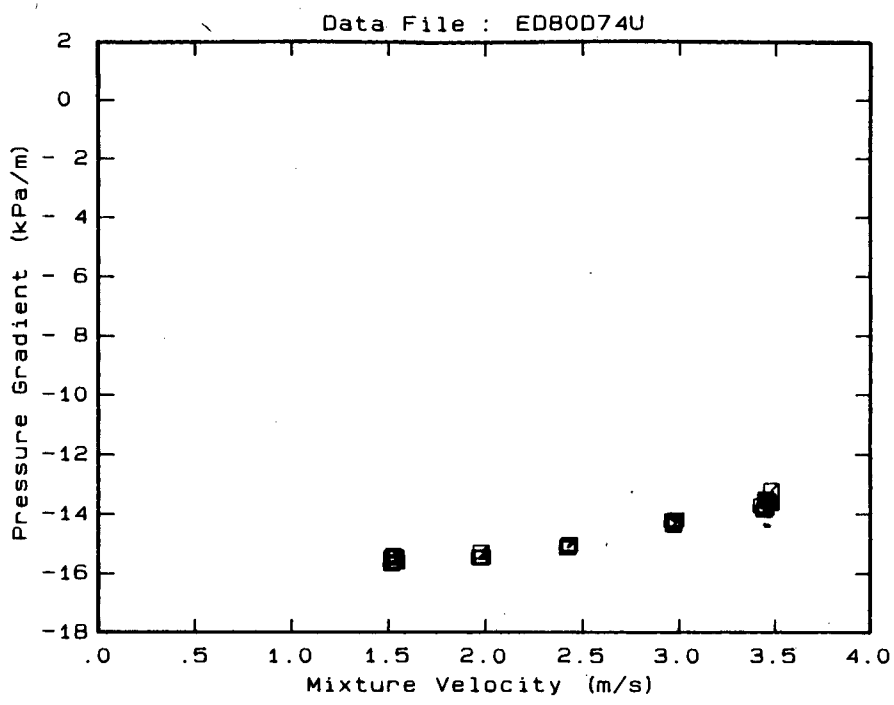

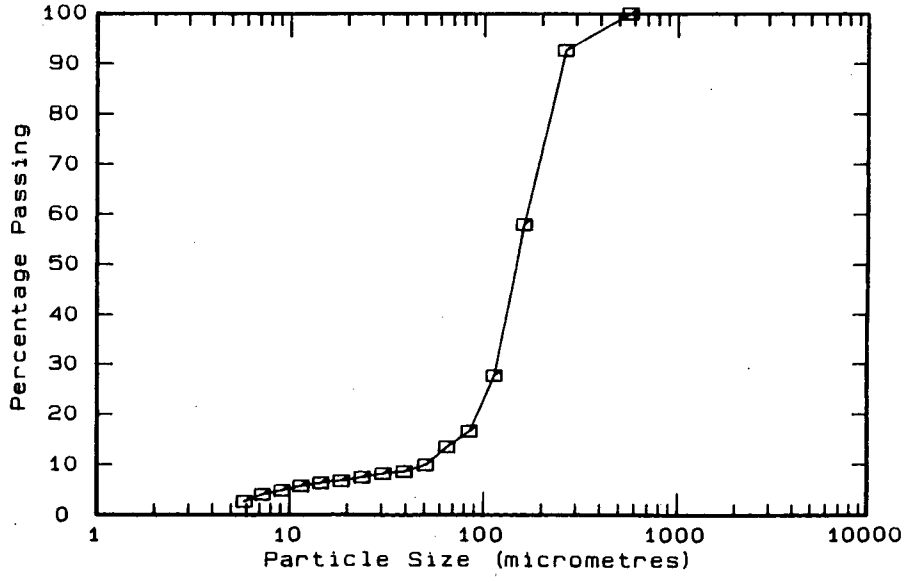

DATA FILE : ED80D79U

Test Facility	UCT 80 mm NB
Test Date	June 1990
Material Description	East Driefontein CCT
Material Relative Density	2.65
Slurry Relative Density	1.79
Solids Volumetric Concentration (%)	47.88
Solids Mass Concentration (%)	70.88
Mean Slurry Temperature (°C)	21.7
Pipe Internal Diameter (mm)	73.40
Pipe Roughness (μm)	84.0
Pipeline Slope	Vertical Down

Mixture Velocity (m/s)	Pressure Gradient (kPa/m)	Slurry Temp. (°C)
3.374	-12.695	20.0
3.346	-12.839	20.2
3.315	-12.909	20.4
3.287	-13.123	20.6
3.280	-13.181	20.7
3.247	-13.077	20.9
3.208	-13.303	21.0
3.128	-13.410	21.1
3.048	-13.487	21.8
3.052	-13.605	21.9
3.062	-13.595	21.9
2.539	-14.268	22.0
2.546	-14.623	22.2
2.548	-14.369	22.2
2.553	-14.177	22.3
2.556	-14.119	22.3
2.087	-14.985	22.3
2.084	-14.951	22.3
2.091	-14.902	22.3
1.547	-15.178	22.2
1.563	-15.339	22.2
1.536	-15.393	22.1
1.550	-15.411	22.1
1.547	-14.706	22.1
1.546	-15.011	22.0
1.031	-13.747	21.9
1.068	-12.044	21.9
1.065	-14.931	21.9
1.055	-12.895	21.8
1.074	-14.996	21.8
1.068	-14.313	21.8
1.079	-14.917	21.7

Particle Size Distribution
Malvern Particle Size Analyser

Size (μm)	% Passing	% Retained
564.0	100.0	.0
261.6	92.3	7.7
160.4	58.3	34.0
112.8	28.4	29.9
84.3	16.9	11.5
64.6	13.8	3.1
50.2	10.3	3.5
39.0	9.0	1.3
30.3	8.6	.4
23.7	7.8	.8
18.5	7.1	.7
14.5	6.7	.4
11.4	6.0	.7
9.1	5.0	1.0
7.2	4.1	.9
5.8	2.6	1.5
Pan	- .2	2.8

OBSERVED FLOW BEHAVIOUR

Velocity (m/s)	Observation (D = 71.0 mm)

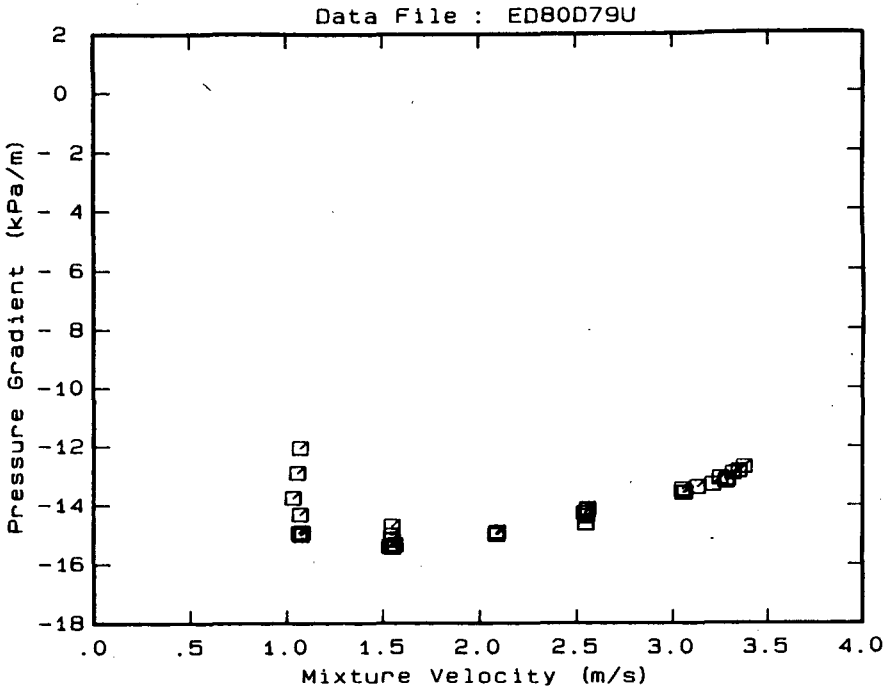

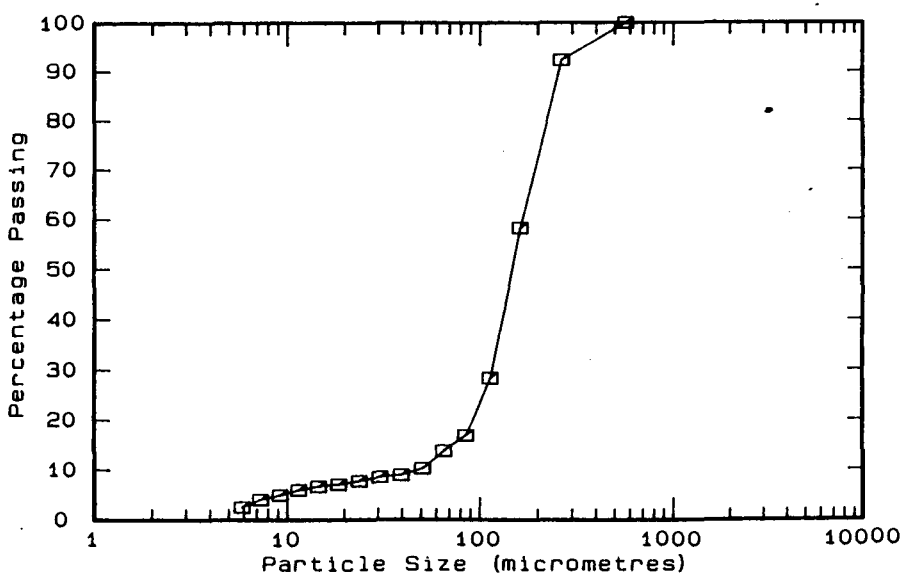

DATA FILE : ED80D84U

Test Facility	UCT 80 mm NB
Test Date	June 1990
Material Description	East Driefontein CCT
Material Relative Density	2.65
Slurry Relative Density	1.84
Solids Volumetric Concentration (%)	50.91
Solids Mass Concentration (%)	73.32
Mean Slurry Temperature (°C)	23.3
Pipe Internal Diameter (mm)	73.40
Pipe Roughness (μm)	84.0
Pipeline Slope	Vertical Down

Mixture Velocity (m/s)	Pressure Gradient (kPa/m)	Slurry Temp. (°C)
2.164	-11.845	21.6
2.249	-11.557	21.8
1.848	-12.815	22.7
1.844	-12.816	22.8
1.846	-12.818	22.9
1.620	-13.559	23.1
1.628	-13.471	23.2
1.629	-13.528	23.3
1.304	-14.406	23.6
1.314	-13.610	23.6
1.302	-14.239	23.7
1.258	-14.159	23.7
1.256	-14.195	23.8
1.017	-14.769	23.9
1.017	-14.869	24.0
1.001	-14.874	24.0
.996	-14.718	24.0
1.018	-14.718	24.1

Particle Size Distribution
Malvern Particle Size Analyser

Size (μm)	% Passing	% Retained
564.0	100.0	.0
261.6	93.9	6.1
160.4	59.8	34.1
112.8	29.9	29.9
84.3	17.9	12.0
64.6	14.6	3.3
50.2	11.4	3.2
39.0	10.0	1.4
30.3	9.5	.5
23.7	8.9	.6
18.5	8.2	.7
14.5	7.6	.6
11.4	6.9	.7
9.1	5.9	1.0
7.2	5.0	.9
5.8	3.3	1.7
Pan	.1	3.2

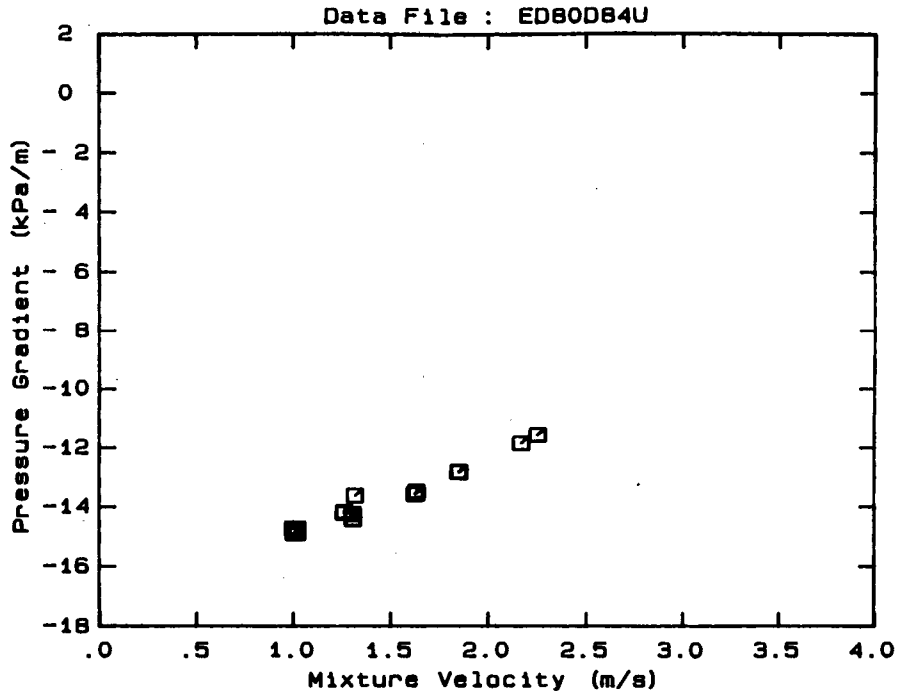

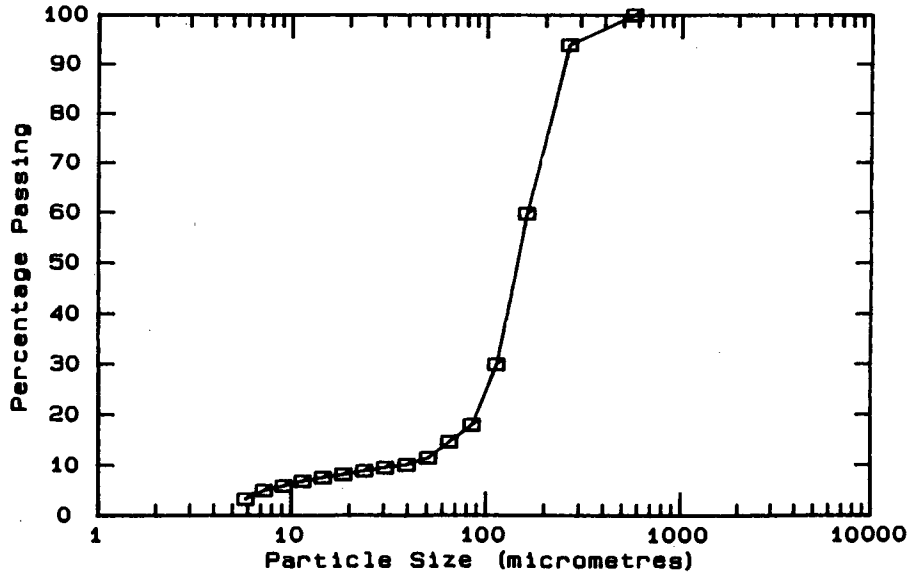

DATA FILE : VR25H55U

Test Facility	UCT 25 mm NB
Test Date	June 1990
Material Description	Vaal Reefs CCT
Material Relative Density	2.65
Slurry Relative Density	1.55
Solids Volumetric Concentration (%)	33.33
Solids Mass Concentration (%)	56.99
Mean Slurry Temperature (°C)	14.5
Pipe Internal Diameter (mm)	26.60
Pipe Roughness (μm)	21.0
Pipeline Slope	Horizontal

Mixture Velocity (m/s)	Pressure Gradient (kPa/m)	Slurry Temp. (°C)
3.390	7.542	14.0
3.406	7.484	14.1
3.448	7.545	14.2
2.942	5.824	14.3
2.939	5.998	14.3
2.949	5.977	14.5
2.488	4.530	14.5
2.487	4.538	14.5
2.489	4.518	14.5
2.085	3.448	14.6
2.077	3.465	14.6
2.086	3.480	14.6
1.670	2.434	14.7
1.672	2.415	14.7
1.539	2.556	14.7
1.246	1.524	14.7
1.235	1.586	14.7
1.224	1.558	14.7

Particle Size Distribution
Malvern Particle Size Analyser

Size (μm)	% Passing	% Retained
564.0	100.0	.0
261.6	90.0	10.0
160.4	54.9	35.1
112.8	34.0	20.9
84.3	23.8	10.2
64.6	20.0	3.8
50.2	16.5	3.5
39.0	13.9	2.6
30.3	12.5	1.4
23.7	10.9	1.6
18.5	9.3	1.6
14.5	8.2	1.1
11.4	6.9	1.3
9.1	5.3	1.6
7.2	4.1	1.2
5.8	2.5	1.6
Pan	.0	2.5

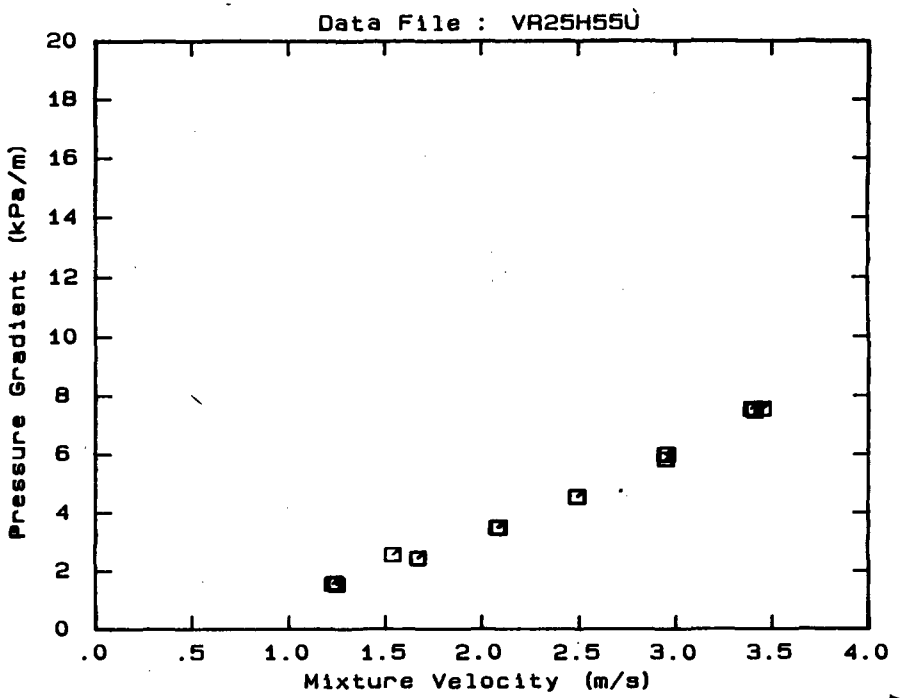

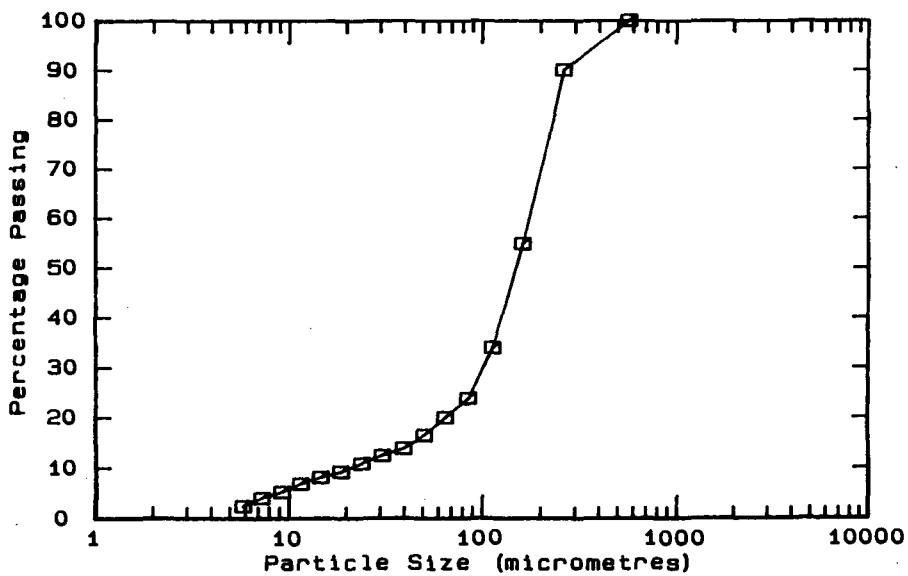

DATA FILE : VR25H66U

Test Facility	UCT 25 mm NB
Test Date	June 1990
Material Description	Vaal Reefs CCT
Material Relative Density	2.65
Slurry Relative Density	1.66
Solids Volumetric Concentration (%)	40.00
Solids Mass Concentration (%)	63.86
Mean Slurry Temperature (°C)	16.4
Pipe Internal Diameter (mm)	26.60
Pipe Roughness (μm)	21.0
Pipeline Slope	Horizontal

Mixture Velocity (m/s)	Pressure Gradient (kPa/m)	Slurry Temp. (°C)
3.278	7.221	15.4
3.244	7.433	15.5
3.266	7.674	15.6
3.279	7.309	15.7
2.940	5.957	15.9
2.869	5.813	16.1
2.925	5.529	16.2
2.565	4.425	16.4
2.536	4.187	16.4
2.548	4.478	16.4
2.546	4.406	16.5
2.146	3.608	16.6
2.143	3.446	16.7
2.150	3.628	16.7
2.161	3.358	16.7
1.696	2.769	16.8
1.690	2.626	16.8
1.693	2.525	16.8
1.287	2.143	16.8
1.297	2.065	16.8
1.275	2.153	16.8

Particle Size Distribution
Malvern Particle Size Analyser

Size (μm)	% Passing	% Retained
564.0	100.0	.0
261.6	89.5	10.5
160.4	53.3	36.2
112.8	31.5	21.8
84.3	21.8	9.7
64.6	18.2	3.6
50.2	15.0	3.2
39.0	12.8	2.2
30.3	11.6	1.2
23.7	10.2	1.4
18.5	8.8	1.4
14.5	7.8	1.0
11.4	6.6	1.2
9.1	5.1	1.5
7.2	4.0	1.1
5.8	2.5	1.5
Pan	- .0	2.5

OBSERVED FLOW BEHAVIOUR

Velocity (m/s)	Observation (D = .0 mm)

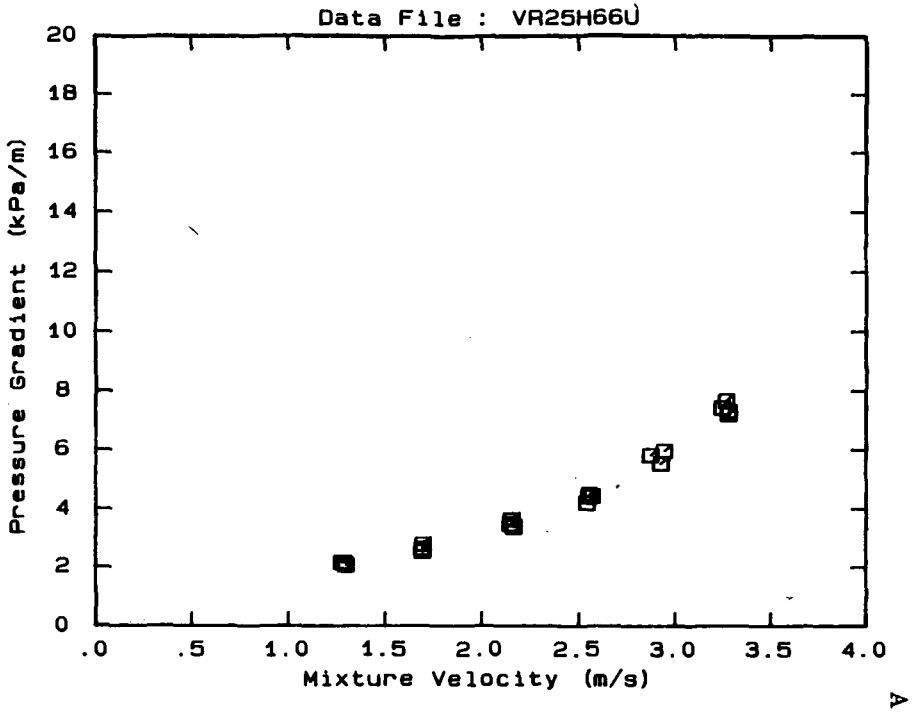

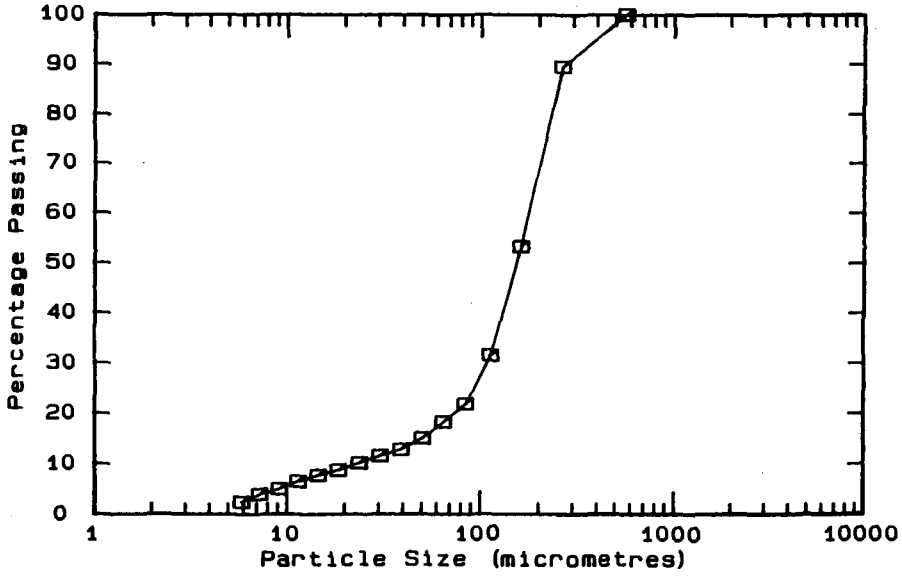

DATA FILE : VR25H75A

Test Facility	UCT 25 mm NB
Test Date	June 1990
Material Description	Vaal Reefs CCT
Material Relative Density	2.65
Slurry Relative Density	1.75
Solids Volumetric Concentration (%)	45.45
Solids Mass Concentration (%)	68.83
Mean Slurry Temperature (°C)	18.3
Pipe Internal Diameter (mm)	26.60
Pipe Roughness (μm)	21.0
Pipeline Slope	Horizontal

Mixture Velocity (m/s)	Pressure Gradient (kPa/m)	Slurry Temp. (°C)
2.816	8.095	17.0
2.767	8.106	17.2
2.733	7.402	17.3
2.598	7.351	17.4
2.633	7.900	17.6
2.469	7.035	18.0
2.463	6.991	18.1
2.469	7.194	18.2
2.111	6.580	18.5
2.105	6.095	18.6
2.105	6.172	18.7
1.696	5.041	18.9
1.693	5.125	19.0
1.697	5.159	19.0
1.276	4.077	19.0
1.268	3.958	19.0
1.270	4.040	19.0

Particle Size Distribution
Malvern Particle Size Analyser

Size (μm)	% Passing	% Retained
564.0	100.0	.0
261.6	89.5	10.5
160.4	53.5	36.0
112.8	30.1	23.4
84.3	21.0	9.1
64.6	17.4	3.6
50.2	14.0	3.4
39.0	12.0	2.0
30.3	11.0	1.0
23.7	9.8	1.2
18.5	8.5	1.3
14.5	7.6	.9
11.4	6.5	1.1
9.1	5.2	1.3
7.2	4.1	1.1
5.8	2.6	1.5
Pan	.1	2.5

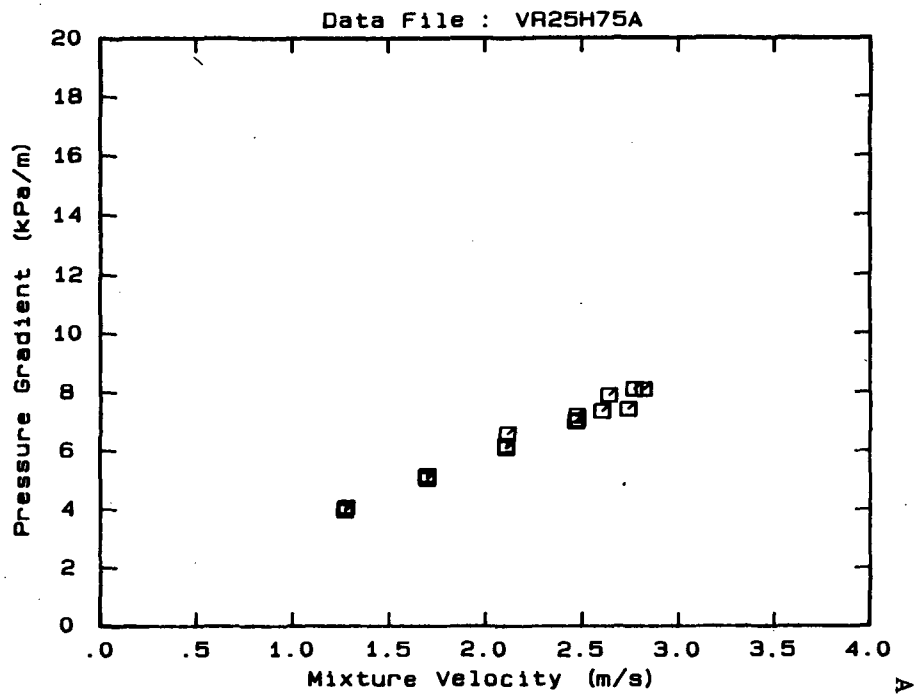

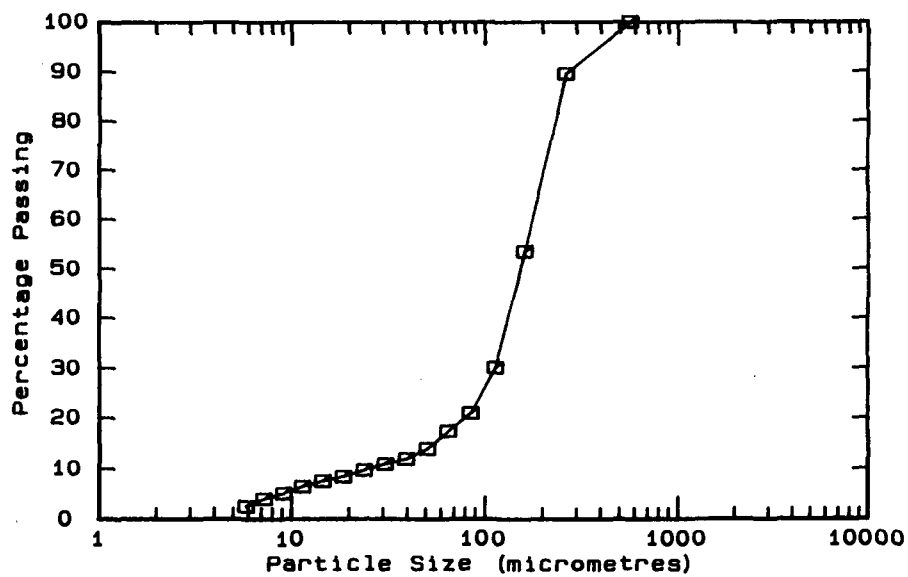

DATA FILE : VR25H75B

Test Facility	UCT 25 mm NB
Test Date	June 1990
Material Description	Vaal Reefs CCT
Material Relative Density	2.65
Slurry Relative Density	1.75
Solids Volumetric Concentration (%)	45.45
Solids Mass Concentration (%)	68.83
Mean Slurry Temperature (°C)	18.0
Pipe Internal Diameter (mm)	26.60
Pipe Roughness (μm)	21.0
Pipeline Slope	Horizontal

Mixture Velocity (m/s)	Pressure Gradient (kPa/m)	Slurry Temp. (°C)
2.448	6.755	17.0
2.784	7.401	17.2
2.789	7.360	17.2
2.801	7.642	17.2
2.812	7.438	17.2
2.817	7.626	17.2
2.814	7.651	17.2
2.532	6.942	17.3
2.558	6.956	17.4
2.552	6.733	17.6
2.536	7.246	18.0
2.121	6.072	18.1
2.114	5.740	18.2
2.091	6.004	18.5
2.086	5.902	18.6
1.681	5.225	18.7
1.674	5.118	18.9
1.680	5.005	19.0
1.679	5.145	19.0
1.254	3.796	19.0
1.256	3.748	19.0
1.250	3.846	19.0

Particle Size Distribution
Malvern Particle Size Analyser

Size (μm)	% Passing	% Retained
564.0	100.0	.0
261.6	88.9	11.1
160.4	51.4	37.5
112.8	29.8	21.6
84.3	20.2	9.6
64.6	16.9	3.3
50.2	13.9	3.0
39.0	11.9	2.0
30.3	10.9	1.0
23.7	9.8	1.1
18.5	8.6	1.2
14.5	7.7	.9
11.4	6.6	1.1
9.1	5.2	1.4
7.2	4.0	1.2
5.8	2.4	1.6
Pan	- .3	2.7

OBSERVED FLOW BEHAVIOUR

Velocity (m/s)	Observation (D = .0 mm)

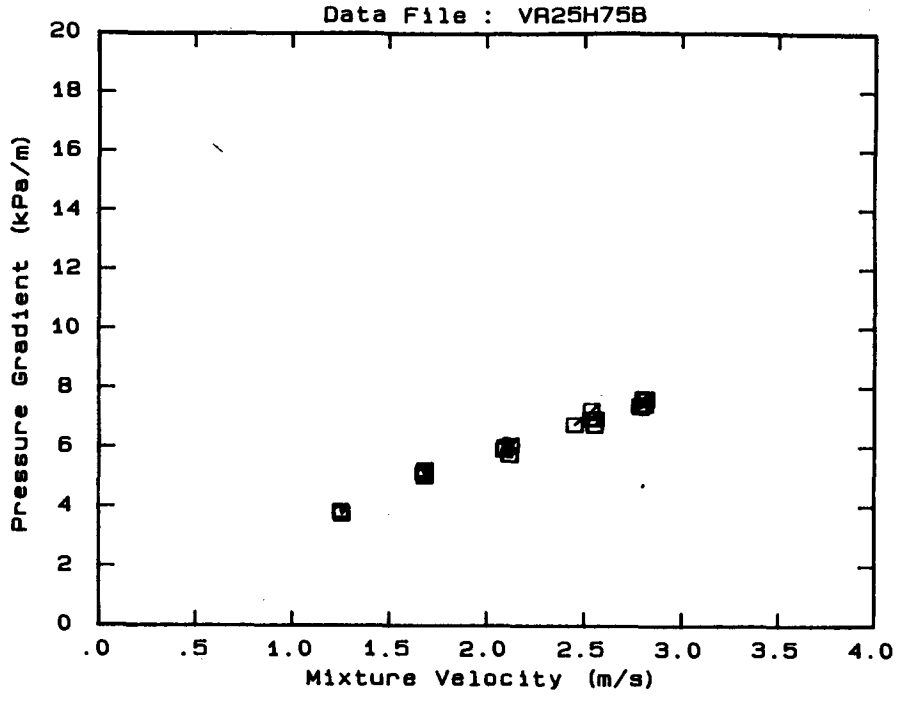

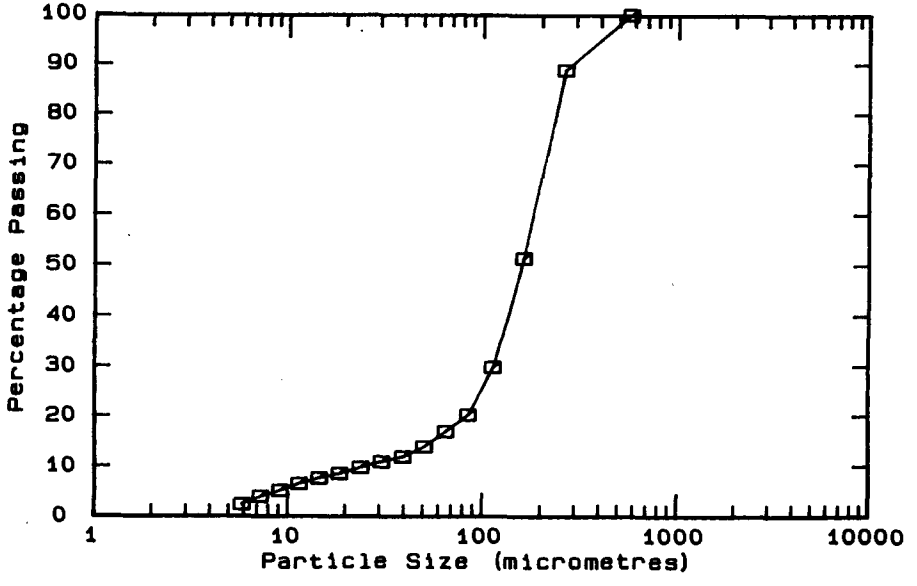

DATA FILE : VR25H77U

Test Facility	UCT 25 mm NB
Test Date	June 1990
Material Description	Vaal Reefs CCT
Material Relative Density	2.65
Slurry Relative Density	1.77
Solids Volumetric Concentration (%)	46.67
Solids Mass Concentration (%)	69.87
Mean Slurry Temperature (°C)	21.2
Pipe Internal Diameter (mm)	26.60
Pipe Roughness (μm)	21.0
Pipeline Slope	Horizontal

Mixture Velocity (m/s)	Pressure Gradient (kPa/m)	Slurry Temp. (°C)
2.677	9.058	20.3
2.713	9.467	20.5
2.701	9.140	20.6
2.513	8.827	20.9
2.511	8.870	21.0
2.503	8.878	21.0
1.704	6.460	21.3
1.691	6.412	21.4
1.694	6.531	21.4
1.686	6.398	21.4
1.684	6.644	21.4
2.119	8.242	21.6
2.123	8.207	21.6
2.127	8.224	21.6
1.274	5.225	21.7
1.274	5.086	21.7
1.271	5.198	21.7

Particle Size Distribution
Malvern Particle Size Analyser

Size (μm)	% Passing	% Retained
564.0	100.0	.0
261.6	88.6	11.4
160.4	52.4	36.2
112.8	31.1	21.3
84.3	21.3	9.8
64.6	18.1	3.2
50.2	15.3	2.8
39.0	13.2	2.1
30.3	12.1	1.1
23.7	11.0	1.1
18.5	9.8	1.2
14.5	8.8	1.0
11.4	7.6	1.2
9.1	6.1	1.5
7.2	4.8	1.3
5.8	3.0	1.8
Pan	.0	3.0

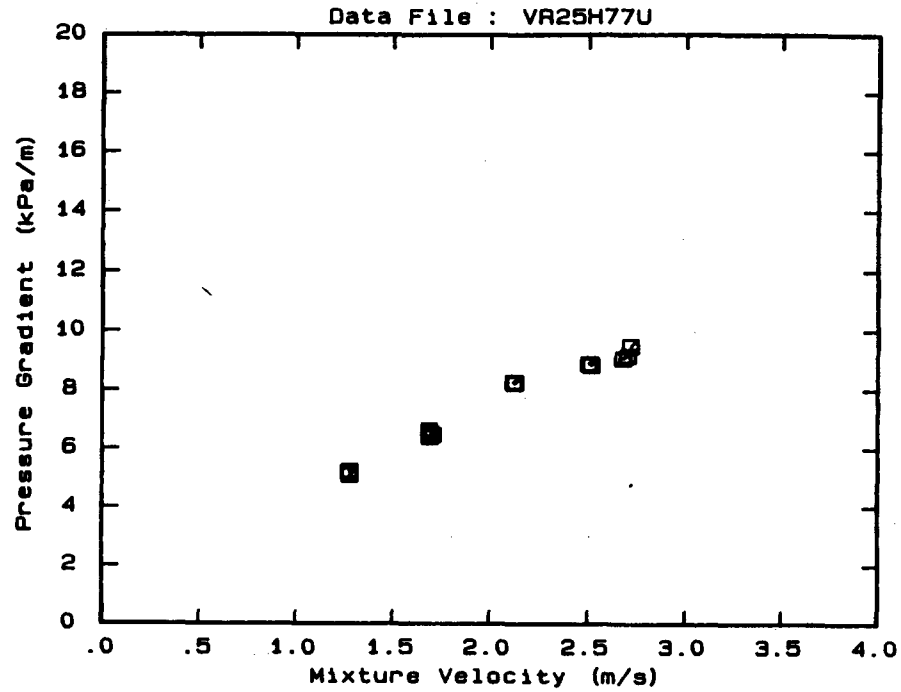

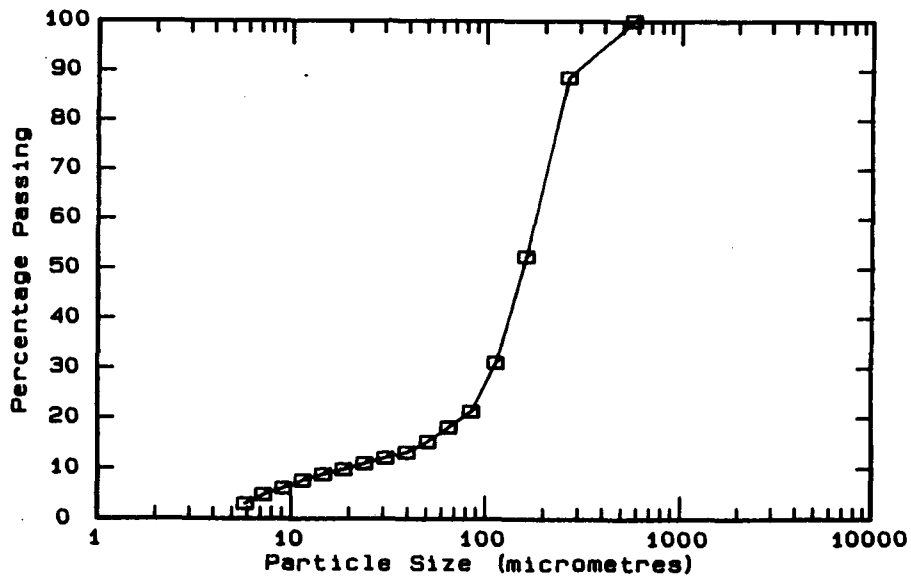

DATA FILE : VR25H86U

Test Facility	UCT 25 mm NB
Test Date	June 1990
Material Description	Vaal Reefs CCT
Material Relative Density	2.65
Slurry Relative Density	1.86
Solids Volumetric Concentration (%)	52.12
Solids Mass Concentration (%)	74.26
Mean Slurry Temperature (°C)	23.5
Pipe Internal Diameter (mm)	26.60
Pipe Roughness (μm)	21.0
Pipeline Slope	Horizontal

Mixture Velocity (m/s)	Pressure Gradient (kPa/m)	Slurry Temp. (°C)
1.321	16.376	23.4
1.331	16.919	23.3
1.329	17.056	23.3
1.350	17.669	23.3
1.265	16.409	23.4
1.258	16.724	23.5
1.241	16.992	23.6
1.191	16.765	23.9
1.162	16.129	23.9
1.150	16.404	23.8

Particle Size Distribution
Malvern Particle Size Analyser

Size (μm)	% Passing	% Retained
564.0	100.0	.0
261.6	90.0	10.0
160.4	56.5	33.5
112.8	32.9	23.6
84.3	22.2	10.7
64.6	19.3	2.9
50.2	16.0	3.3
39.0	13.5	2.5
30.3	12.6	.9
23.7	11.6	1.0
18.5	10.3	1.3
14.5	9.3	1.0
11.4	8.1	1.2
9.1	6.6	1.5
7.2	5.3	1.3
5.8	3.4	1.9
Pan	.1	3.3

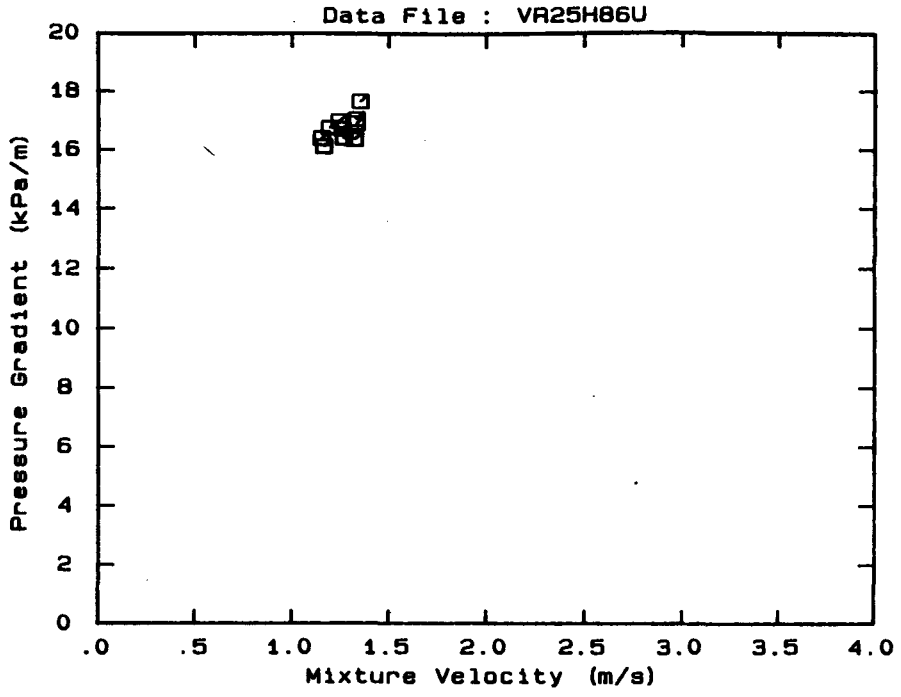

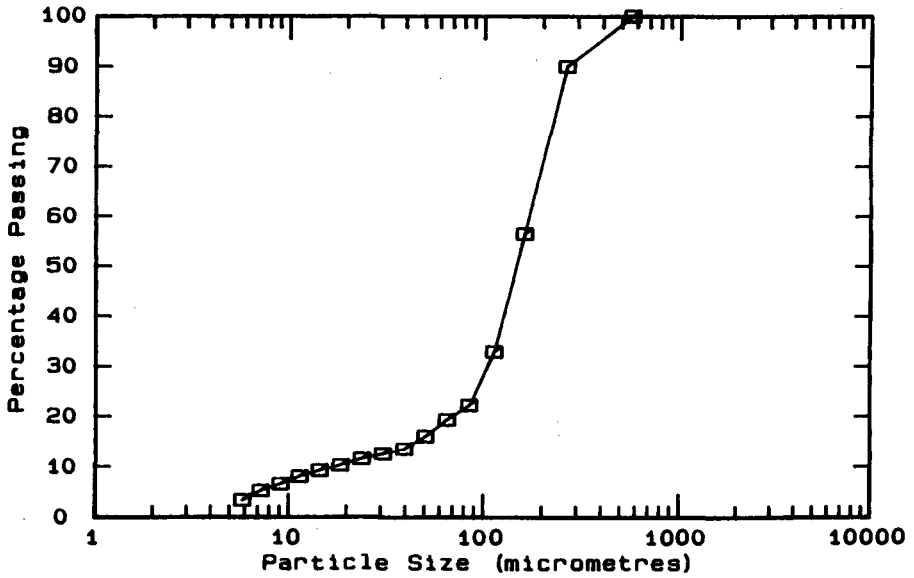

DATA FILE : VR25D55U

Test Facility	UCT 25 mm NB
Test Date	June 1990
Material Description	Vaal Reefs CCT
Material Relative Density	2.65
Slurry Relative Density	1.55
Solids Volumetric Concentration (%)	33.33
Solids Mass Concentration (%)	56.99
Mean Slurry Temperature (°C)	14.5
Pipe Internal Diameter (mm)	26.60
Pipe Roughness (μm)	21.0
Pipeline Slope	Vertical Down

Mixture Velocity (m/s)	Pressure Gradient (kPa/m)	Slurry Temp. (°C)
3.390	- 7.548	14.0
3.406	- 7.670	14.1
3.448	- 7.469	14.2
2.942	- 9.024	14.3
2.939	- 9.326	14.3
2.949	- 9.091	14.5
2.488	-10.597	14.5
2.487	-10.462	14.5
2.489	-10.469	14.5
2.085	-11.671	14.6
2.077	-11.717	14.6
2.086	-11.582	14.6
1.670	-12.800	14.7
1.672	-12.789	14.7
1.539	-13.077	14.7
1.246	-13.833	14.7
1.235	-13.905	14.7
1.224	-13.974	14.7

Particle Size Distribution
Malvern Particle Size Analyser

Size (μm)	% Passing	% Retained
564.0	100.0	.0
261.6	90.0	10.0
160.4	54.9	35.1
112.8	34.0	20.9
84.3	23.8	10.2
64.6	20.0	3.8
50.2	16.5	3.5
39.0	13.9	2.6
30.3	12.5	1.4
23.7	10.9	1.6
18.5	9.3	1.6
14.5	8.2	1.1
11.4	6.9	1.3
9.1	5.3	1.6
7.2	4.1	1.2
5.8	2.5	1.6
Pan	.0	2.5

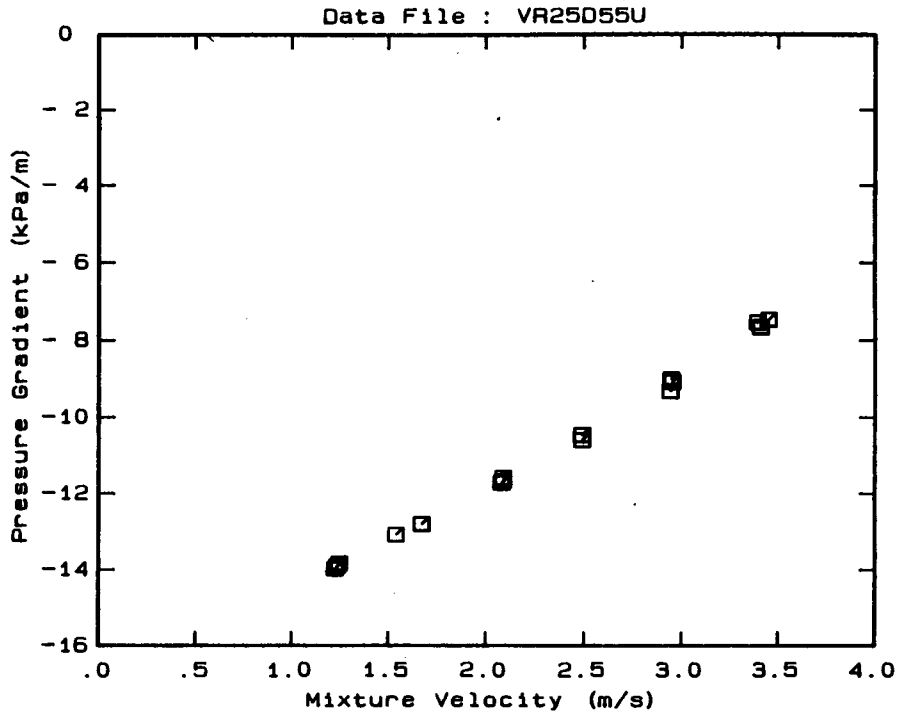

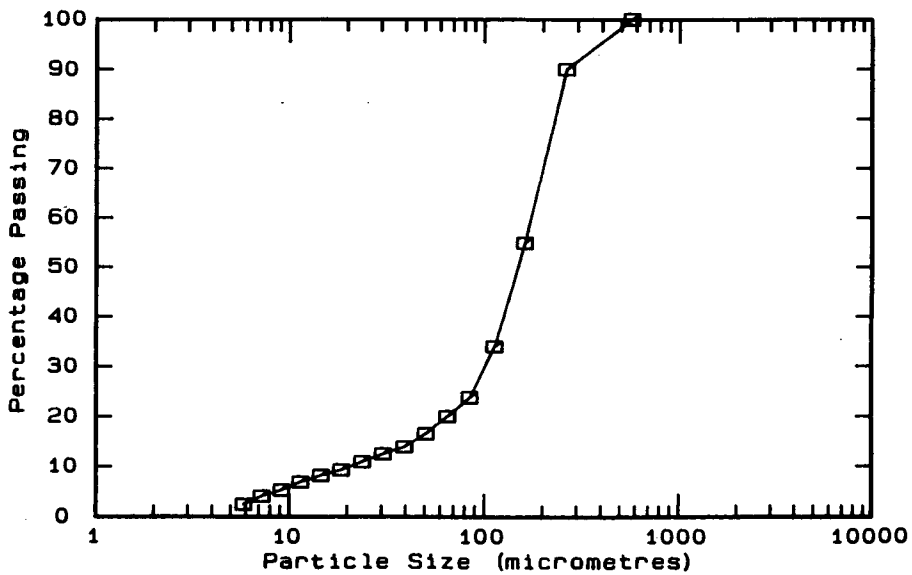

DATA FILE : VR25D66U

Test Facility	UCT 25 mm NB
Test Date	June 1990
Material Description	Vaal Reefs CCT
Material Relative Density	2.65
Slurry Relative Density	1.66
Solids Volumetric Concentration (%)	40.00
Solids Mass Concentration (%)	63.86
Mean Slurry Temperature (°C)	16.4
Pipe Internal Diameter (mm)	26.60
Pipe Roughness (μm)	21.0
Pipeline Slope	Vertical Down

Mixture Velocity (m/s)	Pressure Gradient (kPa/m)	Slurry Temp. (°C)
3.278	- 8.346	15.4
3.244	- 8.434	15.5
3.266	- 9.184	15.6
3.279	- 8.394	15.7
2.940	- 9.482	15.9
2.869	-10.485	16.1
2.925	- 9.863	16.2
2.565	-10.921	16.4
2.536	-11.119	16.4
2.548	-11.202	16.4
2.546	-11.093	16.5
2.146	-12.035	16.6
2.143	-11.937	16.7
2.150	-12.072	16.7
2.161	-11.860	16.7
1.696	-13.262	16.8
1.690	-13.276	16.8
1.693	-13.321	16.8
1.287	-14.288	16.8
1.297	-14.219	16.8
1.275	-14.257	16.8

Particle Size Distribution
Malvern Particle Size Analyser

Size (μm)	% Passing	% Retained
564.0	100.0	.0
261.6	89.5	10.5
160.4	53.3	36.2
112.8	31.5	21.8
84.3	21.8	9.7
64.6	18.2	3.6
50.2	15.0	3.2
39.0	12.8	2.2
30.3	11.6	1.2
23.7	10.2	1.4
18.5	8.8	1.4
14.5	7.8	1.0
11.4	6.6	1.2
9.1	5.1	1.5
7.2	4.0	1.1
5.8	2.5	1.5
Pan	- .0	2.5

OBSERVED FLOW BEHAVIOUR

Velocity (m/s)	Observation (D = .0 mm)

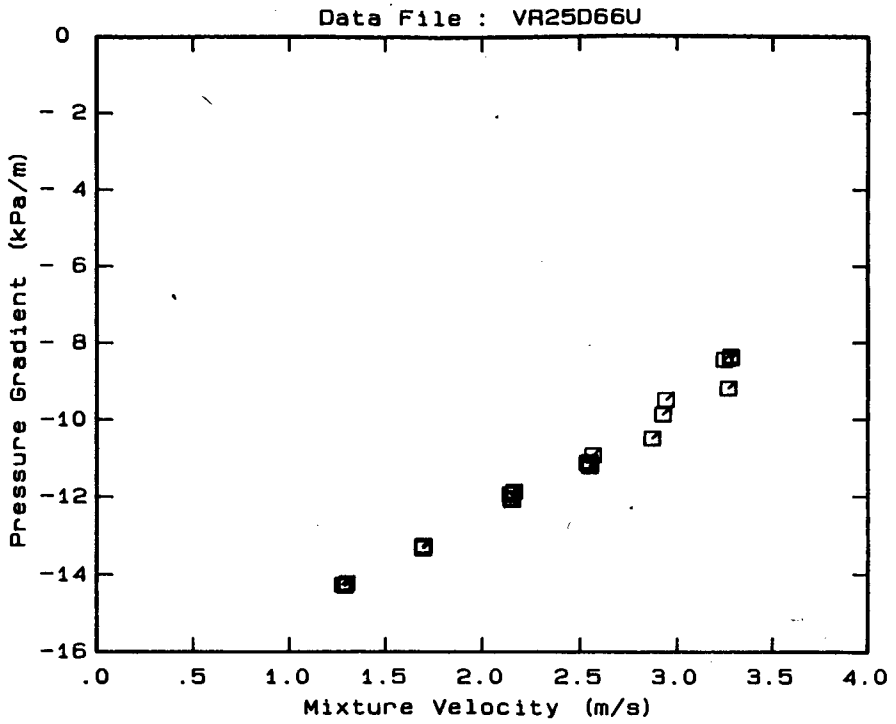

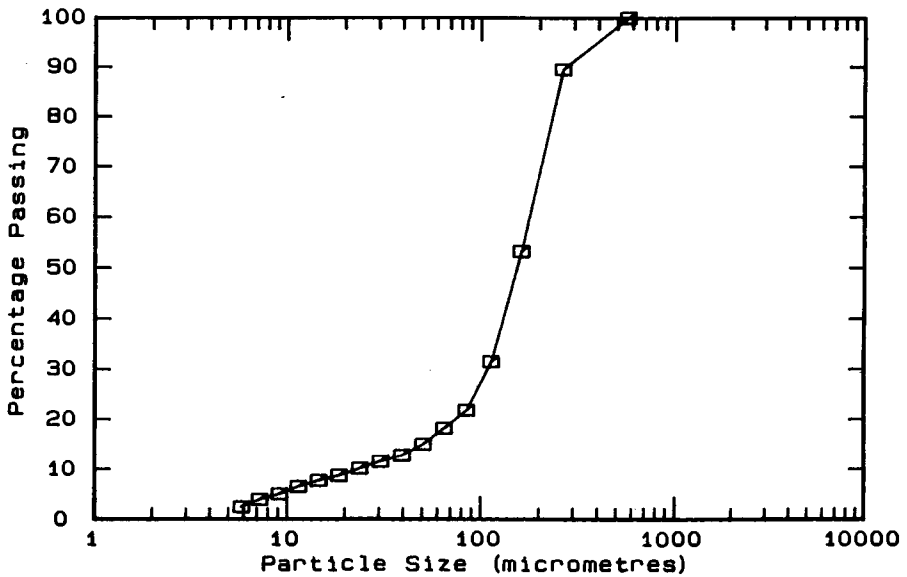

DATA FILE : VR25D75A

Test Facility	UCT 25 mm NB
Test Date	June 1990
Material Description	Vaal Reefs CCT
Material Relative Density	2.65
Slurry Relative Density	1.75
Solids Volumetric Concentration (%)	45.45
Solids Mass Concentration (%)	68.83
Mean Slurry Temperature (°C)	18.3
Pipe Internal Diameter (mm)	26.60
Pipe Roughness (μm)	21.0
Pipeline Slope	Vertical Down

Mixture Velocity (m/s)	Pressure Gradient (kPa/m)	Slurry Temp. (°C)
2.816	- 7.757	17.0
2.767	- 7.707	17.2
2.733	- 7.603	17.3
2.598	- 7.965	17.4
2.633	- 8.023	17.6
2.469	- 8.179	18.0
2.463	- 8.163	18.1
2.469	- 8.231	18.2
2.111	- 9.441	18.5
2.105	- 9.277	18.6
2.105	- 9.344	18.7
1.696	-11.217	18.9
1.693	-11.281	19.0
1.697	-11.166	19.0
1.276	-12.624	19.0
1.268	-12.686	19.0
1.270	-12.587	19.0

Particle Size Distribution
Malvern Particle Size Analyser

Size (μm)	% Passing	% Retained
564.0	100.0	.0
261.6	89.5	10.5
160.4	53.5	36.0
112.8	30.1	23.4
84.3	21.0	9.1
64.6	17.4	3.6
50.2	14.0	3.4
39.0	12.0	2.0
30.3	11.0	1.0
23.7	9.8	1.2
18.5	8.5	1.3
14.5	7.6	.9
11.4	6.5	1.1
9.1	5.2	1.3
7.2	4.1	1.1
5.8	2.6	1.5
Pan	.1	2.5

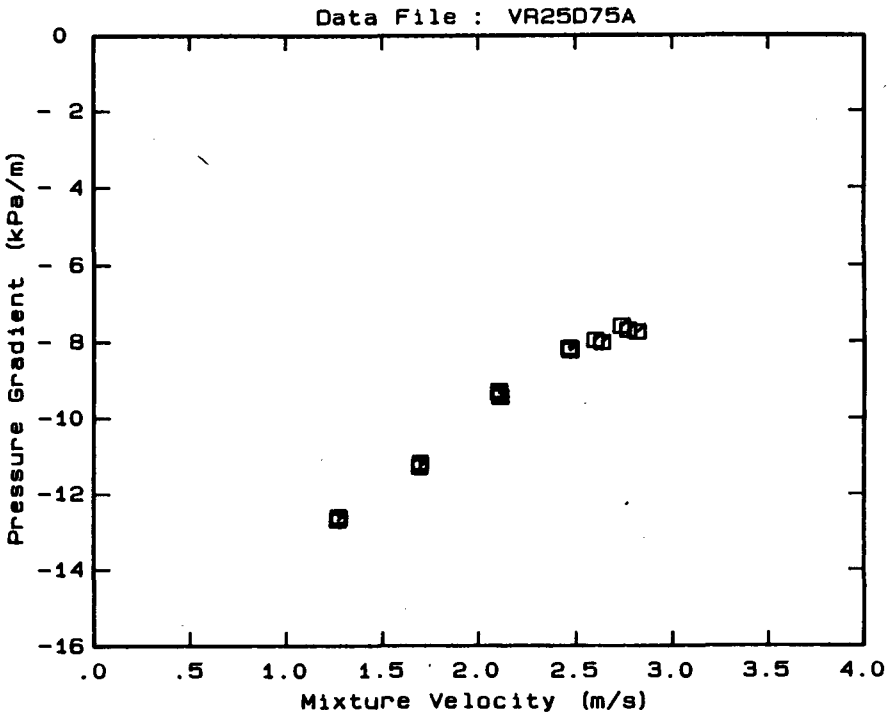

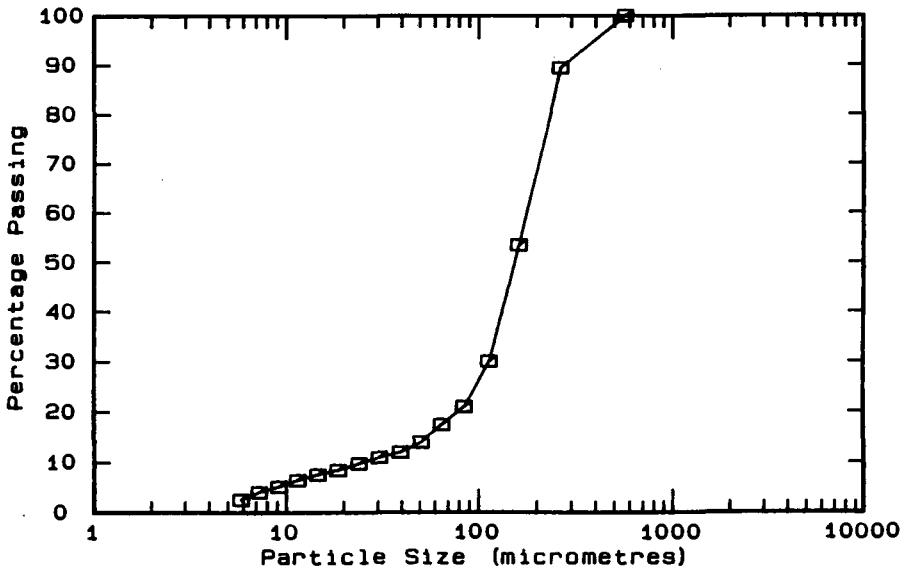

DATA FILE : VR25D75B

Test Facility	UCT 25 mm NB
Test Date	June 1990
Material Description	Vaal Reefs CCT
Material Relative Density	2.65
Slurry Relative Density	1.75
Solids Volumetric Concentration (%)	45.45
Solids Mass Concentration (%)	68.83
Mean Slurry Temperature (°C)	18.0
Pipe Internal Diameter (mm)	26.60
Pipe Roughness (μm)	21.0
Pipeline Slope	Vertical Down

Mixture Velocity (m/s)	Pressure Gradient (kPa/m)	Slurry Temp. (°C)
2.448	- 7.792	17.0
2.784	- 8.350	17.2
2.789	- 8.110	17.2
2.801	- 8.489	17.2
2.812	- 8.305	17.2
2.817	- 8.032	17.2
2.814	- 7.957	17.2
2.532	- 8.771	17.3
2.558	- 9.084	17.4
2.552	- 8.980	17.6
2.536	- 8.779	18.0
2.121	- 9.992	18.1
2.114	- 9.765	18.2
2.091	- 9.793	18.5
2.086	- 9.812	18.6
1.681	-11.448	18.7
1.674	-11.402	18.9
1.680	-11.363	19.0
1.679	-11.237	19.0
1.254	-12.672	19.0
1.256	-12.657	19.0
1.250	-12.698	19.0

Particle Size Distribution
Malvern Particle Size Analyser

Size (μm)	% Passing	% Retained
564.0	100.0	.0
261.6	88.9	11.1
160.4	51.4	37.5
112.8	29.8	21.6
84.3	20.2	9.6
64.6	16.9	3.3
50.2	13.9	3.0
39.0	11.9	2.0
30.3	10.9	1.0
23.7	9.8	1.1
18.5	8.6	1.2
14.5	7.7	.9
11.4	6.6	1.1
9.1	5.2	1.4
7.2	4.0	1.2
5.8	2.4	1.6
Pan	- .3	2.7

OBSERVED FLOW BEHAVIOUR

Velocity (m/s)	Observation (D = .0 mm)

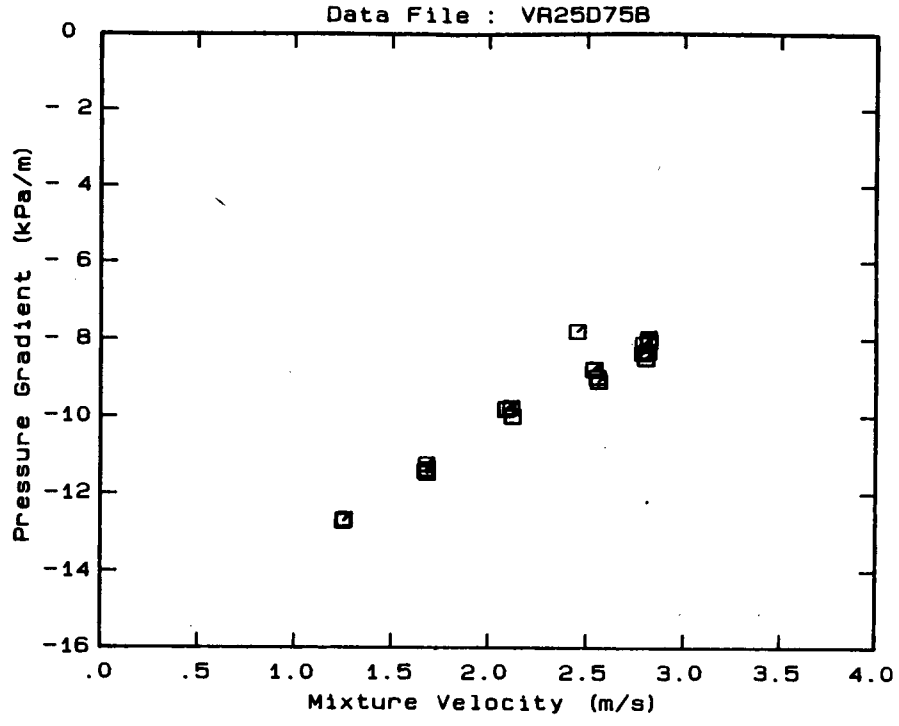

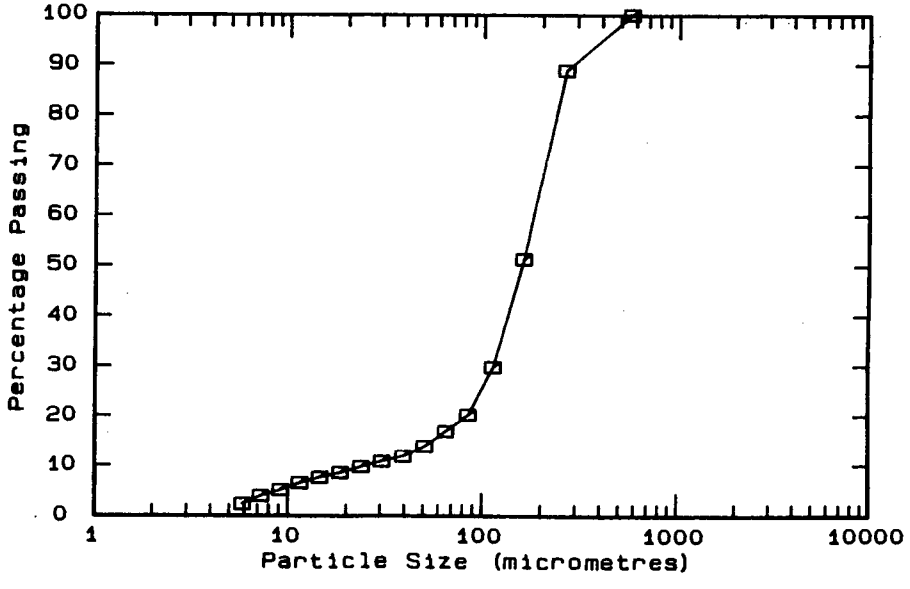

DATA FILE : VR25D77U

Test Facility	UCT 25 mm NB
Test Date	June 1990
Material Description	Vaal Reefs CCT
Material Relative Density	2.65
Slurry Relative Density	1.77
Solids Volumetric Concentration (%)	46.67
Solids Mass Concentration (%)	69.87
Mean Slurry Temperature (°C)	21.2
Pipe Internal Diameter (mm)	26.60
Pipe Roughness (μm)	21.0
Pipeline Slope	Vertical Down

Mixture Velocity (m/s)	Pressure Gradient (kPa/m)	Slurry Temp. (°C)	Particle Size Distribution Malvern Particle Size Analyser Size (μm)	% Passing	% Retained
2.677	- 6.271	20.3	564.0	100.0	.0
2.713	- 6.320	20.5	261.6	88.6	11.4
2.701	- 6.175	20.6	160.4	52.4	36.2
2.513	- 6.837	20.9	112.8	31.1	21.3
2.511	- 6.690	21.0	84.3	21.3	9.8
2.503	- 6.655	21.0	64.6	18.1	3.2
1.704	-10.491	21.3	50.2	15.3	2.8
1.691	-10.491	21.4	39.0	13.2	2.1
1.694	-10.491	21.4	30.3	12.1	1.1
1.686	-10.466	21.4	23.7	11.0	1.1
1.684	-10.439	21.4	18.5	9.8	1.2
2.119	- 8.622	21.6	14.5	8.8	1.0
2.123	- 8.636	21.6	11.4	7.6	1.2
2.127	- 8.356	21.6	9.1	6.1	1.5
1.274	-11.975	21.7	7.2	4.8	1.3
1.274	-11.890	21.7	5.8	3.0	1.8
1.271	-11.966	21.7	Pan	.0	3.0

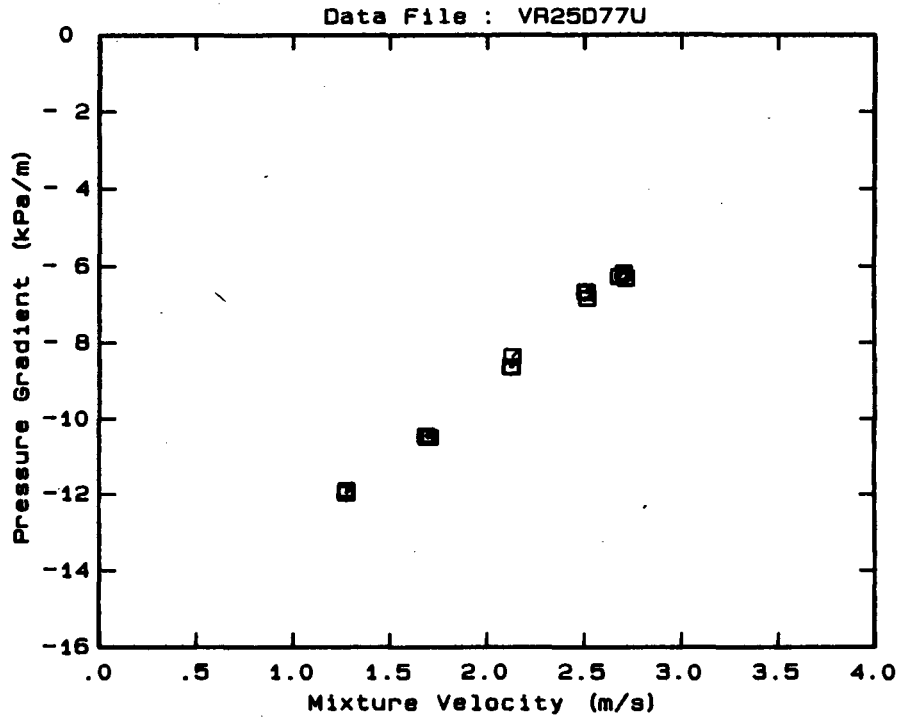

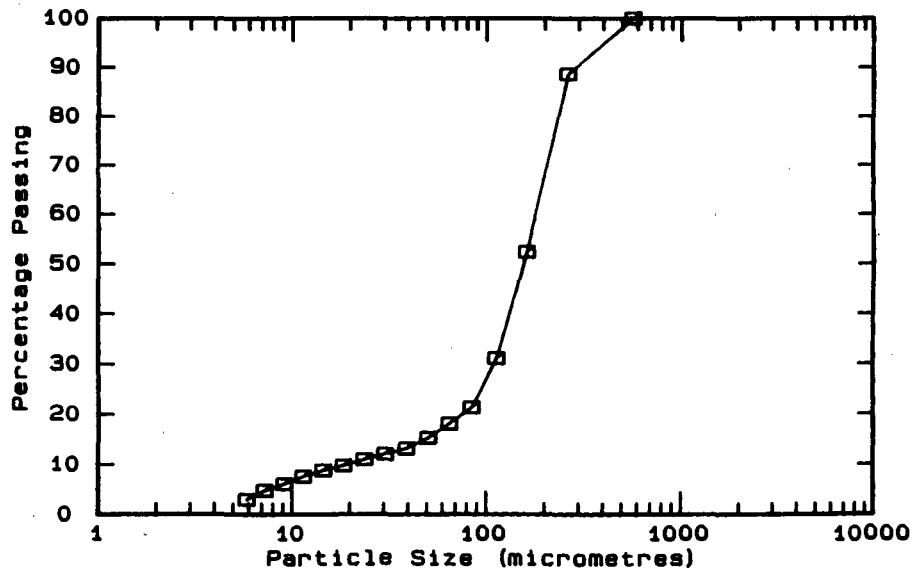

DATA FILE : VR25D86U

Test Facility	UCT 25 mm NB
Test Date	June 1990
Material Description	Vaal Reefs CCT
Material Relative Density	2.65
Slurry Relative Density	1.86
Solids Volumetric Concentration (%)	52.12
Solids Mass Concentration (%)	74.26
Mean Slurry Temperature (°C)	23.5
Pipe Internal Diameter (mm)	26.60
Pipe Roughness (μm)	21.0
Pipeline Slope	Vertical Down

Mixture Velocity (m/s)	Pressure Gradient (kPa/m)	Slurry Temp. (°C)
1.321	- 3.595	23.4
1.331	- 3.254	23.3
1.329	- 2.532	23.3
1.350	- 2.227	23.3
1.265	- 3.066	23.4
1.258	- 2.951	23.5
1.241	- 2.820	23.6
1.191	- 2.754	23.9
1.162	- 2.537	23.9
1.150	- 2.612	23.8

Particle Size Distribution
Malvern Particle Size Analyser

Size (μm)	% Passing	% Retained
564.0	100.0	.0
261.6	90.0	10.0
160.4	56.5	33.5
112.8	32.9	23.6
84.3	22.2	10.7
64.6	19.3	2.9
50.2	16.0	3.3
39.0	13.5	2.5
30.3	12.6	.9
23.7	11.6	1.0
18.5	10.3	1.3
14.5	9.3	1.0
11.4	8.1	1.2
9.1	6.6	1.5
7.2	5.3	1.3
5.8	3.4	1.9
Pan	.1	3.3

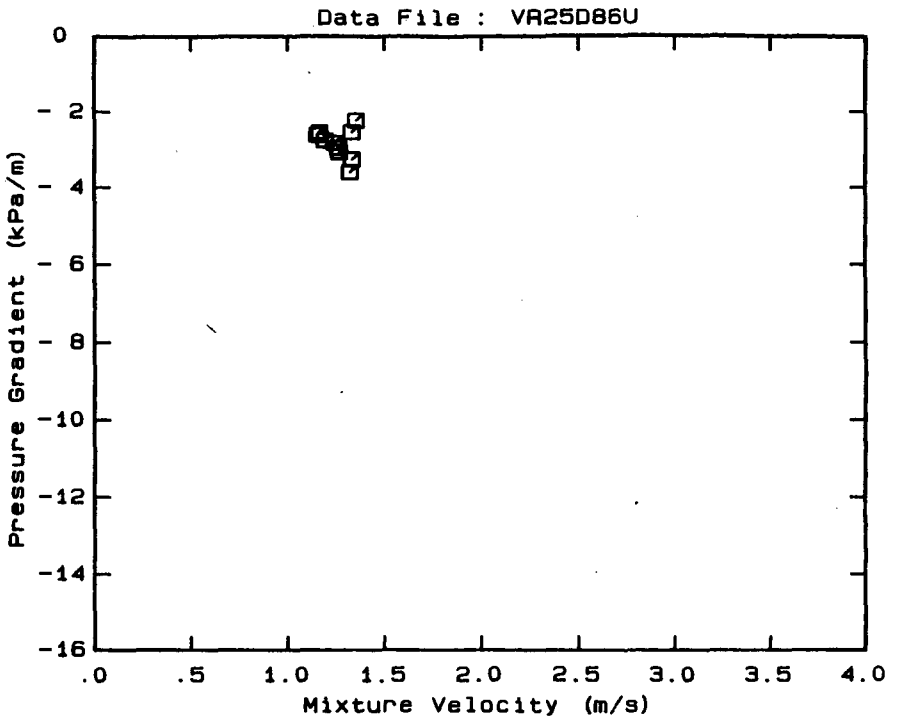

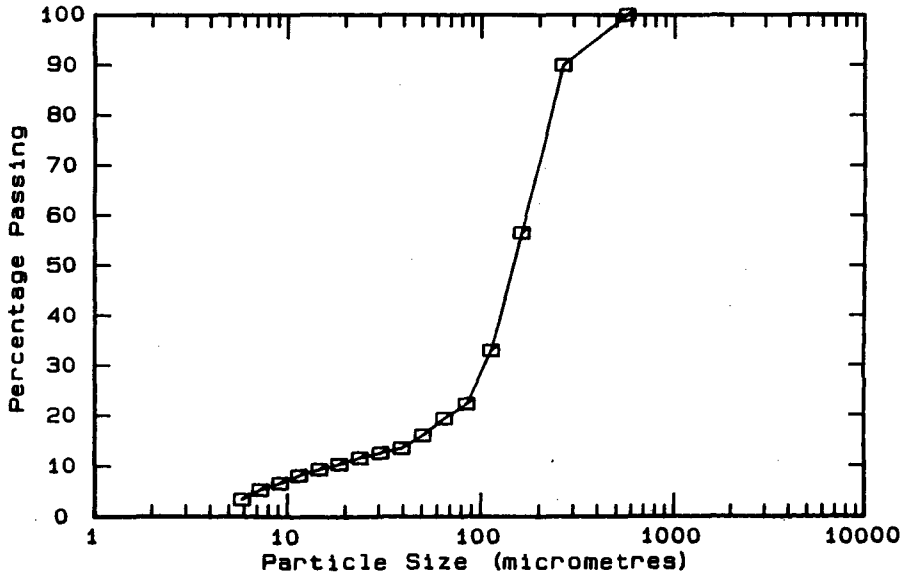

DATA FILE : VR25U55U

Test Facility	UCT 25 mm NB
Test Date	June 1990
Material Description	Vaal Reefs CCT
Material Relative Density	2.65
Slurry Relative Density	1.55
Solids Volumetric Concentration (%)	33.33
Solids Mass Concentration (%)	56.99
Mean Slurry Temperature (°C)	14.5
Pipe Internal Diameter (mm)	26.60
Pipe Roughness (μm)	21.0
Pipeline Slope	Vertical Up

Mixture Velocity (m/s)	Pressure Gradient (kPa/m)	Slurry Temp. (°C)
3.390	22.316	14.0
3.406	22.371	14.1
3.448	22.512	14.2
2.942	20.891	14.3
2.939	20.710	14.3
2.949	20.801	14.5
2.488	19.547	14.5
2.487	19.880	14.5
2.489	19.659	14.5
2.085	18.508	14.6
2.077	18.472	14.6
2.086	18.452	14.6
1.670	17.426	14.7
1.672	17.402	14.7
1.539	17.082	14.7
1.246	16.735	14.7
1.235	16.531	14.7
1.224	16.376	14.7

Particle Size Distribution
Malvern Particle Size Analyser

Size (μm)	% Passing	% Retained
564.0	100.0	.0
261.6	90.0	10.0
160.4	54.9	35.1
112.8	34.0	20.9
84.3	23.8	10.2
64.6	20.0	3.8
50.2	16.5	3.5
39.0	13.9	2.6
30.3	12.5	1.4
23.7	10.9	1.6
18.5	9.3	1.6
14.5	8.2	1.1
11.4	6.9	1.3
9.1	5.3	1.6
7.2	4.1	1.2
5.8	2.5	1.6
Pan	.0	2.5

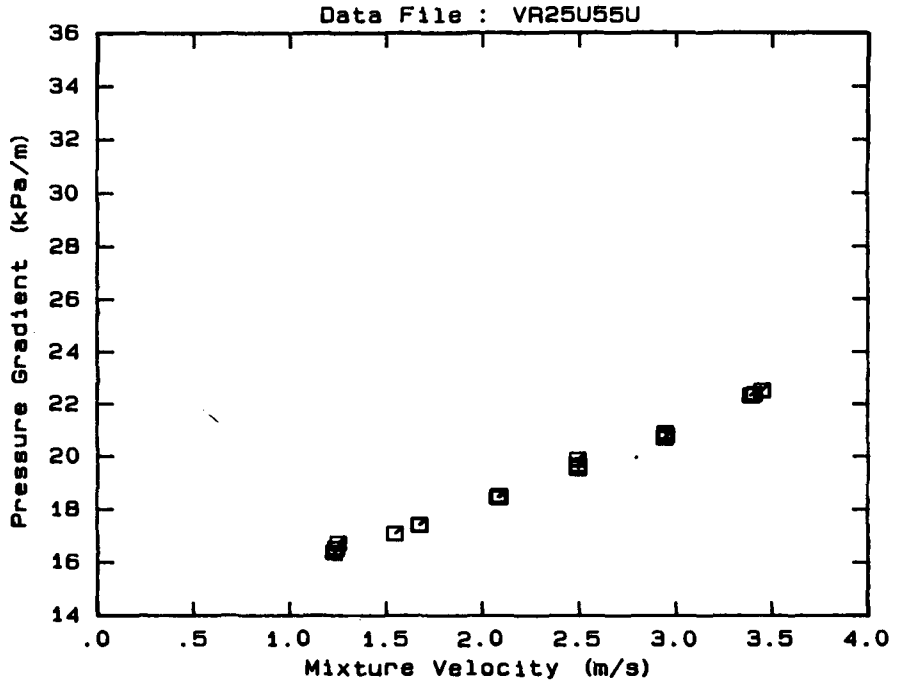

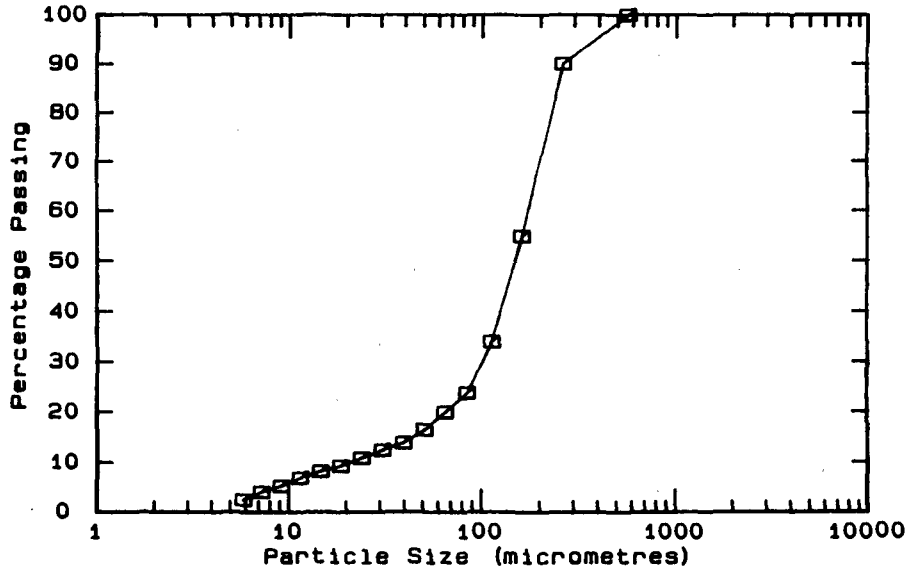

DATA FILE : VR25U66U

Test Facility	UCT 25 mm NB
Test Date	June 1990
Material Description	Vaal Reefs CCT
Material Relative Density	2.65
Slurry Relative Density	1.66
Solids Volumetric Concentration (%)	40.00
Solids Mass Concentration (%)	63.86
Mean Slurry Temperature (°C)	16.4
Pipe Internal Diameter (mm)	26.60
Pipe Roughness (μm)	21.0
Pipeline Slope	Vertical Up

Mixture Velocity (m/s)	Pressure Gradient (kPa/m)	Slurry Temp. (°C)
3.278	23.439	15.4
3.244	22.972	15.5
3.266	23.015	15.6
3.279	23.239	15.7
2.940	21.632	15.9
2.869	20.952	16.1
2.925	21.983	16.2
2.565	19.989	16.4
2.536	20.110	16.4
2.548	20.185	16.4
2.546	20.042	16.5
2.146	19.336	16.6
2.143	19.500	16.7
2.150	19.398	16.7
2.161	19.495	16.7
1.696	18.281	16.8
1.690	18.497	16.8
1.693	18.473	16.8
1.287	17.783	16.8
1.297	17.857	16.8
1.275	17.772	16.8

Particle Size Distribution
Malvern Particle Size Analyser

Size (μm)	% Passing	% Retained
564.0	100.0	.0
261.6	89.5	10.5
160.4	53.3	36.2
112.8	31.5	21.8
84.3	21.8	9.7
64.6	18.2	3.6
50.2	15.0	3.2
39.0	12.8	2.2
30.3	11.6	1.2
23.7	10.2	1.4
18.5	8.8	1.4
14.5	7.8	1.0
11.4	6.6	1.2
9.1	5.1	1.5
7.2	4.0	1.1
5.8	2.5	1.5
Pan	- .0	2.5

OBSERVED FLOW BEHAVIOUR

Velocity (m/s)	Observation (D = .0 mm)

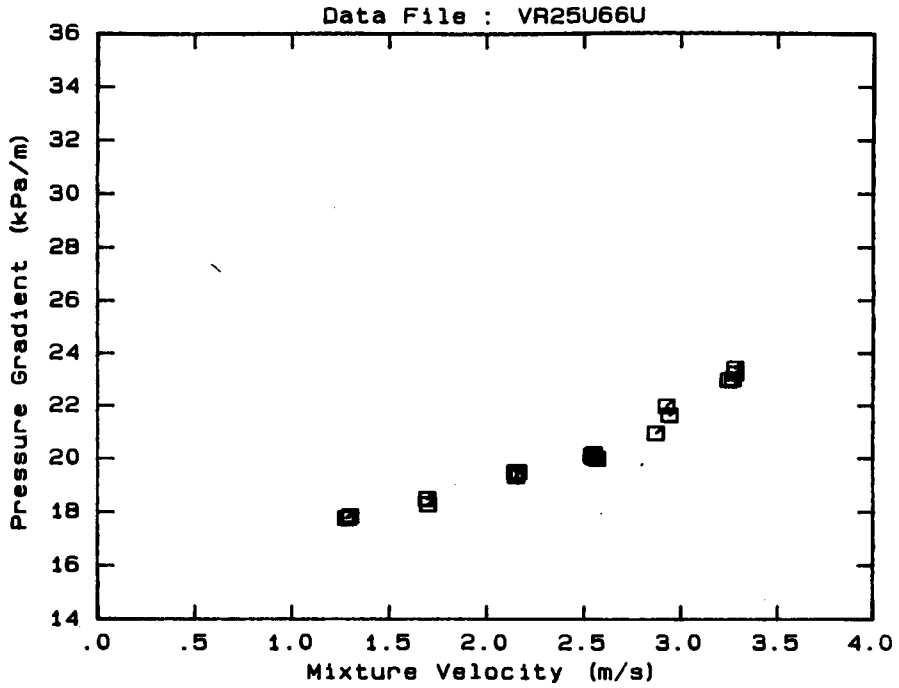

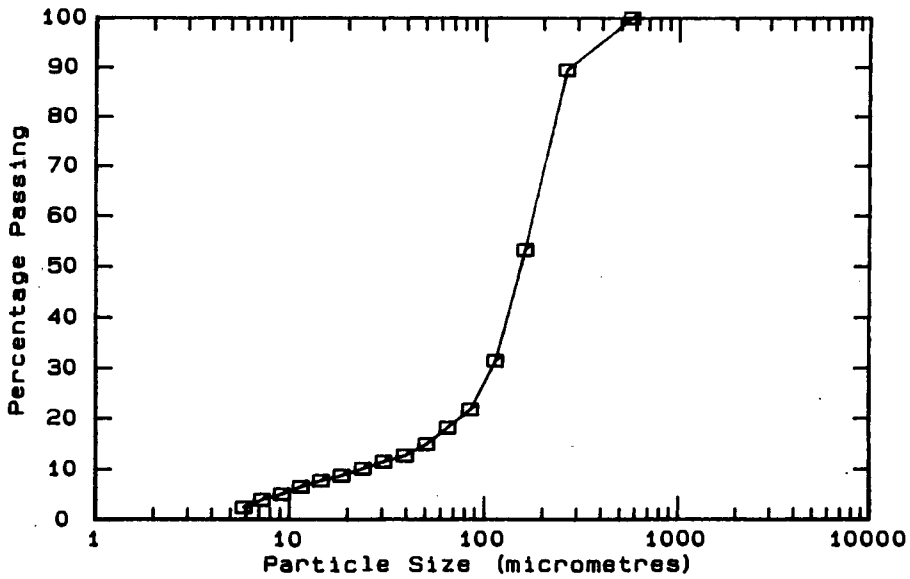

DATA FILE : VR25U75A

Test Facility	UCT 25 mm NB
Test Date	June 1990
Material Description	Vaal Reefs CCT
Material Relative Density	2.65
Slurry Relative Density	1.75
Solids Volumetric Concentration (%)	45.45
Solids Mass Concentration (%)	68.83
Mean Slurry Temperature (°C)	18.3
Pipe Internal Diameter (mm)	26.60
Pipe Roughness (μm)	21.0
Pipeline Slope	Vertical Up

Mixture Velocity (m/s)	Pressure Gradient (kPa/m)	Slurry Temp. (°C)
2.816	24.041	17.0
2.767	23.757	17.2
2.733	24.056	17.3
2.598	23.904	17.4
2.633	23.396	17.6
2.469	23.548	18.0
2.463	24.183	18.1
2.469	23.572	18.2
2.111	22.648	18.5
2.105	23.262	18.6
2.105	22.568	18.7
1.696	21.660	18.9
1.693	21.728	19.0
1.697	21.826	19.0
1.276	20.647	19.0
1.268	20.433	19.0
1.270	20.811	19.0

Particle Size Distribution
Malvern Particle Size Analyser

Size (μm)	% Passing	% Retained
564.0	100.0	.0
261.6	89.5	10.5
160.4	53.5	36.0
112.8	30.1	23.4
84.3	21.0	9.1
64.6	17.4	3.6
50.2	14.0	3.4
39.0	12.0	2.0
30.3	11.0	1.0
23.7	9.8	1.2
18.5	8.5	1.3
14.5	7.6	.9
11.4	6.5	1.1
9.1	5.2	1.3
7.2	4.1	1.1
5.8	2.6	1.5
Pan	.1	2.5

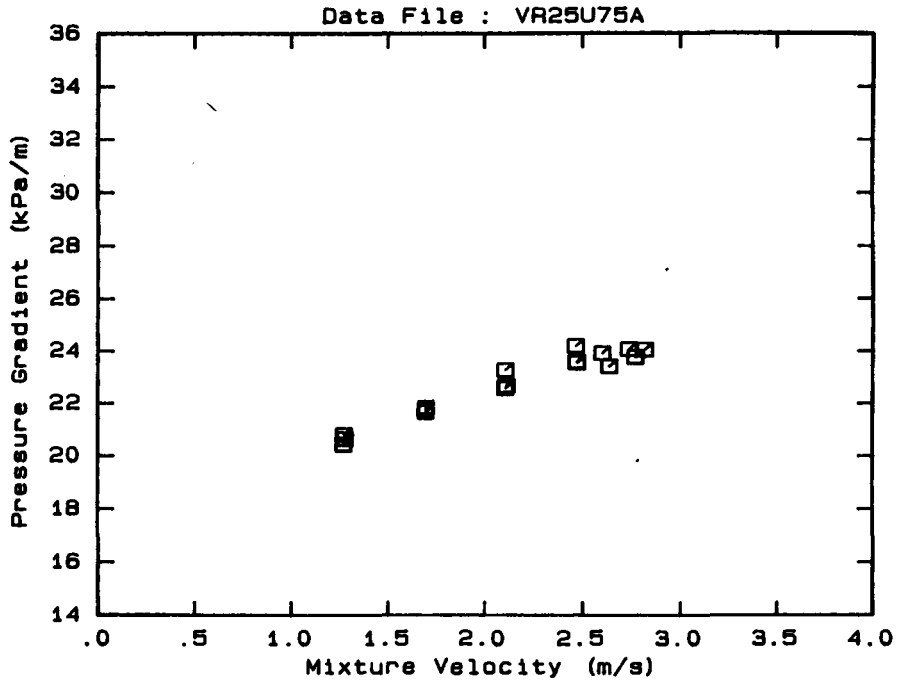

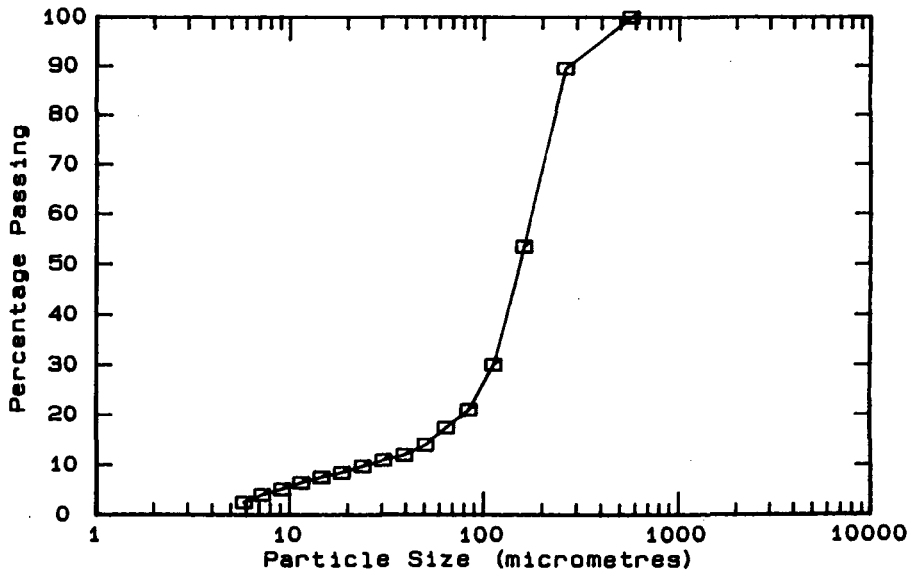

DATA FILE : VR25U75B

Test Facility	UCT 25 mm NB
Test Date	June 1990
Material Description	Vaal Reefs CCT
Material Relative Density	2.65
Slurry Relative Density	1.75
Solids Volumetric Concentration (%)	45.45
Solids Mass Concentration (%)	68.83
Mean Slurry Temperature (°C)	18.1
Pipe Internal Diameter (mm)	26.60
Pipe Roughness (μm)	21.0
Pipeline Slope	Vertical Up

Mixture Velocity (m/s)	Pressure Gradient (kPa/m)	Slurry Temp. (°C)
2.784	23.194	17.2
2.789	24.352	17.2
2.801	23.411	17.2
2.812	23.381	17.2
2.817	24.081	17.2
2.814	24.020	17.2
2.532	23.702	17.3
2.558	22.901	17.4
2.552	23.244	17.6
2.536	23.377	18.0
2.121	22.215	18.1
2.114	22.522	18.2
2.091	22.405	18.5
2.086	22.444	18.6
1.681	21.296	18.7
1.674	21.376	18.9
1.680	21.486	19.0
1.679	21.523	19.0
1.254	20.759	19.0
1.256	20.603	19.0
1.250	20.547	19.0

Particle Size Distribution
Malvern Particle Size Analyser

Size (μm)	% Passing	% Retained
564.0	100.0	.0
261.6	88.9	11.1
160.4	51.4	37.5
112.8	29.8	21.6
84.3	20.2	9.6
64.6	16.9	3.3
50.2	13.9	3.0
39.0	11.9	2.0
30.3	10.9	1.0
23.7	9.8	1.1
18.5	8.6	1.2
14.5	7.7	.9
11.4	6.6	1.1
9.1	5.2	1.4
7.2	4.0	1.2
5.8	2.4	1.6
Pan	- .3	2.7

OBSERVED FLOW BEHAVIOUR

Velocity (m/s)	Observation (D = .0 mm)

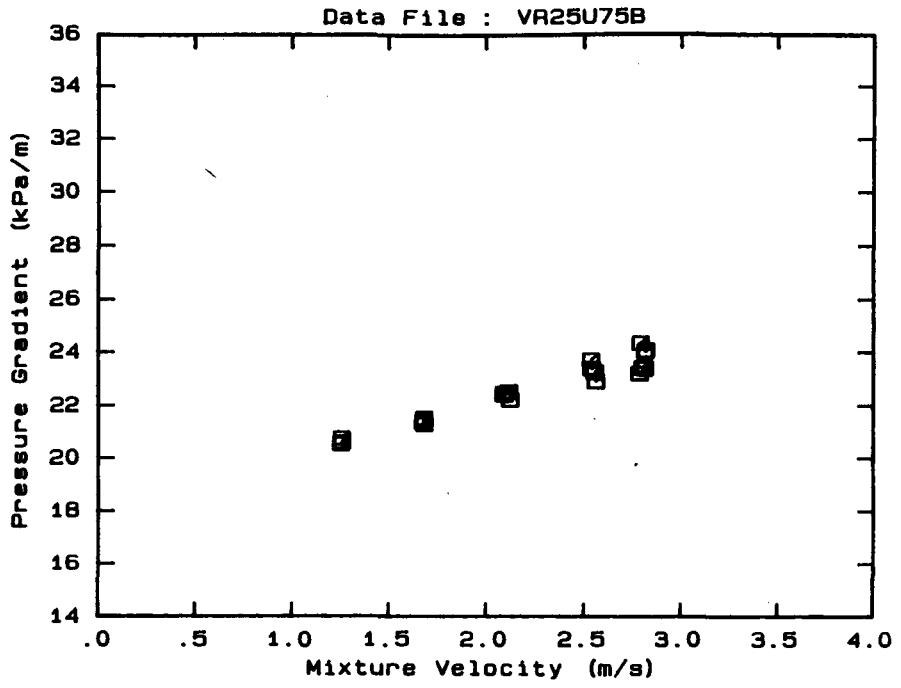

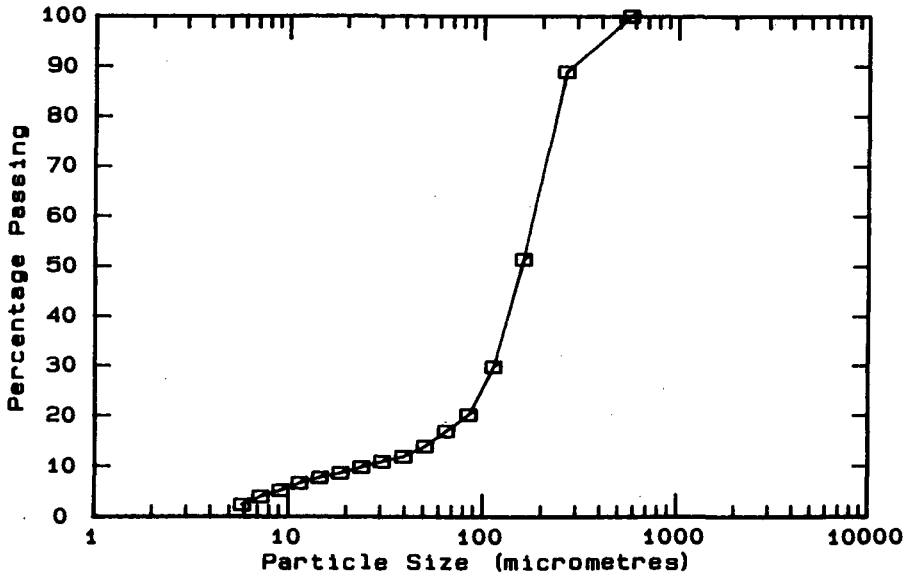

DATA FILE : VR25U77U

Test Facility	UCT 25 mm NB
Test Date	June 1990
Material Description	Vaal Reefs CCT
Material Relative Density	2.65
Slurry Relative Density	1.77
Solids Volumetric Concentration (%)	46.67
Solids Mass Concentration (%)	69.87
Mean Slurry Temperature (°C)	21.2
Pipe Internal Diameter (mm)	26.60
Pipe Roughness (μm)	21.0
Pipeline Slope	Vertical Up

Mixture Velocity (m/s)	Pressure Gradient (kPa/m)	Slurry Temp. (°C)
2.677	25.768	20.3
2.713	25.993	20.5
2.701	25.379	20.6
2.513	25.330	20.9
2.511	25.613	21.0
2.503	25.515	21.0
1.704	23.314	21.3
1.691	23.396	21.4
1.694	23.048	21.4
1.686	23.487	21.4
1.684	23.213	21.4
2.119	24.325	21.6
2.123	24.735	21.6
2.127	25.074	21.6
1.274	21.970	21.7
1.274	22.199	21.7
1.271	22.070	21.7

Particle Size Distribution Malvern Particle Size Analyser		
Size (μm)	% Passing	% Retained
564.0	100.0	.0
261.6	88.6	11.4
160.4	52.4	36.2
112.8	31.1	21.3
84.3	21.3	9.8
64.6	18.1	3.2
50.2	15.3	2.8
39.0	13.2	2.1
30.3	12.1	1.1
23.7	11.0	1.1
18.5	9.8	1.2
14.5	8.8	1.0
11.4	7.6	1.2
9.1	6.1	1.5
7.2	4.8	1.3
5.8	3.0	1.8
Pan	.0	3.0

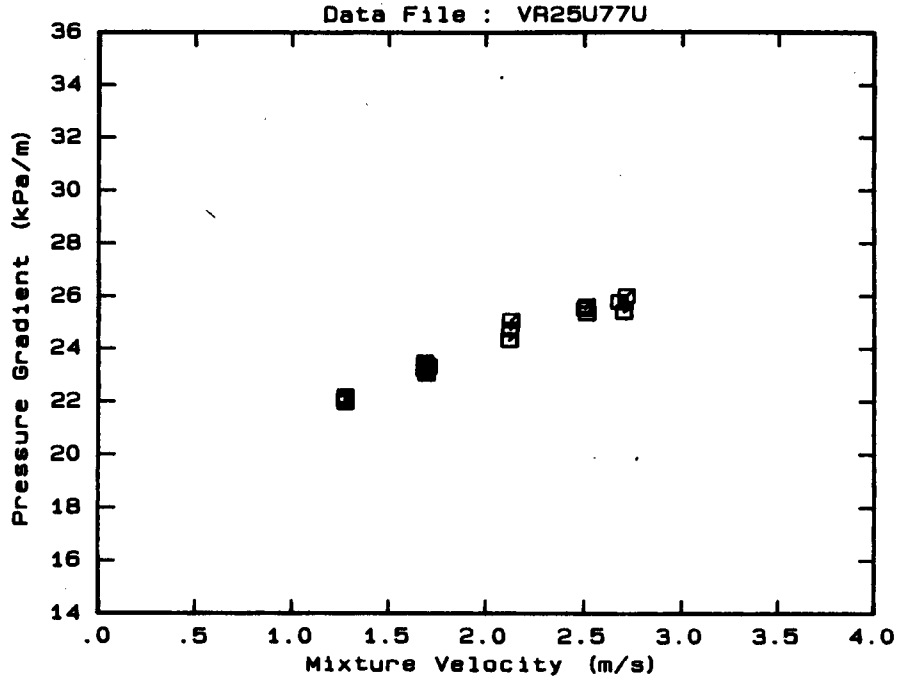

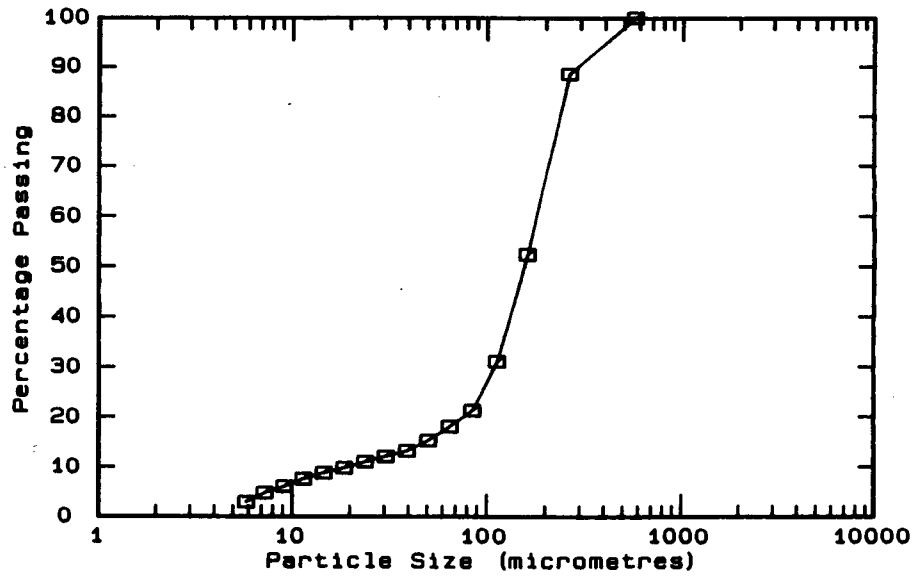

DATA FILE : VR25U86U

Test Facility	UCT 25 mm NB
Test Date	June 1990
Material Description	Vaal Reefs CCT
Material Relative Density	2.65
Slurry Relative Density	1.86
Solids Volumetric Concentration (%)	52.12
Solids Mass Concentration (%)	74.26
Mean Slurry Temperature (°C)	23.5
Pipe Internal Diameter (mm)	26.60
Pipe Roughness (μm)	21.0
Pipeline Slope	Vertical Up

Mixture Velocity (m/s)	Pressure Gradient (kPa/m)	Slurry Temp. (°C)
1.321	32.692	23.4
1.331	33.412	23.3
1.329	33.933	23.3
1.350	34.420	23.3
1.265	33.376	23.4
1.258	33.922	23.5
1.241	33.722	23.6
1.191	33.742	23.9
1.162	34.070	23.9
1.150	33.900	23.8

Particle Size Distribution
Malvern Particle Size Analyser

Size (μm)	% Passing	% Retained
564.0	100.0	.0
261.6	90.0	10.0
160.4	56.5	33.5
112.8	32.9	23.6
84.3	22.2	10.7
64.6	19.3	2.9
50.2	16.0	3.3
39.0	13.5	2.5
30.3	12.6	.9
23.7	11.6	1.0
18.5	10.3	1.3
14.5	9.3	1.0
11.4	8.1	1.2
9.1	6.6	1.5
7.2	5.3	1.3
5.8	3.4	1.9
Pan	.1	3.3

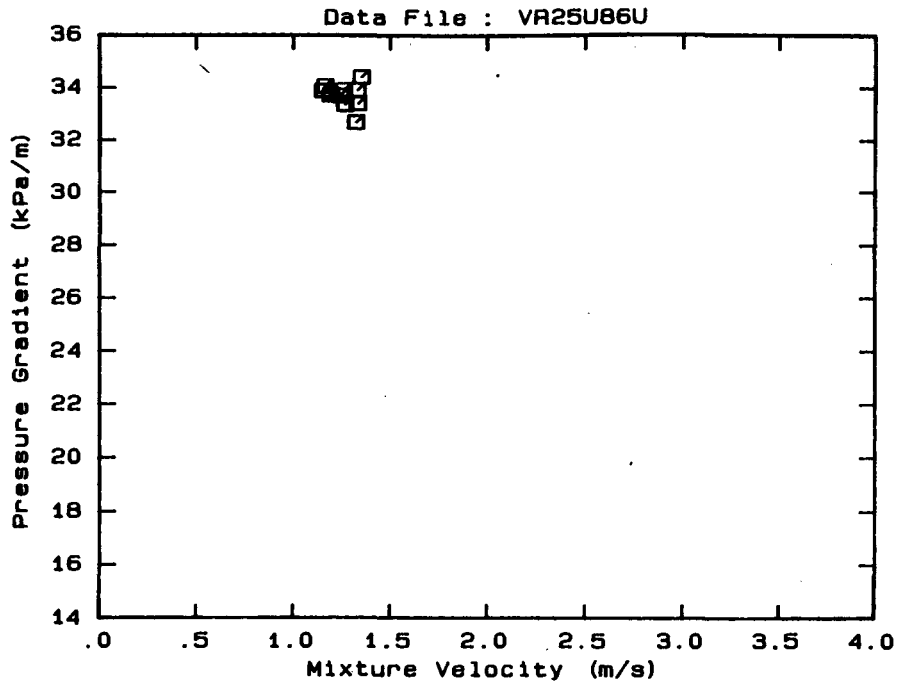

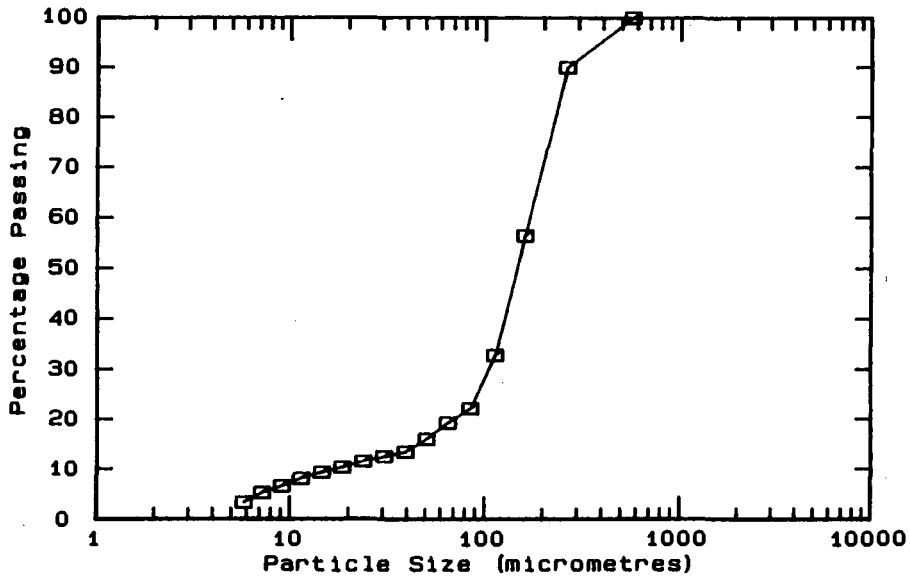

DATA FILE : VR40H71U

Test Facility	UCT 40 mm NB
Test Date	August 1990
Material Description	Vaal Reefs CCT
Material Relative Density	2.65
Slurry Relative Density	1.71
Solids Volumetric Concentration (%)	43.03
Solids Mass Concentration (%)	66.68
Mean Slurry Temperature (°C)	20.1
Pipe Internal Diameter (mm)	40.00
Pipe Roughness (μm)	52.0
Pipeline Slope	Horizontal

Mixture Velocity (m/s)	Pressure Gradient (kPa/m)	Slurry Temp. (°C)
3.788	6.040	19.8
3.788	5.950	19.9
3.774	6.155	20.0
3.775	6.087	20.1
3.767	6.267	20.1
3.795	6.023	20.2
3.212	4.804	20.3
3.208	4.963	20.3
3.217	4.957	20.3
3.219	5.017	20.3
3.221	4.922	20.3
2.717	3.915	20.3
2.716	3.929	20.3
2.711	4.096	20.3
2.716	3.835	20.2
2.167	3.198	20.2
2.164	3.081	20.2
2.160	3.041	20.1
2.158	3.236	20.1
1.662	2.415	20.0
1.678	2.418	20.0
1.671	2.411	20.0
1.666	2.438	20.0
1.103	2.286	19.9
1.097	2.142	19.9
1.101	2.413	19.8
1.124	2.342	19.8
1.123	2.346	19.8
1.115	2.378	19.7

Particle Size Distribution
Malvern Particle Size Analyser

Size (μm)	% Passing	% Retained
564.0	100.0	.0
261.6	86.7	13.3
160.4	48.8	37.9
112.8	29.6	19.2
84.3	19.4	10.2
64.6	16.1	3.3
50.2	13.5	2.6
39.0	12.0	1.5
30.3	10.9	1.1
23.7	9.8	1.1
18.5	8.9	.9
14.5	8.0	.9
11.4	6.8	1.2
9.1	5.4	1.4
7.2	4.3	1.1
5.8	2.7	1.6
Pan	.0	2.7

OBSERVED FLOW BEHAVIOUR

Velocity (m/s)	Observation (D = 46.0 mm)
.87	30% stationary bed
1.28	Asymmetric - slid particles
1.64	Asymmetric - slid particles
2.50	Appears homogeneous
2.45	Appears homogeneous
2.86	Appears homogeneous

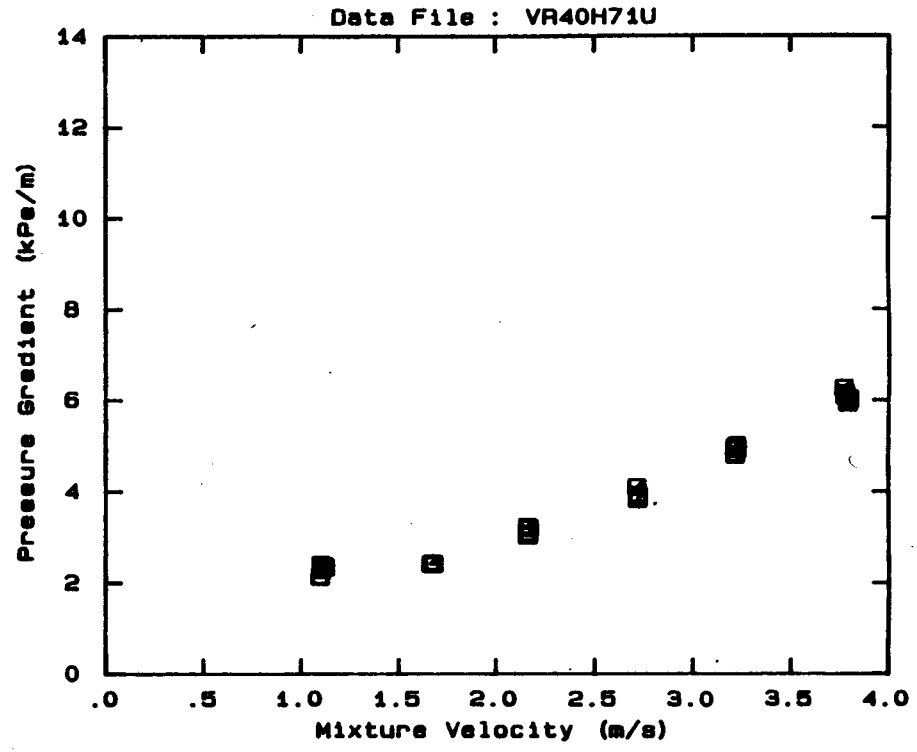

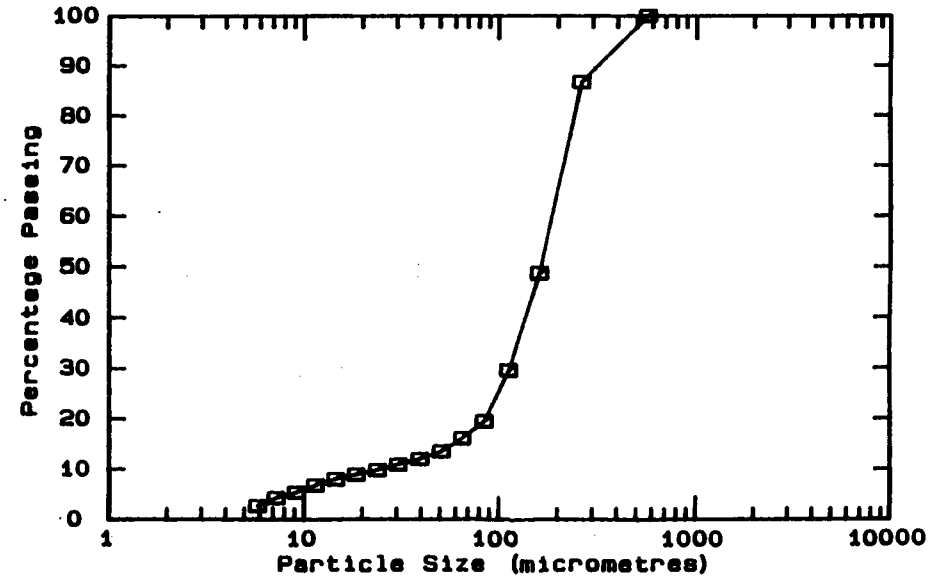

DATA FILE : VR40H75U

Test Facility	UCT 40 mm NB
Test Date	August 1990
Material Description	Vaal Reefs CCT
Material Relative Density	2.65
Slurry Relative Density	1.75
Solids Volumetric Concentration (%)	45.45
Solids Mass Concentration (%)	68.83
Mean Slurry Temperature (°C)	20.9
Pipe Internal Diameter (mm)	40.00
Pipe Roughness (μm)	52.0
Pipeline Slope	Horizontal

Mixture Velocity (m/s)	Pressure Gradient (kPa/m)	Slurry Temp. (°C)
3.897	8.873	19.9
3.918	8.432	20.0
3.931	8.679	20.2
3.897	8.859	20.3
3.947	8.787	20.4
3.228	6.653	20.9
3.230	7.099	20.9
3.232	7.098	21.0
3.238	6.841	21.0
3.236	6.909	21.1
2.681	5.956	21.1
2.677	5.813	21.2
2.673	5.842	21.2
2.675	5.923	21.2
2.116	4.713	21.2
2.116	4.673	21.2
2.111	4.663	21.2
2.119	4.706	21.2
1.628	3.411	21.2
1.626	3.455	21.2
1.627	3.380	21.1
1.616	3.420	21.1
1.007	2.446	21.0
1.000	2.356	21.0
1.001	2.417	21.0
.993	2.400	20.9

Particle Size Distribution
Malvern Particle Size Analyser

Size (μm)	% Passing	% Retained
564.0	100.0	.0
261.6	86.9	13.1
160.4	50.7	36.2
112.8	28.4	22.3
84.3	19.4	9.0
64.6	15.5	3.9
50.2	12.7	2.8
39.0	11.3	1.4
30.3	10.3	1.0
23.7	9.3	1.0
18.5	8.5	.8
14.5	7.7	.8
11.4	6.6	1.1
9.1	5.3	1.3
7.2	4.2	1.1
5.8	2.6	1.6
Pan	- .1	2.7

OBSERVED FLOW BEHAVIOUR

Velocity (m/s)	Observation (D = 46.0 mm)
.79	Asymmetric - slid particles
1.24	Asymmetric - slid particles
1.64	Appears homogeneous
2.05	Appears homogeneous
2.45	Appears homogeneous
2.94	Appears homogeneous

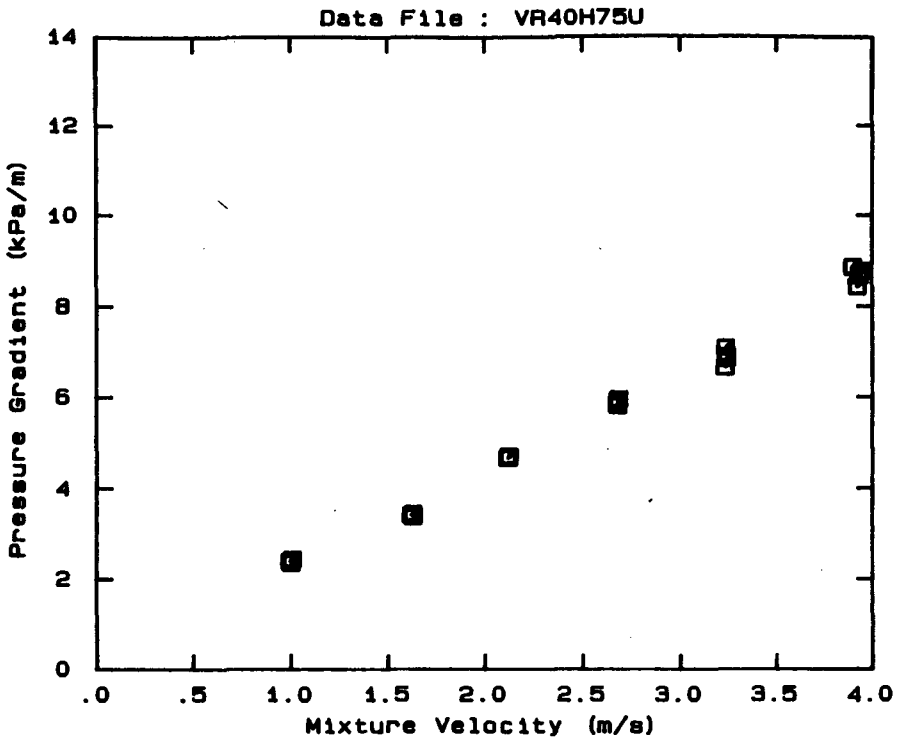

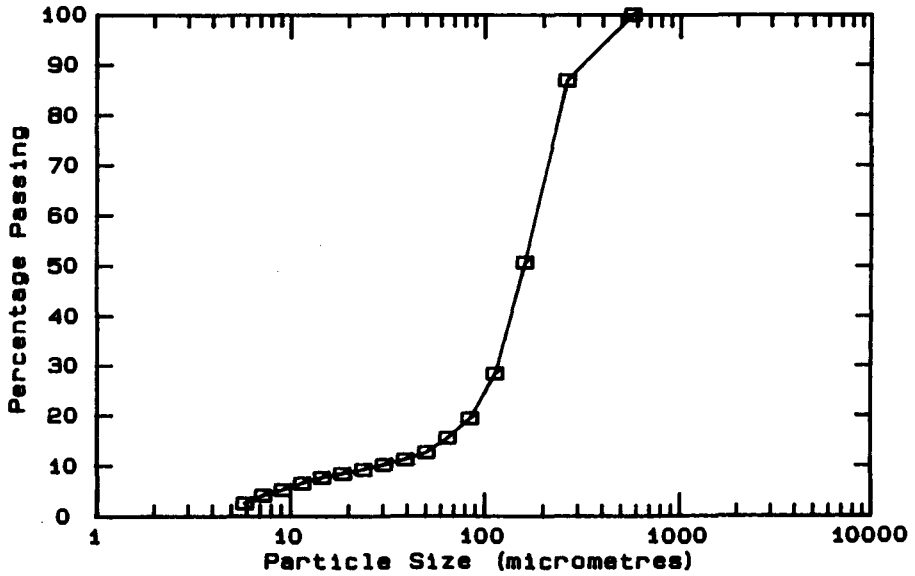

DATA FILE : VR40H80U

Test Facility	UCT 40 mm NB
Test Date	August 1990
Material Description	Vaal Reefs CCT
Material Relative Density	2.65
Slurry Relative Density	1.80
Solids Volumetric Concentration (%)	48.48
Solids Mass Concentration (%)	71.38
Mean Slurry Temperature (°C)	22.5
Pipe Internal Diameter (mm)	40.00
Pipe Roughness (μm)	52.0
Pipeline Slope	Horizontal

Mixture Velocity (m/s)	Pressure Gradient (kPa/m)	Slurry Temp. (°C)
2.987	12.851	21.1
3.003	12.121	21.4
3.014	12.248	21.6
3.023	11.849	21.8
3.035	11.649	22.0
2.613	10.756	22.3
2.611	10.702	22.4
2.618	10.583	22.5
2.619	10.653	22.6
2.093	8.768	22.8
2.085	8.792	22.8
2.085	8.690	22.9
2.086	8.812	22.9
1.624	6.805	22.9
1.618	6.913	22.9
1.616	6.909	22.9
1.615	6.946	22.9
1.044	4.869	22.9
1.008	4.987	22.9
.995	5.088	22.8
.988	5.061	22.8
.981	5.097	22.8
.710	3.922	22.7
.690	3.952	22.6
.669	3.909	22.6
.662	3.896	22.6

Particle Size Distribution
Malvern Particle Size Analyser

Size (μm)	% Passing	% Retained
564.0	100.0	.0
261.6	87.8	12.2
160.4	51.1	36.7
112.8	28.2	22.9
84.3	19.2	9.0
64.6	15.8	3.4
50.2	12.9	2.9
39.0	11.6	1.3
30.3	10.8	.8
23.7	9.7	1.1
18.5	8.9	.8
14.5	8.1	.8
11.4	7.1	1.0
9.1	5.8	1.3
7.2	4.6	1.2
5.8	2.9	1.7
Pan	.1	2.8

OBSERVED FLOW BEHAVIOUR

Velocity (m/s)	Observation (D = 46.0 mm)
.55	Appears homogeneous
.83	Appears homogeneous
1.24	Appears homogeneous
1.60	Appears homogeneous
2.01	Appears homogeneous
2.29	Appears homogeneous

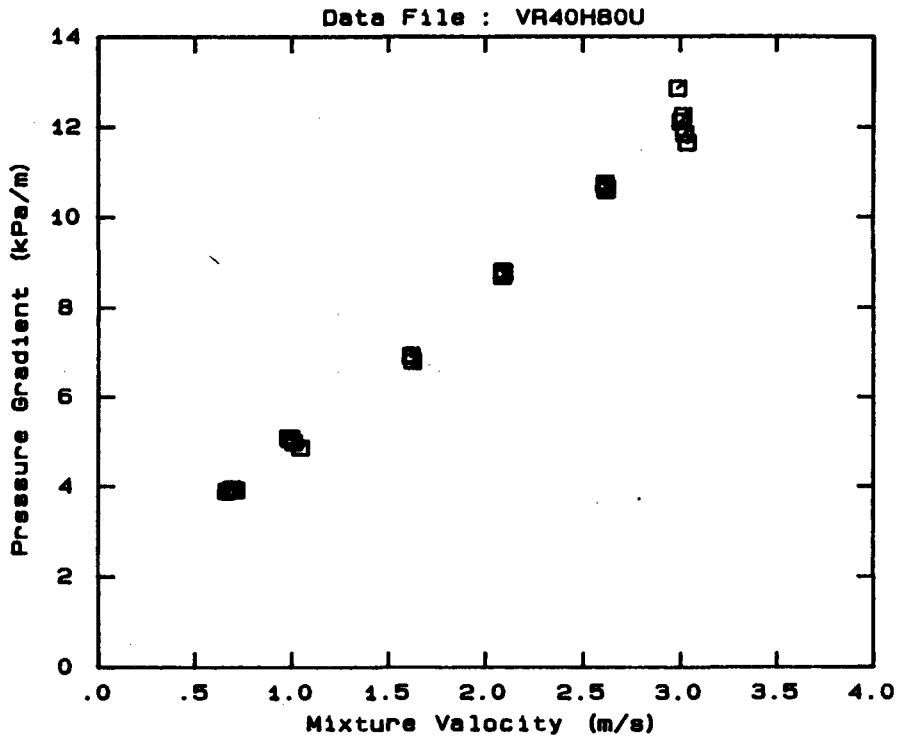

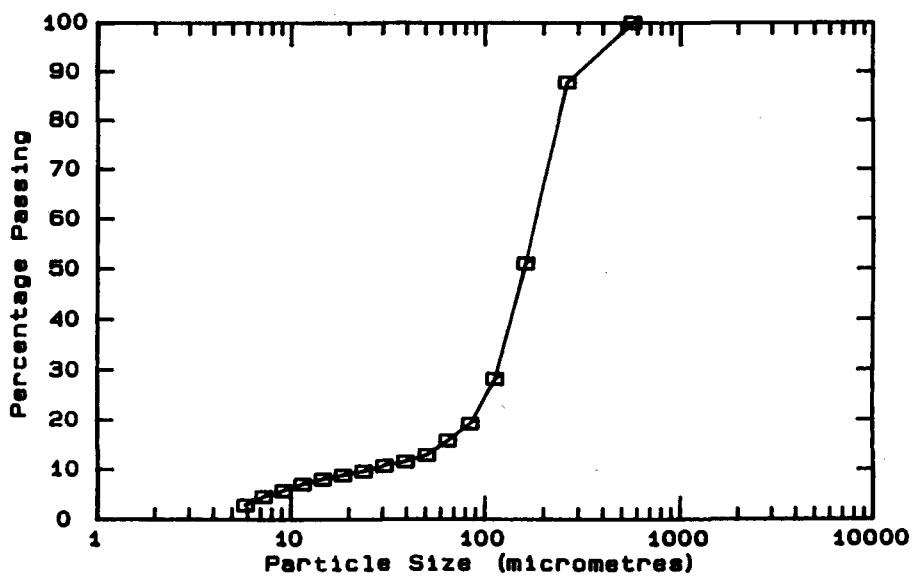

DATA FILE : VR40H83U

Test Facility	UCT 40 mm NB
Test Date	August 1990
Material Description	Vaal Reefs CCT
Material Relative Density	2.65
Slurry Relative Density	1.83
Solids Volumetric Concentration (%)	50.30
Solids Mass Concentration (%)	72.84
Mean Slurry Temperature (°C)	25.9
Pipe Internal Diameter (mm)	40.00
Pipe Roughness (μm)	52.0
Pipeline Slope	Horizontal

Mixture Velocity (m/s)	Pressure Gradient (kPa/m)	Slurry Temp. (°C)
2.282	13.363	24.4
2.275	13.471	24.7
2.270	13.707	24.9
2.301	13.846	25.1
2.310	14.003	25.3
2.304	13.735	25.4
1.853	10.302	25.8
1.841	10.635	25.9
1.840	10.663	26.0
1.853	10.455	26.0
1.851	10.785	26.1
1.851	10.765	26.1
1.348	7.816	26.2
1.331	7.766	26.2
1.318	7.792	26.3
1.320	7.856	26.3
.933	6.539	26.3
.915	6.633	26.3
.903	6.555	26.2
.889	6.508	26.2
.868	6.395	26.2
.596	5.219	26.1
.593	5.239	26.1
.593	5.348	26.1
.600	5.302	26.0
.597	5.195	26.0
.318	3.331	25.9
.286	3.313	25.9
.268	3.296	25.9
.258	3.424	25.8
.257	3.382	25.8

Particle Size Distribution
Malvern Particle Size Analyser

Size (μm)	% Passing	% Retained
564.0	100.0	.0
261.6	87.6	12.4
160.4	49.8	37.8
112.8	28.3	21.5
84.3	17.9	10.4
64.6	14.9	3.0
50.2	12.1	2.8
39.0	10.6	1.5
30.3	9.8	.8
23.7	8.9	.9
18.5	8.1	.8
14.5	7.4	.7
11.4	6.4	1.0
9.1	5.1	1.3
7.2	4.1	1.0
5.8	2.5	1.6
Pan	- .3	2.8

OBSERVED FLOW BEHAVIOUR

Velocity (m/s)	Observation (D = 46.0 mm)
.26	Appears homogeneous
.51	Appears homogeneous
.75	Appears homogeneous
1.03	Appears homogeneous
1.36	Appears homogeneous
1.76	Appears homogeneous

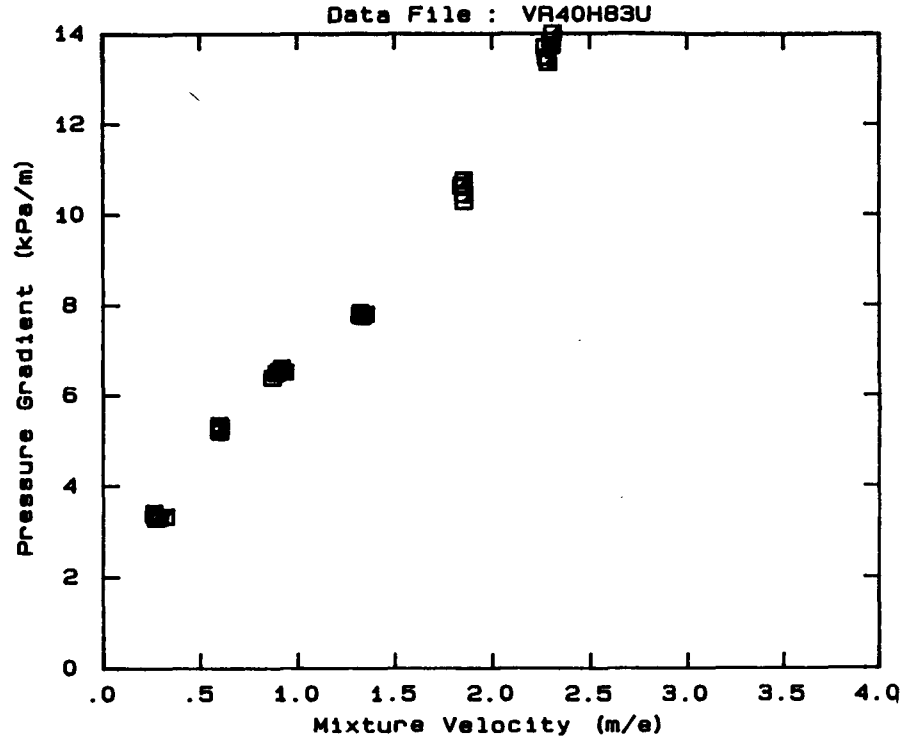

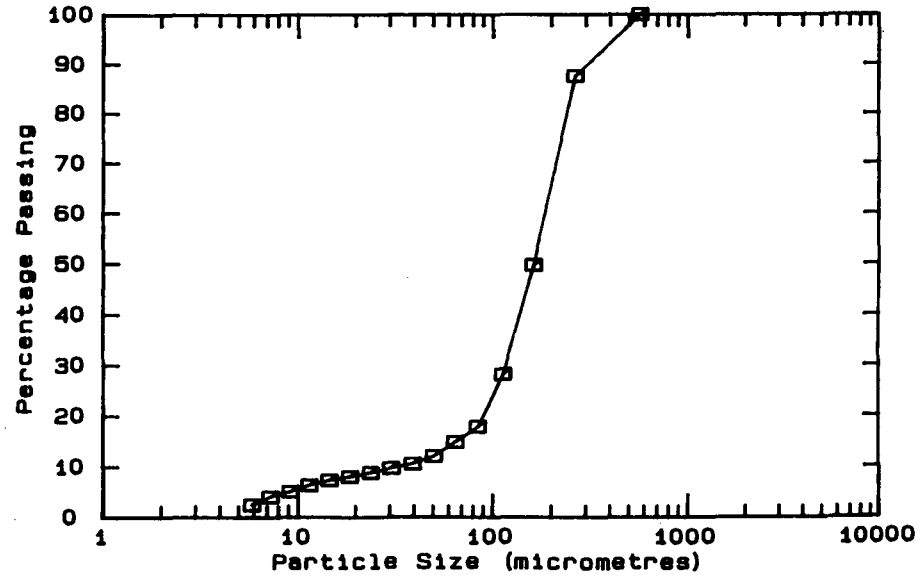

DATA FILE : VR80H79U

Test Facility	UCT 80 mm NB
Test Date	June 1990
Material Description	Vaal Reefs CCT
Material Relative Density	2.65
Slurry Relative Density	1.79
Solids Volumetric Concentration (%)	47.88
Solids Mass Concentration (%)	70.88
Mean Slurry Temperature (°C)	20.1
Pipe Internal Diameter (mm)	73.40
Pipe Roughness (μm)	84.0
Pipeline Slope	Horizontal

Mixture Velocity (m/s)	Pressure Gradient (kPa/m)	Slurry Temp. (°C)
3.371	3.939	19.2
3.382	3.950	19.3
3.387	4.041	19.5
3.401	3.748	19.8
2.920	3.296	19.9
2.925	3.311	20.0
2.925	3.156	20.1
2.930	3.386	20.3
2.449	3.248	20.4
2.455	3.124	20.4
2.453	2.991	20.4
2.457	2.910	20.4
2.462	3.221	20.4
2.461	2.859	20.4
1.953	2.523	20.5
1.947	2.362	20.5
1.950	2.473	20.4
1.525	2.080	20.4
1.512	1.916	20.3
1.518	2.149	20.3
1.515	2.259	20.3
1.513	2.065	20.2
1.034	2.327	20.1
1.043	2.626	20.1
1.046	2.599	20.0
1.047	2.590	20.0
1.041	2.611	20.0

Particle Size Distribution
Malvern Particle Size Analyser

Size (μm)	% Passing	% Retained
564.0	100.0	.0
261.6	89.9	10.1
160.4	52.1	37.8
112.8	28.7	23.4
84.3	18.9	9.8
64.6	15.5	3.4
50.2	12.3	3.2
39.0	10.5	1.8
30.3	9.7	.8
23.7	8.7	1.0
18.5	7.7	1.0
14.5	6.9	.8
11.4	6.0	.9
9.1	4.8	1.2
7.2	3.8	1.0
5.8	2.4	1.4
Pan	- .0	2.4

OBSERVED FLOW BEHAVIOUR

Velocity (m/s)	Observation (D = 71.0 mm)
1.12	Sliding bed
1.61	Asymmetric - slid part
2.10	Asymmetric - slid part
2.63	Appears homgeneous
3.15	Appears homgeneous
3.64	Appears homogeneous

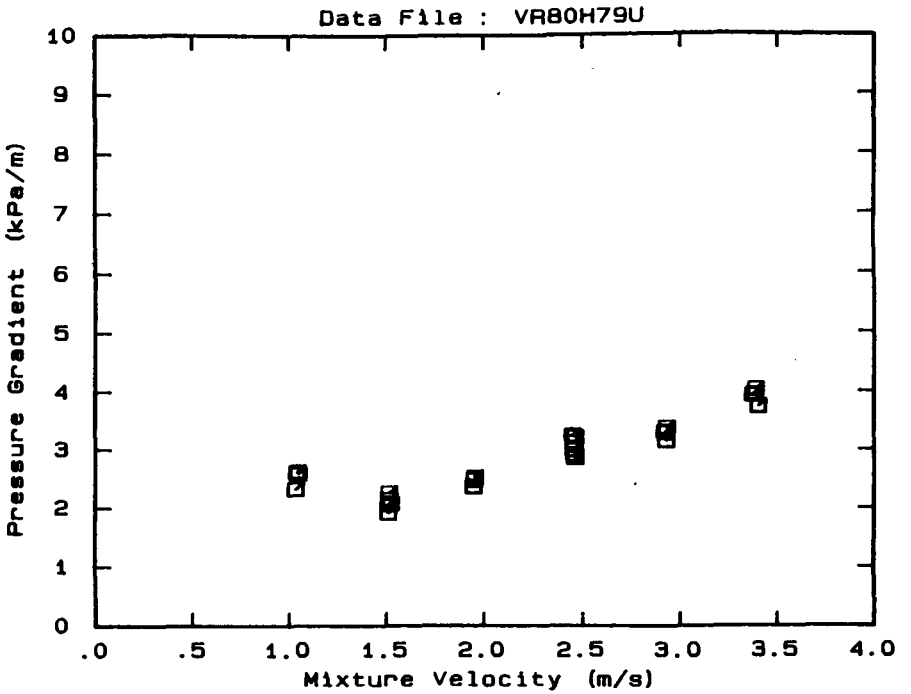

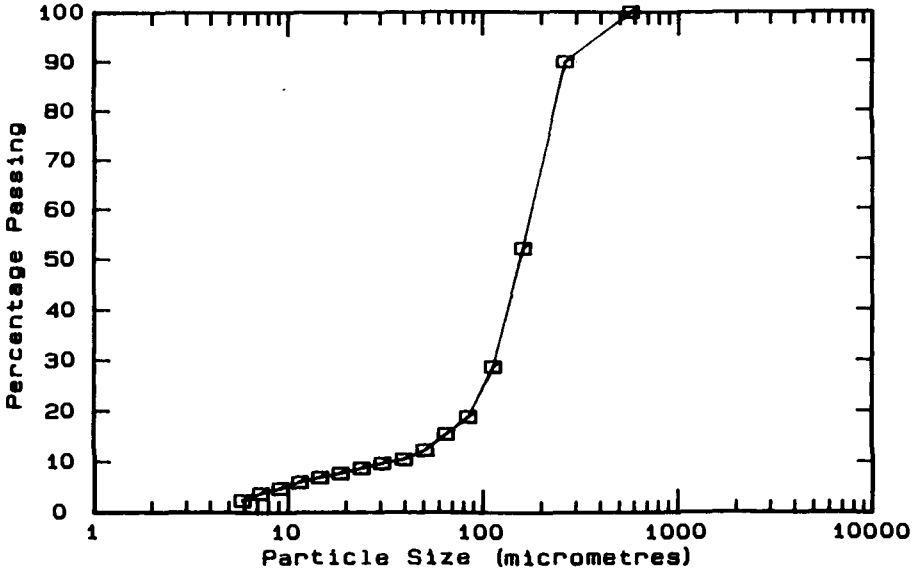

DATA FILE : VR80H81U

Test Facility	UCT 80 mm NB
Test Date	June 1990
Material Description	Vaal Reefs CCT
Material Relative Density	2.65
Slurry Relative Density	1.81
Solids Volumetric Concentration (%)	49.09
Solids Mass Concentration (%)	71.87
Mean Slurry Temperature (°C)	22.3
Pipe Internal Diameter (mm)	73.40
Pipe Roughness (μm)	84.0
Pipeline Slope	Horizontal

Mixture Velocity (m/s)	Pressure Gradient (kPa/m)	Slurry Temp. (°C)
3.319	6.236	20.9
3.330	6.069	21.1
3.343	6.134	21.3
3.366	6.204	21.5
2.966	5.334	21.9
2.981	5.756	22.1
2.982	5.633	22.2
2.995	5.303	22.3
2.470	4.308	22.5
2.466	4.676	22.6
2.465	4.473	22.7
2.465	4.819	22.7
2.467	4.630	22.7
1.990	3.630	22.7
1.989	3.222	22.8
1.984	3.457	22.8
1.988	3.361	22.8
1.984	3.515	22.8
1.481	3.008	22.8
1.480	2.926	22.7
1.478	2.930	22.7
.960	2.442	22.6
.939	2.329	22.5
.919	2.370	22.4
.898	2.356	22.4
.872	2.370	22.3

Particle Size Distribution
Malvern Particle Size Analyser

Size (μm)	% Passing	% Retained
564.0	100.0	.0
261.6	90.9	9.1
160.4	53.0	37.9
112.8	29.7	23.3
84.3	20.0	9.7
64.6	16.5	3.5
50.2	13.4	3.1
39.0	11.5	1.9
30.3	10.6	.9
23.7	9.7	.9
18.5	8.6	1.1
14.5	7.8	.8
11.4	6.8	1.0
9.1	5.5	1.3
7.2	4.4	1.1
5.8	2.8	1.6
Pan	.1	2.7

OBSERVED FLOW BEHAVIOUR

Velocity (m/s)	Observation (D = 71.0 mm)
1.02	Appears homogeneous
1.58	Appears homogeneous
2.14	Appears homogeneous
2.66	Appears homogeneous
3.19	Appears homogeneous
3.57	Appears homogeneous

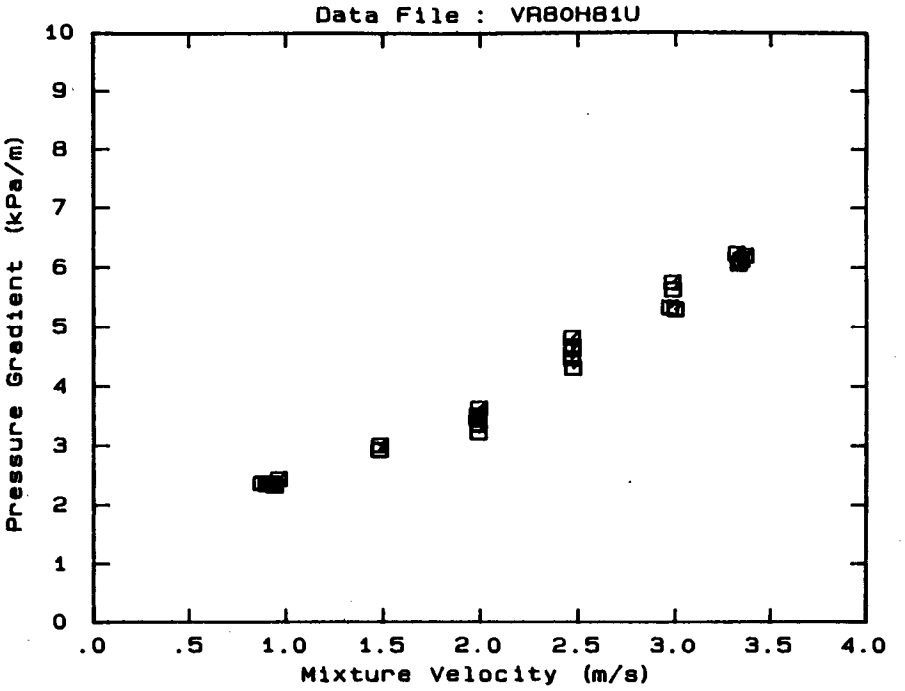

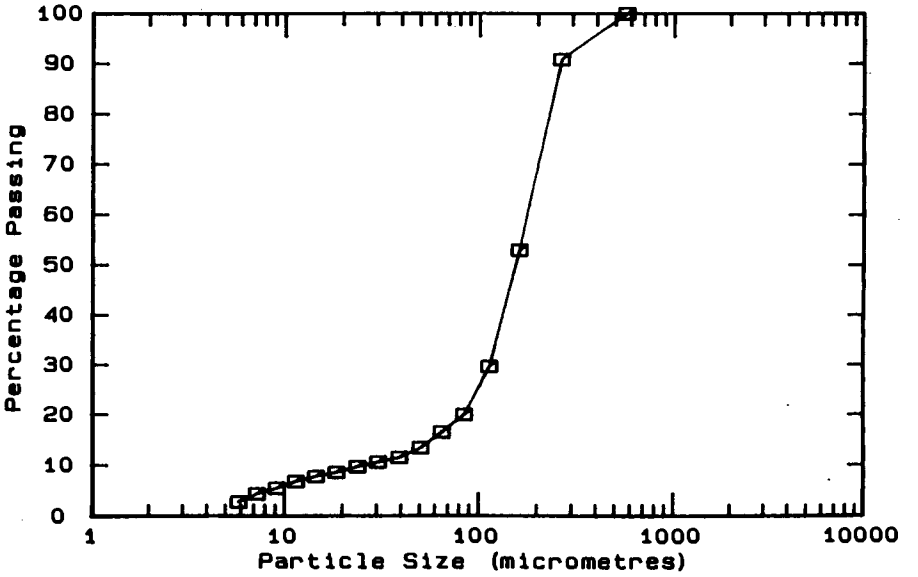

DATA FILE : VR80H85U

Test Facility	UCT 80 mm NB
Test Date	June 1990
Material Description	Vaal Reefs CCT
Material Relative Density	2.65
Slurry Relative Density	1.85
Solids Volumetric Concentration (%)	51.52
Solids Mass Concentration (%)	73.79
Mean Slurry Temperature (°C)	25.0
Pipe Internal Diameter (mm)	73.40
Pipe Roughness (μm)	84.0
Pipeline Slope	Horizontal

Mixture Velocity (m/s)	Pressure Gradient (kPa/m)	Slurry Temp. (°C)
2.426	6.738	22.6
2.476	6.907	22.8
2.524	7.668	23.0
2.531	7.030	23.3
2.519	6.826	23.5
2.094	6.276	24.4
2.127	6.445	24.6
2.140	6.029	24.7
2.131	6.242	24.9
1.656	4.817	25.3
1.656	4.856	25.4
1.657	4.733	25.5
1.364	4.208	25.7
1.351	4.084	25.8
1.337	4.065	25.8
.968	3.427	25.9
.921	3.299	26.0
.879	3.261	26.0
.627	2.859	26.0
.593	2.793	26.0
.556	2.743	26.0
.516	2.779	26.0
.493	2.797	26.0
.587	3.046	25.9

Particle Size Distribution
Malvern Particle Size Analyser

Size (μm)	% Passing	% Retained
564.0	100.0	.0
261.6	89.0	11.0
160.4	50.8	38.2
112.8	28.0	22.8
84.3	19.7	8.3
64.6	16.7	3.0
50.2	13.6	3.1
39.0	12.0	1.6
30.3	11.3	.7
23.7	10.3	1.0
18.5	9.2	1.1
14.5	8.4	.8
11.4	7.4	1.0
9.1	6.0	1.4
7.2	4.8	1.2
5.8	3.1	1.7
Pan	.2	2.9

OBSERVED FLOW BEHAVIOUR

Velocity (m/s)	Observation (D = 71.0 mm)
.53	Appears homogeneous
1.05	Appears homogeneous
1.44	Appears homogeneous
1.75	Appears homogeneous
2.17	Appears homogeneous
2.59	Appears homogeneous

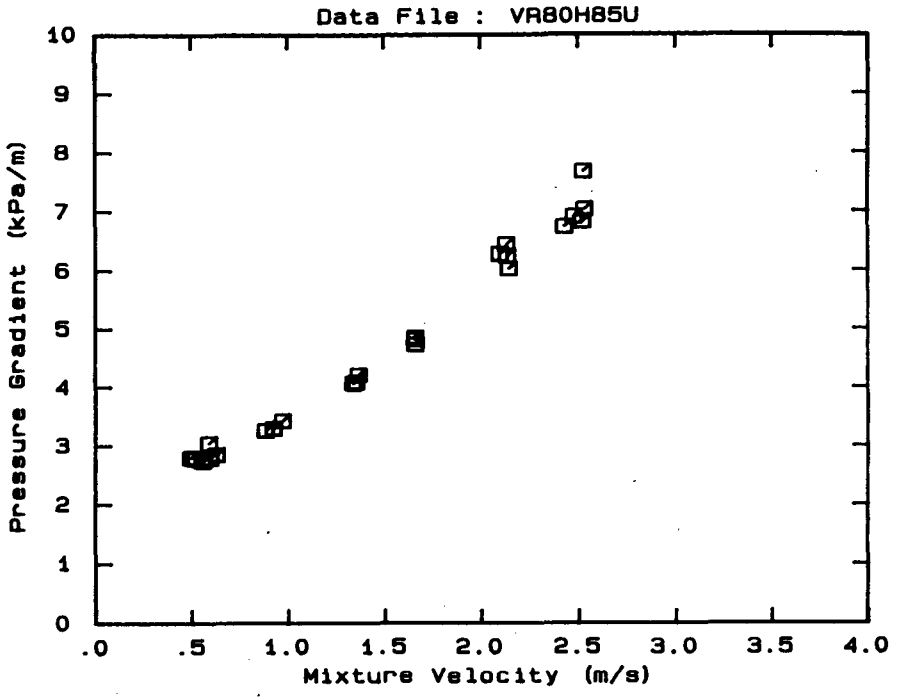

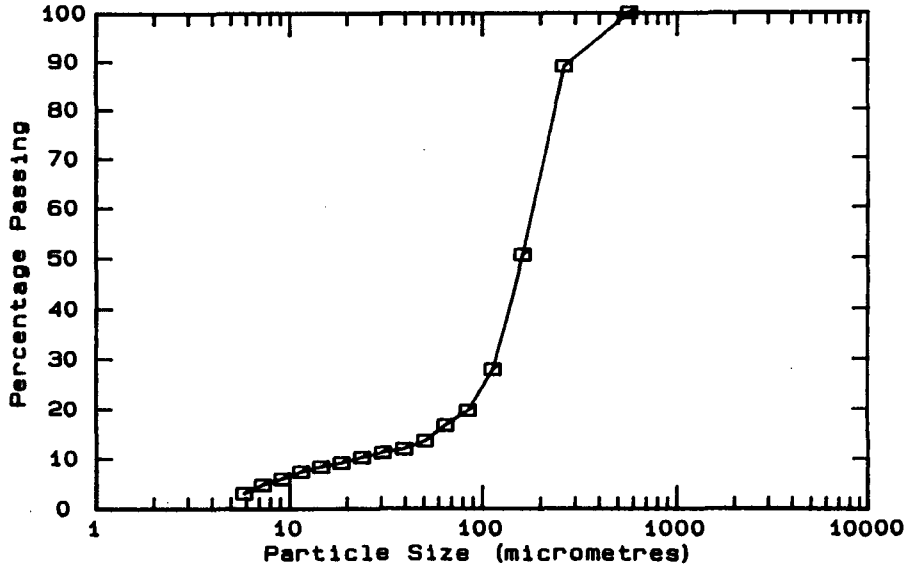

DATA FILE : VR80H89U

Test Facility	UCT 80 mm NB
Test Date	June 1990
Material Description	Vaal Reefs CCT
Material Relative Density	2.65
Slurry Relative Density	1.89
Solids Volumetric Concentration (%)	53.94
Solids Mass Concentration (%)	75.63
Mean Slurry Temperature (°C)	29.3
Pipe Internal Diameter (mm)	73.40
Pipe Roughness (μm)	84.0
Pipeline Slope	Horizontal

Mixture Velocity (m/s)	Pressure Gradient (kPa/m)	Slurry Temp. (°C)
1.307	9.534	29.2
1.298	10.047	29.3
1.278	9.716	29.4
1.264	9.087	29.4
1.246	9.268	29.5
1.239	8.704	29.6
.941	6.466	29.2
.945	6.406	29.2
.931	6.518	29.2
.924	6.510	29.2
.901	6.403	29.2
.908	6.495	29.2
.678	5.722	29.3
.681	5.764	29.4
.681	5.742	29.5
.684	5.712	29.5
.681	5.742	29.4
.442	4.724	29.4
.431	4.634	29.4
.428	4.580	29.3
.422	4.709	29.3
.417	4.725	29.3
.415	4.699	29.3
.412	4.713	29.3

Particle Size Distribution
Malvern Particle Size Analyser

Size (μm)	% Passing	% Retained
564.0	100.0	.0
261.6	90.2	9.8
160.4	52.4	37.8
112.8	29.6	22.8
84.3	20.6	9.0
64.6	17.4	3.2
50.2	14.4	3.0
39.0	12.7	1.7
30.3	12.0	.7
23.7	11.0	1.0
18.5	9.9	1.1
14.5	9.2	.7
11.4	8.1	1.1
9.1	6.6	1.5
7.2	5.3	1.3
5.8	3.4	1.9
Pan	.1	3.3

OBSERVED FLOW BEHAVIOUR

Velocity (m/s)	Observation (D = 71.0 mm)
1.09	Appears homogeneous
1.37	Appears homogeneous
1.58	Appears homogeneous

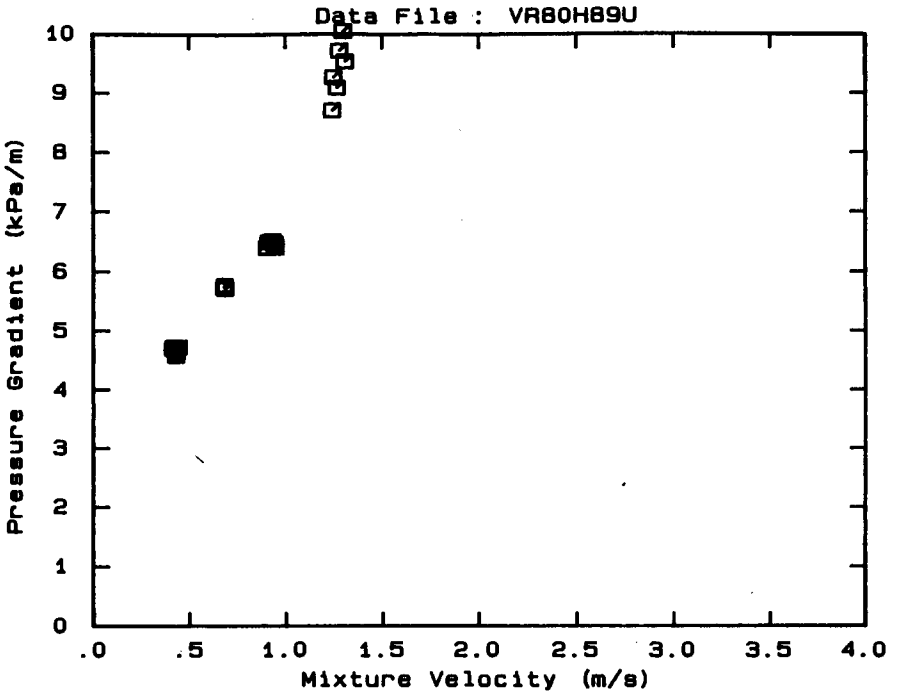

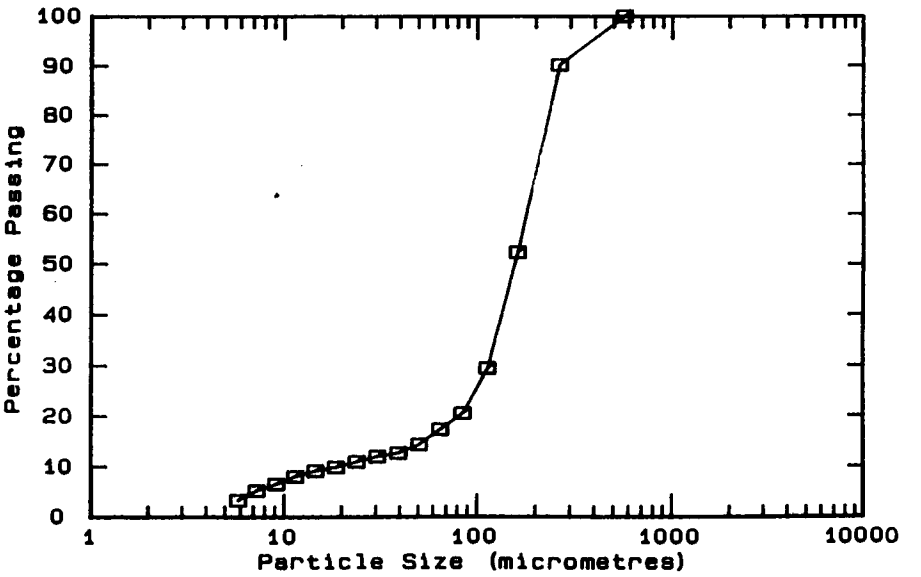

DATA FILE : VR80D70U

Test Facility	UCT 80 mm NB
Test Date	June 1990
Material Description	Vaal Reefs CCT
Material Relative Density	2.65
Slurry Relative Density	1.70
Solids Volumetric Concentration (%)	42.42
Solids Mass Concentration (%)	66.13
Mean Slurry Temperature (°C)	18.2
Pipe Internal Diameter (mm)	73.40
Pipe Roughness (μm)	84.0
Pipeline Slope	Vertical Down

Mixture Velocity (m/s)	Pressure Gradient (kPa/m)	Slurry Temp. (°C)
3.424	-12.629	17.8
3.439	-12.955	17.8
3.445	-12.927	17.9
3.450	-12.890	18.0
3.437	-12.807	18.0
3.447	-13.009	18.1
3.443	-12.920	18.1
2.965	-13.742	18.3
2.951	-13.669	18.3
2.960	-13.769	18.3
2.950	-13.766	18.3
2.439	-14.710	18.4
2.442	-14.698	18.4
2.437	-14.809	18.4
2.012	-15.331	18.3
2.022	-15.412	18.3
2.025	-15.272	18.3
2.023	-15.345	18.3
2.021	-15.361	18.3
1.489	-15.705	18.3
1.484	-15.762	18.3
1.484	-15.746	18.2
1.031	-15.896	18.2
1.038	-15.763	18.2
1.034	-15.873	18.1
1.040	-15.782	18.1
1.031	-15.772	18.1

Particle Size Distribution
Malvern Particle Size Analyser

Size (μm)	% Passing	% Retained
564.0	100.0	.0
261.6	88.2	11.8
160.4	49.9	38.3
112.8	27.1	22.8
84.3	18.0	9.1
64.6	14.6	3.4
50.2	11.5	3.1
39.0	9.8	1.7
30.3	9.0	.8
23.7	8.0	1.0
18.5	7.0	1.0
14.5	6.2	.8
11.4	5.3	.9
9.1	4.2	1.1
7.2	3.3	.9
5.8	2.1	1.2
Pan	.1	2.0

OBSERVED FLOW BEHAVIOUR

Velocity (m/s)	Observation (D = 71.0 mm)

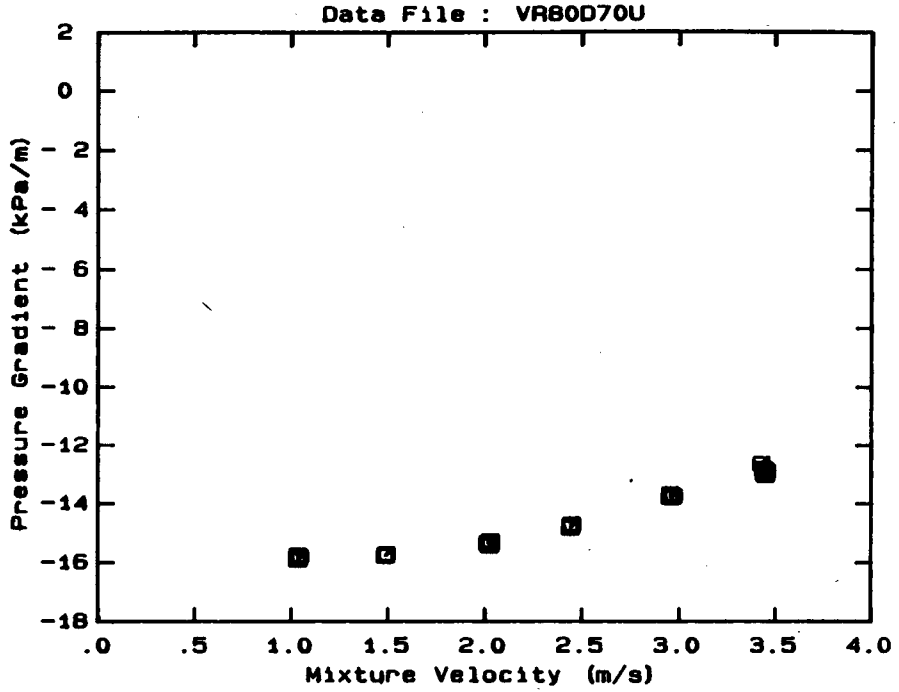

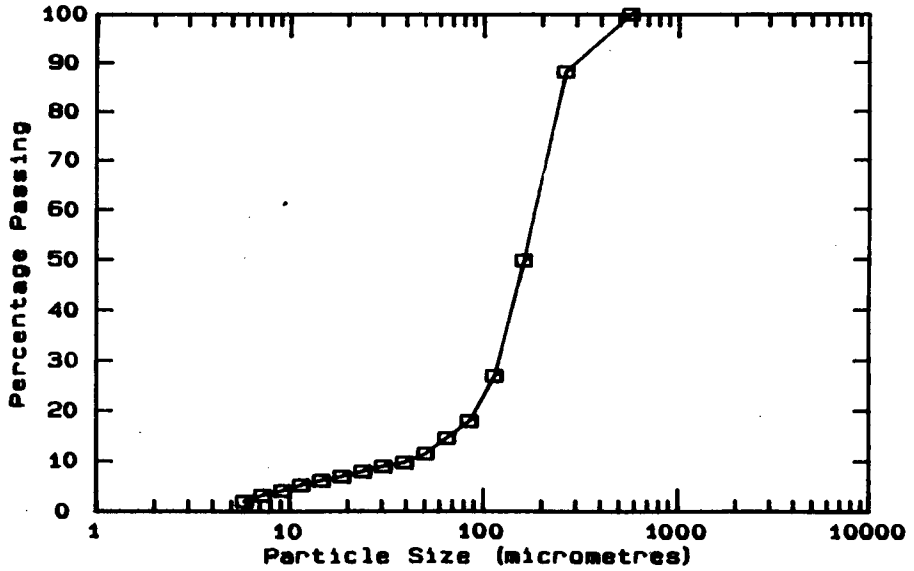

DATA FILE : VR80D75U

Test Facility	UCT 80 mm NB
Test Date	June 1990
Material Description	Vaal Reefs CCT
Material Relative Density	2.65
Slurry Relative Density	1.75
Solids Volumetric Concentration (%)	45.45
Solids Mass Concentration (%)	68.83
Mean Slurry Temperature (°C)	19.0
Pipe Internal Diameter (mm)	73.40
Pipe Roughness (μm)	84.0
Pipeline Slope	Vertical Down

Mixture Velocity (m/s)	Pressure Gradient (kPa/m)	Slurry Temp. (°C)
3.427	-13.869	17.7
3.424	-13.277	17.8
3.430	-13.645	18.0
3.437	-13.806	18.1
3.434	-13.748	18.2
3.440	-13.652	18.3
2.897	-14.396	18.6
2.898	-14.188	18.7
2.897	-14.249	18.8
2.902	-14.305	18.9
2.902	-14.219	18.9
2.454	-14.825	19.1
2.455	-14.781	19.2
2.457	-14.855	19.2
1.962	-15.314	19.4
1.961	-15.318	19.4
1.956	-15.280	19.4
1.473	-15.218	19.5
1.465	-15.524	19.5
1.462	-15.400	19.5
1.463	-15.440	19.5
1.477	-15.460	19.6
1.470	-15.518	19.6
1.004	-15.772	19.6
.996	-16.116	19.6
1.006	-15.976	19.6
1.005	-15.942	19.5

Particle Size Distribution
Malvern Particle Size Analyser

Size (μm)	% Passing	% Retained
564.0	100.0	.0
261.6	87.3	12.7
160.4	49.9	37.4
112.8	28.2	21.7
84.3	19.2	9.0
64.6	16.2	3.0
50.2	13.1	3.1
39.0	11.2	1.9
30.3	10.3	.9
23.7	9.2	1.1
18.5	8.0	1.2
14.5	7.1	.9
11.4	6.1	1.0
9.1	4.8	1.3
7.2	3.7	1.1
5.8	2.2	1.5
Pan	- .2	2.4

OBSERVED FLOW BEHAVIOUR

Velocity (m/s)	Observation (D = 71.0 mm)

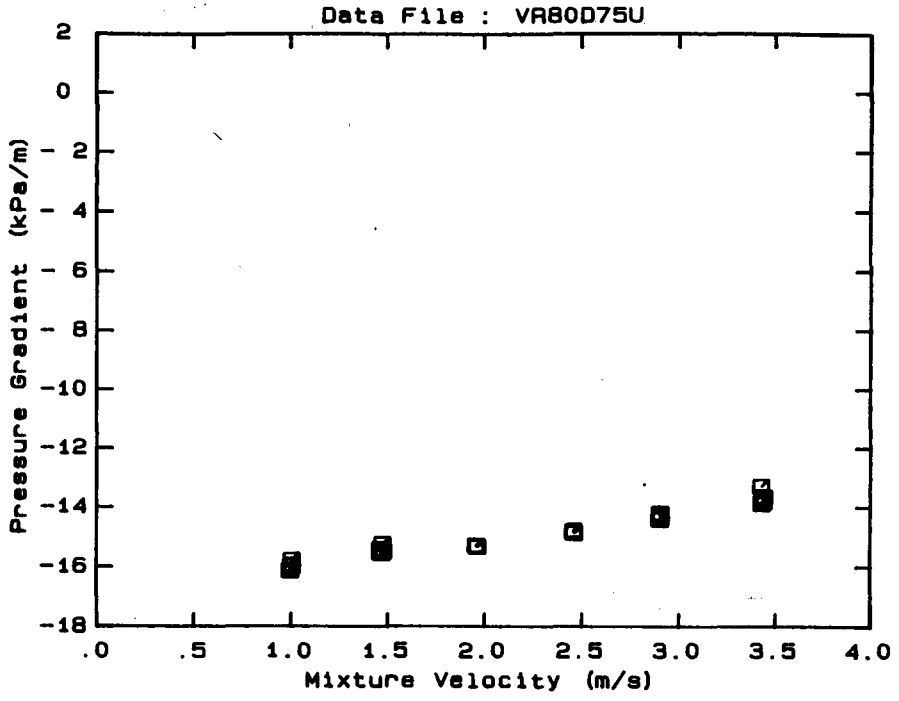

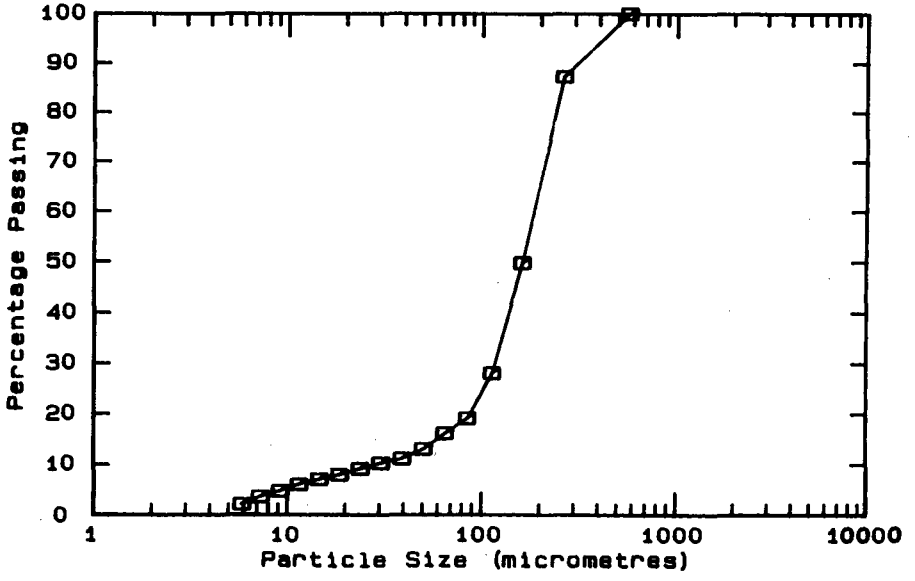

DATA FILE : VR80D79U

Test Facility	UCT 80 mm NB
Test Date	June 1990
Material Description	Vaal Reefs CCT
Material Relative Density	2.65
Slurry Relative Density	1.79
Solids Volumetric Concentration (%)	47.88
Solids Mass Concentration (%)	70.88
Mean Slurry Temperature (°C)	20.1
Pipe Internal Diameter (mm)	73.40
Pipe Roughness (μm)	84.0
Pipeline Slope	Vertical Down

Mixture Velocity (m/s)	Pressure Gradient (kPa/m)	Slurry Temp. (°C)
3.371	-12.816	19.2
3.382	-13.046	19.3
3.387	-12.922	19.5
3.401	-12.705	19.8
2.920	-13.561	19.9
2.925	-13.680	20.0
2.925	-13.721	20.1
2.930	-13.656	20.3
2.449	-14.261	20.4
2.455	-14.219	20.4
2.453	-14.278	20.4
2.457	-14.262	20.4
2.462	-14.429	20.4
2.461	-14.176	20.4
1.953	-14.908	20.5
1.947	-14.817	20.5
1.950	-14.910	20.4
1.525	-15.245	20.4
1.512	-15.267	20.3
1.518	-15.244	20.3
1.515	-15.309	20.3
1.513	-15.306	20.2
1.034	-14.436	20.1
1.043	-13.937	20.1
1.046	-14.573	20.0
1.047	-14.443	20.0
1.041	-14.282	20.0

Particle Size Distribution
Malvern Particle Size Analyser

Size (μm)	% Passing	% Retained
564.0	100.0	.0
261.6	89.9	10.1
160.4	52.1	37.8
112.8	28.7	23.4
84.3	18.9	9.8
64.6	15.5	3.4
50.2	12.3	3.2
39.0	10.5	1.8
30.3	9.7	.8
23.7	8.7	1.0
18.5	7.7	1.0
14.5	6.9	.8
11.4	6.0	.9
9.1	4.8	1.2
7.2	3.8	1.0
5.8	2.4	1.4
Pan	- .0	2.4

OBSERVED FLOW BEHAVIOUR

Velocity (m/s)	Observation (D = 71.0 mm)

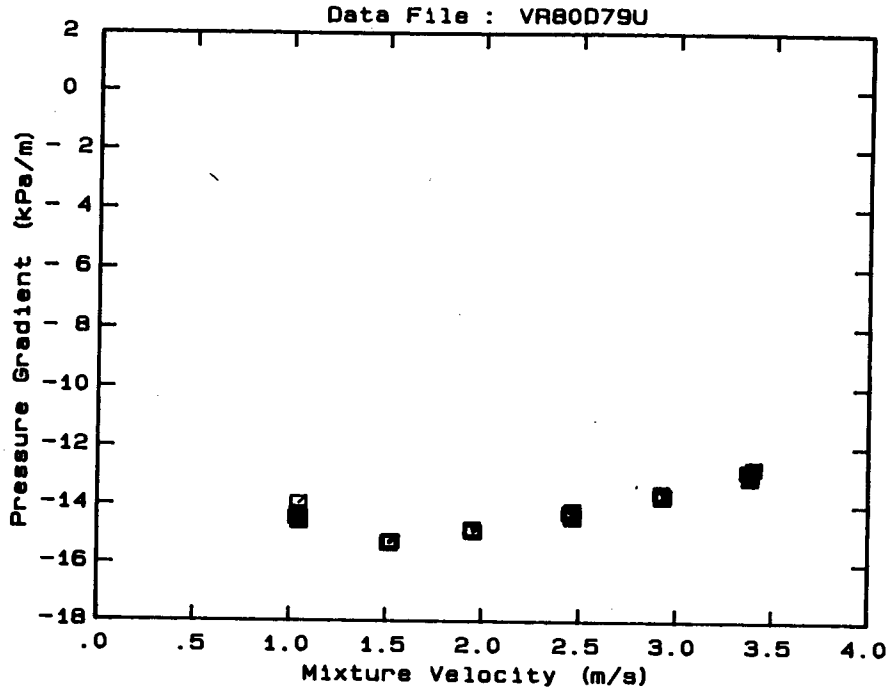

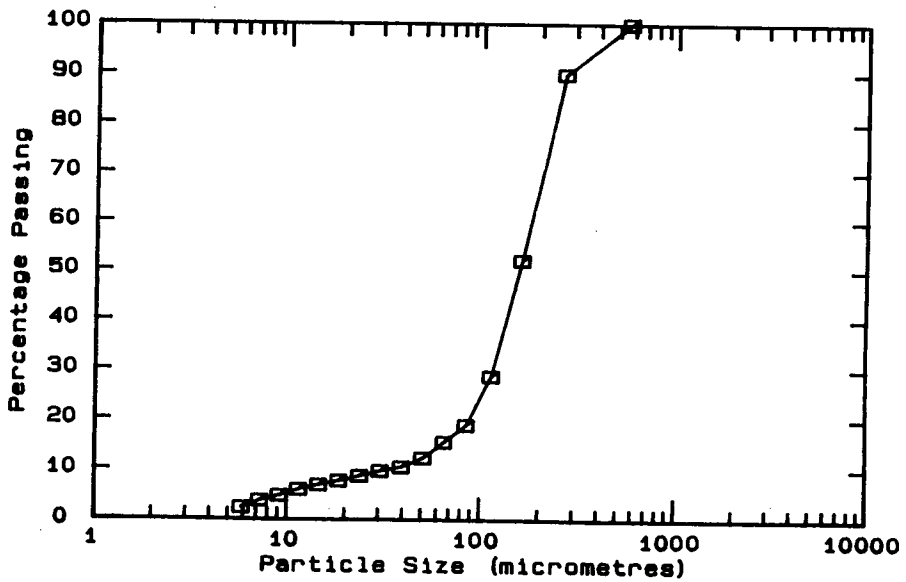

DATA FILE : VR80D81U

Test Facility	UCT 80 mm NB
Test Date	June 1990
Material Description	Vaal Reefs CCT
Material Relative Density	2.65
Slurry Relative Density	1.81
Solids Volumetric Concentration (%)	49.09
Solids Mass Concentration (%)	71.87
Mean Slurry Temperature (°C)	22.3
Pipe Internal Diameter (mm)	73.40
Pipe Roughness (μm)	84.0
Pipeline Slope	Vertical Down

Mixture Velocity (m/s)	Pressure Gradient (kPa/m)	Slurry Temp. (°C)
3.319	-10.301	20.9
3.330	-10.492	21.1
3.343	-10.202	21.3
3.366	-10.410	21.5
2.966	-11.284	21.9
2.981	-11.568	22.1
2.982	-11.544	22.2
2.995	-11.411	22.3
2.470	-12.233	22.5
2.466	-12.502	22.6
2.465	-12.421	22.7
2.465	-12.282	22.7
2.467	-12.366	22.7
1.990	-13.298	22.7
1.989	-13.210	22.8
1.984	-13.227	22.8
1.988	-13.271	22.8
1.984	-13.266	22.8
1.481	-14.156	22.8
1.480	-14.350	22.7
1.478	-14.340	22.7
.960	-15.231	22.6
.939	-15.056	22.5
.919	-15.343	22.4
.898	-14.898	22.4
.872	-14.908	22.3

Particle Size Distribution
Malvern Particle Size Analyser

Size (μm)	% Passing	% Retained
564.0	100.0	.0
261.6	90.9	9.1
160.4	53.0	37.9
112.8	29.7	23.3
84.3	20.0	9.7
64.6	16.5	3.5
50.2	13.4	3.1
39.0	11.5	1.9
30.3	10.6	.9
23.7	9.7	.9
18.5	8.6	1.1
14.5	7.8	.8
11.4	6.8	1.0
9.1	5.5	1.3
7.2	4.4	1.1
5.8	2.8	1.6
Pan	.1	2.7

OBSERVED FLOW BEHAVIOUR

Velocity (m/s)	Observation (D = 71.0 mm)

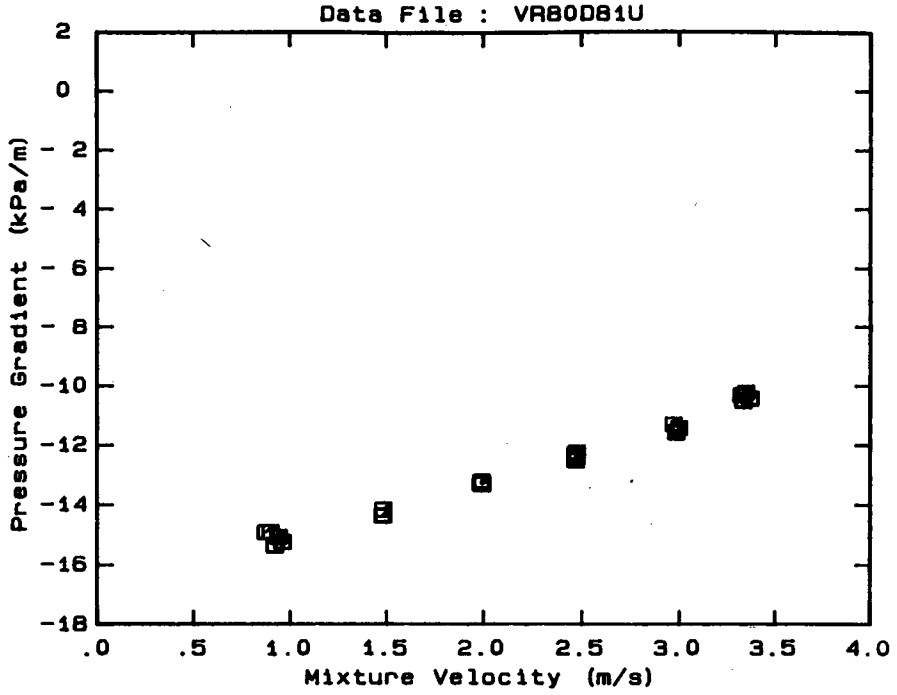

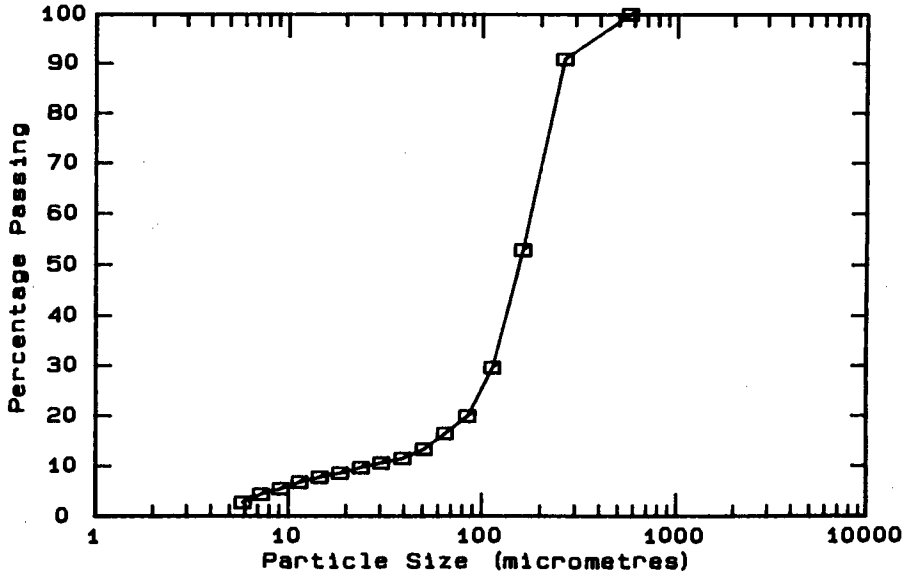

DATA FILE : VR80D85U

Test Facility	UCT 80 mm NB
Test Date	June 1990
Material Description	Vaal Reefs CCT
Material Relative Density	2.65
Slurry Relative Density	1.85
Solids Volumetric Concentration (%)	51.52
Solids Mass Concentration (%)	73.79
Mean Slurry Temperature (°C)	25.0
Pipe Internal Diameter (mm)	73.40
Pipe Roughness (μm)	84.0
Pipeline Slope	Vertical Down

Mixture Velocity (m/s)	Pressure Gradient (kPa/m)	Slurry Temp. (°C)
2.426	- 8.298	22.6
2.476	- 8.300	22.8
2.524	- 8.783	23.0
2.531	- 8.600	23.3
2.519	- 8.535	23.5
2.094	-10.393	24.4
2.127	-10.584	24.6
2.140	-10.041	24.7
2.131	-10.157	24.9
1.656	-12.093	25.3
1.656	-12.116	25.4
1.657	-12.083	25.5
1.364	-13.330	25.7
1.351	-13.313	25.8
1.337	-13.377	25.8
.968	-14.209	25.9
.921	-14.282	26.0
.879	-14.341	26.0
.627	-15.109	26.0
.593	-13.766	26.0
.556	-13.512	26.0
.516	-15.351	26.0
.493	-15.051	26.0
.587	-14.469	25.9

Particle Size Distribution
Malvern Particle Size Analyser

Size (μm)	% Passing	% Retained
564.0	100.0	.0
261.6	89.0	11.0
160.4	50.8	38.2
112.8	28.0	22.8
84.3	19.7	8.3
64.6	16.7	3.0
50.2	13.6	3.1
39.0	12.0	1.6
30.3	11.3	.7
23.7	10.3	1.0
18.5	9.2	1.1
14.5	8.4	.8
11.4	7.4	1.0
9.1	6.0	1.4
7.2	4.8	1.2
5.8	3.1	1.7
Pan	.2	2.9

OBSERVED FLOW BEHAVIOUR

Velocity (m/s)	Observation (D = 71.0 mm)

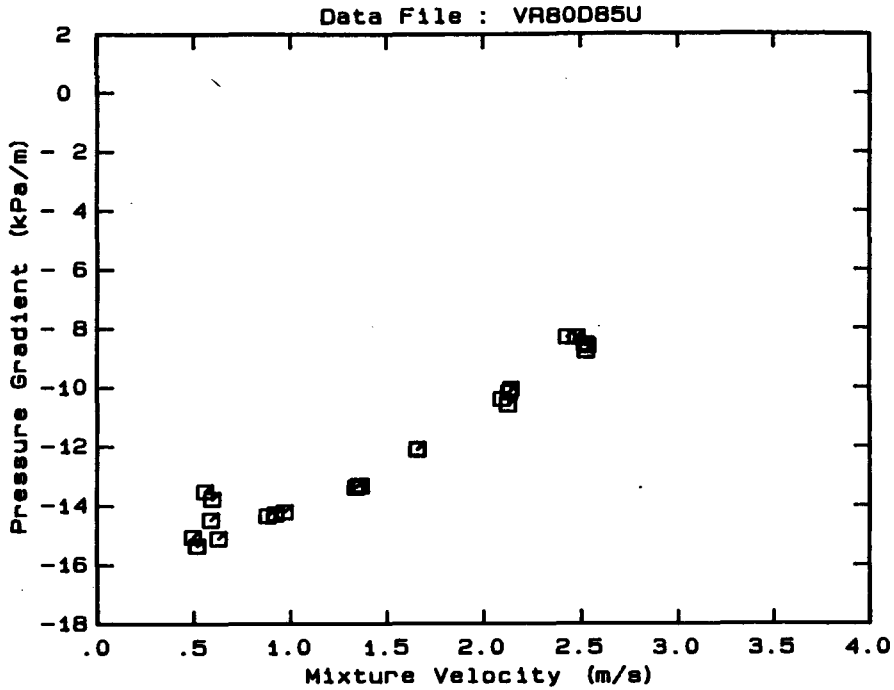

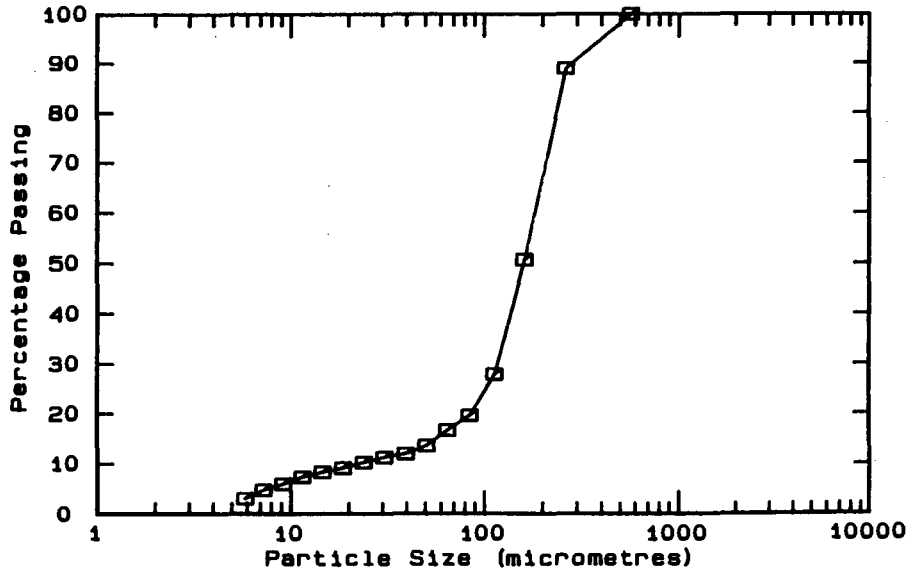

DATA FILE : WD25H67U

Test Facility	UCT 25 mm NB
Test Date	June 1990
Material Description	Western Deeps CCT
Material Relative Density	2.65
Slurry Relative Density	1.67
Solids Volumetric Concentration (%)	40.61
Solids Mass Concentration (%)	64.43
Mean Slurry Temperature (°C)	14.9
Pipe Internal Diameter (mm)	26.60
Pipe Roughness (μm)	21.0
Pipeline Slope	Horizontal

Mixture Velocity (m/s)	Pressure Gradient (kPa/m)	Slurry Temp. (°C)
3.371	9.798	14.3
3.423	10.038	14.3
3.406	9.798	14.4
3.389	9.836	14.5
2.932	7.614	14.7
2.937	7.719	14.7
2.930	7.533	14.8
2.947	7.716	14.8
2.546	5.903	15.0
2.542	5.632	15.0
2.560	5.810	15.0
2.129	3.858	15.1
2.133	3.837	15.1
2.124	3.865	15.1
1.683	2.486	15.2
1.680	2.492	15.2
1.684	2.474	15.2
1.304	1.868	15.2
1.303	1.925	15.2
1.308	1.978	15.3

Particle Size Distribution
Malvern Particle Size Analyser

Size (μm)	% Passing	% Retained
564.0	100.0	.0
261.6	95.9	4.1
160.4	73.6	22.3
112.8	48.7	24.9
84.3	35.8	12.9
64.6	28.9	6.9
50.2	23.7	5.2
39.0	20.8	2.9
30.3	18.4	2.4
23.7	16.2	2.2
18.5	14.6	1.6
14.5	13.2	1.4
11.4	11.6	1.6
9.1	9.6	2.0
7.2	7.6	2.0
5.8	4.8	2.8
Pan	- .0	4.8

OBSERVED FLOW BEHAVIOUR

Velocity	Observation

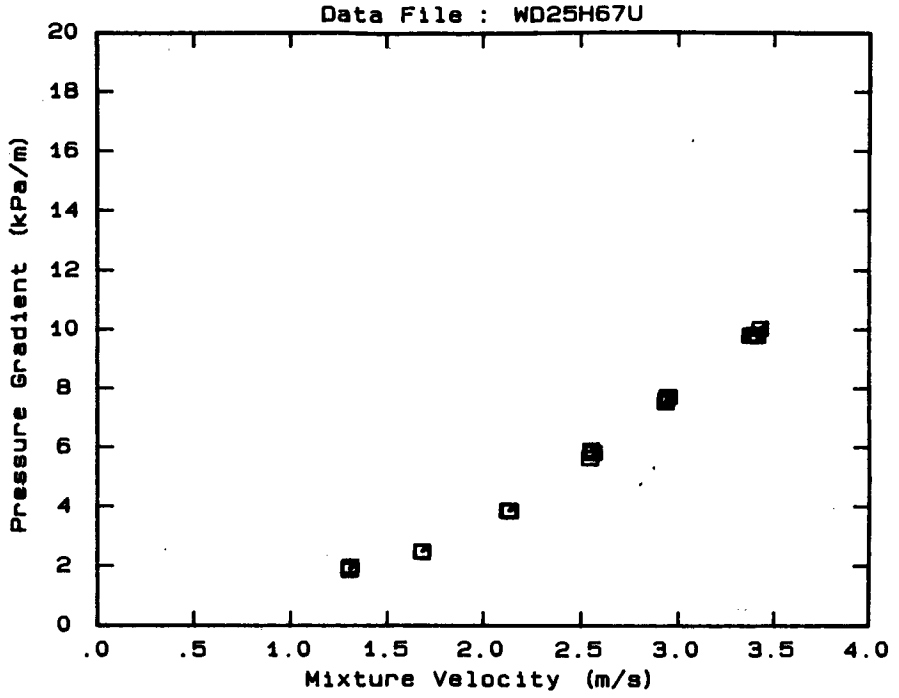

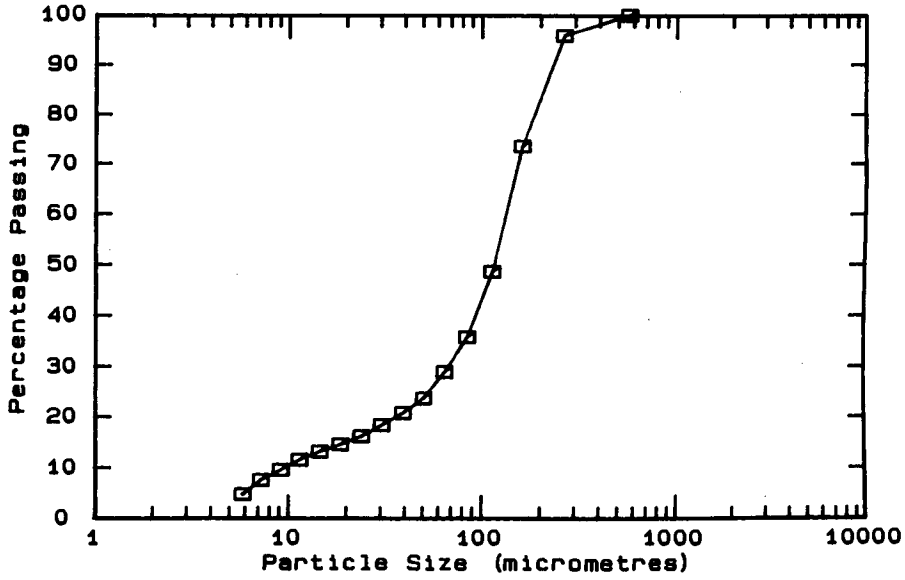

DATA FILE : WD25H73U

Test Facility	UCT 25 mm NB
Test Date	June 1990
Material Description	Western Deeps CCT
Material Relative Density	2.65
Slurry Relative Density	1.73
Solids Volumetric Concentration (%)	44.24
Solids Mass Concentration (%)	67.77
Mean Slurry Temperature (°C)	16.1
Pipe Internal Diameter (mm)	26.60
Pipe Roughness (μm)	21.0
Pipeline Slope	Horizontal

Mixture Velocity (m/s)	Pressure Gradient (kPa/m)	Slurry Temp. (°C)
3.371	8.115	15.5
3.375	8.446	15.6
3.407	8.449	15.6
3.411	8.530	15.7
3.416	8.740	15.8
3.437	8.706	15.9
2.984	6.416	16.0
2.983	6.580	16.1
2.983	6.650	16.1
2.554	5.062	16.3
2.543	5.191	16.3
2.540	5.181	16.3
2.128	4.077	16.4
2.126	4.133	16.4
2.126	4.101	16.4
1.682	3.228	16.4
1.675	3.231	16.4
1.677	3.281	16.4
1.284	2.515	16.5
1.279	2.447	16.4
1.281	2.466	16.4

Particle Size Distribution
Malvern Particle Size Analyser

Size (μm)	% Passing	% Retained
564.0	100.0	.0
261.6	96.3	3.7
160.4	75.3	21.0
112.8	50.5	24.8
84.3	37.0	13.5
64.6	30.5	6.5
50.2	24.9	5.6
39.0	21.6	3.3
30.3	19.3	2.3
23.7	16.9	2.4
18.5	15.3	1.6
14.5	14.0	1.3
11.4	12.3	1.7
9.1	10.3	2.0
7.2	8.2	2.1
5.8	5.2	3.0
Pan	.1	5.1

OBSERVED FLOW BEHAVIOUR

Velocity (m/s)	Observation (D = .0 mm)

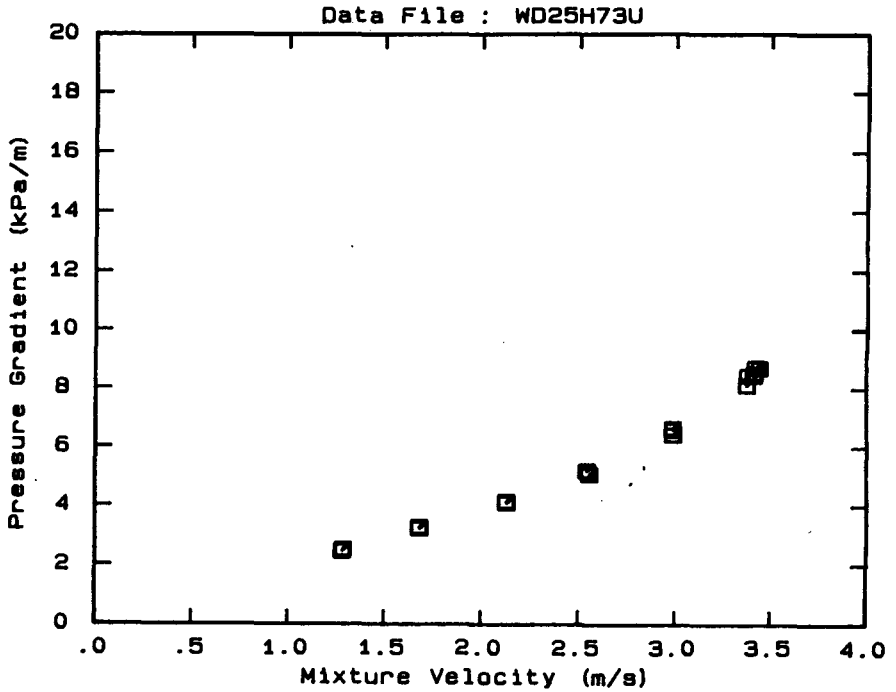

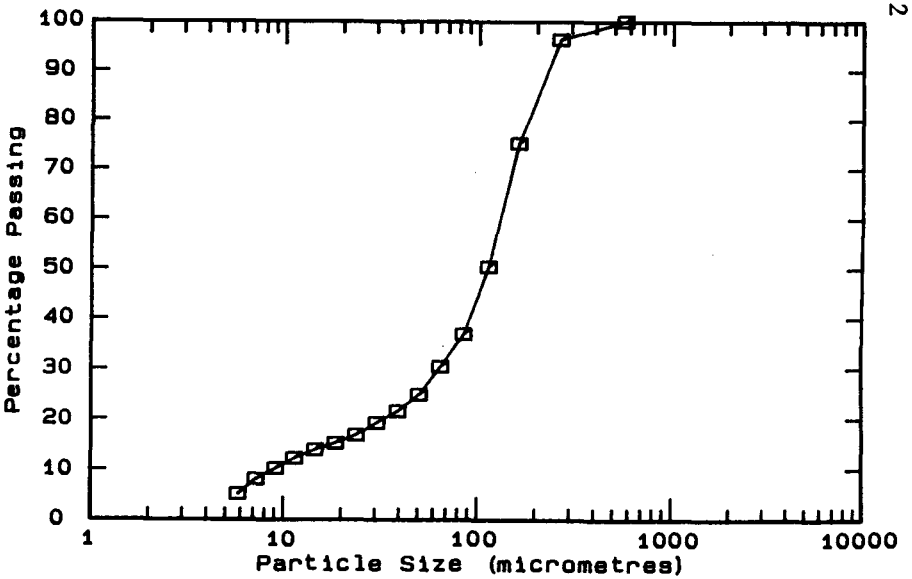

DATA FILE : WD25H76U

Test Facility	UCT 25 mm NB
Test Date	June 1990
Material Description	Western Deeps CCT
Material Relative Density	2.65
Slurry Relative Density	1.76
Solids Volumetric Concentration (%)	46.06
Solids Mass Concentration (%)	69.35
Mean Slurry Temperature (°C)	17.6
Pipe Internal Diameter (mm)	26.60
Pipe Roughness (μm)	21.0
Pipeline Slope	Horizontal

Mixture Velocity (m/s)	Pressure Gradient (kPa/m)	Slurry Temp. (°C)
3.480	10.107	16.8
3.467	10.071	16.9
3.485	10.074	17.0
3.506	10.198	17.1
3.525	10.006	17.1
3.544	10.223	17.2
2.969	8.173	17.5
2.968	8.134	17.5
2.966	8.075	17.6
2.975	8.179	17.6
2.552	6.860	17.7
2.552	7.062	17.7
2.545	6.985	17.8
2.129	5.841	17.9
2.133	5.972	17.9
2.122	5.943	17.9
1.683	4.647	17.9
1.679	4.814	17.9
1.678	4.722	17.9
1.272	3.645	17.9
1.269	3.644	17.9
1.261	3.637	17.9

Particle Size Distribution
Malvern Particle Size Analyser

Size (μm)	% Passing	% Retained
564.0	100.0	.0
261.6	94.9	5.1
160.4	74.0	20.9
112.8	50.9	23.1
84.3	37.0	13.9
64.6	30.9	6.1
50.2	26.4	4.5
39.0	22.7	3.7
30.3	20.2	2.5
23.7	18.4	1.8
18.5	16.4	2.0
14.5	14.8	1.6
11.4	13.1	1.7
9.1	10.9	2.2
7.2	8.6	2.3
5.8	5.4	3.2
Pan	.0	5.4

OBSERVED FLOW BEHAVIOUR

Velocity (m/s)	Observation (D = .0 mm)

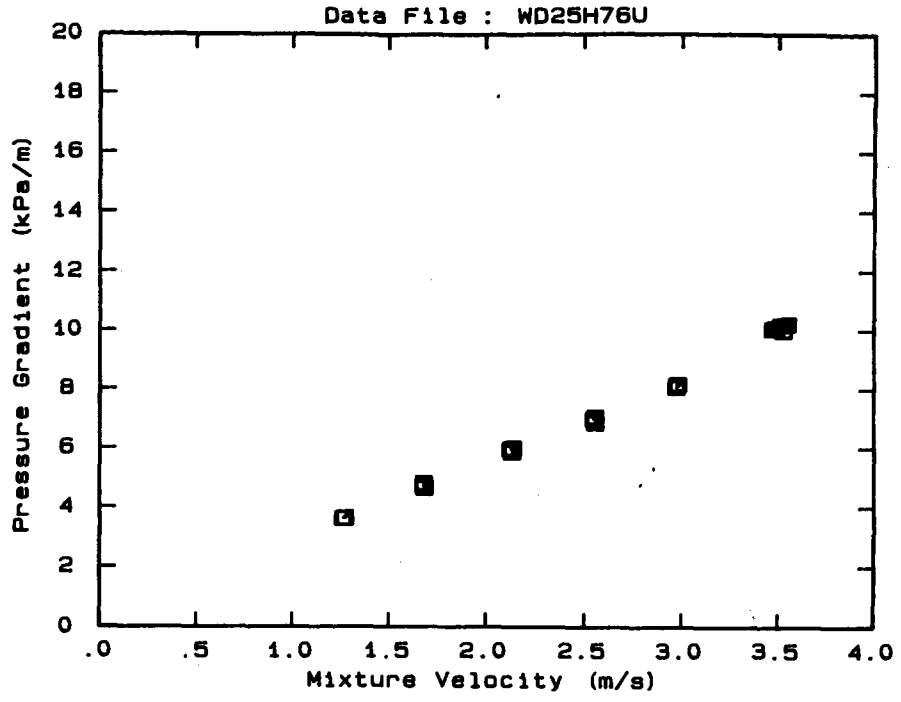

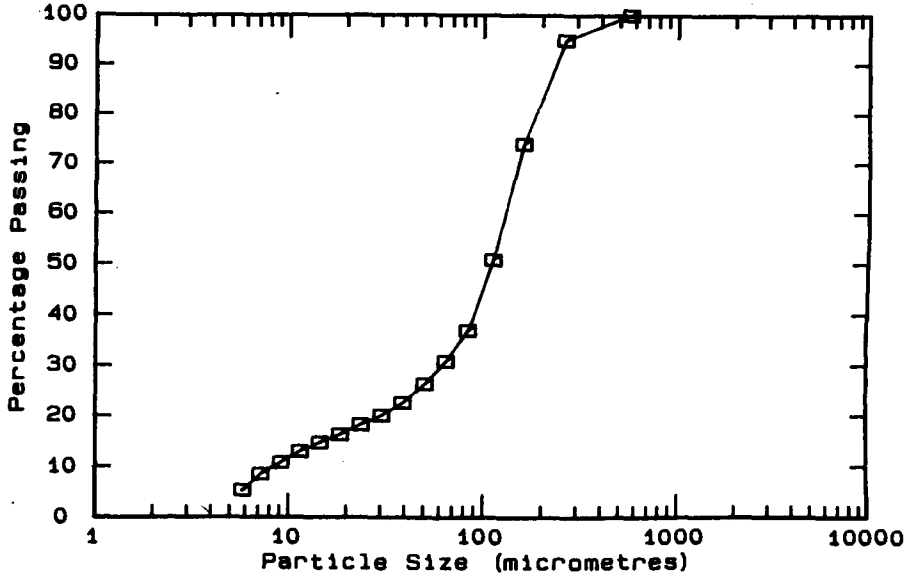

DATA FILE : WD25H79U

Test Facility	UCT 25 mm NB
Test Date	June 1990
Material Description	Western Deeps CCT
Material Relative Density	2.65
Slurry Relative Density	1.79
Solids Volumetric Concentration (%)	47.88
Solids Mass Concentration (%)	70.88
Mean Slurry Temperature (°C)	19.5
Pipe Internal Diameter (mm)	26.60
Pipe Roughness (μm)	21.0
Pipeline Slope	Horizontal

Mixture Velocity (m/s)	Pressure Gradient (kPa/m)	Slurry Temp. (°C)
3.431	12.865	18.6
3.480	13.133	18.7
3.518	13.252	18.8
2.937	10.804	19.3
2.956	11.045	19.3
2.949	11.105	19.4
2.958	10.927	19.5
2.548	9.356	19.6
2.540	9.194	19.7
2.552	9.261	19.7
2.101	7.851	19.8
2.097	7.815	19.8
2.093	8.024	19.8
1.678	6.473	19.8
1.678	6.342	19.8
1.682	6.547	19.8
1.671	6.559	19.8
1.222	4.995	19.8
1.216	5.084	19.8
1.213	5.006	19.7

Particle Size Distribution
Malvern Particle Size Analyser

Size (μm)	% Passing	% Retained
564.0	100.0	.0
261.6	97.6	2.4
160.4	76.9	20.7
112.8	50.7	26.2
84.3	37.4	13.3
64.6	31.0	6.4
50.2	25.6	5.4
39.0	22.1	3.5
30.3	19.9	2.2
23.7	18.0	1.9
18.5	16.1	1.9
14.5	14.6	1.5
11.4	13.0	1.6
9.1	10.8	2.2
7.2	8.7	2.1
5.8	5.6	3.1
Pan	.1	5.5

OBSERVED FLOW BEHAVIOUR

Velocity	Observation

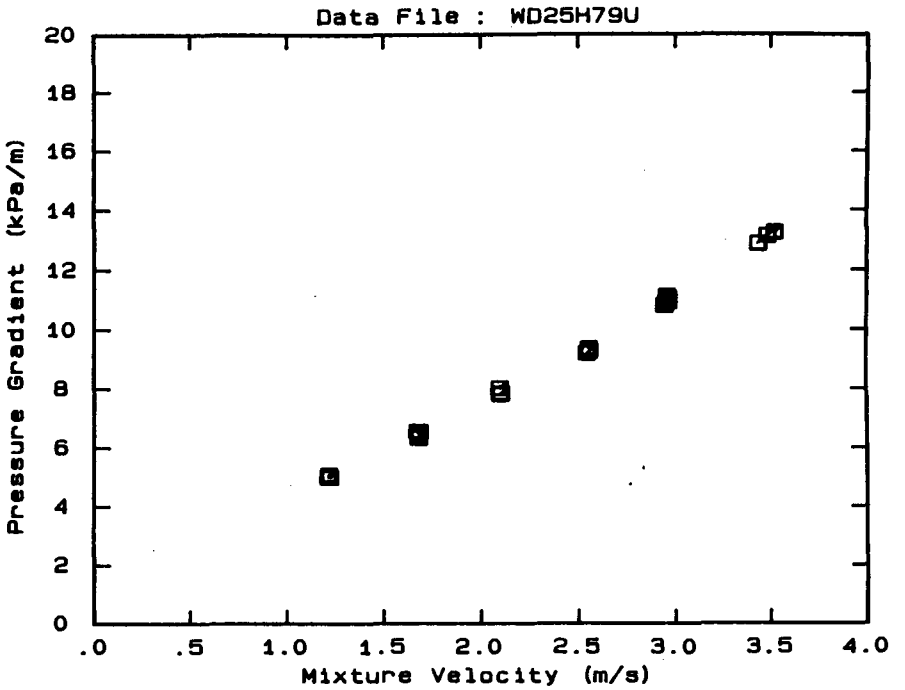

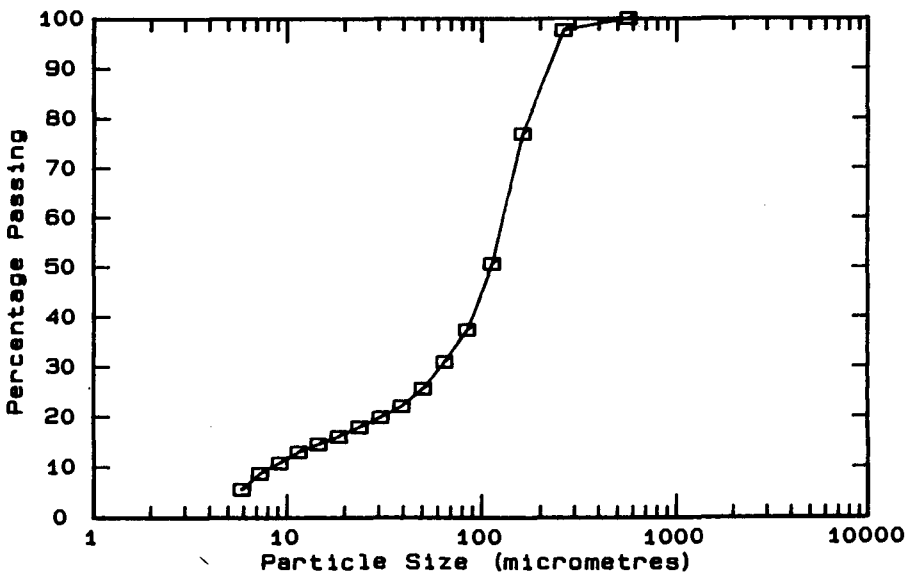

DATA FILE : WD25H82U

Test Facility	UCT 25 mm NB
Test Date	June 1990
Material Description	Western Deeps CCT
Material Relative Density	2.65
Slurry Relative Density	1.82
Solids Volumetric Concentration (%)	49.70
Solids Mass Concentration (%)	72.36
Mean Slurry Temperature (°C)	21.0
Pipe Internal Diameter (mm)	26.60
Pipe Roughness (μm)	21.0
Pipeline Slope	Horizontal

Mixture Velocity (m/s)	Pressure Gradient (kPa/m)	Slurry Temp. (°C)
3.234	15.824	20.0
3.272	16.231	20.1
3.273	16.207	20.2
2.987	14.792	20.6
3.022	15.065	20.7
3.001	14.546	20.8
2.550	12.670	21.1
2.556	12.803	21.1
2.575	12.806	21.2
2.115	10.733	21.3
2.115	10.632	21.4
2.112	10.770	21.4
1.681	8.715	21.4
1.673	8.612	21.4
1.671	8.528	21.4
1.267	7.075	21.4
1.255	7.062	21.4
1.255	7.190	21.4

Particle Size Distribution
Malvern Particle Size Analyser

Size (μm)	% Passing	% Retained
564.0	100.0	.0
261.6	96.7	3.3
160.4	75.6	21.1
112.8	50.3	25.3
84.3	37.2	13.1
64.6	30.5	6.7
50.2	25.0	5.5
39.0	22.2	2.8
30.3	19.9	2.3
23.7	17.4	2.5
18.5	15.9	1.5
14.5	14.5	1.4
11.4	12.7	1.8
9.1	10.6	2.1
7.2	8.4	2.2
5.8	5.2	3.2
Pan	- .3	5.5

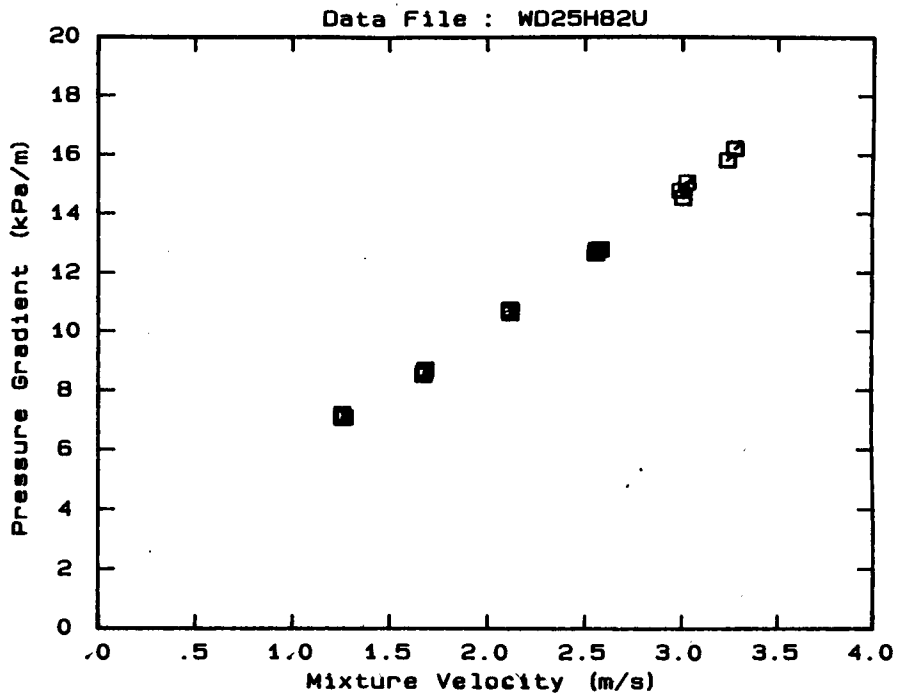

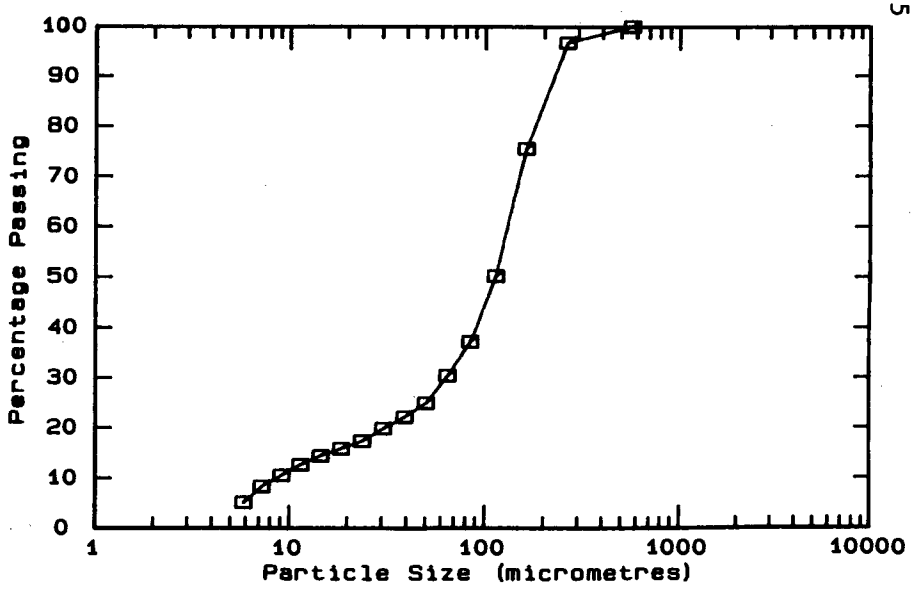

DATA FILE : WD25H85U

Test Facility	UCT 25 mm NB
Test Date	June 1990
Material Description	Western Deeps CCT
Material Relative Density	2.65
Slurry Relative Density	1.85
Solids Volumetric Concentration (%)	51.52
Solids Mass Concentration (%)	73.79
Mean Slurry Temperature (°C)	21.1
Pipe Internal Diameter (mm)	26.60
Pipe Roughness (μm)	21.0
Pipeline Slope	Horizontal

Mixture Velocity (m/s)	Pressure Gradient (kPa/m)	Slurry Temp. (°C)
2.429	16.464	20.0
2.424	16.365	20.1
2.073	14.603	21.1
2.071	14.485	21.2
2.091	14.691	21.3
1.672	12.391	21.4
1.690	12.597	21.4
1.693	12.497	21.4
1.265	10.920	21.4
1.260	11.030	21.4
1.242	11.094	21.4
1.223	11.375	21.4
1.210	11.834	21.4

Particle Size Distribution
Malvern Particle Size Analyser

Size (μm)	% Passing	% Retained
564.0	100.0	.0
261.6	96.4	3.6
160.4	76.0	20.4
112.8	50.7	25.3
84.3	37.6	13.1
64.6	30.6	7.0
50.2	25.3	5.3
39.0	22.2	3.1
30.3	19.8	2.4
23.7	17.7	2.1
18.5	16.0	1.7
14.5	14.6	1.4
11.4	13.0	1.6
9.1	10.9	2.1
7.2	8.7	2.2
5.8	5.5	3.2
Pan	.0	5.5

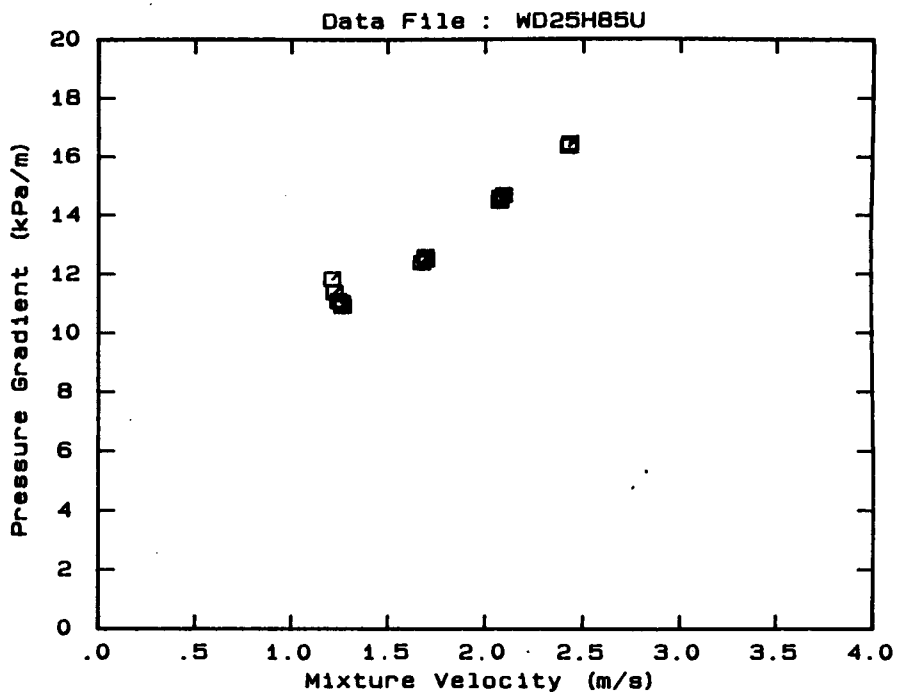

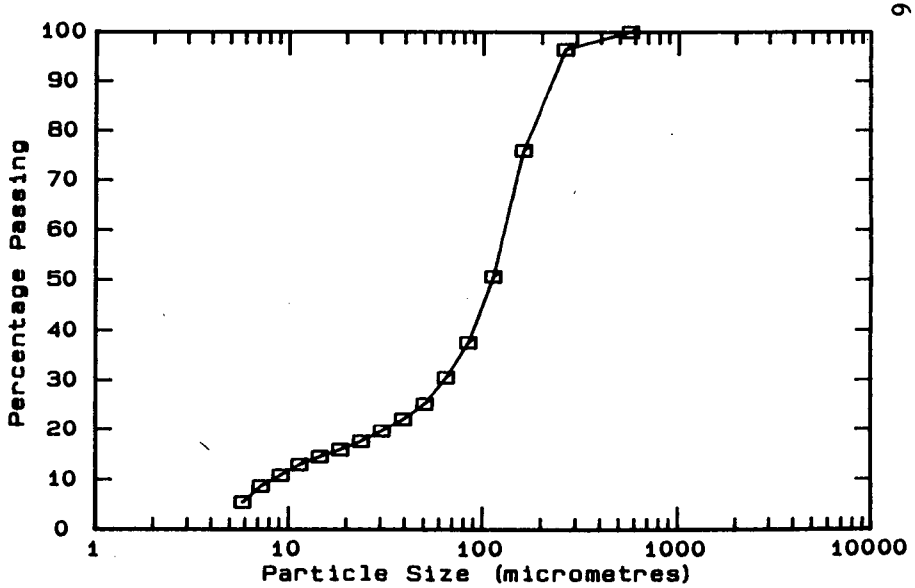

DATA FILE : WD25D67U

Test Facility	UCT 25 mm NB
Test Date	June 1990
Material Description	Western Deeps CCT
Material Relative Density	2.65
Slurry Relative Density	1.67
Solids Volumetric Concentration (%)	40.61
Solids Mass Concentration (%)	64.43
Mean Slurry Temperature (°C)	14.9
Pipe Internal Diameter (mm)	26.60
Pipe Roughness (μm)	21.0
Pipeline Slope	Vertical Down

Mixture Velocity (m/s)	Pressure Gradient (kPa/m)	Slurry Temp. (°C)
3.371	- 7.328	14.3
3.423	- 6.899	14.3
3.406	- 6.923	14.4
3.389	- 7.030	14.5
2.932	- 9.231	14.7
2.937	- 8.773	14.7
2.930	- 9.124	14.8
2.947	- 9.112	14.8
2.546	-10.468	15.0
2.542	-10.459	15.0
2.560	-10.335	15.0
2.129	-12.216	15.1
2.133	-12.248	15.1
2.124	-12.046	15.1
1.683	-13.509	15.2
1.680	-13.192	15.2
1.684	-13.396	15.2
1.304	-14.175	15.2
1.303	-14.246	15.2
1.308	-14.248	15.3

Particle Size Distribution
Malvern Particle Size Analyser

Size (μm)	% Passing	% Retained
564.0	100.0	.0
261.6	95.9	4.1
160.4	73.6	22.3
112.8	48.7	24.9
84.3	35.8	12.9
64.6	28.9	6.9
50.2	23.7	5.2
39.0	20.8	2.9
30.3	18.4	2.4
23.7	16.2	2.2
18.5	14.6	1.6
14.5	13.2	1.4
11.4	11.6	1.6
9.1	9.6	2.0
7.2	7.6	2.0
5.8	4.8	2.8
Pan	- .0	4.8

OBSERVED FLOW BEHAVIOUR

Velocity	Observation

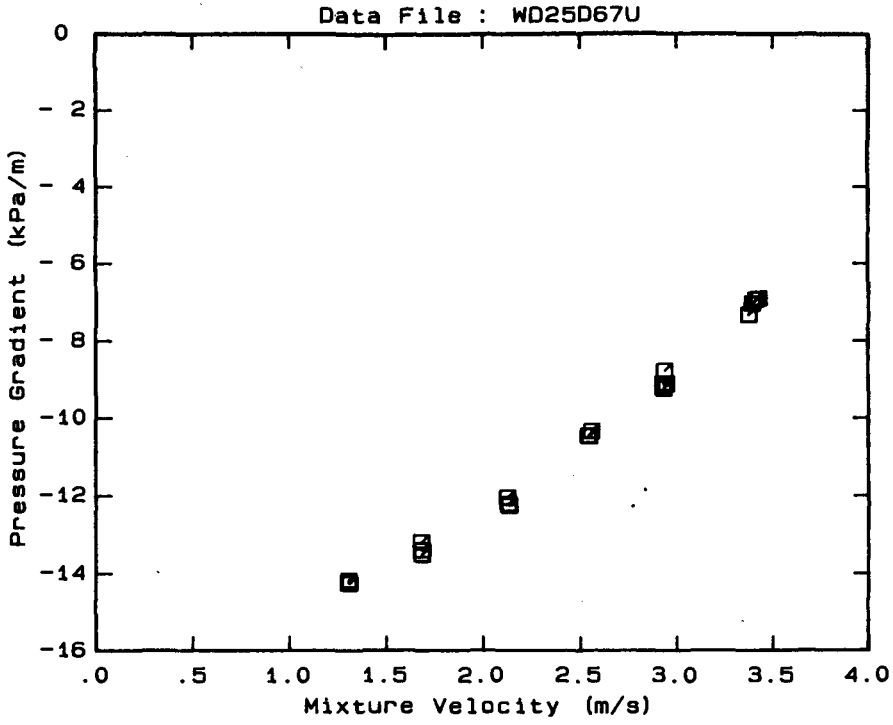

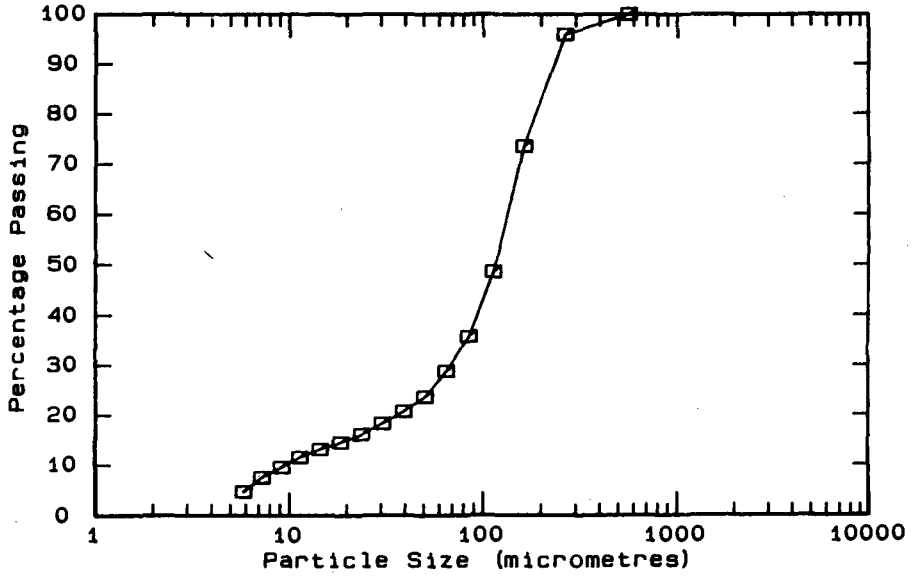

DATA FILE : WD25D73U

Test Facility	UCT 25 mm NB
Test Date	June 1990
Material Description	Western Deeps CCT
Material Relative Density	2.65
Slurry Relative Density	1.73
Solids Volumetric Concentration (%)	44.24
Solids Mass Concentration (%)	67.77
Mean Slurry Temperature (°C)	16.1
Pipe Internal Diameter (mm)	26.60
Pipe Roughness (μm)	21.0
Pipeline Slope	Vertical Down

Mixture Velocity (m/s)	Pressure Gradient (kPa/m)	Slurry Temp. (°C)
3.371	- 5.959	15.5
3.375	- 7.186	15.6
3.407	- 6.475	15.6
3.411	- 6.749	15.7
3.416	- 7.156	15.8
3.437	- 6.548	15.9
2.984	- 8.543	16.0
2.983	- 8.551	16.1
2.983	- 8.632	16.1
2.554	-10.165	16.3
2.543	-10.238	16.3
2.540	-10.264	16.3
2.128	-11.763	16.4
2.126	-11.878	16.4
2.126	-11.740	16.4
1.682	-13.163	16.4
1.675	-13.039	16.4
1.677	-13.085	16.4
1.284	-14.075	16.5
1.279	-14.030	16.4
1.281	-14.057	16.4

Particle Size Distribution
Malvern Particle Size Analyser

Size (μm)	% Passing	% Retained
564.0	100.0	.0
261.6	96.3	3.7
160.4	75.3	21.0
112.8	50.5	24.8
84.3	37.0	13.5
64.6	30.5	6.5
50.2	24.9	5.6
39.0	21.6	3.3
30.3	19.3	2.3
23.7	16.9	2.4
18.5	15.3	1.6
14.5	14.0	1.3
11.4	12.3	1.7
9.1	10.3	2.0
7.2	8.2	2.1
5.8	5.2	3.0
Pan	.1	5.1

OBSERVED FLOW BEHAVIOUR

Velocity (m/s)	Observation (D = .0 mm)

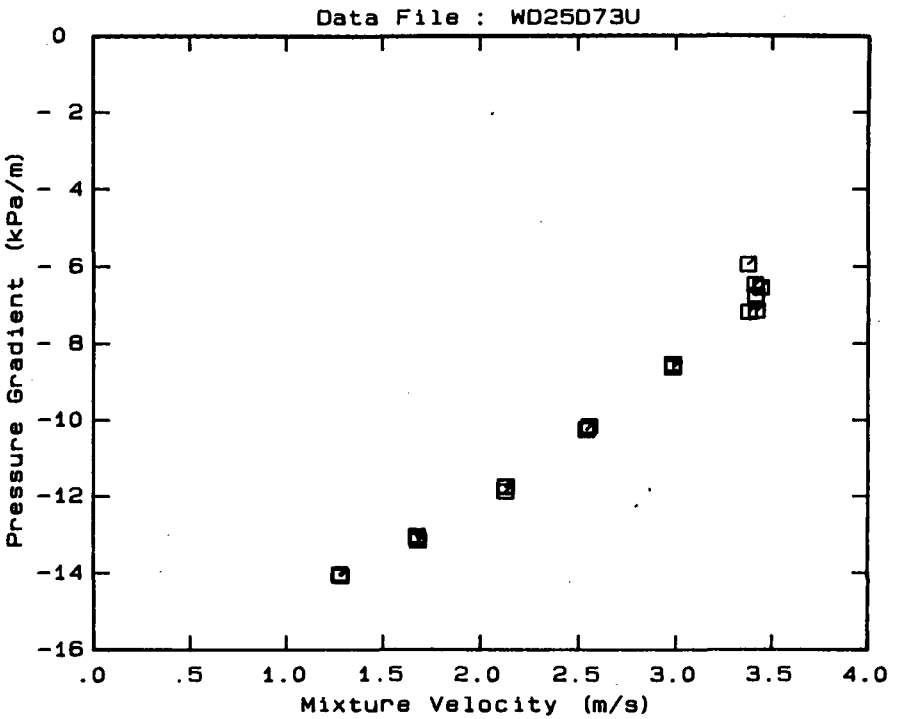

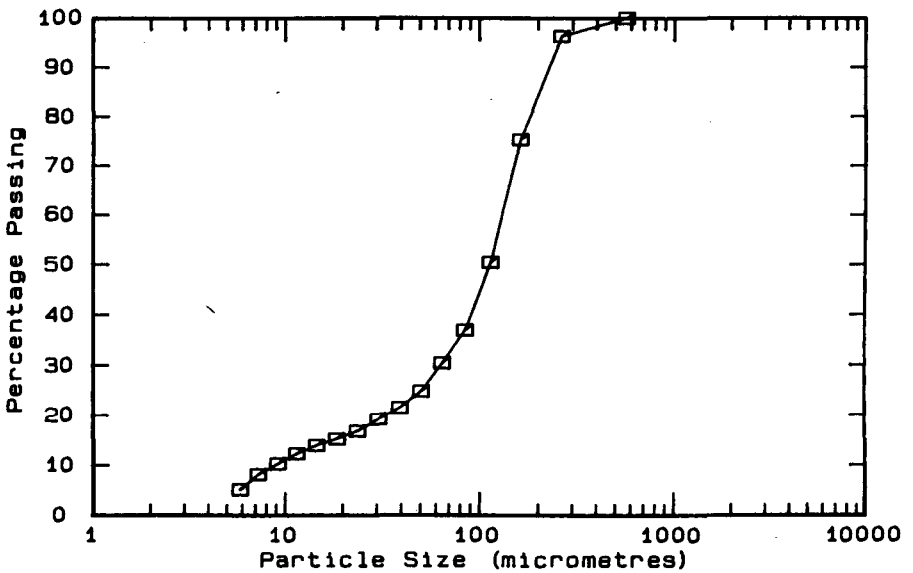

DATA FILE : WD25D76U

Test Facility	UCT 25 mm NB
Test Date	June 1990
Material Description	Western Deeps CCT
Material Relative Density	2.65
Slurry Relative Density	1.76
Solids Volumetric Concentration (%)	46.06
Solids Mass Concentration (%)	69.35
Mean Slurry Temperature (°C)	17.6
Pipe Internal Diameter (mm)	26.60
Pipe Roughness (μm)	21.0
Pipeline Slope	Vertical Down

Mixture Velocity (m/s)	Pressure Gradient (kPa/m)	Slurry Temp. (°C)
3.480	- 5.109	16.8
3.467	- 5.002	16.9
3.485	- 4.546	17.0
3.506	- 4.870	17.1
3.525	- 4.236	17.1
3.544	- 4.836	17.2
2.969	- 7.501	17.5
2.968	- 7.257	17.5
2.966	- 7.320	17.6
2.975	- 7.550	17.6
2.552	- 8.775	17.7
2.552	- 9.012	17.7
2.545	- 8.944	17.8
2.129	-10.568	17.9
2.133	-10.657	17.9
2.122	-10.644	17.9
1.683	-12.092	17.9
1.679	-12.159	17.9
1.678	-12.226	17.9
1.272	-13.384	17.9
1.269	-13.426	17.9
1.261	-13.384	17.9

Particle Size Distribution
Malvern Particle Size Analyser

Size (μm)	% Passing	% Retained
564.0	100.0	.0
261.6	94.9	5.1
160.4	74.0	20.9
112.8	50.9	23.1
84.3	37.0	13.9
64.6	30.9	6.1
50.2	26.4	4.5
39.0	22.7	3.7
30.3	20.2	2.5
23.7	18.4	1.8
18.5	16.4	2.0
14.5	14.8	1.6
11.4	13.1	1.7
9.1	10.9	2.2
7.2	8.6	2.3
5.8	5.4	3.2
Pan	.0	5.4

OBSERVED FLOW BEHAVIOUR

Velocity (m/s)	Observation (D = .0 mm)

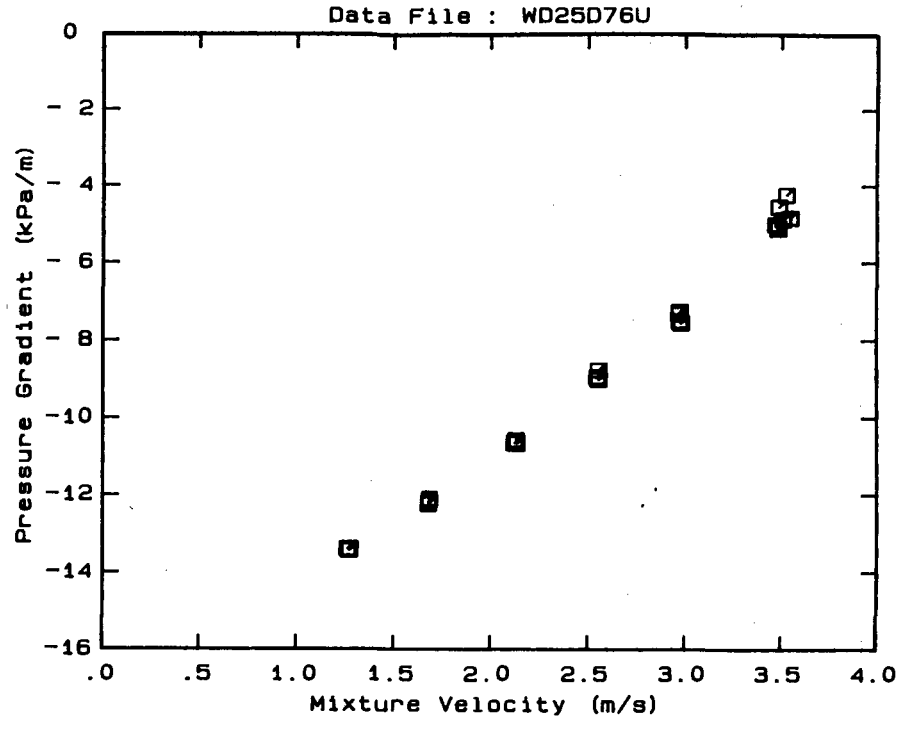

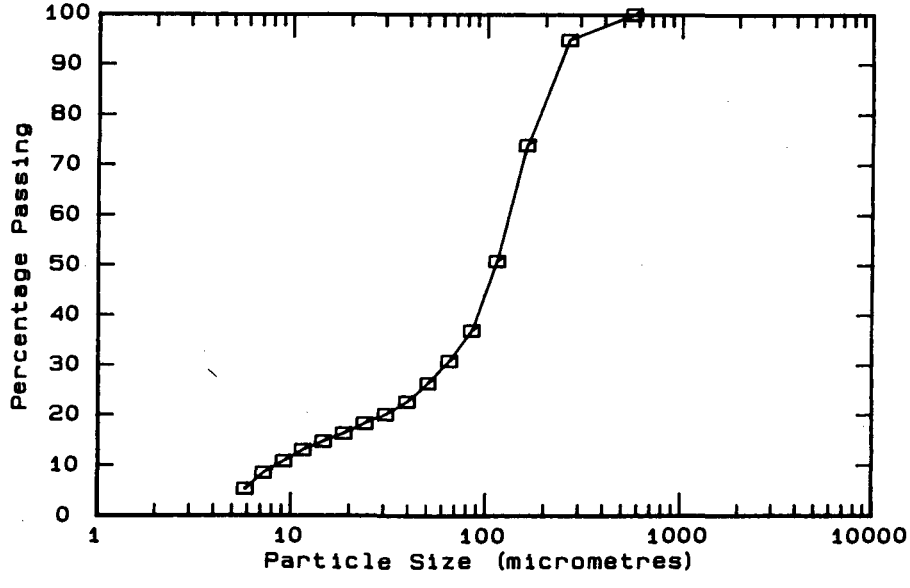

DATA FILE : WD25D79U

Test Facility	UCT 25 mm NB
Test Date	June 1990
Material Description	Western Deeps CCT
Material Relative Density	2.65
Slurry Relative Density	1.79
Solids Volumetric Concentration (%)	47.88
Solids Mass Concentration (%)	70.88
Mean Slurry Temperature (°C)	19.5
Pipe Internal Diameter (mm)	26.60
Pipe Roughness (μm)	21.0
Pipeline Slope	Vertical Down

Mixture Velocity (m/s)	Pressure Gradient (kPa/m)	Slurry Temp. (°C)
3.431	- 1.984	18.6
3.480	- 2.140	18.7
3.518	- 1.915	18.8
2.937	- 4.723	19.3
2.956	- 4.701	19.3
2.949	- 5.033	19.4
2.958	- 4.748	19.5
2.548	- 6.446	19.6
2.540	- 6.444	19.7
2.552	- 6.414	19.7
2.101	- 8.538	19.8
2.097	- 8.451	19.8
2.093	- 8.585	19.8
1.678	-10.260	19.8
1.678	-10.400	19.8
1.682	-10.487	19.8
1.671	-10.366	19.8
1.222	-12.274	19.8
1.216	-12.345	19.8
1.213	-12.319	19.7

Particle Size Distribution
Malvern Particle Size Analyser

Size (μm)	% Passing	% Retained
564.0	100.0	.0
261.6	97.6	2.4
160.4	76.9	20.7
112.8	50.7	26.2
84.3	37.4	13.3
64.6	31.0	6.4
50.2	25.6	5.4
39.0	22.1	3.5
30.3	19.9	2.2
23.7	18.0	1.9
18.5	16.1	1.9
14.5	14.6	1.5
11.4	13.0	1.6
9.1	10.8	2.2
7.2	8.7	2.1
5.8	5.6	3.1
Pan	.1	5.5

OBSERVED FLOW BEHAVIOUR

Velocity	Observation

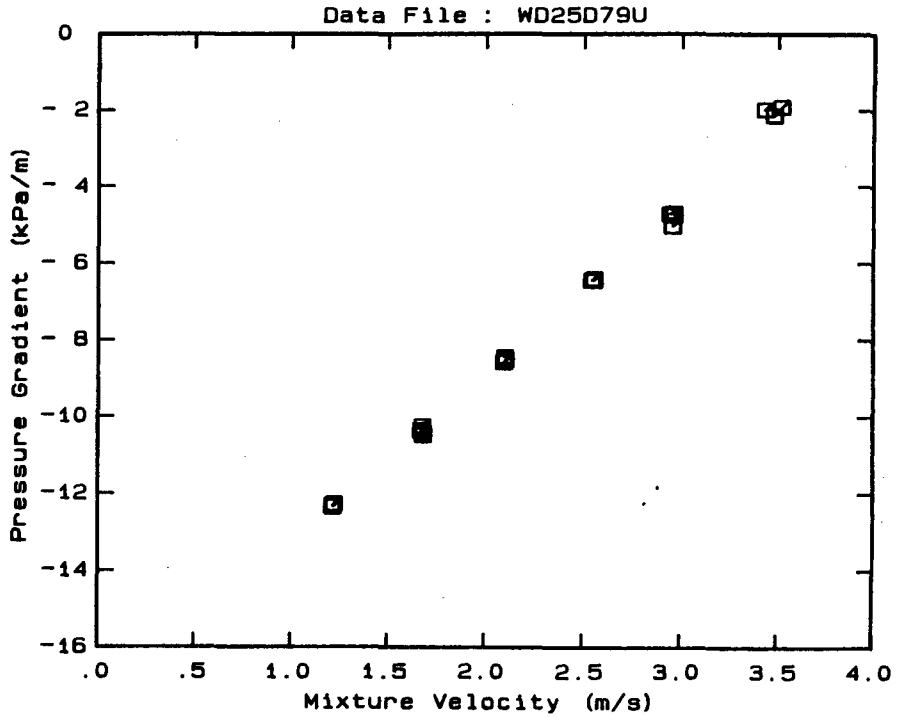

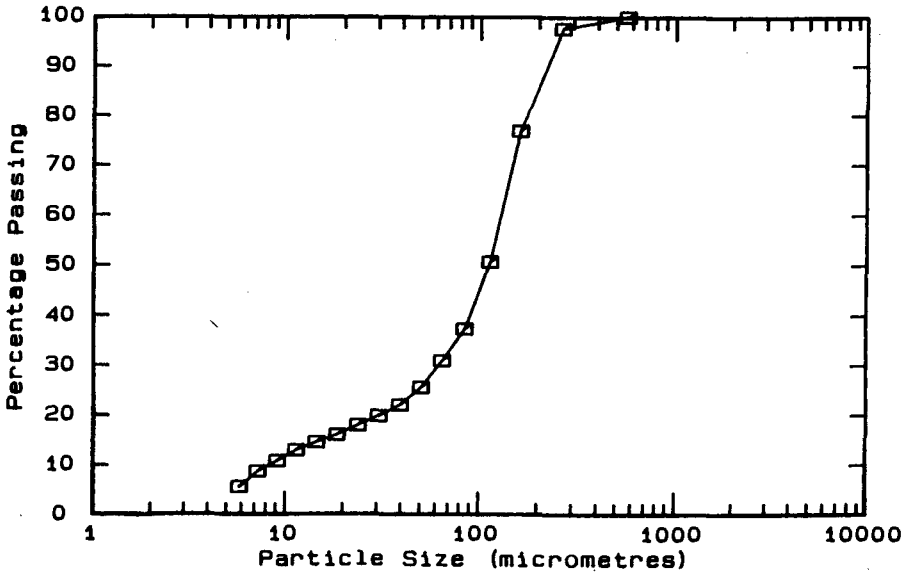

DATA FILE : WD25D82U

Test Facility	UCT 25 mm NB
Test Date	June 1990
Material Description	Western Deeps CCT
Material Relative Density	2.65
Slurry Relative Density	1.82
Solids Volumetric Concentration (%)	49.70
Solids Mass Concentration (%)	72.36
Mean Slurry Temperature (°C)	21.0
Pipe Internal Diameter (mm)	26.60
Pipe Roughness (μm)	21.0
Pipeline Slope	Vertical Down

Mixture Velocity (m/s)	Pressure Gradient (kPa/m)	Slurry Temp. (°C)
3.234	1.609	20.0
3.272	1.813	20.1
3.273	1.981	20.2
2.987	- .088	20.6
3.022	.108	20.7
3.001	- .079	20.8
2.550	- 3.434	21.1
2.115	- 6.295	21.3
2.115	- 6.370	21.4
2.112	- 6.344	21.4
1.681	- 8.455	21.4
1.673	- 8.543	21.4
1.671	- 8.490	21.4
1.267	-10.579	21.4
1.255	-10.533	21.4
1.255	-10.562	21.4

Particle Size Distribution
Malvern Particle Size Analyser

Size (μm)	% Passing	% Retained
564.0	100.0	.0
261.6	96.7	3.3
160.4	75.6	21.1
112.8	50.3	25.3
84.3	37.2	13.1
64.6	30.5	6.7
50.2	25.0	5.5
39.0	22.2	2.8
30.3	19.9	2.3
23.7	17.4	2.5
18.5	15.9	1.5
14.5	14.5	1.4
11.4	12.7	1.8
9.1	10.6	2.1
7.2	8.4	2.2
5.8	5.2	3.2
Pan	- .3	5.5

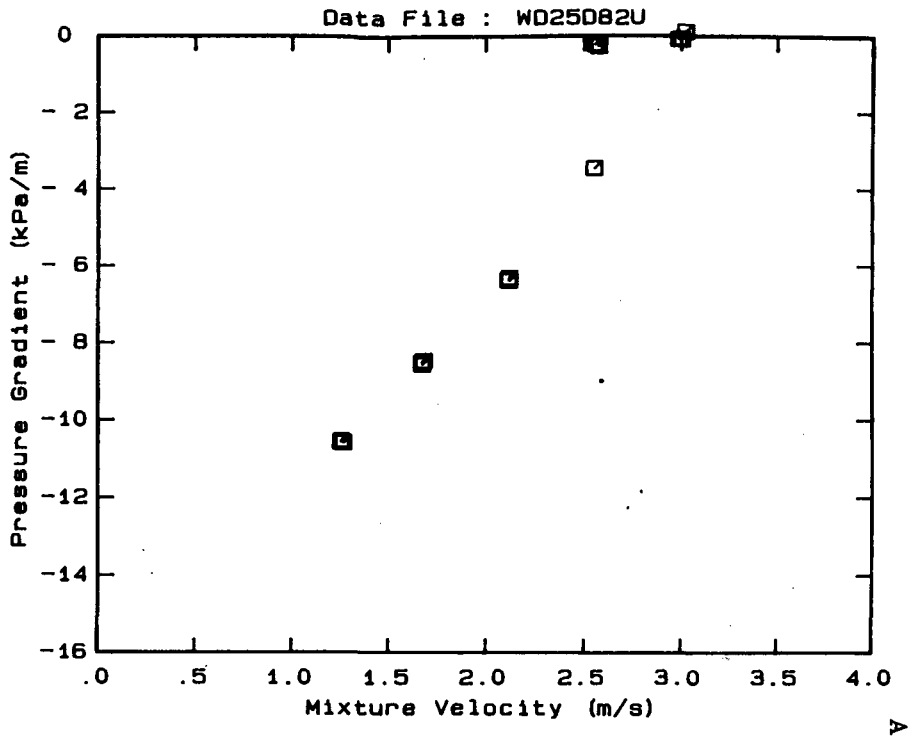

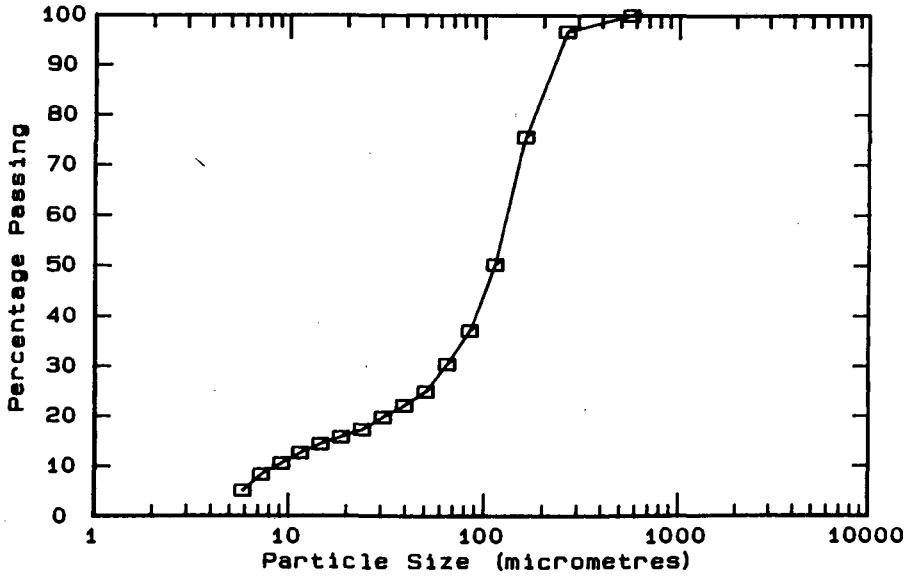

DATA FILE : WD25D85U

Test Facility	UCT 25 mm NB
Test Date	June 1990
Material Description	Western Deeps CCT
Material Relative Density	2.65
Slurry Relative Density	1.85
Solids Volumetric Concentration (%)	51.52
Solids Mass Concentration (%)	73.79
Mean Slurry Temperature (°C)	21.1
Pipe Internal Diameter (mm)	26.60
Pipe Roughness (μm)	21.0
Pipeline Slope	Vertical Down

Mixture Velocity (m/s)	Pressure Gradient (kPa/m)	Slurry Temp. (°C)
2.429	- .761	20.0
2.424	- .309	20.1
2.073	- 2.722	21.1
2.071	- 2.812	21.2
2.091	- 2.544	21.3
1.672	- 5.648	21.4
1.690	- 5.583	21.4
1.693	- 5.609	21.4
1.265	- 6.067	21.4
1.260	- 7.461	21.4
1.242	- 8.124	21.4
1.223	- 8.154	21.4
1.210	- 9.808	21.4

Particle Size Distribution
Malvern Particle Size Analyser

Size (μm)	% Passing	% Retained
564.0	100.0	.0
261.6	96.4	3.6
160.4	76.0	20.4
112.8	50.7	25.3
84.3	37.6	13.1
64.6	30.6	7.0
50.2	25.3	5.3
39.0	22.2	3.1
30.3	19.8	2.4
23.7	17.7	2.1
18.5	16.0	1.7
14.5	14.6	1.4
11.4	13.0	1.6
9.1	10.9	2.1
7.2	8.7	2.2
5.8	5.5	3.2
Pan	.0	5.5

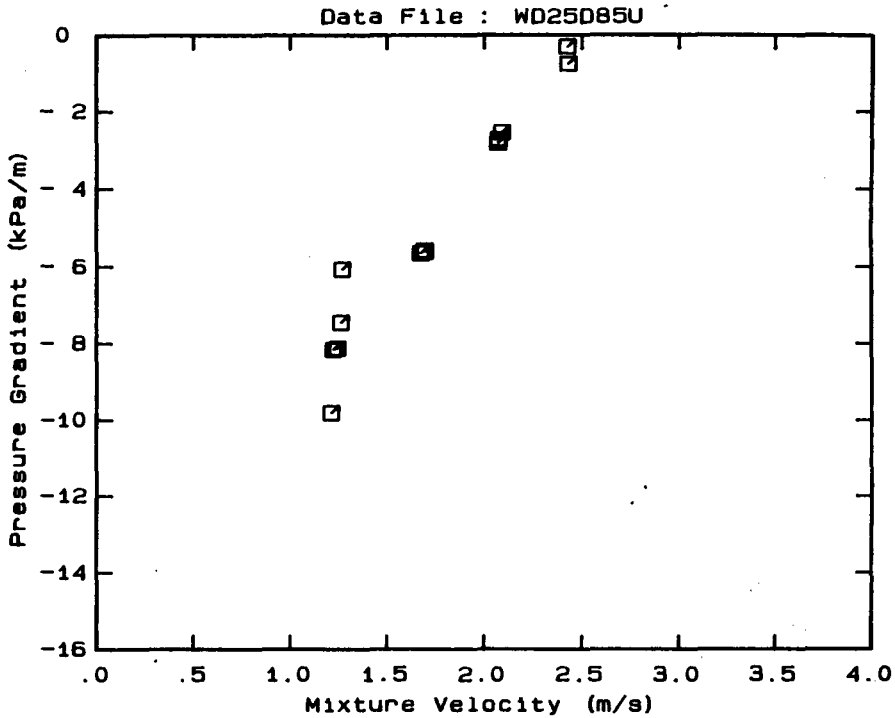

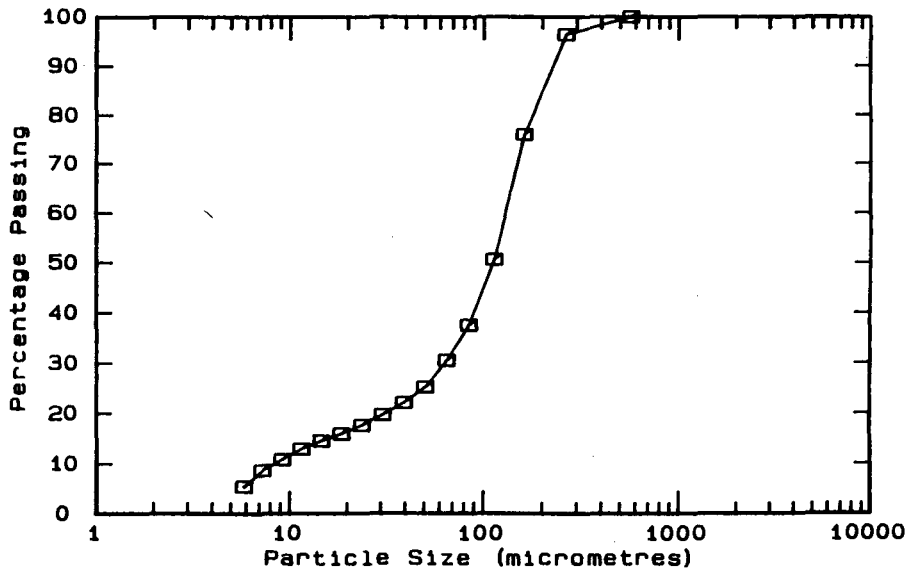

DATA FILE : WD25U67U

Test Facility	UCT 25 mm NB
Test Date	June 1990
Material Description	Western Deeps CCT
Material Relative Density	2.65
Slurry Relative Density	1.67
Solids Volumetric Concentration (%)	40.61
Solids Mass Concentration (%)	64.43
Mean Slurry Temperature (°C)	14.9
Pipe Internal Diameter (mm)	26.60
Pipe Roughness (μm)	21.0
Pipeline Slope	Vertical Up

Mixture Velocity (m/s)	Pressure Gradient (kPa/m)	Slurry Temp. (°C)
3.371	25.528	14.3
3.423	26.542	14.3
3.406	26.476	14.4
3.389	26.258	14.5
2.932	23.973	14.7
2.937	23.911	14.7
2.930	24.120	14.8
2.947	24.044	14.8
2.546	21.919	15.0
2.542	22.234	15.0
2.560	22.084	15.0
2.129	19.657	15.1
2.133	19.660	15.1
2.124	19.793	15.1
1.683	18.538	15.2
1.680	18.579	15.2
1.684	18.539	15.2
1.304	18.162	15.2
1.303	18.061	15.2
1.308	18.092	15.3

Particle Size Distribution
Malvern Particle Size Analyser

Size (μm)	% Passing	% Retained
564.0	100.0	.0
261.6	95.9	4.1
160.4	73.6	22.3
112.8	48.7	24.9
84.3	35.8	12.9
64.6	28.9	6.9
50.2	23.7	5.2
39.0	20.8	2.9
30.3	18.4	2.4
23.7	16.2	2.2
18.5	14.6	1.6
14.5	13.2	1.4
11.4	11.6	1.6
9.1	9.6	2.0
7.2	7.6	2.0
5.8	4.8	2.8
Pan	- .0	4.8

OBSERVED FLOW BEHAVIOUR

Velocity	Observation

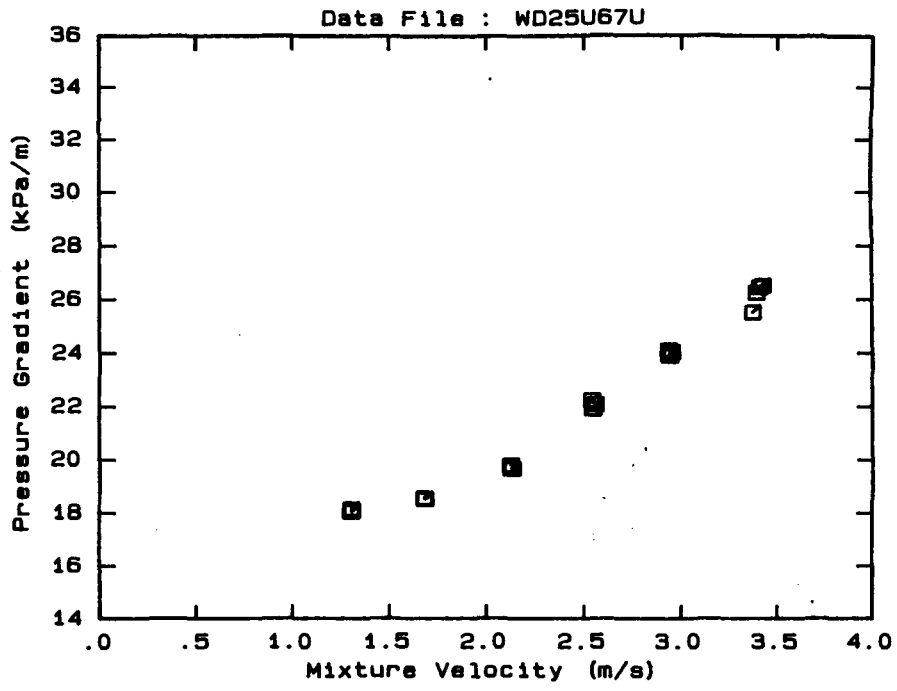

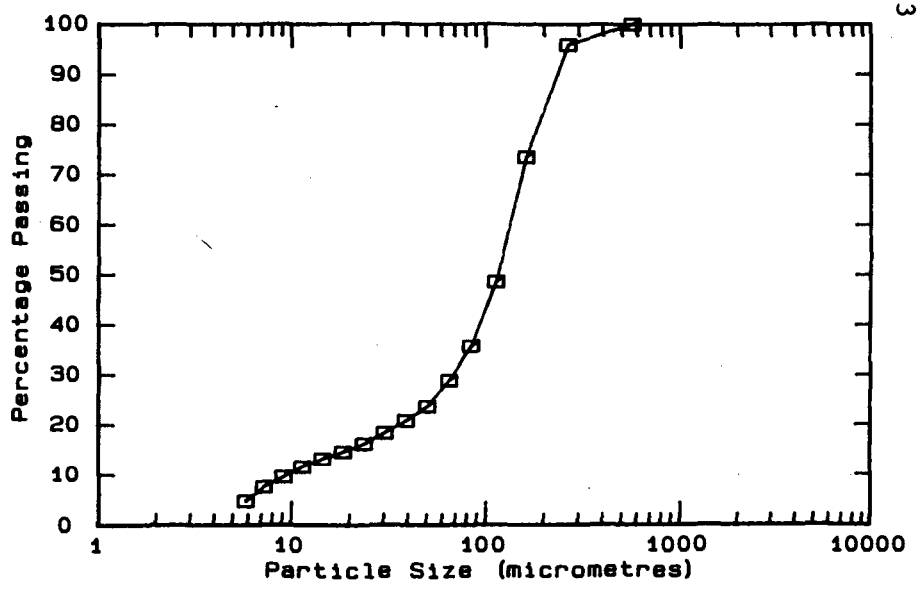

DATA FILE : WD25U73U

Test Facility	UCT 25 mm NB
Test Date	June 1990
Material Description	Western Deeps CCT
Material Relative Density	2.65
Slurry Relative Density	1.73
Solids Volumetric Concentration (%)	44.24
Solids Mass Concentration (%)	67.77
Mean Slurry Temperature (°C)	16.1
Pipe Internal Diameter (mm)	26.60
Pipe Roughness (μm)	21.0
Pipeline Slope	Vertical Up

Mixture Velocity (m/s)	Pressure Gradient (kPa/m)	Slurry Temp. (°C)
3.371	25.640	15.5
3.375	24.841	15.6
3.407	25.560	15.6
3.411	25.078	15.7
3.416	25.129	15.8
3.437	25.236	15.9
2.984	23.388	16.0
2.983	23.209	16.1
2.983	22.961	16.1
2.554	22.022	16.3
2.543	22.180	16.3
2.540	21.728	16.3
2.128	20.982	16.4
2.126	20.833	16.4
2.126	20.948	16.4
1.682	19.993	16.4
1.675	20.215	16.4
1.677	20.037	16.4
1.284	19.179	16.5
1.279	19.278	16.4
1.281	19.132	16.4

Particle Size Distribution
Malvern Particle Size Analyser

Size (μm)	% Passing	% Retained
564.0	100.0	.0
261.6	96.3	3.7
160.4	75.3	21.0
112.8	50.5	24.8
84.3	37.0	13.5
64.6	30.5	6.5
50.2	24.9	5.6
39.0	21.6	3.3
30.3	19.3	2.3
23.7	16.9	2.4
18.5	15.3	1.6
14.5	14.0	1.3
11.4	12.3	1.7
9.1	10.3	2.0
7.2	8.2	2.1
5.8	5.2	3.0
Pan	.1	5.1

OBSERVED FLOW BEHAVIOUR

Velocity (m/s)	Observation (D = .0 mm)

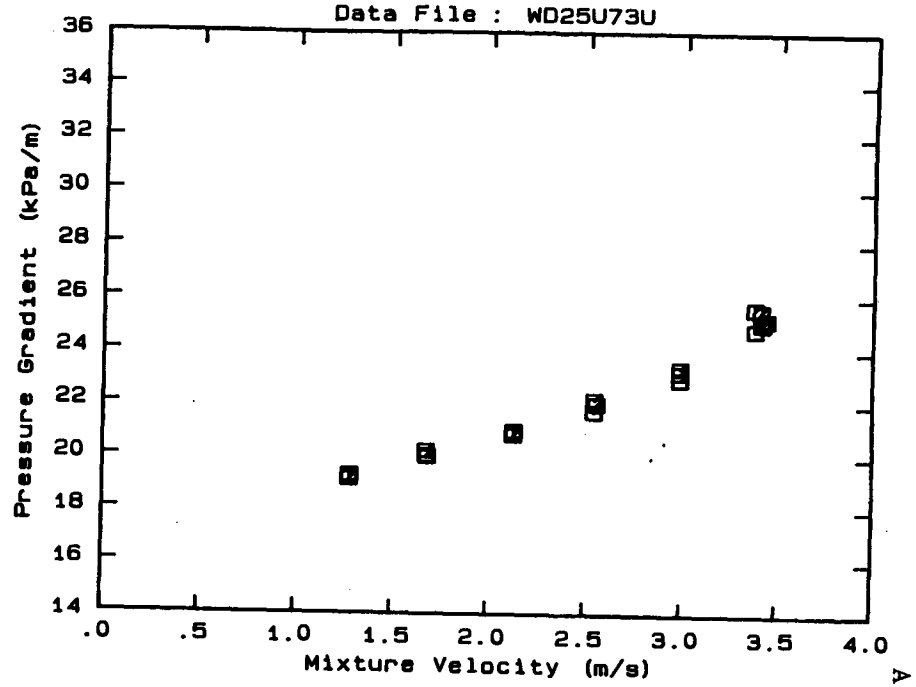

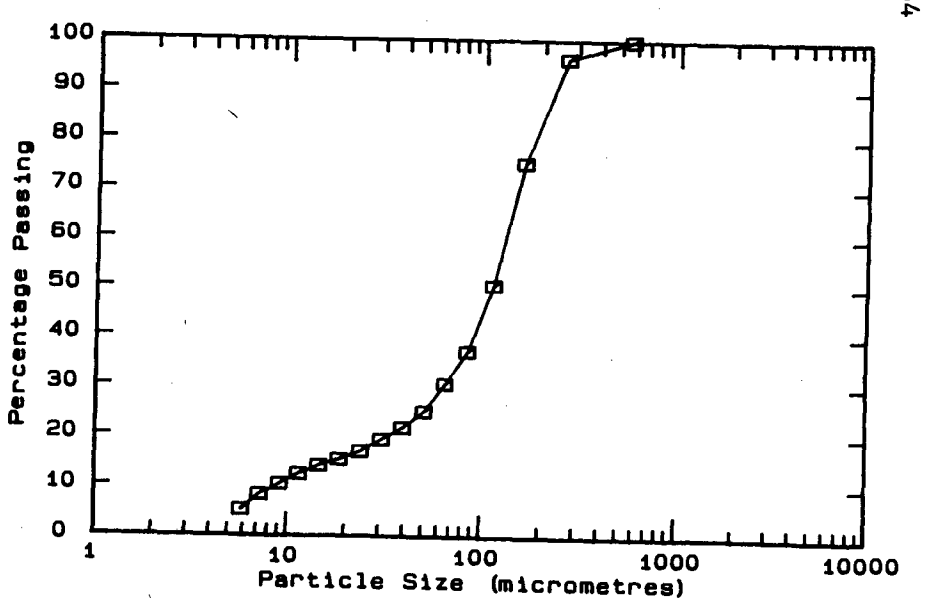

DATA FILE : WD25U76U

Test Facility	UCT 25 mm NB
Test Date	June 1990
Material Description	Western Deeps CCT
Material Relative Density	2.65
Slurry Relative Density	1.76
Solids Volumetric Concentration (%)	46.06
Solids Mass Concentration (%)	69.35
Mean Slurry Temperature (°C)	17.6
Pipe Internal Diameter (mm)	26.60
Pipe Roughness (μm)	21.0
Pipeline Slope	Vertical Up

Mixture Velocity (m/s)	Pressure Gradient (kPa/m)	Slurry Temp. (°C)
3.480	27.695	16.8
3.467	27.102	16.9
3.485	27.617	17.0
3.506	27.232	17.1
3.525	27.658	17.1
3.544	27.755	17.2
2.969	25.578	17.5
2.968	25.642	17.5
2.966	25.444	17.6
2.975	25.233	17.6
2.552	24.518	17.7
2.552	23.996	17.7
2.545	24.237	17.8
2.129	22.891	17.9
2.133	22.908	17.9
2.122	22.837	17.9
1.683	21.453	17.9
1.679	21.478	17.9
1.678	21.478	17.9
1.272	20.510	17.9
1.269	20.395	17.9
1.261	20.699	17.9

Particle Size Distribution
Malvern Particle Size Analyser

Size (μm)	% Passing	% Retained
564.0	100.0	.0
261.6	94.9	5.1
160.4	74.0	20.9
112.8	50.9	23.1
84.3	37.0	13.9
64.6	30.9	6.1
50.2	26.4	4.5
39.0	22.7	3.7
30.3	20.2	2.5
23.7	18.4	1.8
18.5	16.4	2.0
14.5	14.8	1.6
11.4	13.1	1.7
9.1	10.9	2.2
7.2	8.6	2.3
5.8	5.4	3.2
Pan	.0	5.4

OBSERVED FLOW BEHAVIOUR

Velocity (m/s)	Observation (D = .0 mm)

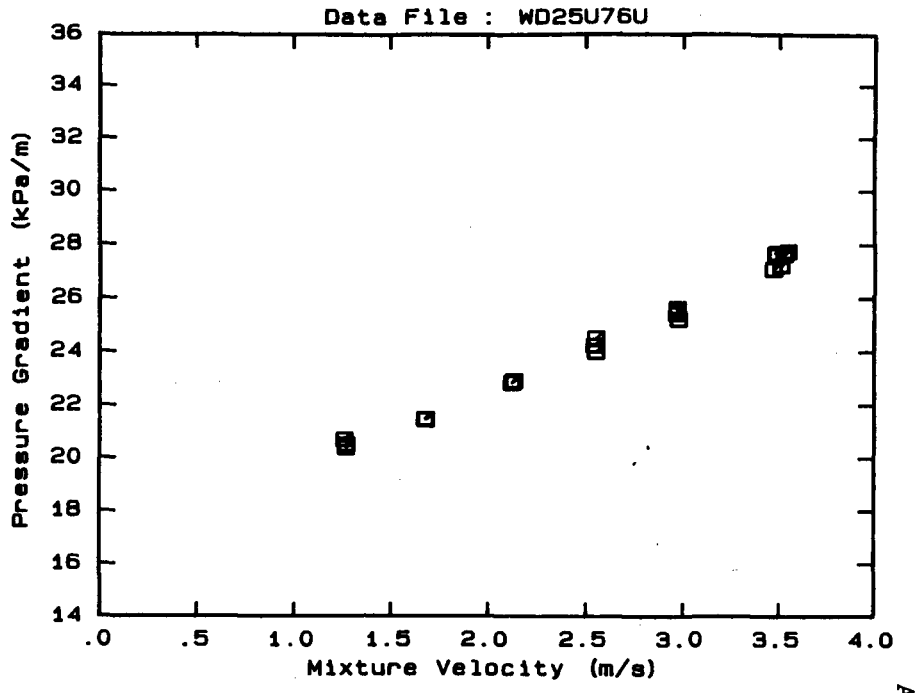

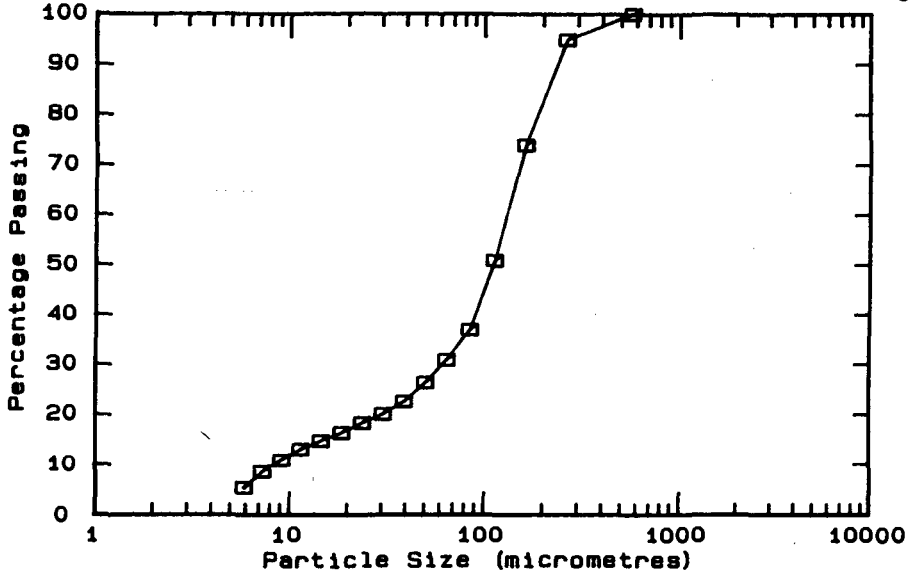

DATA FILE : WD25U79U

Test Facility	UCT 25 mm NB
Test Date	June 1990
Material Description	Western Deeps CCT
Material Relative Density	2.65
Slurry Relative Density	1.79
Solids Volumetric Concentration (%)	47.88
Solids Mass Concentration (%)	70.88
Mean Slurry Temperature (°C)	19.5
Pipe Internal Diameter (mm)	26.60
Pipe Roughness (μm)	21.0
Pipeline Slope	Vertical Up

Mixture Velocity (m/s)	Pressure Gradient (kPa/m)	Slurry Temp. (°C)
3.431	30.874	18.6
3.480	30.739	18.7
3.518	30.785	18.8
2.937	28.233	19.3
2.956	28.428	19.3
2.949	28.114	19.4
2.958	27.947	19.5
2.548	26.731	19.6
2.540	26.577	19.7
2.552	26.687	19.7
2.101	24.818	19.8
2.097	25.048	19.8
2.093	24.931	19.8
1.678	23.606	19.8
1.678	23.507	19.8
1.682	23.543	19.8
1.671	23.464	19.8
1.222	22.504	19.8
1.216	22.214	19.8
1.213	22.481	19.7

Particle Size Distribution
Malvern Particle Size Analyser

Size (μm)	% Passing	% Retained
564.0	100.0	.0
261.6	97.6	2.4
160.4	76.9	20.7
112.8	50.7	26.2
84.3	37.4	13.3
64.6	31.0	6.4
50.2	25.6	5.4
39.0	22.1	3.5
30.3	19.9	2.2
23.7	18.0	1.9
18.5	16.1	1.9
14.5	14.6	1.5
11.4	13.0	1.6
9.1	10.8	2.2
7.2	8.7	2.1
5.8	5.6	3.1
Pan	.1	5.5

OBSERVED FLOW BEHAVIOUR

Velocity	Observation

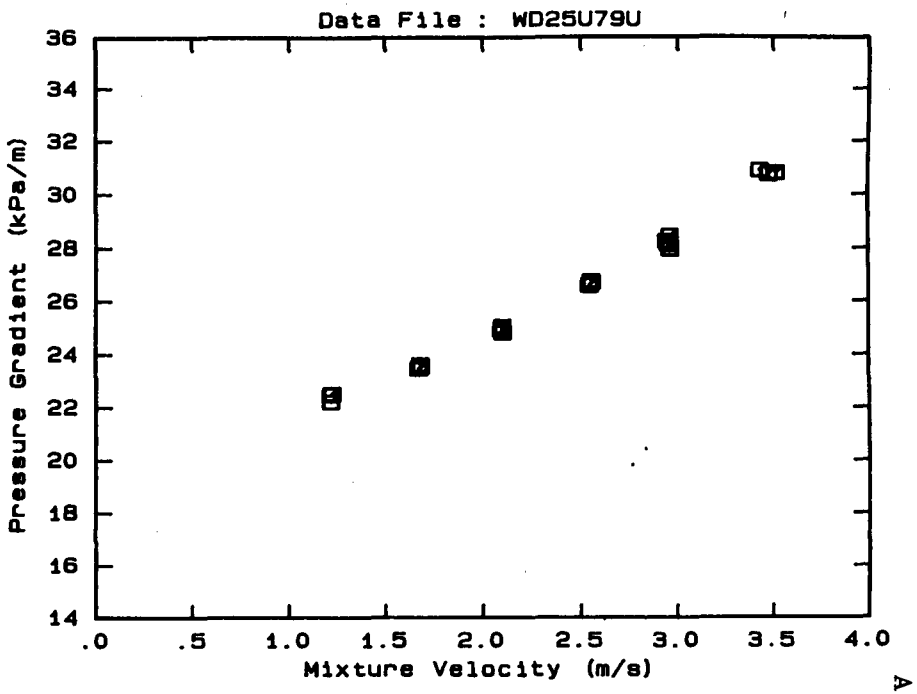

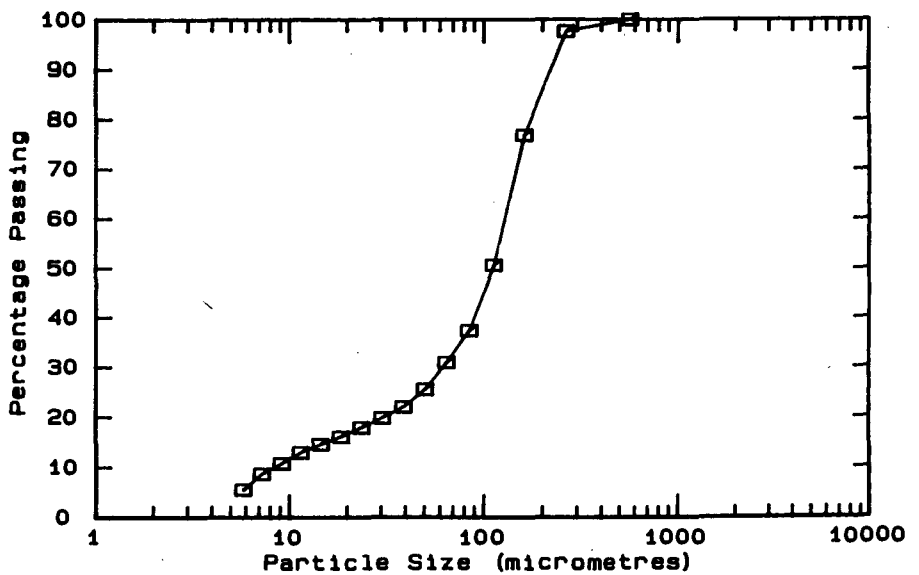

DATA FILE : WD25U82U

Test Facility	UCT 25 mm NB
Test Date	June 1990
Material Description	Western Deeps CCT
Material Relative Density	2.65
Slurry Relative Density	1.82
Solids Volumetric Concentration (%)	49.70
Solids Mass Concentration (%)	72.36
Mean Slurry Temperature (°C)	21.0
Pipe Internal Diameter (mm)	26.60
Pipe Roughness (μm)	21.0
Pipeline Slope	Vertical Up

Mixture Velocity (m/s)	Pressure Gradient (kPa/m)	Slurry Temp. (°C)
3.234	33.351	20.0
3.272	33.344	20.1
3.273	33.474	20.2
2.987	31.945	20.6
3.022	32.258	20.7
3.001	31.826	20.8
2.550	29.605	21.1
2.556	29.900	21.1
2.575	29.532	21.2
2.115	27.828	21.3
2.115	27.716	21.4
2.112	27.800	21.4
1.681	26.368	21.4
1.673	26.091	21.4
1.671	26.140	21.4
1.267	24.621	21.4
1.255	24.842	21.4
1.255	24.676	21.4

Particle Size Distribution
Malvern Particle Size Analyser

Size (μm)	% Passing	% Retained
564.0	100.0	.0
261.6	96.7	3.3
160.4	75.6	21.1
112.8	50.3	25.3
84.3	37.2	13.1
64.6	30.5	6.7
50.2	25.0	5.5
39.0	22.2	2.8
30.3	19.9	2.3
23.7	17.4	2.5
18.5	15.9	1.5
14.5	14.5	1.4
11.4	12.7	1.8
9.1	10.6	2.1
7.2	8.4	2.2
5.8	5.2	3.2
Pan	- .3	5.5

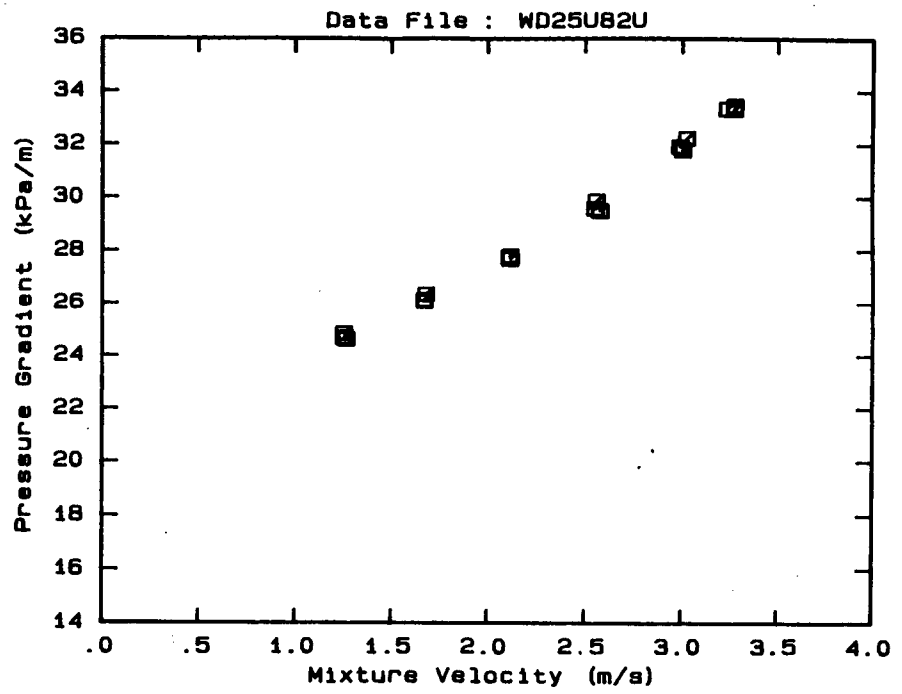

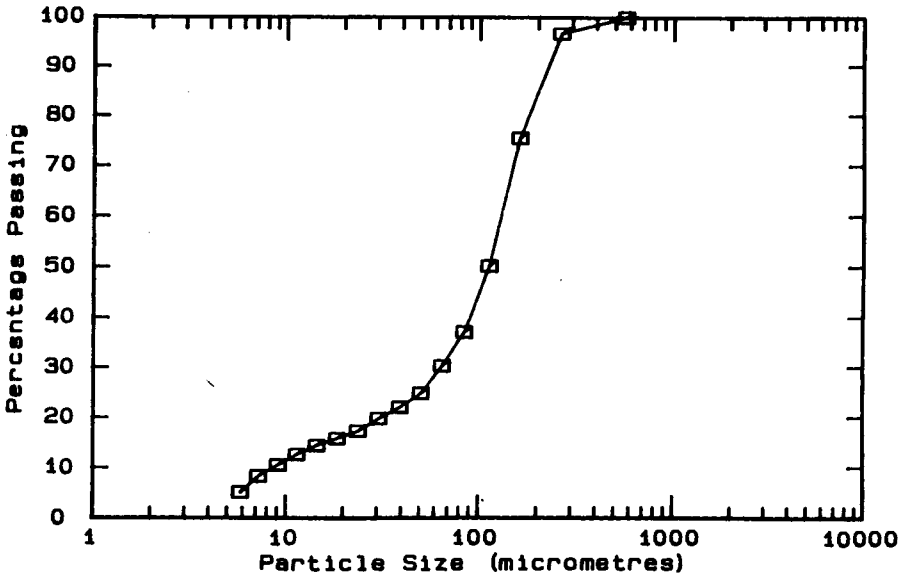

DATA FILE : WD25U85U

Test Facility	UCT 25 mm NB
Test Date	June 1990
Material Description	Western Deeps CCT
Material Relative Density	2.65
Slurry Relative Density	1.85
Solids Volumetric Concentration (%)	51.52
Solids Mass Concentration (%)	73.79
Mean Slurry Temperature (°C)	21.1
Pipe Internal Diameter (mm)	26.60
Pipe Roughness (μm)	21.0
Pipeline Slope	Vertical Up

Mixture Velocity (m/s)	Pressure Gradient (kPa/m)	Slurry Temp. (°C)
2.429	33.901	20.0
2.424	34.304	20.1
2.073	32.839	21.1
2.071	32.658	21.2
2.091	33.078	21.3
1.672	30.766	21.4
1.690	30.304	21.4
1.693	30.642	21.4
1.265	28.100	21.4
1.260	28.121	21.4
1.242	27.990	21.4
1.223	28.464	21.4
1.210	28.552	21.4

Particle Size Distribution
Malvern Particle Size Analyser

Size (μm)	% Passing	% Retained
564.0	100.0	.0
261.6	96.4	3.6
160.4	76.0	20.4
112.8	50.7	25.3
84.3	37.6	13.1
64.6	30.6	7.0
50.2	25.3	5.3
39.0	22.2	3.1
30.3	19.8	2.4
23.7	17.7	2.1
18.5	16.0	1.7
14.5	14.6	1.4
11.4	13.0	1.6
9.1	10.9	2.1
7.2	8.7	2.2
5.8	5.5	3.2
Pan	.0	5.5

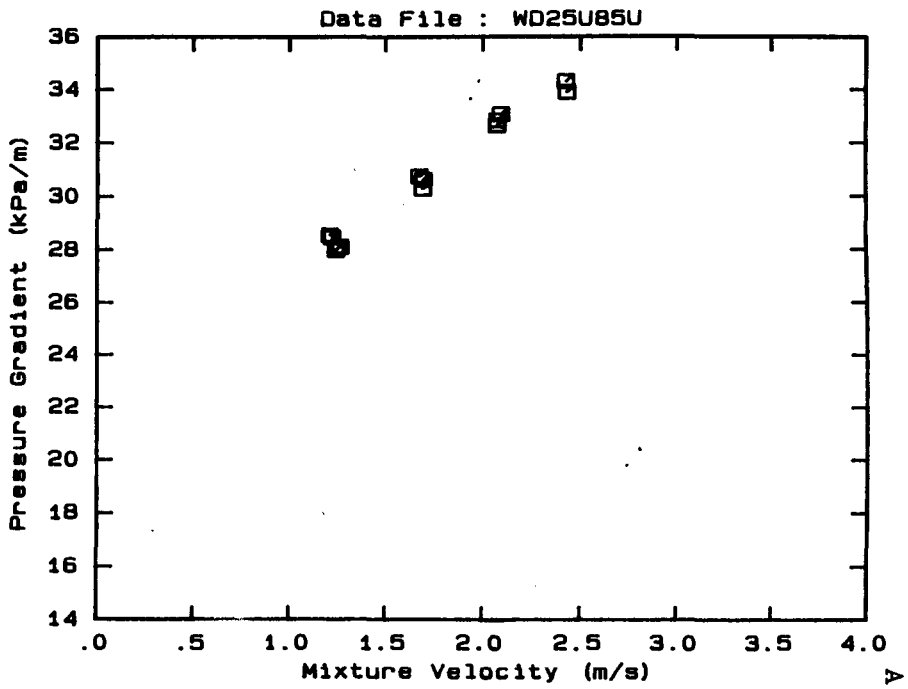

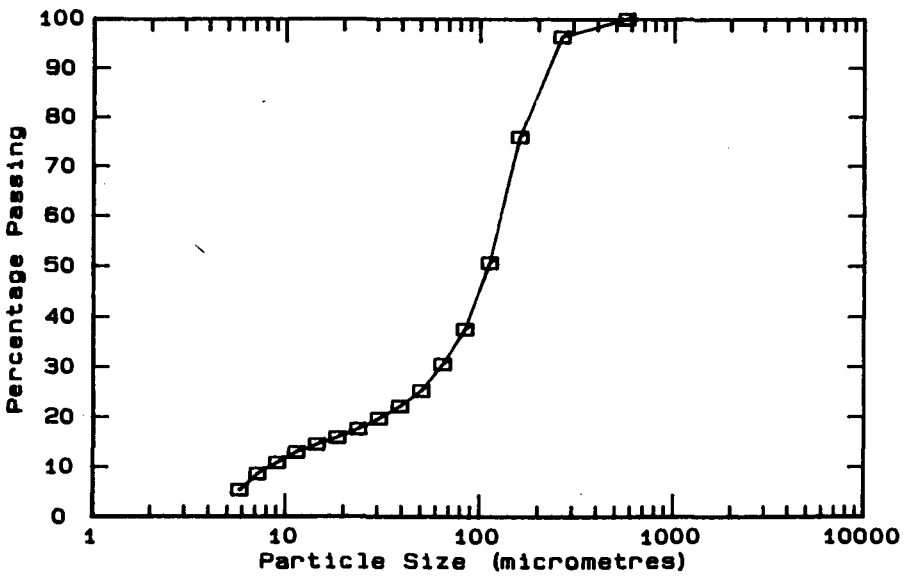

DATA FILE : WD40H63U

Test Facility	UCT 40 mm NB
Test Date	August 1990
Material Description	Western Deeps CCT
Material Relative Density	2.65
Slurry Relative Density	1.63
Solids Volumetric Concentration (%)	38.18
Solids Mass Concentration (%)	62.07
Mean Slurry Temperature (°C)	17.7
Pipe Internal Diameter (mm)	40.00
Pipe Roughness (μm)	52.0
Pipeline Slope	Horizontal

Mixture Velocity (m/s)	Pressure Gradient (kPa/m)	Slurry Temp. (°C)
3.924	8.267	17.1
4.027	9.010	17.2
3.962	8.524	17.3
3.968	8.700	17.4
3.949	8.067	17.5
3.949	8.623	17.6
3.297	6.324	17.7
3.309	6.240	17.8
3.314	6.241	17.8
3.304	6.239	17.8
2.669	4.267	17.9
2.656	4.583	17.9
2.667	4.713	17.9
2.620	4.234	17.9
2.097	2.886	17.9
2.132	2.916	17.9
2.134	3.073	17.9
1.587	1.436	17.8
1.610	1.592	17.8
1.609	1.527	17.8
1.592	1.746	17.8

Particle Size Distribution
Malvern Particle Size Analyser

Size (μm)	% Passing	% Retained
564.0	100.0	.0
261.6	98.4	1.6
160.4	79.8	18.6
112.8	52.5	27.3
84.3	37.2	15.3
64.6	30.1	7.1
50.2	24.8	5.3
39.0	21.5	3.3
30.3	19.1	2.4
23.7	17.0	2.1
18.5	15.3	1.7
14.5	14.1	1.2
11.4	12.4	1.7
9.1	10.1	2.3
7.2	8.2	1.9
5.8	5.3	2.9
Pan	.2	5.1

OBSERVED FLOW BEHAVIOUR

Velocity (m/s)	Observation (D = 46.0 mm)
1.20	Asymmetric - sliding part
1.56	Asymmetric - sliding part
2.01	Slightly aysmetric
2.46	Appears homogeneous
3.03	Appears homogeneous

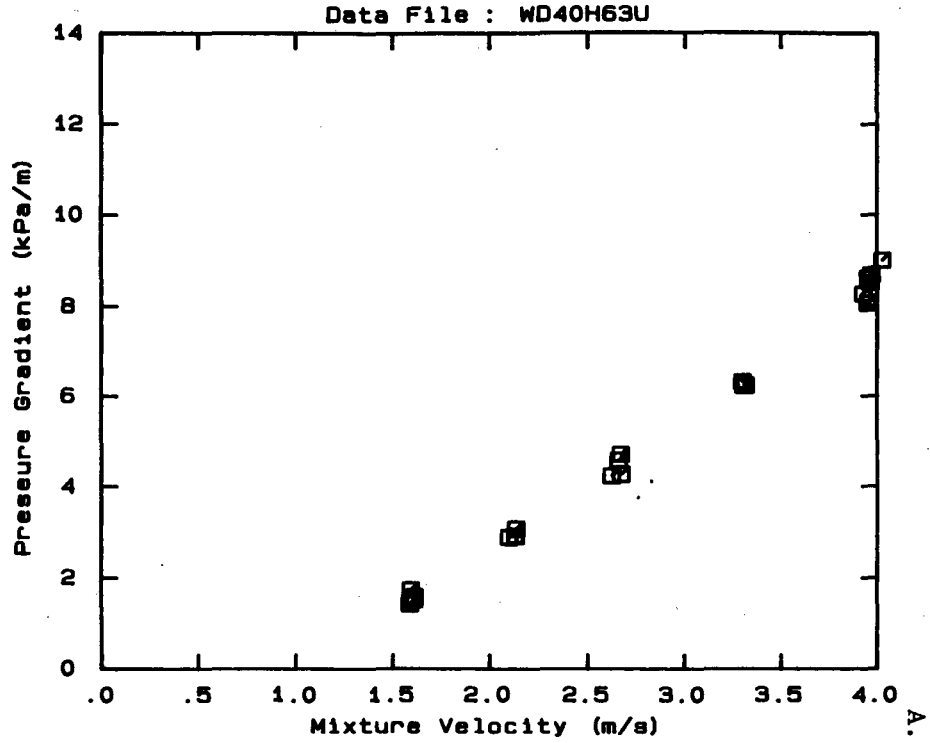

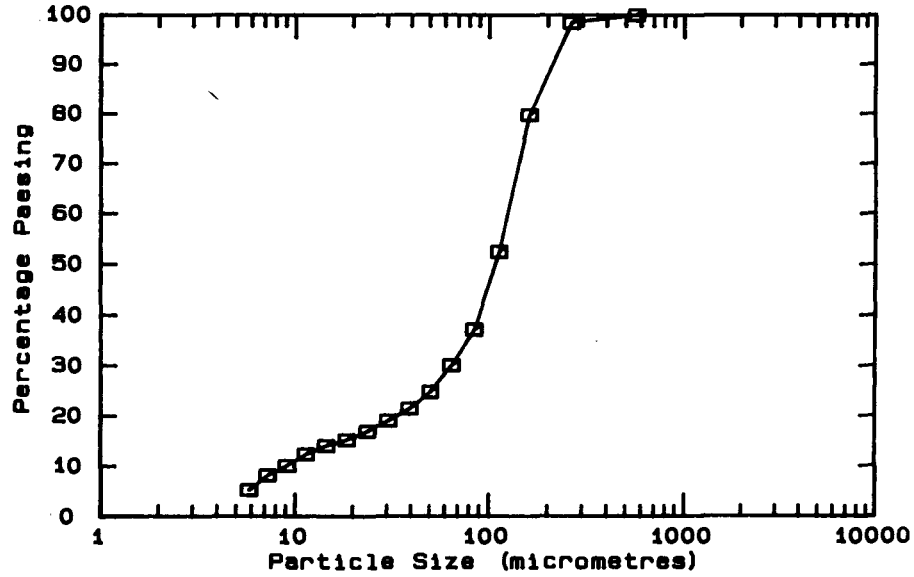

DATA FILE : WD40H71U

Test Facility	UCT 40 mm NB
Test Date	August 1990
Material Description	Western Deeps CCT
Material Relative Density	2.65
Slurry Relative Density	1.71
Solids Volumetric Concentration (%)	43.03
Solids Mass Concentration (%)	66.68
Mean Slurry Temperature (°C)	18.9
Pipe Internal Diameter (mm)	40.00
Pipe Roughness (μm)	52.0
Pipeline Slope	Horizontal

Mixture Velocity (m/s)	Pressure Gradient (kPa/m)	Slurry Temp. (°C)
3.748	8.419	18.0
3.706	8.184	18.2
3.714	8.377	18.3
3.466	7.094	18.5
3.272	6.634	18.7
3.318	6.606	18.8
3.190	7.339	18.8
3.323	6.368	18.9
3.316	6.549	18.9
3.287	6.650	18.9
2.714	4.210	19.0
2.659	3.772	19.0
2.622	4.132	19.1
2.638	3.784	19.1
2.626	4.154	19.1
2.678	3.948	19.1
2.123	2.793	19.1
2.122	2.615	19.1
2.113	2.749	19.1
1.604	2.076	19.0
1.593	1.982	19.0
1.611	2.047	19.0
1.122	1.762	18.9
1.139	1.937	18.9
1.115	1.959	18.9
1.106	1.963	18.9
1.120	1.832	18.8
1.115	1.850	18.8

Particle Size Distribution
Malvern Particle Size Analyser

Size (μm)	% Passing	% Retained
564.0	100.0	.0
261.6	97.8	2.2
160.4	76.3	21.5
112.8	50.6	25.7
84.3	36.3	14.3
64.6	29.1	7.2
50.2	24.1	5.0
39.0	21.0	3.1
30.3	18.7	2.3
23.7	16.7	2.0
18.5	15.1	1.6
14.5	13.8	1.3
11.4	12.0	1.8
9.1	9.9	2.1
7.2	8.0	1.9
5.8	5.1	2.9
Pan	- .1	5.2

OBSERVED FLOW BEHAVIOUR

Velocity (m/s)	Observation (D = 46.0 mm)
.87	20% sliding bed
1.24	Asymmetric - slid particles
1.64	Asymmetric - slid particles
2.05	Appears homogeneous
2.45	Appears homogeneous
2.78	Appears homogeneous

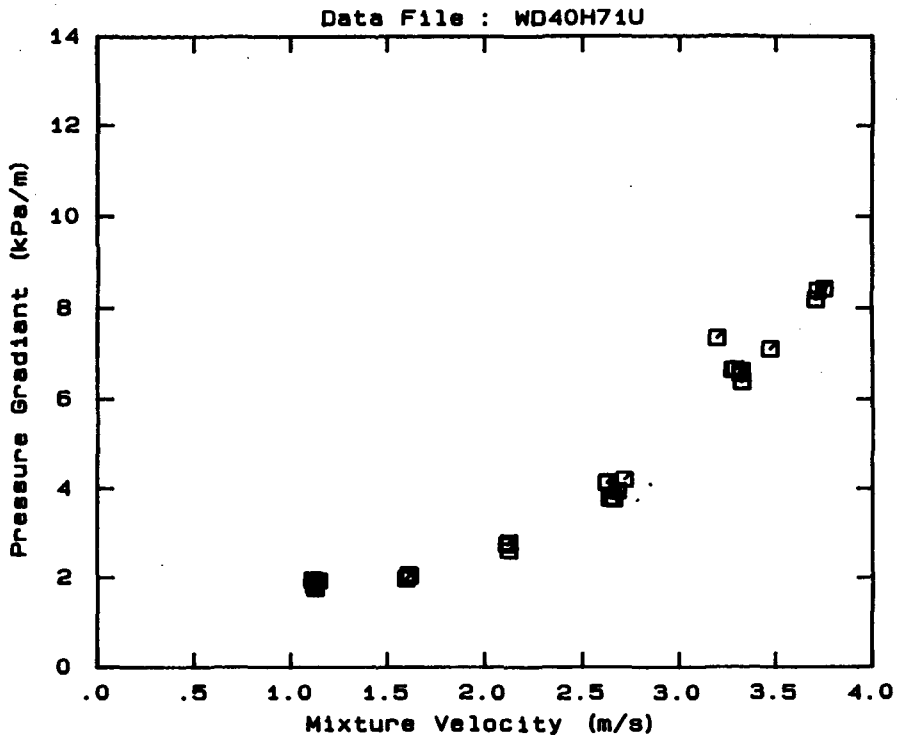

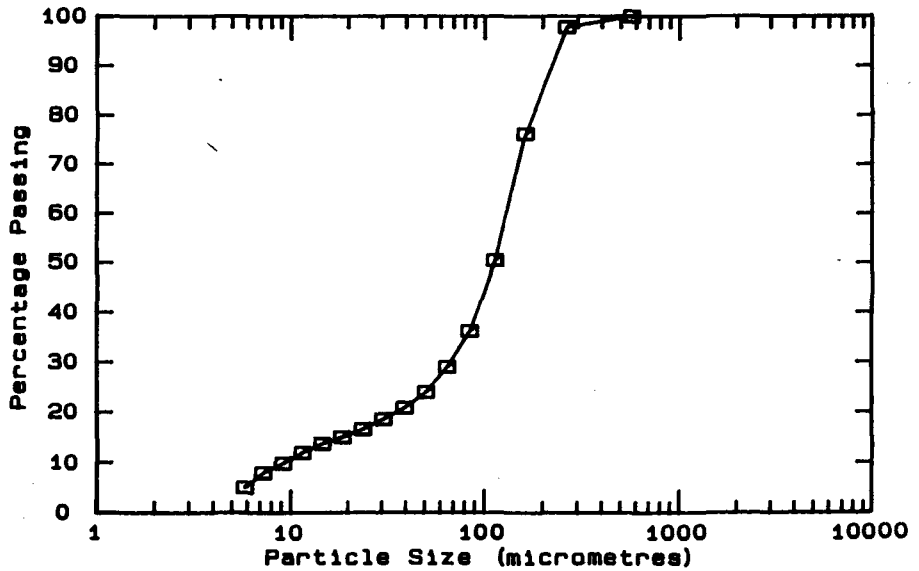

Test Faci
Test Date
Material
Material
Slurry Re
Solids Vo
Solids Ma
Mean Slur
Pipe Inte
Pipe Roug
Pipeline

Mixture Velocity (m/s)	Pres Grad (kPa
1.934	12.2
1.973	11.9
1.969	12.3
1.999	12.2
1.968	12.0
1.975	12.2
1.624	10.5
1.593	10.8
1.558	11.1
1.545	11.6
1.535	11.9
1.001	8.3
.962	8.2
.942	8.2
.944	8.1
.922	8.3
.690	7.3
.678	7.3
.676	7.3
.655	7.2
.758	7.4
.725	7.2

DATA FILE : WD40H76U

Test Facility	UCT 40 mm NB
Test Date	August 1990
Material Description	Western Deeps CCT
Material Relative Density	2.65
Slurry Relative Density	1.76
Solids Volumetric Concentration (%)	46.06
Solids Mass Concentration (%)	69.35
Mean Slurry Temperature (°C)	21.1
Pipe Internal Diameter (mm)	40.00
Pipe Roughness (μm)	52.0
Pipeline Slope	Horizontal

Mixture Velocity (m/s)	Pressure Gradient (kPa/m)	Slurry Temp. (°C)
3.726	7.122	20.2
3.740	7.614	20.3
3.787	7.916	20.4
3.794	7.387	20.5
3.787	7.505	20.6
3.229	6.379	21.0
3.250	6.412	21.1
3.265	6.416	21.1
2.666	5.272	21.3
2.533	5.264	21.3
2.512	5.050	21.3
2.523	5.006	21.3
2.132	4.497	21.4
2.148	4.383	21.4
2.140	4.322	21.4
2.134	4.403	21.3
1.597	3.180	21.3
1.575	3.245	21.3
1.610	3.417	21.3
1.577	3.061	21.2
1.555	3.127	21.2
1.037	2.346	21.1
1.045	2.403	21.1
1.009	2.395	21.1
1.020	2.363	21.1

Particle Size Distribution
Malvern Particle Size Analyser

Size (μm)	% Passing	% Retained
564.0	100.0	.0
261.6	98.9	1.1
160.4	82.9	16.0
112.8	59.6	23.3
84.3	43.5	16.1
64.6	36.4	7.1
50.2	30.9	5.5
39.0	26.8	4.1
30.3	23.9	2.9
23.7	21.5	2.4
18.5	19.4	2.1
14.5	17.8	1.6
11.4	15.5	2.3
9.1	12.6	2.9
7.2	10.4	2.2
5.8	6.6	3.8
Pan	- .3	6.9

OBSERVED FLOW BEHAVIOUR

Velocity (m/s)	Observation (D = 46.0 mm)
.83	Asymmetric
1.24	Asymmetric
1.64	Slightly Asymmetric
2.05	Appears homogeneous
2.45	Appears homogeneous
2.82	Appears homogeneous

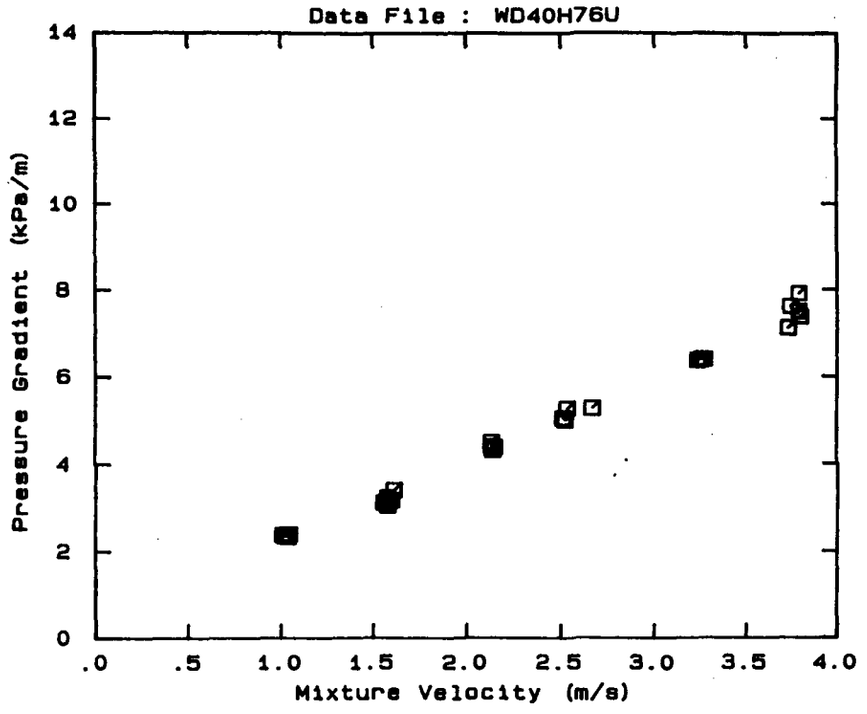

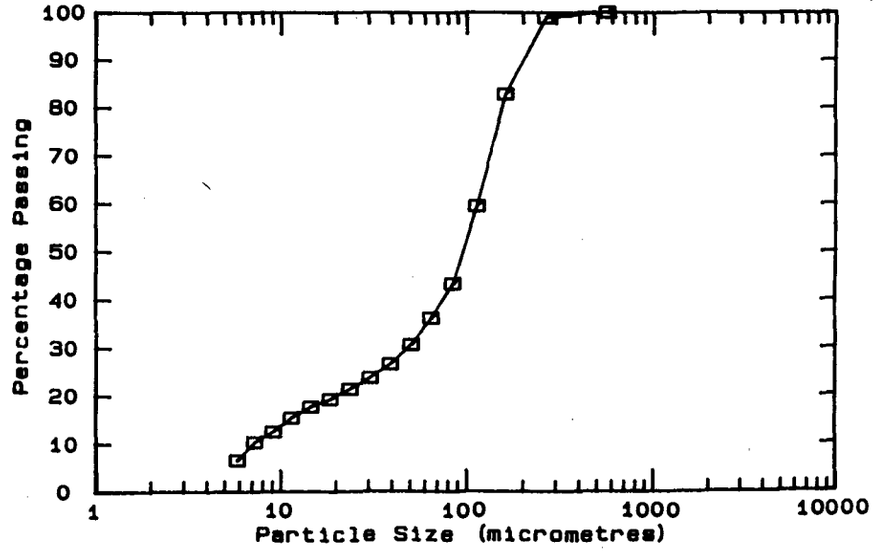

DATA FILE : WD40H88U

Test Facility	UCT 40 mm NB
Test Date	August 1990
Material Description	Western Deeps CCT
Material Relative Density	2.65
Slurry Relative Density	1.88
Solids Volumetric Concentration (%)	53.33
Solids Mass Concentration (%)	75.18
Mean Slurry Temperature (°C)	32.6
Pipe Internal Diameter (mm)	40.00
Pipe Roughness (μm)	52.0
Pipeline Slope	Horizontal

Mixture Velocity (m/s)	Pressure Gradient (kPa/m)	Slurry Temp. (°C)
.736	14.209	30.5
.748	12.968	30.6
.735	12.967	30.9
.716	13.322	32.1
.720	13.650	32.1
.740	13.462	32.2
.569	11.413	33.0
.563	11.490	33.0
.556	11.487	33.0
.556	11.460	33.0
.284	8.108	33.1
.300	8.258	33.1
.304	8.335	33.1
.302	7.906	33.1
.299	8.080	33.1
.170	6.384	33.1
.174	6.448	33.1
.168	6.432	33.1
.167	6.225	33.1
.167	6.237	33.1

Particle Size Distribution
Malvern Particle Size Analyser

Size (μm)	% Passing	% Retained
564.0	100.0	.0
261.6	98.6	1.4
160.4	78.9	19.7
112.8	53.5	25.4
84.3	38.5	15.0
64.6	31.5	7.0
50.2	26.8	4.7
39.0	23.4	3.4
30.3	20.9	2.5
23.7	18.9	2.0
18.5	17.0	1.9
14.5	15.5	1.5
11.4	13.5	2.0
9.1	11.0	2.5
7.2	9.1	1.9
5.8	5.8	3.3
Pan	- .1	5.9

OBSERVED FLOW BEHAVIOUR

Velocity	Observation

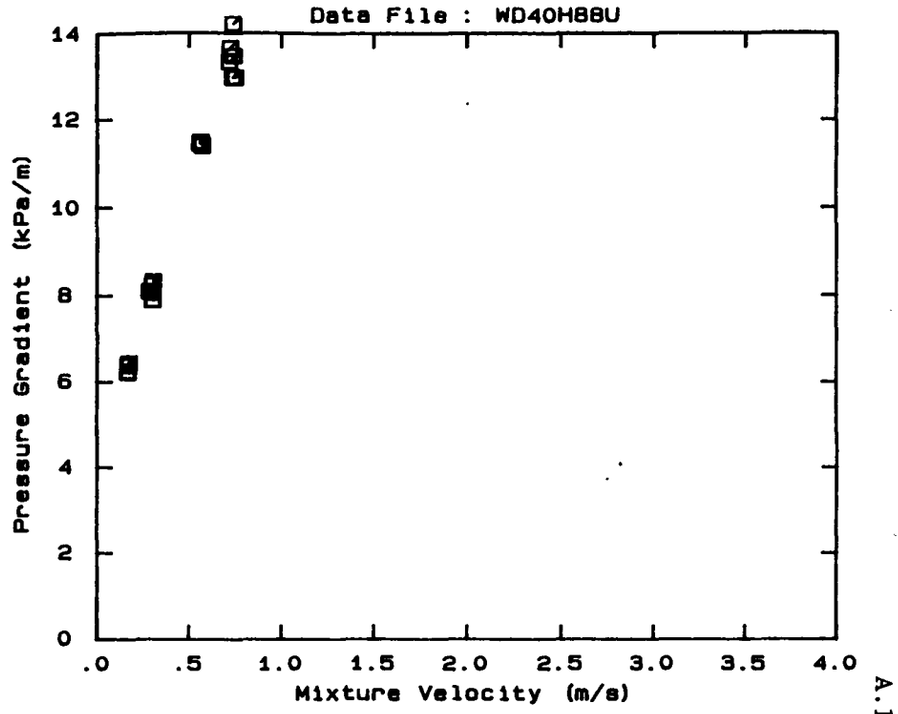

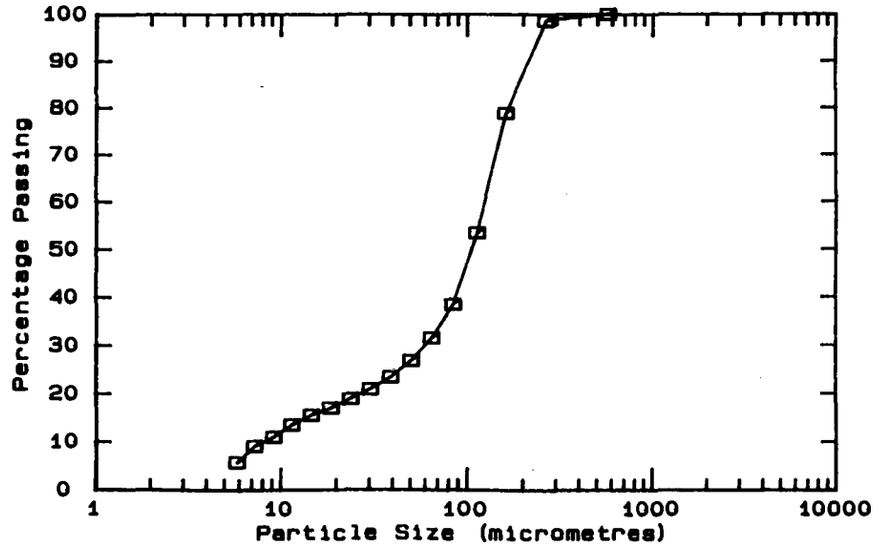

A.144

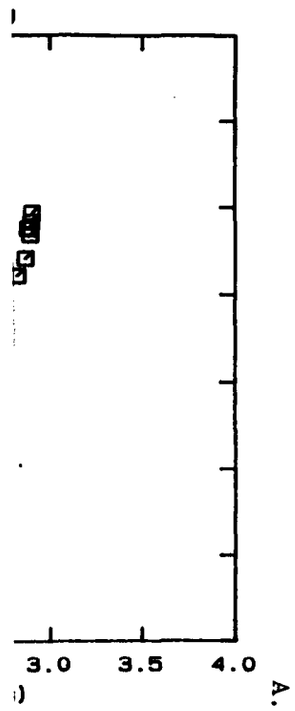

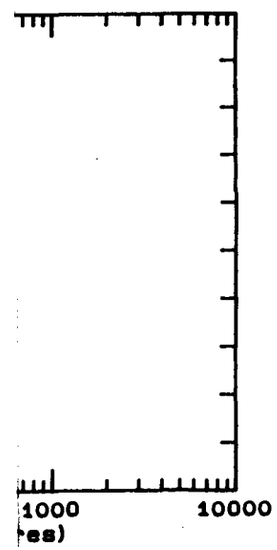

A.142

DATA FILE : WD40D63U

Test Facility	UCT 40 mm NB
Test Date	August 1990
Material Description	Western Deeps CCT
Material Relative Density	2.65
Slurry Relative Density	1.63
Solids Volumetric Concentration (%)	38.18
Solids Mass Concentration (%)	62.07
Mean Slurry Temperature (°C)	17.7
Pipe Internal Diameter (mm)	40.00
Pipe Roughness (μm)	52.0
Pipeline Slope	Vertical Down

Mixture Velocity (m/s)	Pressure Gradient (kPa/m)	Slurry Temp. (°C)
3.924	- 7.805	17.1
4.027	- 7.087	17.2
3.962	- 7.329	17.3
3.968	- 7.237	17.4
3.949	- 7.584	17.5
3.949	- 7.471	17.6
3.297	- 9.423	17.7
3.309	- 9.781	17.8
3.314	- 9.522	17.8
3.304	- 9.755	17.8
2.669	-11.995	17.9
2.656	-11.920	17.9
2.667	-11.679	17.9
2.620	-12.152	17.9
2.097	-13.319	17.9
2.132	-13.297	17.9
2.134	-13.257	17.9
1.587	-15.089	17.8
1.610	-15.282	17.8
1.609	-15.096	17.8
1.592	-15.060	17.8

Particle Size Distribution
Malvern Particle Size Analyser

Size (μm)	% Passing	% Retained
564.0	100.0	.0
261.6	98.4	1.6
160.4	79.8	18.6
112.8	52.5	27.3
84.3	37.2	15.3
64.6	30.1	7.1
50.2	24.8	5.3
39.0	21.5	3.3
30.3	19.1	2.4
23.7	17.0	2.1
18.5	15.3	1.7
14.5	14.1	1.2
11.4	12.4	1.7
9.1	10.1	2.3
7.2	8.2	1.9
5.8	5.3	2.9
Pan	.2	5.1

OBSERVED FLOW BEHAVIOUR

Velocity (m/s)	Observation (D = .0 mm)

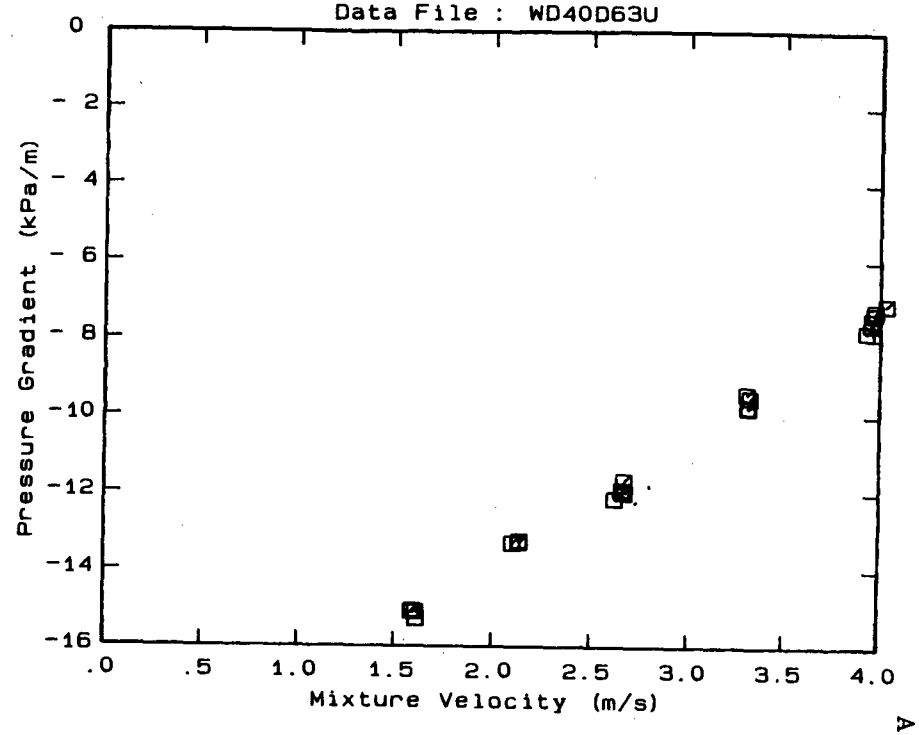

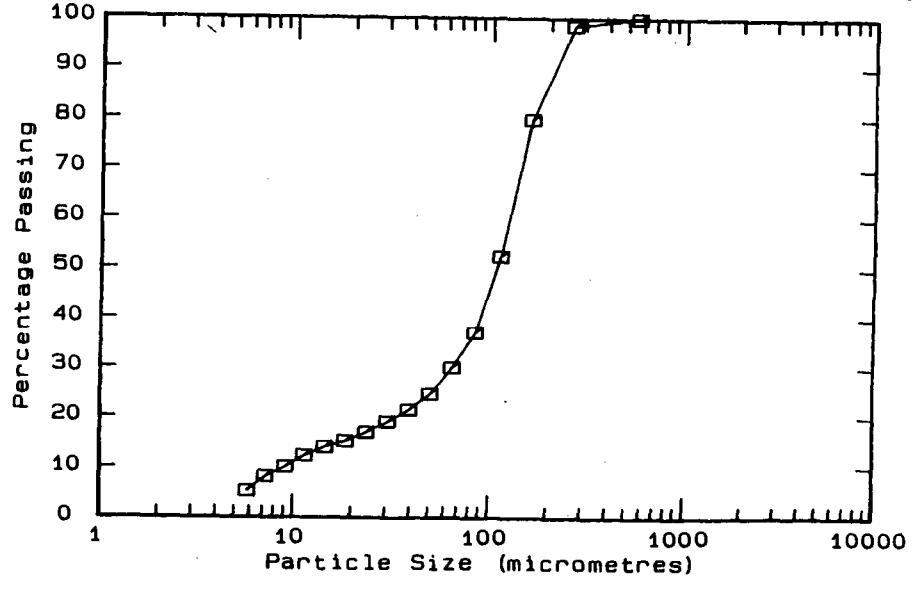

DATA FILE : WD40D71U

Test Facility	UCT 40 mm NB
Test Date	August 1990
Material Description	Western Deeps CCT
Material Relative Density	2.65
Slurry Relative Density	1.71
Solids Volumetric Concentration (%)	43.03
Solids Mass Concentration (%)	66.68
Mean Slurry Temperature (°C)	18.9
Pipe Internal Diameter (mm)	40.00
Pipe Roughness (μm)	52.0
Pipeline Slope	Vertical Down

Mixture Velocity (m/s)	Pressure Gradient (kPa/m)	Slurry Temp. (°C)
3.748	- 8.111	18.0
3.706	- 8.283	18.2
3.714	- 8.385	18.3
3.466	- 8.839	18.5
3.272	-10.986	18.7
3.318	-10.792	18.8
3.190	-11.709	18.8
3.323	-10.830	18.9
3.316	-10.759	18.9
3.287	-10.355	18.9
2.714	-13.993	19.0
2.659	-14.165	19.0
2.622	-14.174	19.1
2.638	-14.187	19.1
2.626	-14.096	19.1
2.678	-13.968	19.1
2.123	-14.579	19.1
2.122	-14.607	19.1
2.113	-14.755	19.1
1.604	-15.118	19.0
1.593	-15.184	19.0
1.611	-15.113	19.0
1.122	-15.343	18.9
1.139	-15.103	18.9
1.115	-15.124	18.9
1.106	-15.287	18.9
1.120	-15.053	18.8
1.115	-15.134	18.8

Particle Size Distribution
Malvern Particle Size Analyser

Size (μm)	% Passing	% Retained
564.0	100.0	.0
261.6	97.8	2.2
160.4	76.3	21.5
112.8	50.6	25.7
84.3	36.3	14.3
64.6	29.1	7.2
50.2	24.1	5.0
39.0	21.0	3.1
30.3	18.7	2.3
23.7	16.7	2.0
18.5	15.1	1.6
14.5	13.8	1.3
11.4	12.0	1.8
9.1	9.9	2.1
7.2	8.0	1.9
5.8	5.1	2.9
Pan	- .1	5.2

OBSERVED FLOW BEHAVIOUR

Velocity (m/s)	Observation (D = .0 mm)

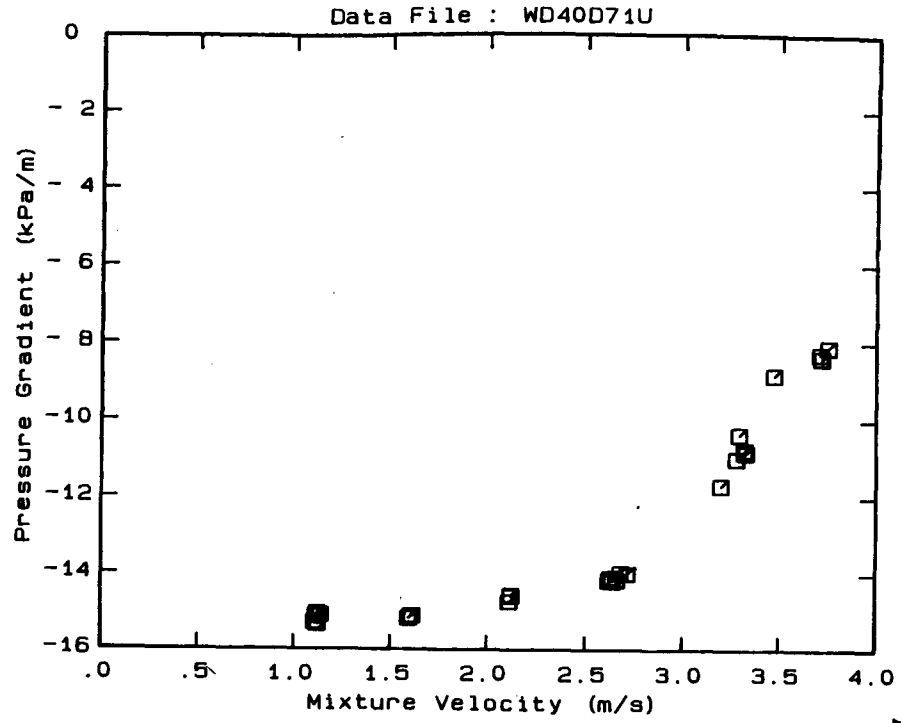

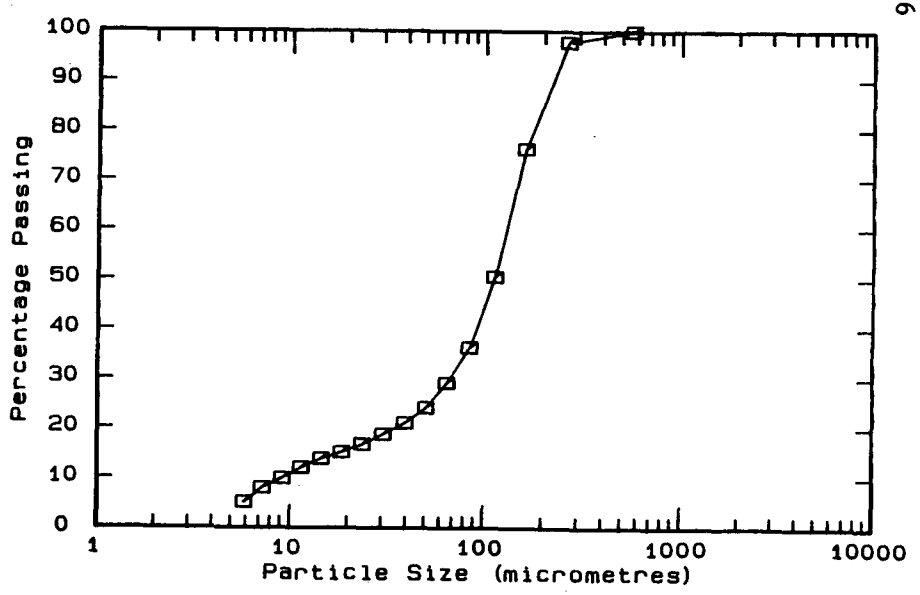

DATA FILE : WD40D76U

Test Facility	UCT 40 mm NB
Test Date	August 1990
Material Description	Western Deeps CCT
Material Relative Density	2.65
Slurry Relative Density	1.76
Solids Volumetric Concentration (%)	46.06
Solids Mass Concentration (%)	69.35
Mean Slurry Temperature (°C)	21.1
Pipe Internal Diameter (mm)	40.00
Pipe Roughness (μm)	52.0
Pipeline Slope	Vertical Down

Mixture Velocity (m/s)	Pressure Gradient (kPa/m)	Slurry Temp. (°C)
3.726	-10.670	20.2
3.740	-10.722	20.3
3.787	-11.254	20.4
3.794	-10.699	20.5
3.787	-10.888	20.6
3.229	-11.749	21.0
3.250	-11.772	21.1
3.265	-11.691	21.1
2.666	-12.754	21.3
2.533	-12.857	21.3
2.512	-12.939	21.3
2.523	-12.859	21.3
2.132	-13.458	21.4
2.148	-13.343	21.4
2.140	-13.347	21.4
2.134	-13.400	21.3
1.597	-14.102	21.3
1.575	-14.189	21.3
1.610	-14.293	21.3
1.577	-14.149	21.2
1.555	-14.298	21.2
1.037	-14.947	21.1
1.045	-14.903	21.1
1.009	-14.902	21.1
1.020	-14.907	21.1

Particle Size Distribution
Malvern Particle Size Analyser

Size (μm)	% Passing	% Retained
564.0	100.0	.0
261.6	98.9	1.1
160.4	82.9	16.0
112.8	59.6	23.3
84.3	43.5	16.1
64.6	36.4	7.1
50.2	30.9	5.5
39.0	26.8	4.1
30.3	23.9	2.9
23.7	21.5	2.4
18.5	19.4	2.1
14.5	17.8	1.6
11.4	15.5	2.3
9.1	12.6	2.9
7.2	10.4	2.2
5.8	6.6	3.8
Pan	- .3	6.9

OBSERVED FLOW BEHAVIOUR

Velocity (m/s)	Observation (D = .0 mm)

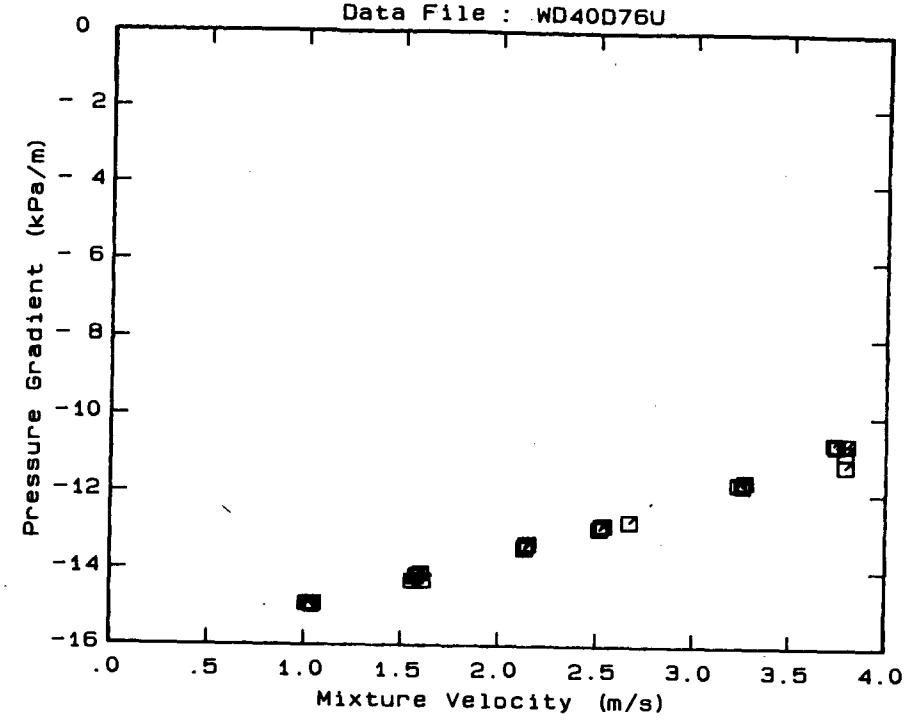

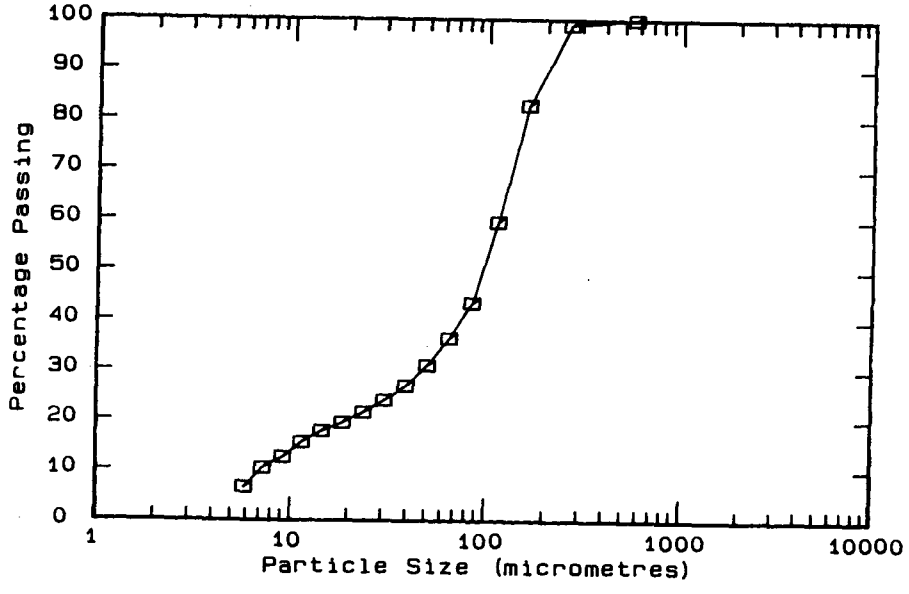

DATA FILE : WD40D86U

Test Facility	UCT 40 mm NB
Test Date	August 1990
Material Description	Western Deeps CCT
Material Relative Density	2.65
Slurry Relative Density	1.86
Solids Volumetric Concentration (%)	52.12
Solids Mass Concentration (%)	74.26
Mean Slurry Temperature (°C)	31.1
Pipe Internal Diameter (mm)	40.00
Pipe Roughness (μm)	52.0
Pipeline Slope	Vertical Down

Mixture Velocity (m/s)	Pressure Gradient (kPa/m)	Slurry Temp. (°C)
1.934	- 6.195	30.2
1.973	- 5.478	30.3
1.969	- 4.628	30.4
1.999	- 5.247	30.5
1.968	- 5.616	30.7
1.975	- 5.195	30.9
1.624	- 7.463	31.5
1.593	- 8.088	31.5
1.558	- 7.609	31.6
1.545	- 7.820	31.6
1.535	- 7.407	31.6
1.001	- 9.030	31.5
.962	- 9.044	31.5
.942	- 9.175	31.5
.944	- 9.228	31.5
.922	- 9.117	31.5
.690	- 9.632	31.2
.678	-10.322	31.1
.676	-10.289	31.1
.655	-10.005	31.0
.758	-10.165	31.0
.725	-10.515	30.9

Particle Size Distribution
Malvern Particle Size Analyser

Size (μm)	% Passing	% Retained
564.0	100.0	.0
261.6	97.3	2.7
160.4	77.2	20.1
112.8	51.4	25.8
84.3	37.1	14.3
64.6	30.1	7.0
50.2	25.3	4.8
39.0	22.1	3.2
30.3	19.8	2.3
23.7	17.8	2.0
18.5	16.1	1.7
14.5	14.7	1.4
11.4	13.0	1.7
9.1	10.8	2.2
7.2	8.6	2.2
5.8	5.4	3.2
Pan	- .0	5.4

OBSERVED FLOW BEHAVIOUR

Velocity (m/s)	Observation (D = .0 mm)

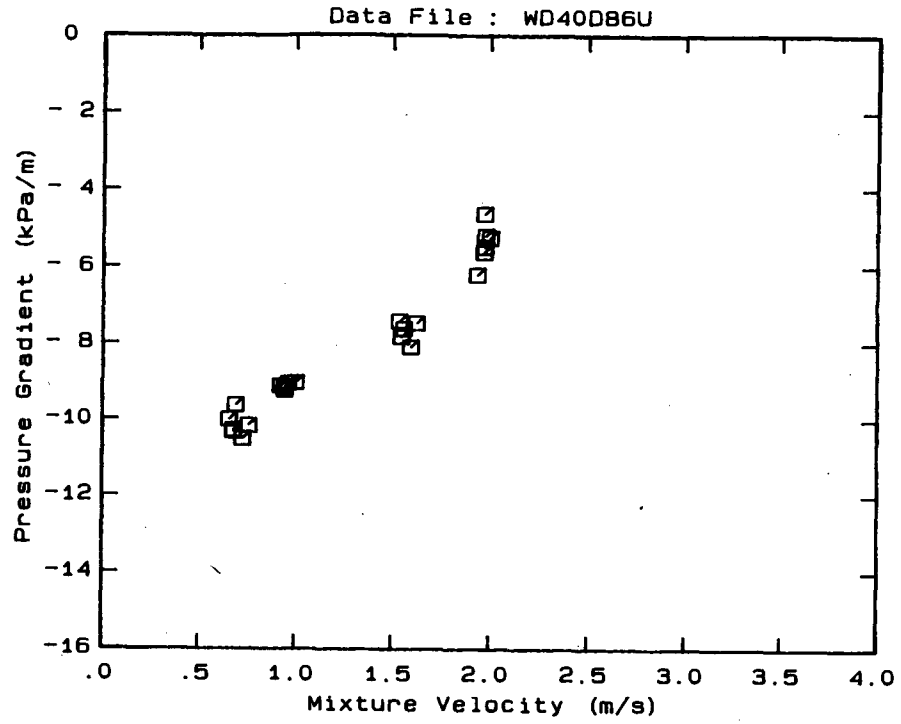

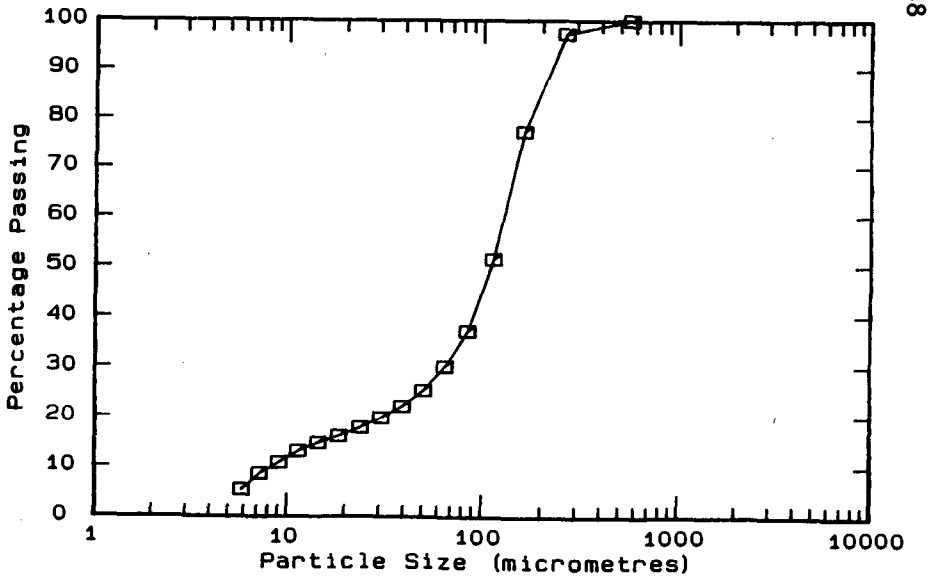

DATA FILE : WD40D88U

Test Facility	UCT 40 mm NB
Test Date	August 1990
Material Description	Western Deeps CCT
Material Relative Density	2.65
Slurry Relative Density	1.88
Solids Volumetric Concentration (%)	53.33
Solids Mass Concentration (%)	75.18
Mean Slurry Temperature (°C)	32.9
Pipe Internal Diameter (mm)	40.00
Pipe Roughness (μm)	52.0
Pipeline Slope	Vertical Down

Mixture Velocity (m/s)	Pressure Gradient (kPa/m)	Slurry Temp. (°C)	Particle Size Distribution Malvern Particle Size Analyser Size (μm)	% Passing	% Retained
.716	- 2.959	32.1	564.0	100.0	.0
.720	- 3.290	32.1	261.6	98.6	1.4
.740	- 3.389	32.2	160.4	78.9	19.7
.569	- 5.255	33.0	112.8	53.5	25.4
.563	- 5.374	33.0	84.3	38.5	15.0
.556	- 5.076	33.0	64.6	31.5	7.0
.556	- 4.926	33.0	50.2	26.8	4.7
.284	- 8.481	33.1	39.0	23.4	3.4
.300	- 9.050	33.1	30.3	20.9	2.5
.304	- 8.782	33.1	23.7	18.9	2.0
.302	- 8.745	33.1	18.5	17.0	1.9
.299	- 8.837	33.1	14.5	15.5	1.5
.170	-11.873	33.1	11.4	13.5	2.0
.174	-11.636	33.1	9.1	11.0	2.5
.168	-11.904	33.1	7.2	9.1	1.9
.167	-12.030	33.1	5.8	5.8	3.3
.167	-11.877	33.1	Pan	- .1	5.9

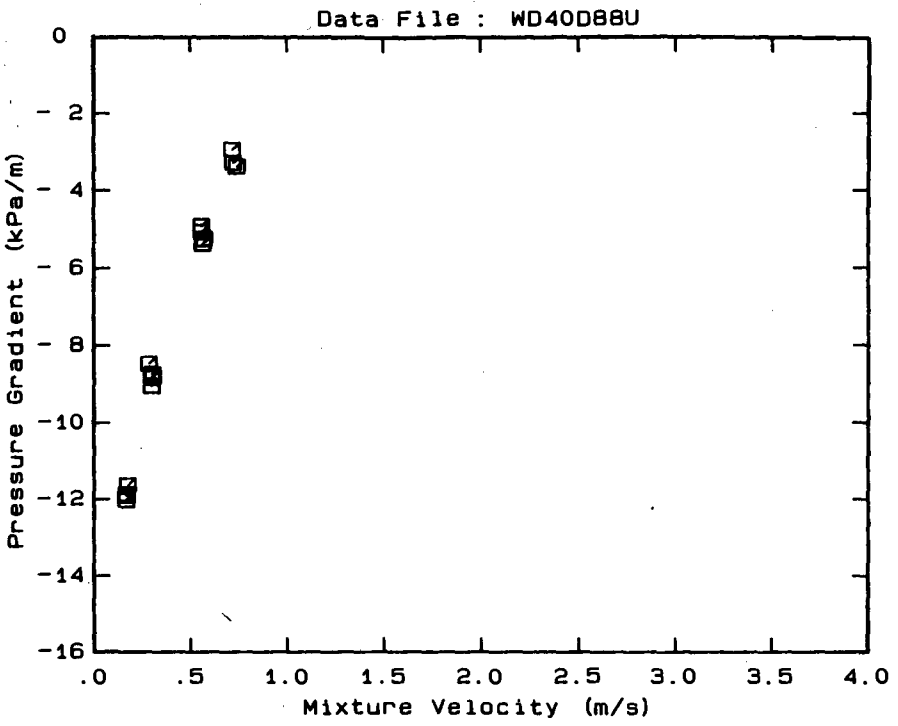

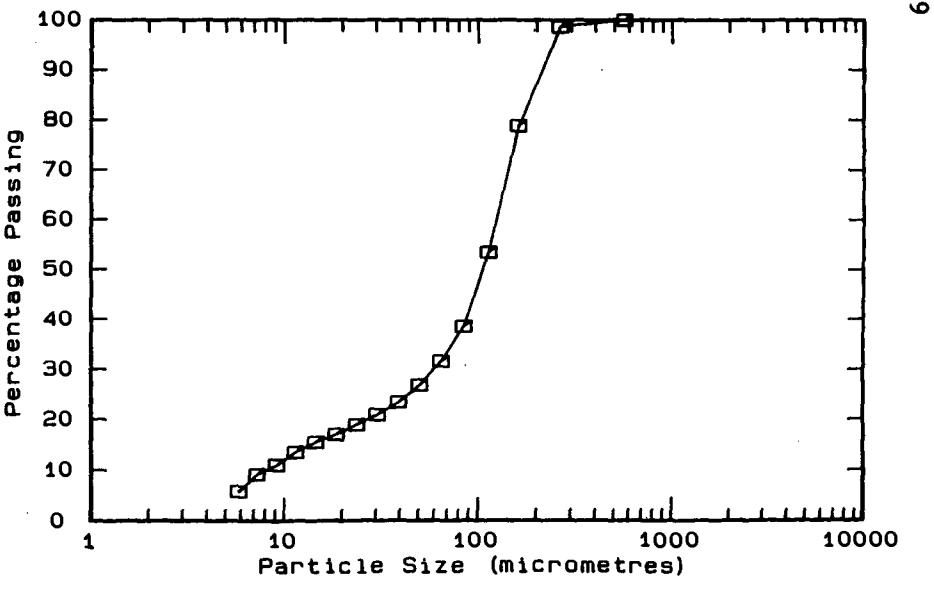

DATA FILE : WD80H69U

Test Facility	UCT 80 mm NB
Test Date	June 1990
Material Description	Western Deeps CCT
Material Relative Density	2.65
Slurry Relative Density	1.69
Solids Volumetric Concentration (%)	41.82
Solids Mass Concentration (%)	65.57
Mean Slurry Temperature (°C)	16.3
Pipe Internal Diameter (mm)	73.40
Pipe Roughness (μm)	84.0
Pipeline Slope	Horizontal

Mixture Velocity (m/s)	Pressure Gradient (kPa/m)	Slurry Temp. (°C)
3.411	3.255	15.6
3.401	3.178	15.7
3.405	3.212	15.8
3.413	3.387	15.8
3.406	3.394	15.8
2.924	2.663	16.0
2.931	2.292	16.3
2.931	2.288	16.3
2.928	2.358	16.4
2.442	1.830	16.4
2.439	1.756	16.4
2.439	1.754	16.5
2.002	1.379	16.5
2.003	1.187	16.5
1.998	1.472	16.5
1.998	1.253	16.5
1.999	.938	16.5
2.006	1.547	16.5
2.011	1.244	16.5
1.485	.955	16.5
1.481	.935	16.5
1.487	.664	16.5
1.486	.981	16.5
1.491	.988	16.5
.985	.871	16.5
.976	.576	16.5
.990	.546	16.5
.998	.235	16.5
1.004	.879	16.4
.991	.779	16.4
.990	.547	16.4
.990	.657	16.4
.991	.661	16.4

Particle Size Distribution
Malvern Particle Size Analyser

Size (μm)	% Passing	% Retained
564.0	100.0	.0
261.6	96.8	3.2
160.4	74.5	22.3
112.8	49.2	25.3
84.3	35.7	13.5
64.6	29.2	6.5
50.2	23.9	5.3
39.0	20.3	3.6
30.3	18.1	2.2
23.7	16.2	1.9
18.5	14.3	1.9
14.5	13.0	1.3
11.4	11.5	1.5
9.1	9.5	2.0
7.2	7.6	1.9
5.8	4.8	2.8
Pan	.0	4.8

OBSERVED FLOW BEHAVIOUR

Velocity (m/s)	Observation (D = 71.0 mm)
1.05	Asymmetric - slid part
1.58	Asymmetric-slid part-pulses
2.14	Asymmetric-slid part-pulses
2.63	Asymmetric - slid part
3.15	Asymmetric ?
3.64	Appears homogeneous

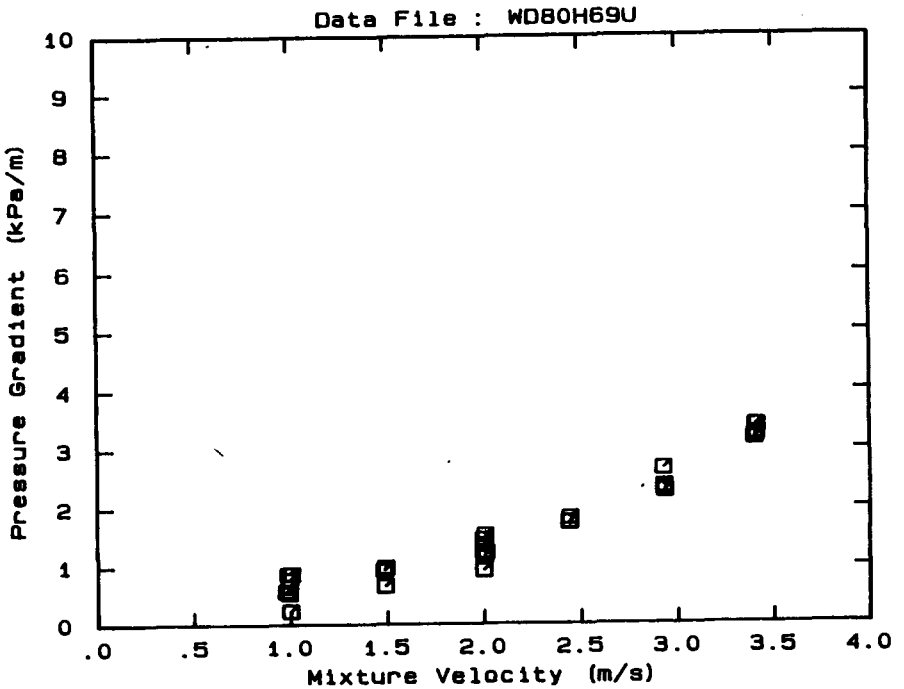

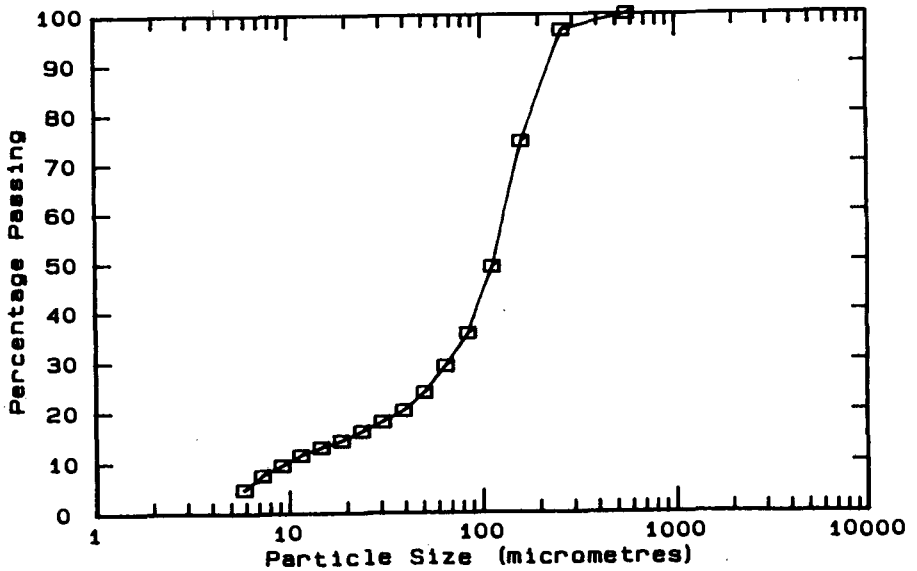

DATA FILE : WD80H73U

Test Facility	UCT 80 mm NB
Test Date	June 1990
Material Description	Western Deeps CCT
Material Relative Density	2.65
Slurry Relative Density	1.73
Solids Volumetric Concentration (%)	44.24
Solids Mass Concentration (%)	67.77
Mean Slurry Temperature (°C)	17.1
Pipe Internal Diameter (mm)	73.40
Pipe Roughness (μm)	84.0
Pipeline Slope	Horizontal

Mixture Velocity (m/s)	Pressure Gradient (kPa/m)	Slurry Temp. (°C)
3.409	3.598	16.4
3.417	3.489	16.5
3.417	3.525	16.6
3.408	3.455	16.7
2.960	3.048	16.9
2.951	2.924	17.0
2.955	2.740	17.0
2.952	2.879	17.1
2.951	2.917	17.1
2.949	2.679	17.1
2.439	1.809	17.2
2.445	1.836	17.2
2.438	1.748	17.2
1.987	1.077	17.3
1.984	1.203	17.3
1.985	1.123	17.3
1.983	1.328	17.3
1.458	1.402	17.3
1.455	1.066	17.3
1.463	.780	17.3
1.457	1.080	17.2
1.464	.830	17.2
1.459	1.580	17.2
1.461	.868	17.2
1.032	.399	17.2
1.034	.364	17.2
1.036	.843	17.2
1.027	.460	17.2
1.038	.199	17.2
.968	1.007	17.2

Particle Size Distribution
Malvern Particle Size Analyser

Size (μm)	% Passing	% Retained
564.0	100.0	.0
261.6	96.2	3.8
160.4	74.9	21.3
112.8	50.9	24.0
84.3	37.4	13.5
64.6	30.7	6.7
50.2	25.7	5.0
39.0	22.2	3.5
30.3	19.7	2.5
23.7	17.6	2.1
18.5	15.7	1.9
14.5	14.2	1.5
11.4	12.5	1.7
9.1	10.4	2.1
7.2	8.2	2.2
5.8	5.1	3.1
Pan	- .2	5.3

OBSERVED FLOW BEHAVIOUR

Velocity (m/s)	Observation (D = 71.0 mm)
1.09	Asym.-15% slid bed-pulses
1.58	Asymmetric-slid part-pulses
2.14	Asymmetric-slid part-pulses
2.63	Appears homo. - slid part
3.19	Appears homogeneous
3.68	Appears homogeneous

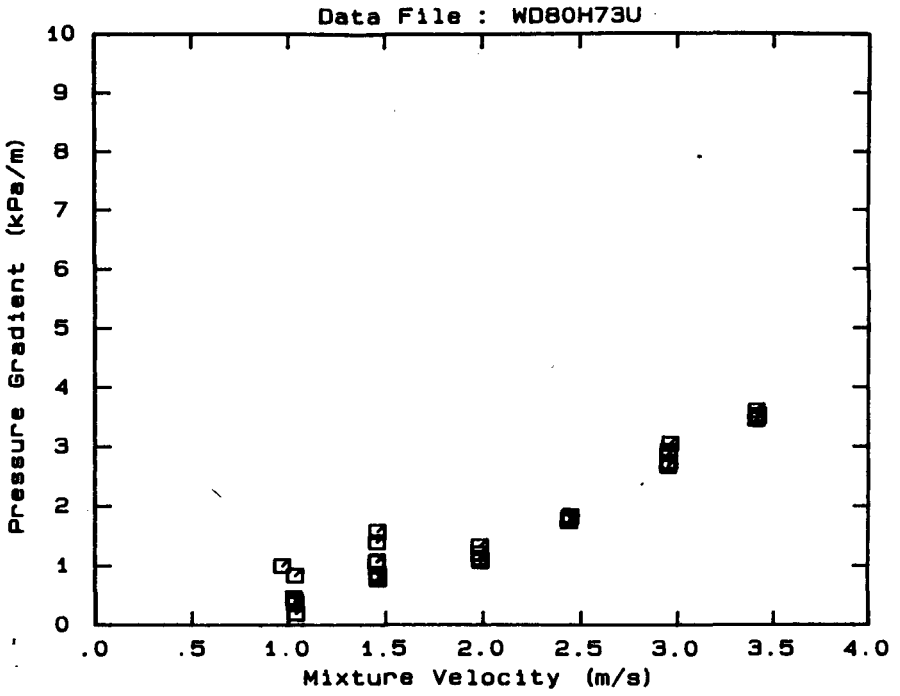

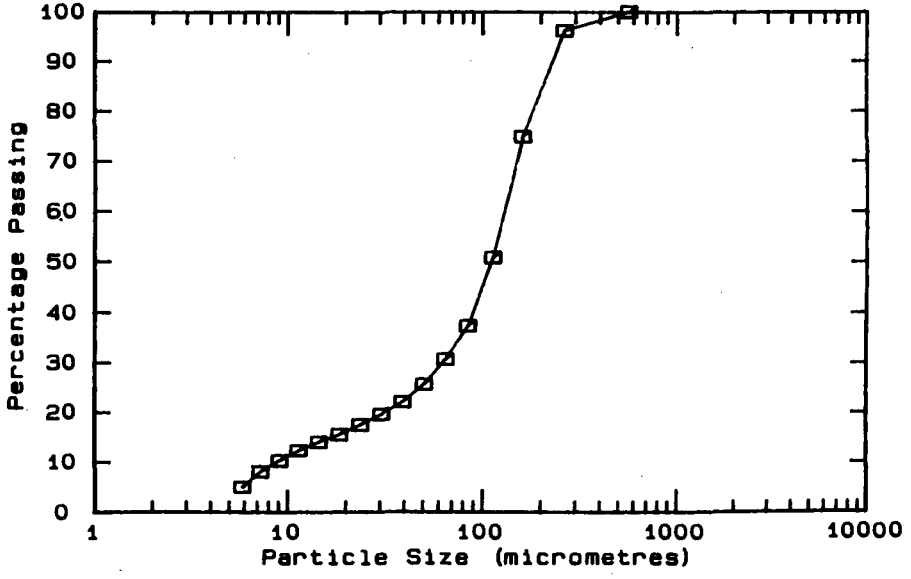

DATA FILE : WD80H78U

Test Facility	UCT 80 mm NB
Test Date	June 1990
Material Description	Western Deeps CCT
Material Relative Density	2.65
Slurry Relative Density	1.78
Solids Volumetric Concentration (%)	47.27
Solids Mass Concentration (%)	70.38
Mean Slurry Temperature (°C)	18.2
Pipe Internal Diameter (mm)	73.40
Pipe Roughness (μm)	84.0
Pipeline Slope	Horizontal

Mixture Velocity (m/s)	Pressure Gradient (kPa/m)	Slurry Temp. (°C)
3.422	3.038	17.6
3.424	3.236	17.7
3.432	3.486	17.7
3.438	3.160	17.8
2.952	2.621	18.1
2.955	2.768	18.1
2.942	2.538	18.1
2.952	2.576	18.2
2.439	2.678	18.3
2.443	2.396	18.3
2.439	2.490	18.3
2.434	2.577	18.4
2.440	2.486	18.4
1.953	1.875	18.4
1.961	1.789	18.4
1.951	1.527	18.4
1.957	1.895	18.4
1.957	1.951	18.4
1.501	1.619	18.4
1.500	1.781	18.4
1.486	1.832	18.3
1.494	2.033	18.3
1.487	1.934	18.3
1.483	2.129	18.3
1.493	2.257	18.3
1.495	2.081	18.3
1.493	1.909	18.3
1.038	1.855	18.3
1.060	1.930	18.2
1.026	1.763	18.2
1.031	1.571	18.2
1.026	1.825	18.2
1.037	1.831	18.2
1.029	1.740	18.2

Particle Size Distribution
Malvern Particle Size Analyser

Size (μm)	% Passing	% Retained
564.0	100.0	.0
261.6	96.4	3.6
160.4	76.3	20.1
112.8	50.4	25.9
84.3	37.1	13.3
64.6	30.3	6.8
50.2	25.1	5.2
39.0	21.3	3.8
30.3	19.0	2.3
23.7	17.3	1.7
18.5	15.2	2.1
14.5	13.7	1.5
11.4	12.2	1.5
9.1	10.1	2.1
7.2	8.1	2.0
5.8	5.1	3.0
Pan	- .1	5.2

OBSERVED FLOW BEHAVIOUR

Velocity (m/s)	Observation (D = 71.0 mm)
1.09	Asymmetric - slid particles
1.61	Asymmetric - slid particles
2.10	Asymmetric - slid particles
2.63	Asymmetric - slid particles
3.15	Asymmetric - slid particles
3.99	Appears homogeneous

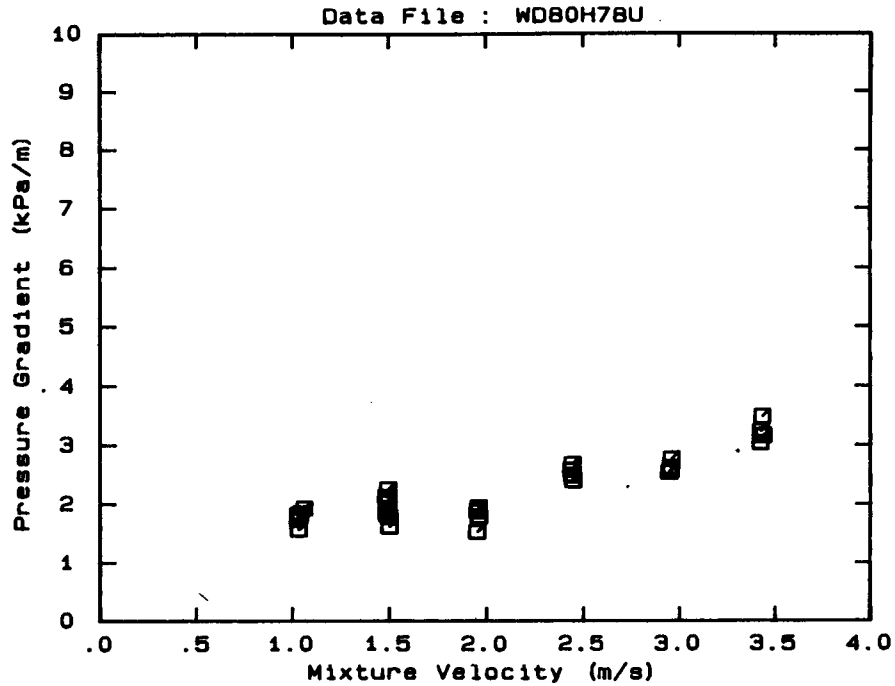

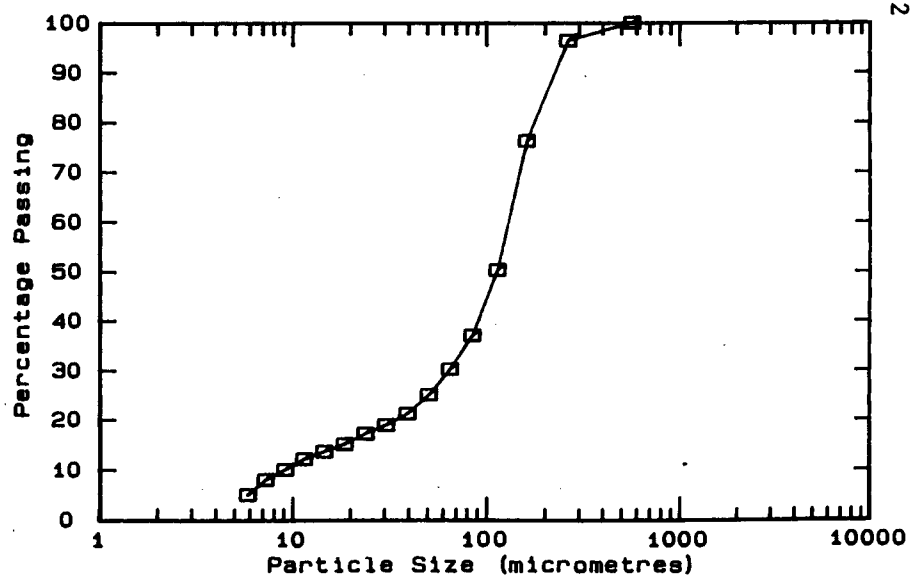

DATA FILE : WD80H81U

Test Facility	UCT 80 mm NB
Test Date	June 1990
Material Description	Western Deeps CCT
Material Relative Density	2.65
Slurry Relative Density	1.81
Solids Volumetric Concentration (%)	49.09
Solids Mass Concentration (%)	71.87
Mean Slurry Temperature (°C)	19.8
Pipe Internal Diameter (mm)	73.40
Pipe Roughness (μm)	84.0
Pipeline Slope	Horizontal

Mixture Velocity (m/s)	Pressure Gradient (kPa/m)	Slurry Temp. (°C)
3.451	5.149	18.6
3.456	4.616	18.7
3.460	4.720	18.9
3.461	4.631	19.0
3.464	4.738	19.1
2.894	3.972	19.7
2.900	3.886	19.8
2.901	4.100	19.8
2.901	3.829	19.9
2.446	3.708	20.0
2.445	3.474	20.0
2.449	3.400	20.1
2.447	3.599	20.1
2.449	3.783	20.1
2.451	3.575	20.1
2.452	3.458	20.1
1.962	3.279	20.2
1.960	3.012	20.2
1.964	3.324	20.2
1.962	3.299	20.2
1.456	2.373	20.1
1.455	2.329	20.1
1.452	2.344	20.1
1.445	2.320	20.1
1.017	1.820	20.0
1.023	1.918	20.0
1.023	1.851	20.0
1.023	1.965	20.0

Particle Size Distribution
Malvern Particle Size Analyser

Size (μm)	% Passing	% Retained
564.0	100.0	.0
261.6	95.5	4.5
160.4	74.7	20.8
112.8	51.5	23.2
84.3	37.1	14.4
64.6	30.7	6.4
50.2	25.9	4.8
39.0	21.8	4.1
30.3	19.5	2.3
23.7	17.6	1.9
18.5	15.6	2.0
14.5	14.1	1.5
11.4	12.5	1.6
9.1	10.4	2.1
7.2	8.2	2.2
5.8	5.1	3.1
Pan	- .2	5.3

OBSERVED FLOW BEHAVIOUR

Velocity (m/s)	Observation (D = 71.0 mm)
1.09	Asymmetric - slid particles
1.61	Asymmetric - slid particles
2.10	Asymmetric - slid particles
2.63	Asymmetric - slid particles
3.15	Appears homogeneous
3.99	Appears homogeneous

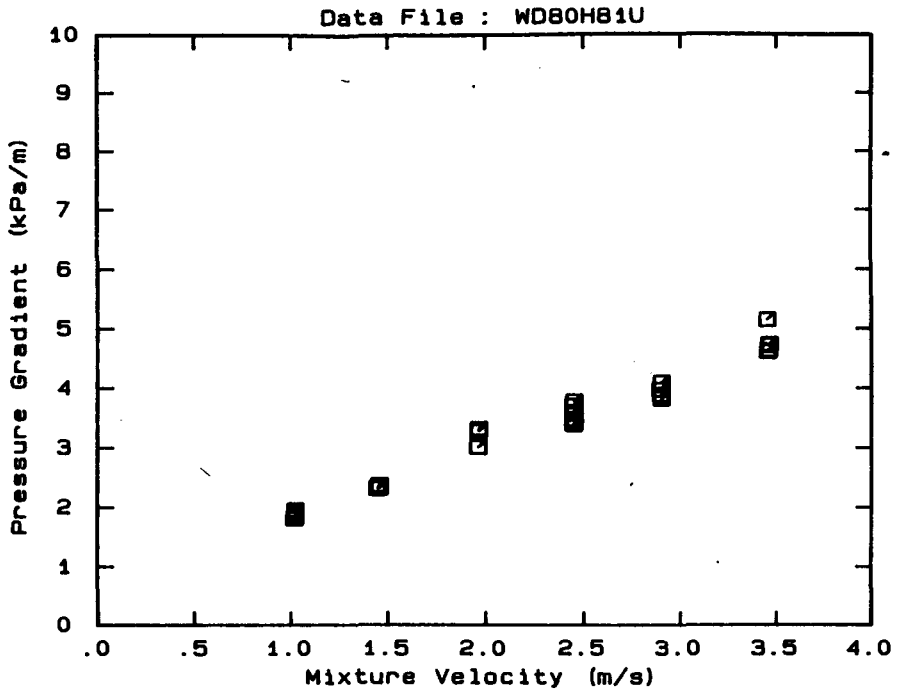

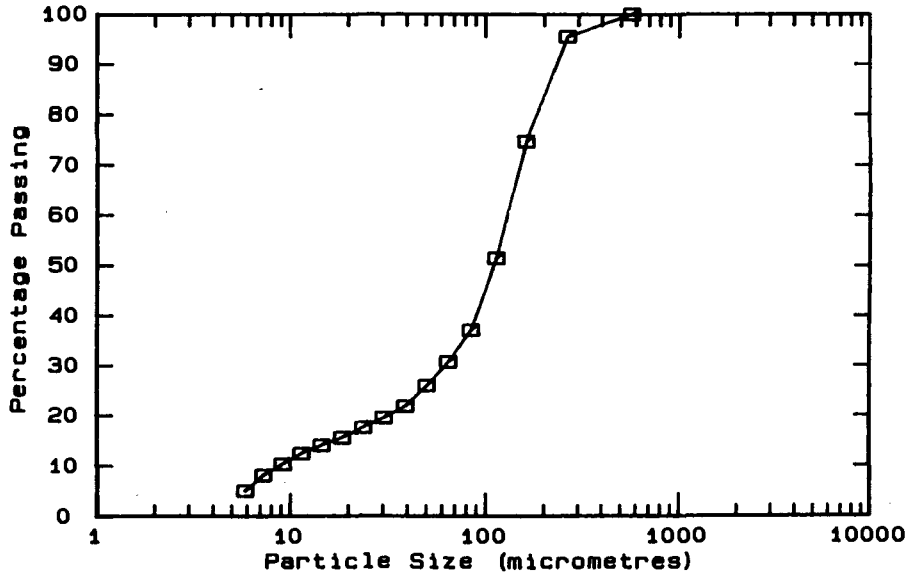

DATA FILE : WD80H86U

Test Facility	UCT 80 mm NB
Test Date	June 1990
Material Description	Western Deeps CCT
Material Relative Density	2.65
Slurry Relative Density	1.86
Solids Volumetric Concentration (%)	52.12
Solids Mass Concentration (%)	74.26
Mean Slurry Temperature (°C)	22.8
Pipe Internal Diameter (mm)	73.40
Pipe Roughness (μm)	84.0
Pipeline Slope	Horizontal

Mixture Velocity (m/s)	Pressure Gradient (kPa/m)	Slurry Temp. (°C)
3.192	9.055	21.1
3.200	8.912	21.3
3.208	8.919	21.5
3.218	8.668	21.7
2.925	8.208	22.1
2.935	7.921	22.3
2.944	8.204	22.4
2.951	8.375	22.5
2.438	7.104	22.8
2.443	7.080	22.9
2.439	7.352	22.9
2.444	7.294	23.0
2.451	7.457	23.0
2.453	7.219	23.1
1.987	6.061	23.2
1.986	6.124	23.3
1.989	6.024	23.3
1.986	6.005	23.3
1.463	4.502	23.3
1.471	4.493	23.3
1.471	4.475	23.3
1.470	4.481	23.3
.991	3.233	23.2
.973	3.157	23.2
.931	3.237	23.1
.906	3.172	23.1

Particle Size Distribution
Malvern Particle Size Analyser

Size (μm)	% Passing	% Retained
564.0	100.0	.0
261.6	96.2	3.8
160.4	76.3	19.9
112.8	52.7	23.6
84.3	38.2	14.5
64.6	31.6	6.6
50.2	26.5	5.1
39.0	22.6	3.9
30.3	20.1	2.5
23.7	18.1	2.0
18.5	16.3	1.8
14.5	14.8	1.5
11.4	13.1	1.7
9.1	11.0	2.1
7.2	8.7	2.3
5.8	5.5	3.2
Pan	.0	5.5

OBSERVED FLOW BEHAVIOUR

Velocity (m/s)	Observation (D = 71.0 mm)
1.09	Slightly asymmetric
1.61	Slightly asymmetric
2.10	Appears homogeneous
2.63	Appears homogeneous
3.15	Appears homogeneous
3.99	Appears homogeneous

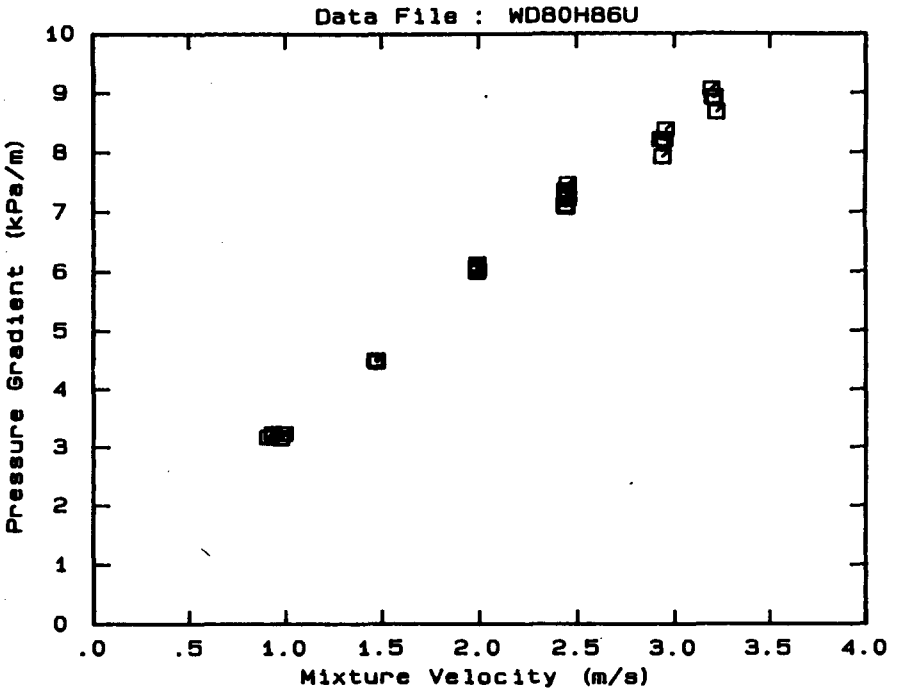

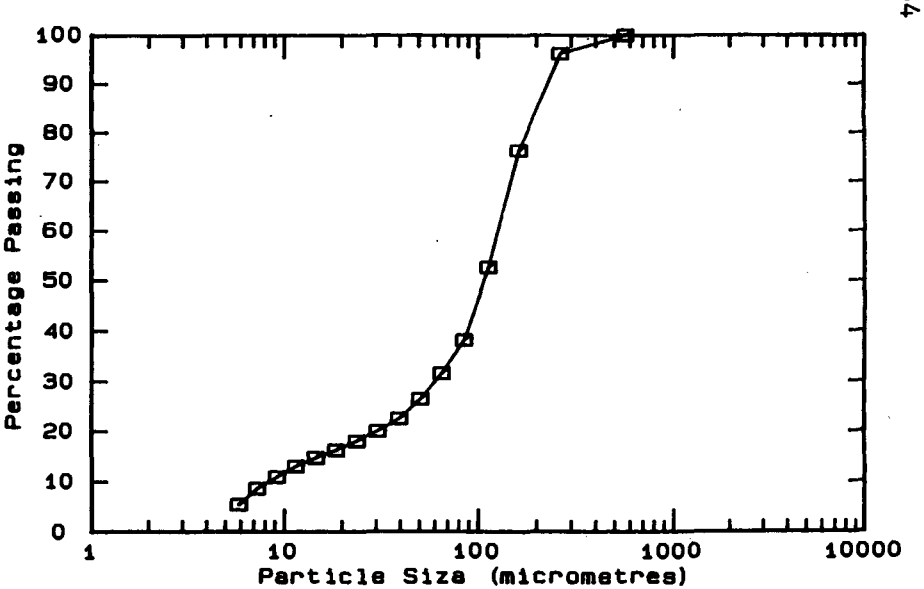

DATA FILE : WD80H90U

Test Facility	UCT 80 mm NB
Test Date	June 1990
Material Description	Western Deeps CCT
Material Relative Density	2.65
Slurry Relative Density	1.90
Solids Volumetric Concentration (%)	54.55
Solids Mass Concentration (%)	76.08
Mean Slurry Temperature (°C)	27.4
Pipe Internal Diameter (mm)	73.40
Pipe Roughness (μm)	84.0
Pipeline Slope	Horizontal

Mixture Velocity (m/s)	Pressure Gradient (kPa/m)	Slurry Temp. (°C)
2.031	9.793	26.0
2.037	10.066	26.2
2.048	9.902	26.4
2.046	10.232	26.6
1.635	8.096	27.1
1.662	8.394	27.2
1.663	8.434	27.3
1.664	8.257	27.4
1.661	8.225	27.4
1.179	7.203	27.6
1.068	6.976	27.8
1.029	6.879	27.9
.984	7.168	27.9
1.001	7.250	27.9
.674	6.026	28.0
.655	6.124	28.0
.675	6.316	28.0
.656	6.180	28.0
.664	6.200	28.0

Particle Size Distribution
Malvern Particle Size Analyser

Size (μm)	% Passing	% Retained
564.0	100.0	.0
261.6	96.9	3.1
160.4	78.0	18.9
112.8	54.1	23.9
84.3	39.5	14.6
64.6	33.0	6.5
50.2	27.7	5.3
39.0	24.1	3.6
30.3	21.5	2.6
23.7	19.3	2.2
18.5	17.5	1.8
14.5	16.0	1.5
11.4	14.2	1.8
9.1	12.0	2.2
7.2	9.6	2.4
5.8	6.1	3.5
Pan	.1	6.0

OBSERVED FLOW BEHAVIOUR

Velocity (m/s)	Observation (D = 71.0 mm)
.74	Appears homogeneous
1.37	Appears homogeneous
1.75	Appears homogeneous
1.89	Appears homogeneous
2.21	Appears homogeneous

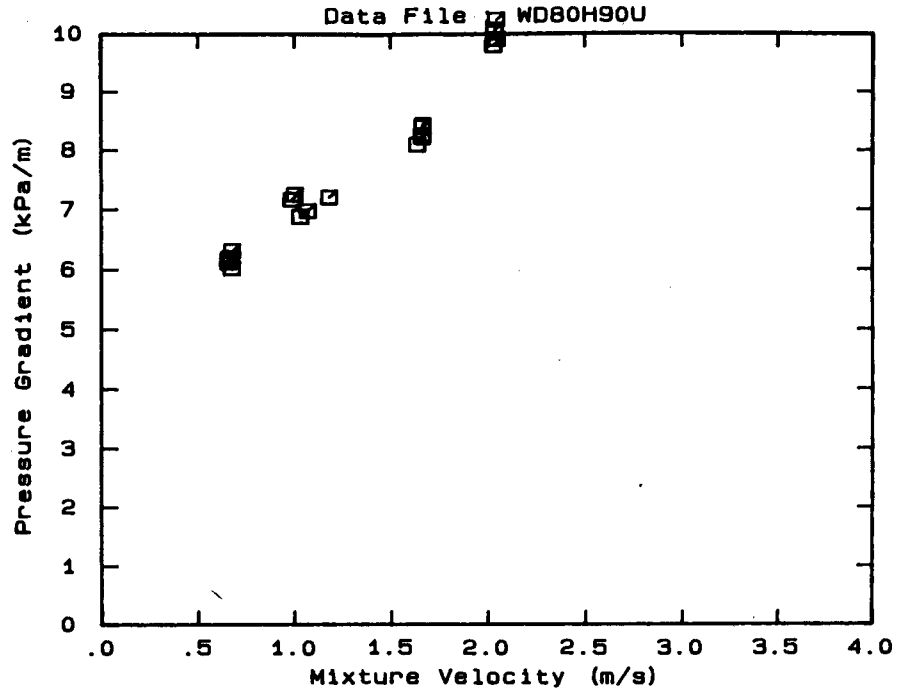

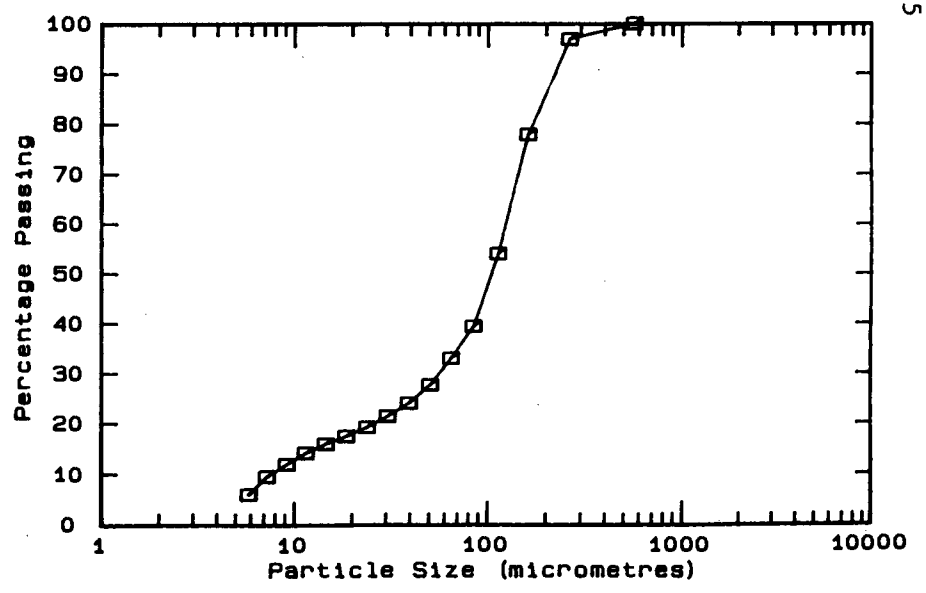

DATA FILE : WD80D69U

Test Facility	UCT 80 mm NB
Test Date	June 1990
Material Description	Western Deeps CCT
Material Relative Density	2.65
Slurry Relative Density	1.69
Solids Volumetric Concentration (%)	41.82
Solids Mass Concentration (%)	65.57
Mean Slurry Temperature (°C)	16.3
Pipe Internal Diameter (mm)	73.40
Pipe Roughness (μm)	84.0
Pipeline Slope	Vertical Down

Mixture Velocity (m/s)	Pressure Gradient (kPa/m)	Slurry Temp. (°C)
3.411	-12.681	15.6
3.401	-12.544	15.7
3.405	-12.642	15.8
3.413	-12.645	15.8
3.406	-12.623	15.8
2.924	-13.601	16.0
2.931	-13.558	16.3
2.931	-13.451	16.3
2.928	-13.652	16.4
2.442	-14.388	16.4
2.439	-14.424	16.4
2.439	-14.385	16.5
2.002	-15.084	16.5
2.003	-15.051	16.5
1.998	-15.183	16.5
1.998	-15.104	16.5
1.999	-15.051	16.5
2.006	-15.070	16.5
2.011	-15.066	16.5
1.485	-15.749	16.5
1.481	-15.825	16.5
1.487	-15.694	16.5
1.486	-15.774	16.5
1.491	-15.776	16.5
.985	-16.101	16.5
.976	-16.072	16.5
.990	-15.969	16.5
.998	-15.917	16.5
1.004	-16.104	16.4
.991	-16.043	16.4
.990	-15.980	16.4
.990	-16.037	16.4
.991	-15.948	16.4

Particle Size Distribution
Malvern Particle Size Analyser

Size (μm)	% Passing	% Retained
564.0	100.0	.0
261.6	96.8	3.2
160.4	74.5	22.3
112.8	49.2	25.3
84.3	35.7	13.5
64.6	29.2	6.5
50.2	23.9	5.3
39.0	20.3	3.6
30.3	18.1	2.2
23.7	16.2	1.9
18.5	14.3	1.9
14.5	13.0	1.3
11.4	11.5	1.5
9.1	9.5	2.0
7.2	7.6	1.9
5.8	4.8	2.8
Pan	.0	4.8

OBSERVED FLOW BEHAVIOUR

Velocity (m/s)	Observation (D = .0 mm)

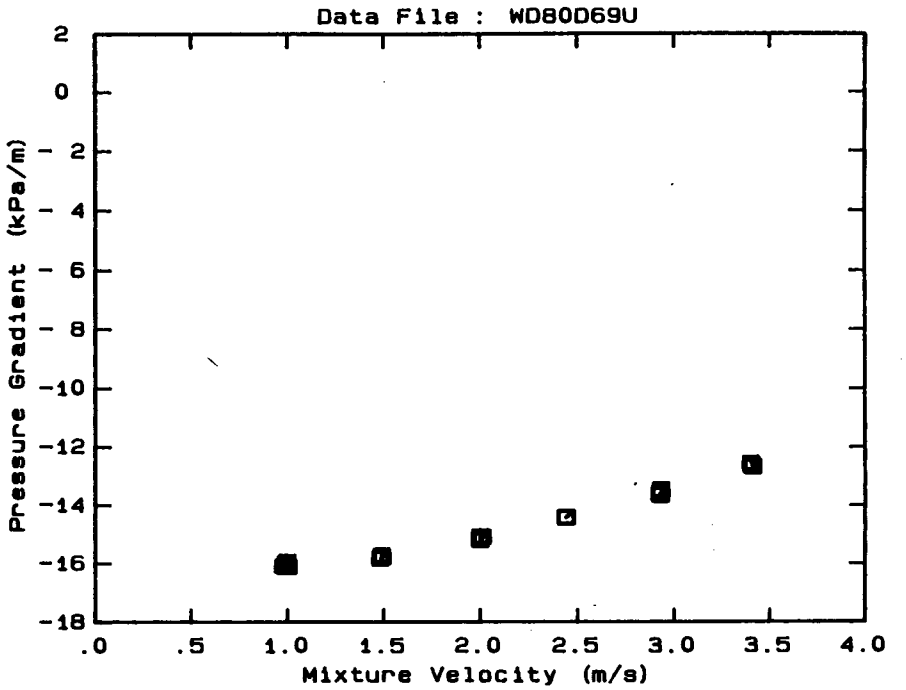

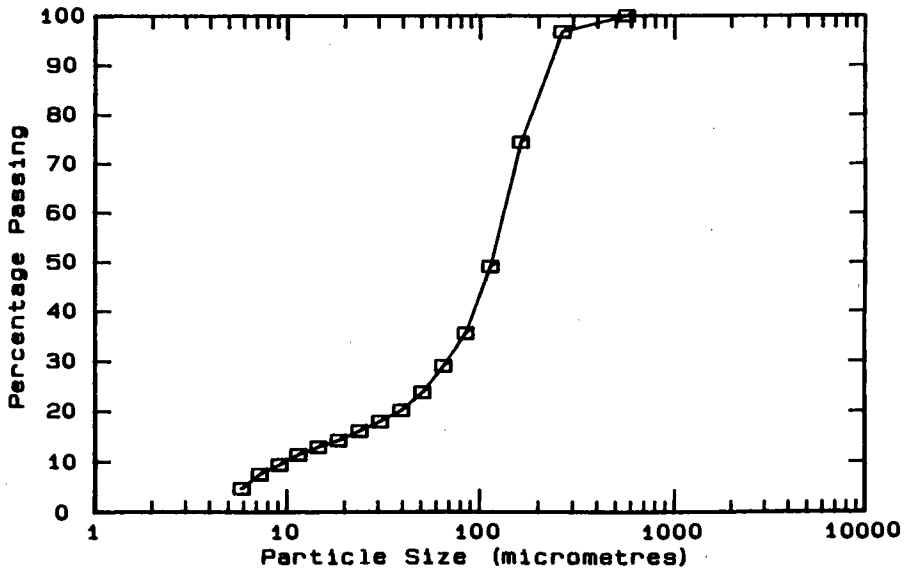

DATA FILE : WD80D73U

Test Facility	UCT 80 mm NB
Test Date	June 1990
Material Description	Western Deeps CCT
Material Relative Density	2.65
Slurry Relative Density	1.73
Solids Volumetric Concentration (%)	44.24
Solids Mass Concentration (%)	67.77
Mean Slurry Temperature (°C)	17.1
Pipe Internal Diameter (mm)	73.40
Pipe Roughness (μm)	84.0
Pipeline Slope	Vertical Down

Mixture Velocity (m/s)	Pressure Gradient (kPa/m)	Slurry Temp. (°C)
3.409	-12.705	16.4
3.417	-12.667	16.5
3.417	-12.646	16.6
3.408	-12.680	16.7
2.960	-13.980	16.9
2.951	-13.678	17.0
2.955	-13.478	17.0
2.952	-13.912	17.1
2.951	-13.636	17.1
2.949	-13.658	17.1
2.439	-14.627	17.2
2.445	-14.602	17.2
2.438	-14.587	17.2
1.987	-15.617	17.3
1.984	-15.761	17.3
1.985	-15.576	17.3
1.983	-15.706	17.3
1.458	-16.084	17.3
1.455	-15.888	17.3
1.463	-15.982	17.3
1.457	-16.078	17.2
1.464	-15.951	17.2
1.459	-16.012	17.2
1.461	-15.936	17.2
1.032	-16.117	17.2
1.034	-16.032	17.2
1.036	-16.116	17.2
1.027	-16.108	17.2
1.038	-16.130	17.2
.968	-16.161	17.2

Particle Size Distribution
Malvern Particle Size Analyser

Size (μm)	% Passing	% Retained
564.0	100.0	.0
261.6	96.2	3.8
160.4	74.9	21.3
112.8	50.9	24.0
84.3	37.4	13.5
64.6	30.7	6.7
50.2	25.7	5.0
39.0	22.2	3.5
30.3	19.7	2.5
23.7	17.6	2.1
18.5	15.7	1.9
14.5	14.2	1.5
11.4	12.5	1.7
9.1	10.4	2.1
7.2	8.2	2.2
5.8	5.1	3.1
Pan	- .2	5.3

OBSERVED FLOW BEHAVIOUR

Velocity (m/s)	Observation (D = .0 mm)

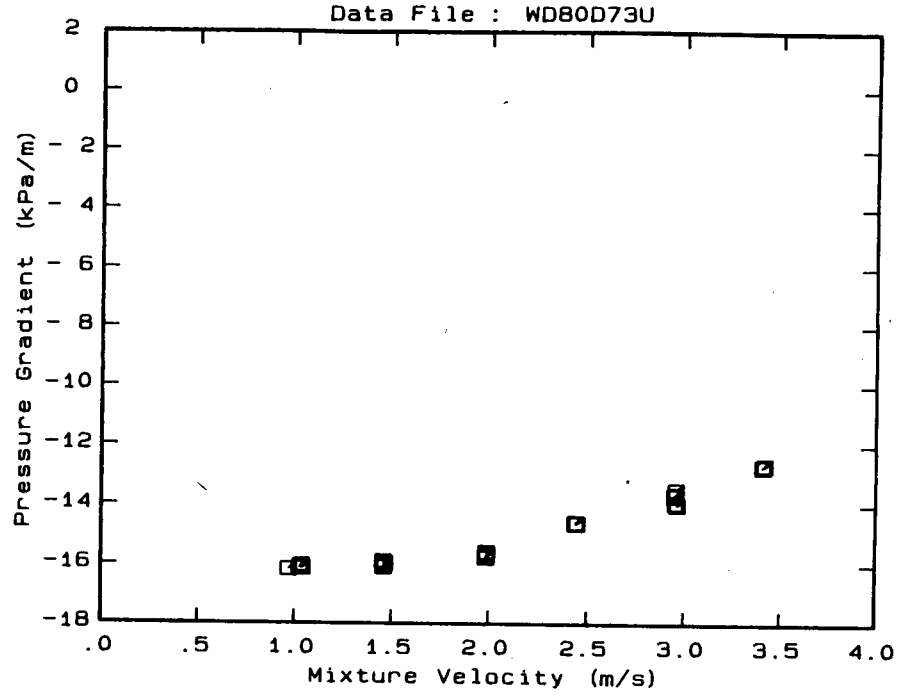

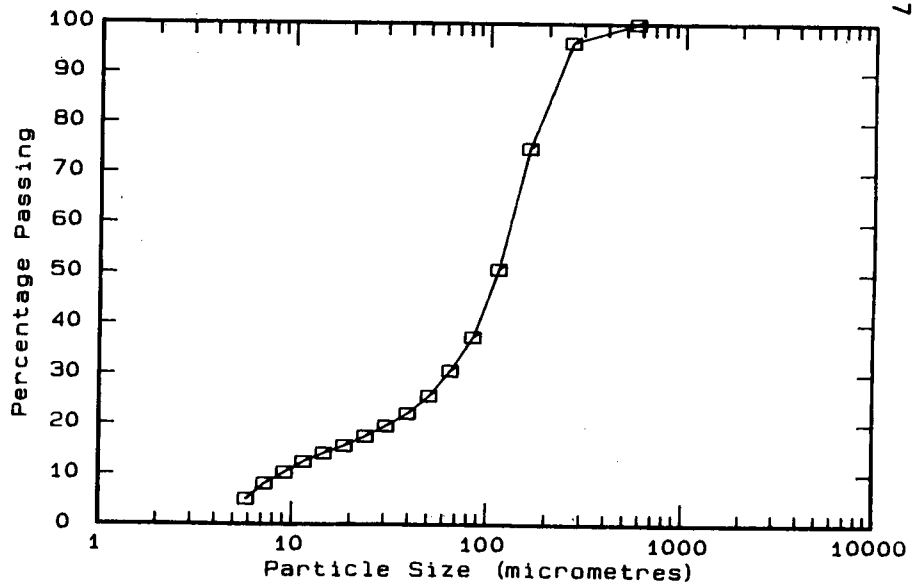

DATA FILE : WD80D78U

Test Facility	UCT 80 mm NB
Test Date	June 1990
Material Description	Western Deeps CCT
Material Relative Density	2.65
Slurry Relative Density	1.78
Solids Volumetric Concentration (%)	47.27
Solids Mass Concentration (%)	70.38
Mean Slurry Temperature (°C)	17.0
Pipe Internal Diameter (mm)	73.40
Pipe Roughness (μm)	84.0
Pipeline Slope	Vertical Down

Mixture Velocity (m/s)	Pressure Gradient (kPa/m)	Slurry Temp. (°C)
3.422	-13.574	16.4
3.424	-13.659	16.5
3.432	-13.654	16.5
3.438	-13.545	16.5
2.952	-14.526	16.5
2.955	-14.443	16.5
2.942	-14.291	16.6
2.952	-14.454	16.7
2.439	-15.137	16.9
2.443	-15.111	17.0
2.439	-15.229	17.0
2.434	-14.994	17.1
2.440	-15.052	17.1
1.953	-15.566	17.1
1.961	-15.546	17.2
1.951	-15.526	17.2
1.957	-15.602	17.2
1.957	-15.597	17.3
1.501	-15.950	17.3
1.500	-15.940	17.3
1.486	-15.975	17.3
1.494	-15.959	17.3
1.487	-15.905	17.3
1.483	-15.867	17.3
1.493	-15.893	17.2
1.495	-15.880	17.2
1.493	-15.869	17.2
1.038	-16.419	17.2
1.060	-15.877	17.2
1.026	-15.977	17.2
1.031	-15.568	17.2
1.026	-15.335	17.2
1.037	-15.432	17.2
1.029	-15.525	17.2

Particle Size Distribution
Malvern Particle Size Analyser

Size (μm)	% Passing	% Retained
564.0	100.0	.0
261.6	96.2	3.8
160.4	74.9	21.3
112.8	50.9	24.0
84.3	37.4	13.5
64.6	30.7	6.7
50.2	25.7	5.0
39.0	22.2	3.5
30.3	19.7	2.5
23.7	17.6	2.1
18.5	15.7	1.9
14.5	14.2	1.5
11.4	12.5	1.7
9.1	10.4	2.1
7.2	8.2	2.2
5.8	5.1	3.1
Pan	- .2	5.3

OBSERVED FLOW BEHAVIOUR

Velocity (m/s)	Observation (D = .0 mm)

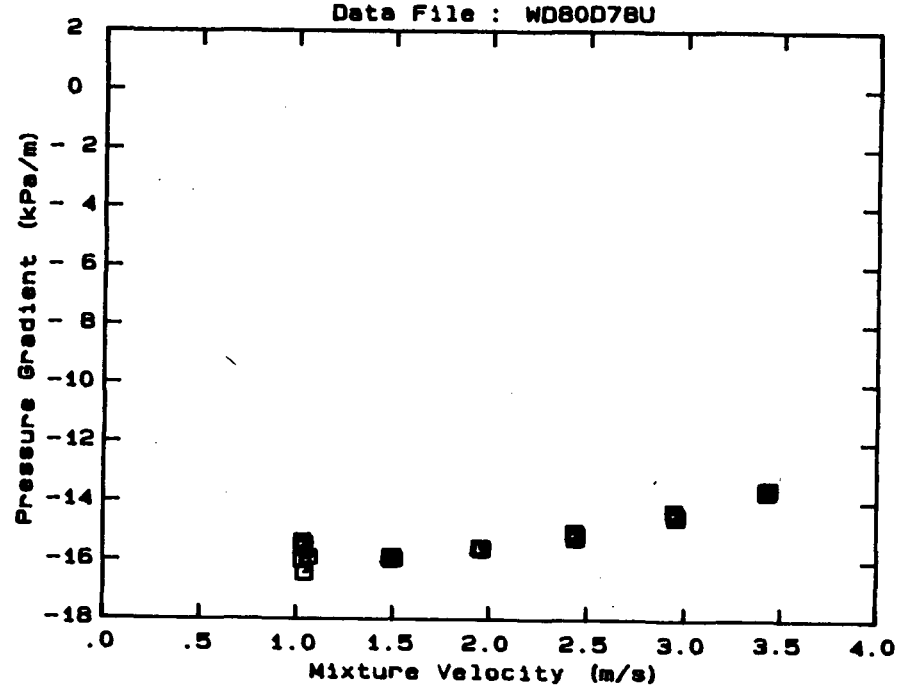

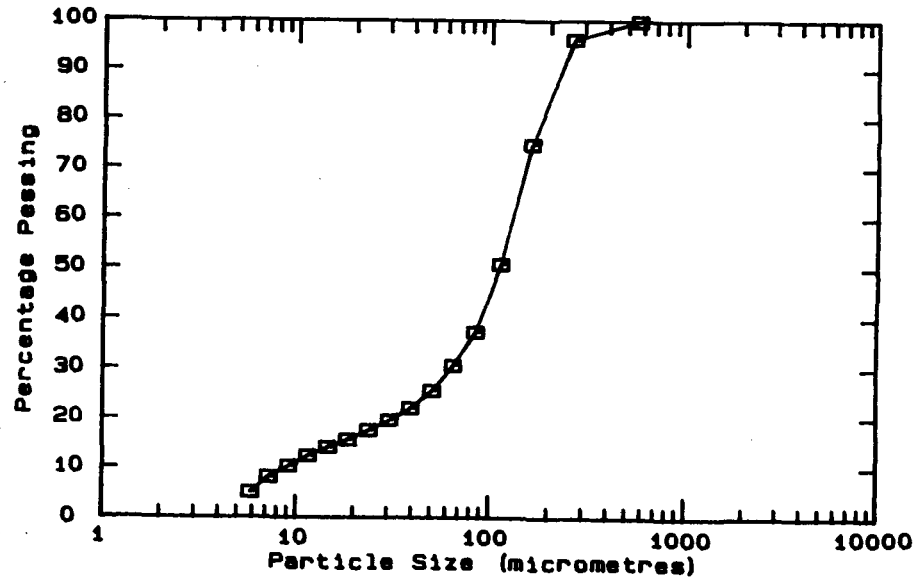

DATA FILE : WD80D81U

Test Facility	UCT 80 mm NB
Test Date	June 1990
Material Description	Western Deeps CCT
Material Relative Density	2.65
Slurry Relative Density	1.81
Solids Volumetric Concentration (%)	49.09
Solids Mass Concentration (%)	71.87
Mean Slurry Temperature (°C)	19.8
Pipe Internal Diameter (mm)	73.40
Pipe Roughness (μm)	84.0
Pipeline Slope	Vertical Down

Mixture Velocity (m/s)	Pressure Gradient (kPa/m)	Slurry Temp. (°C)
3.451	-12.304	18.6
3.456	-12.329	18.7
3.460	-12.524	18.9
3.461	-12.354	19.0
3.464	-12.364	19.1
2.894	-13.343	19.7
2.900	-13.323	19.8
2.901	-13.278	19.8
2.901	-13.219	19.9
2.446	-13.975	20.0
2.445	-13.987	20.0
2.449	-14.022	20.1
2.447	-13.974	20.1
2.449	-13.957	20.1
2.451	-13.948	20.1
2.452	-13.945	20.1
1.962	-14.691	20.2
1.960	-14.565	20.2
1.964	-14.535	20.2
1.962	-14.444	20.2
1.456	-15.200	20.1
1.455	-15.500	20.1
1.452	-15.162	20.1
1.445	-15.165	20.1
1.017	-15.754	20.0
1.023	-15.653	20.0
1.023	-15.643	20.0
1.023	-15.568	20.0

Particle Size Distribution
Malvern Particle Size Analyser

Size (μm)	% Passing	% Retained
564.0	100.0	.0
261.6	95.5	4.5
160.4	74.7	20.8
112.8	51.5	23.2
84.3	37.1	14.4
64.6	30.7	6.4
50.2	25.9	4.8
39.0	21.8	4.1
30.3	19.5	2.3
23.7	17.6	1.9
18.5	15.6	2.0
14.5	14.1	1.5
11.4	12.5	1.6
9.1	10.4	2.1
7.2	8.2	2.2
5.8	5.1	3.1
Pan	- .2	5.3

OBSERVED FLOW BEHAVIOUR

Velocity (m/s)	Observation (D = .0 mm)

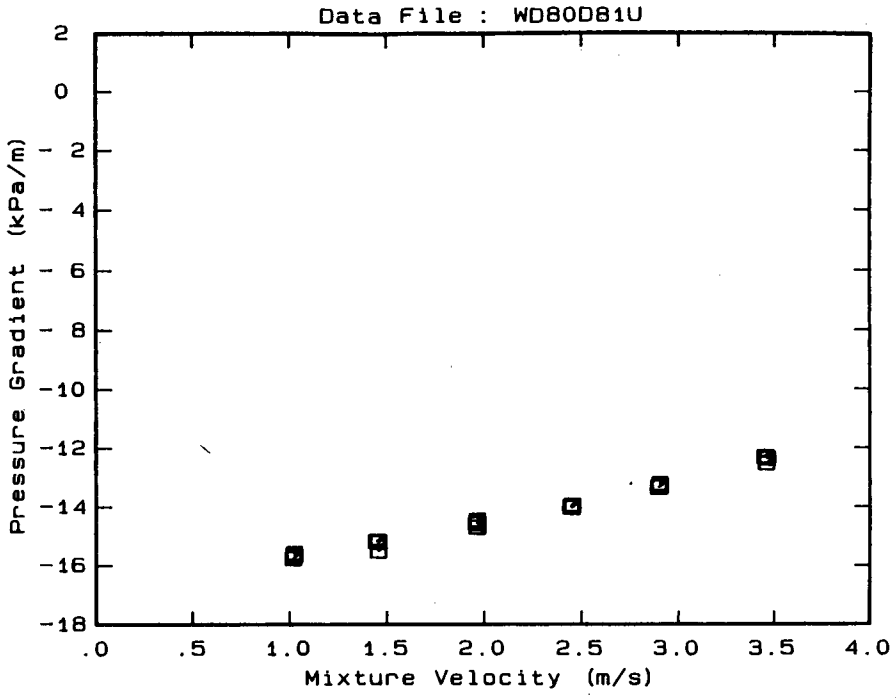

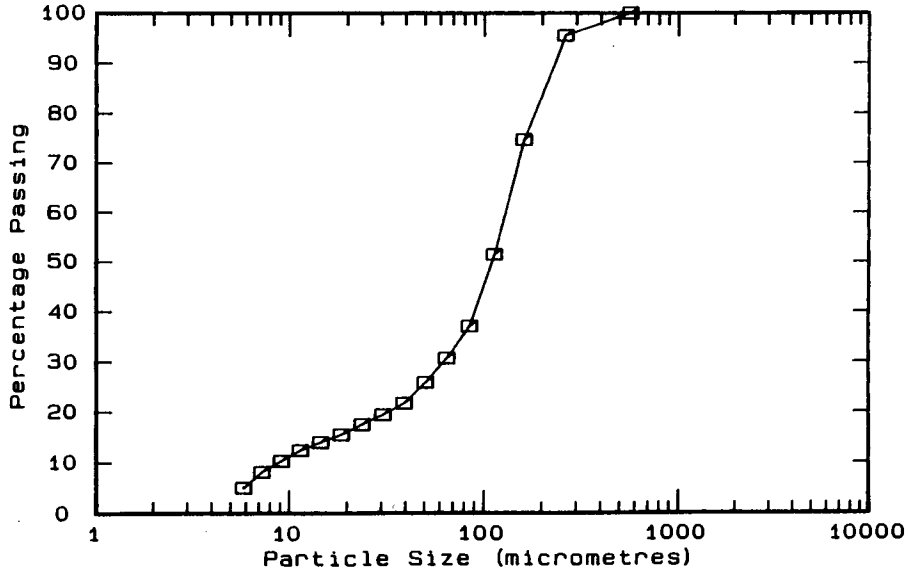

DATA FILE : WD80D86U

Test Facility	UCT 80 mm NB
Test Date	June 1990
Material Description	Western Deeps CCT
Material Relative Density	2.65
Slurry Relative Density	1.86
Solids Volumetric Concentration (%)	52.12
Solids Mass Concentration (%)	74.26
Mean Slurry Temperature (°C)	22.8
Pipe Internal Diameter (mm)	73.40
Pipe Roughness (μm)	84.0
Pipeline Slope	Vertical Down

Mixture Velocity (m/s)	Pressure Gradient (kPa/m)	Slurry Temp. (°C)
3.192	- 9.273	21.1
3.200	- 9.220	21.3
3.208	- 9.221	21.5
3.218	- 9.128	21.7
2.925	-10.381	22.1
2.935	-10.138	22.3
2.944	-10.224	22.4
2.951	-10.373	22.5
2.438	-11.736	22.8
2.443	-11.308	22.9
2.439	-11.408	22.9
2.444	-11.348	23.0
2.451	-11.732	23.0
2.453	-11.605	23.1
1.987	-12.682	23.2
1.986	-12.614	23.3
1.989	-12.510	23.3
1.986	-12.337	23.3
1.463	-13.272	23.3
1.471	-13.297	23.3
1.471	-13.304	23.3
1.470	-13.297	23.3
.991	-14.555	23.2
.973	-14.554	23.2
.931	-14.509	23.1
.906	-14.570	23.1

Particle Size Distribution
Malvern Particle Size Analyser

Size (μm)	% Passing	% Retained
564.0	100.0	.0
261.6	96.2	3.8
160.4	76.3	19.9
112.8	52.7	23.6
84.3	38.2	14.5
64.6	31.6	6.6
50.2	26.5	5.1
39.0	22.6	3.9
30.3	20.1	2.5
23.7	18.1	2.0
18.5	16.3	1.8
14.5	14.8	1.5
11.4	13.1	1.7
9.1	11.0	2.1
7.2	8.7	2.3
5.8	5.5	3.2
Pan	.0	5.5

OBSERVED FLOW BEHAVIOUR

Velocity (m/s)	Observation (D = .0 mm)

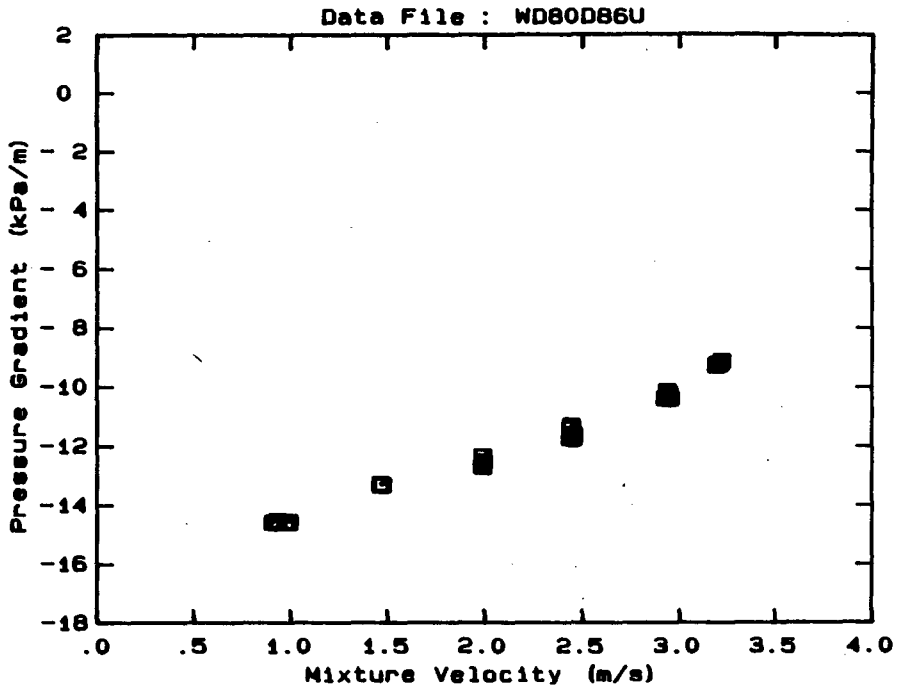

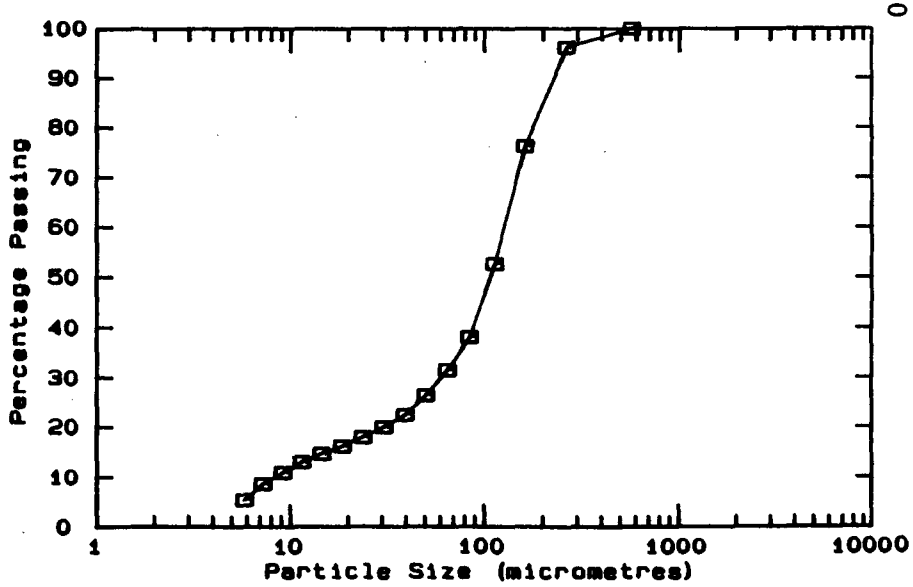

DATA FILE : WD80D90U

Test Facility	UCT 80 mm NB
Test Date	June 1990
Material Description	Western Deeps CCT
Material Relative Density	2.65
Slurry Relative Density	1.90
Solids Volumetric Concentration (%)	54.55
Solids Mass Concentration (%)	76.08
Mean Slurry Temperature (°C)	27.4
Pipe Internal Diameter (mm)	73.40
Pipe Roughness (μm)	84.0
Pipeline Slope	Vertical Down

Mixture Velocity (m/s)	Pressure Gradient (kPa/m)	Slurry Temp. (°C)
2.031	- 5.809	26.0
2.037	- 5.703	26.2
2.048	- 5.830	26.4
2.046	- 5.737	26.6
1.635	- 8.355	27.1
1.662	- 7.942	27.2
1.663	- 8.373	27.3
1.664	- 7.985	27.4
1.661	- 8.132	27.4
1.179	- 9.807	27.6
1.068	-10.301	27.8
1.029	-10.319	27.9
.984	-10.358	27.9
1.001	-10.273	27.9
.674	-11.417	28.0
.655	-11.356	28.0
.675	-11.230	28.0
.656	-11.426	28.0
.664	-11.278	28.0

Particle Size Distribution
Malvern Particle Size Analyser

Size (μm)	% Passing	% Retained
564.0	100.0	.0
261.6	96.9	3.1
160.4	78.0	18.9
112.8	54.1	23.9
84.3	39.5	14.6
64.6	33.0	6.5
50.2	27.7	5.3
39.0	24.1	3.6
30.3	21.5	2.6
23.7	19.3	2.2
18.5	17.5	1.8
14.5	16.0	1.5
11.4	14.2	1.8
9.1	12.0	2.2
7.2	9.6	2.4
5.8	6.1	3.5
Pan	.1	6.0

OBSERVED FLOW BEHAVIOUR

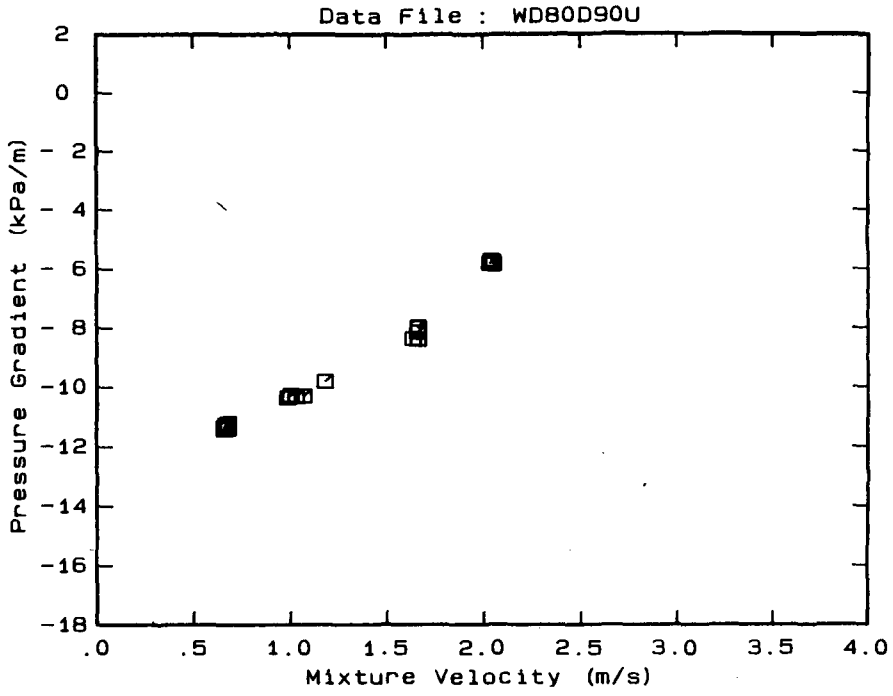

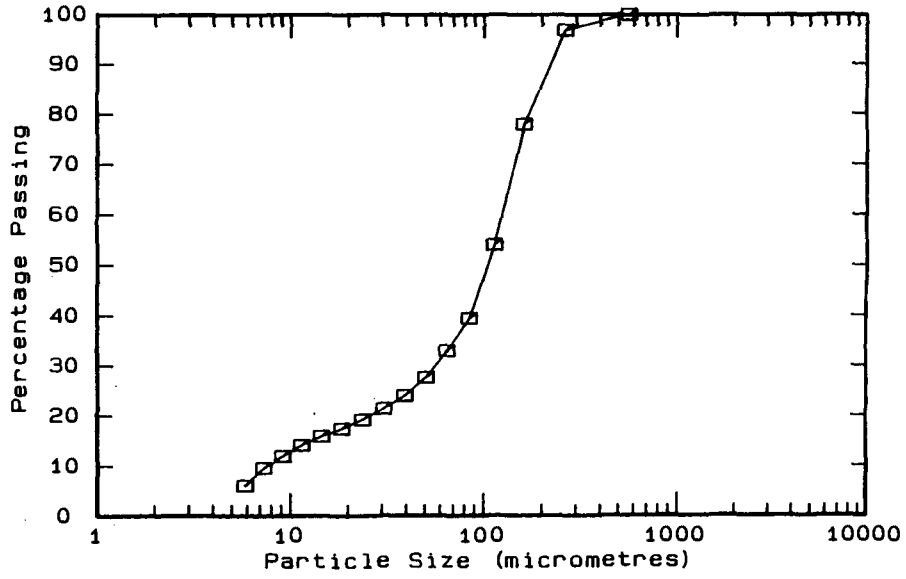

APPENDIX B

EVALUATION OF INTERSTITIAL SEEPAGE FLOW

Nomenclature

A	area	(m^2)
C	concentration by volume	
d	particle diameter	(m)
k	permeability	(m^2)
p	fluid pressure	(Pa)
Q	flow rate	(m^3/s)
Re	particle Reynolds' number	
u	superficial velocity	(m/s)
α	dimensionless paramater	
β	dimensionless parameter	
ϵ	porosity = (1 - C)	
ρ_w	density of fluid	(kg/m^3)
μ	dynamic coefficient of viscosity	(kg/ms)

Darcy's Law

Darcy's law for steady incompressible flow through a porous medium states :

$$u = \frac{k}{\mu} \frac{dp}{dx} \quad . \tag{B.1}$$

The superficial velocity, u is the flow rate divided by the cross-sectional area of the medium, i.e.

$$u = \frac{Q}{A} \quad , \tag{B.2}$$

where A = internal area of pipe, in our case.

The permeability, k is a function of the medium type, packing density and particle Reynolds number. The Ergun empirical correlation may be used to estimate the permeability of the medium (Blevins (1984)) where

$$k = \frac{1}{\frac{\alpha (1-\epsilon)^2}{d^2 \epsilon^3} + \frac{\beta (1-\epsilon) \rho_w}{\epsilon^3 d \mu}} \quad . \tag{B.3}$$

Expression B.3 may be simplified for the two limiting cases of laminar flow and turbulent flow as shown in the following table :

TABLE B.1

LAMINAR FLOW	TURBULENT FLOW
Re < 20	Re > 10^3
$k = \frac{\epsilon^3 d^2}{\alpha (1-\epsilon)^2}$ (B.4)	$k = \frac{\epsilon^3 d\mu}{\beta (1-\epsilon)\rho_w}$ (B.5)

Note that for laminar flow k is independent of the superficial velocity and fluid characteristics. The dimensionless parameters α and β are quoted by Blevins as :

TABLE B.2

	α	β
Rough particles	180	4,0
Smooth particles	180	1,8

Worked Example

To establish the validity of the assumption that the flow of the carrier fluid through the granular matrix of coarse particles is negligible we consider the following example :

Taking water at 15°C as the liquid we have

$\rho_w = 999,1 \text{ kg/m}^3$ and $\mu = 1,140 \times 10^{-3}$ (kg/ms).

A representative particle diameter, $d = 300\ \mu m$

Packing density, $\epsilon = 0,60 \quad (C = 40\%)$

Maximum pressure gradient expected, $\frac{dp}{dx} = 20\ kPa/m$

From Table B.2 for rough particles we get $\alpha = 180$ and $\beta = 4,0$.

Assuming laminar flow, from Table B.1

$$k = \frac{\epsilon^3 d^2}{\alpha (1-\epsilon)} = 6,750 \times 10^{-10}\ m^2$$

$$u = \frac{k}{\mu} \frac{dp}{dx} = 0,012\ m/s$$

and $$Re = \frac{\rho\, ud}{\mu} = 3,114 < 20 \quad \therefore \text{ laminar.}$$

Thus for the "worst case" considered in the above example the seepage velocity of 12 mm/s is clearly negligible compared with a typical mixture velocity of 2 m/s.

APPENDIX C

AREA COORDINATES FOR TRIANGULAR ELEMENTS

Referring to Figure C.1 the position of an arbitrary point P is expressed in terms of three non-dimensional coordinates L_1 , L_2 , L_3 which relate respectively to the sides directly opposite nodes 1, 2 and 3 . By definition each coordinate is the ratio of the perpendicular distance h_i from one side to the altitude h measured from the same side, thus

$$L_i = h_i/h \quad ; \quad i = 1, 2, 3 \ . \tag{C.1}$$

The ratio of A_i to the area A of the whole element is

$$\frac{A_i}{A} = \frac{B\, h_i/2}{B\, h/2} = \frac{h_i}{h} = L_i \quad ; \quad i = 1, 2, 3 \ . \tag{C.2}$$

Thus L_i are termed area coordinates as they define the area of the subtriangles in terms of the complete area of the element. The sum of the three coordinates must always equal one. Also L_i has a value of one at node i and zero at the other two nodes with a linear variation between them. These are exactly the same values that the element shape functions $N_i^{(e)}$ have, thus

$$L_i = N_i^{(e)} \quad ; \quad i = 1, 2, 3 \ . \tag{C.3}$$

Area coordinates are used in place of cartesian coordinates as several formulae exist to facilitate integration. In particular

$$\int_A L_1^a \, L_2^b \, L_3^c \, dA = \frac{a \,!\, b \,!\, c \,!}{(a + b + c + 2) \,!} \, 2A \ , \tag{C.4}$$

where A = area of integration

a, b, c = arbitrary integer powers.

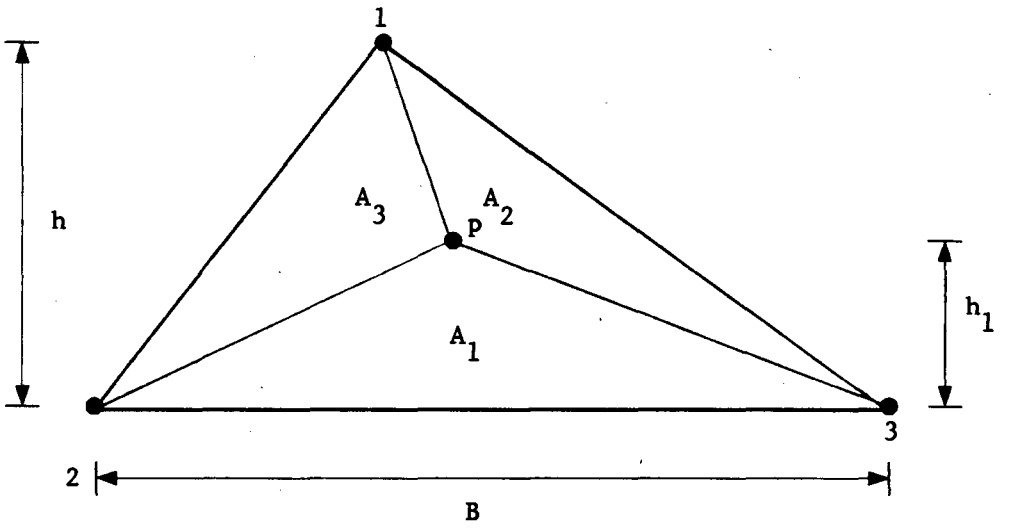

Figure C.1 : Area coordinate definitions

APPENDIX D

ISOKINETIC SAMPLING PROBE FOR SLURRY FLOWS

11th International Conference on the
Hydraulic Transport of Solids in Pipes

HYDROTRANSPORT 11

Stratford-upon-Avon, UK: 19-21 October 1988

PAPER C1

ISOKINETIC SAMPLING PROBE FOR SLURRY FLOWS

R. Cooke, J.H. Lazarus
Hydrotransport Research Unit, Department of Civil Engineering, University of Cape Town, South Africa

Summary

An instrument is described which samples slurry flows isokinetically without requiring a separate measurement of the local velocity. The method utilises the stagnation pressure in the sampling tube as a reference to determine the isokinetic velocity. The sampling probe can determine the local velocity, concentration and particle size distribution within a pipe.

The geometry, layout and the accuracy of the probe is discussed. Measurements were made in a 140 mm internal diameter horizontal pipe conveying a sand-water slurry at a volumetric concentration of 18%.

Nomenclature

a	=	elemental area	(m^2)
A	=	pipe area	(m^2)
c	=	local concentration	
C	=	bulk delivered concentration	
C_b	=	packed bed concentration	
d	=	particle diameter	(m)
d_{50}	=	particle diameter such that 50% by weight of particles are < d_{50}	(m)
D	=	internal pipe diameter	(m)
h	=	head difference measured in units of water	(m)
i	=	hydraulic gradient	(m/m)
ℓ	=	length dimension	(m)
q	=	elemental flow rate	(m^3/s)
Q	=	bulk flow rate	(m^3/s)
r	=	radial distance	(m)
R	=	pipe radius	(m)
S	=	relative density	
S_f	=	particle shape factor	
u	=	local velocity	(m/s)

Held in Stratford-upon-Avon, UK. Organised and sponsored by BHRA, The Fluid Engineering Centre

u_{max} = maximum velocity in an elemental strip (m/s)

u^+ = dimensionless local velocity = $\frac{u}{u_*}$

u_* = local shear velocity (m/s)

U_* = shear velocity = $\sqrt{\frac{\tau_o}{\rho S_m}}$ (m/s)

V = bulk velocity = Q/A

V_t = particle settling velocity (m/s)

V_t' = hindered particle settling velocity (m/s)

y = distance from pipe wall (m)

y^+ = friction Reynolds number = $\frac{U_* y}{\nu}$

ϵ_s = sediment transfer coefficient (m^2/s)

κ = von Karman constant

ν = kinematic viscosity (m^2/s)

ν_e = effective kinematic viscosity (m^2/s)

τ_o = shear stress at pipe wall (N/m^2)

Subscripts

d = delivered
m = solids-liquid mixture
s = solids
v = volume

1. Introduction

To understand the internal mechanisms in a slurry pipeline it is important that measurements are made of internal parameters, such as local velocity, local concentration and local particle size distribution. As part of the ongoing program by the Hydrotransport Research Unit at the University of Cape Town to develop a unified theory for slurry flows, an experimental study is being conducted to develop a probe capable of determining these local parameters.

A method of obtaining a sample of slurry from a pipeline is to use an L-shaped tube pointing into the direction of flow. To ensure that a representative sample is withdrawn from the pipeline, the mixture should be removed through the sampling tube at a velocity equal to the undisturbed local velocity upstream of the tube - this is termed isokinetic sampling. Previous research (Nasr-El-Din *et al* (1984) and Nasr-El-Din and Shook (1987)) used a separate velocity probe to determine the freestream approach velocity and then iteratively adjusted the flow rate through the sampling tube. The probe presented herein utilises the stagnation pressure in the sampling tube as a reference for measuring the freestream approach velocity and thus alleviates the necessity of measuring the local velocity with a separate probe. This technique has been used for gas-liquid flows (Jones (1983)).

2. Experimental Procedure

The experimental investigation is being conducted using the Hydrotransport Research Unit's pipeloop test facility which has been described elsewhere by Lazarus and Sive (1984). Figure 1 shows an overall view of the test facility. Figure 2 depicts the general layout of the isokinetic sampling probe while Figure 3 shows an assembly drawing of the probe.

The experimental procedure has three components:

(i) Determine isokinetic conditions
(ii) Measure the isokinetic velocity
(iii) Determine the local concentration and particle size distribution

2.1 Determining the Isokinetic Condition

The isokinetic sampler (A) is located 70 pipe diameters downstream from the nearest 180° bend. The radial position of the probe is adjustable and the probe can also be rotated about the pipe axis; this allows measurement at any point within the pipe cross section. Only vertical profiles are presented herein. To reduce obstruction of the flow the probe has a 5 degree taper as recommended by Nasr-El-Din *et al* (1984).

The pressure inside the sampling tube is measured by the circumferential pressure tapping (B), and compared with the static pressure at the wall (C). The static pressure tapping is rotatable so that it is always at the same horizontal level as the sampling tube axis. Since the circumferential pressure tapping (B) is positioned a distance ℓ downstream of the static pressure tapping, a correction must be made for the head loss in the sampling tube between section AA and section BB. This is done by measuring the head loss over the same length of pipe, ℓ, of the same diameter as the sampling tube (D).

Figure 2 shows the air-water manometer board (E) where the pressure differences from the isokinetic sampler (A), and the head loss measuring section (D), are measured as head differences h_1 and h_2 respectively. The flow rate through the sampling tube is controlled using the slurry pump (F) and pinch valve (G). When the head difference h_1 equals the head difference h_2 isokinetic conditions exist. The isokinetic velocity may now be measured and the local concentration and particle size determined.

2.2 Measuring the isokinetic velocity

The velocity in the sampling tube is measured using a magnetic flow meter (H). The magnetic flow meter is calibrated by closing valves (G) and (I) to isolate the sampling loop from the 140 mm pipeline, and valves (J) and (K) are opened to allow clear water to flow through the magnetic flow meter. The water from the outlet is diverted to a container and the sampling time and volume are measured to calculate the flow rate.

2.3 Determining the local concentration and particle size distribution

The sampling probe measures the local delivered concentration at section AA. To measure this delivered concentration a sampling loop (L) is used. The sampling loop is based on the same principle as a counter flow meter (Lazarus (1982)). The average of the *in situ* concentration in the riser and downcomer equals the delivered concentration in the pipe. Once isokinetic conditions have been achieved the slurry is diverted to the sampling loop bypass (M) using the L-ported ball valve (N) and valve (O) is closed simultaneously, thus capturing a sample of slurry in the sampling loop. The sample is removed through the drain valve (P).

The volume of the sampling loop is determined by filling it with clear water and measuring the mass of water removed through the drain valve. The concentration is calculated from the oven dry mass of the solids contained in the sampling loop. The particle size distribution is obtained from a sieving analysis.

3. Results and Discussion

3.1 Clear water tests

The results of clear water tests at three mean velocities are presented in Figure 4. The data points are superimposed on a logarithmic turbulent velocity profile given by:

$$u^+ = \frac{1}{\kappa} \ell n\, y^+ + 5{,}5 \qquad \text{valid for } y^+ > 30 \tag{1}$$

where $\kappa = 0{,}40$ for water

$$u^+ = \frac{u}{U_*}$$

$$y^+ = \frac{U_* y}{\nu}$$

$$U_* = \sqrt{\frac{\tau_o}{\rho}}$$

The measured local velocities and the predicted velocity profiles (Figure 4) are in good agreement. Therefore, the head loss between section AA and section BB is the same as the head loss measured across the head loss measuring section (D). These head losses would be expected to differ slightly as the entry conditions are not the same for both cases.

3.2 Sand-water mixture test results

The particle size distribution for the sand used in the test is shown in Figure 5.

For the sand used:

$S_s = 2{,}65$
$d_{50} = 564\ \mu m$
$S_f = 0{,}6$

Figure 6 shows the measured velocity and concentration profiles at a mean mixture velocity (V_m) of 3,34 m/s and a mean delivered concentration (C_{vd}) of 18% by volume. The velocity profile has a maximum velocity of 4,08 m/s which occurs at an upward eccentricity of 12 mm from the pipe axis.

To check the accuracy of the local concentration and velocity profile, the profiles are integrated over the pipe area and compared with the mean delivered concentration and mean velocity. To perform the integration the pipe section is divided into 14 horizontal strips, each 10 mm thick, as shown in Figure 7. The integrated bulk mixture flow rate and bulk solids flow rate is calculated from:

$$Q_m = \sum_{i=1}^{n} q_m = \sum_{i=1}^{n} \bar{u}_i\, a_i \tag{2}$$

$$Q_s = \sum_{i=1}^{n} q_s = \sum_{i=1}^{n} \bar{u}_i\, \bar{c}_i\, a_i \tag{3}$$

where n = 14.

The mean concentration ($\bar{c}_i$) at each horizontal section spanning the pipe is obtained directly from the concentration profile in Figure 6, making the assumption that the concentration at any one level is constant horizontally across the pipe cross section. The method used to estimate the mean mixture velocity ($\bar{u}_i$) at each section of the pipe is described in Appendix A. The results of the integration for the test case shown in Figure 6 are presented in Table 1.

Table 1 shows that the local and bulk concentration values agree to within 2%, the slightly higher value from the integration is probably due to the concentration decreasing towards the pipe wall along a horizontal level. The integrated velocity profile gives a flow rate which is 10% lower than the measured bulk flow rate.

Figure 8 shows sieving analyses of samples removed from different points across the vertical section. The curves show how the local d_{90} particle size at each level increases towards the bottom of the pipe.

Figure 9 presents the variation of local delivered volumetric concentration of different size fractions with vertical position in the pipe cross section. Figure 10 illustrates the same data on a different concentration scale to make the presentation of the curves at lower concentrations clearer. The coarser fraction ($d > 150$ μm) shows an increasing concentration towards the bottom of the pipe while the finer fraction ($d < 150$ μm) decreases in concentration towards the bottom of the pipe.

Figure 11 shows the concentration profile data plotted with 3 concentration profile correlations (see Appendix B for details of correlations). The first order diffusion model was evaluated at y_a = 70 mm and c_a = 17%, the model shows good agreement with the data points over the central portion of the pipe. The second order diffusion model is a poor fit to the experimental data. The Shook correlation (Carleton *et al* (1978))evaluated at y_a = 70 mm and c_a = 17% shows reasonable agreement with the data points and closely predicts the correct profile shape. Note that all the correlations predict zero concentration at the top of the pipe.

4. Conclusions

4.1 The sampling probe can sample accurately up to a local concentration in excess of 50% by volume without requiring the use of a separate velocity probe.

4.2 The measured velocity profiles in clear water show good agreement with the predicted velocity profiles, thus validating the assumption that the head loss between the probe nose and the circumferential pressure tapping is the same as the head loss measured across a pipe of the same length and diameter.

4.3 The integrated concentration and bulk concentration values agree to within 2%.

4.4 The integrated flow rate is 10% lower than the bulk flow rate. The probe will be evaluated further to improve the confidence level when measuring velocity profiles.

4.5 The local delivered concentration of different particle size fractions shows that the concentration of the coarser fraction ($d > 150$ μm) increases towards the bottom of the pipe, while the concentration of the finer fraction ($d < 150$ μm) decreases towards the bottom of the pipe.

4.6 The Shook concentration profile correlation closely predicts the correct profile shape.

5. Acknowledgements

The authors wish to acknowledge financial support received from the following organizations:

Council for Scientific and Industrial Research
East Rand Gold and Uranium Company
University of Cape Town

References

1. Carleton, A.J., Prench, R.J., James, J.G., Broad, B.A., Streat, M. (1978): "Hydraulic transport of large particles using conventional and high concentration conveying". *Proc. 5th International Conference on the Hydraulic Transport of Solids in Pipes* (Hanover, Germany, May 8-11), Cranfield, U.K.: BHRA, Paper D2, p. D2-15 to D2-28.

2. Jones, O.C. (1983). "Two-Phase Flow Measurement Techniques in Gas-Liquid Systems", *Fluid Mechanics Measurements*. ed. Goldstein, R.J., New York: Hemisphere, p. 534-537.

3. Lazarus, J.H., Sive A.W. (1984): "A novel Balanced Beam Tube Viscometer and the rheological characterisation of high concentration Fly Ash slurries". *Proc 9th International Conference on the Hydraulic Transport of Solids in Pipes* (Rome, Italy, October 17-19), Cranfield, U.K.: BHRA, Paper E1, p. 207-226.

4. Lazarus, J.H. (1982) "Pump and Pipeline Instrumentation". *Course Notes, 8th International Conference on the Hydraulic Transport of Solids in Pipes* (Johannesburg, South Africa, Aug, 1982), Cranfield, U.K.: BHRA.

5. Nasr-El-Din, M. and Shook, C.A. (1987): "Effect of a 90 degree Bend on Slurry Velocity and Concentration Distributions". *Journal of Pipelines*, Vol. 6, p. 239-252.

6. Nasr-El-Din, M., Shook C.A. and Colwell, J. (1986): "The Lateral Variation of Solids Concentration in Horizontal Slurry Pipeline Flow". *Proc. International Symposium on Slurry Flow, ASME, winter Annual meeting*, p. 175-180.

7. Nasr-El-Din, M., Shook C.A. and Esmail, M.N. (1984):"Isokinetic Probe Sampling from Slurry Pipelines". *The Canadian Journal of Chemical Engineering*, Vol. 62, April, p. 179-184.

APPENDIX A - EVALUATION OF $\bar{u}_i$ FOR VELOCITY PROFILE INTEGRATION

To estimate the mean velocity ($\bar{u}_i$) as a fraction of the maximum velocity, u_{max} of each horizontal section the velocity defect law is used as follows; Consider a horizontal strip one unit thick.

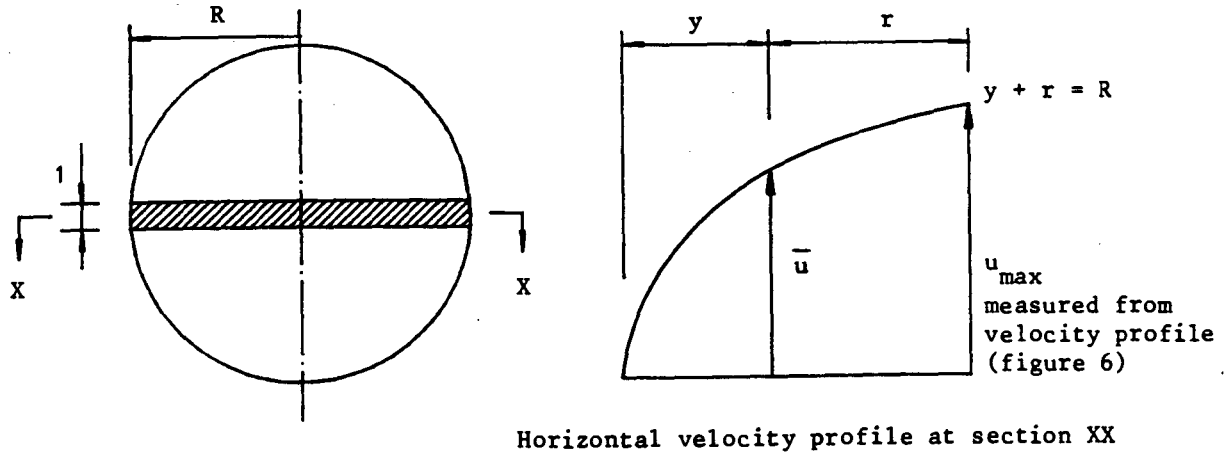

Horizontal velocity profile at section XX

$$u = u_{max} + \frac{u_*}{\kappa} \ln\left(\frac{y}{R}\right)$$

$$q = \int_0^R u\,dr = \int_0^R \left(u_{max} + \frac{u_*}{\kappa} \ln\left(\frac{y}{R}\right)\right) dy$$

$$q = \left[u_{max}\, y + y \frac{u_*}{\kappa} \left(\ln\left(\frac{y}{R}\right) - 1\right)\right]_0^R$$

$$\therefore \quad q = R\left(u_{max} - \frac{u_*}{\kappa}\right)$$

$$\bar{u} = \frac{q}{R} = u_{max} - \frac{u_*}{\kappa} \qquad \text{(A1)}$$

Note that both u_* and κ vary across the pipe cross section since they are concentration dependent. The local shear velocity (u_{*i}) is evaluated using

$$u_{*i} = \sqrt{\frac{\tau_o}{S_m \rho}} \qquad \text{(A2)}$$

where S_m = local relative density of mixture obtained from Figure 6
$= c_i\,(S_s + 1)$
τ_o = shear stress at the pipe wall, assumed to act uniformly over the pipe circumference.

The von Karman value (κ) was calculated over a horizontal level at r = 0 (i.e. approximately constant concentration) using the following two relations

$$u^+ = \frac{2}{\kappa} \ln y^+ - 3{,}05 \qquad \text{valid } 5 < y^+ < 30 \qquad \text{Transition zone} \qquad \text{(A3)}$$

$$u^+ = \frac{u_{max}}{v^*} + \frac{1}{\kappa} \ln\left(\frac{y}{R}\right) \qquad \text{valid } 30 < y^+ \qquad \text{Turbulent zone} \qquad \text{(A4)}$$

where u_{max} is obtained from Figure 6 at y = R,
i.e. the axis of the pipe

κ is found to equal 0,44 by equating equation (A3) and (A4) at $y^+ = 30$. This represents an increase in κ over the clear water value of 0,4. This variation has been reported by others, e.g. Nasr-El-Din *et al* (1986). This value of κ is then used as an average throughout the velocity profile to evaluate equation (A1).

APPENDIX B - CONCENTRATION PROFILE CORRELATIONS

B.1 First order Diffusion Model

$$c(y) = c_a \left[\frac{D/y - 1}{D/y_a - 1}\right]^Z \qquad \text{(B.1)}$$

where $Z = \dfrac{V_t}{\beta \kappa U_*}$ $\qquad \beta \simeq 1$

V_t = settling velocity of d_{50} particles
y = height above pipe floor

B.2 Second order Diffusion Model

$$c(y) = C_b \exp\left[\frac{-V_t'}{\epsilon_s} (y - y_b)\right] \qquad \text{(B.2)}$$

where C_b = packed bed concentration
V_t' = hindered settling velocity of d_{50} particles
ϵ_s = transfer coefficient = 0,052 U_* D

B.3 Shook correlation (Carleton *et al* (1978))

$$c(y) = C_b \left[\left[\tan \frac{y \left[2 g d \left(\frac{S_s - 1}{S_s}\right)\right]^{1/2}}{12 \nu_e}\right]^2 + 1\right]^{-3} \qquad \text{(B.2)}$$

where ν_e = effective kinematic viscosity

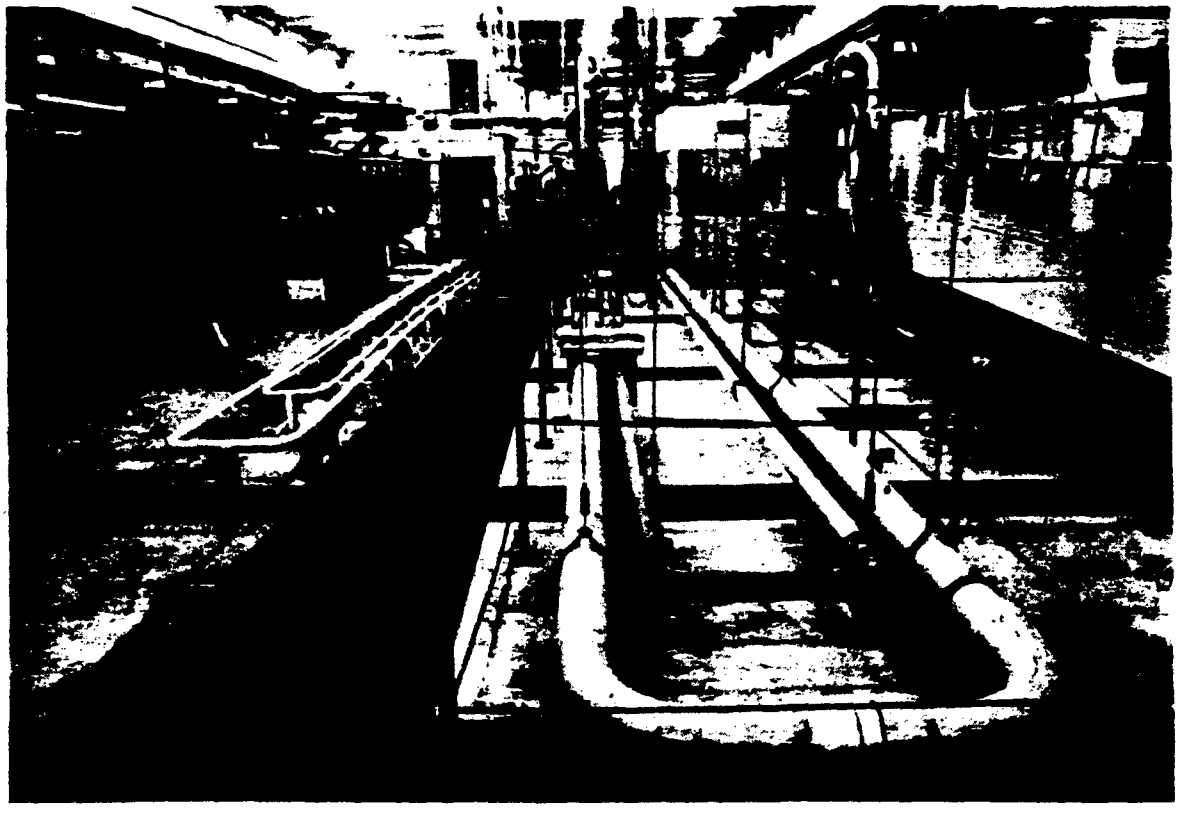

Figure 1 - Overall view of Hydrotransport Research Unit's pipeloop test facility

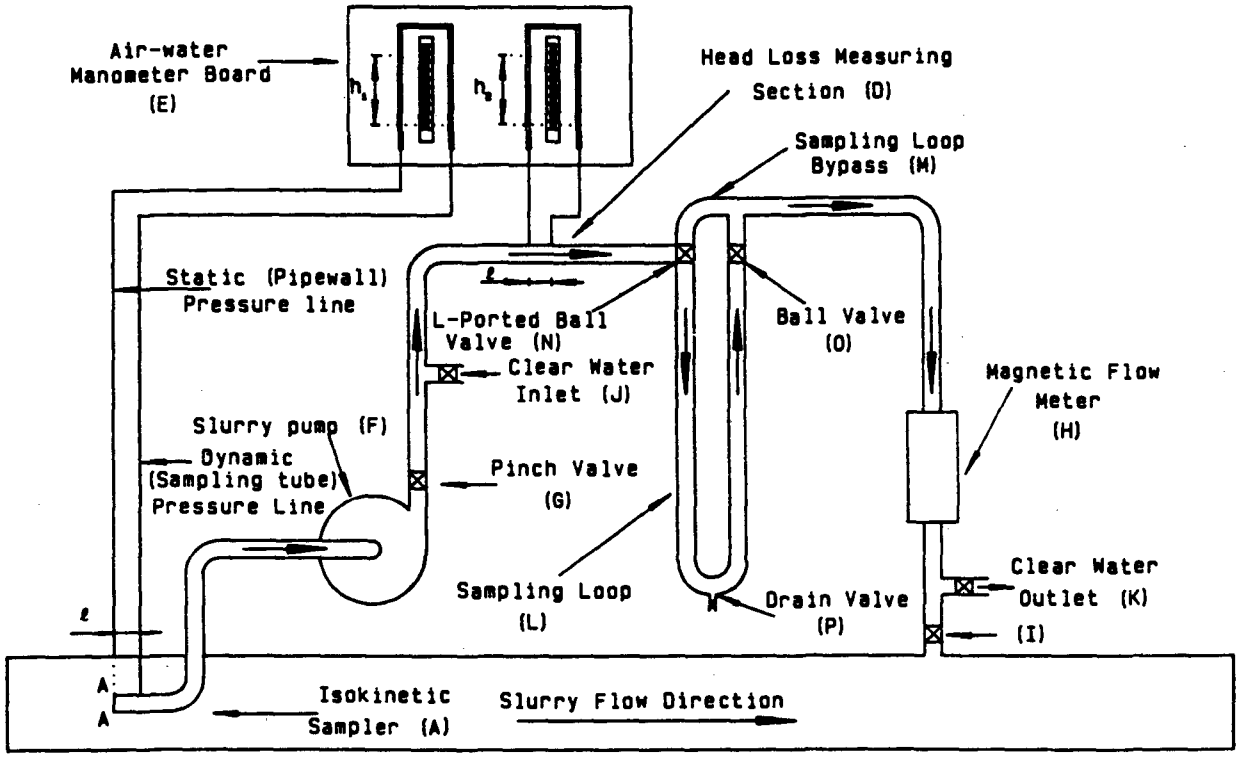

Figure 2 : General layout of isokinetic sampling probe.

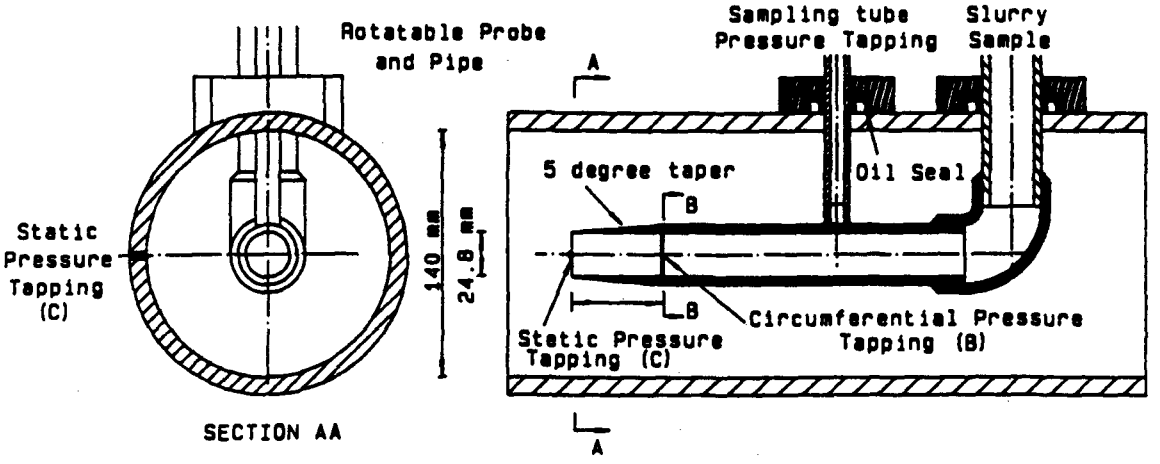

Figure 3 : Assembly drawing of isokinetic probe.

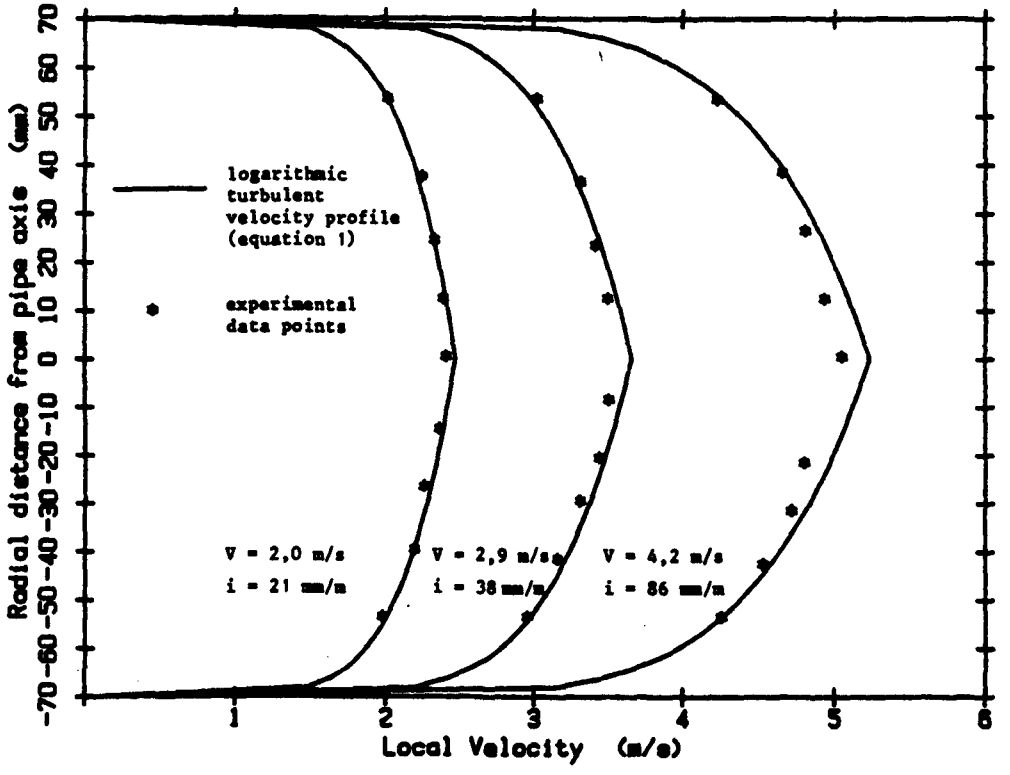

Figure 4 : Clear water test results.

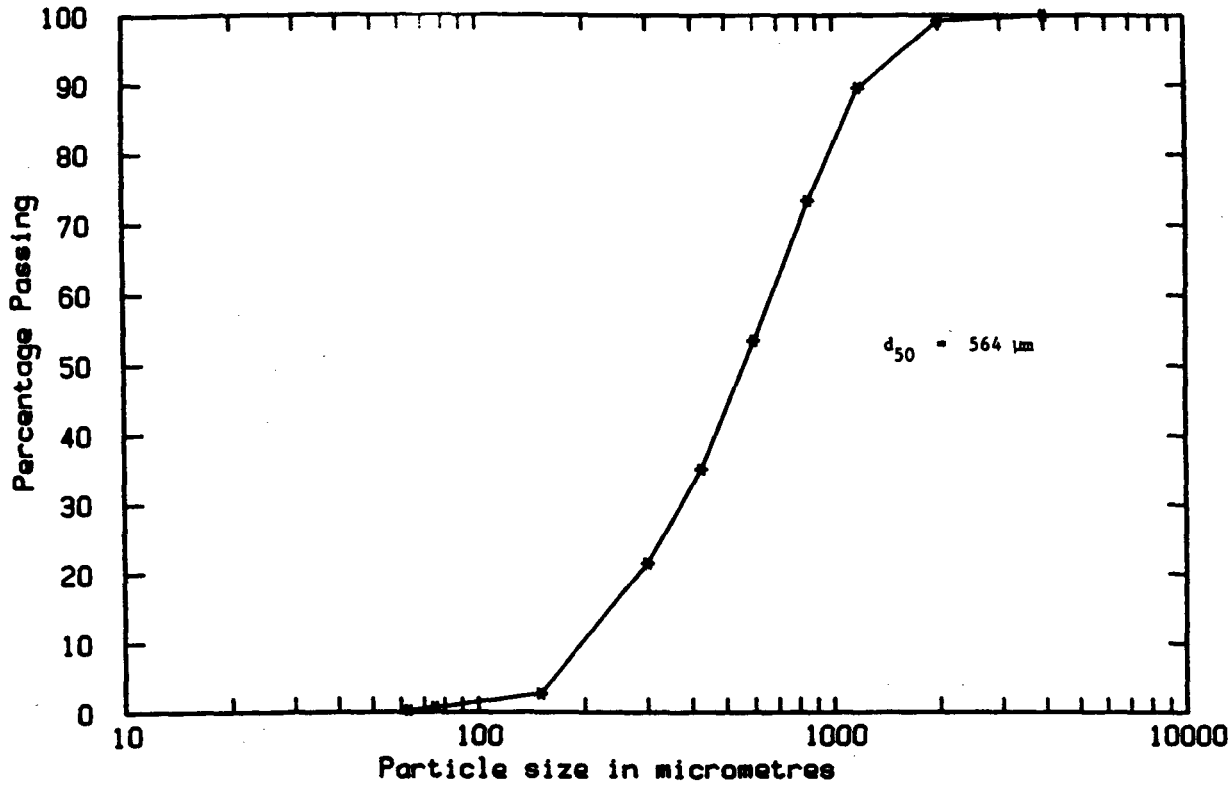

Figure 5 : Sand particle size distribution.

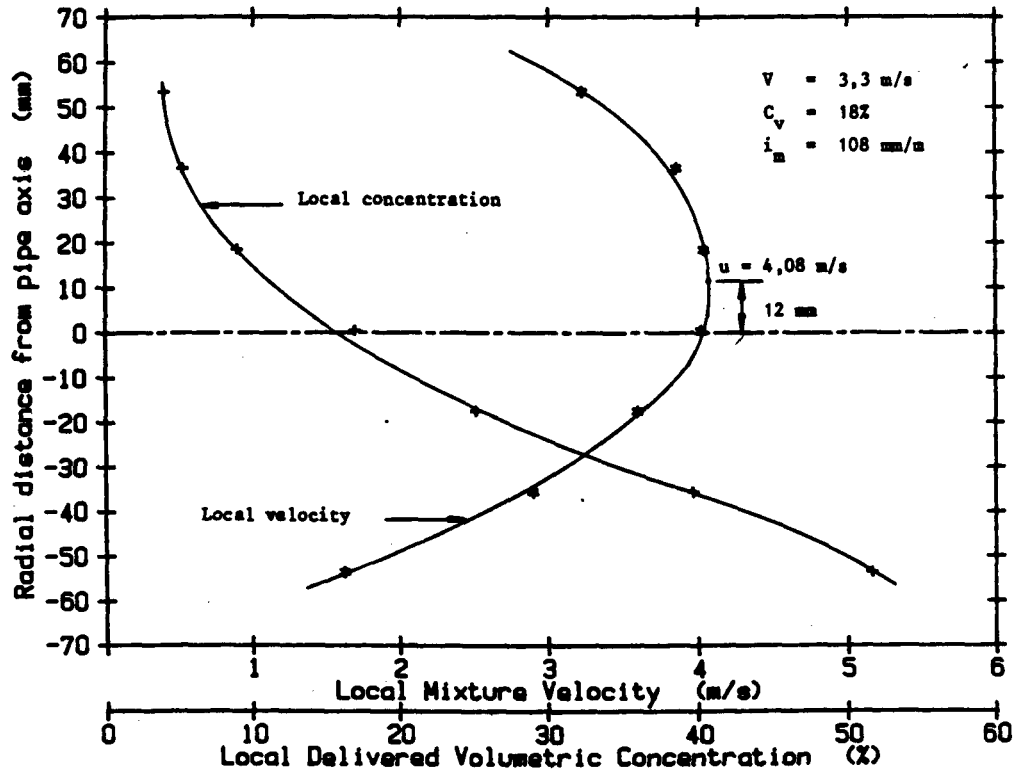

Figure 6 : Measured velocity and concentration profiles.

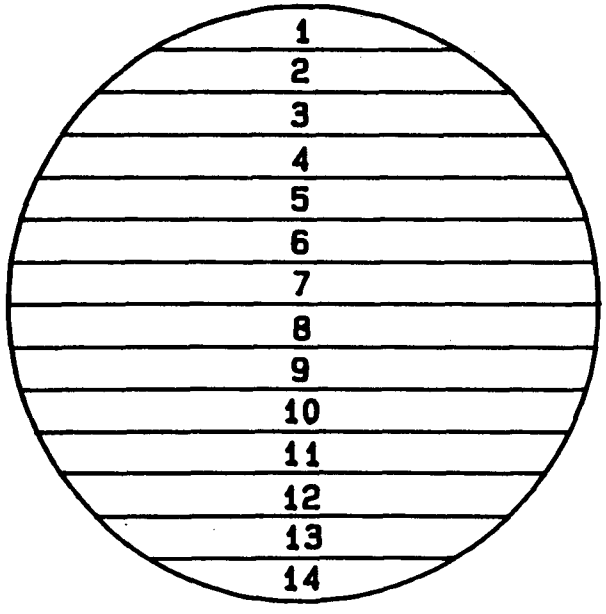

Figure 7: Division of pipe section into horizontal strips.

Table 1: Results of velocity and concentration profile integration

Strip	Area (mm^2)	u (from Fig 6) (m/s)	c (from Fig 6) (%)	$\bar{u}$ (eq A1) (m/s)	q_m (eq 2) (ℓ/s)	q_s (eq 3) (ℓ/s)
1	503	2,76	3,0	2,33	1,17	0,04
2	868	3,16	3,8	2,74	2,37	0,09
3	1 075	3,60	4,6	3,18	3,42	0,16
4	1 215	3,88	5,6	3,46	4,21	0,24
5	1 311	4,01	7,6	3,60	4,71	0,36
6	1 370	4,08	10,6	3,68	5,04	0,53
7	1 399	4,06	15,0	3,67	5,13	0,77
8	1 399	3,94	19,2	3,56	4,98	0,96
9	1 370	3,70	24,0	3,33	4,56	1,10
10	1 310	3,32	30,6	2,96	3,88	1,19
11	1 215	2,92	40,0	2,58	3,14	1,25
12	1 075	2,29	47,0	1,96	2,11	0,99
13	868	1,63	52,0	1,31	1,14	0,59
14	503	1,10	56,0	0,78	0,40	0,22
					46,26	8,49

$\therefore$ $\Sigma q_m = 46{,}26$ ℓ/s Bulk $Q_m = 51{,}82$ ℓ/s

i.e. Σq_m is 10,7% less than the bulk Q_m

$\Sigma q_s = 8{,}49$ ℓ/s $C_{vd} = \frac{\Sigma q_s}{\Sigma q_m} = 18{,}35\%$ Bulk $C_{vd} = 18\%$

i.e. integrated C_{vd} is 1,9% greater than the bulk C_{vd}

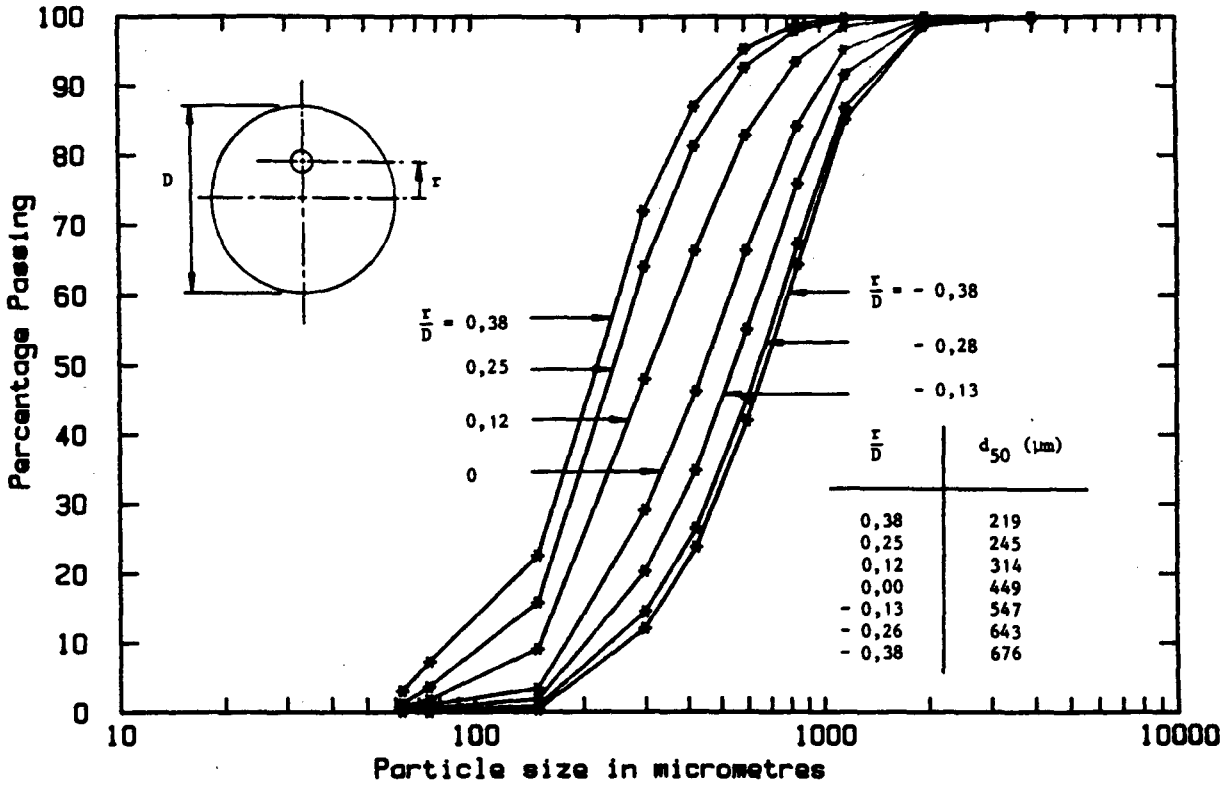

Figure 8 : Particle size distribution at different vertical points within pipe cross section.

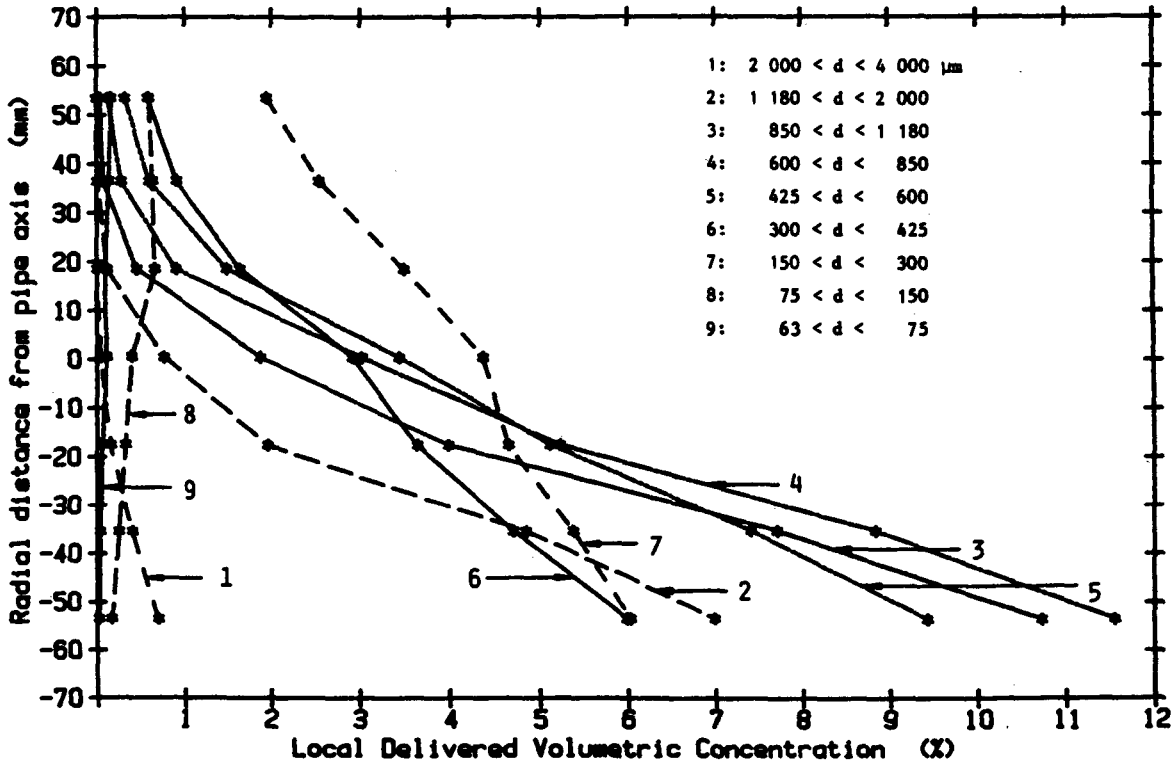

Figure 9 : Variation of local concentration of different size fractions.

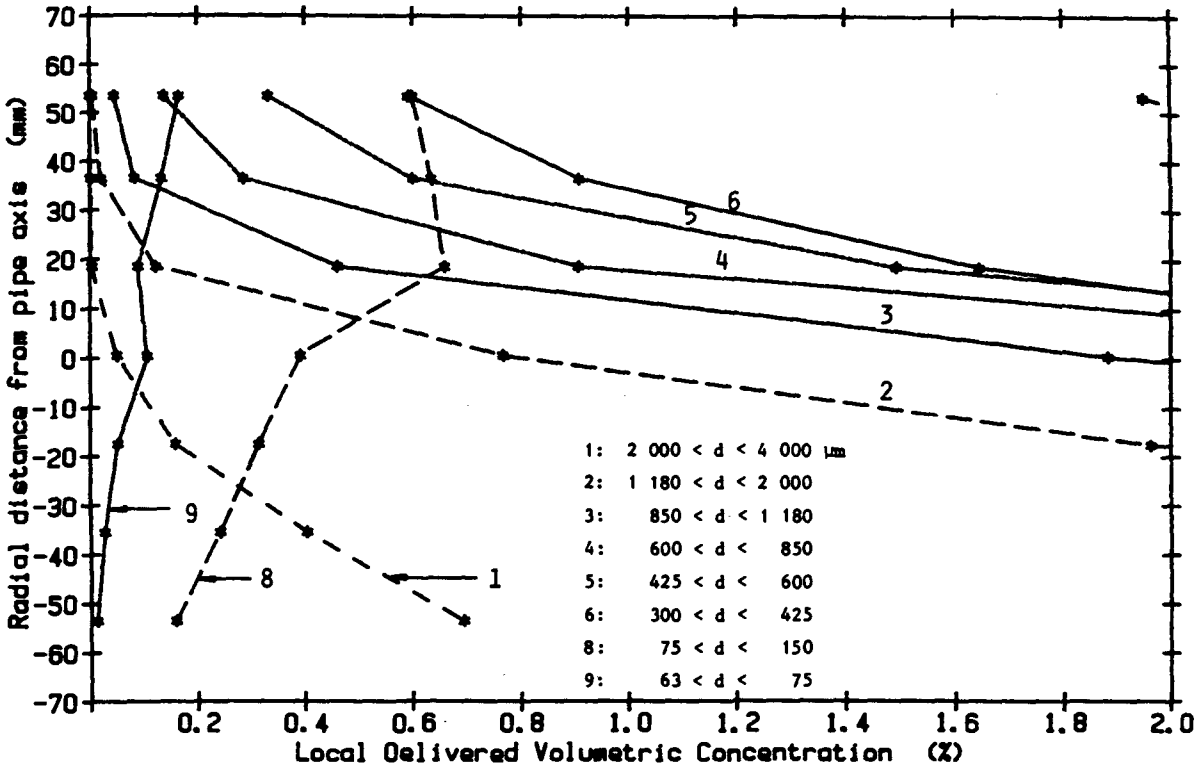

Figure 10 : Variation of local concentration of different size fractions.

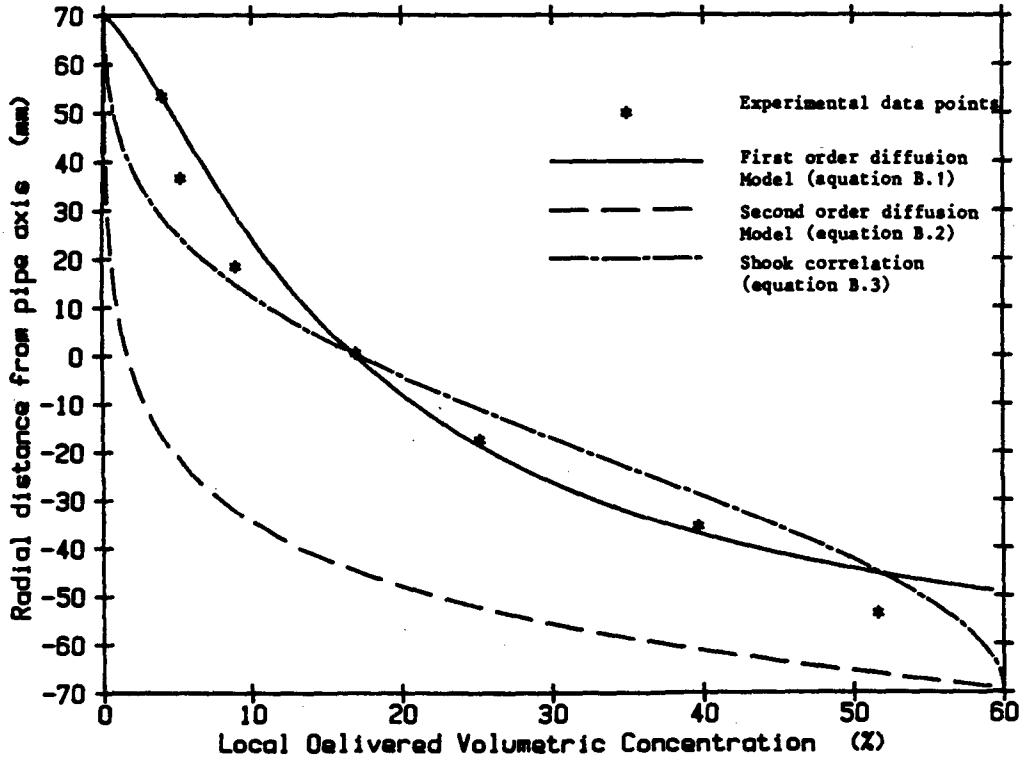

Figure 11 : Experimental data points and concentration correlations.

APPENDIX E
COMPUTER PROGRAM LISTING

```
!*****************************************************************************

!                                  D P F L O W

!Pressure gradient computation for the dense phase flow of classified tailings

!*****************************************************************************

library "PRINTER.TRC"          ! Printer output routines
library "SPLOT.TRC"            ! Screen plotting routines
library "VELOCITY.TRC"         ! Finite element method routines

declare def LOCATE
option angle degrees

public Cc,DIAM,dpdx,dpdxL,G,h,Ko,Mum,Muslid,Phi,Rho,Sm,SmV,Ss
public dp,Cv,Cvehicle,dT,Pt,drep,Ccmin,Ccmax,Delta,CmaxF,Sf,Vs,Vcorr
public Taumixw,Tauliqw,Tausfailw,TauwSp,TauwSW,V,TotalMum,WallMum
public TEST_FILE$,XINT,XMIN,XMAX,YINT,YMIN,YMAX,VDISTLOOP
public DATA_NUM,KROUGH,MESHDATA$,MEAN_VELOCITY,Rinter

dim D(25)                       ! Particle Size Distribution diameters
public DPDATA(50)               ! dp/dx data points
dim OBS$(10)                    ! Flow observations
dim PASS(25)                    ! Percentage passing
dim RET(25)                     ! Percentage retained
dim TEMPDATA(50)                ! Slurry temperature data points
public VDATA(50)                ! Velocity data points
dim VO(10)                      ! Flow observation velocities
dim VdP(1,2)


open #1: printer

!*****************************************************************************
! PROGRAM DRIVER :

call INITIALISE
call WATER_PROP
let Cv = (Sm-Sw)/(Ss-Sw)
call VEHICLE_PROP
call SOLID_PROP
call PRINT_START
let LOOP = 0
let MinDP = DPmin*1000 - Sm*Rho*G*sin(Phi)
let MaxDP = DDPmax*1000 - Sm*Rho*G*sin(Phi)
    for dp = MinDP to MaxDP step (MaxDP-MinDP)/(CALCNUM-1)
        let LOOP = LOOP + 1
        let dpdx = dp + Sm*Rho*G*sin(Phi)
        let dpdxL = abs( dp - Cc*(Ss-SmV)*Rho*G*sin(Phi) )
        let A = abs( dpdx - Sm*Rho*G*sin(Phi) )
        let B = Ko*dpdxL*tan(Delta)
        let C = Rho*G*(Ss-SmV)*Cc*cos(Phi)*tan(Delta)
            if abs(Phi) = 90 then
                let Rinter = ( B + (DIAM*C/2) ) / ( (A/2) + C )
                let MESHDATA$ = "25NODE.PRN"
            else
                let MESHDATA$ = "172NODE"
            end if
        call FEM_DRIVER
        let V = MEAN_VELOCITY
        call PRINT_OUTPUT
        let VdP(LOOP,1) = V
        let VdP(LOOP,2) = dp
    next dp
call PRINT_END
call SCREEN_AXES
call SDATA_PLOT
call LOG_STANDARD_ERROR
```

```
    for i = 1 to LOOP
        let TotaldP = ( VdP(i,2) + Sm*Rho*G*sin(Phi) ) / 1000
        plot VdP(i,1),TotaldP;
    next i
        for VV = 1 to 3
            call VELOCITY_PRESSURE( VdP(,),Fricdp,VV,CALCNUM)
            print #1: "Friction gradient at ";VV;"m/s = ";Fricdp
        next VV

!*************************************************************************
sub DATA_READ

open #10: name DATA_FILE$

input #10: TEST_FILE$
input #10: FACILITY$
input #10: DAT$
input #10: MAT$
input #10: Ss
input #10: Sm
input #10: DIAM
input #10: KROUGH
input #10: SLOPE$

let KROUGH = KROUGH/1e6
if SLOPE$ = "Horizontal" then let Phi = 0
if SLOPE$ = "Vertical Down" then let Phi = -90
if SLOPE$ = "Vertical Up" then let Phi = 90

let DIAM = DIAM/1000
let DPmin = 0
let DPmax = 0
let DDPmax = -20

input #10: DATA_NUM
      for i = 1 to DATA_NUM
          input #10: VDATA(i),DPDATA(i),TEMPDATA(i)
          let SUMTEMP = SUMTEMP + TEMPDATA(i)
             if DPDATA(i) < DPmin then let DPmin = DPDATA(i)
             if DPDATA(i) > DPmax then let DPmax = DPDATA(i)
             if DPDATA(i) > DDPmax then let DDPmax = DPDATA(i)
      next i
let Temp = SUMTEMP/DATA_NUM

input #10: PSD_NUM
      for k = 1 to PSD_NUM
          input #10: D(k),RET(k)
          let SUMRET = SUMRET + RET(k)
          let PASS(k) = 100 - SUMRET
      next k

input #10: OBS_NUM
    if OBS_NUM <> 0 then
        input #10: DOBS
        for j = 1 to OBS_NUM
           input #10: VO(j),OBS$(j)
        next j
    end if
let YMAX = 0
let YMIN = 0
    select case DPmax
        case 0
            let YMAX = 0
        case 0 to 10
            let YMAX = 10
            let YINT = 1
        case 10 to 20
            let YMAX = 20
            let YINT = 2
        case else
```

```
            let YMAX = 40
            let YINT = 5
    end select
        select case DPmin
            case 0
                let YMIN = 0
            case -10 to 0
                let YMIN = -10
                let YINT = 1
            case -20 to -10
               let YMIN = -20
               let YINT = 2
         end select

end sub
!*************************************************************************
sub LOG_STANDARD_ERROR

let SUM = 0
    for i = 1 to DATA_NUM
        let V = VDATA(i)
        call VELOCITY_PRESSURE( VdP(,),Fricdp,V,CALCNUM)
        let FricdpDATA = DPDATA(i)*1000 - Sm*Rho*G*sin(Phi)
        let SUM = SUM + ( log10(abs(FricdpDATA)) - log10(abs(Fricdp)) )^2
    next i
let LSE = sqr(SUM) / (DATA_NUM - 1)
print #1: " LSE : ";
print #1 ,using "###.####": LSE

end sub
!*************************************************************************
sub INITIALISE

mat D = 0
mat DPDATA = 0
mat PASS = 0
mat RET = 0
mat TEMPDATA = 0
mat VDATA = 0
mat VO = 0
mat VdP = 0
    do
        let ERR = 0
            when error in
                input prompt "Data File Name ? ":FIL$
                let DATA_FILE$ = "C:\UCTDATA\"&FIL$&".PRN"
                call DATA_READ
                clear
            use
                print "Error";EXTYPE;":";EXTEXT$
                let ERR = 1
            end when
    loop until ERR = 0
let CALCNUM = 10                    ! Number of calculated data points
let Ccmin = .44
let Ccmax = .6
let CmaxF = .74                     ! maximum packing of fine fraction
let Coeffa = 1.4
let G = 9.81                        ! gravitational acceleration
let LOOP = 0
let Sf = .70                        ! particle settling shape factor
let SUMTEMP = 0
let XMAX = 4                        !m/s
let XINT = .25
let XMIN = 0
let Vs = 1e-3                       ! settling velocity for psd split

mat redim VdP(CALCNUM,2)
```

```
end sub
!*****************************************************************************
sub SOLID_PROP

let Cc = (1-Pt)*Cv
let Delta = 23.529*Cv + 17.882
let Muslid = tan(Delta)/2
let Ko = ( Cc/Ccmax )^(15)
let Pcrep = Pt + (1-Pt)/2                          ! d50 of Coarse Fraction
call DIAMETER(drep,Pcrep*100,D,PASS)
let drep = drep*1e-6
    if Cc >= Ccmin then
        let hHi = drep/2
        let hLo = 0
        let KCcmin = Ccmin*(drep^3)
            do
                let h = (hHi+hLo)/2
                let KCc = Cc*( 6*(h^2)*drep^2 - 4*(h^3) )
                    if KCc > KCcmin then
                        let hHi = h
                    else
                        let hLo = h
                    end if
            loop until abs(KCcmin-KCc) < 1e-14
    else
        let h = drep/2
    end if

end sub
!*****************************************************************************
sub VEHICLE_PROP

let dt = 10e-6          ! Starting value for iteration
    do
        let dttrial = dt
        call PERCENTAGE(dttrial*1e6,P,D,PASS)
        let Pt = P/100
        let Cvehicle = Pt*Cv/(1+Cv*(Pt-1))
        let SmV = Sw + Cvehicle*(Ss -Sw)
        let Vcorr = ( 1 - (Cvehicle/CmaxF) )^(-2.5)          ! Landel et al.
        let Mum = Mu*Vcorr
        let dt = sqr( (Vs*18*Mum) / (Rho*G*Sf*(Ss-SmV)) )
    loop until abs(dt-dttrial) < 1e-7
let TVcorr = ( 1 - (Cv/Ccmax) )^(-3.5)                   ! Landel et al.
let TotalMum = Mu*TVcorr

end sub
!*****************************************************************************
sub WATER_PROP

let Rho = 1004.166 * exp(-.0002958 * Temp)
let Sw = Rho/999.1

    if Temp < 23 then
        let Mu = (1.732 * exp(-.028 * Temp)) * 1e-3
    else if Temp < 43 then
        let Mu = (2.516 - .505 * log(Temp)) * 1e-3
    else
        let Mu = (15.971 * Temp^(-.863)) * 1e-3
    end if

end sub
!*****************************************************************************
end
!*****************************************************************************
sub DIAMETER(PDIAM,P,D(),PASS())

let i = 0
    do
        let i = i + 1
```

```
        let P1 = PASS(i)
    loop until P1 < P
let Ld1 = log10(D(i))
let Ld2 = log10(D(i-1))
let P2 = PASS(i-1)
let m = (P2-P1) / (Ld2-Ld1)
let LPDIAM = ((P-P1)/m) + Ld1
let PDIAM = 10^LPDIAM

end sub
!*****************************************************************************
sub PERCENTAGE(PDIAM,P,D(),PASS())

let i = 0
let Ld = log10(PDIAM)
    do
        let i = i + 1
        let Ld1 = log10(D(i))
    loop until Ld1 < Ld
let Ld2 = log10(D(i-1))
let P1 = PASS(i)
let P2 = PASS(i-1)
let m = (P2-P1) / (Ld2-Ld1)
let P = m*(Ld-Ld1) + P1

end sub
!*****************************************************************************
sub VELOCITY_PRESSURE(VdP(,),dp,VEL,DATANUM)
! Routine to determine the pressure gradient corresponding to a specified
! velocity from the pressure gradient curve stored in array
! VdP(V,dp) using linear interpolation.

let i = 0
let Vmax = 0
    for k = 1 to DATANUM
        if VdP(k,1) > Vmax then let Vmax = VdP(k,1)
    next k
        if Vmax >= VEL then
                do
                    let i = i + 1
                    let V2 = VdP(i,1)
                loop until V2 >= VEL
            let dP2 = VdP(i,2)
                if i = 1 then
                    let V1 = V2
                    let dP1 = dP2
                    let M = 0
                else
                    let V1 = VdP(i-1,1)
                    let dP1 = VdP(i-1,2)
                    let M = ( dP1 - dP2 ) / ( V1 - V2 )
                end if
            let K = dP1 - M*V1
            let dp = M*VEL + K
       else
            let dp = 0
       end if

end sub
!*****************************************************************************
! Definition of LOCATE function used in routines GLOBAL, GAUSS and
! BACKSUBS in module VELOCITY

def LOCATE(i,j,NEQUNS) = .5 * (j-i) * (2*NEQUNS+1-j+i) + i

!*****************************************************************************
```

```
!*************************************************************************
module VELOCITY

! This module contains all the routines used to calculate the velocity
! distribution in a slurry pipeline. The finite element mesh is specified
! by the data file name MESHDATA$.

!*************************************************************************

library "FNTDLIB.TRC"                    ! Trigonometric functions degrees
declare def acos
declare def LOCATE
declare public Cc,DIAM,dpdx,dpdxL,G,h,Ko,Mum,Muslid,Phi,Rho,Sm,SmV,Ss
declare public dp,Cv,Cvehicle,dT,Pt,drep,Ccmin,Ccmax,Delta,CmaxF,Sf,Vs,Vcorr
declare public TauwSp,TauwSW,V,MEAN_VELOCITY,VDISTLOOP
declare public KROUGH,Rinter,TotalMum,FlowRegime$
declare public Taumixw,Tausfailw,Tauliqw
share A,B,K,BANDWIDTH,NBOUNDARY,NELEMENT,NEQUNS,NNODE,ORDER,Tausfail
share R,Rapp,Rh,Rw,XMIN,XMAX,ps,VelB,MESHDATA$,Beta,dpfric
share AREAS(1)
share C(3)
share D(3)
share ELEMENT(1,1)
share ELEMENTCOORD(3,3)
share FORCE(1)
share GLOBALSTIFF(1)
share LOCALFORCE(1)
share LOCALSTIFF(1,3,3)
share NODECOORD(1,1)
share NODE(3)
share SOLUTION(1)
share VELOCITY(1)
share #1,#2,#10

open #1: PRINTER
open #2: SCREEN 0,1,0,1

!*************************************************************************
sub FEM_DRIVER

option angle degrees

let Rw = DIAM/2
let Rh = Rw - h
let dpfric = dpdx - Sm*Rho*G*sin(Phi)
let A = dpfric
let B = Ko*dpdxL*tan(Delta)
let K = Rho*G*(Ss-SmV)*Cc*cos(Phi)*tan(Delta)

if abs(Phi) = 90 then
    let MESHDATA$ = "19MESH.PRN"
    let Tausfail = B
    let Tausfailw = B * (Muslid/tan(Delta))
    let Taumixw = dpfric*Rw/2
    let Tauliqw = Taumixw - Tausfailw
        if Tauliqw =< 0 then
            let MEAN_VELOCITY = 0
        else
            let VelB = Tauliqw*h/Mum
            let Taumixh = dpfric*Rh/2
            let Tauliqh = Taumixh - Tausfail
                if Tauliqh =< 0 then
                    let FlowRegime$ = "PLUG"
                    let MEAN_VELOCITY = VelB * (Rw^2 + Rh^2) / (2*Rw^2)
                else
                    let FlowRegime$ = "SYM. CORE"
                    let VDISTLOOP = VDISTLOOP + 1
                    let ps =  2*Rh*Tauliqh / ( Rh^2 - Rinter^2 )
                        if VDISTLOOP = 1 then
                            call MESHREAD
```

```
                                call NODEPLOT
                            end if
                        call BOUNDARY_VALUES
                        call LOCAL
                        call GLOBAL
                        call GAUSS
                        call BACKSUBS
                        call VELCALC
                            if VDISTLOOP = 1 then call VERT_AXIS
                        call VERTPLOT
                        call INTEGRATE
                    end if
        end if
else
   let MESHDATA$ = "91MESH.PRN"
        if B >= A*Rw/2 then
            let FlowRegime$ = "PLUG"
            let Tausfailw = (B + K*Rw)*Muslid/tan(Delta)
            let Taumixw = A*Rw/2
            let Tauliqw = Taumixw - Tausfailw
                if Tauliqw =< 0 then
                    let MEAN_VELOCITY = 0
                else
                    let VelB = Tauliqw*h/Mum
                    let MEAN_VELOCITY = VelB * (Rw^2 + Rh^2) / (2*Rw^2)
                end if
        else
                if (B+2*Rw*K) < A*Rw/2 then
                    let FlowRegime$ = "ASYM. CORE"
                    let VDISTLOOP = VDISTLOOP + 1
                    let Tausfailh = B + K*Rw
                    let Taumixh = dpfric*Rh/2
                    let Tauliqh = Taumixh - Tausfailh
                    let Ytop = ( B + K*Rw) / ( (A/2) + K )
                    let Ybot = ( B + K*Rw) / ( -(A/2) + K )
                    let ps = 2*Rh*Tauliqh/( (Rh^2) - ((Ytop-Ybot)^2)/4 )
                else
                    let FlowRegime$ = "SLID. BED"
                    let VDISTLOOP = VDISTLOOP + 1
                    let Ywall = Rw - ( (A*Rw/2) - B )/K
                    let Ycent = ( B + K*Rw) / ( (A/2) + K )
                    let Beta = acos(-Ywall/Rw)
                    let Taumixh = dpfric*Rh/2
                    let Forceh = 0
                    let dAngle = ( 180 - Beta ) / 10
                        for Angle = Beta to 180 step dAngle
                            let Y = -Rw*cos(Angle)
                            let Tausfailh = B + K*(Rw-Y)
                            let Tauliqh = Taumixh - Tausfailh
                            let localFh = Tauliqh*Rh*dAngle*Pi/180
                            let Forceh = Forceh + localFh
                        next Angle
                    let Denom = Pi*Rh^2 - ( (Ycent-Ywall)*Rh*sin(Beta) +
Beta*(Rh^2)*Pi/180 - Ywall*Rh*sin(Beta) )
                    let ps = 2*Forceh/Denom
                end if
                    if VDISTLOOP = 1 then
                        call MESHREAD
                        call NODEPLOT
                    end if
            call BOUNDARY_VALUES
            call LOCAL
            call GLOBAL
            call GAUSS
            call BACKSUBS
            call VELCALC
                if VDISTLOOP = 1 then call VERT_AXIS
            call VERTPLOT
            call INTEGRATE
        end if
```

```
end if

end sub
!*************************************************************************
sub MESHREAD

! This routine reads the nodal coords, nodal conectivity and number of
! boundary nodes from data files MESHDATA$.

open #10: NAME MESHDATA$
input #10: NNODE,NBOUNDARY
mat redim NODECOORD(NNODE,2)
    for i = 1 to NNODE
        input #10: NUM, R,THETA
        let NODECOORD(i,1) = ((DIAM-2*h)/2)*R*sin(THETA)
        let NODECOORD(i,2) = ((DIAM-2*h)/2)*R*cos(THETA)
    next i

input #10: NELEMENT
mat redim ELEMENT(NELEMENT,3)
    for k = 1 to NELEMENT
        input #10: ELEMNUM, ELEMENT(k,1), ELEMENT(k,2), ELEMENT(k,3)
    next k
let ORDER = NNODE - NBOUNDARY
close #10

end sub
!*************************************************************************
sub NODEPLOT
! Routine to plot the mesh elements at their nodal coordinates. This provides
! a visual check that the mesh data input is correct.

set mode "HERCULES"
clear
let XMIN = -0.05*(DIAM/2)
let XMAX = 1.05*(DIAM/2)*2.464
let YMIN = -1.05*(DIAM/2)
let YMAX = - YMIN
set WINDOW XMIN,XMAX,YMIN,YMAX

for EL = 1 to NELEMENT
   for j = 1 to 4
      if j = 4 then let ELNODE = 1 ELSE let ELNODE = j
      let NOD = ELEMENT(EL,ELNODE)
      let X = NODECOORD(NOD,1)
      let Y = NODECOORD(NOD,2)
      plot X,Y;
   next j
   plot X,Y
next EL

end sub
!*************************************************************************
sub BOUNDARY_VALUES

mat redim SOLUTION(NNODE)
mat SOLUTION = 0
let Taumixw = dpfric*Rw/2

if abs(Phi) = 90 then
        for Bnode = ORDER+1 to NNODE      ! Boundary nodes with prescribed
values
            let SOLUTION(Bnode) = VelB
        next Bnode
else if FlowRegime$ = "SLID. BED" then
        let Betarad = Beta*Pi/180
        let Tauswbed = ( Rho*G*(Ss-SmV)*Cc*Rw*(Betarad-sin(Beta))/Betarad +
Ko*dpdxL ) * Muslid
        let Tauliqwbed = Taumixw - Tauswbed
            if Tauliqwbed =< 0 then
```

```
                let Vbed = 0
            else
                let Vbed = Tauliqwbed*h/Mum
            end if
                for Bnode = ORDER+1 to NNODE
                    let Y = NODECOORD(Bnode,2)
                    let Angle = acos(-Y/Rw)
                        if Angle =< Beta then
                            let SOLUTION(Bnode) = Vbed
                        else
                            let Tausfailw = ( B + K*(Rw-Y) )*Muslid/tan(Delta)
                            let Tauliqw = Taumixw - Tausfailw
                                if Tauliqw =< 0 then
                                    let SOLUTION(Bnode) = 0
                                else
                                    let SOLUTION(Bnode) = Tauliqw*h/Mum
                                end if
                        end if
                next Bnode
else
        for Bnode = ORDER+1 to NNODE
            let Y = NODECOORD(Bnode,2)
            let Tausfailw = ( B + K*(Rw-Y) )*Muslid/tan(Delta)
            let Tauliqw = Taumixw - Tausfailw
                if Tauliqw =< 0 then
                    let SOLUTION(Bnode) = 0
                else
                    let SOLUTION(Bnode) = Tauliqw*h/Mum
                end if
        next Bnode
end if

end sub
!*************************************************************************
sub LOCAL
! This routine calculates the element stiffness matrices and load vectors
! which are stored in LOCALSTIFF and LOCALFORCE respectively.

mat redim LOCALFORCE(NELEMENT)
mat redim LOCALSTIFF(NELEMENT,3,3)
mat redim AREAS(NELEMENT)

for NEL = 1 to NELEMENT
       for j = 1 to 3
           let NODE(j) = ELEMENT(NEL,j)
           let ELEMENTCOORD(j,1) =1   !Modifying matrix for area calculation
           let ELEMENTCOORD(j,2) = NODECOORD(NODE(j),1)
           let ELEMENTCOORD(j,3) = NODECOORD(NODE(j),2)
       next j
   let AREA = ABS( DET(ELEMENTCOORD) / 2 )
   let AREAS(NEL) = AREA
   let C(1) = ELEMENTCOORD(2,3) - ELEMENTCOORD(3,3)
   let C(2) = ELEMENTCOORD(3,3) - ELEMENTCOORD(1,3)
   let C(3) = ELEMENTCOORD(1,3) - ELEMENTCOORD(2,3)
   let D(1) = ELEMENTCOORD(3,2) - ELEMENTCOORD(2,2)
   let D(2) = ELEMENTCOORD(1,2) - ELEMENTCOORD(3,2)
   let D(3) = ELEMENTCOORD(2,2) - ELEMENTCOORD(1,2)
       for i = 1 to 3
           for j = 1 to 3
               let STIFF = ( C(i)*C(j) + D(i)*D(j) ) / (4*AREA)
               let LOCALSTIFF(NEL,i,j) = STIFF
           next j
       next i
   let X1 = ( ELEMENTCOORD(1,2) + ELEMENTCOORD(2,2) ) / 2
   let X = .5*( ELEMENTCOORD(3,2) - X1 ) + X1
   let Y1 = ( ELEMENTCOORD(1,3) + ELEMENTCOORD(2,3) ) / 2
   let Y = .5*( ELEMENTCOORD(3,3) - Y1 ) + Y1
   let R = sqr( (X^2) + (Y^2) )
       if ( B + K*(Rw-Y) ) > A*R/2 then
           let GAMMA = 0
```

```
        else
            let GAMMA = ps/TotalMum
        end if
    let LOCALFORCE(NEL) = (AREA/3) * GAMMA
next NEL

end sub
!*************************************************************************
sub GLOBAL
! Routine to perform the global assembly of local stiffness matrices
! and load vectors into GLOBALSTIFF and FORCE.

let NEQUNS = NNODE
let SIZ = LOCATE(1,NEQUNS,NEQUNS)
mat redim GLOBALSTIFF(SIZ)
mat redim FORCE(NEQUNS)
mat GLOBALSTIFF = 0
mat FORCE = 0
let BANDWIDTH = 0

for NEL = 1 to NELEMENT                          !Loop through the elements
   for ELNODEI = 1 to 3                          !Local row
      let NODEI = ELEMENT(NEL,ELNODEI)           !Global node i
      if NODEI <= NEQUNS then
         let FORCE(NODEI) = FORCE(NODEI) + LOCALFORCE(NEL)
            for ELNODEJ = 1 to 3                    !Local column
               let NODEJ = ELEMENT(NEL,ELNODEJ)     !Global node j
               if NODEJ <= NEQUNS then
                  let DIFF = NODEJ - NODEI
                     if DIFF >= 0 then
                        if DIFF > BANDWIDTH then let BANDWIDTH = DIFF
                        let POSITION = LOCATE(NODEI,NODEJ,NEQUNS)
                        let GLOBALSTIFF(POSITION) = GLOBALSTIFF(POSITION) +
LOCALSTIFF(NEL,ELNODEI,ELNODEJ)
                     end if
               end if
            next ELNODEJ
      end if
   next ELNODEI
next NEL

! Modifing force vector for nodes with prescribed values
    for i = 1 to ORDER                          ! Rows of force vector
        for Bnode = ORDER+1 to NNODE            ! Boundary nodes
            let POSITION = LOCATE(i,Bnode,NEQUNS)
            let FORCE(i) = FORCE(i) - GLOBALSTIFF(POSITION)*SOLUTION(Bnode)
        next Bnode
    next i

end sub
!*************************************************************************
sub GAUSS
! Routine to perform Gauss reduction on GLOBALSTIFF and FORCE.

for EQUN = 1 to ORDER
   let BANDPOS = EQUN + BANDWIDTH
   if BANDPOS > ORDER then let BANDPOS = ORDER
   let POS = LOCATE(EQUN,EQUN,NEQUNS)
   let PIVOT = GLOBALSTIFF(POS)
   let ROWSTART = EQUN + 1
      for ROW = ROWSTART to BANDPOS
      let POS = LOCATE(EQUN,ROW,NEQUNS)
      let FACTOR = GLOBALSTIFF(POS) / PIVOT
      if FACTOR <> 0 then
            for COL = EQUN to BANDPOS
               if ROW <= COL then
                  let POSA = LOCATE(ROW,COL,NEQUNS)
                  let POSB = LOCATE(EQUN,COL,NEQUNS)
                   let    GLOBALSTIFF(POSA)    =    GLOBALSTIFF(POSA)    -
FACTOR*GLOBALSTIFF(POSB)
```

```
            end if
          next COL
        let FORCE(ROW) = FORCE(ROW) - FACTOR*FORCE(EQUN)
      end if
   next ROW
next EQUN

end sub
!*****************************************************************************
sub BACKSUBS
! Routine to calculate nodal values from reduced GLOBALSTIFF and FORCE.
! Nodal values are stored in SOLUTION.

let NEQUN1 = ORDER + 1

for EQUN = 1 to ORDER
   let NBACK = NEQUN1 - EQUN
   let POS = LOCATE(NBACK,NBACK,NEQUNS)
   let PIVOT = GLOBALSTIFF(POS)
   let RESID = FORCE(NBACK)
   let DIFF = ORDER - NBACK
   if DIFF <> 0 then
       let NBACK1 = NBACK + 1
       let BANDPOS = NBACK + BANDWIDTH
       if BANDPOS > ORDER then let BANDPOS = ORDER
          for COL = NBACK1 to BANDPOS
             let POS = LOCATE(NBACK,COL,NEQUNS)
             let RESID = RESID - GLOBALSTIFF(POS)*SOLUTION(COL)
          next COL
   end if
let SOLUTION(NBACK) = RESID / PIVOT
next EQUN

end sub
!*****************************************************************************
sub VELCALC
! Routine to calculate the nodal velocity values from the matrix SOLUTION.
! The nodal velocity values are stored in VELOCITY.

mat redim VELOCITY(NNODE)

for NOD = 1 to NNODE
    let VELOCITY(NOD) = SOLUTION(NOD)
next NOD

end sub
!*****************************************************************************
sub VERT_AXIS

set MODE "HERCULES"
clear
let XMAX = 8
let XMIN = 0
let YMAX = DIAM/2
let YMIN = -YMAX
set WINDOW XMIN,XMAX,YMIN,YMAX
plot XMAX,YMIN;XMIN,YMIN;XMIN,YMAX;XMAX,YMAX;XMAX,YMIN;
   for i = 1 to XMAX
      plot i,YMIN;i,YMIN + YMAX/10
   next i
plot XMIN,0;XMAX,0

end sub
!*****************************************************************************
sub VERTPLOT
! Routine to plot the vertical axis velocity and distribution from VELOCITY

   for i = 1 to NNODE
      let X = NODECOORD(i,1)
      let Y = NODECOORD(i,2)
```

```
      let VEL = VELOCITY(i)
      if X = 0 then
         if Y >= 0 then plot VEL,Y;
      end if
   next i
   plot 0,DIAM/2

   for i = 1 to NNODE
      let X = NODECOORD(i,1)
      let Y = NODECOORD(i,2)
      let VEL = VELOCITY(i)
      if abs(X) < 1e-16 then
         if Y <= 0 then plot VEL,Y;
      end if
   next i
   plot 0,-DIAM/2

end sub
!*****************************************************************************
sub INTEGRATE
! Routine to integrate the nodal velocity values over each element to
! obtain the mean mixture velocity.

let MIXTUREFLOW = 0
let FLOW_AREA = 0

for NEL = 1 to NELEMENT
   let N1 = ELEMENT(NEL,1)
   let N2 = ELEMENT(NEL,2)
   let N3 = ELEMENT(NEL,3)
   let Y1 = NODECOORD(N1,2)
   let Y2 = NODECOORD(N2,2)
   let Y3 = NODECOORD(N3,2)
   let AVVEL = VELOCITY(N1) + (2/3)*( ( ( VELOCITY(N2) + VELOCITY(N3) )/2 )
- VELOCITY(N1) )
   let MIXTUREFLOW = MIXTUREFLOW + AVVEL*AREAS(NEL)
   let FLOW_AREA = FLOW_AREA + AREAS(NEL)
next NEL

let MEAN_VELOCITY = MIXTUREFLOW / FLOW_AREA

! NB ADD IN ANULAR FLOW AS WELL

end sub
!*****************************************************************************
end module
!*****************************************************************************
```

```
!*****************************************************************************
module printer                  ! print routines

declare public Cc,DIAM,dp,dpdx,dpdxL,G,h,Ko,Mum,Muslid,Phi,Rho,Sm,SmV,Ss
declare public Taumixw,Tauliqw,Tausfailw,TauwSp,TauwSW,V,TEST_FILE$
declare public Cv,Cvehicle,dT,Pt,drep,Ccmin,Ccmax,Delta,CmaxF,Sf,Vs,Vcorr
declare public TVcorr,TotalMum,Mu,MATPROP$
open #1: printer
share #1

!*****************************************************************************
sub PRINT_END

print #1: chr$(192);
call PRINT_LINE
print #1: chr$(217)
print #1:

end sub
!*****************************************************************************
sub PRINT_LINE

for i = 2 to 79
     print #1: chr$(196);
next i

end sub
!*****************************************************************************
sub PRINT_OUTPUT

print #1: chr$(179);
print #1 ,using "####.#":Tauliqw;
print #1: tab(8);
print #1 ,using "#####.#":Tausfailw;
print #1: tab(16);
print #1 ,using "#####.#":TauwSW;
print #1: tab(24);
print #1 ,using "#####.#":TauwSp;
print #1: tab(32);
print #1 ,using "  ###.#":Taumixw;
print #1: tab(40);
print #1 ,using " #####.#":dpdxL;
print #1: tab(48);
print #1 ,using " #####.#":dp;
print #1: tab(56);
print #1 ,using " #.####":Ko;
print #1: tab(64);
print #1 ,using "#####.#":dpdx/1000;
print #1: tab(72);
print #1 ,using " ##.##":V;
print #1: tab(80);chr$(179)

end sub
!*****************************************************************************
sub PRINT_START

print #1:
print #1: "Material Properties : ";MATPROP$
print #1: TEST_FILE$,"D:";DIAM,"Phi:";Phi,"Date:";date
print #1: "Ss:";Ss,"Sm:";Sm,"SmV:";SmV
print #1: "C:";Cv,"Cvhcl:";Cvehicle,"Cc:";Cc
print #1: "dt:";dT,"Pt:";Pt,"drep:";drep,"Mus:";Muslid
print #1: "Ccmin:";Ccmin,"Ccmax:";Ccmax,"Delta:";Delta
print #1: "CmaxF:";CmaxF,"Sf:";Sf,"Vset:";Vs,"h:";h
p       r       i       n       t                       #       1       :
"Muw:";Mu,"Vcorr:";Vcorr,"VVisc:";Mum,"TVcorr:";TVcorr,"TVisc:";TotalMum
print #1: chr$(218);
call PRINT_LINE
print #1: chr$(191)
print #1: chr$(179);" TwF";tab(8);"  TwS";tab(16);" TwSW";tab(24);" TwSp";
```

```
print #1: tab(32);" Tw";tab(40);" dpdxL";tab(48);"dpfric";tab(56);"    Ko";
print #1: tab(64);"  dP/dx";tab(72);"   Vm";tab(80);chr$(179)

end sub
!*****************************************************************************
end module
!*****************************************************************************
```

```
!*****************************************************************************
module SPLOT          ! Routines for plotting on screen

declare public TEST_FILE$,XINT,XMIN,XMAX,YINT,YMIN,YMAX
declare public VDATA(),DPDATA(),DATA_NUM,LSE
share X,XRANGE,Y,YRANGE

!*****************************************************************************
sub SCREEN_AXES

clear
let XRANGE = XMAX - XMIN
let YRANGE = YMAX - YMIN

set mode "HERCULES"
set window -.2*XRANGE,XMAX,YMIN-.2*YRANGE,YMAX
set text justify "center","half"

box lines XMIN,XMAX,YMIN,YMAX
   for i = XMIN to XMAX step XINT
       if A=0 then let A=1 else let A=0
       if A=1 then plot text, at i,(YMIN-YRANGE/20):using$("#.##",str$(i))
       plot i,YMIN;i,(YMIN+YRANGE/50)
       plot i,YMAX;i,(YMAX-YRANGE/50)
   next i
plot text, at XRANGE/2,(YMIN-YRANGE/10):"VELOCITY (m/s)"

   for i = YMIN to YMAX step YINT
       if B=0 then let B=1 else let B=0
       if B=1 then plot text, at (XMIN-XRANGE/30),i:using$("##.#",str$(i))
       plot XMIN,i;(XMIN+XRANGE/100),i
       plot XMAX,i;(XMAX-XRANGE/100),i
   next i
set text justify "left","half"
plot text, at (XMIN-.2*XRANGE),YMIN+.65*YRANGE:"PRESS"
plot text, at (XMIN-.2*XRANGE),YMIN+.55*YRANGE:"GRAD "
plot text, at (XMIN-.2*XRANGE),YMIN+.45*YRANGE:"kPa/m"

end sub
!*****************************************************************************
sub SDATA_PLOT

let TITLE$ = "Data File : " & TEST_FILE$
set text justify "center","half"
plot text, at .5*XMAX,YMIN+.95*YRANGE: TITLE$
for i = 1 to DATA_NUM
   let X = VDATA(I)
   let Y = DPDATA(i)
       call SDATA_LABEL
next i

end sub
!*****************************************************************************
sub SDATA_LABEL  ! Square

let DX = XRANGE/180
let DY = YRANGE/140

plot X,Y;X+DX,Y+DY;X-DX,Y+DY;X-DX,Y-DY;X+DX,Y-DY;X+DX,Y+DY

end sub
!*****************************************************************************
sub SLSE_WRITE
let TITLE$ = "LSE : " & str$(LSE)
set text justify "center","half"
plot text, at .1*XMAX,YMIN+.85*YRANGE: TITLE$
end sub
!*****************************************************************************
end module
!*****************************************************************************
```